DEPARTMENT OF DEFENSE HANDBOOK

FIRE CONTROL SYSTEMS—GENERAL

This handbook is for guidance only.
Do not cite this document as a requirement.

AMSC/NA   FSC 12GP

FOREWORD

1. This handbook is approved for use by the Department of the Army and is available for use by all Departments and Agencies of the Department of Defense.

2. This handbook is for guidance only. Do not cite this document as a requirement. If it is, the contractor does not have to comply.

3. This handbook was developed to provide guidance and general approaches to the development of fire control systems. In particular, the handbook has been prepared to aid the designers of Army fire control equipment and to serve as a reference guide for all military and civilian personnel who may be interested in the design aspects of such materiel. The guidance in this handbook is based on the fundamental parameters of the fire control problem and its solution. Primary emphasis is placed on the systematic approach required in the design of present-day fire control equipment and systems. This approach involves thorough analysis of the particular fire control problem at hand, establishment of the most suitable mathematical model, and computerization and mechanization of the mathematical model.

4. This handbook was developed under the auspices of the US Army Materiel Command's Engineering Design Handbook Program, which is under the direction of the US Army Industrial Engineering Activity. Research Triangle Institute was the prime contractor for this handbook under Contract No. DAAA09-86-D-0009. The development of this handbook was guided by a technical working group chaired by Ms. Robin Gullifer of the Fire Support Armament Center of the US Army Armament Research, Development, and Engineering Center.

5. Beneficial comments (recommendations, additions, deletions) and any pertinent data which may be of use in improving this document should be addressed to Commander, US Army Armament Research, Development, and Engineering Center, ATTN: AMSTA-AR-EDE-S, Picatinny Arsenal, NJ 07806-5000, by using the Standardization Document Improvement Proposal (DD Form 1426) appearing at the end of this document or by letter.

CONTENTS

CHAPTER 1
INTRODUCTION TO FIRE CONTROL SYSTEMS

CHAPTER 2
THEORETICAL ASPECTS OF THE FIRE CONTROL PROBLEM
AND ITS SOLUTION

CHAPTER 3
FUNCTIONAL ELEMENTS OF FIRE CONTROL EQUIPMENT

CHAPTER 4
DESIGN PHILOSOPHY

CHAPTER 5
DESIGNING FOR RELIABILITY, MAINTAINABILITY,
EASE OF OPERATION, AND SAFETY

CHAPTER 6
FIRE CONTROL SYSTEM DESIGN

CHAPTER 7
NUCLEAR, BIOLOGICAL, AND CHEMICAL
CONTAMINATION SURVIVABILITY

APPENDIX A
GENERAL BALLISTIC EQUATIONS

APPENDIX B
FILTERING AND PREDICTION

APPENDIX C
PROBABILITY THEORY

LIST OF ILLUSTRATIONS

LIST OF TABLES

LIST OF ABBREVIATIONS AND ACRONYMS

AA = aptitude area
= antiaircraft
ADC = air data converter
ADL = armament datum line
ADSS = air data system
ADS = air data servo system
AFAS = advanced field artillery system
AFAS-C = advanced field artillery system cannon
AFQT = Armed Forces Qualification Test
AGL = above ground level
AHARS = attitude and heading reference system
AHIP = Attack Helicopter Improvement Program
AL = azimuth lead angle
ALU = arithmetic logic unit
AMC = US Army Materiel Command
AOA = angle of attack
APDS = armor-piercing discarding sabot
APFSDS = armor-piercing, fin-stabilized, discarding sabot
APFSDS-T = armor-piercing, fin-stabilized, discarding sabot, tracer
AR = Army Regulation
= autoregressive
ARDEC = US Army Armament Research, Development, and Engineering Center
ARU = attitude reference unit
ASI = additional skill identifier
ASVAB = Armed Services Vocational Aptitude Battery
ATE = automatic test equipment
AWS = area weapon system
BAT = balanced area tracker
BC = ballistic computer
BCD = binary-coded decimal
BCS = battery computer system
BFW = Bradley fighting vehicle
BIT = built-in test
BITE = built-in test equipment
BOIP = basis of issue plan
BOIPFD = basis of issue plan feeder data
BRL = Ballistic Research Laboratory
BRU = boresight reticle unit
BUCS = backup computer system
C^2I = command, control, and intelligence
C^3 = command, control, and communications
CD = compact disk
cdf = cumulative distribution function

CFOV = center of the field of view
CGPSE = commander's GPS extension
CID = commander's integrated display
CITV = commander's independent thermal viewer
CMB = computer memory board
COFT = conduct of fire trainer
CPG = copilot/gunner
CPU = central processing unit
CRT = cathode-ray tube
CTDR = Commercial Training Device Requirement
DAP = display adjustment panel
DCT = digital control transformer
DELACC = delivery accuracy
DEU = display electronic unit
DFT = discrete Fourier transform
DIVAD = division air defense
DMA = direct memory access
DS2 = decontaminating solution No. 2
DSC = DIVAD system controller
DT = development test
DTB = data transmission board
DTV = daytime video
DU = depleted uranium
DVO = direct view optics
E = target elevation angle
ECCM = electronic counter-countermeasures
ECM = electronic countermeasures
EKF = extended Kalman filter
EMI = electromagnetic interference
EMP = electromagnetic pulse
EOM = end of message
ERDEC = Edgewood Research, Development, and Engineering Center
ESPAWS = enhanced self-propelled artillery weapon system
ETAS = elevated target acquisition system
EU = electronic unit
FAAD = forward area air defense
FADAC = field artillery digital automatic computer
FAMAS = field artillery meteorological acquisition system
FCC = fire control computer
FCP = fire control processor
FDLS = fault detection location system
FE = fire elevation angle
FFAR = folding fin aerial rocket
FFT = fast Fourier transform
FIST = fire support team

FISTV = fire support team vehicle
FLIR = forward-looking infrared
FLOT = forward line of own troops
FM = frequency modulation
FOG-M = fiber-optic guided missile
FOV = field of view
GAS = gunner's auxiliary sight
GBM = gun ballistics module
GD = soman
GDU = graphics display unit
GFE = Government-furnished equipment
GFT = graphical firing table
GLAADS = gun low-altitude air defense system
GLLD = ground laser location designator
GPM = gun processor module
GPS = gunner's primary sight
= global positioning system
GRC = gyro-reticle compensation
GTD = gun/turret drive
G/VLLD = ground/vehicular laser location designator
HARS = heading and attitude reference system
HD = mustard
HDU = helmet display unit
HEAT = high-explosive antitank
HEAT-MP-T = high-explosive, antitank, multipurpose, tracer
HEIT = high-explosive incendiary tracer
HELP = Howitzer Extended Life Program
HEP = high-explosive plastic
HFEA = Human Factors Engineering Analysis
HFHTB = human factors howitzer test bed
HHA = Health Hazard Assessment
HIP = Howitzer Improvement Program
HMD = helmet-mounted display
HMMS = Hellfire modular missile system
HOGE = hovering out of ground effects
HOV = hover
IAT = image automatic tracking
ICVS = infantry combat vehicles
IFF = identification, friend or foe
iff = if and only if
IFV = infantry fighting vehicle
IHADSS = integrated helmet and display sight system
IHU = integrated helmet unit
ILS = integrated logistics support
INTAAWS = integrated air-to-air weapons system

IO = input-output
IPT = initial production test
IR = infrared
J-STARS = Joint Air Force/Army Surveillance and Target Attack Radar System
KE = kinetic energy
KIAS = knots indicated airspeed
KTAS = kt airspeed
LED = light-emitting diode
LHX = light helicopter, experimental
LHX-U = light utility transport
LIFO = last in, first out
LMC = linear motion compensator
LOS = line of sight
LOS-F-H = line of sight forward heavy
LOS-R = line of sight rear
LRF = laser range finder
LRF/D = laser range finder/designator
LSI = large-scale integration
MANPRINT = manpower and personnel integration
MAP = maximum a posteriori probability estimation
MBT = main battle tank
MECA = microprogrammable emulation computer architecture
MEPSCAT = Military Entrance Physical Strength Capacity Test
METT = mission, enemy, terrain, and troops
MFOV = medium field of view
MGEM = modern gun effectiveness model
ML = maximum likelihood estimation
MLRS = multiple launch rocket system
MMS = mast-mounted sight
MMSE = minimum mean square error
MOPP = mission-oriented protective posture
MOS = metal oxide semiconductor
= military occupational specialty
MPE = mean probable error
MPT = manpower, personnel, and training
MRS = muzzle reference sensor
MSG = message
MSI = medium-scale integration
MTBF = mean time between failures
MTDF = modified three degrees of freedom
MTI = moving target indicator
MTTR = mean time to repair
mux = multiplexer
MVND = multivariate normal distribution
MW = main weapon

MWFCS = multiweapon fire control system
NASA = National Aeronautics and Space Administration
NATO = North Atlantic Treaty Organization
NBC = nuclear, biological, and chemical
NDRC = National Defense Research Commission
NEMA = National Electrical Manufacturers Association
NFOV = narrow field of view
NLOS = nonline of sight
NMS = new manning system
NOE = nap of the earth
NASTRAN = NASA advanced finite element structural analysis system
NSTDR = Nonsystem Training Device Requirement
OAS = omnidirectional airspeed sensor
ORD = Operational Requirements Document
ORT = optical relay tube
OT = operational test
P = pilot
PADS = position and azimuth determining system
PC = personal computer
PCMCIA = personal computer memory card international association
p.d. = positive-definite
pdf = probability density function
PGW = precision-guided weapon
PIVADS = product-improved Vulcan air defense system
PM = program manager
POS/NAV = position and navigation
PNVS = pilot night vision system
PSD = power spectral density
p.s.d. = positive-semidefinite
PTF = pulse transfer function
PVC = polyvinyl chloride
QQPRI = quantitative and qualitative personnel requirements information
RAM = random access memory
= reliability, availability, and maintainability
RAM-D = reliability, availability, and maintainability-durability
RF = radio frequency
RIG = rate-integrating gyro
ROM = read-only memory
ROR = range-only radar
R&M = reliability and maintainability
rms = root mean square
RP = radar processor
RPM = rocket processor module
rpm = revolutions per minute
rss = root sum square

RT = receive traffic
RTF = ready to fire
SACMFCS = small arms common module fire control system
SADARM = search-and-destroy armor
SCB = servo controller board
SDF = six degrees of freedom
SDT = statistical decision theory
SEU = sight electronics unit
SGA = standards of grade authorizations
SGS = swiveling gunner station
SINCGARS = single-channel ground and airborne radio system
SMASH = Southeast Asia multisensor and armament system for helicopter
SOS = stabilized optical sight
SOTAS = standoff target acquisition system
SP = self-propelled
SQI = special qualification identifier
SSU = stabilized sight unit
= sensor survey unit
SSWG = System Safety Working Group
STB = supertropical bleach
TAA = total Army analysis
TAADS = The Army Authorization Documents System
TACFIRE = tactical fire direction system
TACOM = US Army Tank-Automotive and Armaments Command
TAD = target audience description
TADS = target acquisition and designation system
TCS = turret control system
TDF = three degrees of freedom
TDNS = Training Device Needs Statement
T&E = test and evaluation
TEMP = test and evaluation master plan
TIS = thermal imaging sight
TOE = table of organization and equipment
TOF = time of flight
TOW = tube-launched, optically tracked, wire guided
TP-T = training, practice, tracer
TPCSDS-T = training, practice, cone-stabilized, discarding sabot, tracer
TRADOC = US Army Training and Doctrine Command
TSU = telescopic sight unit
TTHS = trainee, transient, holdee, and student
TTS = tank thermal sight
TV = television
TWGSS = tank weapon gunnery simulation system
TWS = thermal weapon sight
UAV = unmanned aerial vehicle

US = United States
UV = ultraviolet
VADS = Vulcan air defense system
VATLS = visual airborne target location system
VDU = visual display unit
Vh = own ship velocity
Vmax = maximum own ship velocity
VTSS = virtual target scoring system
WFOV = wide field of view
WWI = World War I
WWII = World War II
YAG = yttrium aluminum garnet

CHAPTER 1
INTRODUCTION TO FIRE CONTROL SYSTEMS

The evolution of propelled and self-propelled weapons is reviewed. Weaponry terms, applications, and require-ments are described, and the problems associated with weapon systems development are discussed. Modern weapon systems for ground, sea, and airborne targets are reviewed.

1-1 DEFINITION AND NATURE OF FIRE CONTROL

1-1.1 GENERAL

This chapter defines and describes the nature of fire control, chronologically covers development of Army fire control equipments, discusses recent developments in Army fire control, and summarizes the applications of fire control to modern warfare. Hopefully, this information will both interest the fire con-trol designer and be of direct value to him by providing knowledge of past developments and present trends.

1-1.2 DEFINITION AND GOALS OF FIRE CONTROL

Fundamentally, all fire control problems are variations of the same basic situation: launching a projec-tile from a weapon station to hit a selected target. The target or the weapon station or both may be mov-ing. Fire control is the science of offsetting the direction of weapon fire from the line of sight to the target in order to hit the target as illustrated in Fig. 1-1. The angle of offset is called the prediction angle, i.e., the angle between the line of sight (the line from the weapon station to the target at the instant of firing) and the weapon line (the extension of the weapon axis). It represents the fire control system prediction of the best solution to the fire control problem using the available information. As discussed subsequent-ly, the prediction angle is achieved as the result of offset components in elevation and azimuth.

With guns and rocket launchers, solution data are applied up to the instant of firing, whereas with guid-ed missiles, solution data are also applied at intervals or continuously after firing. The fire control series is concerned with weapons laying before and during firing and does not cover in-flight control of guided missiles, although many of the same principles apply.
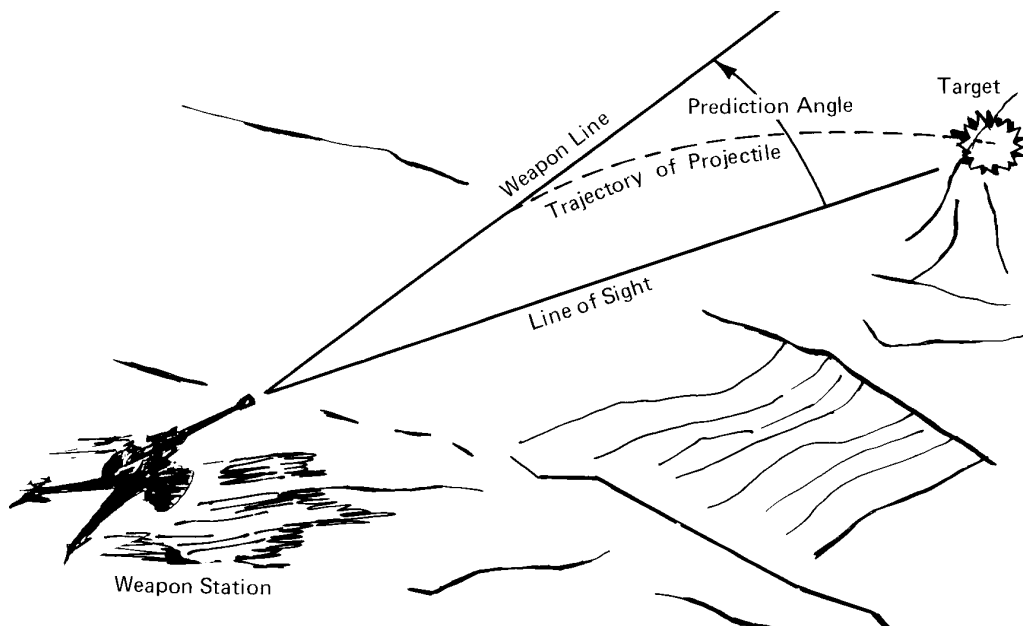
Figure 1-1. Fire Control Scenario (Ref. 1)

Fire control is accomplished by (1) accumulating appropriate input data, (2) calculating the elevation and azimuth components required for the projectile to intersect the target, and (3) applying these components to the fire control mechanisms to position the weapon correctly. These three functions are primarily associated, respectively, with (1) acquisition and tracking systems, (2) computing systems, and (3) weapon pointing systems.

In some situations fire control includes solution of two additional problems: (1) maintaining cognizance of the weapon-target situation and controlling the time and volume of fire to achieve maximum effectiveness of fire and minimize waste of ammunition and (2) causing projectiles to explode when they reach the vicinity of the target by means of time fuzes preset with the aid of a fuze-time computer. The latter problem, however, does not occur with impact and proximity fuzes.

Thus fire control may be broadly defined as quantitative control over one or more of the following to deliver effective weapon fire on a selected target:

    1. The direction of launch

    2. The time and volume of fire

    3. The detonation of the missile.

Fire control , however, is primarily concerned with Item 1, the direction of launch, and the fire control series is concerned mainly with this aspect.

Throughout the Army community, the terms "weapon fire control" and "weapon control" are used interchangeably with the expression "fire control". To indicate specific applications to certain types of weapons, terms such as "gun fire control" and "missile fire control" are frequently used.

1-1.3 SUMMARY OF FIRE CONTROL METHODS

The fundamental problem of fire control is to orient a weapon so that the projectile it fires will hit the selected target. For weapons of the present era fire control varies in complexity from the simple aiming of a pistol to the intricate problem of destroying an intercontinental ballistic missile in flight.

Two general methods of fire control are used with Army weapons: direct fire control and indirect fire control.

1-1.3.1 Direct Fire Control

Direct fire control is used to control weapon fire delivered at a target that can be observed e.g., by optical or electro-optical instruments, either from the weapon itself or from nearby elements, i.e., as in a director-controlled type of weapon system. When the target is visible from the weapon, a line of sight is established between the gun and the target. The weapon can then be aimed in elevation and azimuth with reference to this line of sight either with sighting instruments mounted on the weapon or with a director fire control system.

The following types of direct fire are used in Army combat situations:

    1. Antiaircraft fire

    2. Small arms weapon fire, e.g., rifles and machine guns

    3. Tank weapon fire

    4. Airborne weapon fire

    5. Field artillery weapon fire.

Types 1 through 4 are typical direct fire situations. On the other hand, fire from field artillery weapons (Type 5) is direct fire only under exceptional short-range conditions.

1-1.3.2 Indirect Fire Control

Indirect fire control is used for the control of weapon fire delivered at a target that cannot be observed from the weapon position. When the target is not directly visible from the weapon, e.g., when it lies behind a hill, an indirect method of observation is established. Fire control intelligence is then obtained and firing data computed for the gun at a fire direction center. The transmission of firing data to the weapon

may be verbal or digital by radio, wire, or cable. In the digital case the gun may be pointed in azimuth and in elevation automatically in accordance with the established firing data.

The following types of indirect fire are used in Army combat situations:

1. Mortar fire
2. Field artillery weapon fire
3. Tank weapon fire.

The first two types are typical indirect fire situations (No. 2 can be direct fire in exceptional circumstances.); by contrast, No. 3 only occasionally involves the use of indirect fire.

1-1.3.3 Geometry of Typical Fire Control Problem

Fig. 1-2 shows the fundamental geometry of a typical direct fire control problem in terms of the prediction angle, i.e., the total offset angle measured from the present line of sight to the weapon line. As indicated, it has an elevation component and an azimuth component. The prediction angle is uniquely determined at each instant of the fire control situation by two factors:

1. The motion of the target relative to the weapon
2. The exterior ballistics affecting the path of the projectile after the weapon is fired.
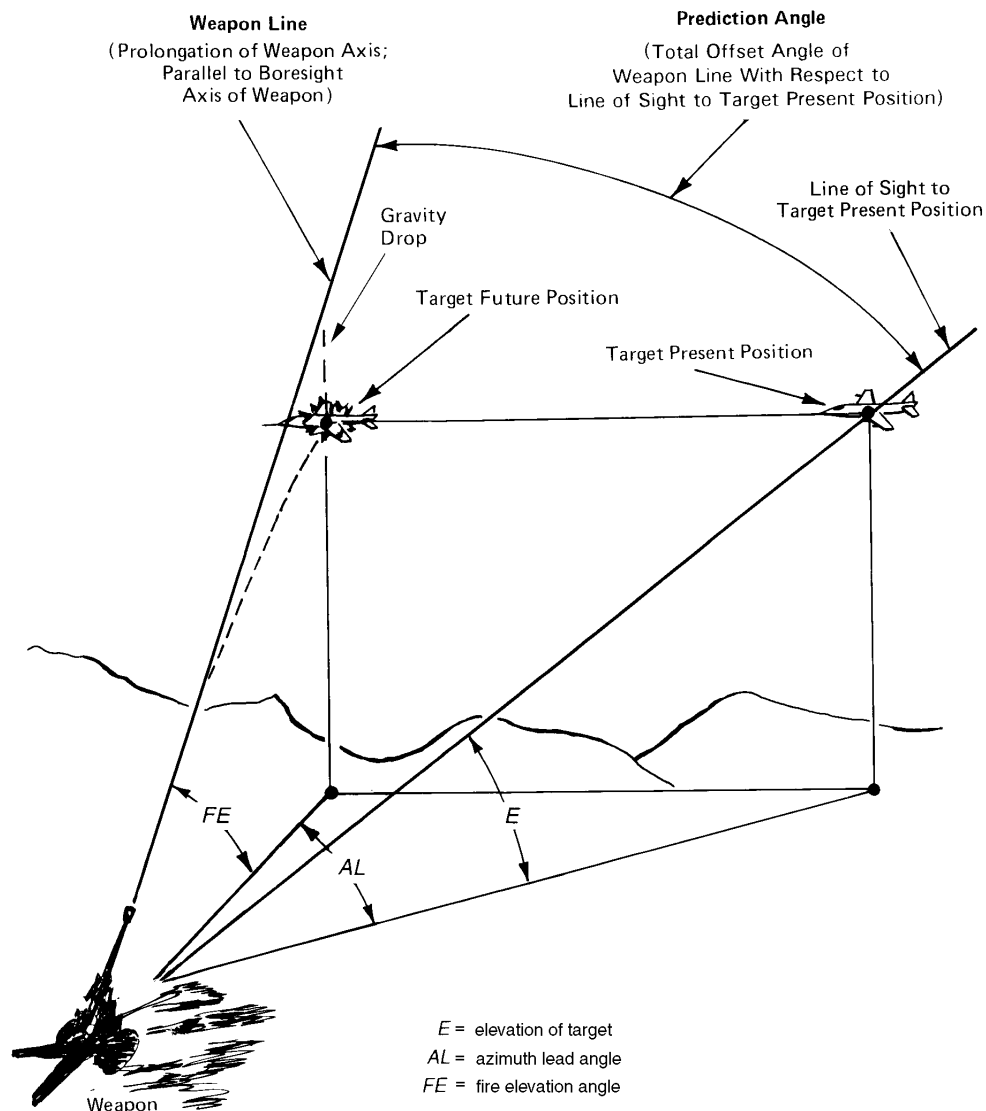
Figure 1-2. Fundamental Geometry of a Typical Fire Control Problem for Surface-to-Air Fire (Ref. 1)

The theoretical fire control problem consists of finding the magnitude of the required prediction angle between the weapon line and the line of sight, together with the direction of the axis about which it represents a rotation, as functions of measurable physical quantities. Because of practical considerations involved in achieving the required offset of the weapon line from the line of sight, the prediction angle is defined in terms of and implemented by means of two separate components—an elevation component and an azimuth component—the combination of which yields the required offset angle. For example, in the illustrative fire control problem depicted in Fig. 1-2, the elevation component of the prediction angle is equal to the fire elevation angle (FE) minus the target elevation angle (E). FE is the vertical angle between the axis of the weapon bore (the weapon line) and its projection onto the horizontal plane, and E is the vertical angle between the line of sight to the present target position and its projection onto the horizontal plane. The azimuth component of the prediction angle in Fig. 1-2 is equal to the azimuth lead angle (AL), the angle between the horizontal projections of the weapon line and the line of sight to the present target position.

A practical fire control design effort analyzes the fire control problem, establishes a mathematical model, and mechanizes this model. The end product is equipment suitable to receive the available inputs for particular fire control applications and generate the correct prediction angle as the output. This practical design problem is discussed in Chapters 3, 4, and 6.

1-1.4 CLASSIFICATION OF FIRE CONTROL EQUIPMENT

Fire control objectives are achieved by the use of specially designed aids, instruments, and systems. One or more of these basic operations may be involved: electrical, electronic, mechanical, optical, hydraulic, or combinations of these.

Fire control aids are devices that help the aimer judge or correct the prediction angle. They include such items as rifle sights and, in a broader sense, the use of tracer bullets. Fire control instruments are used for more exact quantitative acquisition, calculations, and application of data than aids. They include range finders, compasses, telescopes, and radars; predictors, directors, and other computers; and servos and other devices used to position the weapon in azimuth and elevation. A fire control system is defined as an assemblage of interacting or interdependent fire control equipment that receives data concerning the present position and motion (if any) of a selected target, calculates the future target position, correlates this information with information concerning projectile flight (exterior ballistics data), and controls the aiming of the weapon to bring effective fire upon the target. Human operators may be considered elements of a system, and in any evaluation of overall system effectiveness they should be so considered.

Fire control equipment is frequently classified by its location as either on-carriage or off-carriage equipment.

On-carriage describes instruments such as sighting telescopes and range finders that are mounted directly on the weapon or weapon carriage.

Off-carriage equipment includes all fire control instruments that are not mounted on weapons or weapon carriages. Off-carriage instruments might include some types of range finders, radars, position-locating systems, computers, and illuminating devices.

Depending on the application, most fire control instruments can fall into either classification.

1-1.5 APPLICATIONS OF MODERN FIRE CONTROL SYSTEMS

The various types of weapon fire that are controlled by fire control equipment may be classified by establishing the relationship of the physical location of the weapon fire to the physical location of the target. Thus the various types of weapon fire covered in this handbook may be classified as

      1. Surface-to-surface

      2. Surface-to-air

      3. Air-to-surface

      4. Air-to-air.

Each classification applies to all of the types of weapon fire implied by the name of the classification. That is, the classifications do not differentiate the type of weapon or launcher; the type of projectile, warhead, or propellant; or the type of fire control system used; or the type of target; or stationary and moving target. In this handbook it is also assumed that air-to-air and air-to-surface classifications are limited to aircraft available to the US Army, notably rotary wing aircraft or helicopters.

With respect to the type of warhead fired, there is a wide variety of so-called "kill mechanisms". Simple high-explosive warheads are intended to inflict damage by means of the overpressure created by the blast. On the other hand, fragmentation rounds distribute a large number of small shell fragments over an area.

Antitank warheads are designed to penetrate the armor of a tank by using kinetic or chemical energy and to inflict injury on the crew and damage to the ammunition, fuel, or tank equipment.

Some antipersonnel munitions contain a cargo of small projectiles, i.e., flechettes. When the munition is fired or the high-explosive charge detonates, the projectiles are propelled into a controlled area at very high velocity. These projectiles, although light in weight, are capable of producing damage to the targets struck.

With respect to targets, small, singular targets are referred to as point targets, e.g., a vehicle, an aircraft, a soldier. A target with larger extension, e.g., a formation of vehicles, aircraft, or troops, generally is referred to as an area target. Obviously, the fire control accuracy required and the kill mechanism used depend upon the type of target being engaged.

1-1.5.1 Surface-to-Surface

The classification of surface-to-surface weapon fire includes all projectiles, except guided missiles, that are fired from the surface of the earth and whose purpose is to destroy a target also on the surface of the earth.

The destructive intent of surface-to-surface cannon fire is directed in defense and attack against either of the two basic categories of targets: the stationary target and the moving target. With respect to the stationary target, the firing data required for accurate weapon laying is based on providing the required projectile trajectory in accordance with known ballistic data, information on variables of the firing situation, such as wind, and information concerning the location of the target relative to the location of the weapon. Target position relative to weapon position is generally determined by sight but can also be obtained from other sources. An increase in the range of fire between the gun and the target generally results in an increase in the errors of gunfire.

With respect to moving surface targets, information on present position and motion is usually derived from direct observation of the target. Firing data are based on predicting the future target position and then providing a projectile trajectory that passes through that position. From the time a projectile is fired, i.e., exits the gun tube, its trajectory is irrevocably dependent on projectile ballistics, atmospheric effects, rotation of the earth, and gravity. Also a finite time is required for the projectile to reach the target. Accordingly, if the time of flight is short and the target motion is slow, the probability of a hit is reasonably good. On the other hand, if the target is moving rapidly with a high degree of maneuverability, the probability of destruction is low. Inadequate target observation and inaccurate range measurement correspondingly reduce the hit probability (See Chapter 4 for a discussion of hit probability.).

Surface-to-surface weapon fire with rockets includes any rocket-propelled missile whose trajectory cannot be controlled during flight, that is launched from the surface of the earth, and whose purpose is to destroy a target also on the surface of the earth. The comments on surface-to-surface cannon fire apply to rockets also. Essential differences between cannons and rockets are mainly in the important characteristics of the military rocket. Military rockets use a method of propulsion that, unlike the gun-fired projectile, results in the propellant and its gases traveling with the rocket during the period of propellant burning. Military rockets also are characterized by relatively low velocity, which results in greater time of flight to target and thus provides the target greater time to maneuver with a concomitant reduction in the

probability of obtaining hits. Dispersion of single-warhead rockets as a result of in-flight turbulence of the burning propellant, inaccuracies in the symmetry or alignment of the rocket nozzle, and the use of stabilizing fins limit their ground use largely to area targets.

In the tactical employment of military weapons, cannons are generally used where great accuracy and range flexibility are required; rockets are limited in both respects. Conversely, the volume, rate of fire, and high mobility of rocket weapons justify their use against area targets or large troop concentrations, although rockets are not suited for a high rate of fire over extended periods due to logistic constraints. Used in antitank weapons for direct fire by infantrymen at short ranges, the rocket is well suited to deliver a small, light shaped-charge warhead at low velocity that is capable of destroying a tank.

1-1.5.2   Surface-to-Air

The classification of surface-to-air weapon fire includes any projectile, exclusive of guided missiles, that is fired from the surface of the earth and whose purpose is to destroy a target in the air. This classification also includes any rocket-propelled missile launched from the surface of the earth whose trajectory cannot be controlled during flight and whose purpose is to destroy an airborne target. The advantages and disadvantages discussed in subpar. 1-1.5.1 with regard to free-flight rocket employment apply here as well.

The mission of air defense is (1) counterair, (2) preemptive air defense, and (3) point defense of critical assets. Because of the high speed, the maneuvering capabilities in three dimensions, and the relatively small size of airborne targets such as rotary or fixed wing aircraft, the unique problem of this type of fire control is determination of the future position of the target. The fire control problem in surface-to-air gunfire therefore consists of (1) predicting the future course of the target on the basis of its behavior in the time just preceding the firing of the gun, (2) determining the probable position of the target at the end of the time of flight, and (3) preparing the firing data required to place a projectile at that point at that time.

Of major significance in this category of weapon fire is that computation of a single set of firing data will not suffice for application to the aiming point. Rather firing data suitable for any instant must be available during the entire period of time the target is flying within the range of the weapon being employed. This period may be short; therefore, firing data must be produced rapidly and continuously throughout the interval. Further, since the target capability to quickly change direction and speed reduces its vulnerability, the maximum practicable volume of fire must be used in a minimum amount of time to increase the probability of target destruction.

1-1.5.3   Air-to-Surface

The classification of air-to-surface weapon fire includes all projectiles, except guided missiles, that are fired from an aircraft and whose purpose is to destroy a target on the surface of the earth. This includes stationary and moving targets, both point and area. The high velocity of the airborne launching platform adds to the muzzle velocity, has a major impact on the trajectory, and further complicates weapon pointing calculations. For moving targets all of the aspects of prediction mentioned in subpar. 1-1.5.2 must also be considered.

Rockets fired from fast-moving aircraft are more effective than those launched from the ground because of their greater accuracy, which results from the additional speed with respect to the air that the high-speed forward movement of the aircraft imparts to the rocket at launching. The accompanying aerodynamic effects on the rocket fins result in increased stability of the rocket and thereby tend to minimize dispersion and permit relatively accurate fire at point targets. Unfortunately, launching from helicopters traveling at low speeds does not fully realize such advantages. Further, because of helicopter vertical and traverse flight motion, the air mass passing across the launcher causes rocket tip-off, i.e., the rocket reorients into relative wind when launched. Rotor downwash causes a similar tip-off effect.

1-1.5.4 Air-to-Air

The classification of air-to-air weapon fire includes all projectiles, except guided missiles, that are fired from an aircraft and whose purpose is to destroy an aerial target. The fire control problem is essentially the same as the air-to-ground moving target case; the primary difference is the higher speed and vertical maneuverability of the target. This results in a more difficult acquisition and tracking function as well as greater uncertainties in prediction. It also creates a major aircraft steering problem when fixed rocket launchers are used. When fixed launchers are used, the aircraft pilot must "aim" the aircraft at the maneuvering target, a task that is difficult at best.

1-1.6 THE INPUT-OUTPUT (IO) CONCEPT

Fire control may be viewed in terms of certain measured quantities that are used as inputs and certain outputs that are required to position a weapon for firing at a stationary or moving target. The input-output (IO) concept is implied at once when consideration is given to gathering data on the position of a target, calculating the target future position, correlating exterior ballistics information, and controlling the aiming of a weapon to fire on the target.

Basic input data can be enumerated as range, elevation, azimuth, and motion of the target, all measurable with respect to weapon position. Supplementary input data include information on the wind and such items affecting initial projectile velocity as gun barrel erosion and propellant temperature. In any fire control system all available input data are used to the extent of the capability of the system to produce as outputs such firing data as are applicable to the aiming of the weapon being controlled.

1-1.6.1 Primary Factors in Establishing Input-Output Relationships

There are two main categories:

1. Factors affecting the projectile path
2. Target motion with respect to the weapon.

These factors are discussed in some detail in Chapter 2 but are summarized in the paragraphs that follow to clarify the input-output concept. Each of these factors must be considered an integral part of each individual fire control problem. The emphasis allotted to a given factor in establishing the solution to a particular fire control problem is determined primarily by its relative effect on the outputs and by the accuracy requirements of the fire control system. Chapter 3 describes the various functional elements of fire control systems and cites functional arrangements that provide desired input-output relationships for specific fire control systems. Chapter 4 presents the conceptual approach used to achieve the actual designs of these fire control systems most effectively.

1-1.6.1.1 Factors Affecting the Projectile Path

The factors that affect projectile motion are both external and internal to the projectile. The external factors include gravity and the medium, usually air, through which the projectile travels. The internal factors are the projectile mass distribution, shape, size, and spin as well as initial velocity. The external and internal factors are not independent of each other but rather are coupled to produce what are sometimes called rigid-body effects. These effects are described by a set of nonlinear differential equations that cannot be solved in closed form because of the velocity-dependent nature of the coefficients that appear in these equations and are obtained from empirical data. In addition to giving rise to a path, that is not parabolic, rigid-body effects can also explain the deviation of projectile motion from the plane of fire. The term "six-degree-of-freedom model" is often used to describe this set of equations. These equations have been thoroughly verified by comparison with live firing results.

1-1.6.1.2 Target Motion With Respect to the Weapon

Obviously, anything projected at a moving target, whether it is a projectile from a weapon or a football rifled at a fast-moving end, must incorporate some allowance, or lead, to account for target motion if a

hit is to be achieved. If all of the other conditions of a fire control situation remain unchanged, the amount of lead required to correct for target motion increases with the magnitude of the target velocity and varies with the relative direction of the target; a target traveling at right angles to the line of sight requires a larger lead angle than a target traveling at the same speed on some other path.

Target range and projectile time of flight also affect lead. The required lead increases as time of flight increases, or the greater the projectile velocity, the less lead required.

1-1.6.2 Secondary Factors in Establishing Input-Output Relationships

The firing tables that form the basis of correcting for the individual characteristics of projectile trajectories are of necessity computed by assuming certain standard conditions. In an actual fire control problem, various nonstandard conditions must be corrected for if their omission would seriously affect the fire control solution. The following nonstandard conditions are typical:

    1. Corrections to elevation firing data are made to account for
        a. Differences in projectile weight
        b. Increase or decrease in muzzle velocity
        c. Ballistic head winds and tailwinds
        d. Air density and temperature
        e. Shell surface friction effects
        f. Rotation of the earth.
    2. Corrections to azimuth firing data are made to account for
        a. Crosswind
        b. Drift
        c. Rotation of the earth.

Because of the constant improvement that is being made in fire control equipment, sources of error that were considered insignificant may become significant as grosser errors are eliminated. Examples of these are the corrections for cant and gun tube distortion, which are now required for modern tank fire control systems due to the introduction of accurate ranging equipment.

1-2 CHRONOLOGICAL DEVELOPMENT OF ARMY FIRE CONTROL

1-2.1 INTRODUCTION

Missile hurling was a skilled craft thousands of years before writing was developed, and ballistics—the study of the motion and behavior characteristics of projectiles—was elevated from a technical art to a science following the introduction of firearms to Western Europe in the 15th century A.D. On the other hand, fire control reached scientific status quite recently; accurate fire control became practical only with the development of accurate weapons in the last century and a half. The vastly increased ranges of weapons and mobility of targets during the same period made accuracy a practical necessity.

1-2.2 PRE-19TH CENTURY FIRE CONTROL

1-2.2.1 A Word on Nomenclature

Originally, the term artillery was applied to all devices used to propel missiles through the air. With the initial development of firearms, however, all guns were called cannon to distinguish them from mechanically operated missile-throwing weapons. As firearms developed further, those using projectiles of small diameter were termed small arms, whereas all other firearms retained the original terminology of cannon. Eventually, the term artillery came to mean cannon in this sense and to identify the arm of the Army that mans and operates cannon. (See Refs. 2 and 3 for modern definitions of gun, cannon, small arms, howitzer, and mortars, etc.)

1-2.2.2 Control of Weapons Prior to Firearms

A large variety of missile weapons was used from the Stone Age through the Middle Ages, ranging from the earliest hurled stones, spears, and javelins to weapons using stored energy (e.g., the simple bow and later the longbow) and weapons that were elastically operated and mechanically retracted (e.g., the catapult, ballista, and later the crossbow). Control over the accuracy of all of these weapons, however, was primarily a matter of skill and judgment.

1-2.2.3 Development and Control of Early Firearms

The medieval Chinese invention of gunpowder probably became known in the Near East early in A.D. 1200 to Moslems who had fought with Mongols during the reign of Genghis Khan. Gunpowder led eventually to the invention of firearms in the form of heavy, crude cannon that were introduced into warfare in Western Europe about A.D. 1310.

The end of the 14th century witnessed the appearance of the earliest hand firearm, the hand cannon, which was devised from the early crude cannon. The hand cannon evolved as a simple wrought iron or bronze tube of large caliber and smooth bore mounted on a crude stock. It was muzzle loaded, had no trigger or sight, and was fired by lighting a touchhole of exposed powder. Weapon fire was, of course, quite inaccurate.

Weapon improvements in the early days of ordnance engineering were primarily refinements in the ignition of powder charges for small arms and were exemplified by the introduction of triggering devices and the elimination of the objectionable match by the invention of the flintlock. These developments resulted in only small improvements in the accuracy of weapon fire, however. For example, as late as the Battle of Bunker Hill, the Continental troops ensured effectiveness of fire against the British by the simple expedient of holding it until they could see the "whites of their eyes".

Until the 19th century control of gunfire from cannon as from small arms was rudimentary. It consisted chiefly of aligning the cannon with the target for azimuth control and elevating it by eye, even though the gunner's quadrant was invented by Tartaglia about 1545. Sometimes the curvature of the trajectory was allowed for by "sighting along the line of metal". This was accomplished by aligning the top of the muzzle with the point of aim and thus the cannon was elevated by the amount of taper from breech to muzzle.

As early as the 16th century, mathematicians had established approximate solutions for the trajectory of projectiles. Galileo, Tartaglia, Newton, Bernoulli, Euler, and others prepared the foundations for accurate weapon laying in their treatises by bringing theoretical ballistics "to a degree of perfection capable of directing fire in all circumstances" (Tartaglia). Many of the mathematicians of this period were even able to prepare rudimentary forms of firing data from range observations. In the 17th century both a gunner's quadrant and a gunner's level were in limited use.

Through the 18th century, however, inconsistent gun performance and lack of interest of military authorities combined to prevent any advance in fire control corresponding to the advances in the science of ballistics. Little attempt was made to regulate initial velocity because powder charges were estimated and the projectile load was variable. These inaccuracies, combined with poor workmanship on the guns and human fallibility in laying them, severely limited the accurate range. Battle ranges were spoken of as pistol shot (about 46 m) and half pistol shot (about 18 m). Targets were slow; the fastest was a charging troop of cavalry. Fire control is not mentioned in tactical treatises or directives of the period.

1-2.3 DEVELOPMENTS IN THE 19th CENTURY

1-2.3.1 Improvements in Weapons

In the 19th century weapons improved so much in consistency of performance, rapidity of fire, and range that improved fire control became both practical and necessary. Techniques improved generally in manufacturing powder and in fabricating gun components with greater precision and durability. Perhaps the most significant developments, however, were rifling and breech loading.

Rifling imparts rotation to the projectile. It thus gives the projectile stability in flight, prevents tumbling, and reduces dispersion. Rifling has been used in small arms since the late 18th century in such more or less single-shot applications as hunting. As long as muzzle loading was used, however, rifling was impractical in military weapons because of the difficulty of devising a projectile that could be loaded through a fouled bore (especially after rapid firing) and at the same time fit closely enough to expand into the rifling when fired.

Then came the development of percussion primers, which used a new powder that exploded when crushed, and metal cartridge cases that would "obturate", i.e., close up, the gun breech to prevent propellant gases from escaping. These made breech loading and hence rifling practical for artillery. The first workable rifled artillery appeared about 1846. Five years later an elongated bullet with an expandable lead base was developed, which led to the cylindrical-ogival artillery projectile with a rotating band of copper or soft metal alloy to engage the spiral grooves of the gun.

Breech loading not only made rifling practical, it also made rapid fire safe for the first time.

1-2.3.2 Improvements in Fire Control

The first practical gunsights, introduced during the Napoleonic Wars, consisted of fixed front and rear sight points parallel to the bore of the gun. They were mainly suitable for leveling the gun at the point of aim.

Rifling introduced a drift to the right during flight that resulted from the combined effects of right-hand twist (All rifling in US weapons is right-handed.) and gravity. In big guns it was first approximately compensated for by inclining the rear sight bracket. However, during and after the Civil War, increases in range and consistent performance of guns made graduated and adjustable gunsights a necessity. The simple gunsight evolved to the tangent sight, which consisted of a fixed foresight near the muzzle and a rear sight movable in the vertical plane. The reference point—a notch or aperture—of the rear sight was supported on a swinging leaf. Vertical movement of the rear sight was restricted to permit it to follow a drift curve cut out in the sight leaf, which thereby compensated for any lateral deviation of the projectile due to drift. Further refinements permitted lateral adjustment to correct for the effects of wind.

Toward the end of the 19th century, fire control was further improved by adding the sight telescope, which was mounted on the gun so that its line of sight could be offset from the axis of the bore of the gun to correct for the effects of range, drift, and relative motion between gun and target. Elevation scales were graduated in accordance with ordnance proving ground data, and the weight and composition of powder charges were carefully regulated. A final improvement in operation was obtained by installing two sights and dividing the responsibility for keeping the line of sight on target between (l) the pointer, who controlled gun elevation, and (2) the trainer, who controlled gun azimuth.

By the end of the 19th century, refinements in the manufacture of guns, detailed studies of trajectories, and simple fire control sighting equipment had made possible much more accurate long-range shooting than had been possible at the start of the century.

1-2.4 DEVELOPMENTS IN THE 20TH CENTURY THROUGH WORLD WAR II

Until recently fire control concepts could be mastered through a detailed study of actual fire control systems, but the increasing number and complexity of weapons and weapon systems—and hence of the associated fire control systems—have now made it impractical to learn general concepts by this method.

On the other hand, as a background for the approach pursued in the fire control series, a brief exposure to the "hardware", in the form of a survey of fire control development during the 20th century, should be helpful. Sufficient detail is provided to indicate operation of the equipment and functioning of the various mechanisms involved. Detailed information on its use with particular weapons is contained in the appropriate manuals.

1-2.4.1 Field Artillery Fire Control Equipment

Field artillery weapons were and are used primarily in the indirect fire mode of operation. As a result, the weapons must be directed by the use of data collected externally to the weapon, which is reduced to weapon azimuth, elevation, charge, and fuze setting.

During the period prior to the end of World War II (WWII), the individual weapons were under the control of a battalion that had three firing batteries, each consisting of four or six weapons depending on caliber. In the usual operation all relevant data were received by the battalion fire direction center and transformed into data pertaining to the direction of the weapons in each of the three batteries. Ordinarily, as each battery would engage a different target, three sets of firing data would be produced.

Field artillery was generally used against area targets, such as troops in an open field; therefore, firing data were based only on the geographic center of each of the batteries. All weapons in the battery were then laid parallel to the firing line. This pattern produced widely dispersed fire in the target area.

The conditions described were those most prevalent. As tactics demanded, one or more batteries could be detached from the battalion and operated as independent units. Also, if the target was relatively small, such as a bridge, the fire emanating from the individual weapons in the battery could be made to converge on the target.

To bring effective fire on a target requires the following:

1. Data describing the position of the target relative to the weapon must be acquired. Prior to the advent of sophisticated terrestrial position and angular measuring devices, determining target position relative to the weapon with any degree of accuracy was quite difficult unless both target and weapon positions were obtained from a survey. Although maps, flash ranging, and sound ranging were useful tools, the system depended on the availability of a forward observer. The forward observer first estimated his own position relative to the weapons and then the position of the target relative to himself. Generally, the only equipment the observer was able to carry was a magnetic compass, a pair of binoculars, and possibly an aiming circle. Manuals contained instructions for "pacing off" distances. There are many systems taught and described in the literature, but many cleverly improvised methods used to obtain the desired data were devised by alert personnel. During WWII aerial observers could be used by the field artillery if and when they were available. (Mortality rates in such units were extremely high.) Since the aerial observer had no specialized equipment for making measurements, his value was primarily in finding potential targets, estimating the positions of targets, and reporting the effectiveness of the resulting fire. Following the collection of data obtained by the various methods, it was the responsibility of the battalion fire direction center to transform this data by using plotting equipment into range, height differential, and azimuth between weapons and targets.

2. After determination of target position with respect to each of the battery centers, a human operator known as the battery computer combined these data with the weapon ballistics from a firing table to arrive at the firing angles of the weapons and the fuze setting. Included in the input data used were the effects on the firing angles introduced by nonstandard conditions such as wind, air temperature and density, shell weights, powder temperature, etc. To perform these calculations quickly and accurately requires a modern digital computer, so the data arriving at the weapons were somewhat inaccurate no matter how precise the battery computer's computation.

3. The next step was to position the weapon tube in accordance with the data generated and to set the fuze. Voice communication was used to transmit data and tactical orders between all elements. Needless to say, the probability of the initial round fired from the weapon hitting the target was low, so a procedure known as "registration" was performed. This involved using data accumulated to direct one of the weapons in each of the batteries at a known location, which was at the approximate center of the target area. (Actual targets were not used in order to preserve an element of surprise.) This spot was called the "registration point". The location of the resulting burst relative to the registration point would be estimated by the forward observer, who would relay this information to the fire direction center. When subsequent

rounds were sufficiently close to the registration point, firing data corrections were determined for the cumulative effects of all nonstandard conditions. With these corrections applied to the firing data, a battery could engage any accurately located target within range of its cannon and have a first-round fire-for-effect capability.

However, the limitations imposed by this inexact and cumbersome system were acceptable since field artillery was not generally meant for use against point targets. Moreover, the projectiles fired were not expected to impact a point target such as a tank; they were expected to bring the projectile to a point over the target area at which the shell would detonate and shower the area with shell fragments and the metallic particles loaded in the shell. The function of the time fuze was to assure this detonation at the proper location. Artillery fire was designed to neutralize the troops by either destroying them or forcing them to take cover.

1-2.4.1.1   Instruments Used in Target Location

1-2.4.1.1.1   Binoculars

Binoculars are used in many situations that required augmente observation. They are militarized versions of this familiar instrument used by sportsmen. The advantages of using such an instrument as compared with viewing objects with the naked eye are these:

1. They provide magnification and thus enhance viewing.

2. Because of the size of the aperture, light gathering is enhanced and thus allows operations at lower light levels.

3. The large separation of the objective lenses enhances the viewer's ability to sense the depth and hence separation of objects.

4. The binoculars are provided with a collimated reticle used to measure the angular separation of objects in the field of view.

Numerous models of these instruments provide a wide variety of apertures, fields of view, and magnifications.

1-2.4.1.1.2   Magnetic Compass

This handheld instrument is a militarized version of a device commonly used in civilian life. It contains a magnetized needle, which, when properly leveled, is capable of indicating the direction of the magnetic pole, a sight for pointing the instrument at an object, and scales that read the direction of the object from north. These scales are adjustable to allow correction for the known deviation between true and magnetic north. It contains a circular level vial that assists leveling this handheld device. By rotating the body of the instrument from the horizontal to the vertical plane, it is possible to read the angular elevation of a point of interest with respect to the observer.

The magnetic compass has many uses in directing field artillery weapons. One is providing the forward observer with a lightweight means to locate points in azimuth and elevation with respect to himself. It also allows orienting weapons when no better means are available.

1-2.4.1.1.3   Maps and Plotting Boards

As noted, a large amount of geographical data was needed to determine the position of the firing battery with respect to the target. This included the information accumulated by the forward observer in locating himself as well as his sensings of the "registration" rounds. Prior to the introduction of automated computation, reducing these data by hand calculation under field conditions was a difficult task. Thus establishing the firing line in polar coordinates was accomplished by means of a graphical solution. This graphical computation was done by using a wide variety of equipment that depended on the problem to be solved and the material available. The procedure included tacking maps or blank sheets of paper to drafting boards where plotting and reading were accomplished with pins, calibrated straight edges, and

protractors. However, there was standardized plotting equipment designed specifically for the task, which proved to be quite useful. One such instrument that was widely used was the M10 Plotting Board. It was used primarily when the observer knew his position with respect to the weapon and his relationship to the target.

In addition to plotting boards designed for the solution of commonly encountered problems, there were boards designed for use in highly specialized applications. These included the M5 Plotting Board, used solely for the solution of the flash ranging problem, and the M1A1 Plotting Board, used with sound ranging.

1-2.4.1.1.4 Sound and Flash Ranging

Sound and flash ranging systems were designed to pinpoint the locations of hostile artillery weapons that had just been fired by measuring the timing of the sound produced by the weapon firing and the direction to the flash emanating from the weapon muzzle. Conceptually the flash ranging system was by far the simpler. It involved the accurate positioning and orientation of observation instruments at points from which the flash of the weapon could be observed and the direction to the observed flash measured and recorded. In theory this data gathering could be accomplished by two observers reporting data about one event. In practice, however, it was necessary to use at least six observers reporting data on at least six flashes. This number was required for many reasons, including the fact that all observations may not have been made on the same flash. In addition to the location of targets, the system could be used during "registration" to measure the deviation of the location of a high burst from its predicted location. The intersection formed by these observations was established by using the M1A1 Plotting Board.

Sound ranging, on the other hand, was quite complex in both theory and practice. Six evenly spaced microphones were emplaced on the ground along a baseline that was oriented perpendicularly to a line joining the center of the base with the expected target. Generally, the baseline was straight, but occasionally a curved base was used because of the terrain. Sounds received by the six microphones were recorded, and the time difference between the arrival of the sound at two adjacent microphones measured. With the relative locations of the two microphones (expressed in sound seconds) as well as the difference between the times of arrival of the sound, it is possible to plot a hyperbola describing all of the possible locations of the target. To find the actual location of the target, a similar procedure is followed using the data produced by pairing the other four microphones. The intersection of the five resulting hyperbolas is the location of the target. Unfortunately, determining the intersection of five hyperbolas under combat conditions was not easy.

1-2.4.1.1.5 Aiming Circles

The aiming circle is a device with a function analogous to that of a theodolite used by surveyors. It is, however, considerably less accurate and less expensive than a theodolite but is rugged enough to endure the harsh environment in which it is used. It was provided with a calibrated azimuth motion that may be rotated through 3200 mils*. By the use of a calibrated micrometer knob, azimuths were readable to about 0.5 mil. In the case of Aiming Circle M1, elevation is measured by leveling the line of sight of the straight telescope and reading elevation with reticle graduations placed along a vertical crosshair. In a later version the aiming circle, the M2, was provided with a small elbow telescope with elevation motion that can be read directly with a scale and vernier. Instrument lights were provided in both instruments for night reading of scales, reticles, and levels.

The aiming circle could be leveled using a circular bubble and was provided with a magnetic compass and means to enter magnetic deviation. It was always used in conjunction with a tripod, which provided the necessary leveling adjustments. The aiming circle was oriented by use of the magnetic compass, by

---

*A mil is a unit of angular measurement equal to 1/6400 of 360 deg. It is used in gunnery applications, and it is convenient because one mil subtends approximately 1 m at 1000 m.

reciprocal laying with other similar devices, or by observing a point of known direction (if the location of the aiming circle was known). For example, if an object of known direction was to be used for orientation, the aiming circle azimuth scales and micrometer were set to the azimuth of the point. The entire instrument was rotated with respect to the tripod until the vertical crosshair in the telescope lay on the aiming point. Because the mass of the instrument was 9 kg without the tripod, it could be carried by the forward observer to his advanced position where it provided better measurements of elevation and azimuth than could be obtained from the magnetic compass.

1-2.4.1.1.6 Battery Commander's Telescope

The battery commander's telescope, developed during World War I (WWI), was a binocular instrument designed in a periscopic configuration that allowed an observer to view the effects of artillery fire while concealed from enemy view. The M65 was the instrument most widely used during WWII and beyond. It was used in a variety of applications, including observation by the forward observer and flash ranging. Because of the stereoscopic vision provided, the M65 was effectively used to spot the effects of artillery fire.

The M65 had two independent telescopic assemblies mounted permanently in a vertical position. Each assembly was 0.4 m long from eyepiece to objective with a 6-deg field of view and 10-power magnification. The right-hand telescope contained a reticle with a pattern allowing measurement of azimuth and elevation from its center to ±50 mils.

The base of the instrument resembled an aiming circle without a magnetic compass. It had a circular level vial and a mechanism to rotate the entire assembly in azimuth with a scale and vernier that could be read to about 0.5 mil elevation. The instrument could be used with two types of tripods. One was of standard height and thus permitted observation by a standing man; the other was a short ground mount that allowed viewing in a prone position. The optical system of the instrument provided adjustment for focus and interpupillary distance. Filters and night lighting were provided.

1-2.4.1.1.7 Optical Range Finders

By far the most difficult part of target location, until the development of the laser range finder, was measurement of the distances between points. Early and unsuccessful attempts to measure distance involved the use of stadiametric and two-station range-finding principles. Stadiametric methods involved bracketing the outside dimensions of a target of presumably known size with a pair of parallel reticle lines. Because the size of the target was known, the distance between the reticle lines was a function of range. The difficulties in the practical application of the device included that (1) the outline of the target might be obscured, e.g., a tank standing in high grass, and (2) if a target such as a tank turned so as to change its aspect, knowing its true length was of little value. (Because of these difficulties, most stadia reticles now use the vehicle height—not length or width.) In the two-station range-finding system, angle-measuring instruments were located at two carefully surveyed and oriented points and simultaneously pointed at the target. The distances and angles involved could then be computed. This system was of course stationary and subject to errors such as observers not simultaneously pointing at the same target.

Using the properties of right triangles, Army ordnance engineers began to design more dependable and more mobile optical range finders. The self-contained instruments that resulted contained a baseline of fixed length with prisms at each end of the base. The prism at the left end of the base was fixed in angle and rotated the incoming image of the target through a 90-deg angle. The prism at the opposite end of the base could be rotated. When the lines of sight from the two ends of the base converged onto the target at the apex of the right triangle, range could be determined by measuring the angle of the right-hand prism with respect to the baseline. The longer the baseline, the more accurate the determination of range. Lengthening the base increased the instrument size, cost, and weight and lowered dependability. As a result, the design of such instruments was a compromise of the various factors involved.

Optical range finders fell into two categories that depended on which of two types of optical presentations were provided to the single operator using the instrument. These presentations required the operator to accomplish distinctly different tasks during performance of the ranging function. One type of optical presentation was known as a coincidence range finder, whereas the other was called a stereoscopic range finder. By adjustment, separate images seen through the two eyepieces of a coincidence range finder can be made to coincide. A reading of the adjustment gives the distance. A stereoscopic range finder is a telescopic instrument that gives correct ranges when the object sighted on appears at the same distance or depth as an image or crosshair marked on the lens.

1-2.4.1.2 Ballistic and Meteorological Data

The flight path followed by a free-flying projectile fired from a weapon tube is known as its ballistic trajectory. Computation of the trajectory requires a set of input data that is too lengthy to be adequately covered in this discussion. A brief sample of weapon-related data includes elevation of the weapon, velocity of the projectile as it emerges from the weapon tube, and the resistance offered by air that slows down the projectile during its flight. Also needed are data relating to the environment at the time of firing. These include propellant temperature, air density and temperature, and wind direction and speed.

When all required data have been assembled, it is necessary to solve a set of simultaneous differential equations in order to calculate the proper elevation and azimuth required to produce a projectile trajectory that will pass through the target. An appropriate fuze time setting could also be calculated.

For practical reasons, the firing tables issued to the troops in book form were constrained to an approximation of actual conditions. These tables were of varying complexity and completeness, depending upon the range of the weapon and the importance of the mission. A typical table might give the elevation required to destroy a target at a given range and altitude; the table might also give the effect on range of a unitary change of conditions. For example, if a correction were to be made for a head wind, the operator would multiply the shortening of range produced by a unit of head wind as given in the table to determine the resulting loss of range. This change would then be added to the true range of the target and elevation would be recomputed.

It was rarely possible to compute the so-called cross effects, such as the change in range due to head wind if the projectile were being slowed down by a higher than standard air density. Some firing tables did actually contain some of the cross effects, but they were too bulky and the computations too time-consuming to enable timely delivery of fires. In addition to the elevation effects, there were the lateral effects on the trajectory, such as crosswind and projectile drift due to the spin imparted by gun tube rifling. For extremely long-range weapons the effect of earth rotation during the time the projectile was in the air was given.

In addition to the fact that the computation of firing data did not include all variables, the use of firing tables contained in books was complicated and subject to a wide variety of computational errors. As a result, the so-called graphical firing table was developed during the 1940s. It was essentially a piece of wood with a scale glued to it. When the desired range was determined, a cursor would be set over a range mark unit, and weapon elevation and the unit effects of nonstandard conditions were read.

The fielding of militarized, high-speed digital computers such as the M18 field artillery digital automatic computer (FADAC) during the 1960s alleviated some of these problems.

During WWII all weather-related information was received from the Army Signal Corps, which accumulated it periodically (at 3- or 4-h intervals) by releasing a balloon carrying instruments to measure air pressure and temperature at various levels. These measurements were transmitted back to the ground by radio. Tracking the balloon by ground-based observation instruments produced wind data at various levels. The firing table data included the maximum height of the projectile trajectory; therefore, it also specified which of the altitude levels transmitted by the Signal Corps should be used.

1-2.4.1.3 Entering Elevation Data Into the Weapon

At various times the Army has used a wide variety of field artillery weapons of various designs and calibers. Each of these weapons was provided with a set of fire controls specifically tailored to the military requirements in effect at the time and the restrictions imposed by design of the carriage. Nevertheless, the design principle for all such equipment was identical. Although the on-carriage fire control devices described here are those used in connection with weapons of the WWII period, the same underlying design theory applies to the fire control used by all field artillery weapons. It should also be noted that most of the carriages produced near the end of WWII used a two-man laying system in which the gunner, positioned to the left of the weapon, controlled the azimuth setting, and the number two man, positioned on the right, controlled elevation. Weapon azimuth and elevation data computed by the battery fire direction center are in a level coordinate system, but field artillery weapons are rarely level. Thus the on-carriage fire control systems must be able to compensate for the out-of-level condition of both the vertical and horizontal axes of rotation of the tube, or cant. This adjustment is known as cant correction.

1-2.4.1.3.1 Gunner's Quadrant

The gunner's quadrant M1 was developed for use by the field artillery prior to WWII. Operation of this device is based on the principle of offsetting a spirit level with respect to its leveling feet. The gunner's quadrant M1 is shown in Fig. 1-3. When the device is used to set the elevation of a weapon tube, it is used in conjunction with two hardened pads embedded in the breechblock of the weapon that are known as gunner's quadrant pads. The spacing of these pads is identical to that of the feet on the gunner's quadrant. At time of weapon manufacture they were carefully machined to lie in a plane that is parallel to both the axis of the bore of the weapon and its axis of elevation (trunnion). Any deviation from the axis of elevation is inscribed on the breech.

The gunner's quadrant is now used to boresight and safety weapons and to provide extreme accuracy in elevation when required.

1. Elevation Scale, 800-1600 mils (Right Side) (Hidden)
2. Frame
3. Elevation Scale, 0-800 mils (Left Side)
4. Frame Shoe (Four Places)
5. Reference Surface, 800-1600 mils
6. Knob
7. Micrometer Mask
8. Micrometer Scale
9. Left Radial Arm Plunger Plate
10. Radial Arm Plunger
11. Reference Surface, 0-800 mils
12. Radial Arm
13. Name Plate
14. Cover
15. Level Vial
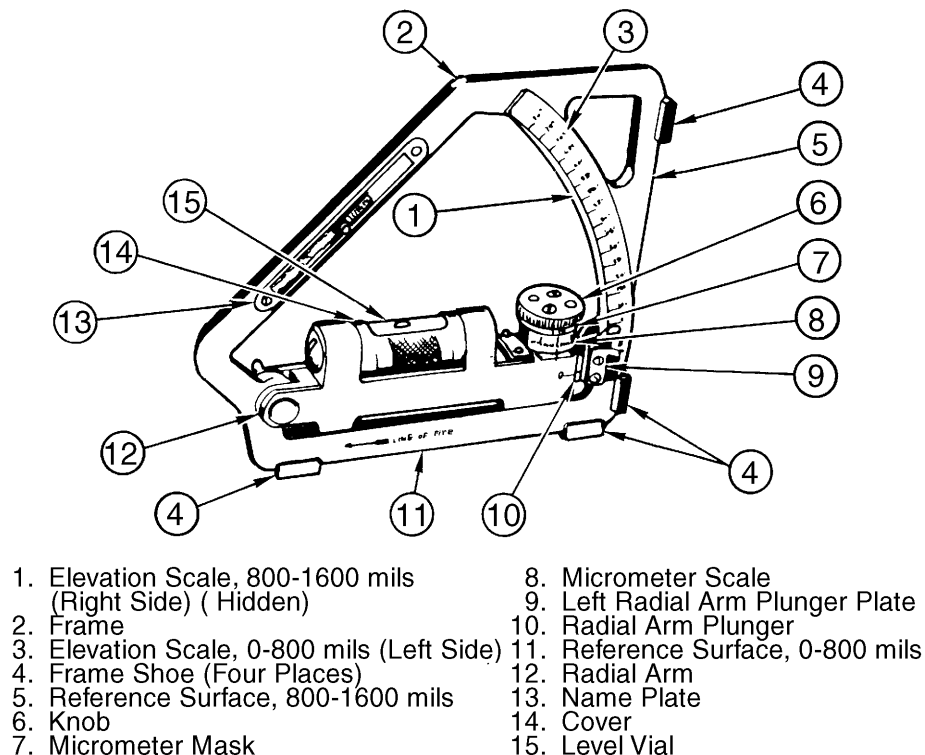
Figure 1-3. Gunners Quadrant M1A1 (Ref. 4)

1-2.4.1.3.2 Elevation and Range Quadrants

The instrument most generally used during WWII to set weapon elevation under combat conditions was the elevation quadrant. Instruments of this type are capable of accurately setting elevation of the weapon with respect to level in a vertical plane. The heart of the device is an axis (gun bar) that was carefully adjusted at the time of weapon assembly to be parallel to the axis of the weapon and moves in elevation with the weapon. A housing that is cross-leveled about the gun bar contains a level vial whose angular offset from the gun bar in the plane of the instrument may be measured by a scale and vernier. After receipt of weapon elevation from the fire direction center, the instrument is cross-leveled and the vial displaced from the gun bar by the required elevation. The weapon is then elevated until the bubble in the vial is centered.

The principle of operation of the range quadrant is the same as that of the elevation quadrant. The difference between the two is that the range quadrant is provided with a long helical scale that is graduated in range. Entering a range setting displaces the level vial with respect to the gun bar by the amount of elevation needed to engage a target at the range shown. Thus the weapon may be set in elevation when a complete fire direction center is not available. Of course, this procedure is quite inaccurate because the only correction that can be made prior to registration is for the angular difference in height between the weapon and the target.

1-2.4.1.4 Entering Azimuth Data Into the Weapon

The basic on-carriage fire control device for setting the azimuth into the weapon is the panoramic telescope. This instrument was built in the form of a periscope with a ventricle offset between the eyepiece and the objective that is long enough to permit the gunner to observe all of the elements of the battery important to the operation, i.e., aiming circle and aiming posts. For weapons without side armor or roofs, the panoramic telescope M12 with an offset of about 0.2 m met this criterion, and during WWII it became the most widely used of these instruments. In contrast, panoramic telescopes used with post-WWII roofed and armored self-propelled artillery required lengths of almost one meter for the sight line to clear the edges of the roof.

1-2.4.1.5 Fuze Setters

As previously described, if field artillery fire is to be effective, it is necessary to detonate the projectile at a point where it sprays unprotected troops and material with shell fragments or shrapnel. The fuzes used are set to a time computed by the fire direction center. One type of fuze was based on the burning of a powder train, whereas another used a mechanical clock.

Time was set by rotating the top of the nose cone with respect to the bottom until an index on the upper half pointed to the correct time reading on the lower half. Two types of devices were employed to rotate the top. One type of device was a special wrench having a circular tapered hole and notches for engaging ribs on the fuze. After the safety pin in the fuze was removed, the wrench was placed over the upper part of the cone and turned until the desired reading appeared on the time scale. This was somewhat awkward because reading the scales on the fuze could be difficult after the fuze had been attached to the shell. A better method of setting fuzes was devised during WWII that involved a device with which the desired time could be entered into the setter prior to placing it over the nose cone. After engaging the lugs in the fuze, the inner part of the setter was turned.

1-2.4.1.6 Direct Fire Optical Instruments

Direct fire by field artillery during WWII was a secondary mission, i.e., used primarily for defense against close-in targets that could be seen from the weapon. As a result, the equipment supplied for this mission was minimal. The gunner would rotate the line of sight of the panoramic telescope to its boresight position and then traverse the weapon until the vertical crosshairs of the reticle pattern lay on the target. The number two man to the right of the weapon tube was provided with a simple telescope, usually of 10

power, that was affixed to the elevation quadrant. An important function of this telescope was to provide the number two man with a way to elevate the axis of the weapon to be above the line of sight to the target to compensate for the gravity drop of the projectile. This angle, presented in the firing table, is a function of range. There were several ways to accomplish this compensation. Mechanically, the simplest way was to provide the telescope with a ballistic reticle having range graduations spaced below the horizontal cross. Thus after estimating range the weapon would be elevated until the range graduation fell on the target. These graduations were extended horizontally on both the right and left sides of the vertical crosshair for use when the gunner might be leading a moving target. Telescopes of this type were of either straight or elbow configuration.

1-2.4.2   Tank Fire Control Equipment

The British built and used the first tank during WWI in an effort to break the stalemate of trench warfare that prevailed during that war. Subsequently, in the period between the two world wars, much effort was devoted to tank development, particularly by the European countries. World events during the 1930s emphasized the importance of the tank in modern warfare. US Army ordnance engineers also directed considerable attention toward the end of that decade to the problems of tank warfare. Three of the major fire control problems that were stressed during years of development through World War II were sighting, range finding, and tank stabilization functions.

1-2.4.2.1   Sighting Equipment

The use of rapidly moving tanks and armored vehicles confronted ordnance engineers with two basic sighting requirements:

1. To design fire control sighting equipment that would enable guns to be aimed more rapidly at swiftly moving tank targets

2. To develop observing and sighting devices for tanks.

As a result of the first requirement, antitank reticles were devised that allowed the gunner to apply proper target lead and range adjustment at the same time. The M6 telescopic sight was adopted as standard in 1938 for use with the 37-mm antitank gun. Later other sighting telescopes using antitank reticles were developed that permitted antiaircraft weapons to be brought to bear on ground targets.

The second requirement—improved means of observation by tank crews—posed serious design problems for Army ordnance designers. Prior to 1940 targets were sighted through narrow openings in the turret. These direct-vision slots weakened tank armor and increased the danger to the tank crew from projectile fragments; also the limited visibility forced the crew to open the turret hatch to make observations and thus exposed them to enemy fire. (Despite the hazards, however, most crews reportedly preferred this technique because it allowed them greater visibility, and they could engage the enemy more quickly.)

To solve these problems, experimentation with many sighting devices based on the principles of the periscope was undertaken. At first these devices were unsuitable because the observer had so little room to move his head in the narrow confines of the tank interior. Late in 1940, however, Army weapons design engineers integrated the periscope with a telescope in an effort to give both the instrument and observer some degree of protection. Two experimental tank periscopes, the T1 and the T2, that incorporated a straight-tube telescope for gun sighting were designed. A linkage mechanism to the gun enabled the gunner to aim the weapon for direct fire simply by centering the proper telescope reticles on the target without moving his head since the line of sight moved with the gun. The optical line of sight was adjustable in deflection and elevation for boresighting the weapon, but adjustment proved difficult. The two periscopes were standardized in 1941: the M1 for the 75-mm gun and the M2 for the 37-mm gun.

Early in 1942 a more complex and expensive but also more accurate periscope, the T8, was developed and was a major improvement over the M1 and M2 units. This periscope had a high-powered telescope on the right-hand side to sight distant targets, whereas the periscope itself, on the left-hand side, had a reflex reticle to sight nearby targets. Despite the high costs of manufacture inherent in the optical and

mechanical features of the design, the evident superiority of the instrument warranted its acceptance and standardization as the M10 in 1944.

The upper end of the telescopic periscopes projected above the armor plate of tanks; accordingly, a chance hit would shatter the exposed window, mirror, and body of the unit. Therefore, additional direct-sighting capability was subsequently provided the tank crew by means of a small, straight-tube telescope that permitted sighting through a tiny opening in the turret. This instrument, the M70, was standardized in 1943 on the basis of its acceptable optical characteristics, i.e., adequate magnification and a wide field of view, and a size small enough to allow accommodation of the space limitations inside a tank. The small aperture in the tank turret used with this sighting instrument minimized danger to the tank crew from enemy fire. Later improvements increased telescopic power from 3 power to 5 power in the M71, which became standard equipment on most tanks by 1945. The M71 manifested a wider field of view and better light-gathering power than the M70.

A variable-power telescope was later developed that could be readily adjusted to provide either 4-power magnification with a relatively wide field of view or 8-power magnification with a much narrower field. This major innovation, the M83, was adopted near the end of World War II. It was uniquely adaptable for aiming at close-in targets by using its 4-power capability and for sighting on distant targets with its 8-power adjustment.

1-2.4.2.2 Ranging Equipment

During World War II the fire control capabilities of the tank were limited by the lack of satisfactory range-finding equipment. The M71 used a ballistic reticle. The tank gunner first estimated range by eye and then elevated the weapon until the proper range graduation of the reticle was placed on the target. The deflection pattern of the ballistic reticle permitted the gunner to make allowance for target motion. The same principle was used in tank periscopes, such as the M4A1.

Accordingly, ordnance engineers in 1944 and 1945 applied themselves to the task of developing an integrated tank fire control system that would properly combine ranging, computing, and aiming functions. The project was still in the development stage at the end of the hostilities. Optical range finders, however, were later devised that constituted the primary sighting system for the next generation of medium tanks.

1-2.4.2.3 Stabilization Equipment

The African Campaign in World War II revealed the need for a stabilized tank gun to fire accurately from a tank moving over rough terrain. Crews were forced to stop the tanks momentarily to aim accurately and thereby provide enemy gunners with convenient sitting targets. Shortly thereafter the Westing-house elevation stabilizer was placed in the Medium Tank M4, the series of tanks that included the Light Tank M5 and the Medium Tank M26.

Maximizing the advantages of high-powered tank sighting systems for gun laying while a tank was in motion became a paramount objective of Army weapon design engineers during World War II. The ultimate goal was a stable platform to stabilize tank weapons completely during travel over rough terrain. The gyrostabilizer, the stable element used by the Navy to lay guns of a ship in accordance with computed orders (to obviate the need to fire only in the middle of a ship's roll), provided the Army with the logical answer to the tank fire control problem.

1-2.4.3 Air Defense Fire Control Equipment

The defense of United States territory by seacoast gun batteries (established in the latter part of the 19th century) and antiaircraft gun batteries (established in the early part of the 20th century) emphasized the need to develop fire control equipment and systems for these weapons. These systems were the fore-runners of modern air defense systems. The evolution of faster moving, more heavily armored vessels was paralleled by formidable improvements in the rate of fire, range, and accuracy of coastal artillery weapons. The problems of seacoast artillery were unique: (1) targets were often below gun elevation, (2) ships

maneuvered at sea and thus presented a field of fire that offered no reference points, and (3) because of the techniques then current for acquiring accurate gun-firing data, gun batteries were separated from fire direction centers, so the transmission of firing data was complicated, and the time of fire was delayed. Antiaircraft artillery introduced additional complications because the targets moved in three dimensions and were much faster and more maneuverable than ships.

1-2.4.3.1 Target Data

Although seacoast defense had experienced the need to obtain target data, even under the moving target situation, seagoing vessels were relatively slow and incapable of significant maneuver. The aircraft, however, presented a versatile target capable of altering velocity in three dimensions. Observation and tracking devices in use at the time were not effective against this relatively high-speed target. Special attention would have to be given to this new threat, not only in terms of measuring target position and velocity but also in terms of using the data to calculate gun orders in a timely manner.

1-2.4.3.1.1 Target Angles and Rates

Although target velocity was known to be an important factor in the solution of the seacoast fire control problem and was considered essential in the plotting board calculation, in the antiaircraft treatment it could be the single most critical factor involved. The position error incurred in the tracking process was not particularly significant in itself. It was the manner in which these errors propagated into estimates of velocity during the differentiation process that concerned the designers. In fact, the entire process of extracting target state estimates from measured data is still of major concern and has been the object of innumerable filter studies. Early approaches depended upon measurement of sight or track radar gimbal angles to provide estimates of angular orientation. Coupled with range information, the target present position could then be computed in an earth-referenced inertial Cartesian coordinate set. Under the assumption of constant target velocity, variations in the differential target position would be readily identified as noise and filtered out. The advancements made in measurement of target motion and the techniques used to extract useful estimates and generate target predicted position are discussed during the review of air defense gun systems.

1-2.4.3.1.2 Target Illumination and Sound Location

Before the advent of radar during World War II, both light and sound were used to locate aircraft targets approaching under cover of darkness, fog, or smoke. Systems comprising searchlights, control stations for the searchlights, sound locators, and allocated power equipment were used. The purpose of the sound locator was to provide initial information on the general position of the target. The control station was located about 60 m from the searchlight so that the controlling observer's view of the target would not be obscured by the diffused light within the beam. A typical searchlight control station used sound to place the narrow pencil beam of the searchlight on or near the target initially.

1-2.4.3.1.3 Optical Range Finder

Just before World War II stereoscopic height finders were used extensively by antiaircraft artillery. (These instruments were made obsolete by radar during World War II.) This type of height finder was, in effect, a stereoscopic range finder with an additional optical wedge system—comprised of two optical wedges and associated mechanical parts—to measure aircraft altitudes. The additional components solved the right triangle in which the angle of elevation and measured slant range were known quantities.

Since the director solved the fire control problem in the earth-referenced coordinate frame, the target altitude or height was required. Both the target range and elevating measurements were available at the height finder, so the target height was generated there before being sent to the director. Because the height was assumed constant, it could be readily filtered.

1-2.4.3.1.4 Early Radar

Although the optical range finder (or height finder) served its purpose reasonably well, it still required an operator to track the target continuously optically while attempting to focus the image properly in accordance with target range. In addition to human error the mechanical tolerances of the instrument introduced errors proportional to the square of the range; thus accuracy of the curvature of the ballistic trajectory and the target motion compensation fell off rapidly when a longer range target was engaged. Early in 1941 the details of the British breakthrough in radar efficiency became available to fire control designers, and steps were immediately taken to incorporate the technology into existing systems. A range-only radar version was incorporated into the later series directors, and the antenna was slaved to the optical telescope of the director. This linkage eliminated the need for the height finder operator and offered accurate range information, and any tracking errors were virtually independent of range. A later full track radar was developed for the M9 electrical director that was used when targets were not visible (See subpar. 1-2.4.3.3 for a detailed discussion.).

1-2.4.3.2 Mechanical Computers

The plotting boards and range deflection correction devices used by seacoast artillery to determine manually target range and azimuth (present and predicted) and secondary ballistic corrections were unsuitable for accurate, reliable calculations. The resulting human error factor and the time lag between error data acquisition and correction setting induced the coast artillery to draw up specifications for computers that would automatically produce firing data.

One of the earliest firing data computers was the Mechanical Computer M1917, developed by the French for antiaircraft purposes and adopted as standard during World War I by the United States. It represented an initial approach to the complex gunnery fire control problems that were beginning to extend beyond the reach of human performance capabilities and was considered one of the best of its kind in 1917.

However, it did not allow for nonstandard conditions, and worse, it required time to transmit and apply the firing data to the gun since at that time electrical transmission of data to guns had not yet been achieved. Instead firing data were telephoned to the gun often from remote locations. Thus the concept of instantaneous and continuous calculation of data and its application to the weapon were largely invalidated by these disadvantages.

Before and during World War I the British Admiralty mastered the principle of director fire, by which a battery of guns on a ship could be positioned for firing from a remote location. Satisfactory gun directors based on those principles were designed and built by the English Vickers Corporation for the British Navy. Soon afterward, other directors became available for British military ordnance. US Army ordnance, borrowing a leaf from its Navy counterpart, adopted as standard a Vickers-designed director designated M1. The design of this director was based on the target angular-rate-of-travel method (See subpar. 2-3.3.2 for a description.) used to determine lead. It was the semiballistic type, i.e., there was a partial correction for the nonstandard conditions involved in projectile flight.

For the next two decades the search by ordnance engineers for automatic computing devices that would eliminate human error and save time and manpower culminated in the development of the standard M2, M3, and M4 directors, which fully corrected for nonstandard ballistic conditions. These equipments were designed to use the target linear speed method for determining lead and to compute ballistic data by means of three-dimensional cams. They were classified as universal directors because they could be used against air, land, and seagoing targets and their field of operation included 360 deg of traverse, 10 deg of depression, and 80 deg of elevation. They were particularly useful against aircraft targets. Because aircraft targets are small and move rapidly in three dimensions, a system of automatic computation and transmission of firing data to the gun battery had become necessary to the satisfactory solution of the antiaircraft fire control problem. (The development of data transmission equipment is covered in subpar. 1-2.4.4.4.)

1-2.4.3.3 Electrical Directors

As work on the 90-mm and 120-mm antiaircraft (AA) guns progressed in 1940, scientists at the Bell Telephone Laboratories proposed an electrical gun director. Enthusiasm over the plan mounted later in the year when it appeared feasible to use the newly developed principles of radar for tracking purposes.

Army ordnance designers, Bell Laboratories, and the National Defense Research Commission (NDRC) collaborated to develop, design, construct, and standardize the mathematically complex M9 electrical director early in 1942. Manufacture was simplified by the use of standard components. The M9 director, however, which was developed for the 90-mm AA gun, and later the M10 director, which was developed for the 120-mm AA gun, represented formidable and extremely complicated devices that were suitable only for large AA guns. Because of their mass (about 1600 kg), these directors were installed in trailers separate from the guns, yet they manifested many distinct advantages over the mechanical directors:

1. They eliminated many of the inherent errors of mechanical prediction.
2. They provided complete solutions for the prevailing nonstandard ballistic conditions.
3. They effected a shorter minimum slant range and an increase in maximum horizontal range.
4. They improved target tracking.

Each electrical director consisted of a tracker, a computer, an altitude converter, and power elements that were all interconnected by a cable system. For visible targets the tracker provided the computer with range, elevation, and azimuth data. The radar system was used when the target was not visible. The raw data defining the position of the target in polar coordinates, i.e., range, azimuth, and elevation, were converted into rectangular coordinates in the computer. The computer also determined the target velocity in order to account for the time element and thereby provide for lead. It then searched its ballistic references for firing data and corrected for nonstandard conditions. It continuously computed all firing data automatically and electrically; these data were transmitted to the gun continuously and almost instantaneously.

1-2.4.3.4 Data Transmission

As work on gun computers and directors progressed, researchers sought to minimize the time consumed and errors committed in transmitting firing data by telephone from observation posts to plotting rooms and finally to gun positions. During the 1930s, direct electrical transmission of data was adopted, and effective use of director-type automatic and continuous fire control systems began. Time was clearly the most essential factor in the application of such systems. For example, for the most probable type of aircraft target, an enemy bomber, the future positions of the target had to be accurately and continuously determined, the firing data automatically computed, and the necessary shots fired to destroy the target— all within the brief time interval that commenced shortly before the target came within firing range and ended shortly before the target was in a position to drop its bombs effectively.

Two basic types of data transmission systems were devised to solve the time problem: the direct current, step-by-step system and the alternating current, self-synchronous, system which was adopted as standard by the US Army. In both systems a displacement of the transmitter rotor was compensated for automatically by a corresponding displacement of the receiver rotor when an excitation current was supplied. Thus it became possible to provide the means, sought as far back as 1919 by the coast artillery, for the continuous and instantaneous transmission of fire control data between two or more remote units.

1-2.4.3.5 Weapon Laying

The inception of the 90-mm AA gun in 1938 and the standardization of the 120-mm, high-velocity AA gun, the M1, in 1944 created an array of design problems. The 90-mm gun was initially designed without the automatic controls required for rapid elevation and traverse of the gun. This factor precluded the use of adequate gun director control. In 1940 a power control servo system for the gun was developed by the Sperry Gyroscope Company. It was a complex of electrical, mechanical, and hydraulic units that, despite

minor defects, provided the gun with a relatively accurate means of aiming at targets moving at high angular speeds. It had the outstanding feature of aiming effectively at targets at close ranges for which manual tracking was difficult because of high angular rates and accelerations. The typical manual gun control operation required two operators, one for each axis, to use handwheels with high mechanical advantage gear trains to drive the weapon in accordance with commands from the director. A synchro differential, accepting synchro transmitter signals of the command and feedback position of the weapon, was used to display the error signal the operator attempted to null.

1-2.4.4 Small Arms Fire Control

During the American Revolutionary War battle at Bunker Hill, infantry individual weapon fire was effective. "Don't fire until you see the whites of their eyes!" expresses the tactic of short-range, massed fire that was used. In the early part of the 20th century, however, a trend toward the use of a few weapons against a few point targets began.

The sighting mechanism supplied with rifles in the 1880s consisted of a forward and a rear vertical bar (as it does in the 1990s except with an aperture sight vice the rear bar), which were to be aligned with one another and with the target. Although optical sights were widely and successfully used with larger weapons, the "iron sight" has persisted in rifles.

1-2.4.4.1 Optical Sights

Snipers using rifles attempt to hit point targets at long range. Often, aiming the weapon is the most difficult task. During WWII the Army began to experiment with optical telescopic sights as aids to snipers. Various magnifications were tried, and it was found that relatively high magnifications improved performance for supported weapons. For soldier-supported weapons, however, the involuntary "wander" of the hands and arms limited the magnification that could be used to advantage. Although this work continued after WWII, there has been no broad acceptance of the concept of providing all soldiers with optical sights.

1-2.4.4.2 Active Infrared Night Sights

To aid night vision, near-visible infrared (IR) searchlights were investigated as a source of illumination. Providing the troops with sensors that detect the IR energy enables them to view a scene at night. Although this concept was adopted in armored vehicle applications, it was never implemented to aid fire control for small arms. The major drawback is that an enemy can equip his forces with similar detectors.

1-2.4.5 World War II Air-to-Ground and Air-to-Air Fire Control Development

During WWII the sophistication in fire control achievable through the use of gyro stabilization and analog computation was reserved for development of the Norden and Sperry bombsights. The bombsight was highly classified, and precaution was always taken to assure that its design was not compromised. It provided the crews with the means to deliver bombs accurately on point targets from high altitude; however, delivery was constrained by the need to fly at a constant altitude and speed for several minutes while setting the bombsight for bomb release. During this period the bomber formation was particularly vulnerable to antiaircraft fire and fighter attack. The principle defense against the fighter was maintenance of a tight formation, which assured that the maximum number of guns could be used to defend a single bomber.

The cal .50 machine gun was deployed on bombers either in pairs for turret application or in a single configuration for pintle-mounted waist window use. In the pintle-mounted case the crewman would stand behind the weapon and control its aim through use of a metal ring sight. The operators seated in the nose, top, tail, or ball turrets traversed in accordance with lateral hand control motion; hand control vertical motion elevated the guns. A projected reticle of concentric circles indicated to the operator where the boresighted guns were pointed. The lead to compensate for relative target motion was introduced by

tracking off-target in angle magnitude and direction as conditioned by judgment and hour after hour of gunnery training. Tracers gave the operator the means to observe the stream of projectiles and refine his aim. Fighter pilots employed the same technique using a projected reticle sight and controlled the fixed cal .50 machine gun fire by pointing the aircraft. This type of sight was resurrected for initial use in the helicopter during the aircraft weaponization program in the early 1960s.

In 1941 General Electric developed a revolutionary aircraft fire control system. The system was based on a small computer, which could correct automatically for altitude, airspeed, temperature, and target range. The gunners controlled the gun turrets from remote locations, i.e., they were not located in the gun turrets. This system was incorporated into the first B-29 heavy bombers. In the B-29 the bombardier controlled two forward gun turrets, one on top and one on the bottom of the fuselage. The left-side gunner controlled a turret on top that was mounted toward the rear of the middle of the fuselage, and the right-side gunner controlled a gun turret mounted on the bottom toward the rear. Also the computer had a central control mechanism that enabled any of these gunners or the central fire control gunner to control more than one of the four turrets at one time. This computerized gun system was eliminated to save weight when the B-29Bs were fielded. (Ref. 5)

1-2.5 POST-WWII DEVELOPMENTS

1-2.5.1 General

By the end of World War II, the "law of diminishing returns" was beginning to affect the methods of weapon and fire control technology that had achieved such dramatic results earlier in the war. Sophisticated engineering designs, often achieved at great expense and effort, produced only minor improvements. Clearly, fresh approaches based on new concepts in technology were needed to extend the capability to engage targets with minimum risk to US personnel.

Accordingly, efforts in the late 1940s and the 1950s concentrated on developing new weapons that would markedly increase striking range, reduce susceptibility to countermeasures, and achieve a greater destructive effect. These efforts resulted in the development of guided missiles, capable of ranges from a few kilometers to intercontinental spans, as a means for defense or attack. Guided missiles can strike a rapidly maneuvering, high-speed target with predictable accuracy and probability of kill.

Missiles that could be guided in flight, i.e., whose course and speed could be altered to match target maneuvers and compensate for initial errors, opened up new fire control approaches and new magnitudes of destructive potential. At the same time, these missiles, as well as the new high-performance aircraft developed after World War II, were targets of a higher order of speed and maneuverability, and conventional fire control methods and weapons would not suffice against them. In missile guidance and control systems, all or part of the intelligence and control elements were transposed from the aiming point of a weapon to the missile.

Even for antiaircraft applications, however, the need to develop conventional weapons along with their fire control system has continued into the 1990s partly because of the need to complement guided missiles at shorter ranges in which engagement times, i.e., the time to detect, interrogate, acquire, fire at, and destroy a target, are critical. Breakthroughs in computer and electro-optical technology expanded the options for fire control software and hardware implementation. The storage and speed of digital processing permitted the use of an array of mathematical techniques in the real-time solution of the fire control problem, particularly in terms of filtering, ballistics, and prediction. The availability of lasers for ranging, angle tracking, and target designation led to a host of new weapon system developments. The remote, high-resolution imagery provided by television cameras and forward-looking infrared (FLIR) sensors opened up a complete new world of day and night, passive operations. The application of this technology upgraded older fire control systems and formed the basis of completely new systems. These applications will be shown as the fire control described in the paragraphs that follow is reviewed.

1-2.5.2 Artillery Fire Control

Since the days when artillery fire began to exceed the range of the gunner's eye, a more positive means of delivery of an effective "first round" has been the artilleryman's greatest desire. These are the six major functions upon which this accuracy still depends:

1. Knowledge of the location of the battery, including each cannon location
2. Knowledge of the location of the target
3. Knowledge of the direction of an azimuth reference, usually north
4. Completeness of meteorological data
5. Accuracy of trajectory computation
6. Accuracy of weapon lay.

The first and fourth functions were considered given information by the fire control developer. The equipment the forward observer used to locate targets for battery fire and to provide corrections for adjusted fire was imprecise. The determination of gun orders based on target position information, meteorological data, and gun and round ballistics was a problem in terms of accuracy and time required for computation. Laying the weapon, particularly in an out-of-level condition, was a time-consuming operation.

Studies were conducted to identify the shortcomings that had led to excessive errors and long reaction times. These studies uncovered the sources of the problems, but many were attributable to fundamental hardware limitations and human errors. The advent of new technologies—such as digital processing, electro-optical sensors, inertial components, advanced control theory, and sophisticated software algorithms—finally provided progress toward realization of the artilleryman's early desire: a first-round hit.

Subsequent paragraphs follow the advances made in the targeting, position finding, and computational and gun-laying functions since World War II. This presentation leads to a discussion of integrated fire control systems and concepts of autonomous weapon systems placing accurate indirect fire on a moving target while continuously relocating. Such is the need for mobility and fire power on the battlefield.

Only equipment associated with the so-called "technical fire control" is described. The tactical fire direction system (TACFIRE), which provides computerized digital communications, automated processing of normal fire support information (e.g., fire planning, conduct of fire, and target data), and rapid dissemination of the results of processing and feedback, is essentially a tactical fire control element providing command and control and is not covered. The battery computer system (BCS), which is the technical fire control, is discussed.

A general discussion of the command and control functions as they relate to advanced concepts is included in the comments on the Advanced Field Artillery System (AFAS) in subpar. 1-2.5.2.6.

1-2.5.2.1 Computational Systems

The most challenging computational problem associated with artillery fire control has always been determination of the projectile trajectory. Unlike the ballistic solution generally used in the direct fire application, the complete trajectory is needed through a range of extreme values of elevation and range. The long flight time of the projectile allows environmental factors more time to influence the trajectory path and emphasizes the need for inclusion of these factors in any solution formulation. Early use of firing tables was, in fact, an admission by fire control designers that the ballistic solution could not be accomplished at the weapon. Integration of the governing differential equations was accomplished by analog equipment of such size and complexity and over such an extended period of time that on-site operation was impossible.

In time, however, the differential equation solution was stated in various approximating algebraic or trigonometric forms that could be solved in the field by using analog devices or computers. Eventually, with the advent of the high-speed digital computer, an approximating form of the ideal differential equation model could be solved in the field. The time required for solution was acceptable only because of

other time delays in the weapon-laying process. It is a matter of time, however, until a virtually real-time solution of the ideal trajectory equations will be accomplished on-site.

Over time the overall artillery fire control problem has changed; motion of the target and, more recently, consideration of the motion of the artillery weapon system have brought new dimensions to the solution. The processing of data for the filter algorithms associated with target prediction, weapon system navigation, and application of advanced control theory materially increases the computational workload. The continuous advances in computer technology ensure that these problems will be solved.

1-2.5.2.1.1 Graphical Firing Tables

In the beginning the determination of firing data was made directly from tabular firing tables. These tables were generated by the US Army Ballistics Research Laboratory, Aberdeen Proving Ground, MD, by solving the approximating three-degree-of-freedom differential equation on a mechanical analog computing device at the University of Pennsylvania. The device used variable gear ratios to set values of ballistic parameters and ball/disc devices for integration. This device was later replaced by the ENIAC, the first electronic digital computer in the world, developed under a joint effort by the Ballistics Research Laboratory and the University of Pennsylvania. Since then, a progression of increasingly more advanced digital computers has provided solutions to ever more sophisticated trajectory representations. Today the full six-degree solution (discussed in Chapter 2) using aeroballistic data taken from wind tunnel tests is obtained as a matter of course.

Use of the tabular firing tables by the fire direction personnel, however, introduced problems in look-up time and human errors. An alternative was the use of a special circular slide rule that obtained the information contained in the firing table in an analog manner. The design depended upon the representation of the desired variable, e.g., gun elevation was found in terms of arbitrary single-valued functions of input variables such as range and muzzle velocity in a multiplicative relationship. The arbitrary functions were obtained by a curve fit of firing data. The application of logarithms put the results in the form of a known sum relationship that could be implemented on adjacent members of a circular slide rule. Considerable ingenuity was required to achieve full firing table representation.

The circular rules were subsequently converted to graphical firing tables (GFTs), as shown in Fig. 1-4. A GFT is designed in the form of a linear slide rule and has one or more scales of varying ranges on either surface and a plastic cursor with a matte finish to receive pencil markings of range corrections and a printed hairline. It is used to determine data used in firing, such as quadrant elevation, angle of site, and drift, and to calculate the trajectory of a projectile in relation to a target. It usually contains various scales in meters, mils, and seconds. For field artillery applications the GFT is used in conjunction with a surveyed firing chart from which the range to the target is obtained. Target range is the entry for all subsequent calculations using a GFT.

When GFTs were the primary means of computing firing data, the fastest way to compute the data was to place a GFT "fan" over the range scale on a range-deflection protractor, which is used to measure angles and distances on the firing chart. Once the target was plotted on the chart, all the basic firing data could be read from one instrument.
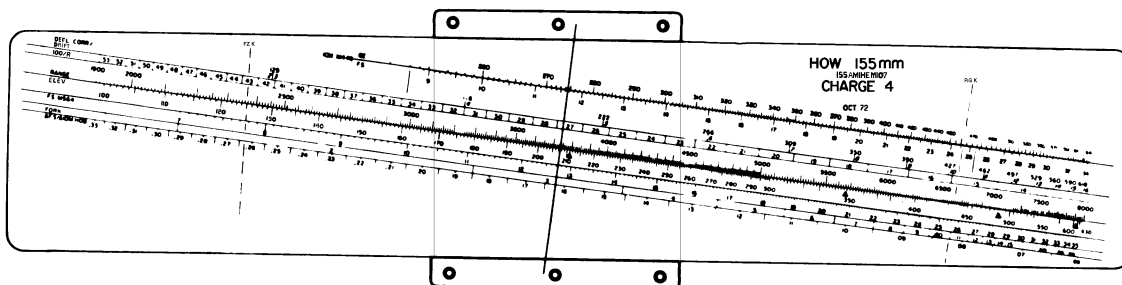
Figure 1-4. Graphical Firing Table (GFT) (Ref. 6)

1-2.5.2.1.2   T-29E2 Computer

An early effort to relieve the artilleryman of the burden of using firing tables or manipulating graphical firing tables, both of which often resulted in the introduction of human errors, was the development of the electromechanical analog T-29E2 field artillery computer. It used electrical resolvers and feedback amplifiers to solve a set of equations in a closed loop fashion that was generated by fitting a curve to the tabular firing table data. The equations—one for the elevation axis and one for the azimuth axis—represented the desired gun orders. Trigonometric functions determined target range and azimuth. Arbitrary coefficients were structured as functions of the ballistic parameters, muzzle velocity, air density and temperature, ballistic wind, powder temperature, and projectile weight. These were manually introduced into the computer, which used an electrical resolver to solve a truncated Fourier series for the quadrant elevation. The virtually instantaneous solution output of gun elevation and azimuth appeared on counters for immediate application to the weapon. Provision was made to introduce the forward observer's impact data comment, which resulted in display of the corrected solution for adjusted fire. However, the success of the digital approach to the solution resulted in the phasing out of this computer.

1-2.5.2.1.3   Field Artillery Digital Automatic Computer (FADAC)

The shortcomings of the manual techniques used to generate firing data continued to dominate the error budget and reaction time. An imaginative scientist investigated the potential of using digital techniques to integrate the governing differential equations and associated geometry. Thus initial consideration was given to using the digital differential analyzer, which was well suited to solving the equation. Digital computer technology, however, had progressed to the point at which trajectory integration could be accomplished in an acceptable time. This technology could also maintain the flexibility required to treat the geometrical aspects and could do all of this in a reasonably sized package. This program ultimately produced the M-18 Gun Direction Computer, commonly referred to as the field artillery digital automatic computer (FADAC). FADAC, along with ancillary equipment that greatly expanded its capabilities, was thoroughly tested and type classified. It was used from the 1960s until the early 1980s.

FADAC was a portable, solid-state, general-purpose computer specifically designed to withstand the rigors of rough transportation and varying climatic conditions. The efficiency of the computer and ancillary equipment remained unimpaired when it was operated in severe rain, salt-laden air, or dust storms. The construction of the FADAC was modular. At the time, the FADAC represented the ultimate in simplicity of computer operation. Switches, controls, keyboards, and all displays were directly in front of the operator, so a minimum of movement was required of him. The FADAC performed computations that had formerly been done manually and stored other information that had formerly been in written form. Inputs to the FADAC were received by the operator by voice or written message and were entered into the computer by the operator. Meteorological information was entered manually or with a perforated-tape reader.

Although FADAC computation time was reasonable, the algorithm used required two-thirds of the time of flight to compute initial firing data. Therefore, faster manual procedures using a chart and a GFT fan were used for the initial rounds fired at targets of opportunity, and subsequent rounds were fired using FADAC data.

1-2.5.2.1.4   Battery Computer System

The battery computer system (BCS) is a high-speed, digital network that integrates all artillery echelons from forward observer to battalion. It can also operate independently with only the forward observer and battery. In a matter of seconds the BCS accepts a fire request from the forward observer, computes all firing data, and displays firing commands for each weapon that are then transmitted electronically to the guns.

As many as 12 howitzers or guns can receive their individual commands almost simultaneously from a

single BCS. In fact, three separate, concurrent missions can be executed with this system. It makes corrections based on meteorological data, individual weapon location, and muzzle velocities. Its storage capabilities cover multiple fire plans, mission data, and the applications of standard and nonstandard ballistic parameters. In addition to basic survey routines, the BCS contains maintenance and diagnostic routines.

The BCS is a fully tested, field-qualified, and general-purpose unit that can be used for many different applications. For example, it is used to compute multiple launch rocket system (MLRS) fire commands and could be used as the central processor in the field artillery meteorological acquisition system (FA-MAS).

It provides artillery units with a capability to compute firing data for first-round accuracy with simple, reliable operation. The individual mechanical and electronic components are compact, rugged, and watertight and have plug-in modules. Computer-prompted displays minimize operator errors, and self-paced training for the operator is embedded. With highly visible displays, digital controls, a standard typewriter keyboard, and the ability to isolate a malfunction, it is resistant to operator error.

1-2.5.2.1.5 Commercial Adaptations

The Army also attempted to modify commercially available, handheld calculators to meet its field calculation requirements. Some of these are described in this paragraph.

The backup computer system (BUCS) is a portable, lightweight, battery-powered computer system capable of calculating fire control data for a number of howitzer systems and for the Lance missile. BUCS also provides an automated means for conducting field artillery survey computations, datum-to-datum transformations, and planning of nuclear fire missions. BUCS is used as a backup to the battery computer system. BUCS is implemented on the Hewlett-Packard HP 71B handheld computer, and each weapon application software is embodied in a set of one to four plug-in EPROM chip modules. When inserted into the computer, the modules determine the weapon system for which fire missions can be processed.

There are two configurations for BUCS:

1. *General.* Consists of the Hewlett-Packard HP 71B handheld, battery-operated calculator with standard typewriter keyboard, numerical keypad, and a one-line (22-character) liquid crystal display (LCD)

2. *Special.* Same as the general but also includes the Hewlett-Packard HP 2225B printer with battery pack, adapter, and charger and an HP-IL interface module with associated cables.

Software development for the initial BUCS Materiel Release (Revision 0) was conducted in-house by the Fire Control Division at the US Army Armament Research, Development, and Engineering Center and has been transferred to the Life Cycle Software Engineering Center for postdeployment software support. The cannon user's manual currently in the field describes the operation of this software application.

The key modifications made for Revision 1 were to provide faster solution times, operator charge selection, and life cycle software documentation for postdeployment support. Many of the BASIC routines used are common to all BUCS cannon applications. Some routines are common only to 155-mm applications with corresponding common routines for 105-mm applications. These "common" routines were developed by the Fire Control Division and provided to a contractor for development of the "weapon-specific" routines on some applications.

With the fielding of BUCS, field artillery batteries had an inexpensive backup system during periods that the BCS is nonoperational. BUCS replaced the programmable handheld calculator TI-59, which is no longer being produced, and BUCS also served as an interim replacement for the FADAC.

The M23 mortar ballistic computer provides fully automated fire direction, computation, communications, and display capabilities for 60-mm, 81-mm, and 107-mm (4.2-in.) mortar units. It is a handheld, lightweight, battery-powered unit capable of rapidly computing ballistic trajectories for mortars. When used with TACFIRE, the M23 can receive incoming digital messages from a forward observer or the artillery fire direction center and can perform all required computations for firing up to 18 individual weapons.

1-2.5.2.2 Target Location

1-2.5.2.2.1 Laser Range Finders

Of all of the problems presented to the designers of fire control equipment, the design of equipment to measure range had been the most challenging and, until the 1970s, the most frustrating. In general, two basic techniques are available to the designers of range-measuring devices. The first technique, which is used in optical range finders, solves a right triangle in which the length of one side (i.e., the baseline) is fixed, and an angle is measured to determine range. The second technique involves transmission of a pulse of energy, such as a radar pulse, and measurement of the time required for it to return after being reflected from a target.

Although the ability to improve baseline range finders did exist, the problems inherent in this type of design, e.g., excessive errors at long ranges and lack of capability at night, made the time measurement technique much more attractive. Because the time measurement technique was so successful in microwave radars used against aerial targets, a program to develop the tank Range Finder T44 on this principle was initiated during the early 1950s. Unfortunately, the reflection of signals from the numerous objects that normally surround ground targets could not be overcome and the program was dropped. In the late 1950s an effort was made to measure range in the microwave region for the field artillery application, and some success eliminating clutter effects was experienced by using a unique processing of the sum and difference signals. The investigation into microwave radar, however, led to interest in the so-called pulsed light type of range finder. A rather large mirror was used to focus light from a high-energy source that was electrically switched to provide pulses on the target. Since the light was incoherent, it could not be propagated to the distances considered necessary for practical deployment. For the pulse approach a breakthrough in the field of lasers provided a coherent light source that permitted the development of range finders of required range and accuracy. The laser range finder proved superior to existing optical range finders for the following reasons:

1. *Small Size.* It was now possible to install range finders in vehicles that were previously too small to accommodate them.

2. *Economy.* It was more economical to produce in quantity than the Range Finder M17 (the latest production type of optical range finder).

3. *Ease of Use.* It was extremely simple to use compared with existing optical range finders.

4. *Accuracy.* Accuracy was independent of range (only to pulse timing). The error in the baseline range finder increased as the square of the range increased.

The announcement of the development of the first ruby laser, i.e., the first practical laser, in 1960 immediately raised the expectation at Army laboratories that the much-awaited coherent light source for a pulsed range finder had arrived. For the most part, design was accomplished through experimentation to determine critical cavity parameters, e.g., ruby rod length, level of rod chromium doping, rotating mirror speed, and cavity geometry. Laser investigations continued and the ruby was replaced with a neodymium rod. Eventually this configuration went into a production range finder, and it has been used since by artillery forward observers to measure target range. A handheld version of the laser range finder, weighing only 2.3 kg (5 lb) and with an accuracy of 10 m out to 10,000 m, was developed in the late 1970s primarily to increase the accuracy of mortar fire.

1-2.5.2.2.2 Ground Laser Location Designator (GLLD)

The ground laser location designator (GLLD) is the principal ranging and laser designation device for Army artillery forward observers working with laser-guided weapons. In operation, the observer ranges the target, calls the request to the fire direction center, and when told, paints the target with a coded laser spot on which the projectile seeker homes in. Although primarily used with Copperhead, it can also mark targets for the Hellfire antitank missile and precision-guided Air Force ordnance. The stabilized mast-mounted sight (MMS) on the OH-58 scout helicopter incorporates the same coded designator for

an airborne alternative to the ground version of the laser. For Hellfire, the AH-64S Apache onboard target acquisition designator system (TADS) incorporates a stabilized version of the same laser designator for autonomous operation.

In all cases the demands of placing virtually all of the laser energy on the target most of the time are severe. This demand imposes stringent requirements on the tracking system, as well as the need to maintain alignment between the laser transmitter and the line of sight. In the airborne application the tracking accuracy requirement necessitates use of a video-passive autotracker. A fallout of the 10 to 20 pulses per second repetition rate provided by the neodymium designator is a range measurement data rate consistent with the fire control requirement of virtually all conventional fire applications.

1-2.5.2.2.3 The Fire Support Team Vehicle (FISTV)

The fire support team vehicle (FISTV) M981 is an M113 series armored personnel carrier equipped for use by artillery forward observers in mechanized and armored units. Although the vehicle is not designed to fire a weapon, the crew provides the target acquisition and direction for artillery firing batteries. In the FISTV an armored pod that normally houses the twin tube-launched, optically tracked, wire-guided (TOW) missile launcher of the M901 improved TOW vehicle is fitted with a ground/vehicular laser location designator (G/VLLD) combination (discussed in subpar. 1-2.5.2.2.2). The turret raises, lowers, and rotates in the same manner as the M901. In addition to the G/VLLD, onboard fire control equipment consists of a commander's viewing device, targeting station control and display, north-seeking gyrocompass, image transfer assembly, and a night sight. In addition to conventional fire control, the FISTV provides coded laser designation and tracking for both Copperhead projectiles and Hellfire missiles.

1-2.5.2.2.4 Airborne Observation

Since the beginning of artillery, the advantages associated with locating targets from an elevated platform have been exploited. Although light aircraft and the helicopter replaced the free air balloon as the observation vehicle, little had been done to improve the original observer's technique until recent years. The human eye, with or without optical assistance, was used to find the target, terrain features were related to map features, target coordinates were passed on to the artillery, and adjustments were made when rounds impacted the ground. In the early 1950s, however, steps were taken to change this process through development of the visual airborne target location system (VATLS). A stabilized sight with variable high-powered magnification was used to locate targets and establish a track long enough that the target position was known with respect to the aircraft. Ground radar track of the VATLS aircraft provided the means to locate the target in an earth-referenced coordinate system for transmission to the artillery fire direction center. A laser range finder was eventually added to the system when it was reconfigured for testing on an observation helicopter. Despite the high potential of the system, it was too expensive, and it was not until three decades later that a similar capability was fielded for an observation helicopter, this time in the form of the mast-mounted sight. The concept here uses television (TV) and FLIR remote sensors, and the reference frame is carried in the helicopter by an inertial package. The laser that is used in the Attack Helicopter Improvement Program (AHIP) provides additional airborne designation capability.

The standoff target acquisition system (SOTAS) appeared to have the potential to locate targets for artillery engagement from an aerial platform. It featured a helicopter-borne moving target indicator (MTI) radar that tracked the movement of enemy vehicles and displayed the information in real time in a decision command post. The platform was the basic UH-60 Blackhawk utility helicopter fitted with onboard system display terminals and a large rotating antenna mounted beneath the fuselage. The program was terminated in the early 1980s.

Considered a less expensive alternative to artillery spotting and laser designation by aircraft and helicopters and one that is firmly under the control of the ground commander, the unmanned aerial vehicle (UAV) is in development. The sensor package of the UAV is the integrated unit that contains a daylight

TV camera and FLIR sensor for surveillance and could contain a target tracker and laser device for ranging and designation of targets.

With an airframe about 1.8 m long and a wing span of about 3.7 m, the UAV generates virtually no signature for enemy radar or other sensors to detect. Its ground speed is in excess of 160 km/h, and it has a cruising duration of 3 to 12 h. The ground control station is manned by a commander, a controller for the air vehicle, and a crew member who operates the UAV. The laser device can be stabilized in its line of sight so that targets can remain fixed by the boresighted laser, and good images can be obtained even during violent maneuvering. Recording equipment can play back the video imagery for later use.

Although the elevated target acquisition system (ETAS) was not developed as an airborne observation vehicle, it is based upon the principle that there is a decided advantage to put a sensor package in the air, in this case on a mast about 20 m high. An airborne version has been fielded. A full complement of available state-of-the-art sensors has been placed in a mast-mounted sight on several versions of the OH58 helicopter. These sensors include low-light level TV, FLIR, laser range finder and designator, and radio frequency (RF) interferometers. The targeting data obtained from the variety of sensors are processed and displayed to exploit fully the spectral characteristics of each sensor. Automatic target tracking and target position prediction are potential additional system functions. ETAS is expected to replace most of the present family of moving target surveillance radars that use active emitters, which are vulnerable to enemy detection, and that have inadequate detection and recognition capability. The program, however, has suffered schedule slippage partly due to concern whether the vulnerability of the system is justified by the small increase in look angle provided by the 20-m mast.

1-2.5.2.3 Weapon Laying Equipment

The mechanical fire control associated with the M109 series howitzer (M109 through M109A5) requires a variety of manual and visual operations in response to verbally received firing data or data transmitted digitally to the gun where it is displayed. The nature of the present system requires that the weapons must be deployed in close proximity to each other. Due to the use of off-carriage aiming and azimuth reference devices and the need for surveyed positions from which to shoot, fire units must remain in fixed locations for extended periods of time, and thereby are subjected to potential counterfire, or expend excessive time relocating, and thereby do not provide continuous fire support.

Generally speaking, fire control instrumentation at the weapon has not changed appreciably since World War II. Instruments have been improved and are more accurate, but the basic principles have remained the same. In fact, one of the newest weapons in the inventory, the M198 155-mm towed howitzer, has been fielded with a new set of fire control instruments based on these same principles. This situation has begun to change, however, with the fielding of the M109A6 howitzer. Recent developments in gyro and computer technology that were coupled with gun drive servos made totally on-carriage fire control a viable approach to weapon position and tube pointing and thus have provided a true shoot-and-scoot capability.

In 1980 much of the future direction of cannon artillery seemed to be based on an Army conceptual study called the enhanced self-propelled artillery weapon system (ESPAWS), directed toward defining the ideal self-propelled gun for the 1990s and beyond, as well as its modes of operation.

The ultimate objective of ESPAWS was a self-propelled gun system suitable for autonomous operations, doing away with vulnerable battery positions in an intense electronic warfare environment, and offering greater responsiveness and volume of fire without increasing manpower or the number of tubes.

Although the M109 was officially in the ESPAWS picture, it was not considered a realistic candidate because its deficiencies, even in the improved models, gave rise to the program in the first place. The belief was that the M109 series, which was first fielded in 1959-60, was not capable of the kind of major improvements envisioned, although the study might lead to interim changes.

The M109 lacked the automotive performance for the shoot-and-scoot mode of operation (ESPAWS

was to be able to fire eight rounds and move 300 m within two minutes.), could not easily accommodate an automatic loader (a first-minute rate of fire of ten rounds per minute), and offered insufficient protection against direct fire weapons and chemical and radiological effects.

Other ESPAWS requirements included onboard data processing devices that allow self-survey, the autonomous solution of the gunnery problem, range to 30 km with better accuracy than the M109, projectile and propellant magazines, improved optics, improved reliability, self-diagnostic equipment, on- and off-board fuze setters, aids for the driver and sensors to monitor the state of the ammunition supply and such ballistic factors as gun cant, powder temperature, and muzzle velocity.

The ESPAWS concept was also dependent on improved ammunition supply systems—the higher rates of fire required improved field logistics—and on the development of secure, high-speed communications to service the remote fire control processors.

The results of the M109 study, however, led to a series of product improvement recommendations oriented to achieving some of the ESPAWS objectives. Many of these were considered in the Howitzer Extended Life Program (HELP) that followed.

1-2.5.2.4 Howitzer Extended Life Program (HELP)

The M109 family of weapons is one of medium weight, self-propelled (SP), fully tracked howitzers. They have a ballistic aluminum armored hull and cab to enable air transportability while providing crew protection. A 155-mm cannon and a hydropneumatic, variable recoil mechanism are mounted in a cab with full 360-deg traversing capabilities. Power is provided by a diesel engine coupled to a semiautomatic transmission. The track-driven hull has an independent torsion-bar-type suspension with 14 road wheels. Secondary armament is provided by a cal .50 M2 machine gun.

The US Army fleet of M109s was converted by modification kit to the M109A1 configuration between 1973 and 1980. The objective of this modification was to increase range. The kit consisted of a new gun tube, i.e., M185 tube assembly, a modified traverse mechanism, new travel lock, a different direct fire sight reticle, and a new equilibration system. Conversion of the US Army M109A1s to the M109A3 configuration occurred from 1980 to 1984. This conversion applied several midlife product improvements including the M178 gun mount and turret bustle projectile stowage rack kits. These improvements provided increased reliability, availability, and maintainability (RAM); improved crew safety features; onboard storage for long wheelbase projectiles and the M712 Copperhead; and onboard boresight alignment capability (M140).

After the fielding of the M109A2—the production version of the modification—and M109A3, comments from the field, equipment improvement reports, and sample data collection reports on these howitzers pointed out continuing deficiencies in system RAM. This program was succeeded by the HIP program.

1-2.5.2.5 Howitzer Improvement Program (HIP) and the M109A6

HELP analyses resulted in the determination of the functional characteristics of the M109A2/A3 howitzer improvement program (HIP) required to remedy the deficiencies identified. The M109A4 incorporated nuclear, biological, and chemical (NBC) and RAM improvements, whereas the M109A5 incorporated the NBC, RAM, and M284 cannon improvements.

Howitzer battalions, such as the M109 series, are organized, manned, and equipped principally to perform the direct support mission for the heavy division, separate armored and mechanized brigade, and armored cavalry regiments. In addition, they are capable of performing field artillery standard tactical missions of reinforcing, general support reinforcing, general support, and nonstandard tactical missions. These battalions predominantly provide close support fire against targets posing a threat to the committed combat operations and long-range fire to augment the attack by other fire support systems on threat forces before they can influence the battle.

HIP-type units, equipped with the M109A6, normally deploy in firing platoon position areas with support centralized in a battery support area. HIP batteries and subordinate platoons and individual howit-

zers are located in-depth between 3 and 15 km behind the forward line of own troops (FLOT). Specific distances vary with the tactical situation, the mission, and the terrain; however, to the extent possible, platoon position areas are 1000 to 4000 m apart, so that individual howitzer sections, consisting of the howitzers and the companion ammunition resupply vehicle, are in position areas of up to 1000 m in diameter (an area considered the typical Russian counterfire footprint). This semiautonomous mode of operation is the cornerstone of the improvement in system survivability provided by the M109A6.

The M109A6, the HIP howitzer, is an armored, fully tracked howitzer carrying 39 complete, conventional geometry rounds and two oversized projectiles onboard. It is operated by a crew of four, including the driver. The M109A6 main armament consists of the M284 cannon—a modified version of the 39-caliber M185 cannon assembly, a modified elevation-equilibration cylinder, and an M182 gun mount—a modified M178. The cannon range is 30 km for rocket-assisted projectiles and 24 km for unassisted projectiles. Forced-air cooling of both the cannon and gun mount permits longer sustained firing rates.

The fire control system is fully automated and provided with onboard accurate position location and azimuth reference, onboard ballistic solutions of fire missions (with external backup), and computer-controlled gun drive through servos with manual backup. These features permit flexibility in employment and enhance responsiveness and firing rates (emplaced first-round firing rate of 30 s and first round within 60 s of receipt of a fire mission while on the move). Digital and voice communications using either the AN/VRC-64 radios with KY57 communication secure hardware or the single-channel ground and airborne radio system (SINCGARS) with embedded encryption enable dispersed operations and missions from one firing unit to multiple howitzers.

1-2.5.2.6 Advanced Field Artillery System (AFAS)

An appreciation of the AFAS can be obtained by review of the purpose for development, which is summarized in the paragraphs that follow.

A need exists for a lightweight, self-propelled indirect fire weapon system capable of meeting the fire support needs of the close combat force, battle task force, and land battle force. The 1980 fire support mission area analysis and the 1980 mission element need statement addressed the deficiencies of the current M109 series of self-propelled howitzers. The howitzer modernization program, which included the HIP, addressed M109 deficiencies in responsiveness, armament, reliability, maintainability, range, and survivability. Product improvements to the M109 do not, however, address the major requirements for improving the weapon system mobility and agility, increasing its lethality, and decreasing the manpower required for ammunition handling. The Army needs a new generation of indirect fire weapon systems that can meet all of the requirements and use emerging technology to leap ahead of any threat.

The new weapon system must include technological advances to improve operational availability by using composite materials and prognostic test equipment; incorporate advanced propulsion technologies to increase range, rate of fire, and ammunition lethality; and improve mobility and survivability. A major requirement for the AFAS program is to achieve "leap-ahead" capabilities while realizing substantial personnel saving through the use of robotics and automation technologies.

The advanced field artillery system-cannon (AFAS-C) is being developed to displace the M109A6 howitzer in the forward-deployed and heavy contingency forces. It will incorporate liquid propellant that provides a greater degree of flexibility in system design and simplifies crew operations, and it will include a fully automated ammunition handling system. Fire control will probably be enhancements of the revolutionary improvements on the M109A6.

1-2.5.3 Combat Vehicle Fire Control

Immediately after World War II, the U.S. devoted considerable research and development to overcoming weaknesses revealed in tank fire control systems during the war. These were the chief shortcomings:

    1. Visual estimation of range

2. Lack of correction of such secondary (but still significant) effects as wind, range, muzzle velocity change, and cant

3. Accommodation of only one range-elevation relationship on the ballistic reticle

4. Lack of effective devices for night acquisition and tracking.

Obviously, with such rudimentary fire control the probability of a first-round hit on opposing armor was unacceptably low, time for engagement was too long, and operations were limited to daytime. Because of these deficiencies, a number of studies were conducted immediately following World War II to determine what could and should be done to improve tank fire control systems. One such study, conducted during 1947, was particularly effective in establishing the desirability of more sophisticated fire control than had previously been provided. Moreover, the study indicated that the greatest single improvement in accuracy could be achieved by providing an instrument capable of measuring range.

Unfortunately, the developmental cycle of tank range finders was not completed before the Korean conflict. Therefore, the first vehicles produced during that emergency could not be equipped with range finders. For that reason the fire control for the medium tank M46 consisted of a direct fire telescope T152 and a periscope of the M10 or M16 series, both of which were similar to those used during World War II.

1-2.5.3.1 M47 and M48 Tanks

It was not until 1952, when the medium tank M47 was produced, however, that tank fire control systems which were appreciably better than those used during World War II became available. The M47 tank used the gunner-operated range finder M12 (developed as the T41) as a primary fire control system.

The fire control systems for the M48 Tank and the M60 tank used many of the same principles as the M47 system, but they also included new features, the most important of which were ballistic corrections. The system for the M47 tank used the M12 stereoscopic range finder, which converted range into superelevation within the range finder, whereas the systems for the M48 and M60 tanks used the M13 range finder with a separate ballistic computer, the M13A1D, for this function.

1-2.5.3.2 M60A3 Tank

The fire control for the M60 tank was the next standardized tank fire control system produced for the US Army. Included in this system is the range finder M17C. In outward appearance it closely resembles the M13, but it is a coincidence type of instrument. Coincidence range finders have an inherent instability due to mechanical distortions caused by bending and thermal effects. Heavy construction can minimize these, but space limitations in the M60 vehicle ruled out this solution. Instead a manually operated compensating device was provided that corrected these distortions. The success of this modification was demonstrated by user acceptance.

In addition to the M13A1D ballistic computer and the range finder M17C, the fire control system for the M60 tank also included the gunner's periscope M32, which provides alternative 8-power visible sighting and 8-power active infrared sighting and unity-power visible viewing. The periscope M35, which also provides for active infrared viewing, may be substituted for the M32 because, in conjunction with the M14 reticle projector, it incorporates internal projection of reticle data. At the commander's station is the periscope M34 which is an 8-power, visible binocular instrument, and the periscope M36, which functions like the periscope M32.

Obviously, considerable progress had been made, but much remained to be done. For example, the fire control system of the M60 was far superior to that of the M48, but it was still deficient in the following respects:

1. Although the best available techniques were used in this design, the M17 type of range finder did not completely satisfy the requirements for such a device. One of its principal shortcomings was excessive errors at ranges over 2000 m.

2. Although many factors other than range should enter into determination of weapon elevation,

range alone was used as the basis for generating a solution for weapon elevation. In addition, there was no compensation for lateral effects.

      3. Although the equipment provided the gunner and driver in the M60 tank offered some night operation capability, they required an active searchlight, which is undesirable for security reasons. Also the range of the night vision periscope was inadequate.

These three problems were solved in the product-improved M60A3 fire control system. It features the ballistic computer system that provides a full fire control solution, the AN/VVG-2 laser range finder (LRF) to supply accurate target range, and the tank thermal sight (TTS) for passive, high-resolution night viewing capability.

1-2.5.3.2.1   Ballistic Computer

The ballistic computer system has the M21 ballistic computer. This system computes fire control corrections to compensate for zeroing and the effects of gravity, drift, crosswind, horizontal target motion, ammunition temperature, altitude, air temperature, gun wear, trunnion cant, gunner's and commander's sight parallax, and gun jump. The computer system processes the information in analog form and provides a mechanical analog shaft rotation as an elevation output, an optical reticle displacement to the gunner's sight, electrical rate commands to the stabilization system, and servo signals to the commander's sight as an azimuth output. In addition to the correction computations, the system accumulates estimated gun wear information and is capable of self-test and fault isolation to the unit level.

1-2.5.3.2.2   Laser Range Finder

The AN/VVG-2 laser range finder (LRF) was designed for use as a primary component of the M60A3. The ranging function is accomplished by directing a pulse of laser light at the target, receiving target-reflected light from this pulse, and converting the elapsed time between transmittal and reception to range data.

The LRF is located in the commander's station, and either the tank commander or gunner can operate the LRF system from his battle station. The system has both manual and automatic operating modes. A range reply from targets or nontargets along the line of sight of the system dual-power sighting telescope can be either automatically processed or displayed for operator evaluation as to whether they are either real or false targets. The reflected signal from the automatically acquired or operator-selected target and other objects along the line of sight are received and accepted as return pulses. These pulses are identified and converted into measured target ranges.

In the manual mode these replies are stored for selection by the operator. On command each stored target range is displayed for evaluation. The selected range is then processed into an input form acceptable to the M21 computer. In the automatic mode target range is automatically fed to the M21 computer if the range reply conforms to established "acceptability" criteria.

The receiver-transmitter unit is mechanically supported on end bearings mounted on the tank turret with their axes at right angles to the gun line of sight. A ballistic drive link coupled from the gun trunnion to the left end of the receiver-transmitter causes the unit to rotate in a vertical plane on its support bearings. The receiver-transmitter optical sighting path is thereby compensated for gun elevation movement. Superelevation correction (for ammunition-type ballistics) is subtracted from the optical sight elevation position through the gun mechanical drive linkage connected to the receiver-transmitter.

As the gunner rotates the tank turret and gun in azimuth to follow the target, the receiver-transmitter optical sight follows accordingly. The azimuth lead angle for the gun is computed by the M21 computer, which then deflects the receiver-transmitter azimuth mirror in the opposite direction from the desired gun lead angle. When the sight is again laid on the target, the resulting turret movement causes the gun to lead the target by an appropriate angle.

During operation of the LRF system power supply circuitry transforms, converts, and regulates the tank

battery power and controls its distribution within the system. Prior to and during system use, system test and protection features permit system self-test and provide malfunction indications. System protective features include interlocks and voltage-monitoring circuits.

1-2.5.3.2.3 Tank Thermal Sight

The tank thermal sight (TTS) uses visible and infrared frequencies that use unity power optics, eight-power optics, infrared optics, and video-processing electronics. The IR optics include the head mirror and drive, IR afocal assembly, the front side of the scan mirror, the IR imager, and the cooled detector, i.e., Dewar. The video-processing electronics consist of the video preamplifier, video postamplifier/driver, and light-emitting diode (LED) array. Visible optics for IR processing include the back side of the scan mirror, the visual collimator, the LED optics, the reticle combiner, the roof prism, the image intensifier, and the binocular eyepiece assembly.

The afocal assembly reduces the image in the selected field of view to a size compatible with the optical aperture of the IR imager and collimates the received IR radiation so it reaches the scan mirror in parallel rays. The mirror reflects the collimated radiation into the IR imager, which focuses the scanned image onto the cooled detector elements located in the detector (Dewar) assembly. The detectors convert the IR energy into electrical signals that are processed by the video-processing electronics and converted into visible light by the light-emitting diode array. The visual collimator transmits the light to the back side of the scan mirror where it is reflected to the LED optics through the reticle combiner/beam splitter and into the gunner's and commander's displays. The image viewed at the eyepiece is a direct visible reproduction of the IR scene.

1-2.5.3.3 M1 Tank

The M1 main battle tank (MBT) went into production in the spring of 1980. It was officially christened the "Abrams" after the late Gen Creighton W. Abrams, Chief of Staff of the Army during 1972-74 and a well-known tank commander during World War II.

The fire control, which accounts for about a fifth of the unit cost, allows the main gun to be fired accurately to the limit of the effective range of the ammunition, day or night, with some degradation when moving. The fire control system consists of all of the equipment provided for target sighting, aiming, and firing the main gun, the 7.62-mm coaxial machine gun, the commander's cal .50 machine gun, and the loader's 7.62-mm machine gun. The general arrangement of the major fire control components and their configuration within the turret, as viewed from the turret rear looking forward, is shown in Fig. 1-5.

The primary optical sighting instruments are the gunner's primary sight and the optical relay extension to the commander. This periscope is mounted to the upper turret structure and incorporates servopositioned reticles for complete ballistic solutions with day and night vision imaging. It is linked in the elevation axis with the main armament through resolver follow-up electrical devices. The laser range finder transceiver, the thermal night vision subsystem, and the gyro-stabilized, line-of-sight platform are integrated within the gunner's primary sight. The objective opening of the sight is protected ballistically by an armored steel cover with doors that can be opened or closed from inside the turret.

The gunner also has an auxiliary sight in the simple, rugged telescope affixed directly to the main armament mount. The commander has a three-power, fixed focus periscope for general surveillance and for firing the weapon mounted in his station.

The ballistic computation system is an accurate and flexible digital system that continuously controls reticle and gun offsets. It consists of the digital computer memory processor and associated input/output devices within an electronic unit mounted under the main armament and a gunner's control panel. An ion-drift wind sensor is mounted at the rear of the turret bustle roof, and a pendulum static cant sensor is located in the center of the turret roof on the inside. The outputs of these sensors are automatically fed to the computer along with the laser range finder data.
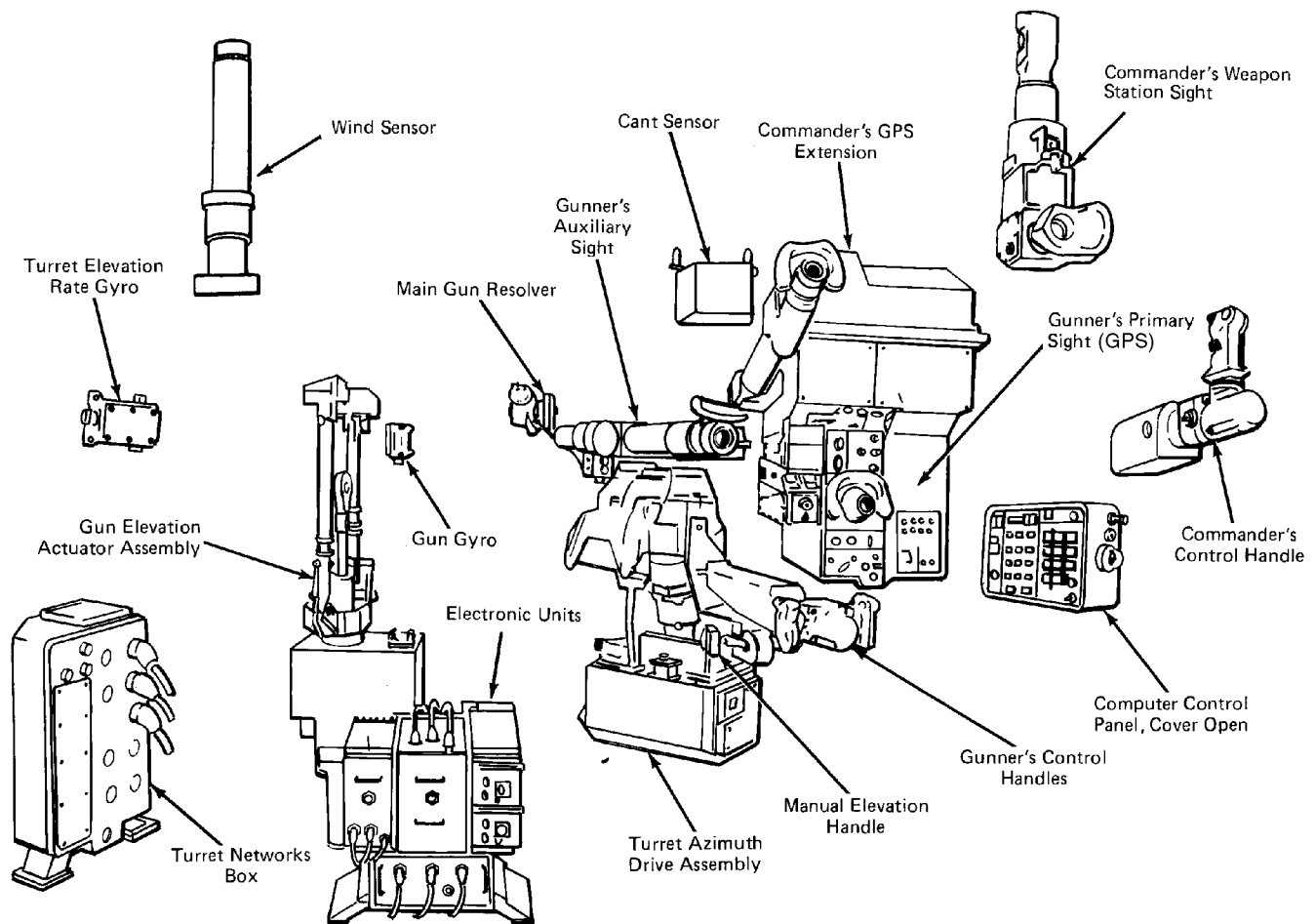
Figure 1-5. M1 Fire Control Components

The gun and turret drive subsystem is electrohydraulic. Its power is provided by an engine-driven pump through a slip ring at the turret/hull interface to the two power valves in a manifold beneath the main gun. Engine-off hydraulic power is provided through the slip ring by a hull-mounted, battery-driven hydraulic pump. Space stabilization in the azimuth plane is accomplished through gyroscopic sensors and servocontrolled valving in the azimuth drive gear assembly. The gun and turret drive subsystem consists principally of

1. An azimuth drive assembly located directly in front of the gunner
2. The elevation actuator assembly located left of the main gun
3. An electronic unit located under the main armament
4. The gyroscopic sensors located on the turret and gun and in the hull
5. The gunner's and commander's main weapon control handles.

The overall design of the fire control system includes a substantial amount of redundancy to provide survivability through alternate modes of operation if the primary system becomes damaged during combat. Examples of this redundancy include the following:

1. Availability to the commander of the gunner's primary sight extension
2. Availability of the gunner's auxiliary sight if the gunner's primary sight is inoperable
3. Direct slaving of the gunner's primary sight to the main gun in elevation if the stabilization system fails
4. Manual elevation and azimuth control if both turret power and auxiliary hydraulic power are lost

5. Design of the computer controls to provide early operator identification and nulling of malfunctioning inputs

6. Provision in the computer design for manual inputs if desired in lieu of automatic sensor inputs

7. Dual controls for the gunner, that include two power control handles, two parallel laser buttons, two parallel palm switches, and two parallel weapon triggers

8. An override control handle at the commander's station that is complete with laser button, palm switch, and weapon trigger

9. Manual main gun firing even with the total loss of vehicle electrical power.

The M1 has been upgraded to the M1A1 and the M1A2. The M1A2 includes many improvements in fire control such as the commander's independent thermal viewer, the commander's and the driver's integrated displays, the gunner's control and display panel, improved fire control and hull electronic units, and integration of position and navigation sensors. The M1 is also discussed in Chapter 6 in detail as an example of tank fire control.

1-2.5.3.4 M2 Infantry Fighting Vehicle and M3 Cavalry Fighting Vehicle

Although support for an infantry fighting vehicle (IFV) centered on the antitank capability that was designed into the vehicle at a late stage in development, the infantry considers it the primary means to keep the infantry alive and effective on a tank-dominated battlefield. Instead of a simple infantry carrier like the M113, the Army has a vehicle that could make mounted combat the norm for the mechanized infantry squad.

Principal design requirements for the IFV (The cavalry fighting vehicle is a variation of the IFV.) included mobility equal to the most modern tanks, such as the M1, and main armament powerful enough to handle enemy light armor and support the infantry squad when dismounted action is necessary.

The main gun for the M2 IFV is the M242 25-mm "chain gun". This is an externally powered weapon cycled by an electrically driven chain drive. Both armor-piercing discarding sabot (APDS) and high-explosive ammunition are available. The dual feed mechanism on the gun can fire either type of ammunition in any combination and allow the gunner to switch instantly to the type of ammunition required to destroy the target. The 7.62-mm coaxial machine gun, located to the right of the main gun, is the M240C. It is mounted in its own separate gas-proof box with trouble light.

The dual-tube TOW missile launcher, housed in an armored rectangular box, is hinged to the left side of the turret, folds flat against the turret for traveling, and is raised through a 90-deg arc for firing. The high firing position allows the missile to be fired while the vehicle hull is behind cover, i.e., in defilade, a capability facilitated by the separate elevation mechanism that permits a 20-deg depression and 30-deg elevation. The IFV carries seven TOW missiles. Two TOWs are in the launch tubes, and five are inside the IFV.

The turret stabilization system that allows the main armament to be fired while the vehicle is moving is considered one of the most accurate of its kind. Contributing to this accuracy are the relatively low turret mass, the large number of gyros used, and the fact that the gun is mounted close to the vehicle centerline.

The main gun can be elevated 60 deg (a North Atlantic Treaty Organization (NATO) requirement) to engage aircraft and depressed 10 deg. The turret drive has a minimum tracking rate of 0.05 mil per second for extremely accurate laying of the main armament and a maximum slew rate of 60 deg per second for rapid engagement of alternate targets. The all-electric turret drive and stabilization system was chosen over hydraulic and hybrid models because they are subject to flash fires.

The fire control system features an integrated day and night sight, the night vision component of which has the same thermal-imaging infrared device used with the TOW ground mount. The sight incorporates a 12-power magnification missile sight, a 4-power sight for the main gun, a target acquisition sight, and an optical relay that allows the commander to see the same sight picture as the gunner in the turret alongside him. The commander, who is seated on the right side of the turret, can override all turret and fire controls.

Unlike the M1 tank the system does not incorporate a ballistic computer or range finder. This omission complicated the effort to improve fire control in order to provide effective fire against aerial targets. An even more fundamental drawback, however, is the absence of a means to offset the sight line from the gun line to introduce kinematic lead, i.e., a gimbal system.

The fire control systems of the M3 cavalry fighting vehicle are identical to those of the M2 IFV. The M2 and M3 are referred to as Bradley fighting vehicles (BFVs). The current versions of the BFVs are the M2A2 and the M3A2, which incorporate improved armor protection.

1-2.5.4 Air Defense Fire Control Systems

Between World War II and the early 1960s, the Army devoted much effort to the improvement of antiaircraft fire to keep pace with the increasing speed of modern aircraft. Special emphasis was placed on developing lightweight, mobile, automatic, radar- controlled tracking systems for use in the forward area.

Formidable difficulties were encountered, particularly in tracking low-flying aircraft. No radar was able to discriminate these aircraft from ground clutter consistently enough to lock on the target and track it automatically. Computers of the era were unable to process the rapidly changing inputs of target range and angular velocity, and they were cumbersome and difficult to maintain in the field. Combinations of optical and radar systems were evaluated, and simplifications were made to increase the usefulness of frontline weapons.

Although some of the weapon systems proved effective against some kinds of targets, none achieved the required percentage of hits on high-speed maneuvering targets at low altitude.

One of the systems developed, the Vigilante, had highly sophisticated fire control to direct the 50 rounds/s fire of a 37-mm Gatling gun, but it was never fielded. In 1962 it was decided to phase out development of the Vigilante in favor of the Mauler forward area defense missile system. At this time, the man-portable, shoulder-launched Redeye missile system with an IR homing seeker had already been fielded. It appeared then that the guided missile was to dominate air defense. The Mauler program, however, was later terminated due to unreliability, and the Redeye was to have shortcomings in reaction time and false target lock-on difficulties. A program initiated to provide an interim gun solution resulted in development and fielding of the Vulcan air defense system (VADS).

By the late 1970s the results of a series of gun air defense effectiveness studies provided sufficient justification for product improvement of the VADS. Modification kits were developed to improve VADS performance to meet the product-improved Vulcan air defense system (PIVADS) requirements. Prior to PIVADS the requirements for the division air defense (DIVAD) system were released. Studies had been devoted to weapon characteristics such as optimum gun caliber, fire control configuration, and mobility needs and to the suitability of foreign systems. After limited testing, the DIVAD system, named SGT York, went into production. However, in an extensive user field test it was found to be deficient in several areas, and the program was canceled. This decision may have been influenced by the fact that neither the SGT York nor any gun air defense system would be effective against a standoff helicopter threat. After cancellation of the SGT York, a replacement study was begun to determine how to produce air defense system(s) capable of defeating the updated air threat in the short time frame.

For a variety of reasons (Some of which are noted with the system descriptions that follow.), few of the air defense gun systems developed by the Army reached full production.

1-2.5.4.1 Self-Propelled 40-mm

During World War II the increased activity of enemy aircraft in ground support and reconnaissance brought a demand for a light, forward area antiaircraft system to defend Army field forces. Since the 40-mm cannon was being produced in large numbers, it was used as the basic weapon, and on-carriage target-indicating and target-designating systems were developed. Near the end of the war a self-propelled twin 40-mm gun mount with a mechanical computing sight was introduced for use in forward areas.

Between 1947 and 1950 a program to improve 40-mm AA fire control resulted in the drive controller T26, which used a ball resolver type of tracking head as the gunner's control.

1-2.5.4.2   T33/M33

In the 1950s a number of different AA fire control systems were developed for weapons of various sizes. The most prolifically produced systems were the rather large AA weapons, and these were designed originally to be fully automatic, the T33 and M38 (Skysweeper).

The T33 was developed in 1949 and 1950 as an electromechanical system designed to detect any aircraft and compute the firing data necessary to control 90- or 120-mm guns. It included two radars: a tracking radar and an acquisition radar. The tracking radar and its associated parts—tracking console, tracking antenna, tactical console, computer, data junction box, and early warning plotting board—were installed on a trailer, whereas the acquisition radar—with antenna, antenna drive unit, antenna RF unit, and modulator unit—was set up separately from the tracking radar but controlled from it. The T33 system is discussed in Ref. 7.

Although the M33 system, introduced in 1952, was like the T33, it had an improved acquisition antenna enclosed in a fiberglass dome that was transported in and emplaced from a flatbed trailer. The M33 system is discussed in Ref. 7.

1-2.5.4.3   M38 Skysweeper

The M38 Skysweeper was specifically designed to provide fully automatic fire control for a 75-mm AA gun against low-flying, high-speed aircraft. This system was produced, tested, and used over a seven-year period from 1951 to 1958. Many deficiencies were discovered and eliminated during the test program and in the field. It was recommended that production be severely curtailed until the "bugs" were eliminated.

The Skysweeper included a medium-range, 75-mm cannon with on-carriage fire control equipment that included an electromechanical computer, radar tracker, periscope, power control, target selector, cable system, and wiring set. The gun had automatic loading and ramming. Thus the whole unit formed a rapid-fire, completely integrated AA weapon system.

The computer was mechanically connected to the radar tracker and to the azimuth power controls via ground reference shafting. The modularly constructed computer had two converters to convert angular data from the radar to rectangular coordinates. A prediction unit in the computer—with constant-speed motor, inverter, and ballistic unit with cam—determined target rate and multiplied it by the time of projectile flight. Target lead distance and present position were then added in each coordinate and converted to future angular data. A ballistic unit added elevation and corrected time of flight.

The computer output was put in synchro form for transmission to the power controls. Data on wind, muzzle velocity, and air density could be inserted.

Skysweeper was effective against targets approaching or moving away at constant, moderate speeds and altitudes, but its effectiveness decreased rapidly against targets at higher speeds or those with changes in speed and direction and at low altitudes. For example, one series of tests produced 67% hits on targets moving perpendicularly to the line of sight at 277 m/s (540 knots). When target speed increased to 417 m/s (810 knots), accuracy dropped to 17%. It was speculated that the trouble might be inadequate computer capability.

At low altitudes the lack of a Doppler element in the radar made detection difficult; no target signal return was detected when ground clutter signals exceeded target signals in intensity. In a series of low-altitude tests, detection of low targets was approximately 50%. Lock-on also proved exceedingly difficult, i.e., 28% vs 70% for the M33; the difficulty was probably due to the complex tasks of detection and lock-on being performed by a single operator. Once lock-on was achieved, however, tracking was more satisfactory. The M38 system is discussed in Refs. 8 and 9.

1-2.5.4.4 T50 Raduster

In the early 1950s a fully automatic off-carriage radar and computer antiaircraft fire control system, the Rattrap, was developed for towed and self-propelled 40-mm AA weapons, especially the twin 40-mm, self-propelled M42 Duster. This system, however, proved to be too cumbersome and complex for use in forward areas. A similar system with relaxed requirements, the Mousetrap, was abandoned after a design study, and effort was concentrated on the T50 AA fire control system, referred to as the T50 Raduster.

The T50 Raduster was an on-carriage system designed for optical tracking and radar range input. It consisted basically of a range radar, optical sight, computer, and range servo. The system depended on visual detection, acquisition, and directional tracking of a target; estimated range could be introduced manually if the radar was not functioning properly. The computer generated angular leads on the basis of inputs from the optical equipment and radar.

Ref. 10 is a complete report on the Raduster development program. Refs. 11 and 12 provide a report on radar test results and further discussions.

1-2.5.4.5 Vigilante

The Vigilante, developed during 1959 through 1962, was another effort in the series that began with the use of mechanical computing sights for twin 40-mm AA guns at the end of World War II. Experience in the intervening years had shown that

1. Doppler radar was far superior to pulse radar in discriminating moving targets, i.e., low-flying aircraft, in ground clutter.

2. The optimum system for detecting and tracking high-performance tactical aircraft should use radar detection, range-only radar tracking, and optical position tracking.

The Vigilante was developed as an on-carriage system with a multibarrel, 37-mm Gatling gun. Two systems were developed: the towed and the self-propelled. The problem of producing enough power for both self-propulsion and turret operation, however, was never entirely overcome. Only one of each system was actually produced, and the program was phased out in favor of the Mauler and Redeye. The Vigilante was designed as a forward area system. It was located in a turret that could be mounted on either the self-propelled or the towed carriage. The turret was capable of 360 deg rotation. It contained the operator's compartment together with the controls and indicator, radar, computer, periscope, hydraulic power servos, and the main slip ring assembly. The turret also contained the cannon and the ammunition feed assembly.

From the seat in the operator's compartment, all controls essential to operation of the radar, computer, sight, and gun were accessible. A single eyepiece presented visual information from the radar and the periscope. Provision was also made to acquire "targets of opportunity" by means of an open sight.

The radar was a pulse-Doppler system that detected only moving targets. It provided a search and range tracking capability for the operator. A track-while-scan feature allowed automatic azimuth tracking of a target while the antenna was scanning 360 deg.

The fire control computer and sight provided the required automatic range and angular tracking capability. The azimuth hydraulic power servo drove the turret and gun to the predicted azimuth of the moving target, and the elevation power servo positioned the gun to the predicted target elevation. The computer provided primary and secondary ballistic inputs to position the power control servos to the predicted target position. The Vigilante system is discussed in Refs. 13 and 14.

1-2.5.4.6 Vulcan Air Defense System

After cancellation of Vigilante and Mauler, the Army did not have a forward area air defense system, so it canvassed industry for an available solution to the problem. In response a supplier using a 20-mm Gatling gun, which had been developed for an aircraft application, and a World War II vintage lead computing sight, the MK 20, as the principal elements put together a prototype for test. It was called the Vul-

can air defense system (VADS). Another contractor offered a modified twin 40-mm Duster with a new gun and turret drive system and a modified sight. A third contractor delivered an available single-barreled, 20-mm system prototype with a lead computing sight serving as the fire control. The accuracy of these systems was limited by the lack of range measurement. A shoot-off was conducted at Aberdeen Proving Ground, and VADS was selected for development. The system that was to be developed and produced in both self-propelled and towed configurations, however, included a range-only radar.

The M61 lead computing gunsight (derived from the MK 20) is a sealed unit containing the lead computing gyroscope and associated circuits and an optical system to project the reticle image. The gunsight used the disturbed reticle principle, which is used to compute a lead angle by offsetting a collimated reticle image, representing the line of sight, from the axis of the gun line. When the gunner is tracking a moving target with the reticle, the gun ideally will lead the target to compensate for target motion and will be properly elevated to correct for trajectory curvature. The term "disturbed reticle" originated from the fact that in this type of sight in the course of normal target tracking, the gunner may see the reticle abruptly move off target. This movement occurs because the sight is mounted on the turret/gun base, and any motion of the base is experienced at the sight reticle. The physical introduction of the gun lead angle is the principal cause of this type of disturbance. If the fire control is off-carriage or if the sight line is isolated from gun/turret motion through inertial stabilization, this can be avoided. (See subpar. 1-2.5.4.8 for further discussion.)

The range-only radar (ROR) is an X band coherent Doppler with moving target indicator. It is gimballed in elevation and azimuth and driven by servos to follow up on the sight line orientation. The radar, which uses the Doppler principle to discriminate stationary targets (clutter), searches ranges from 200 to 5000 m and locks onto and range tracks low-flying aircraft maneuvering within this range. The radar set measures target range along the line of sight and measures range rate. These measurements are used to compute target motion lead angles. Thus, when the gunner tracks the target optically by using the gun drives, the proper lead angle and superelevation are established to hit the target.

In practice, VADS gunners had difficulty maintaining consistently high-performance tracking on high-speed maneuvering targets. This problem was caused by the disturbed reticle implementation that included the gun/turret servo control in the track loop. Also contributing to system error were the approximations used in the analog solution and its sensitivity to component variation. To overcome the rather large systematic error, the barrels of the 20-mm Gatling gun were offset to introduce a dispersion sufficiently large to increase burst hit probability. The product-improved Vulcan air defense system (PIVADS) was initiated to improve system performance.

1-2.5.4.7 Gun Low-Altitude Air Defense System (GLAADS)

The successful development of the laser range finder and FLIR imaging system resulted in consideration of their use in the forward air defense role for both day and night applications. Accordingly, the GLAADS program (Ref. 15) was structured to provide an experimental prototype that would demonstrate improved performance over contemporary domestic and foreign systems by using these electro-optical sensors as well as an advanced fire control equation formulation and digital computer. Key performance objectives included a projectile intercept capability to at least 3000 m with a radial probable error of less than 3 mils and a hit probability of greater than 0.5 per unit for a 30-round burst against a fighter aircraft. The prototype incorporated a pair of hydraulically driven 25-mm, self-powered dual feed guns. The program was terminated after development of the prototype.

The fire control subsystem was mechanized to provide options for use in particular phases of the engagement. Chief among these options were automatic (passive video) or manual sight line pointing during target acquisition and tracking and the use of the FLIR, visual telescope, or the acquisition/track sensor. The fire control computer generated the lead angle commands and the gun and rate-aided tracking signals from the sensor range measurements and the line of sight rate data.

1-2.5.4.8   Product-Improved Vulcan Air Defense System (PIVADS)

After well-instrumented field trials, experiments against simulated targets, and analysis, the shortcomings of VADS were identified, and the scope of the required modifications was established. The product improvement program, PIVADS, called for the design, manufacture, and installation of a modified fire control subsystem on existing VADSs. (Ref. 16)

The modification required improvement or replacement of the VADS computing sight with a director sight and replacement of the analog subsystem with a digital processor. It was decided that the AN/VPS-2 ROR would be retained and integrated with the modified fire control.

In accordance with requirements, the VADS computing sight was changed to a stabilized director sight to replace the disturbed reticle.

The PIVADS is in the field in two versions: the self-propelled M163A2 and the towed M167A2. The system has improved tracking, gun pointing, and computer predictions of future target position. A combination of an improved sight, a microprocessor, and a turret drive reduces the gunner's workload to making rate corrections once the target is acquired. Once a target track is established, the computer drives the turret based on target prediction and ballistic solution data. An azimuth gear drive virtually eliminates backlash and wear.

1-2.5.4.9   Division Air Defense System (DIVAD)

In 1977 after reviewing proposals for a new division air defense gun system to replace the VADS, the Army awarded two development contracts. Each contractor was to build a complete DIVAD prototype, and the winner of the follow-on production contract would be determined by a competitive firing test. The Army evaluated the results of the firing against modestly maneuvering fixed and rotary wing aircraft and found both systems to be comparable and acceptable. The Army's source selection evaluation board eventually selected one contractor in the spring of 1981. A production contract for 50 DIVADs was awarded one year later. In the fall of 1985 the DIVAD program was canceled because it performed poorly in realistic engagement scenarios during field tests.

DIVAD was a mobile, radar-controlled, all-weather gun system intended to replace the Vulcan and provide close-range, low-altitude air defense for armored and mechanized units. It featured a turret-mounted twin automatic cannon mated to the M48 tank chassis, which the Army had specified for the program. The philosophy of the program was to use proven components where feasible. Accordingly, the design used a 40-mm Bofors gun with an integrated search-and-track radar derived from the F-16 fighter aircraft radar. The armored turret also contained the computer, optical/electro-optical fire control components, ammunition, environmental conditioning equipment, the turret/gun drive that aimed the primary weapon, and the necessary controls and displays. The chassis contained the electrical and hydraulic power generation equipment for the turret and automotive subsystem. An ammunition storage and feed subsystem stored and delivered the required rounds to each gun in accordance with the programmed firing schedules. The system had a three-man crew: a squad leader, gunner, and driver. A fourth crew member was to be stationed at the organizational support level for noncombat functions.

Fig. 1-5 shows the major software elements of the fire control system. The three major software elements of the fire control system were resident in the DIVAD system controller (DSC), the fire control computer (FCC), and the radar processor (RP). The RP was contained in the portions of the radar subsystem shown in the upper right corner of the diagram. There was also software in the attitude reference unit (ARU), the graphics display unit (GDU), and the receiver and antenna electronics (parts of the radar subsystem).

The basic function of the DSC was to coordinate and direct the activities for all other system elements. As Fig. 1-6 shows, the DSC had more devices connected to it than any other component. It set up and managed the seven operational modes of the system. In addition, it performed the following functions for all system modes: (1) monitored and controlled system power, (2) maintained the system reference clock, (3) synchronized system execution cycles, (4) controlled data transfers over the multiplex bus, (5) controlled all operator interfaces, (6) provided real-time control and task sequencing, and (7) provided operability and control of all subsystems, i.e., gun feed/fire, turret, sights displays, and hull terminal.

The FCC was the system calculator. All real-time solutions to fire control equations, target prioritization, and gun pointing and target display were performed by this software. The first resided in the digital signal processor (DSP). It removed clutter from the radar returns and performed Doppler target detection. The second resided in the radar computer (RC) and supervised operation of the radar hardware. Operating under mode and submode selections received from either the control panel or the fire control computer, it generated operating commands for the remaining 13 radar units, which controlled signal generation, reception, and processing within the radar set. It computed target and other relevant data from the radar returns, and it transmitted computed data to the fire control computer.
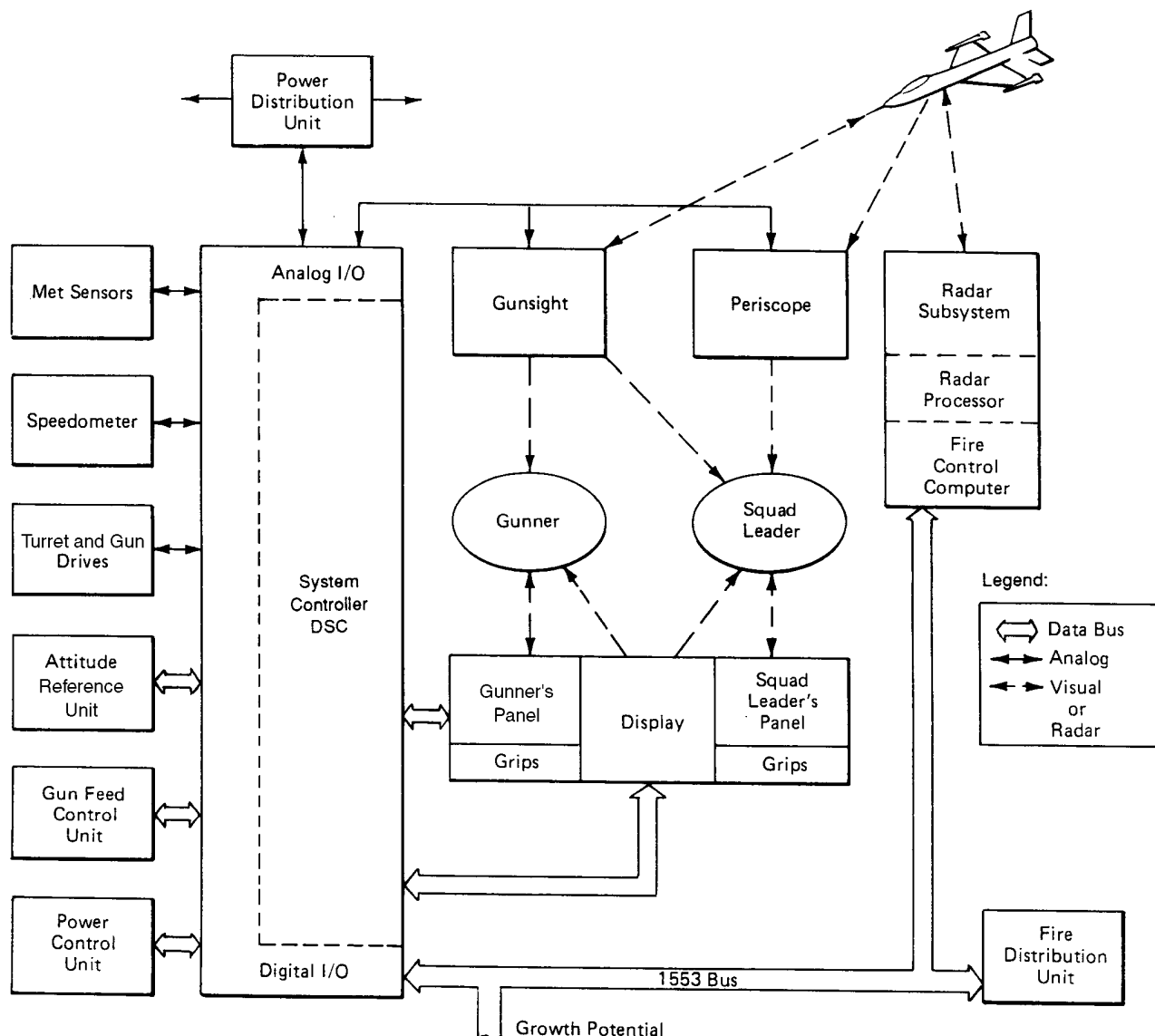
Figure 1-6. SGT York Fire Control System

The fire control subsystem was comprised of those elements shown in Fig. 1-7. The principal elements of the fire control subsystem, the flow of information between them, and the flow of information between the fire control system and the operators are shown in Fig. 1-8. The paths between the operators and the fire control subsystem were visual by way of the plasma display, the gunsight, the periscope, and the manual interface with the control panels and the associated handgrips. The other data paths shown in the figure are electrical (via cable). The principal data path is the MIL-STD-1553 serial digital data bus, which transmits all the measurements, control signals, and commands among the radar, the FCC, and the other elements of the system through the system controller. The communication links from the system controller to the other elements of the fire control subsystem are slower serial digital buses (to the ARU, control panels, and plasma display), parallel digital (with the laser in the gunsight), analog signals (the gun and feed control, the turret and gun drive, the speedometer and meteorological sensors, the hand controls, the gunsight, and the periscope), and discrete signals on individual wires for critical control signals.
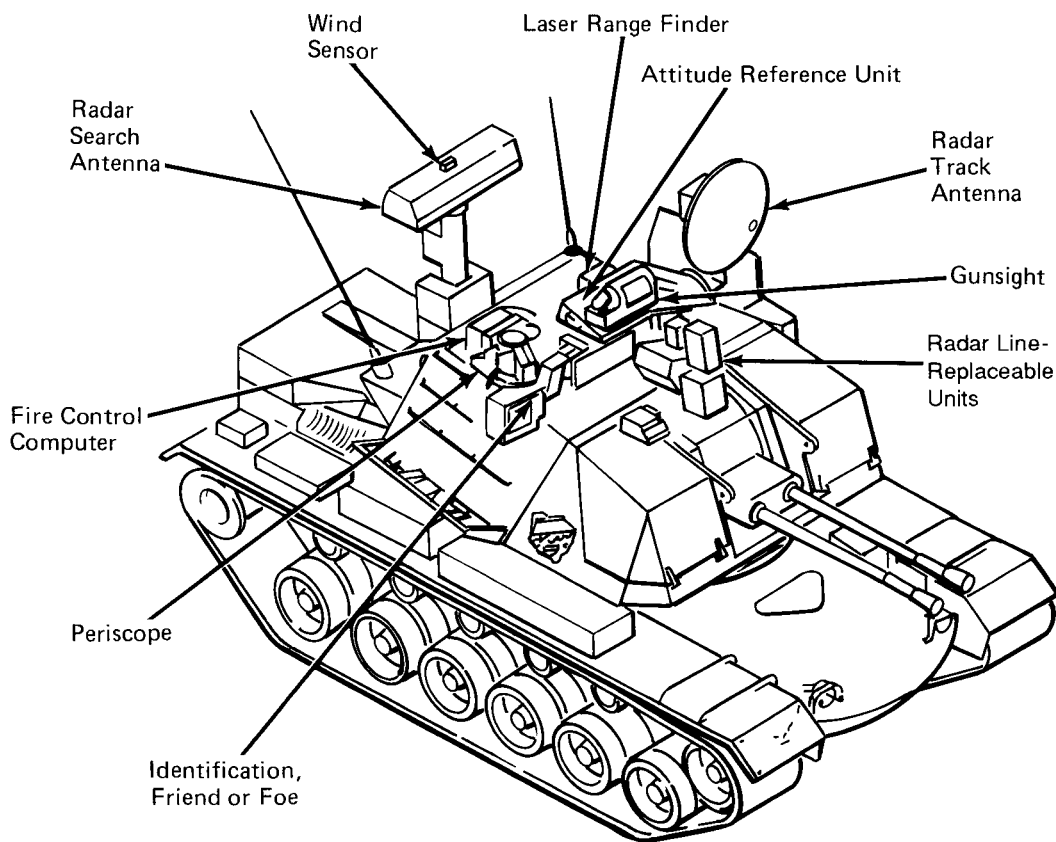
Figure 1-7. SGT York Control Subsystem

The radar was capable of continuous search while tracking a target. The simultaneous search-and-track functions were accomplished by time-sharing the radar electronics (i.e., transmitter, low-power RF, and radar processor) between the search antenna and the track antenna. The switching circulators (waveguide circulators) direct the transmitter output to either the search or track antenna.

The tracking radar monopulse was configured for single-target tracking with a dedicated tracking antenna whose gimbal coverage was compatible with the extreme angle requirements of the gun. The signal processing of track data was time interleaved with search signal processing so that continuous tracking was performed while targets were being detected within the full search volume.
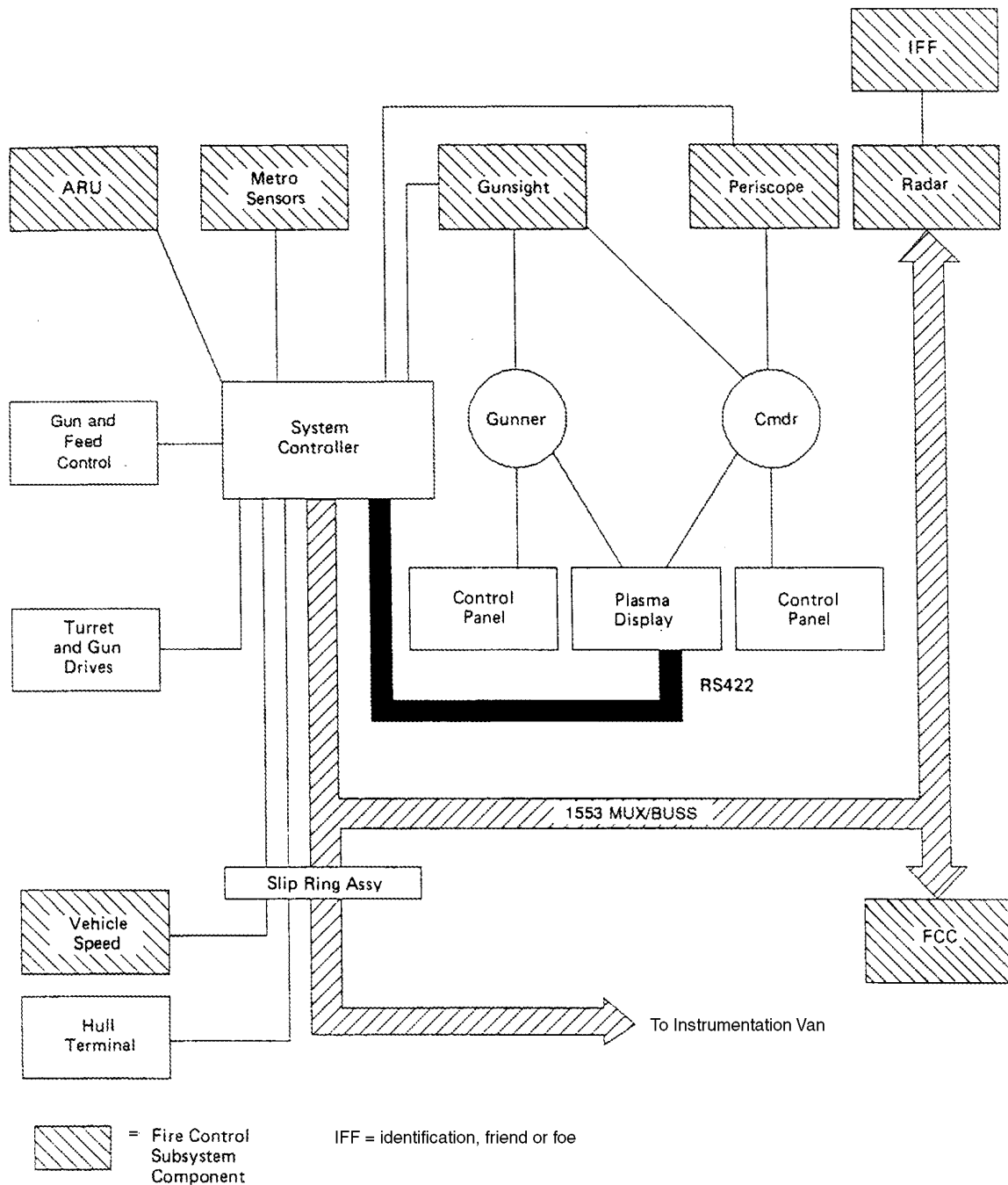
Figure 1-8. Fire Control Block Diagram

For a tracked target, the slant range, radial velocity, and direction cosines were to be used in an integrated fire control system. Therefore, provisions were included to enable the radar to acquire a target that had been detected by a sensor other than the radar. In this mode of operation the radar maintained electronic silence until an acquisition command was received, at which time the transmitter was enabled.

The search mode detected targets using pulse Doppler processing. Complete clutter rejection was achieved in both the stationary and moving environments by incorporating a highly stable, digitally controlled frequency source and other cancellation circuitry.

The search-and-track functions were time interlaced along with a continuous, automatic real-time calibration of critical radar functions. This connection was intended to ensure that the radar performed under battlefield conditions without requiring skillful involvement by the crew.

The gunsight was composed of three major subsystems: the telescope, the laser range finder, and the stabilized sight unit. The gunsight and the commander's periscope were the optical equivalent of the radar system; their primary function was to back up the radar, particularly in the aerial engagement mode. The optical subsystems, however, had additional capabilities over and above those of the radar, i.e., they could be used in ground engagements in either an active or passive surveillance mode of operation.

The gunsight was the counterpart of the tracking radar and had approximately the same field coverage. Range could be obtained by means of the laser range finder. Although the primary function of the sight was to back up the radar when it was down, the sight also assisted the radar and enhanced the system capability.

The stabilized sight unit (SSU) was mounted to the top of the turret, and it directed the line of sight of the telescope to the position commanded by the operator or computer. To maintain high optical resolution and permit accurate tracking, the telescope was inertially stabilized to isolate it from external disturbances caused by gun firing, engine vibrations, and the dynamics of a moving vehicle.

The heart of the SSU was the gimbal assembly that housed a gyro-stabilized inertial platform, two orthogonal gimbals that provided pitch and yaw motions, a pointing mirror, an inertial balancer, and a band drive mechanism. Each of the two axes contained a torque motor and an angular resolver to drive the gimbals and read out angular position, respectively. A single, two-axis tuned rotor gyro, common with the ARU and the squad leader's SSU, maintained the inertial reference of the stabilized platform.

The periscope was composed of two major subassemblies: the telescope and the stabilized sight unit. The periscope was the optical counterpart of the search radar and had approximately the same field coverage. It provided the capability for detection and acquisition of air and ground targets while the crew was protected by armor. The armored SSU was mounted to the turret roof directly over the telescope, which was located within the crew compartment. The magnification, field of view, and stabilization of the periscope were configured as cost-effective companions to the gunsight. Targets were detected by the squad leader with the periscope and handed off to the gunner for identification and tracking with the gunsight. The 4-power, 12-deg, field of view night vision system in the periscope was similar to that in the gunsight. Also the squad leader's SSU was similar to the gunsight SSU.

The primary function of the ARU was to supply the fire control subsystem with geodetic referenced turret attitude and attitude rate information. Also supplied by the ARU were the horizontal components of the turret linear accelerations in the form of digital, quantized incremental velocities and vehicle north and east horizontal velocities.

The meteorological sensors consisted of the wind sensor, the atmospheric pressure sensor, and the temperature sensor. All three sensors supplied analog inputs, in either dc voltage or frequency, to the DSC. In the DSC these analog inputs were converted to digital signals and fed to the fire control computer to be used in the fire control solution.

The DSC was based on a multiprocessor architecture consisting of three central processing unit (CPU) cards, a 6-kB (kilobyte) random access memory (RAM) card used as a data storage buffer, and a 192-byte nonvolatile memory used to store calibration and status data.

The major data interface in the launch system was the MIL-STD-1553 data bus. This 1.0-MHz serial bus is capable of transferring data and commands at a 37.5-kB/s rate among as many as 32 terminals connected to it.

The SGT York air defense gun system, i.e., DIVAD, was never fielded and was terminated by the Secretary of Defense in August 1985. It performed poorly in realistic field tests.

1-2.5.4.10 Forward Area Air Defense (FAAD)

Following the cancellation of the DIVAD gun program, the Army developed a five-part plan to meet its requirements for air defense of its divisions. The knowledge obtained in the field test of SGT York against the simulated Soviet air threat not only exposed the inadequacy of SGT York but also highlighted the

need to continue the analysis of the projected threat. The Army and the Defense Intelligence Agency based their projections of advances in threat helicopter operations on the Apache attack helicopter. The threat MI-28 Havoc helicopter is available and has sophisticated weapon systems. The antitank and anti-helicopter Havoc will be equipped with advanced antitank missiles similar to the laser-guided Hellfire missile. The increased threat use of remotely piloted vehicles as platforms for target sensors is anticipated.

The five phases of the Army forward air defense program are the command, control, and intelligence (C^2I); nonline of sight (NLOS); line of sight forward heavy (LOS-F-H); line of sight rear (LOS-R); and combined arms initiatives. The weapons are based on using available hardware initially. The C^2I will manage and coordinate all actual weapon systems. It will consist of active radar installed in both airborne and ground installations with passive identification systems. The C^2I will communicate target information to those weapon systems the Army plans to equip with passive sensors. The Army plans to evaluate manned aircraft, remotely piloted vehicles, helicopters, balloons, and airships for its airborne sensor platform. With both radar and weapon systems in the same communication net, target data as well as radar and weapon system location will be available to all users in virtually real time. Presumably, the passive sensors at the weapon systems will provide the required target track data for missile launch and gun fire control solution. These sensors would include visual optics, TV, FLIR, and laser range finder and designation.

As the name implies, the NLOS phase is concerned with targets out of weapon system line of sight, including the standoff helicopter. A leading candidate for this new indirect fire air defense role is the fiber-optic guided missile (FOG-M). The 320-km/h missile is launched vertically and guided by an operator to obscured targets. Its range is up to 10 km. The operator guides the missile using an image provided by the missile TV or IR sensor via the fiber-optic cable.

The LOS-F-H weapon system is similar to the canceled SGT York gun system. In response to a request to industry for information on a suitable configuration, the large majority of replies recommended a hybrid gun/missile weapon. The missile would handle the targets at long range, and the gun would complement its close-in coverage.

The LOS-R weapon system is the Avenger air defense system, which has eight pedestal-mounted Stinger missiles and a cal .50 machine gun mounted on the high-mobility, multipurpose wheeled vehicle. The Avenger has its own passive target tracker and fire control system.

The final segment of the five-part FAAD plan is the combined arms initiative. The initiative included installing air-to-air Stinger missiles on Army attack and scout aircraft and expanding the role of guns and rockets to the air-to-air mission. The BFV was to be provided with improved fire control to direct its 20-mm gun in the air defense role. The lack of a gimballed platform to introduce lead angles and to point a laser range finder complicates this improvement. Also intended is evaluation of the use of tank rounds against helicopters as well as other air targets. Performance would of course be limited by the tank kinematic lead angle implementation. Because of its three-dimensional mobility, the threat helicopter can often establish an offensive position where a line of sight can be established to a tank while the helicopter remains out of the line of sight to the protecting LOS-F-H weapon system.

1-2.5.5 Small Arms Fire Control

Although effective firing of small arms requires solution of the same fire control problem all weapons have, less effort has been devoted to application of technical devices in small arms. The rifle fire control of the 1980s, for example, is basically little different from the rifles used in the American Civil War. Although not a very efficient process, riflemen are required to acquire targets, estimate range, point, and aim their weapons without aid. This lack of sophisticated fire control aids is due in part to the costs involved in providing fire control equipment to large numbers of soldiers. In addition, there are problems in providing equipment that is small, lightweight, rugged, and operable under battlefield conditions.

However, there have been some relatively recent efforts devoted to providing improved sighting equipment for the small arms user.

1-2.5.5.1 Optical Sights

For more than a hundred years, the typical military rifle has been equipped with what is referred to as an "iron sight". The sight consists of two vertical elements on the top of the barrel of the rifle, one at the rear of the barrel and one near the muzzle. The infantryman's aiming task is to align the front and rear sights with each other and with the target.

Snipers (as well as sport hunters) have used optical sights for many years. The sniper's task is different from the typical infantryman's task. The sniper may be firing at long range, and he needs to aim for a hit in a particular location on a target. (A human target at 500 m is only 1 mil in width.) He does know, however, where the target will appear, and he generally has ample time to shoot. Under these circumstances an optical sight, perhaps with magnification of ≈3 power and an integral reticle, has been thought to be advantageous.

There has been interest in the U.S. and in other countries in providing optical sights to infantrymen at large to improve their rifle shooting performance. Tests have been conducted to determine performance with optical sights compared to performance with iron sights. As of this writing, the U.S. has not adopted optical sights for general infantry use.

1-2.5.5.2 Image Intensifier Night Sights

As early as the 1950s, tanks were provided with the capability to operate at night. The early systems used a xenon searchlight and an IR viewing device, and snipers were provided so-called "starlight" scopes. These scopes consisted of the viewing device only and were useful at short ranges in good viewing conditions. Development of these night sights depended upon use of the image intensifier tube.

In the early 1960s considerable effort was devoted to providing passive night viewing devices for use with infantry weapons. Image intensifier tubes do not operate in the absence of light; they operate at low light levels. Typical night light levels vary from approximately 0.3×10^{-2} candela/per square meter (cd/m^2) in moonlight conditions to approximately 0.3×10^{-5} cd/m^2 in overcast starlight. Typical image intensifier tubes obtain luminance gains of the order of 10^6 and higher over these night light levels. Thus the devices are very useful.

In general, these tubes achieve high gains by means of serial stages of electron multiplication or by amplifying secondary electron emission. They are available with either electrostatic or electromagnetic focusing. More recent versions make use of so-called microchannel plates and current amplifiers. In all cases the electrons are finally focused on a phosphor screen, which is viewed by the user.

With advances in tube designs new viewing devices were designed and were designated as second generation, third generation, etc. The improvements involve not only better sensitivity and resolution but also reductions in the size, weight, and power supply requirements of the devices. Additional information on the design characteristics of image intensifier tubes and viewing devices is available from the Program Manager, Night Vision and Electro-Optics, Fort Belvoir, VA.

Although currently in wide use, image intensifier night sights are not issued to all users of small arms. They are still not very rugged and are relatively expensive and bulky.

The image intensifiers currently in use are the AN/PVS-4 individual served weapon sight, which is designed primarily for the M16A2 rifle but can also be used on the M60 machine gun, and the AN/PVS-10 sniper night sight. The AN/PVS-4 sight uses a 25-mm, second-generation image intensifier that produces an image that is brighter and 3.5 times larger than that otherwise viewed through the naked eye. The scene is imaged on the MX9644/UV image intensifier tube by a 95-mm f/1.3 catadioptric lens, and the output is viewed through a six-element, 10-power eyepiece. An illuminated reticle is projected directly on the face of the intensifier through the center of the catadioptric objective. The AN/PVS-10 is an integrated day and night sight for the M24 sniper rifle. This sight uses third-generation technology and the same mil-dot reticle the existing Leupold day scope uses. The magnification for day and night operation is 8.5 power.

Although not specifically designed for this use, other image-intensifying devices used for small arms

fire control are the AN/PVS-5A night vision goggles, which are binocular and use second-generation image intensifiers, and the AN/PVS-7 series night vision goggles, which are monocular and use third-generation image intensifiers.

1-2.5.5.3 Infrared Night Sights

Some image intensifiers are sensitive in the 0.7- to 1.0-μm region of the spectrum, often referred to as the "near-IR". This subparagraph discusses systems that are sensitive at wavelengths between 8 and 12 μm, often called "thermal IR". At this wavelength band, detectors can "see" in day and night conditions not only through the atmosphere but also to some extent through smoke, dust, and haze. They are not dependent upon amplification of ambient light but upon the viewing of reflected and radiated source energy.

These systems detect and image differences in radiation between objects and their backgrounds. Developed in the late 1950s, the earliest systems of this type were intended to be mounted in aircraft. They were designed to look at an area forward of the position of the aircraft over the ground, and were called forward-looking infrared, or FLIR, an acronym that is still used.

In Vietnam these systems were placed on aircraft platforms and were very successful. Because they detect thermal differences in the scene, they were ideally suited for detecting small cooking fires on the ground.

The Army first became interested in applications of this type of sensor in the 1960s. The first application was in armored vehicles, and the systems were called thermal sights. In the M1 Abrams tank the thermal sight is the commander's primary sight for surveillance and target acquisition in daylight as well as night.

The Army developed thermal sights as a group of modules, all of which could be common with other systems. This concept is called the common module approach. Each detector, preamplifier, and video amplifier is a module that can be used in a variety of systems. This interchangeability results in considerable economy.

The AN/PAS-13 thermal weapon sight (TWS) is a lightweight, self-contained, day and night thermal imaging device. The sight uses advanced sensor design and a solid-state thermoelectric cooler. It consists of a common sensor body with interchangeable telescope assemblies and a disposable power source. There are three configurations: light, medium, and heavy.

The system consists of a matrix of detectors. Each detector represents a picture element or pixel, which is a resolution-limiting element. For example, a 280 x 180 matrix of detectors results in a television-like picture of 280 ×180 resolution elements. Each detector has dedicated amplification electronics and is scanned sequentially in horizontal line fashion similar to television. The output of each pixel corresponds to the average temperature "seen" by the detector. Additional information on the design characteristics of FLIRs or thermal sights is included in Refs. 18 and 19.

FLIR systems are used in armored vehicles as well as in aircraft and in antiaircraft applications, in which they displace radar in detecting and tracking targets.

1-2.5.6 Aircraft Fire Control

The emergence of the helicopter as a weapon delivery platform presented new challenges to the fire control developer. Its capability to hover, fly forward or backward, left or right, and up or down, as well as to fly like a conventional aircraft, created new opportunities. The main rotor blade motion, however, restricts the field of fire, creates downwash that disturbs projectile trajectories, and introduces vibrations that influence optical system design.

The early efforts to place weapons on helicopters that had been developed for utility and observation missions suffered from a lack of understanding of the fire control problem. Helicopter crews used grease pencil crosses on the canopy to aim weapons fixed to the aircraft. Pointable machine guns were fired from windows and used tracer ammunition to assist aiming. The equipment and tactics used by these early

armed helicopters were acceptable in Vietnam because there was little antiaircraft ground threat. Later, the engineering development community became involved, and turreted weapons and optical sighting devices were provided.

Simultaneously, effort was underway in the development community to exploit emerging technologies in fire control system design. These technologies included digital computation, laser, FLIR, TV, radar, stabilization and control, passive video autotrackers, and software advances in filtering, prediction, modeling, and simulation. Success in these areas laid a sound foundation for follow-on attack helicopter fire control development. The view that a single, sophisticated fire control system representing a major part of the weapon system investment could and should be used to direct all weapons fire became accepted. The weapon system is considered an integration of airframe, flight controls, navigation, weapons, and fire control.

The helicopter, which was once considered by many a highly vulnerable vehicle with low survivability, has become a major force. The firepower and agility of the attack helicopter make it a formidable and elusive threat that is often beyond the capability of existing air defenses to defeat. Attack helicopters are being augmented with air-to-air weapons to defeat their enemy counterparts.

1-2.5.6.1 Aircraft Weaponization

The feasibility of firing guns and rockets from utility and observation helicopters had been demonstrated. This soon led to an orderly Army program to develop armament for helicopter application.

A variety of gun and rocket configurations was developed specifically for the OH6, OH58, UH1, and the early version of the AH-1. These included fixed forward and flexible arrangements of the cal .50 and 7.62-mm machine guns, 20- and 30-mm automatic weapons, and a turreted 40-mm grenade launcher. Associated with the weapons was a full selection of rounds, e.g., high explosive, point detonating, tracer, and practice. Initially, the fire control used with all configurations was limited to a simple, single-power reflex sight mounted either to the aircraft cockpit structure or to a cockpit linkage that permitted elevation and azimuth motion.

Several different versions of the 70-mm (2.75-in.) rocket, rocket launcher, warhead, and fuze were developed and deployed during this period. These included fragmentation, flechette, shaped-charge, inert, chemical, and smoke warheads and point-detonating, proximity, and inertial fuzes. Rocket selection and rate of fire were controlled by an intervalometer. The fixed, simple reflex sight was used to point the aircraft and hence the rocket launcher. Use of this type of sight was justified to some extent by the unavailability of a reasonably accurate range finder to eliminate range as an error source. Flight tests of optical baseline range finders and stadia devices proved them to be unsuccessful in the role, and it was not until emergence of the laser range finder that this fundamental need was satisfied. The other major error source that dominated the error budget for the case of stationary targets was the error attributable to the motion of the helicopter. This error source was not eliminated until development of the M-28 armament subsystem for the AH-1G Cobra. Examples of installations on the OH-1 and the OH-6 are shown in Figs. 1-9 and 1-10.

The helicopter sight, XM70E1, shown in Fig. 1-9 has the following characteristics:

1. Unity magnification
2. Reflex sight with a reticle pattern presented at infinity
3. Pilot operated.
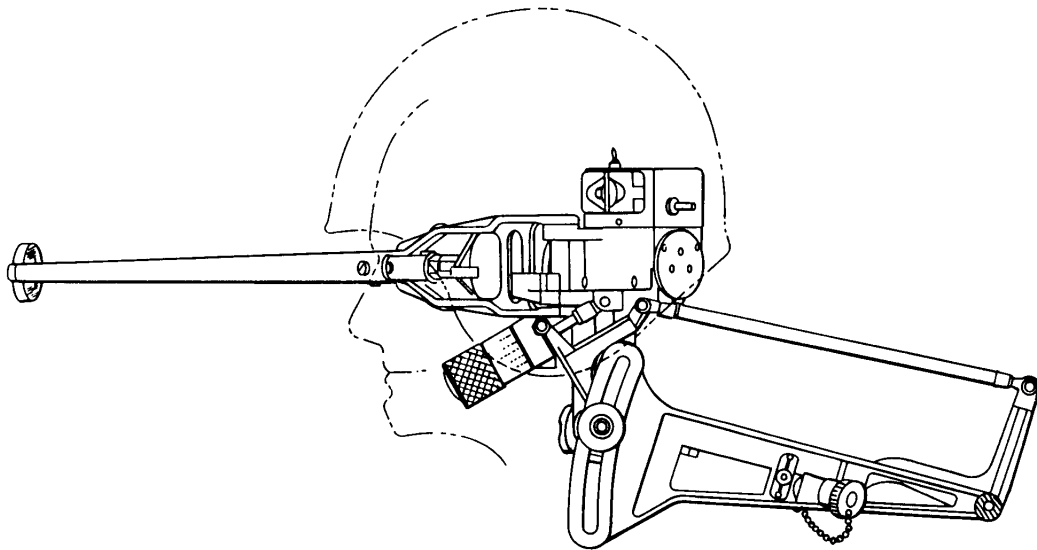
Figure 1-9. Helicopter Sight, Reflex, XM70E1

The helicopter 7.62-mm machine gun M134 shown in Fig. 1-10 has the following characteristics:
1. Mounted on left side of helicopter
2. Maximum effective range: 1100 m
3. Muzzle velocity: 838 m/s
4. Rate of fire: 2000 or 4000 rounds/s
5. Elevation: OH-6A: –24 deg to 10 deg
OH-58A: –20 deg to 5 deg
6. Traverse: none
7. Sight: pilot-operated XM70E1 type.
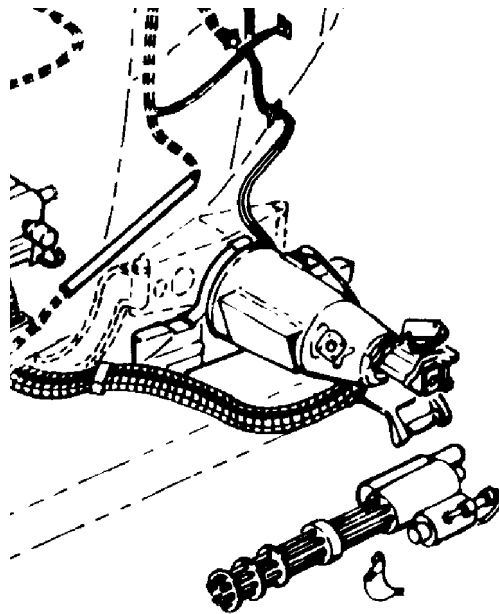
Figure 1-10. 7.62-mm Helicopter Machine Gun M134 (Ref. 20)

The French-developed SS-11 was a wire-guided, solid propellant, antitank missile fired from the ground and from helicopters. The need for magnification to improve the gunner's tracking capability while controlling the SS-11 guided missile highlighted the need for stabilization of the image against helicopter vibration. The antioscillation sight XM-58 was to provide a 6-power stabilized image for the OH-1 gunner through the use of a gyro-stabilized monocular. Development of the first of a series of handheld sights for target acquisitions and identification followed; the first of which was the variable magnification XM-76 antioscillation sight. The image in this sight was stabilized by the adjustable thickness of a liquid prism, which was controlled by a gyro sensor input. These were the simple forerunners of the highly stabilized performance sensor platforms that were developed to guide the sophisticated missile systems of attack helicopters.

1-2.5.6.2   Experimental Prototypes

In the late 1960s and early 1970s, flight-test programs that examined the feasibility of including experimental hardware in follow-on attack helicopter developments were commonplace. Helicopter fire control was a new field and not as well-developed as other areas of fire control. There also were several new technological breakthroughs to be exploited at the time. Further, an aggressive, foresighted Army aviation leadership, intent on showing that the helicopter was a survivable and valuable element on the battlefield, pushed for development. As a result, the applicability of new hardware technology to helicopter fire control was investigated vigorously.

Some of the more significant efforts are discussed in the subparagraphs that follow. Other improvement efforts included a stabilized monocular to improve the gunner's SS-11 missile guidance, active and passive stabilized binoculars for target acquisition and identification, helmet sights with mechanical linkage and IR sensor pickoffs, passive video autotrackers, automatic target cueing from video imagery, optical detection augmentation, rotor blade detection radar, kinematic ranging using velocity and angle rate, closed loop fire control with sensing of round miss distance for automatic solution correction, a television bombsight, optical bombsight adaptation for acoustic sensor battlefield emplacement, low light level TV (active and passive) sight sensor, and pintle-mounted intensifier night sights. For the most part, the flight-test programs were a combination of Army and industry efforts specifically directed at implementing a concept and advancing the hardware so tests would be productive.

1-2.5.6.2.1   Multiweapon Fire Control System (MWFCS)

In the early days of placing weapons on helicopters, fire control was considered to be little more than a sighting appendage to the weapon. The MWFCS Program was an effort to demonstrate that fire control should be viewed as a major subsystem and integrated with the airframe, flight controls, and navigation to control all aircraft weapons. An experimental prototype was developed for the UH-1 originally, but it was later modified and installed in the AH-1 Cobra, where flight tests verified the feasibility and practicably of the system concept.

This endeavor marked the first time that many of the devices now considered commonplace in attack helicopters were used. They included a high-performance, modular, two-power stabilized optical sight (SOS) with ports for a laser range finder, a night vision device, and a damage assessment camera. Because the various devices use different spectral bands, sharing of common optical elements that included the stabilized head prism was possible. An image intensifier whose range depended upon ambient light offered some degree of night vision capability. An adaptation of the ruby artillery range finder, which was liquid cooled to supply a 3-pulse-per-second repetition rate and aligned to the visual line of sight through use of a unique boresight technique, provided range input for the computer. Sight gimbal pickoffs and stabilization gyros measured sight line orientation and inertial angular rates, which, when coupled with the range and helicopter airspeed, provided the necessary data for a full fire control solution. It was assumed in the solution that target acceleration was zero. A curve fit to the 20-mm ammunition trajectory data was used in the computer to calculate ballistic leads as well as projectile time of flight to intercept.

The digital format offered the means to store the curve fit parameters of the ballistics for all rounds considered for use.

Air data sensors measured temperature, pressure, and helicopter airspeed. Air density was calculated from the first two. Because the fire control solution took place in the air mass reference space only, helicopter velocity with respect to the air mass was required. The fixed increment digital computer, which used metal oxide semiconductor (MOS) large-scale integrated circuitry, provided the first Army real-time implementation of a helicopter fire control system. The system, configured for the Cobra, demonstrated an accuracy of about 5 mils on ground targets when using the 20-mm turreted gun and the SOS mode of operation. Pilot and copilot helmet sights, used primarily for target acquisition and remote SOS pointing, offered a snapshot mode for close-in targets. The successful results of this program were cited as justification for the weapon accuracies specified in the Cheyenne requirements.

1-2.5.6.2.2   Integrated Rocket Delivery Systems

A large inventory of the 70-mm (2.75-in.) folding fin aerial rocket (FFAR) made the rocket a likely candidate for the helicopter application. Early firings from a helicopter platform using a simple projected reticle sight, however, resulted in large errors, which were attributed to a dispersion that would virtually eliminate this rocket as a viable area weapon candidate except for close-in ranges. In fact, the errors were due in large measure to the effects of downwash and relative wind. Subsequent tests revealed that the actual dispersion was less than 10 mils rather than the 25 mils originally obtained and that the rocket might be successfully used at longer ranges if the tip-off (angular momentum acquired due to the action of gravity as the forward supports of the rocket leave the launcher before the aft supports) errors could be compensated for effectively. Compensation required that the downwash and relative wind across the launcher be measured and an indication provided to the pilot of their impact on launcher pointing so that the proper helicopter steering commands could be given. A pilot's head-up display with a reticle driven by computer-generated compensation for the tip-off and trajectory curvature formed the basis for the development of the prototype integrated rocket delivery system.

Simulation was conducted to assure that the flight controls and helicopter response enabled the pilot to keep the driven reticle on target by steering the aircraft even though the reticle command generated by the computer changed with the aircraft attitude. Relative wind across the launchers was measured by an innovative airspeed device, and the position of the collective control provided a measure of downwash magnitude. A neodymium laser range finder mounted internally and controlled from the cockpit by the gunner using the pantograph sight described in subpar. 1-2.5.6.3.2 provided range for computer input. Solution of the fire control equations yielded the commands to drive the pilot sight reticle in azimuth and elevation. Successful firing of the rocket under field test conditions provided the impetus for a development program that was adapted to improve the fire control on the AH-1 Cobra. Credibility peaked when the Commanding General of the US Army Aviation Center, personally flying the system, scored a hit on each of two passes while firing a pair of rockets at a tank target at 3000 m, an event that came to be known as the "Miracle of Yuma".

1-2.5.6.2.3   Southeast Asia Multisensor and Armament System for Helicopter (SMASH)

On the AH-1 the SMASH represented the marriage of two major sensor subsystems that were developed to give night and all-weather targeting to Army aircraft in the late 1960s. An MTI radar, the AN/APQ 137, provided the long-range, all-weather capability for detection of ground targets. A set of range-gated clutter reduction filters enabled the operator to observe vehicles moving at speeds as low as 1 m/s and personnel moving at 1.5 m/s. The operator manually controlled the orientation of the antenna in azimuth and elevation while viewing the azimuth and range presentation. Complementing the radar was an imaging FLIR system. The scene was scanned over a linear array of 360 mercury-doped germanium detectors, which provided a 0.25-mil resolution and a differential sensitivity of 0.5 deg C in the 5-deg nar-

row field of view. The FLIR, which operated in the 8- to 14-μm spectral region, offered the means to recognize and identify targets handed off from the radar or acquired initially by the FLIR. Pickoffs on the FLIR stabilized gimbal measured line of sight orientation while the radar, operating in a slaved mode, measured target range. When coupled with navigational and environmental data, this basic target information generated azimuth and elevation commands for the 30-mm gun turret servo.

It was planned to send SMASH to Southeast Asia where it would be used to intercept troops and supplies moving under the cover of darkness. However, before the systems could be delivered, the end of the Vietnam War eliminated the requirement. Successful development of the FLIR led to an immediate change in the specifications for the proposed Cheyenne attack helicopter, i.e., an active low light level TV was replaced with a FLIR. FLIR is recognized today as the standard approach to night viewing in sophisticated weapon systems.

1-2.5.6.2.4 Aerial Artillery

The vulnerability of emplaced artillery to counterbattery fire had been recognized as a reality. The need for mobility had become a necessity, and the helicopter became a candidate to achieve this mobility. Concepts that included mounting the weapons on the helicopter with fire conducted in the air or only on the ground were examined for feasibility. Although the ability of the airframe to survive weapon firing effects, i.e., recoil and blast, was paramount and the most visible cause for concern, the ability to achieve accurate fire under battlefield conditions was also high risk. The physical direct laying of the weapon presented a large fire control problem. Of more theoretical interest was determination of helicopter position, attitude, and velocity, which were required to generate initial conditions for trajectory computations and to lay the weapon in the indirect fire mode. Both software and hardware investigations were directed primarily to use the M204 105-mm howitzer on the CH47 helicopter. The program, however, was terminated before a full system demonstration could be accomplished.

1-2.5.6.2.5 Mast-Mounted Sight

The mast-mounted sight was conceived as a means to enable the helicopter and rotor blades to be hidden from observation while the helicopter maintains full target surveillance and engagement capabilities. Mounted on a platform above the main rotor of a helicopter, the mast-mounted sight allows the helicopter to mask itself and the rotor blades behind natural or man-made defilade and to observe and track a target without being detected from the target area. This concept reduces the vulnerability of the helicopter to enemy detection and increases its battlefield survivability, a capability that makes the mast-mounted sight ideally suited for scout helicopters with forward area missions.

Feasibility efforts were directed at demonstrating that a scout helicopter could perform targeting functions from defilade without detection under simulated conditions of threat radar and visual observation devices. Initially, a television camera was mounted on the mast as the sight. It was necessary that the resolution of the TV camera not be degraded by mast vibration and that an integral laser designator could be accurately pointed.

Early flight-test demonstrations used an available nonrotating, mast-mounted platform developed for a UH-1 helicopter terminal communications system. Several stabilized sight configurations of varying sophistication were installed. One configuration included a laser designator boresighted to the line of sight. In each configuration the pointing of the sight reticle was controlled remotely from the cockpit by the gunner while he observed the scene on a monitor. The pilot, who also observed the display, was able to position the helicopter to take greatest advantage of the defilade while maintaining a clear line of sight to the target. The results of the flight tests were surprisingly good since sight stabilization had not been optimized for this application. In nearly all test trials, strategically emplaced radar and optical devices could not locate the helicopter. The successful demonstration led to development of performance specifications for a prototype stabilized sight and laser designator and a mast mount specifically for the OH-58 scout helicopter that had a significantly higher vibrational level at the mast than the UH-1. Subsequent flight

tests demonstrated compliance with the specifications. The concept, with the addition of FLIR and a passive automatic tracker, was then adopted. These additions provided night viewing and an improved tracking capability for the product-improved OH-58.

1-2.5.6.3 Attack Helicopters

1-2.5.6.3.1 Cheyenne

The Cheyenne represented the Army's first attempt to develop an attack helicopter. The Cheyenne helicopter is shown in Fig. 1-11. The airframe, fire control, navigation, and flight controls were to be optimized to satisfy the weapon system requirements. These requirements included effective fire of the TOW missile, the 30-mm turreted gun, and 70-mm (2.75-in.) rockets on ground targets. The heart of the fire control was the swiveling gunner station (SGS), which provided the relative target data to the digital computer. The electro-optical sensors, TV, imaging IR, TOW tracker, laser range finder, and the visual sight objective were mounted along an optical bench that was inertially stabilized and controlled about an azimuth axis. An elongated precision-stabilized mirror provided the elevation deflection of each sensor line of sight. A gimbal, slaved by servos to follow up on the optical bench around the azimuth axis, carried the gunner station with its relay optics and eyepiece, manual tracking controls, and gunner's seat. "Submil" tracking accuracy was obtained under both day and night conditions and was compatible with the TOW tracker and laser range finder pointing requirements.
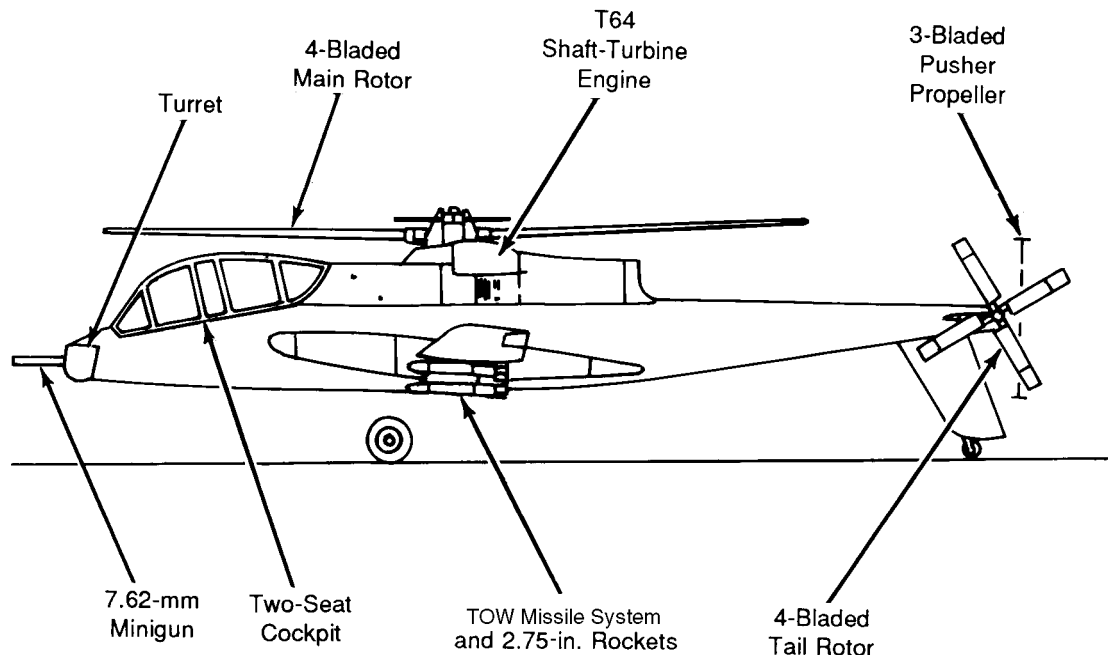
Figure 1-11. Cheyenne Helicopter

Sight gimbal angles and sight line rates measured by stabilization gyros and laser range were transmitted to the computer and then smoothed by using fixed gain filters. These were used along with helicopter velocity and attitude data obtained from the navigational subsystem to solve ballistic and kinematic lead equations expressed in the stabilized sight line frame of reference. Constant target velocity was assumed. The ballistic equations were developed by a curve fit to trajectories generated by a six-degree-of-freedom representation. Azimuth and elevation commands were then computed and used to drive the weapon turret.

Some development problems were experienced in obtaining a producible liquid-cooled ruby laser and

the 8- to 14-μm FLIR. Maintenance of alignment between the electro-optical elements and the visual line of sight and maintenance of mirror flatness over temperature variations were also problems. The image quality of the visual optical telescopes was poor. Difficulty was also experienced in curve fitting the gun ballistics to the accuracy required over the full effective range of the weapons. Notwithstanding the fire control problems, the Cheyenne program was terminated because of safety considerations associated with the airframe.

1-2.5.6.3.2 Cobra

Using the basic rotor system, engine, and drivetrain of the UH-1 utility helicopter but with a streamlined, thin-profile fuselage, the AH-1A went into production in 1967 and was widely used in Vietnam. The Cobra helicopter is shown in Fig. 1-12. Since then, a series of product improvements has increased the sophistication of the navigation, airframe, fire control, and weapon suite until it now can be considered a modern attack helicopter weapon system. The initial weapon configuration was the M28 armament system. A hydraulic turret that accepted a 20-mm machine gun and/or a 40-mm grenade launcher was controlled by the output of a cockpit-mounted pantograph sight and an analog ballistic network. This network compensated for helicopter velocity and ballistic curvature but used a manual input of gunner-estimated range. System accuracy, even against stationary ground targets, was severely limited by this manual range input. The pilot fired 70-mm rockets using a cockpit-mounted reflex sight on which elevation was set by using a reference card that gave elevation as a function of airspeed, estimated range, and altitude.
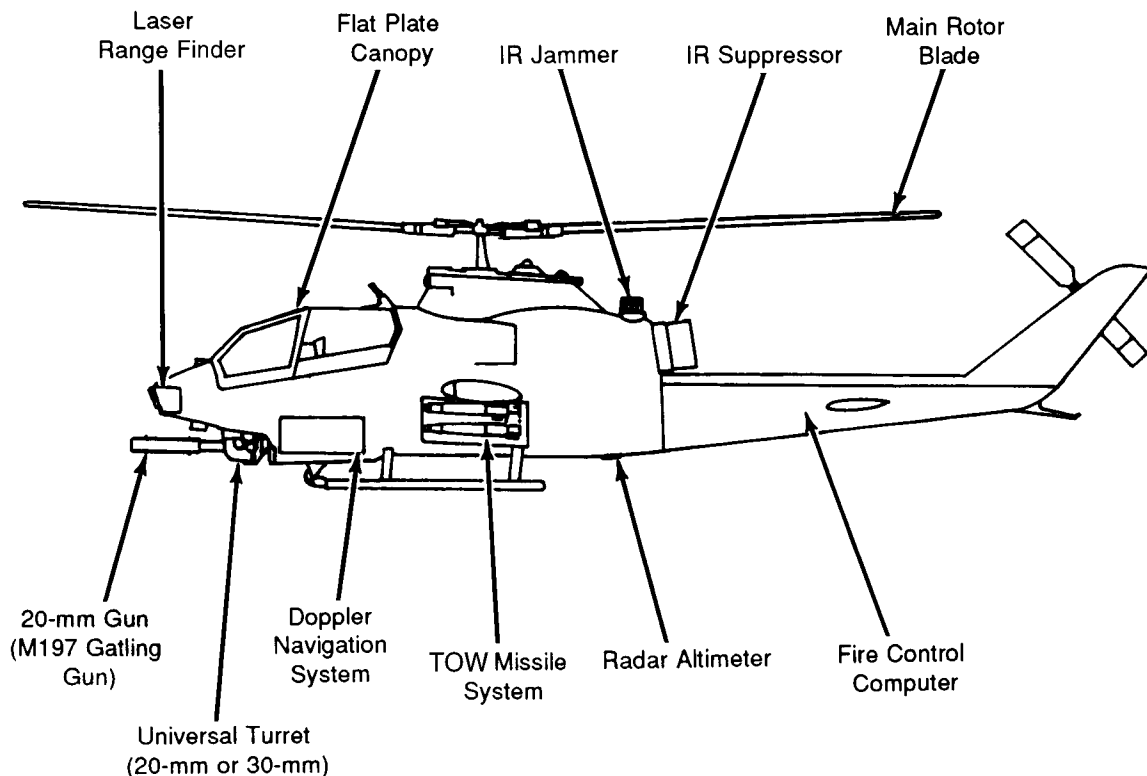
Figure 1-12. AH-1 Cobra Helicopter

The requirement for a heliborne antiarmor missile system led to integration of the ground-qualified TOW missile subsystem into the Cobra in 1972. Effective firing of the TOW from the helicopter required a high-accuracy optical tracking system that could keep a TOW missile IR tracker sighted on target. This

need was satisfied by development of the telescopic sight unit (TSU), which used 12-power optics and was inertially stabilized by rate-integrating gyros. Image quality and pointing stability were adequate to satisfy target identification and tracking requirements. Not only did the TSU meet the onboard missile needs, but it also offered an excellent source of target angular position and rate measurement for conventional fire control application.

In 1977 the AH-1S modernized Cobra development program took advantage of the existence of the TSU, a lightweight Doppler navigator, and a universal turret subsystem to upgrade the Cobra to achieve a full fire control solution for the 20-mm gun and the 70-mm (2.75-in.) rockets. The lack of accurate range information for both conventional fire control use and assurance that the TOW is not fired beyond guided wire length was rectified by integration of a neodymium laser range finder in the TSU. An air data subsystem that uses a swiveling pitot-static probe to sense the local airflow magnitude and direction, the free stream air temperature, and the static pressure was introduced into the system. A heads-up display that presents symbology to the pilot to enable him to align the aircraft for TOW missile delivery and to aim the aircraft for rocket fire was also added. A digital fire control computer solves the gun and rocket ballistic equations. The gun ballistic equations are expressed in the sight line reference frame, whereas the rocket ballistic equations are expressed in the aircraft coordinate reference frame.

1-2.5.6.3.3 AH-64 Apache

The Apache advanced attack helicopter is a 4-bladed, main rotor, twin engine, tandem-arranged, two-man-cockpit aircraft with a maximum all up weight of about 8200 kg and the capability to carry an ordnance load of about 1220 kg. The Apache helicopter is shown in Fig. 1-13. This ordnance load could consist of 16 Hellfire antitank missiles, up to 76, 70-mm (2.75-in.) rockets, up to 1200 rounds for the 30-mm cannon, or combinations of these. The 180-mm (70-in.) diameter Hellfire is equipped with a semiactive laser guidance seeker. The guidance system requires a laser beam to be positioned on the target during the terminal phase of missile flight. This positioning can be accomplished autonomously from the helicopter or remotely by another ground or airborne laser designator. Both direct and indirect firing modes can be used to enhance weapon system operational versatility. Secondary armament, which consists of a 30-mm gun and 70-mm (2.75-in.) rockets, is provided to engage light armor and area targets, respectively.
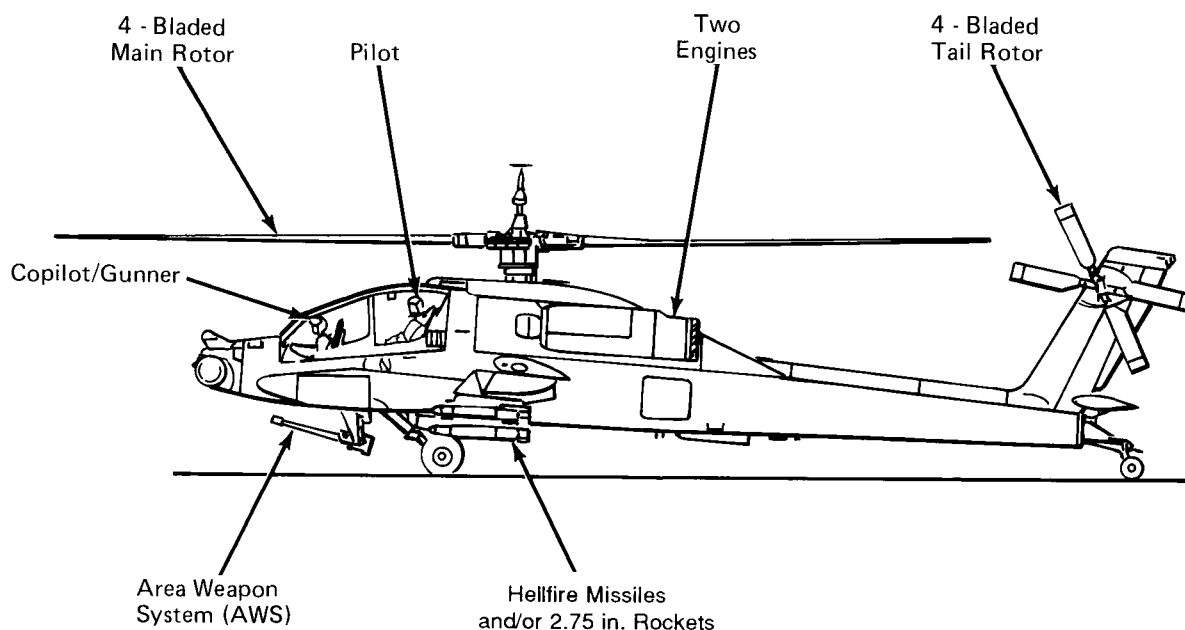
Figure 1-13. AH-64 Apache Configuration

The 30-mm gun is a fully flexible weapon mounted in a belly turret behind the sighting subsystem. This mounting prevents the optics from being obscured or distorted by the gun blast.

Fire control is provided by a high-speed digital computer, an integrated self-contained navigation subsystem, a two-axis air data sensor, all digital mode control electronics, and three advanced vision subsystems. The vision subsystems are the gunner's TADS, a pilot night vision system (PNVS), and an integrated helmet and display sight system (IHADSS) for both crew members.

The TADS is a stabilized, multisensor targeting platform that contains direct view optics, day television, a FLIR imaging sensor, a laser designator/range finder, and a laser spot tracker. By looking through the TADS eyepiece and using the sensors he selects, the gunner is able to acquire, identify, track, and designate targets either day or night at extended ranges. A passive automatic tracker provides a high-performance alternative to the manual track mode through the processing of either TV or FLIR imagery. The laser spot tracker warns the crew if the helicopter is being subjected to laser irradiation. The PNVS contains a FLIR sensor integrated into a highly flexible turret that permits the aircraft to be flown at nap-of-the-earth altitude in darkness and in degraded weather conditions. The IHADSS provides both crew members with a heads-up display for viewing either the PNVS or the TADS sensor displays and for presenting stores status and flight symbology information. The flight information includes commands for rocket and Hellfire launch. The IHADSS also contains mode logic to enable quick target handoff and to control of the gun turret for snapshot fire. The principal elements of the navigation subsystem are the AN/ASN-128 Doppler, i.e., a strapped down inertial heading and attitude reference system, and the air data sensor.

The AH-64 armament, navigation, and fire control subsystems are integrated through a dual redundant digital multiplex system. A distributed digital system architecture has been implemented using subsystem embedded microcomputers. The data buses and the embedded microcomputers are controlled by a central executive fire control computer. This high-speed hybrid computer, which was designed specifically for the AH-64, controls the operations associated with delivery of all weapons and performs computational functions for gun and rocket fire control solutions. When the fire control computer is inoperative, control of the buses reverts to a backup bus control computer. This backup bus controller is capable of performing all essential flight avionics and navigation functions and of providing sufficient fire control to permit all weapons to be operated in a degraded mode.

Further discussion of the Apache fire control design and performance is included in Chapter 6.

1-2.5.6.3.4 Light Helicopter, Experimental (LHX)

To replace its light helicopter fleet, the Army has initiated a program to develop a family of advanced lightweight aerial vehicles. Known as the LHX project, the effort calls for development and procurement of two basic aircraft, a scout/attack vehicle known as the LHX-SCAT—now officially designated the RAH-66 Comanche armed reconnaissance helicopter—and a light utility transport designated LHX-U. Both aircraft are expected to share the same dynamic components including engines, transmissions, rotors, and electronics systems such as flight control, communications, navigation, and sensors.

The Comanche will undertake scout functions, i.e., reconnaissance, target acquisition, designation, and surveillance. The same basic vehicle will also be capable of performing attack missions against armored vehicles and other targets, escorting utility transports, and undertaking defense suppression against airborne and ground targets. The Army envisions the Comanche aircraft will replace the AH-1 Cobra series of attack helicopters and the OH-6 and OH-58 light observation helicopters and supplement the OH-58D scout force.

The Comanche will have a 1260-nautical-mile self-deployment range, a minimum dash speed of 170 knots, a 2.5-h operational endurance, and a minimum vertical climb in excess of 500 ft/min at high-altitude/hot-day standard design conditions (4000 ft and 35°C). The system includes lightweight composite airframe structures, a protected antitorque subsystem, a low-vibration, high-reliability rotor subsystem, second-generation target acquisition and night vision sensors, and advanced electronics architecture.

Comanche armament includes air-to-ground (Hellfire) and air-to-air (Stinger) missiles, 70-mm (2.75-in.) rockets, and a turret-mounted 20-mm cannon. The fire control includes a night vision pilotage system, a helmet-mounted display, an electro-optical target acquisition and designation system, aided target recognition, an improved data modem for exchange of digital data with other weapons systems, and integrated displays.

Because of budgetary constraints, the Comanche program has been reduced to development of two prototypes.

The utility model of the LHX family will have the same engines, transmissions, and other major systems as the Comanche, but it will have a wider, larger volume fuselage enabling it to transport a tactical team of four to six soldiers or up to 680 kg of cargo or equipment. LHX-U missions would include cargo and troop transportation, command and control, artillery observation, and liaison activities. The LHX-U requirements follow:

1. A high degree of maneuverability and sustained flight performance under high-altitude/hot-day conditions

2. Endurance, i.e., the length of time it can remain airborne with a specified amount of fuel, in the 2.5- to 3-h range

3. A lightweight weapons system capable of engaging and defeating armor, area targets, ground defenses, and airborne threats

4. Small size with reduced radar, infrared, acoustical, and visual signatures to minimize the probability of enemy detection

5. Reduced aircraft vulnerability to threat systems including ballistic projectiles, NBC weapons, and other anticipated threats

6. An adaptable design that can be modified to perform many different missions and counter new threats.

To achieve these mission goals and desired capabilities, the LHX will have to incorporate the latest advances in composite structures, advanced propulsion, rotor design, fiber-optic flight control systems, integrated digital avionics, and other technical areas.

1-2.5.6.4   Helicopter Air-to-Air Fire Control

In the late 1970s Army proposals to extend the performance of fire control to the air-to-air role to anticipate a similar counterthreat were disapproved as an Army infringement on the Air Force mission. By the early 1980s the Air Force position changed—a defensive air-to-air posture was now acceptable. Subsequently, both defensive and offensive operations became permissible. Accordingly, a concerted effort was initiated, driven in part by threat activity in the area, to evaluate the performance of the existing fire control and weapons for the air-to-air mission. Cost-effective modification of existing weapons and the suitability of other armament have also been examined.

The effort to improve the accuracy of the AH-1S Cobra 20-mm turreted cannon began in 1978 when improvements in onboard computational power made it possible to solve the fire control problem for airborne threats. It was thought a simple model of the air-to-air engagement geometry would be sufficient, i.e., a linear target state assumption would suffice in the most probable engagements. General Electric engineers developed improved filter algorithms for position, velocity, and acceleration and a linear prediction algorithm. They also modified the 3-barrel, 20-mm Gatling gun to provide dual rates of fire, 750 and 1500 rounds per minute. Other improvements included a ship motion sensor and a laser range finder (4 and 10 pulses per second). A flight test was conducted in October 1979, and the results indicated that constant velocity airborne targets could be successfully engaged by the attack helicopter. At the time this was a monumental accomplishment because until then the gun was assumed to be only an area weapon and therefore not capable of engaging the so-called "point targets". This test proved the gun could indeed be used to engage airborne targets.

The effort demonstrated

    1. The successful engagement of a towed target between 500 and 2000 m

    2. The feasibility of a hovering engagement at a high rate of fire

    3. The computer processing capability on AH-1S-type aircraft can satisfy air-to-air software requirements.

    4. The tracking system was able to engage crossing targets for constant velocities up to 80 knots.

    5. The tracking system performance was degraded during firing due to obscuration from weapon recoil effects.

    6. The long tracking filter settling time (about 6 s) needs to be reduced for combat situations.

Deficiencies found during the test led to "full up" air-to-air system development, i.e., a reduction of settling time and an increase in the capability to engage maneuvering targets. Teledyne Systems Company won a competitive bid to develop improved fire control equations and algorithms and a simulation model. To develop a fire control system for the US Army attack helicopter turreted weapon that would provide the capability of accurate engagements of enemy airborne threats, the critical issues that had to be addressed were

    1. Analytical representation of sensors

    2. Threat and engagement assessment

    3. Improved ballistics

    4. Effectiveness criteria

    5. Investigation of filter alternatives

    6. Gun and turret dynamics

    7. Determination of the impact of these more complicated equations on FCC resources.

By accomplishing all of the goals identified by the critical issues, Teledyne developed the ARTOAR Simulation Model. In the model, sensors were represented by transfer functions that operated by degrading the true value by a random bias and correlated noise. Sensors modeled were the sight unit (TADS for Apache and telescopic sight unit), navigation sensors (attitude and heading reference system (AHARS)), laser range finder, air data sensor, and Doppler radar. Also included in the model were threat and engagements for ground targets, helicopter flight paths, and target flight paths. Ballistics (the so-called "BRL '80 ballistics" were later modified in 1983 to include symmetrical roll properties and used for the HYDRA 70 rocket integration for Cobra.) were provided by Mr. Harold Breaux of the US Army Ballistics Research Laboratory (BRL) at Aberdeen Proving Ground, MD. These BRL equations were further modified to strip out the linear prediction algorithm. A second-order $(1/2)at^2$ prediction equation was developed and used as a separate entity. Miss distance was computed by using the EXBAL4 model of real-world ballistics and compared to the simulated flyout of the onboard ballistics. EXBAL 4 was a 4-degree-of-freedom version of the 6-DOF EXBAL 6. These models were developed by Mr. Tom Hutchings, US Army Armament Research, Development, and Engineering Center (ARDEC), and were based on the BRL TRAJ models. Miss distance was used as the effectiveness criterion but was computationally difficult, so the alternative "time to go to nearest approach" method was used. This method exhibits a parabolic function, i.e., a definite minimum value, as opposed to a miss distance calculation where minimum range is reached quickly and is very nearly indeterminate.

Two different target state filter alternatives were selected. One was the variable coefficient alpha, beta, gamma, and the other was the seven-state Kalman that was similar to the GE approach but with preprogrammed gains. Both were capable of estimating target states of position, velocity, and acceleration and thus providing sufficient data to the second-order filter in terms of the "a" value of acceleration.

One area that was inadequate in the simulation models was the representation of gun turret dynamics. The model included only first-order effects and none of the more important second-order parameters, such as gear backlash, saturation, etc. There has always been vast improvement potential in this area. Assessment of FCC resources indicated that 209 words of additional memory were required for the more

complicated fire control software, but the Cobra and Apache onboard computers would be able to accommodate this burden.

There was no further work done to improve the Cobra fleet. There was no validation flight test to ensure that these new equations, i.e., target state estimation, ballistic, and prediction algorithms, actually improved the accuracy of the Cobra or to verify the simulation. However, the work was used as a starting point for the integrated air-to-air weapons system (INTAAWS) program for the Apache. In addition, there were several analysis efforts that used the ARTOAR model which fed into the LHX (Comanche) requirements development.

Finally, with some very minor modifications the seven-state Kalman filter and second-order prediction algorithms will be installed into the Apache Longbow helicopter. It can be argued that this early work led directly to the formulation of the Comanche because the Cobra and Apache programs had shown the feasibility of air-to-air helicopter engagements.

The tactics to be used by the attack helicopter and threat aircraft are central to this investigation. These tactics are, in turn, dependent upon the fire control performance that is achievable. The projected performance of attack helicopters in the air-to-air combat mission has been studied. Such studies assume that the fire control system, armament, and threat aircraft are performing at a high level. Evaluation criteria are derived from user-stated requirements. An important objective of these studies is the determination of shortcomings in fire control coupled with an estimate of the cost to eliminate these shortcomings. Some of the more critical factors are the behavior of the targeting sensor under maneuvering conditions, the sensor data filtering, target future position prediction, accuracy of the ballistic equations, weapon control, computer speed and storage capability, and reaction times. A sensitivity error analysis provides the means to determine where the emphasis in improvement should be directed and, when coupled with cost data, indicates what the increased cost of an increment of improved effectiveness is.

Another analytical tool that has been used in air-to-air fire control studies is subsystem simulation. Engagement scenarios in the form of interacting attack helicopter and target paths are generated (or reproduced from flight-test data) and used to drive the simulation. Values of all of the fire control parameters of interest are derived from the engagement geometry and perturbed by error functions to represent sensor input to the set of equations representing fire control computer functions. These functions include filtering, prediction, and ballistic equations. The real-world ballistics as represented by the governing six-degree-of-freedom solution is used to fly the round out. The orientation of the gun or launcher is established by the response of the gun turret to computer commands or by the pilot/flight control/aircraft reaction to the steering direction presented to the pilot. In the late 1980s the 70-mm (2.75-in.) rocket with a flechette warhead, wass considered for this mission array prior to computed impact. A high-explosive round fired from a 30-mm gun has been studied. Also air-to-ground guided missiles, such as TOW or Hellfire, are being considered.

The man-portable Stinger ground-to-air guided missile, which uses an IR homing seeker, is a candidate for the attack helicopter mission. The missile is normally fired by the operator from a shoulder launcher using a boresighted ring sight for aircraft target acquisition and track. An audio tone tells the operator that the target is "locked on" within the boresighted seeker field of view and ready for fire. The sight, launcher, and seeker boresight are then offset by the operator to compensate for trajectory curvature and target velocity. Thus an initial lead is introduced into the seeker. This simplifies the proportional navigational task of the missile while it is airborne. These same functions could be implemented for helicopter delivery, but the pilot sight would be remote from the pylon-supported missile launcher. Also the pilot would steer the aircraft to put the sight and boresighted missile seeker on target for initial lock-on. Consideration is being given to modifying the missile seeker so the gimbals may be driven remotely and their orientation with respect to the airframe sensed. Remote control of seeker gimbals would simplify the pilot's steering task to achieve initial seeker lock-on. The display on the pilot's head-up sight of the sensed gimbal positions would indicate what the seeker had locked onto and therefore would reduce the number of false targets.

1-2.5.7 Common Module Fire Control

The existing trend in the development of combat platform weapon systems has been toward fire control system application uniqueness because of vehicle mission, weight, packaging volume, and cost constraints. This uniqueness has propagated into an undesirable proliferation of logistics, training, and maintenance specialization. State-of-the-art technology improvements incorporated into the basic weapon system designs to increase hit probability and improve operator interface have increased the number of system variations requiring support.

The commanders' ability to maintain a weapon system advantage during battlefield engagements is directly proportional to their ability to keep the systems operational, to correct malfunctions rapidly, and to incorporate flexibility into personnel training. This combat advantage can be achieved through reduction of weapon system variations and simplification of system operation and maintenance. One approach to accomplishing this objective is development of generic modules that can be used as building blocks to develop weapon systems. Obviously, the utopian goal of achieving 100% commonality is impossible. A 70 to 80% commonality of modules, however, would significantly reduce the integrated logistic support and training burdens.

A study to define the universal modules required for the Army fire control system application used the top-down, system-to-component approach. The implementation of the fire control functions on existing weapon systems and proposed conceptual systems to accomplish their missions was analyzed. The system specification analysis contained the requirements for direct point fire, accurate engagement range up to 3000 m, day and night operational capability, performance in all weather and battlefield-induced environments, and the ability to fire while on the move. System specifications also reflected the ability of weapon platforms to accomplish secondary objectives, such as area fire, close-in target engagements (i.e., less than 1000 m) using primary or alternate weapons, and manual engagement during loss of vehicle power or fire control damage conditions.

Refined system specifications were used to define subsystem performance. The subsystems were the result of system partitioning, which reflected the requirements of the fire control functions. Each subsystem provided a generic category that was used to perform the initial tradeoff analysis for life cycle cost, which included integrated logistic and training support.

The primary objective of developing common components for Army fire control systems can be accomplished by the additional partitioning of the subsystems into modules. This modular component level provides the weapon platform similarity required by the combat commander to maintain high readiness and efficiency. Modular design alternatives were also evaluated for their life cycle cost, simplicity of operation and maintenance, and universality in the development of future weapon systems.

1-2.6 Conclusions

The following conclusions can be drawn from the history of fire control development, particularly from the crash programs of World War II, Korea, and Vietnam and from the sustained program in the years that followed:

1. Like most technical development for weapon programs, fire control development occurs most rapidly during the times of greatest need. During the stress of wartime, i.e., when something workable must be provided quickly, normal development and test procedures are often dispensed with. Equipment so produced tends to have a life expectancy far beyond that intended originally.

2. In the tactical weapon system arena the possibility that a major new development initiative will eventually be produced and fielded remains relatively low. Since WWII, only the M60 and M1 MBTs and the AH-64 Apache attack helicopter have reached that status; systems such as Cheyenne, Vigilante, Mauler, SGT York, and ESPAWS never made it. The tendency appears to be to take the less risky and less costly option of product improvement, particularly to raise the level of fire control performance.

3. It was estimated in the 1960 edition of this handbook that the average lead time required for the

Army to develop new weapon systems and bring them to operational status was about 10 years. The hope at the time that reorganizations within the Army would result in a significant reduction in this lead time has not been realized.

4. The ever-increasing capability of digital processing has permitted full application of the latest modeling and simulation procedures to fire control system synthesis and analysis. These modeling and simulation results, however, do not always correlate with the data obtained from realistic field tests. A satisfactory explanation of any differences is required to assure valid design and product performance.

1-3 NONTRADITIONAL MUNITIONS FIRE CONTROL

As stated previously, "guided missiles" are not addressed in this handbook. "Guided missile" refers generally to a missile for which launch and flight are established and maintained by its own propulsion system and for which the trajectory can be altered in flight. Guided projectiles are missiles that derive their energy for flight from initial thrust, e.g., a gun. Guided missiles and projectiles are further defined as those for which guidance data are applied during flight. However, there are applications in which the fire control system blends so well with the guidance system that distinctions are difficult. (This blend is also found in some guidance and fuzing systems.) There are additional instances in which fire control is required to enable the guidance to be effective. Three such applications are described in the subparagraphs that follow.

1-3.1 GUIDED PROJECTILES

Guided projectiles are those fired from a gun and provided with onboard means for adjusting their trajectory. A typical example is the 155-mm cannon-launched guided projectile, M712, called Copperhead. This projectile is in service with the US Army and US Marine Corps. It is fired from a conventional 155-mm gun tube.

The target is illuminated by a laser designator, which may be ground- or air-based. A seeker at the nose of the projectile locks on to the laser illumination reflected from the target, and corrections are calculated onboard to adjust the trajectory of the projectile so it will impact the illuminated area. A correction is applied aerodynamically by adjusting the fins. Fig. 1-14 is a sketch of a Copperhead projectile and shows the guidance, warhead, and control sections.

The principal advantage of Copperhead is it provides conventional artillery with a first-round point target hit capability. Because the time of flight of the gun-fired projectile is less than that of a comparable rocket, the observer and designator are exposed to enemy observation and fire for a shorter time. Furthermore, less correction for target movement is required since the projectile reaches the target more quickly.

The primary disadvantage of Copperhead is it does require precise designation of the target until impact and thus exposes the designator team to enemy fire throughout the period. Copperhead II should overcome this disadvantage.

Copperhead II is currently a conceptual weapon, that is to use either an electro-optical or millimeter wave sensor for target location. The projectile would therefore be self-sufficient and eliminate the need for the designator, but it would retain all of its advantages.

In any such weapon there is a limited angle within which its sensor, of whatever type, can "see". The function of the fire control system therefore is to put the projectile within that window, in azimuth and elevation, when the sensing system is activated.
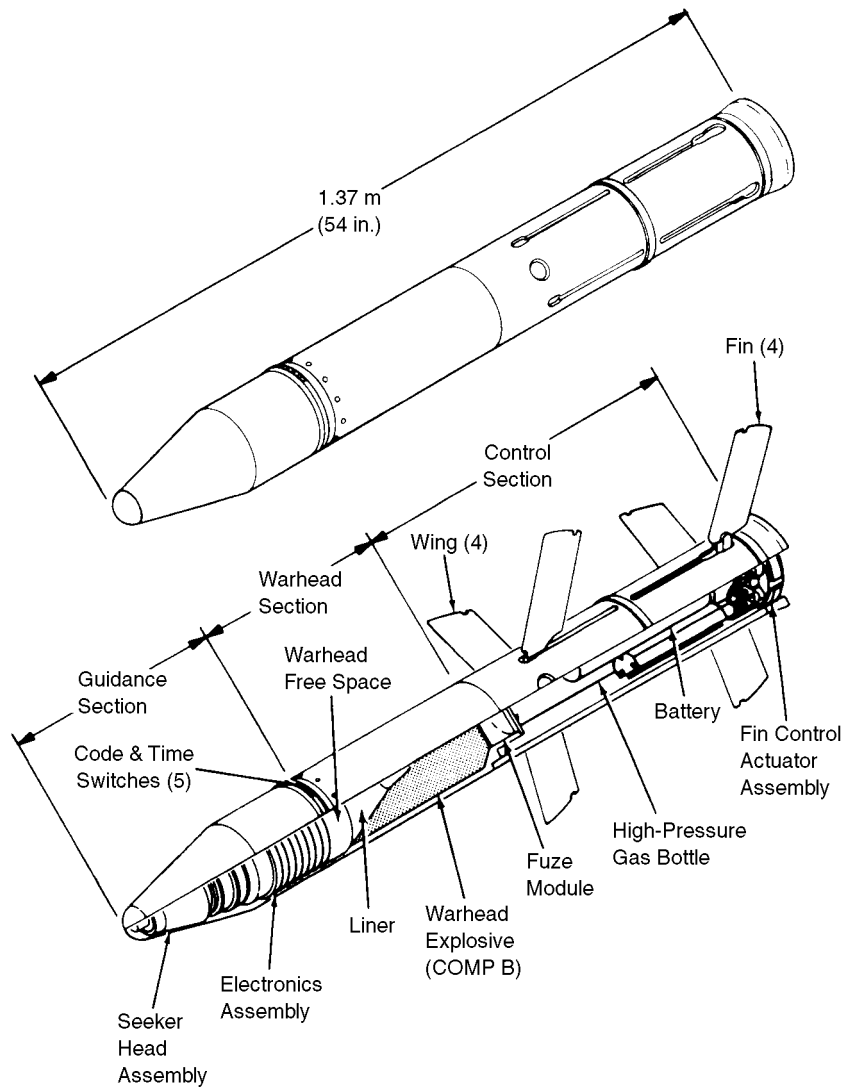
Figure 1-14. Projectile 155-mm, Cannon-Launched, Guided, M712 Copperhead (Ref. 21)

1-3.2 MANEUVERING PROJECTILES

Maneuvering projectiles are defined here as those fired from a gun and responsive to commands from a remote sensing system to change trajectory. Guided projectiles have an onboard sensing system, but maneuvering projectiles do not. As of this writing, these projectiles are developmental.

An air defense artillery fire control radar normally tracks the target prior to weapon firing to enable the system to develop the prediction angle. For a maneuvering projectile the radar would continue to track the target aircraft after projectile firing and would also track the projectile. If the target aircraft were to make a sudden maneuver after the projectile was fired, the prediction angle, even if initially perfect, would become incorrect. Based on the tracking of target and projectile, however, an updated prediction could be calculated on the ground, and commands could be transmitted to the projectile over a suitable communication link. If the projectile is equipped with a means to change its trajectory by executing the commands, it will correct its course to intercept the target aircraft. A similar concept has been studied for application to tanks.

1-3.3 PRECISION-GUIDED WEAPONS

Precision-guided weapons (PGW) consist of submunitions, which are carried to a target area by another projectile, and released. Each PGW contains its own autonomous target search and detection sensor pack-

age. An example is the search-and-destroy armor (SADARM), which is scheduled to be fielded in 155-mm and MLRS versions..

The projectile carrying the SADARM weapons is fired from an artillery gun or by a rocket. The concept relies on intelligence regarding the location of a concentration of targets. The projectile flies to the area in which the targets are located, and an expulsion charge separates the submunitions from the projectile or rocket. Upon separation each PGM deploys a parachute, and each PGW has a target search and detection sensor in its nose section. As the PGWs descend, they search the ground for targets. Upon detecting a target and by using the dual-mode millimeter wave and infrared sensor, the PGW fires an explosively formed penetrator through the top of the target. Since many targets, especially armored targets, are most vulnerable on their top surface, these weapons can be quite effective.

As can be deduced from this discussion, the artillery fire control system must be suitable for the delivery of the projectile to a target area. The PGWs then convert this accuracy to a point target attack. In addition, those elements of the fire control system employed to calculate the detonation parameters and set the fuze must be capable of the accuracy required to ensure separation of the submunitions at the proper location and altitude above the target.

REFERENCES

1. W. Wrigley and J. Hovorka, *Fire Control Principles*, McGraw-Hill Book Company, Inc., New York, NY, 1959.

2. JCS Pub 1-02, *Department of Defense Dictionary of Military and Associated Terms*, 1 December 1989.

3. *Ordnance Technical Terminology*, Special Text ST 9-152, US Army Ordnance School, Aberdeen Proving Ground, MD, June 1962.

4. TM 9-2300-216-10, *Operator's Manual for Gun, Self-Propelled 175-mm, M107, Howitzer, Heavy, Self-Propelled, 8-in., M110, and Howitzer, Heavy, Self-Propelled, 8-in., M110A1*, Department of the Army, 22 December 1978.

5. T. Collison, *The Superfortress is Born*, Duell, Sloan, & Pearce, New York, NY, 1945, pp. 82-9.

6. FM 6-40, *Field Artillery Cannon Gunnery*, Department of the Army, 6 November 1981.

7. J. E. Benfield, *Report on AAFCS T33 and M33 Testing Program*, Report No. DPS/FA1/58/57/1, Electronic Control and Guidance Division, Aberdeen Proving Ground, MD, August 1959.

8. T. E. Burke and Gearge Pettit, *Report on Radar Comparison Tests*, Report No. DPS/TRI-1051/1, Electronic Control and Guidance Division, Aberdeen Proving Ground, MD, October 1959.

9. J. Campbell and W. Roberts, *Effects of Target Speed and Direction on the Accuracy of the AAFCS M38 (Skysweeper Computer)*, Report No. DPS/TRI-1020-18, Electronic Control and Guidance Division, Aberdeen Proving Ground, MD, June 1959.

10. *Improvement of Standard 40-mm Antiaircraft Material, Development of Antiaircraft Fire Control System T50*, Report No. R2314, Research and Development Group, Frankford Arsenal, Philadelphia, PA, June 1959.

11. *Antiaircraft Fire Control System T50*, Report No. FCEE-321, Notes on Developmental-Type Material, Frankford Arsenal, Philadelphia, PA, February 1959.

12. Gearge Pettit, *Investigation of Antiaircraft Techniques (Raduster)*, Report No. DPS APG Misc 301, Electronic Control and Guidance Division, Aberdeen Proving Ground, MD, August 1959.

13. *Final Report for the Vigilante Antiaircraft Weapon System*(U), Report No. E1-228-8221, Sperry Utah Company, July 21, 1961, (THIS DOCUMENT IS CLASSIFIED CONFIDENTIAL).

14. *Evaluation of the Vigilante Forward Area Air Defense System*(U), Report of Evaluation, Project No. GM-162, 20 September 1962, (THIS DOCUMENT IS CLASSIFIED CONFIDENTIAL).

15. *GLAAD-Gun Low-Altitude Air Defense Fire Control Test Bed*, **Ford Aerospace & Communications Corporation, Newport Beach, CA, March 1976.**

16. *The PIVADS Advantage*, **Lockheed Electronics Company, Plainfield, NJ, 1985.**

17. *DIVAD System Overview Computer Software/Firmware*, **Ford Aerospace, Newport Beach, CA, 1 October 1982.**

18. **AMCP 706-127, Engineering Design Handbook,** *Infrared Military Systems, Part One*, **April 1971.**

19. **AMCP 706-128, Engineering Design Handbook,** *Infrared Military Systems, Part Two*, **May 1974.**

20. **TM 9-1090-202-20P,** *Organizational Maintenance Repair Parts and Special Tools List, Armament Subsystem, Helicopter, 7.62-mm Machine Gun–2.75-in. Rocket Launcher: M21*, **Department of the Army, 14 August 1970.**

21. **TM 43-0001-28,** *Army Ammunition Data Sheets for Artillery Ammunition: Guns, Howitzers, Mortars, Recoilless Rifles, Grenade Launchers, and Artillery Fuzes*, **Department of the Army, 30 August 1991.**

BIBLIOGRAPHY

Aircraft Weaponization, Subsystem Photographs and Description, **US Army Aviation Command, St. Louis, MO, 1972.**

AN/VVG-2 Laser Range Finder for the US Army M60A-1 Main Battle Tank, **Hughes Aircraft Company, Culver City, CA, September 1974.**

J. G. Tappert, "An Empirical Approach to the AA Prediction Problem", *Second Antiaircraft Fire Control Working Conference*(U), **BRL Report No. 932, March 1955, p. 62, US Army Ballistics Research Laboratory, Aberdeen Proving Ground, MD, (THIS DOCUMENT IS CLASSIFIED SECRET.).**

R. E. Bassler, Jr., and J. R. Mathias, *Investigation of a Possible Method of Stabilizing a 90-mm Tank Gun*(U), **Instrumentation Laboratory Report No. T-28, Massachusetts Institute of Technology, Cambridge, MA, August 1952, (THIS DOCUMENT IS CLASSIFIED CONFIDENTIAL.).**

W. B. Boyd and B. Rowland, *US Navy Bureau of Ordnance in World War II*, **Bureau of Ordnance, Department of the Navy, Washington, DC, 1953.**

Coast Artillery, **Military Service Publishing Company, Harrisburg, PA, 1942.**

Elements of Armament Engineering, **Department of Ordnance, US Military Academy, West Point, NY, 1954.**

Green, Thomson, and Roots, *US Army in World War II, The Ordnance Department: Planning Munitions for War*, **Office of the Chief of Military History, Department of the Army, Washington, DC, 1955.**

C. R. Hanna and L. B. Lynn, "Gyroscopic Stabilizer for Tank Guns", Electrical Engineer 63, (October 1944).

T. J. Hayes, *Elements of Ordnance*, **John Wiley & Sons, Inc., New York, NY, 1938.**

Integrated Fire Control System for Tank, Light, T-41, **Vol. 1, Engineering Department, Vickers, Inc., Division of the Sperry Corporation, Great Neck, NY, 1 May 1951.**

A. S. Locke et al, *Guidance*, **G. Merrill, Ed., D. Van Nostrand Company, Inc., Princeton, NJ, 1955.**

NAVPERS 16116-B, *Naval Ordnance and Gunnery*, **prepared by the Department of Ordnance and Gunnery, US Naval Academy, Annapolis, MD; Published by the Bureau of Naval Personnel, Department of the Navy, Washington, DC, September 1950.**

NAVWEPS OP 3000, *Weapons Systems Fundamentals, Basic Weapons Systems Components*, **Vol. 1, Bureau of Naval Weapons, Department of the Navy, Washington, DC, 1960.**

OP 1140, *Basic Fire Control Mechanisms*, **Bureau of Ordnance, Navy Department, Washington, DC, September 1944.**

J. Pimlott, *B-29 Superfortress*, **Prentice-Hall, Inc., Englewood Cliffs, NJ, 1983.**

Requirements of a Tank Stabilization System, **Report of D.I.C., Servomechanism Laboratory, Massachusetts Institute of Technology, Cambridge, MA, 6 March 1945.**

W. Sperling, *Optical Instrumentation for US Armored Vehicles*, **Unpublished paper dated 12 June 1962 for presentation to a NATO conference.**

Tank, 75-mm Gun, T41 Integrated Fire Control Systems and Comparative Test of Tank Gun Stabilizers, **Office of the Chief of Ordnance, Department of the Army, Washington, DC, 29 January 1952, (THIS DOCU- MENT IS CLASSIFIED CONFIDENTIAL.).**

TM **9-1240-398-34**, *Sight, Tank Thermal AN/VSG-2*, **Department of the Army, Washington, DC, November 1987.**

Technical Development Plan for the Common Module Fire Control Programs, **US Army Armaments Research and Development Command, Dover, NJ, May 1982.**

XM-21 Tank Fire Control Ballistic Computer System, **Hughes Aircraft Company, Culver City, CA, December 1974.**

CHAPTER 2
THEORETICAL ASPECTS OF THE FIRE CONTROL PROBLEM AND ITS SOLUTION

Three main subjects are presented in this chapter: the fire control problem, the frames of reference used in fire control, and the flight of projectiles. Four coordinate reference frames are explained, i.e., the inertial, earth, air mass, and stabilized weapon station. The reasons for choosing specific reference frames for use in different elements of the solution are delineated. All of the factors that influence the flight of projectiles are defined and are presented in quantitative form.

2-0   LIST OF SYMBOLS

A_f = **firing azimuth, measured clockwise from true north, rad**

A_o = **target azimuth, measured clockwise from true north, rad**

$\dot{A}_o$ = **time rate of change of A_o, or azimuth angular rate of target, rad/s**

a = **effective lever arm between projectile center of gravity and center of pressure, m**

C = **aerodynamic coefficient, dimensionless**

C_A = **approximate kinetic azimuth lead correction, rad**

$\mathbf{D}$ = **drag, N**

E_o = **target elevation angle with respect to horizontal, rad**

$\dot{E}_o$ = **time rate of change of E_o, rad/s**

$\mathbf{F}_{ar}$ = **resultant aerodynamic force due to air resistance, N**

$\mathbf{g}$ = **acceleration due to gravity (9.80665), m/s^2**

h_o = **target height above the horizontal xy-plane, m**

$\dot{h}_o$ = **time rate of change of h_o, m/s**

h_p = **predicted target height above the xy-plane, m**

K = **ballistic coefficient, dimensionless**

K_{Di} = **coefficient of drag, dimensionless (i = 1, 2, 8, T108)**

$\mathbf{L}$ = **lift, N**

$\mathbf{M}$ = **applied torque vector, N·m**

$\mathbf{P}$ = **vector force of air pressure, N**

QE = **quadrant elevation angle, rad**

R = **ogival radius, cal**

$\mathbf{R}_o$ = **present slant range vector from weapon to target, m**

R_o = **target slant range, or magnitude of $\mathbf{R}_o$, m**

R_1, R_2, R_3 = **slant ranges from weapon to Targets 1, 2, and 3, m**

$\mathbf{R}_{F(AM)}$ = **future weapon-to-target slant range vector (air-mass-referenced), m**

$\mathbf{R}_{F(E)}$ = **future weapon-to-target slant range vector (earth-referenced), m**

$\mathbf{R}_{F(WS)}$ = **future weapon-to-target slant range vector (weapon-station-referenced), m**

r_o = **projection of slant range R_o to present target position T_o onto horizontal plane, m**

r_p = **projection of slant range to future target position T_{P_2} onto horizontal plane, m**

$\mathbf{S}$ = **spinning projectile angular momentum vector, kg·m^2/s**

s = **location of trajectory summit, dimensionless**

T_o = **present target position, dimensionless**

T_p = predicted future target position, dimensionless

t = time, s

t_o = projectile time of flight to present target position, s

t_p = projectile time of flight to predicted future target position, s

$\mathbf{V}_o$ = muzzle velocity vector, m/s

x = range for sight setting, m

x_o, y_o, z_o = present target coordinates, m

$\dot{x}_o, \dot{y}_o$ = time rate of change of x_o and y_o, m/s

x_I, y_I, z_I = axes of geocentric inertial reference frame, m

x_{am}, y_{am}, z_{am} = axes of air mass reference frame, m

$x_{E(i)}, y_{E(i)}, z_{E(i)}$ = axes of various earth reference frames, m:

$i = geo$: geocentric earth

$i = stab$: stabilized weapon station

$i = unstab$: unstabilized weapon station

$i = veh$: vehicle-centered

x_p, y_p, z_p = predicted target position coordinates, m

$x_\Omega, y_\Omega, z_\Omega$ = coordinates of Ω (point of impact or burst), m

$x(\mathbf{E}), y(\mathbf{N})$ = east and north axes, respectively, m

α = quadrant angle of departure, rad

β = angle of fall, rad

δ = angle of yaw (instantaneous angle between projectile line of motion and centerline), rad

ε = angle of sight, direct fire (target sighted), rad

= angle of site, indirect fire (target sited by position), rad

ϕ = angle of orientation, rad

ψ = superelevation angle, mil

Ω = point of projectile impact or burst (if antiaircraft fire), dimensionless

ω = precession angular velocity vector, rad/s

2-1 INTRODUCTION

The problem of control over weapon fire and its solution as discussed in the Fire Control Series does not apply to those projectiles known as "guided missiles". Instead the term projectile—which includes bullets, shells, and rockets—is used here in a more limited sense. For information on fire control as it applies to guided missiles, refer to the Ballistic Missile Series of the Engineering Design Handbooks, AMCP 706-281(SRD), -283, -284, and -286.

Par. 2-2 states the fire control problem and then follows the statement with a summary of generalized fire control theory.

Par. 2-3 discusses the solution of the fire control problem in general terms in a manner that parallels par. 2-2. The solution of the fire control problem is broken down into three distinct phases, and each phase is treated separately.

A broad discussion of the functional elements used in the solution of the fire control problem and examples of how such elements are used in actual systems is reserved for Chapter 3.

2-2 THE FIRE CONTROL PROBLEM

2-2.1 STATEMENT OF THE FIRE CONTROL PROBLEM

The general fire control problem may be stated as follows: "How can a projectile be fired from a weapon (that may be in motion) at a target (that may also be in motion) in such a way as to enable the projectile

to hit the target?". Implicit in this problem statement is the fact that the effects of certain phenomena, if they are encountered, will produce errors in weapon fire. These phenomena, which are common to all types of weapons, can sometimes be reduced to correctable terms when defined by a suitable analytical approach.

It is obvious that the path of the projectile must be made to intersect the path of the target at some point in time so that a hit is obtained. (If the target is stationary, the target path reduces to a point, and the fire control problem is considerably simplified.) Inasmuch as there is usually a finite period of time during which the required intersection of paths can be obtained, there is no single solution but rather a different solution for each moment in real time. Thus an implicit part of many fire control problems is the determination of when fire can profitably be opened and when it should be stopped and how to make the most of the opportunity for fire.

2-2.2 GENERALIZED FIRE CONTROL THEORY

2-2.2.1 Basic Concepts

Analysis of the overall problem of controlled weapon fire brings out an important concept: *There is basically only one fire control problem.* All fire control problems resolve into variations of a single fundamental situation, i.e., the launching of a projectile from a weapon to hit a defined target.

To solve the fire control problem, the element of probability must be taken into account. For example, based upon observations of present target motion, the future target position at the time of hit must be predicted if the effects associated with the phenomenon of relative target motion are to be adequately addressed. In addition, the concept of prediction is associated with the in-flight characteristics of a projectile during its time of flight (TOF). During the projectile TOF, the projectile is entirely under the influence of natural phenomena, e.g., gravity drop and drift, that lie beyond the control of operating personnel. From the time the projectile is fired, its trajectory is irrevocably dependent on gravity, the environment, and the ballistics of the projectile. Thus, because the exact nature of these quantities and their interplay cannot be exactly predicted, the element of probability must be considered in this connection also.

To compensate for the effects of the various phenomena that affect the fire control problem, the use of certain corrective measures is necessary. Determination of the required corrective measures by fire control equipment is made possible by the application of suitable analytical approaches. These approaches, which are primarily algebraic in nature, may be expressed in terms of various types of models and are dealt with in Chapter 4, "Design Philosophy".

2-2.2.2 The Geometrical Approach

To understand the true nature of the fire control problem, however, it has been found to be more effective to treat generalized fire control theory in geometrical terms rather than in algebraic terms. This approach can be taken because the basic fire control problem is a kinematic and dynamic problem, i.e., one involving the relative motion between points in space (weapon, projectile, and target) and the forces acting on the projectile. It therefore lends itself to expression in terms of the pertinent kinematics (velocities) and dynamics (forces) rather than to a purely numerical treatment. The algebraic approach must be applied, of course, in the actual solution of any particular fire control problem.

The geometry involved is not a matter of triangulation but one of vectors related by the laws of physics. Vector diagrams and vector operations may be used extensively, therefore, to relate the physical parameters of the fire control problem. For a complete, unified treatment of the basic physics and geometry applicable to any fire control problem, see Appendix A and Ref. 1.

2-2.2.3 Common Geometrical Factors

Three concepts that remain constant regardless of the reference coordinate frame selected for expression of the fire control problem are as shown in Fig. 2-1:

    1. *Line of Sight* (LOS)—the straight line between the weapon and the target. It should be noted that the LOS does not necessarily represent a line of visibility between weapon and target. When such visibility is present, direct fire control applies; otherwise, a requirement for indirect fire control exists. (See subpars. 1-1.3.1 and 1-1.3.2 for a discussion of direct and indirect fire.) In indirect fire control the
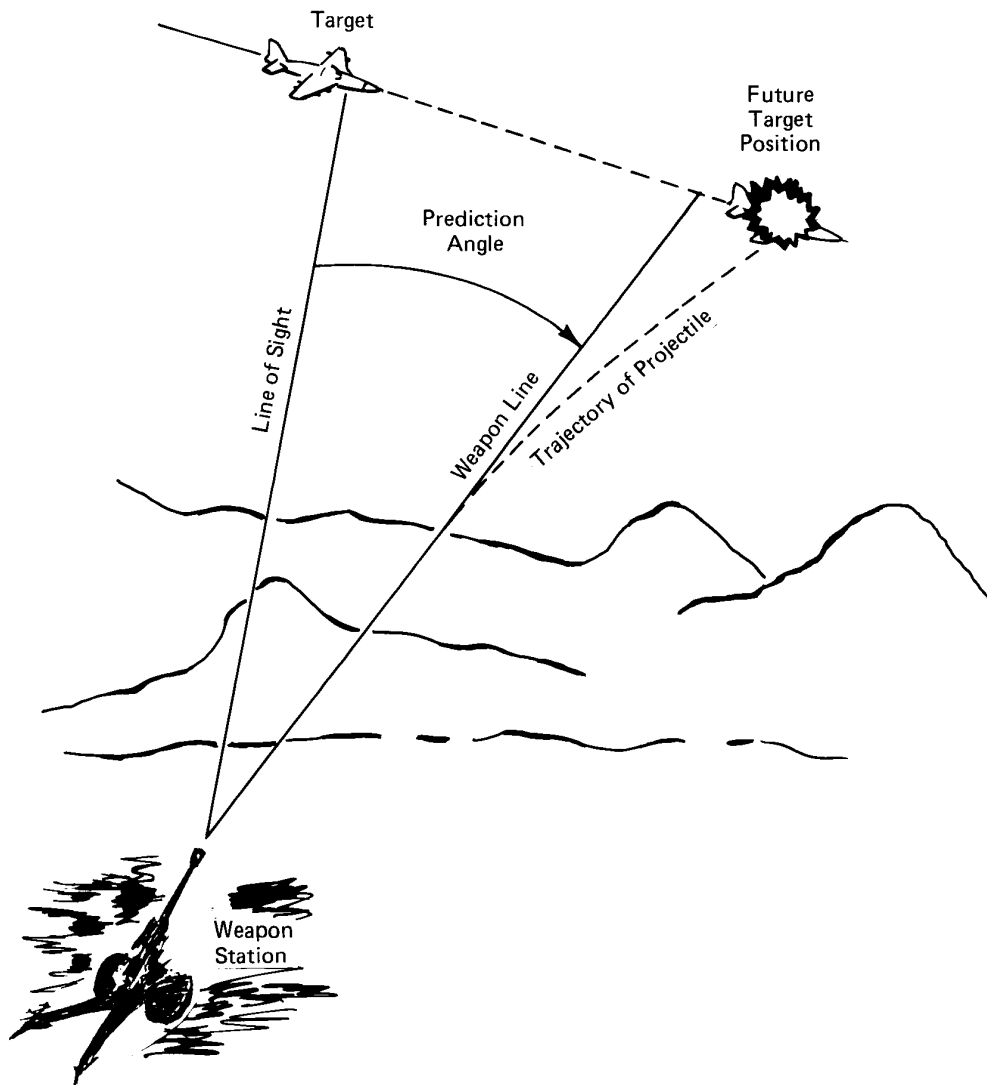
Figure 2-1. Fundamental Geometry of a Typical Fire Control Problem

straight line between the origin of the trajectory and the target is referred to as the "line of site".

    2. *Weapon Line*—the prolongation of the weapon axis. It is a straight line along the direction in which the projectile should be fired to hit the target.

    3. *Prediction Angle*—the total offset angle between the LOS and the weapon line. As used in the Fire Control Series, the term is a general designation that for moving targets corresponds to "lead angle" plus any supplementary corrections for gravity drop and drift. As mechanized in the solution of the fire control problem, the prediction angle is equal to the combination of the angle of elevation and the angle of azimuth.

2-2.3 COORDINATE FRAMES FOR FIRE CONTROL

    As has been noted, the fire control problem is inherently kinematic and dynamic by nature. The solution is, therefore, readily expressible in geometric terms by means of vectors related by the laws of physics.

    Certain vectors, e.g., velocity, require a coordinate reference frame so they may be properly specified. For instance, although airspeed and ground speed both may be considered to be vector velocities, they differ as vectors simply because the frame of reference in each case is different; airspeed must be associated with an air-mass reference frame and ground speed must similarly be associated with a ground reference frame. Unless some reference frame is specified, the concept of velocity can have no meaning.

Among the general cases of fire control, the weapon as well as the target may be in motion, e.g., a moving tank firing at another tank in motion; therefore, the specification of vectors may also be made with respect to moving coordinates.

In general, there are two broad classes of coordinate reference frames:

    1. One class is used to state the fire control problem without reference to actual fire control equipment.

    2. The other class is used to in solve the fire control problem and, accordingly, pertains to reference frames that are fixed in relation to the fire control equipment itself.

A variety of reference frames has been used in connection with fire control. The paragraphs that follow describe the more important reference frames and classify them according to the aforementioned scheme.

2-2.3.1   Primary Coordinate Frames Used to State the Fire Control Problem

There are four primary coordinate reference frames in which the fire control problem can be defined. The first is an inertial reference frame, which usually is referred to simply as "inertial space". This is the framework in which the laws of physics are expressible in their simplest form. An inertial reference frame generally is considered to be unaccelerated, i.e., of constant velocity and nonrotating, with respect to the so-called "fixed stars". For convenience, it is generally taken with its center at the center of the earth. This inertial frame, referred to as a geocentric inertial reference frame (shown in Fig. 2-2), is taken as a reference only for those fire control problems in which the TOF of the projectile is so long that the effects of the diurnal rotation of the earth cannot be ignored, for example, long-range weapon fire.
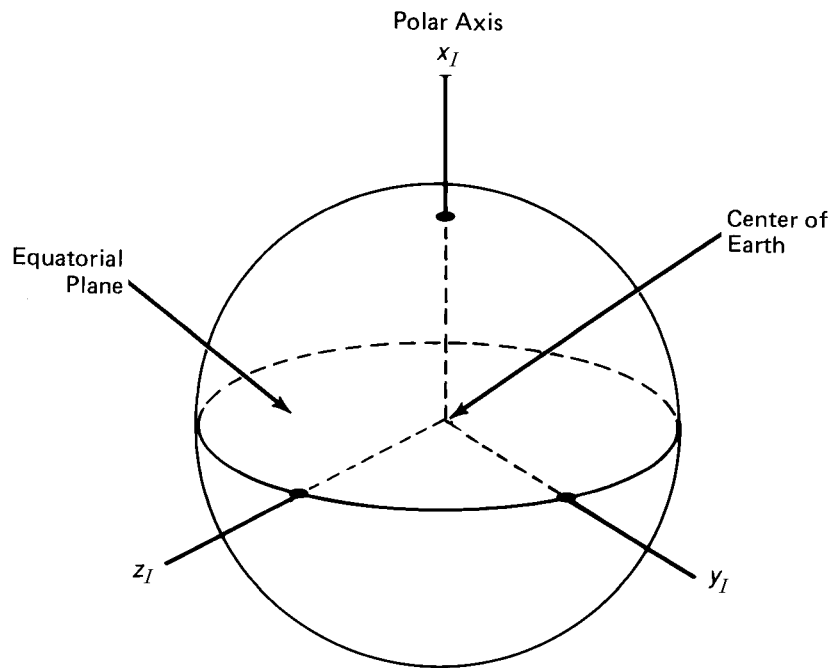
Figure 2-2. Geocentric Inertial (Nonrotating) Reference Frame (Ref. 1)

A second useful reference system is an earth coordinate system, which may be considered fixed with respect to the earth but not necessarily centered at the center of the earth. If the frame of reference has its origin at the center of the earth and rotates with the earth as in Fig. 2-3(A), it is referred to as a geocentric earth reference frame. If the frame of reference is centered at some convenient point on or near the surface of the earth, shown in Fig. 2-3(B), it is referred to as a vehicle-centered earth reference frame. In general, the earth reference frame is extremely useful for those fire control problems in which the weapon is either stationary or is moving slowly at ground level. This reference frame is therefore applicable to most Army fire control problems.

(A) Geocentric Earth Reference Frame   (B) Vehicle-Centered Earth Reference Frame
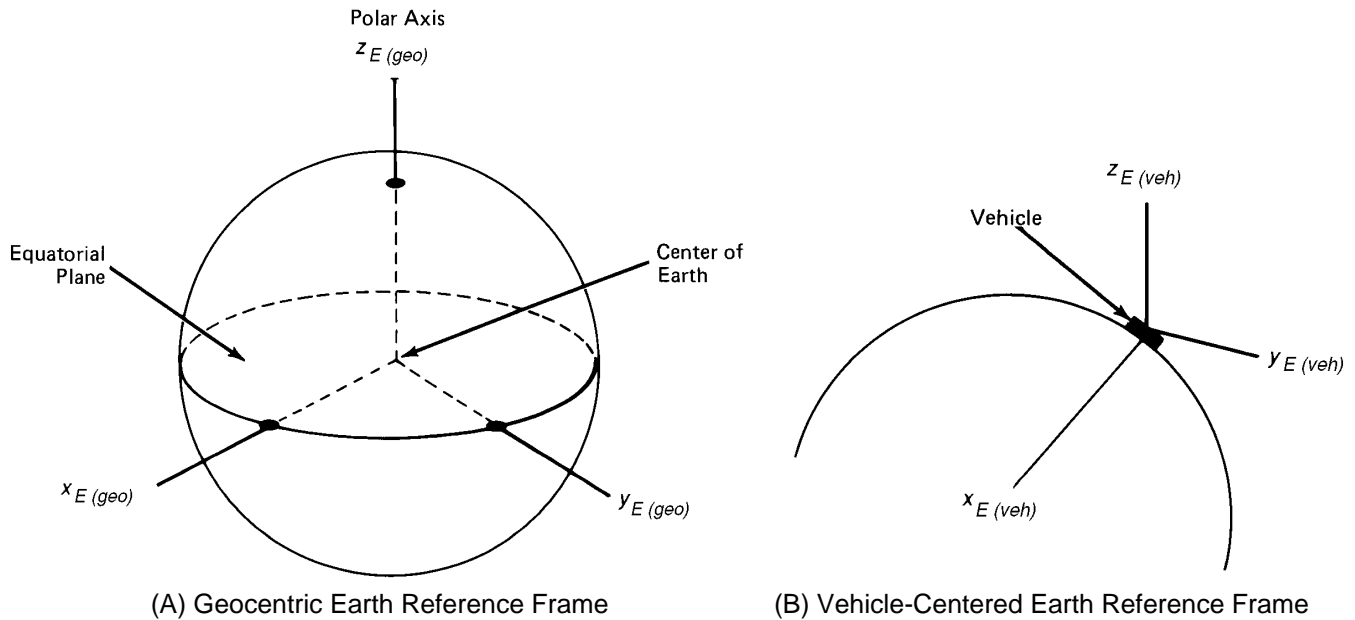
Figure 2-3 Geocentric and Vehicle-Centered Earth (Rotating) Reference Frames (Ref. 1)
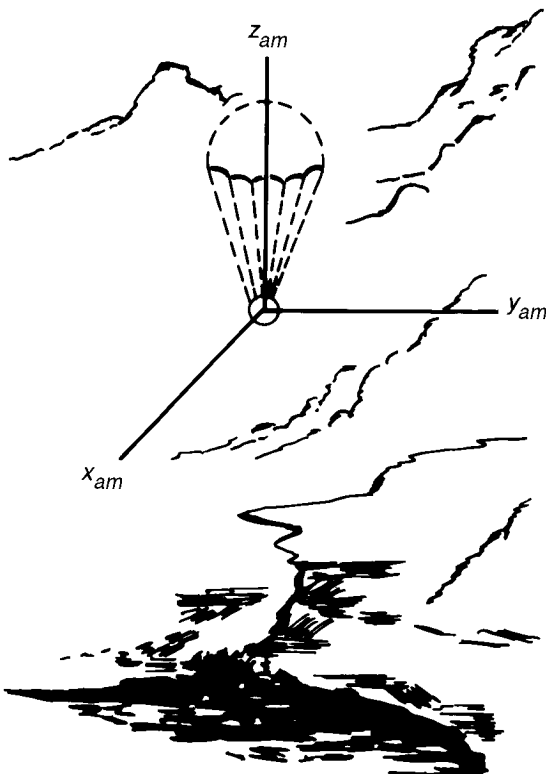
Figure 2-4. Air-Mass Reference Frame (Ref. 1)

A third useful reference frame may be described as an air-mass coordinate system, in which the frame is considered fixed in the air mass. The air-mass reference frame (shown in Fig. 2-4) may be visualized as a frame fixed in a free balloon. This frame is particularly useful for problems associated with airborne fire control, e.g., a helicopter fire control system. In this type of fire control problem the times of flight are generally short; hence the air mass is considered to be inertial. In the air-mass reference frame the ballistics of a moving projectile reduce to their simplest analytic form.

The fourth useful frame of reference is the stabilized weapon station coordinate system (shown in Fig. 2-5). This frame of reference has its origin centered in the weapon station and translates with the vehicle that carries the weapon. The frame is considered, however, to be free of any of the rotational motion of the weapon-carrying vehicle, i.e., motion about the reference coordinate axes in the roll, pitch, and yaw modes. This inertial reference frame is generally useful when the linear motion of the vehicle is readily distinguishable from the roll, pitch, and yaw of the vehicle. Thus the stabilized weapon station coordinate system is useful for a tank weapon system designed to fire while the tank is in motion.

$$
\left.\begin{array}{l} x_{(stab)} \\ y_{(stab)} \\ z_{(stab)} \end{array}\right\} = \text{x-,y-,z-Axes of the Stabilized Weapon Station Coordinate System}
$$

$$
\left.\begin{array}{l} x_{(unstab)} \\ y_{(unstab)} \\ z_{(unstab)} \end{array}\right\} = \text{Set of x-,y-,z-Axes Fixed to Weapon Station and Hence Unstabilized}
$$
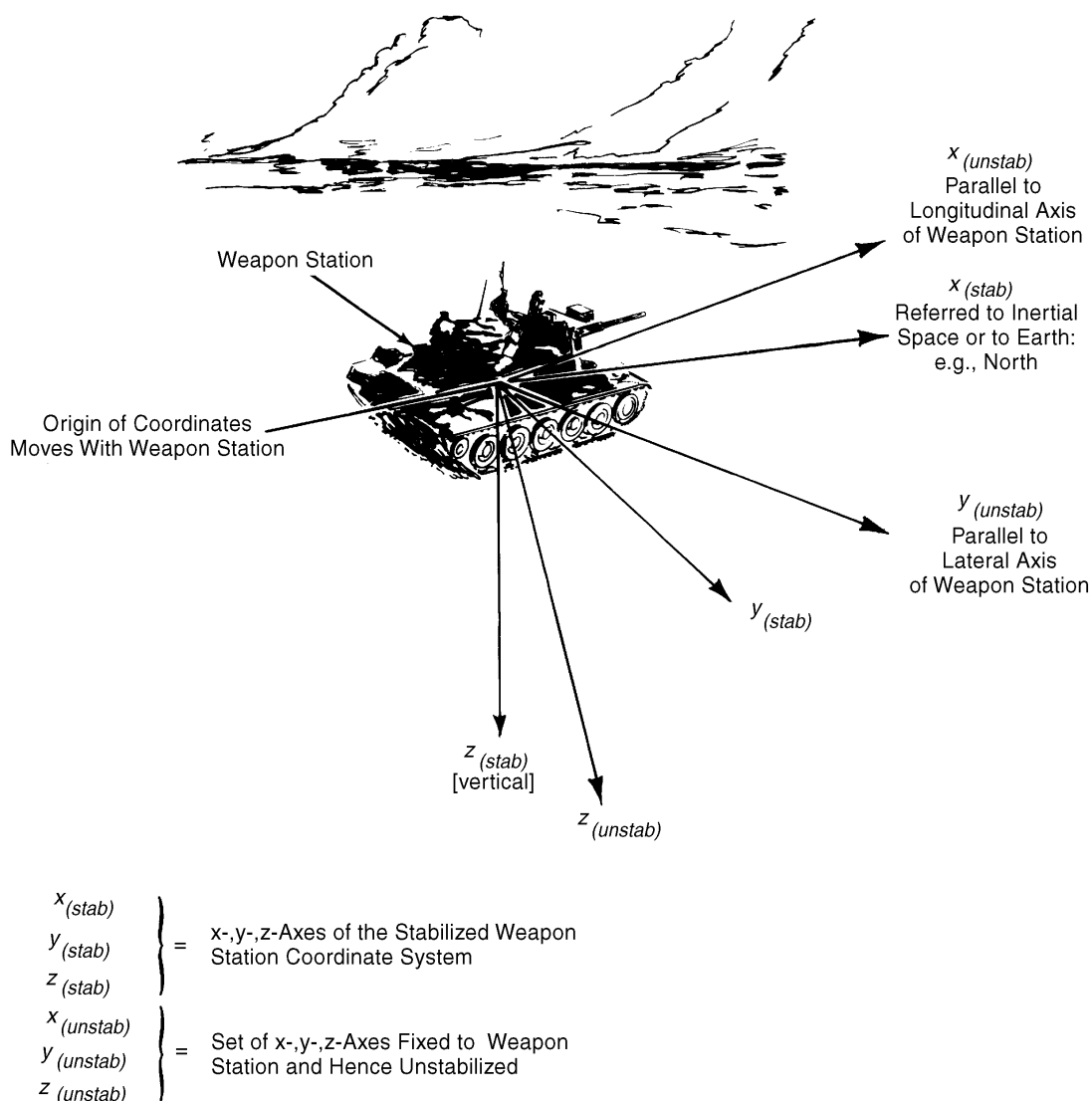
Figure 2-5. Stabilized Weapon Station Coordinate System (Ref. 1)

2-2.3.2 Coordinate Frames of Use in Data Handling and Computing

As indicated in subpar. 2-2.2.3, the basic parameters of the fire control problem are the LOS, the weapon line, and the prediction angle. In the mechanization of the solution to the fire control problem, actual indications of the LOS are provided by some physical tracking mechanism. This indicated LOS usually is referred to as the tracking line. The weapon line of course is coincident with the axis of the weapon tube. Accordingly, both the tracking line and the weapon line represent driven lines firmly fixed with respect to physical equipment in any particular weapon system. Each of these lines must intrinsically have reference coordinate frames associated with them, i.e., there must be a reference frame for the data-gathering function of the acquisition and tracking portions of the fire control system and a reference frame for the data utilization function of the weapon-pointing system. These two frames may or may not be identical. The computed prediction angle must also be generated in a reference coordinate frame. For the sake of distinction, this frame is sometimes referred to as the computation reference frame. This computing frame largely dictates the choice of the other coordinate frames used to carry out the solution of a given fire control problem.

Because the computation reference frame is the frame in which the fire control problem is actually solved, it is necessary in the design of a fire control system that this frame be selected in advance even though—because the selection is sometimes obvious—it is not always explicitly stated by the system design

agency. It is also obvious that the computation reference frame selected should be one that is naturally suited to the fire control problem at hand rather than one into which the fire control solution is forced. For example, two suitable types of earth reference frames and their applications to practical antiaircraft fire control problems are discussed in subpar. 2-3.3. The applications of these same reference frames, plus another alternate reference frame, to the data-gathering function associated with sighting and ranging are discussed in par. 2-3.2.1.

Computation reference frames can be classified into either of two basic types:

1. A reference frame in which both the tracking line and the weapon line may be rotating with respect to the coordinate axes of the frame. Generally, this type of frame is fully stabilized geometrically with respect to the earth. The instantaneous orientations of the tracking line and the weapon line are then specified by numerical angular measurements relative to the coordinate axes of the frame.

2. A reference frame in which one of the three coordinate axes is chosen to be coincident with either the tracking line or weapon line. The line that is not aligned with one of the coordinate axes is then measured relative to the other line.

2-2.3.3 Effect of the Reference Coordinate Frame on the Prediction Angle

In the previous discussion of the coordinate reference systems used in the solution of fire control problems, it was noted that from a geometrical approach certain vectors require a frame of reference in order to be properly specified. Because error-producing effects and their assignable corrective measures, e.g., target motion and the associated kinematic lead correction, are reducible to vectors, they must be considered in relation to a specified, albeit arbitrary, reference coordinate frame. As shown by Fig. 2-6, kine-

*The projectile line is the direction of the initial velocity of the projectile.
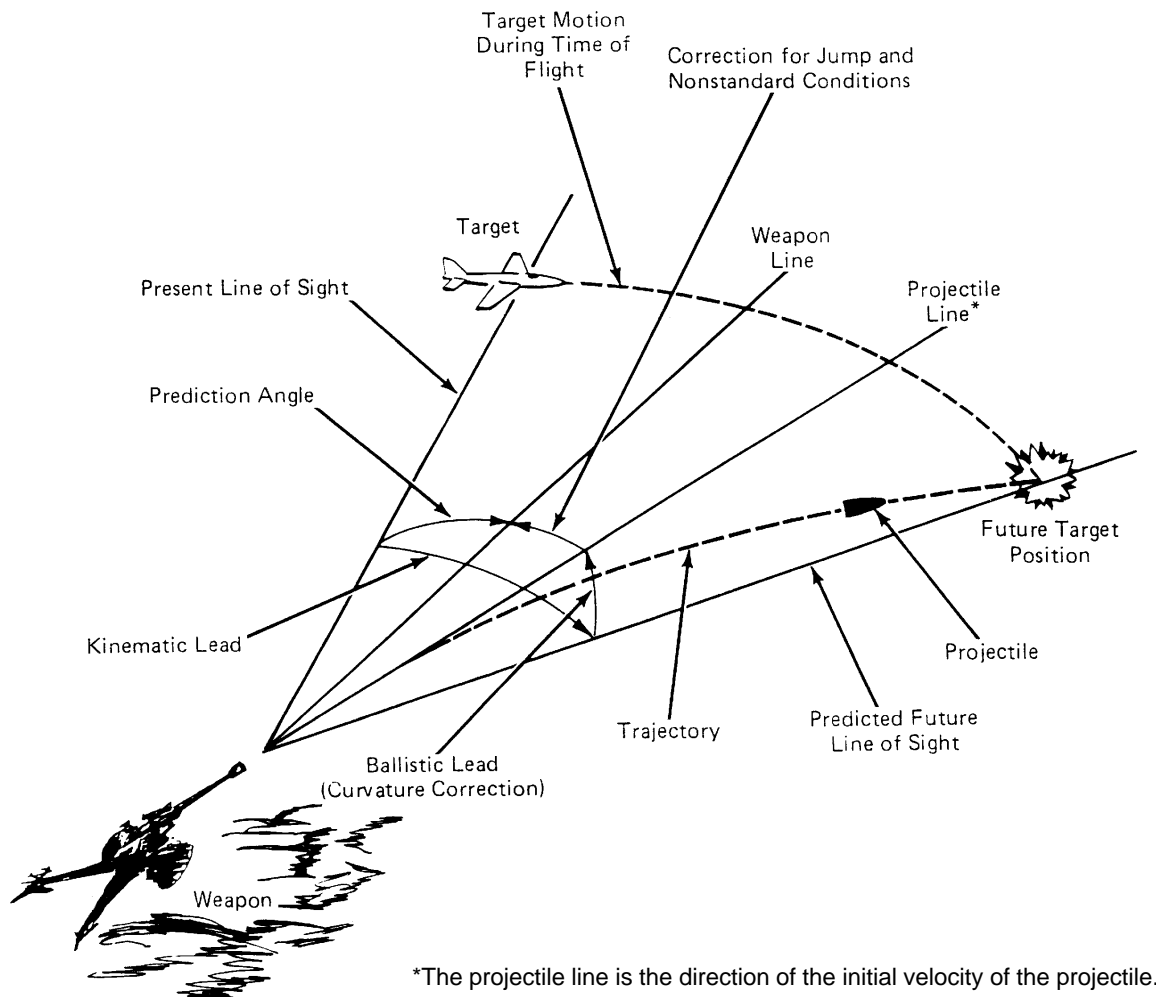
Figure 2-6. Prediction Angle and Its Major Components (Ref. 1)

2-8

matic lead is the angle between the present and future LOSs. The present LOS is the direction from the weapon station to the target at the instant of firing; accordingly, it is invariant with the reference coordinate frame selected. The weapon line defines the axis of the gun tube immediately prior to firing. The projectile line defines the projected line of the projectile at the instant it exits the muzzle. The weapon line and the projectile line differ from each other due to jump and other nonstandard conditions. On the other hand, the future LOS varies with the reference coordinate frame that is chosen. (For example, the future LOS from a moving tank to a stationary target is different for a reference frame fixed to the tank than it is for a reference frame fixed to the earth.) In general, the future LOS is a straight line from the weapon to its target at the instant of projectile impact. Fig. 2-7 represents the future range vector in relation to the present range vector R_o as it might appear from the standpoint of earth $R_{F(E)}$, air-mass $R_{F(AM)}$, and weapon station $R_{F(WS)}$ coordinates, respectively. To illustrate the effect of weapon station velocity, the weapon station is depicted as a high-speed jet aircraft. Therefore, lead is also dependent upon the reference frame chosen. Similar considerations apply to the other components of the prediction angle, e.g., ballistic lead and the correction for jump.

On the other hand, the prediction angle need not be considered in relation to a specified reference coordinate frame because its definitive limits—the LOS and the weapon line—are determined by quantities that are not influenced by the selection of the reference space. For example, the weapon line is coincident with the gun bore in the case of guns; in rocket launchers, it bears a similar significance. Since the weapon line represents a physical, extensible line on the weapon, its specification is independent of the reference coordinate frame. The LOS, as already noted, is similarly invariant with the reference coordinate frame selected. Therefore, the prediction angle also remains invariant with the reference frame se-
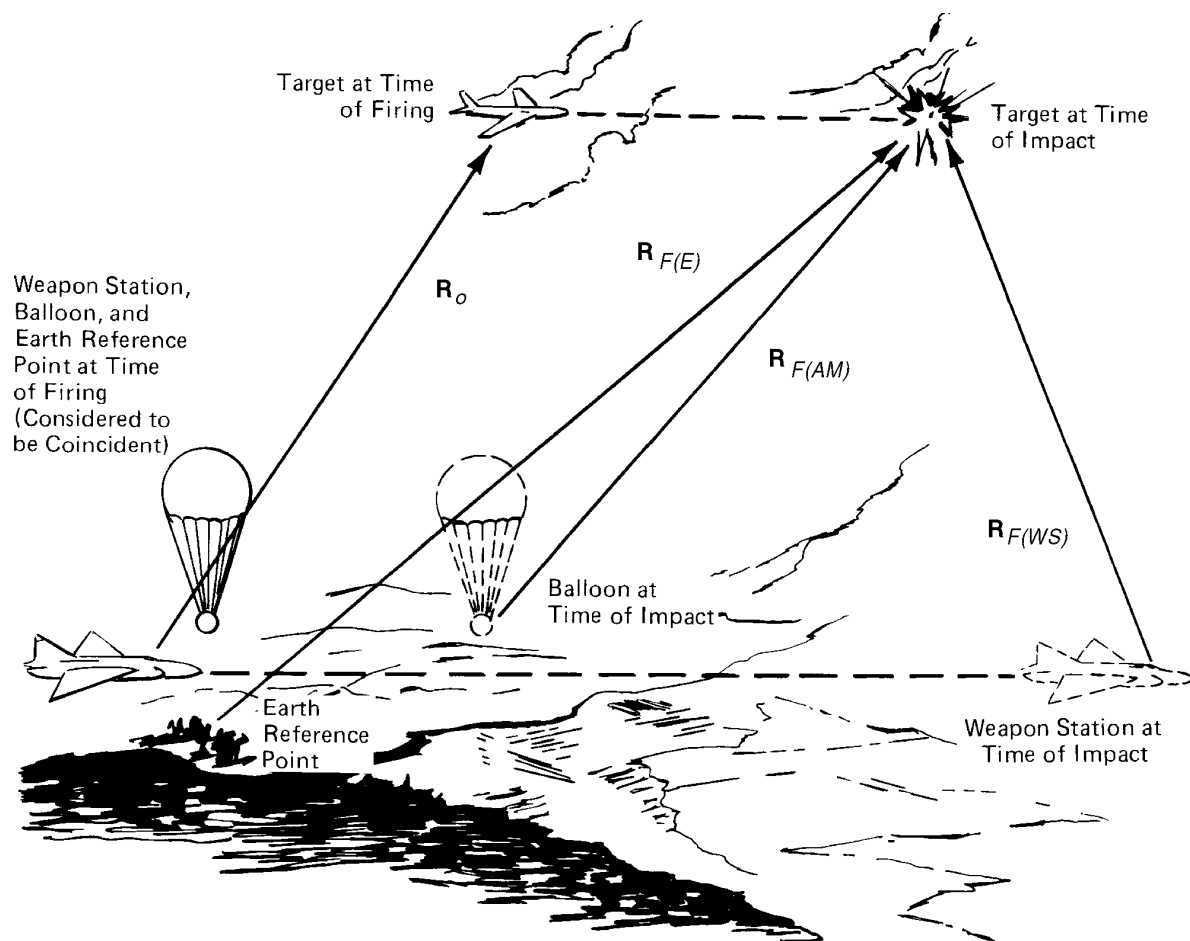
Figure 2-7. Relationship Between the Future Range Vector and the Present Range Vector from the Standpoint of Earth, Air-Mass, and Weapon Station Coordinates, Respectively (Ref. 1)

lected, i.e., irrespective of the coordinate system chosen, the prediction angle is seen to be the same to the observer in any selected reference frame.

For a more detailed discussion of the effect of the reference coordinate frame and illustrative examples, see Appendix A and Ref. 1.

2-2.4 EXTERIOR BALLISTICS

Exterior ballistics is the science that relates to the motion of a projectile in flight after it leaves the muzzle of the gun. To design a modern fire control system, a knowledge of exterior ballistics is a necessity. An understanding of the complicated motion of a spinning projectile fired crosswind from a moving vehicle and the accurate prediction of such motion are also essential.

An appreciation of the magnitudes of aerodynamic forces and moments that act on a projectile in flight can be obtained from an example given by Norwood (See Ref. 2.). It is almost incredible that the aerodynamic drag on the 20-mm M56 round fired at sea level at 1220 m/s is about 89 N and that the lift force at right angles to the velocity vector is about 40 N if the angle of attack (AOA) of the projectile is 3 deg. The 20-mm round itself has a mass of only 0.10 kg and, therefore, a gravitational force of 0.98 N. The effect of the lift, and other smaller forces, is to deflect the motion of the projectile away from its initial direction of motion; as a rule of thumb, this deflection is one milliradian per initial degree of angle of attack. In this example, the windage jump is 3 mils, and one might ask how it is that a 40-N force acting at right angles to the velocity vector of a 0.10-kg projectile produces only a 3-mil deflection? The answer is that the lift force precesses with the projectile about the velocity vector and nearly cancels out.

The deviations from straight line motion of a spinning projectile in flight are due to complicated interactions of aerodynamic forces and moments, gravity, and gyroscopic effects. These effects are incorporated during the development of ballistic equations, which, when properly solved, yield the trajectory solution. A discussion in subpar. 2-2.4.1 of the general ballistic equations, as represented by the six-degree-of-freedom mathematical model, provides an insight into the nature of the forces and moments acting on the projectile in flight and their relationship to the trajectory solution. This discussion is followed in subpar. 2-2.4.2 by a review of the less complex point mass equation that omits consideration of the rigid body effects, i.e., no moments are involved. (Both the six- and three-degree-of-freedom equations taken from the Ballistics Research Laboratory (BRL) representation given in Ref. 3 are provided in Appendix A with clarifying discussion.) Trajectories are then reviewed in terms of the factors that must be considered and compensated for in the fire control application, i.e., curvature, effects of jump, and variations from standard conditions.

2-2.4.1 The General Ballistic Equation

The aerodynamic forces and moments that act on a projectile in flight result from frictional forces and pressure distributions over the projectile body, which in turn result from the motion of the projectile through the air mass. A complete and accurate solution for projectile motion therefore would involve solution of the equations of fluid flow around the projectile. In practical applications this is beyond the capabilities of any available computer, but fortunately, solution of the fluid flow equations is not necessary. The alternative is a semiempirical approach whereby aerodynamic forces and moments are measured in wind tunnels and by means of free-flight tests. These aerodynamic data are modeled in a form suitable for computer use and are used along with the gravitational force in trajectory calculations. The equations of motion, derived from Newton's laws, which relate the three components of the force and moment system to the accelerations, are then used to generate projectile position and attitude as a function of elapsed time. Although projectile attitude is of no practical interest to the fire control designer, it is required input for the positional solution.

Arguments based on dimensional analysis and symmetry are used to derive the functional form of the aerodynamic forces and moments in terms of the aerodynamic or ballistic coefficients C and K, respectively, of the projectile. (C and K are the two different notations currently used to describe the force and moment system.) Dimensional analysis identifies certain restrictions imposed by nature upon the functional form of the mathematical relation describing such laws. Rotational symmetry and mirror symmetry are used to gain further insight into the functional form of the force and moment system.

The K notation is used in this handbook since most of the source material is given in this notation. A description of the K notation is given in Appendix A. The coefficients are functions of measurable quantities that describe the motion of the projectile through the air, e.g., components of linear and angular velocity, the speed of sound in air, and projectile shape. The form of the coefficient function is materially simplified when these quantities are structured as dimensionless products of Mach number, Reynolds number, dimensionless spin, dimensionless force, and yaw angle. By this approach, in which the force and moment system is mathematically modeled through the use of dimensional analysis and symmetry considerations, specific force and moment terms are developed. These can then be identified in familiar physical terms, e.g., drag, lift, and Magnus force. All possible forces and moments are uncovered as opposed to an approach in which the structure is assumed and the existence of some parameters might be overlooked.

The individual forces and moments can be identified and are known to be functions of Mach and Reynolds numbers, dimensionless spin, and the yaw angle. Attempts to derive the form of the functions from fundamental theory have not been productive. It is necessary to measure them in wind tunnels for various combinations of the dimensionless variables or by means of free-flight tests. There is a problem, however, in the use of these data in trajectory computation. A means of interpolation between data points is required. Polynomial curve fits have been applied to the data in the past, but the more recent practice is to generate look-up tables with accompanying interpolation procedures. Experience has shown that many of the coefficients are virtually independent of Reynolds number, and many are independent of dimensionless spin. This independence greatly eases the function definition problem.

Because the ballistic differential equation has no analytic closed form solution, numerical integration methods must be used. The numerical solution requires, in addition to the aeroballistic package, a set of initial conditions, e.g., the projectile initial velocity, angular velocity, yaw, and precession angle. The fire control application requires the direction in which the weapon should be oriented so that the projectile will pass through a given point in space. This direction, the muzzle velocity, and the weapon velocity determine the projectile initial velocity. In effect, therefore, the required orientation is part of the initial conditions. An iterative process is used, and an initial orientation is assumed. The projectile velocity is calculated based on muzzle velocity and weapon velocity and is applied as an initial condition. The amount by which the projectile misses the given point in space is then used to correct the theoretical orientation of the weapon. This process must be repeated until the miss is zero and should be accomplished in near real time if engagement motion is involved. When the target is in motion, the value of the TOF of the projectile to the predicted point in space is also required. This topic is discussed further in subpar. 2-2.5, which deals with target motion.

Although accurate six-degree-of-freedom projectile trajectories can be calculated directly from Newton's laws of motion, computations of this type currently are not believed to be feasible in most fire control applications even with digital computers because too much computation time is required. Careful study, however, leads to the selection of appropriate algorithms that yield trajectory data within the error budget allotted to exterior ballistics calculations and that can be used in fire control applications. This subject is discussed in subpar. 2-2.4.2, which follows.

2-2.4.2 Point Mass Equations

Many approximations of the six-degree-of-freedom equations have been developed over the years in order to compute trajectories in the laboratory within the tolerances required for the type of application of interest. At the Firing Tables Branch of the Fire Control Division of the US Army Armaments Research, Development, and Engineering Center (the Army's official source for firing tables) located at Aberdeen Proving Ground, it has been found that the solution of the so-called "modified point mass equations" provides the accuracy necessary for all but aircraft applications. The effect of initial yaw causes the difficulty in aircraft applications. Most of these representations, however, like the basic six-degree-of-freedom equations, are not solvable in real time with existing digital implementation.

One exception is the three-degree-of-freedom point mass representation, in which the projectile mass is considered to be concentrated at a point. Only the zero yaw drag coefficient is now a factor; the moment equations no longer apply. The attitude of the projectile is not a consideration. In most applica-

tions, however, the solutions must be modified by corrective terms that arise from projectile attitude and spin, but generally these are relatively small. This representation was used for many years to generate firing tables before the advent of high-speed digital computers. It then served the artillery application starting with the use of the field artillery digital automatic computer (FADAC) in the 1960s. Since then, the representation has been used in two air defense gun applications: gun low altitude air defense system (GLAADS) and SGT York. In these applications only the flat portion of the trajectory is of interest. As discussed in the six-degree-of-freedom case, the inverse of the solution required for the fire control problem is obtained; the weapon orientation needed for fire control is an input to trajectory generation.

In all fire control applications to date, with the exceptions previously mentioned, a curve fit to the trajectory has been used. With the analog computer approach the curve fit structure was usually selected based upon the ease of implementation of the analog representation used. The digital approach affords more freedom to express the relationships and permits full use of mathematical routines. Some imagination and ingenuity are generally required to generate a structure for the fit, and significant processing—usually least squares—is required to determine arbitrary parameters. The accuracy of the fit, particularly for LOS weapons, can usually be obtained to an acceptable tolerance. The advantage of the curve fit process over the differential equation solution is that it directly provides the weapon orientation as a function of desired aim point and requires far less solution time. The curve fit process initially required, however, may be time-consuming and costly, and it is possible that the accuracy requirements cannot be achieved. Examples of ballistic relationships obtained this way are discussed in Chapter 6. As digital computational speed and storage increase, greater dependence is expected upon the differential equation solution in the fire control implementation.

A three-degree-of-freedom representation, a reduced form of the six-degree-of-freedom representation, is given in Appendix A. References are indicated in Appendix A that provide a discussion of the numerical integration approaches applicable to digital implementation.

2-2.4.3 Curvature of the Trajectory

The extent of the trajectory that must be considered in the fire control solution depends largely on the type of weapon system application under design.

Fig. 2-8 shows the components of the projectile trajectories required to be known for various typical weapon fire situations in order for the projectiles to hit their respective targets. In each case the trajectory is determined by (1) the position of the origin of fire, i.e., the location of the weapon, (2) the conditions under which the projectile is fired from the weapon, i.e., the quadrant angle of elevation and the initial velocity, and (3) the characteristics of the air through which the projectile must travel in order to reach the target.

Fig. 2-8(A) illustrates the trajectory of a projectile fired from a field artillery weapon that has a high initial velocity and a small quadrant angle of departure. Fig. 2-8(B), on the other hand, represents the trajectory of a projectile fired from a field artillery weapon that has a much lower initial velocity and a large quadrant angle of departure. These two examples represent direct fire and indirect fire situations, respectively.

Fig. 2-8(C) shows the type of trajectory associated with antiaircraft fire. In antiaircraft fire the whole trajectory is generally considered to comprise the ascending branch since the descending branch has no significance. This case is in contrast to the trajectories associated with air-to-ground weapons fire; these trajectories are represented by Fig. 2-8(D). For such trajectories only the descending branch is used; there is no ascending branch.

All four representative trajectories are shown projected on the plane of departure. This plane is the xy-plane of the coordinate system customarily used in the computation of trajectories. In this system the x-axis is horizontal and the y-axis is vertical. The z-axis lies in a horizontal plane and is perpendicular to the plane of departure.
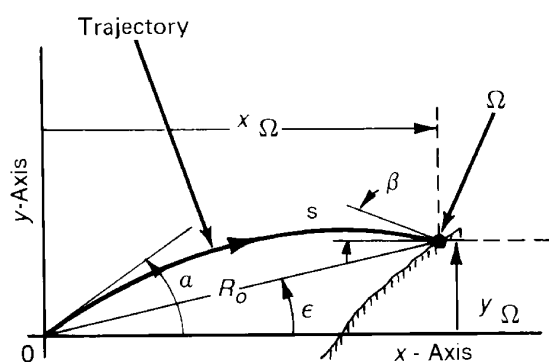
(A) Trajectory Associated With a Direct Fire
Field Artillery Situation
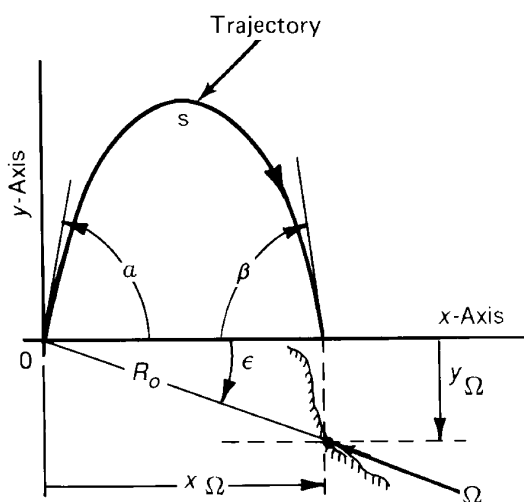
(B) Trajectory Associated With an Indirect Fire
Field Artillery Situation
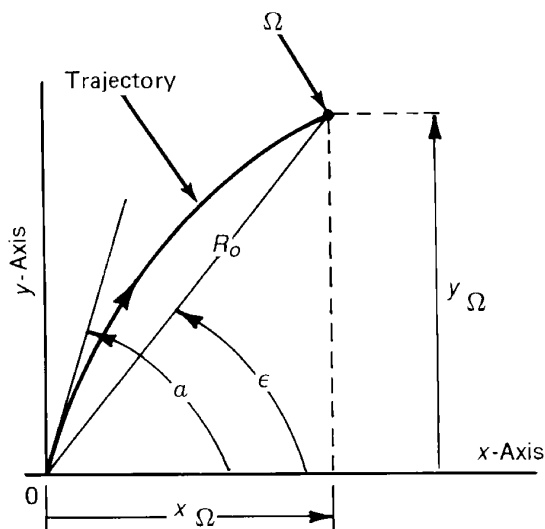
(C) Trajectory Associated With
Antiaircraft Fire
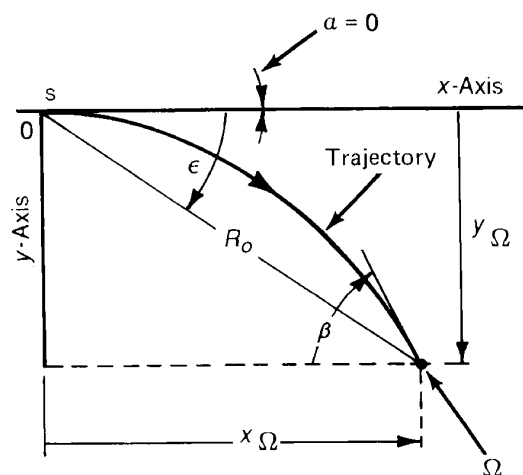
(D) Trajectory Associated With
Air-to-Ground Weapons Fire
by Bombs or Rockets

0 = origin of trajectory

Ω = point of impact, or point
of burst in antiaircraft fire

s = summit of trajectory

a = quadrant angle of departure

β = angle of fall

ϵ = angle of site (indirect fire)
= angle of sight (direct fire)

x_Ω = horizontal range

R_o = slant range

y_Ω = altitude of burst or impact
with respect to weapon

Figure 2-8. Typical Trajectories Projected onto the Plane of Departure (Ref. 4)

2-13

Since the usual trajectory is three dimensional in nature, it does not lie entirely in the xy-plane but also has a projection onto the xz-plane. This projection is represented in Fig. 2-9; the projectile deflection shown in the xz-plane, however, is exaggerated for the purpose of illustration. As indicated, the z-coordinate of the point of impact or burst is designated by the symbol z_Ω and is called the deflection. Deflection is due to the effects of nonstandard wind conditions on the projectile and drift, which is the lateral deviation of the trajectory caused by the gyroscopic precession of the spinning projectile.
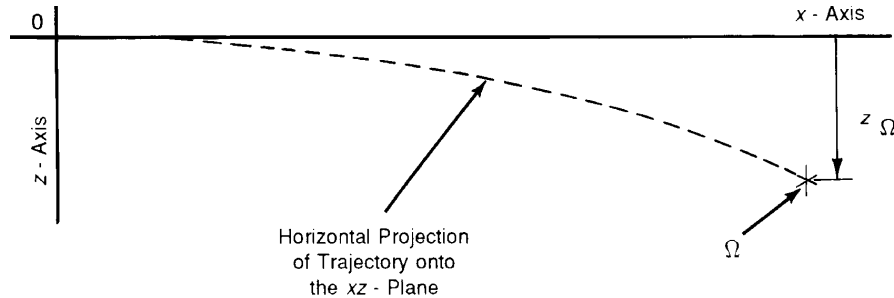
Figure 2-9. Horizontal Projection of a Typical Trajectory

The curvature of the trajectory of a projectile in motion is caused by many forces that act on the projectile during its TOF. The principal influences of the shape of the trajectory are the gravitational field of the earth and the characteristics of the air through which the projectile travels (See subpars. 2-2.4.3.1 and 2-2.4.3.2 for discussion.). Other effects contributing to the form of the projectile path include air mass motion and meteorological conditions. These effects are considered in subpar. 2-2.4.5, "Variations from Standard Conditions".

The force of gravity and air resistance are both generally considered with respect to an air structure referred to as the standard atmosphere. This standard structure provides a mathematical point of departure from which essential ballistic data can be obtained by applying corrections to the variations that may exist in the actual air structure at a particular time.

2-2.4.3.1 Gravity

Gravity is a primary factor that influences the path of a projectile in motion. If a projectile were fired in a vacuum and in the absence of a gravity field, it would maintain a constant direction and continue to travel indefinitely at a constant velocity and would be dependent only on the muzzle velocity V_o and the angle of departure from the weapon (as shown in Fig. 2-10). The kinetic energy that imparts this motion would produce both vertical and horizontal components of velocity, the combined effect of which would form a resultant velocity along the straight line path of projectile motion.
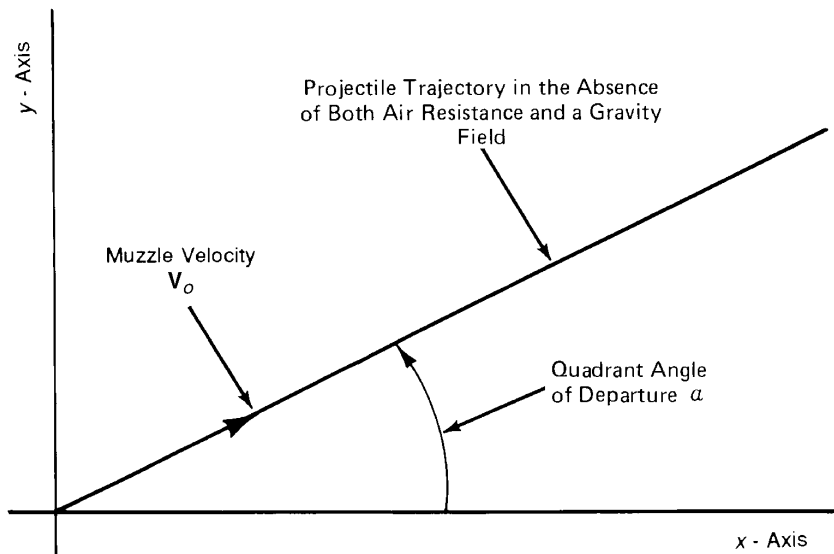
Figure 2-10. Trajectory of a Projectile Fired in a Vacuum and in the Absence of a Gravity Field

With only gravity effects considered, the flight path changes as shown in Fig. 2-11. Because no air resistance would be encountered in the vacuum, the horizontal component of velocity would remain constant. On the other hand, because the projectile would be acted upon by the force of gravity during the TOF, the vertical component of velocity would diminish at the rate of about 9.8 m/s^2. Thus this component would first reduce to zero, at which time the projectile could no longer rise with respect to the sur-
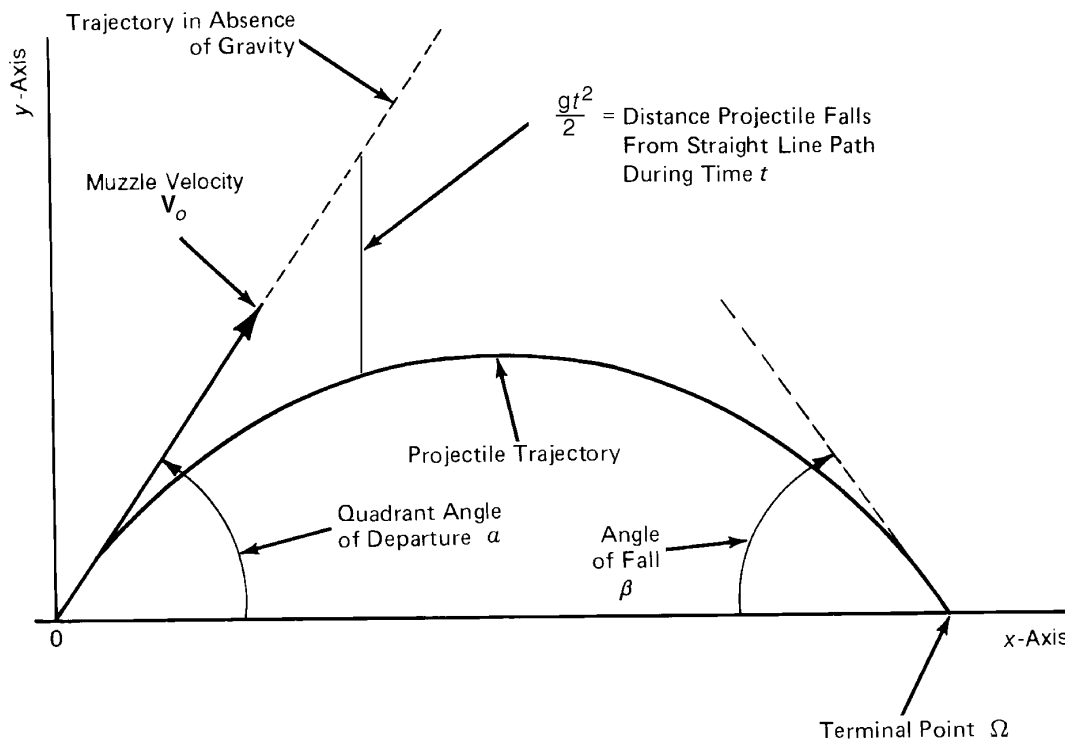
Figure 2-11. Trajectory of a Projectile Fired in a Vacuum With Gravity Effects Considered

face of the earth. Thereafter, gravity would cause the projectile to fall back toward the earth. The form of the path generated by the projectile under such theoretical conditions would be a perfect parabola with the angle of fall exactly equal to the angle of departure and with the summit midway between the origin and terminal points. Also the striking velocity at the terminal is equal to the muzzle velocity, and the maximum range is obtained with a quadrant angle of departure of 45 deg.

2-2.4.3.2   Air Resistance

The trajectory described by a projectile under standard atmospheric conditions becomes a more complex curve than it would in a vacuum. The air resistance acting along the axis of the projectile produces a retarding force component that adds to the effect of gravity on the vertical component of projectile velocity during the ascending portion of the trajectory and subtracts from the effect of gravity during the descending portion. The air resistance also acts to decrease the horizontal component of projectile velocity over the entire trajectory. The net results are that the trajectory is not a true parabola and the angle of fall becomes greater than the angle of departure, the summit is displaced closer to the point of impact than to the origin, the striking velocity is less than the muzzle velocity, and the range of the projectile is greatly reduced. Shown in Fig. 2-12(A) is a projection of a typical standard trajectory on the plane of departure.

Resistance of the air to the forward motion (range motion) of a projectile greatly influences both the shape of the trajectory in elevation and the azimuth direction of the projectile. This influence is shown in Fig. 2-12(B), which is a projection of a typical standard trajectory on the horizontal plane, and is caused by lift forces acting in the plane of yaw; the yaw results from the spin of the projectile.

The factors that must be considered to ascertain the difference between the trajectory characteristics of a projectile fired in air and those of one fired in a vacuum follow:

1. *Density of the Atmosphere.* The air offers resistance to the projectile, which substantially alters the characteristics of the trajectory. Since the density of the atmosphere differs from time to time in accordance with changes in temperature and barometric pressure and with altitude, air resistance varies as the projectile travels the course of its trajectory.

2. *Characteristics of the Projectile.* The specific characteristics of a projectile that influence retardation in passing through air of given density are (1) weight, (2) cross-sectional area, and (3) shape. A pro-
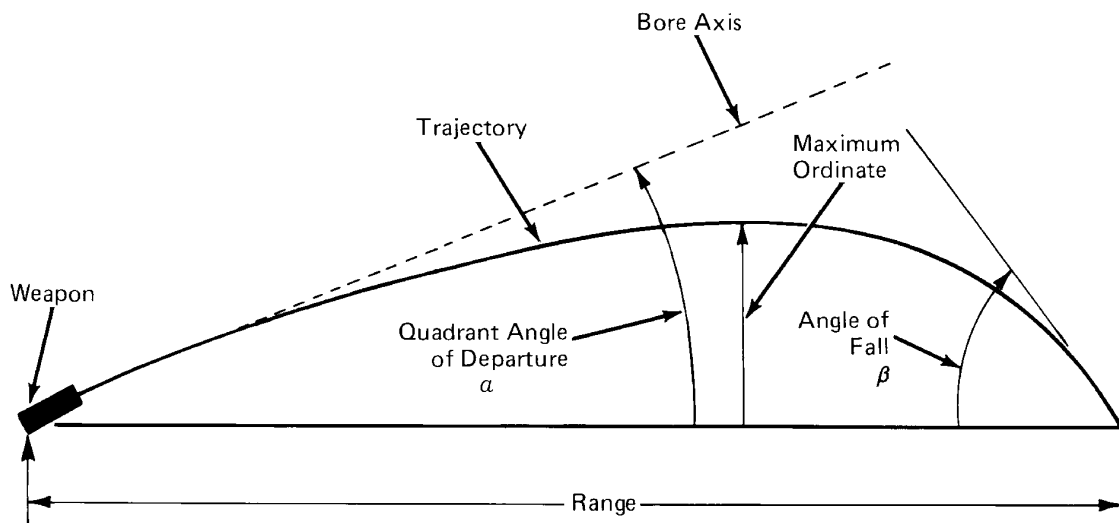
(A) Projection of a Typical Standard Trajectory onto the Plane of Departure
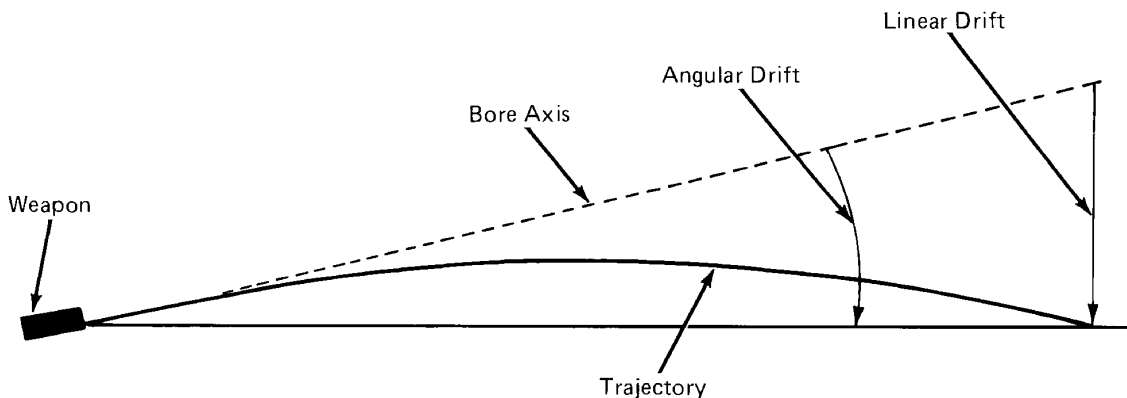
(B) Projection of a Typical Standard Trajectory onto the Horizontal Plane

Figure 2-12. Trajectory of a Projectile Fired Under Standard Atmospheric Conditions (Both Gravity and Air Resistance Present)

jectile that has a streamlined front end encounters less resistance than one with a short, blunt nose. The shape of the base also affects the air resistance encountered by the projectile.

　　3. *Initial Velocity.* If the air density and the design of the projectile are considered to remain constant, the initial velocity of the projectile affects the characteristics of the trajectory because the amount of resistance offered by the air is a function of the projectile velocity.

　In general, air resistance is considered to be a resultant vector force, but many significant force and moment factors make up the total effect that causes retardation and misdirection of the projectile in flight (See Ref. 4 for summary of these factors.). The resultant aerodynamic force that acts on a moving projectile as a result of air resistance can be treated as two component forces, as shown in Fig. 2-13.

　　1. *Lift* L—lies in the plane formed by the tangent to the trajectory and the axis of the projectile (the plane of yaw) and has a direction perpendicular to the direction of projectile motion.

　　2. *Drag* D—a force acting in the same plane as the lift force that has a direction parallel and opposite to the direction of projectile motion.

　Since the attitude of the projectile varies with respect to the instantaneous direction of motion of the projectile over the course of the trajectory, the direction of the lift force also varies. In addition, the magnitude of the lift force increases as the angle of yaw increases. As indicated in Fig. 2-13, the attitude of a projectile with respect to the direction of motion of the projectile is completely specified at any particular instant by the angle of yaw and the angle of orientation. Figs. 2-14 and 2-15 show typical variations of these quantities with time and with respect to one another. The train of events pictured is from a combi-

nation of projectile precession (discussed in subpar. 2-2.4.3.3) and the resulting variations of air pressure on the projectile nose. To meet projectile stability criteria, the oscillations in yaw (called nutation) must be damped out, as shown in Fig. 2-14. (For a summary of how to design projectiles to achieve appropriate control of their flight characteristics, refer to Refs. 5 and 6.)
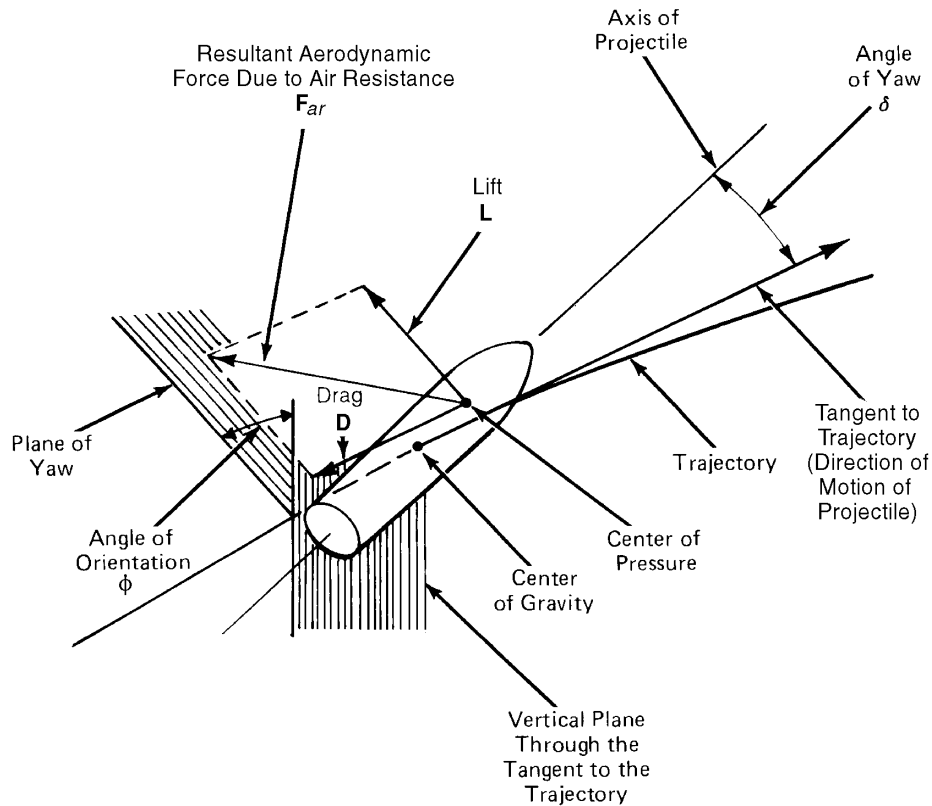
Notes:
1. The plane of yaw is an instantaneous plane formed by the tangent to the trajectory and the axis of the projectile.
2. The dihedral angle between the plane of yaw and the vertical plane through the trajectory is known as the angle of orientation ϕ. The angular motion of a projectile about its center of gravity in three dimensions is described in terms of the angle of yaw δ and the angle of orientation ϕ.

Figure 2-13. Forces on a Projectile Moving in Still Air
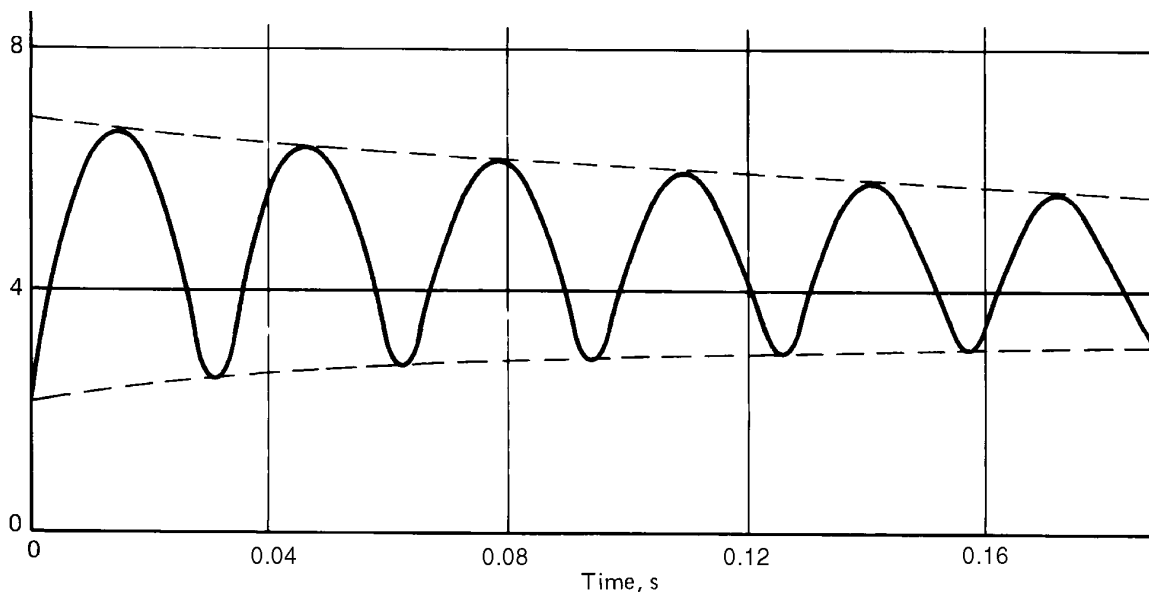
Note: The projectile experiences this damped oscillation condition as it exits the gun and also when its direction changes at the peak of the trajectory.

Figure 2-14. Curve of Yaw Versus Time (Ref. 4)
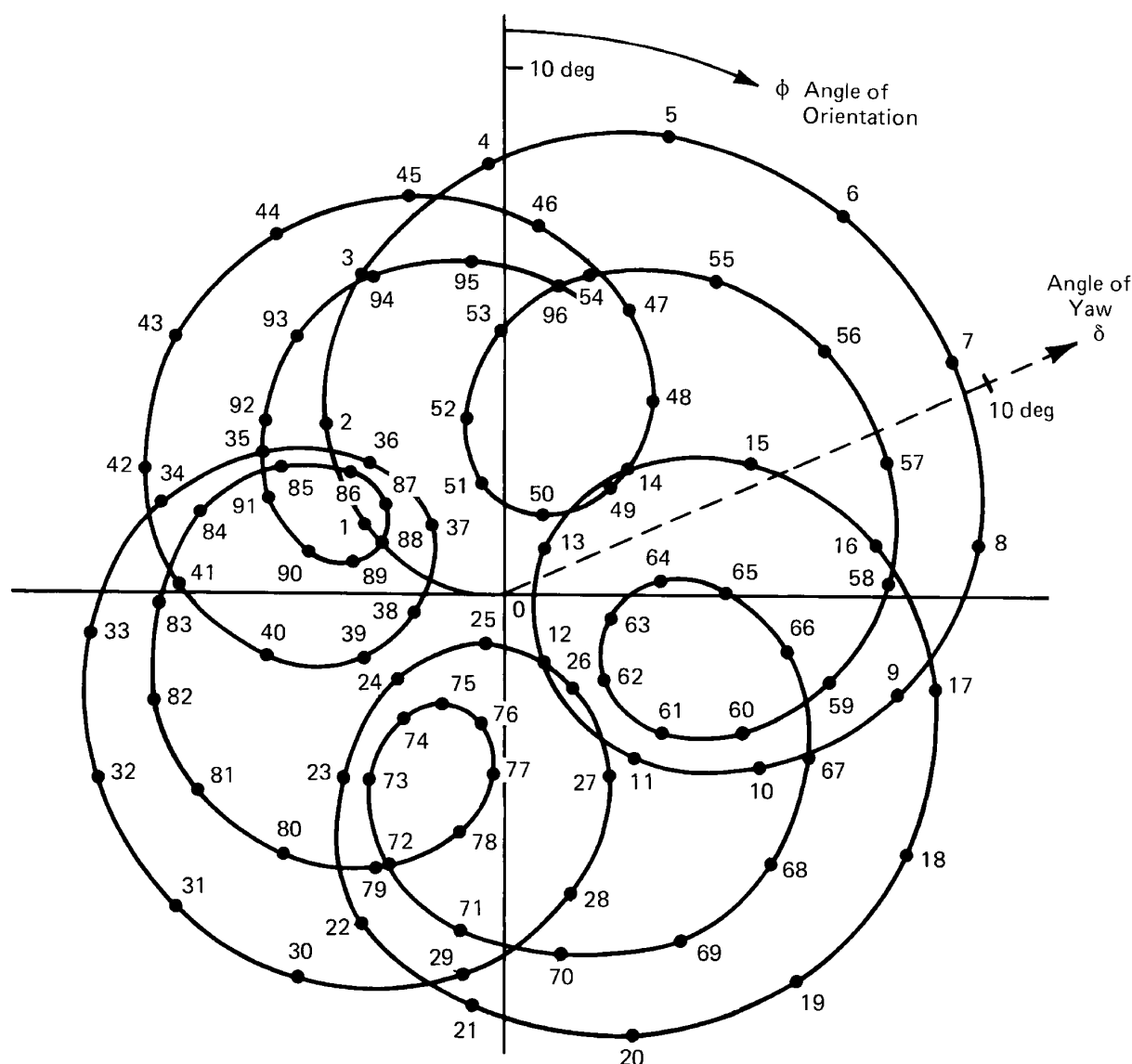
Figure 2-15. Polar Plot of Angle of Orientation Versus the Angle of Yaw With Time (Ref. 4)

Drag, the force component of the total air resistance that acts in the direction opposite to the direction of motion of the projectile, is generated by the resistance of the projectile nose, the skin friction caused by translation and rotation, and the formation of eddy currents and a partial vacuum at the base of the moving projectile. The behavior of airflow over the surface of the projectile during its passage through the air is affected by the form of the projectile, e.g., a blunt-nosed projectile encounters greater air resistance than a projectile with a pointed nose. Similarly, a square-based projectile offers more impedance to air flow than a tapered-based projectile. Projectile size also influences drag. The larger the diameter of the projectile, the larger the surface area exposed to the air and, consequently, the greater the drag effect on the projectile for a given mass. Again, the larger the projectile, the greater the volume of air that must be displaced from the path of the projectile. A portion of the kinetic energy imparted to the projectile at the instant of firing must be used to perform the work of displacing this air.

Skin friction also is an effective component of drag. A rough surface on the projectile increases air resistance and accordingly decreases the range. As the projectile penetrates the air at high speed, the vis-

cosity of the air affects projectile motion. Layers of air adjacent to the surface of the projectile are dragged along with it; other layers of air above and contiguous with these are less affected. The air therefore submits to this layer-sliding action with a reluctance that is manifested by shearing stresses on the projectile surface. Here again drag retards the forward motion of the projectile.

The velocity of the projectile along its curved trajectory also influences drag, as shown in Fig. 2-16 for various projectile shapes. Below the speed of sound, skin friction constitutes the primary retardation effect, and drag is approximately proportional to the square of the velocity of the projectile. With increasing projectile velocities in the subsonic range, the retarding effect also increases but at a faster rate. As the projectile velocity approaches the speed of sound, a sudden increase in drag occurs as a result of local velocities on the surface of the projectile that exceed the speed of sound and a shock wave being set into motion. Since energy is required to establish and maintain any wave motion set up in the air by the projectile, the energy that is contained in the shock wave is derived from the kinetic energy imparted to the projectile at the instant of firing. Thus the shock wave represents an energy loss that is continuously being dissipated through compression and irreversible heating of the air passing through the shock wave. The

(A) Typical Projectile Shapes
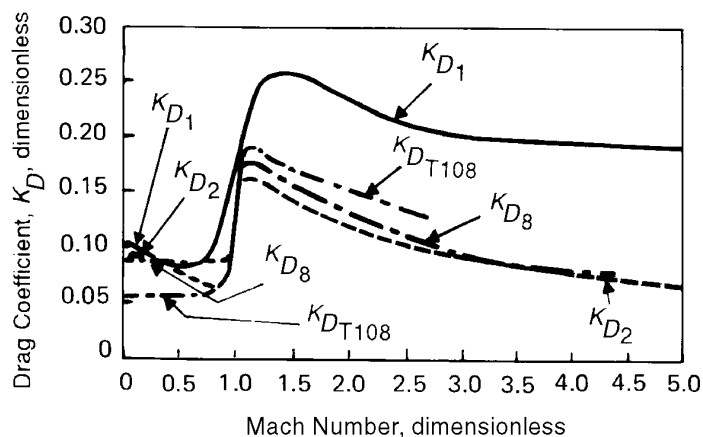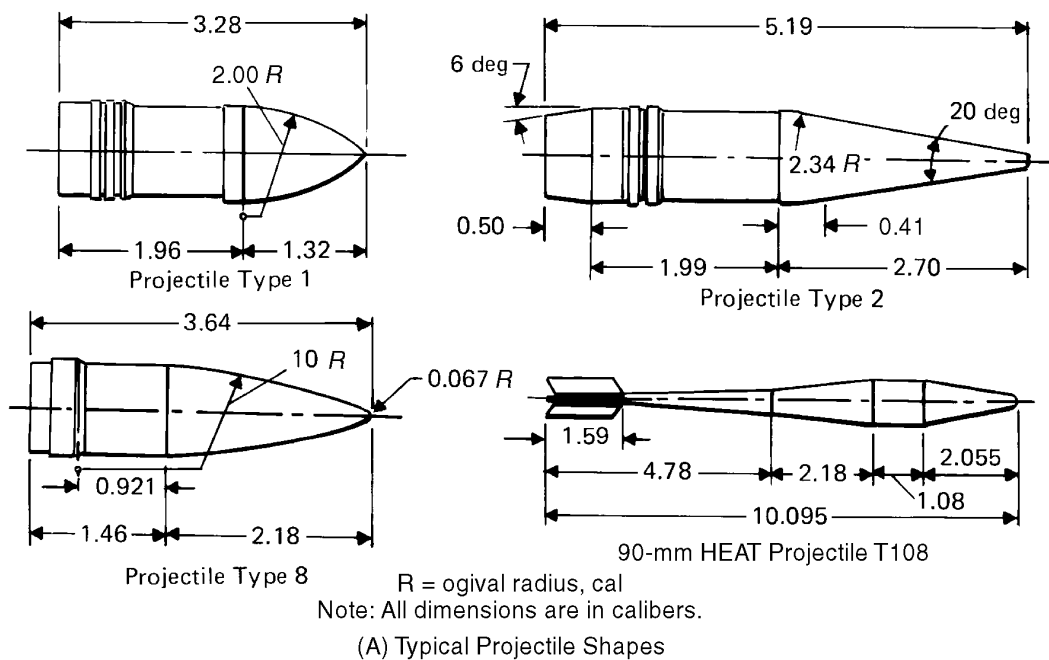
(B) Drag Coefficient vs Mach Number for the Projectile Shapes Shown in (A)

Figure 2-16. Influence of Projectile Velocity on Drag for Various Projectile Shapes (Ref. 7)

continuous drain of energy at this velocity obviously contributes to the retardation of the projectile. Furthermore, as the velocity of the projectile increases beyond the speed of sound, the airstream passing over the surface is unable to effect closure behind the case of the projectile. This inability creates increased turbulence, or wakes, behind the projectile. At supersonic velocities more shock waves are generated that add further drag or retardation effects. The total effect of friction, wake, and shock waves therefore alters the range of the projectile.

A final factor that influences drag is yawing, which, because of aerodynamic effects, results in a motion that fails to present the projectile to the air point first and thus requires the projectile to move through the air with a projected area greater than its diameter. If the angle of yaw exceeds 2 or 3 deg, the air resistance increases sufficiently to induce an increased retarding effect.

In addition to the dominant aerodynamic forces of drag and lift that act on a projectile as a result of air resistance, a dominant moment, called the overturning moment, must also be considered. (Other moments, such as the Magnus moment and the yawing moment—both of which are due to yawing—can normally be neglected.) The overturning moment is the moment of the resultant aerodynamic force $\mathbf{F}_{ar}$, which acts through the center of pressure of the projectile, about the center of gravity of the projectile, as shown in Fig. 2-13, and varies with the sine of the angle of yaw.

2-2.4.3.3 Drift

As indicated in Fig. 2-12(B), the trajectory of an elongated, rotating projectile deviates laterally from the plane of departure so that the horizontal trace of the trajectory is a curved, rather than a straight, line. This lateral deviation is called drift and is measured as the perpendicular distance from the end of the trajectory to the plane of departure. It is sometimes referred to as linear drift in order to differentiate it from angular drift, i.e. the angle subtended by the linear drift between the plane of departure and the vertical plane containing the line of site.

Drift may be considered to result from the following three causes:
1. Gyroscopic action
2. Magnus effect
3. Cushioning effect.

It is reasonably certain, however, that the combined effect of the last two causes named is minor compared with the effect of the first.

The part played by gyroscopic action is considered first. When certain projectiles are fired from weapons, they are given a rotating motion of spin about the longitudinal axis by the rifling, i.e., the lands and grooves of the tube. This spinning action prevents tumbling of the projectile during flight. In US Army weapons, rifling is always a right-hand twist; consequently, the projectiles spin clockwise when viewed from the base of the projectile. The spinning action is accomplished at a rotational speed sufficient to make the projectile behave as a gyroscope during its TOF. Although this gyroscopic behavior stabilizes the projectile in flight, it simultaneously subjects the spinning projectile to gyroscopic precession. Gyroscopic precession is a change in the orientation of the spin axis of a rotating body that takes place as the result of an applied torque. The direction in which the rotating body will turn, or precess, is that which will bring the spin axis into alignment with the axis about which the torque is applied (as shown in Fig. 2-17). The precession of concern here results from the interaction of the torque produced by the air pressure on the underside of the projectile nose, which acts at the center of pressure of the projectile, with the angular momentum of the spinning projectile.

The gyroscopic precession of a projectile occurs as a result of the curvature of the flight path due to gravity (as discussed in subpar. 2-2.4.3.1). Because of the stability of the projectile arising from its spin, the projectile tends to maintain its original flight orientation in space even though the trajectory does curve. Thus, as gravity causes the projectile to drop away from the initial flight direction, the nose of the projectile points slightly above the trajectory. The air pressure now acting on the underside of the nose of the spinning projectile causes the projectile to precess clockwise (as viewed from above the trajectory). This shift of the longitudinal axis of the projectile now exposes the left side of the nose (as viewed from above the trajectory) to the air pressure. Continuing gyroscopic behavior then precesses the spinning projectile still more, and it is once again positioned with the underside of the nose exposed to the pressure

Applied Torque
Direction

S

Projectile
Spin
Direction

P   CP

CG a

M

Precession
Direction

CG = projectile centroid
CP = center of pressure
 P = vector force of air pressure
       (acting on underside of projectile nose), N
 a = effective lever arm, m
 S = angular momentum vector, kg·m^2/s
 M = applied torque vector, N·m
 ω = precession angular velocity vector, rad/s

ω
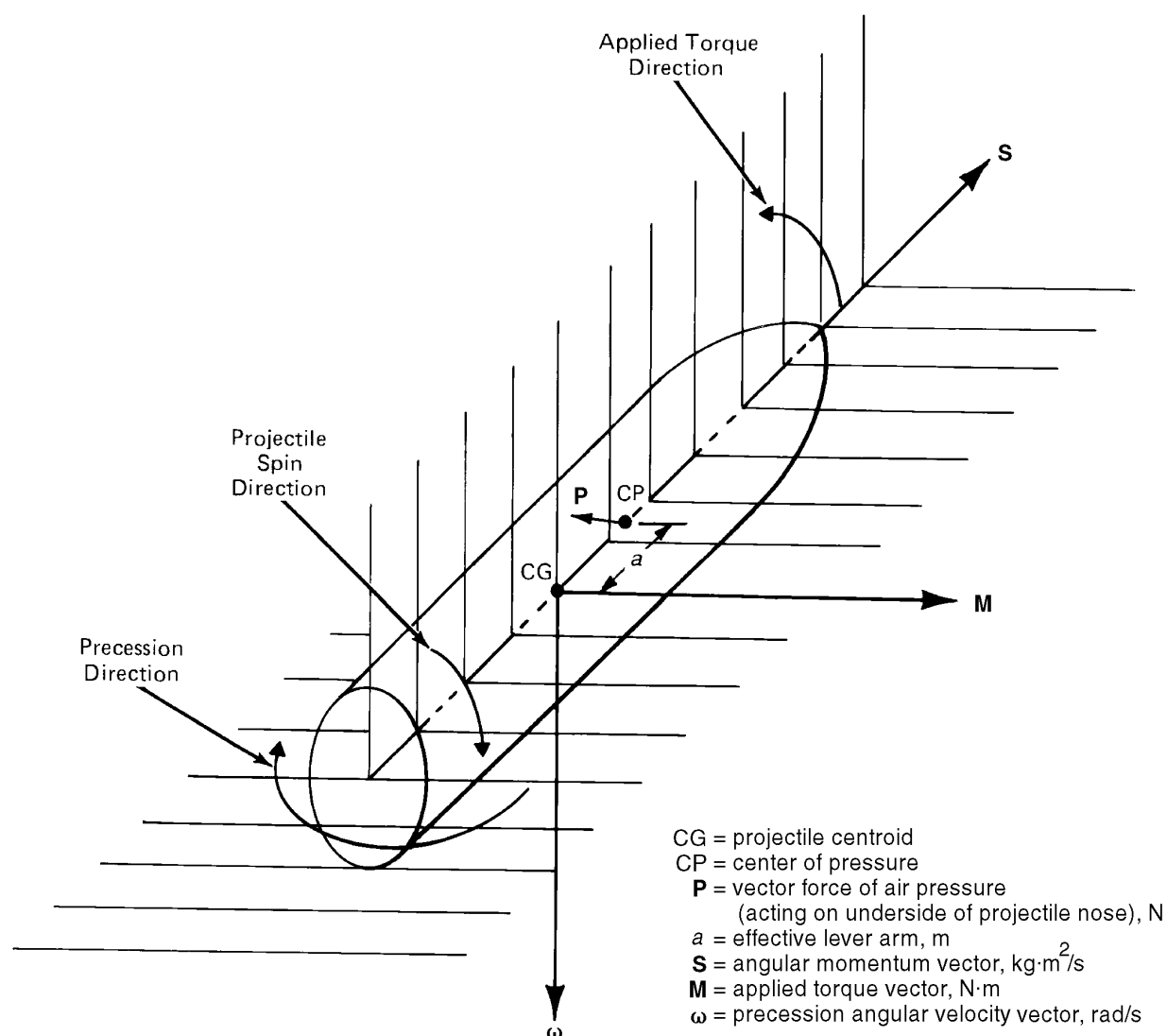
Figure 2-17. Gyroscopic Precession of a Spinning Projectile

of the air. This sequence of events continues and causes the axis of the projectile to oscillate about the instantaneous tangent to the trajectory. The oscillating cycle repeats itself with diminishing effect, as shown in Figs. 2-14 and 2-15.* The predominant orientation of the projectile nose, however, is upward. Therefore, since the maximum air pressure is always on the underside of the projectile, the net precession is always toward the right.

The trajectories of antiaircraft weapons consist of high-elevation ascending legs. These trajectories are relatively flat. Consequently, the pitch angle, the angle between the projectile spin axis and the tangent to the trajectory, remains small. Therefore, the torque produced by air pressure on the underside of the projectile nose and the resulting precession remain small. Most other trajectories, however, are less flat (such as ground weapons firing at ground targets). The pitch angles tend to be larger. Therefore, the torque produced by air pressure in these other trajectories and the resulting precession tend to be large. As a result of this crabwise movement, the lateral component of air resistance continues to push the projectile farther toward the right and thereby causes the projectile to drift to the right from the initial vertically oriented plane of firing. The magnitude of the drift—expressed as a lateral distance on the ground—is dependent on the rotational speed of the projectile, the curvature of the flight path due to gravity, air resis-

*Liquid-filled projectiles or projectiles that are assymetrical about the longitudinal axis may have increased oscillations (precession and nutation) and therefore may become unstable in flight.

tance, and the time duration of flight. The amount of precession, and hence drift, varies inversely with the rotational speed of the projectile. Drift increases with an increase in the other factors, however.

As has already been noted, the initial tendency of a projectile to maintain the original direction of its axis as it falls away from the axis of the weapon tube causes the airstream to strike the lower side of the projectile. The airstream then splits. Part goes past the projectile on the left-hand side (as viewed from the rear of the projectile) and part goes past on the right-hand side. Because of this and the right-hand spin of the projectile, the air adhering to the right-hand side of the projectile meets and opposes that part of the airstream passing on the right-hand side of the projectile, and there is a resulting increase in pressure on that side. At the same time, there is a corresponding rarefaction on the left-hand side of the projectile. This results from the fact that the air adhering to the left-hand side of the projectile is moving in consonance with that part of the airstream passing on the left-hand side of the projectile. Accordingly, the projectile tends to move to the left, the side of less pressure. This effect, known as the Magnus effect, is the same phenomenon that causes a golf ball to hook or to slice when mishit. The Magnus effect can be important in the descending end of a trajectory for a projectile fired at high elevations of the weapon tube because the steepness of the descent causes the airstream to hit the projectile nearly perpendicular to its spin axis and, therefore, with maximum Magnus effect. The Magnus effect opposes the gyroscopic effect.

The cushioning effect is the piling up of air on the underside of the projectile that forms a cushion. The projectile tends to roll on this cushion because of its spin and the friction existing between the projectile and the cushion. This rolling movement is to the right for a projectile with right-hand spin. Thus the cushioning effect opposes the Magnus effect but adds to the gyroscopic effect.

2-2.4.4 Effects and Sources of Jump

The combination of factors that determine the total velocity of the projectile is responsible for creating the phenomenon of jump. Jump is the difference between the initial projectile velocity direction and the direction in which the weapon is aimed. When a projectile is launched from a gun, the phenomenon of a jump usually occurs as a combination of a vertical jump effect and a horizontal jump effect.

The following factors affect both horizontal and vertical jump:

1. The gun dynamic response to firing is driven by the offsets between the center of gravity of recoiling parts and the center of pressure of propellant gases, by expansion of the tube against bearings in the recoil system, by reaction to recoil or elevation cylinders or springs, and by motion of the projectile down the tube. The gun tube motion directly influences pointing direction and crossing velocity at shot exit, and it interacts with the projectile as it accelerates.

2. The projectile dynamic response as it accelerates down the tube is influenced by gun curvature due to gravity, manufacturing tolerances, dynamic response, and thermal distortion. For full bore rounds the resulting balloting of the projectile determines its dynamic state at shot exit. The presence or absence of rifling affects balloting. For sabot rounds the vibration of the projectile within the sabot adds additional degrees of freedom.

3. Once the projectile is free of the gun tube, a number of gas dynamic factors influence the trajectory. Muzzle blast can perturb slow-moving fin-stabilized mortar rounds. Sabot discard significantly alters the trajectory of tank ammunition. Finally, aerodynamic jump and asymmetric jump cause deviations for all rounds.

2-2.4.5 Variations from Standard Conditions

The factors that determine the motion of a projectile are related to certain presupposed conditions that involve the weather, the weapon, the projectile, and a motionless earth. Such conditions are referred to as standard conditions. Because these conditions do not necessarily exist at a particular time of weapon firing, variations from the assumed and accepted standard conditions introduce differences that influence the behavior of the projectile. These variations are referred to as nonstandard conditions. It should be noted that although some of the factors that make up nonstandard conditions are not natural phenomena, they are generally treated as variations from the norm.

Nonstandard conditions include

1. Propellant characteristics

   2. Projectile weight
   3. Air density
   4. Air temperature
   5. Differences in muzzle velocity
   6. Wind
   7. Effects of the rotation of the earth
   8. Nonrigidity of the trajectory.

Each of these nonstandard conditions is discussed in the subparagraphs that follow.

2-2.4.5.1 Propellant Characteristics

The characteristics of propelling charges used to fire projectiles vary from standard conditions because of differences in propellant temperature, packing consistency, and moisture content. These differences cause variations in ignition, rates of burning, gun tube temperature, and seating of the projectile that produce variations in muzzle velocity. Consequently, variations in range result.

2-2.4.5.2 Projectile Weight

Projectiles of the same design are specified as having a standard weight. However, variations from standard, i.e., heavier than standard or lighter than standard, often occur among projectiles. A heavier-than-standard projectile acquires about the same amount of energy from the propellant as a lighter projectile; thus the heavier projectile leaves the muzzle with a muzzle velocity less than that possessed by a projectile of standard weight. Because of the greater sectional density, however, the heavier projectile has an improved ballistic coefficient, and the effect is toward an increase in range. For heavier-than-standard projectiles the net effect of the two factors is to decrease the range over short TOFs and increase the range over longer TOFs, whereas for lighter-than-standard projectiles the reverse is true.

2-2.4.5.3 Air Density

The density of the air is an important factor related to drag because any increase in air density causes greater resistance to the forward motion of the projectile, which results in a decrease in projectile velocity and range. Air density, however, also influences the path of the projectile and its TOF because it is a measure of the mass that must be displaced by the projectile along its flight path. The greater the density of the air, the more kinetic energy must be consumed to overcome the compactness of the air and, consequently, the greater the retardation of the projectile. Over long TOFs such as those in artillery fire, the projectile may pass through several layers of air having different densities, which may have a significant effect on range. For short times of flight such as battle tank fire, the range effects due to density variations in the atmosphere are less important.

2-2.4.5.4 Air Temperature

Nonstandard temperature affects the path of a moving projectile in an oblique manner. Air temperature influences air density, and it was established in the discussion of factors relating to drag that air density affects the retardation of the projectile. Therefore, since a variation in temperature brings about a variation in density, temperature can cause a variation in range. As the temperature of the air increases, the range of the projectile may increase or decrease, depending on the velocity of the projectile. The relationship of drag to the Mach number of the projectile, i.e., projectile velocity/velocity of sound, changes abruptly when the projectile velocity is in the vicinity of Mach 1. As the velocity approaches the speed of sound, the effect of drag increases, but as the air temperature increases, the velocity of sound also increases. In this way the differential effects of air temperature influence the location of the point on the trajectory at which the change in retardation due to the initial speed of sound occurs.

2-2.4.5.5 Differences in Muzzle Velocity

Among the deviations from the standard conditions that cause a projectile to impact or burst at some point other than the target are variations in muzzle velocity. The muzzle velocity is the maximum speed attained by a projectile while under the influence of the propellant gases, and it occurs shortly after the projectile leaves the muzzle of the weapon. The greater the muzzle velocity of a projectile, the greater the range it can attain. Accordingly, variations in the actual muzzle velocity from the standard value upon

which a particular set of firing tables is based result in range inaccuracies.

Variations in muzzle velocity result from a number of causes, which can be summarized as follows:

1. As noted in subpars. 2-2.4.5.1 and 2-2.4.5.2, respectively, variations in propellant characteristics, e.g., temperature, packing consistency, and moisture content, and variations in projectile weight contribute to changes in muzzle velocity.

2. Erosion of the weapon tube enlarges the bore. This increased size allows propellant gases to escape and thereby reduces gas pressure and hence the muzzle velocity.

3. Lack of hard, uniform ramming of separate-loading ammunition from round to round causes variation in the seating of the projectile. This results in nonuniform velocities at the muzzle.

4. Rough surfaces on the rotating band of a projectile prevent proper seating. As a result, the propelling gases escape, and the muzzle velocity decreases.

5. Even such minor factors as manufacturing tolerances and oily weapon tubes result in minor and abnormal variations in the muzzle velocity of the projectile.

2-2.4.5.6 Wind

The lateral nonstandard deviation of a projectile from its standard trajectory results chiefly from wind. For purposes of practicality a theoretical wind assumed to be constant is sometimes used for correction purposes. This constant wind, termed ballistic wind, is expected to have the same effect on a projectile during its flight as the varying winds actually encountered.

The ballistic wind is considered to be horizontal. Therefore, in general, it has components parallel and perpendicular to the line of fire. Accordingly, the ballistic wind generally influences both the range and direction of a projectile trajectory. The component of ballistic wind that blows at right angles to the line of fire is called the crosswind, or lateral wind, and causes the projectile to be displaced laterally with respect to the line of fire. On the other hand, the component of ballistic wind that blows in the plane of fire is referred to as range wind.

With respect to the relationship between the projectile velocity and the velocity of the air adjacent to the projectile, range wind may produce positive or negative effects. If the air moves with the projectile, i.e., if a tail wind is present, the velocity relative to the air is reduced, the projectile encounters less air resistance and, therefore, less drag, and a longer range results. On the other hand, if the air moves in a direction opposite to the forward motion of the projectile, i.e., if a headwind exists, the velocity relative to the air is increased, drag is increased, and the range decreases.

The crosswind component does not affect the trajectory range; it deflects the trajectory into a different vertical plane. The direction and magnitude of this deflection are dependent on the azimuth and velocity of the wind.

The effect of the ballistic wind has minimal influence on flight paths that have a short time duration. Conversely, considerable effect on the accuracy of weapons fire results for flight paths of long time duration. For air defense artillery, field artillery (especially in high-angle fire), and mortar fire, computations incorporate information from meteorological messages that includes ballistic wind direction, speed, air temperature, and air density for altitude zones above the surface of the earth. These data are weighted averages of the conditions that exist from the surface up through the altitude zones indicated and back to the surface.

2-2.4.5.7 Effects of Rotation of the Earth

The rotation of the earth is a factor that affects both the range and azimuth of the terminal point of projectile trajectory. Because the earth rotates from east to west at an angular velocity of 15 deg/h (This rotation produces a tangential velocity of 1670 km/h at the equator.), the effect of the rotation of the earth on the movement of a projectile fired to a high altitude on a very long-range trajectory is highly significant from the standpoint of accuracy. Unless the angular velocity of the earth is accounted for in the differential equations of motion for the projectile, errors in trajectory calculations result. These equations are in subpar. A-2.2 and par. A-4.

For very long-range trajectories two other factors are involved: the variations of gravity with altitude and the curvature of the earth. Rotation of the earth is considered a nonstandard condition that involves the factors of direction of fire, angle of departure, and velocity of the projectile and the aspects of longi-

tude and latitude, i.e., the relative positions of weapon and target with respect to geographic location. For long ranges these aspects represent a departure from the standard. Here projected motion can no longer be considered from the standard conditions of air resistance, a flat earth, and a homogeneous field of gravitation. The variations of gravity with altitude and the curvature of the surface of the earth influence projectile motion in the following ways:

1. The influence of the variation of gravity with altitude is a minor deviatory effect on long-range projectiles. Only when the maximum ordinate of the trajectory reaches 160 km or more is this factor significant. At this altitude at the equator, the acceleration due to gravity decreases approximately 5%; this decrease would increase the range beyond the predicted values obtained under standard conditions.

2. The curvature of the earth affects computation of the trajectory in two ways. In the first place, the direction of the downward force of gravity is established at the origin of the trajectory. At long range the direction of the force of gravity at the point of impact is not parallel to the gravity force at the origin. In the second place, under short-range, standard conditions the coordinates of the particular target are determined on the basis of a horizontal plane. At long ranges the curvature of the earth must be accounted for in computing the point of fall. Because the curvature of the earth changes at a rate of approximately one degree for each 111 km, the range of a projectile over a long trajectory increases over the range computed by simplified solutions. The influence of the curvature of the earth and variations in the gravitational field always act on a given projectile path irrespective of the direction of fire.

2-2.4.5.8   Nonrigidity of the Trajectory

In the standard structure assumed and accepted as the basis of weapons fire, the standard trajectory of a projectile is referred to as the horizontal plane that passes through the weapon and the fixed target. In actual weapons fire, however, the target may be located at heights above or below the horizontal plane and at different values of range; these differences result in various angles of sight. For small angles of sight it is satisfactory to rotate the trajectory about the origin through these small vertical angles in the plane of fire. In theory, this rotation may be accomplished without materially influencing the curvature of the trajectory (as shown in Fig. 2-18). This assumption, known as the theory of rigidity of the trajectory, is generally applicable to tanks and small arms fire and introduces significant range error only when the ratio of target height to target range is large so that the angle of sight is large. In particular, the assumption is not applicable to antiaircraft fire and long-range artillery fire.

2-2.5   EFFECT OF TARGET MOTION

The motion of the target during the TOF of the projectile between the time of launching and the mo-
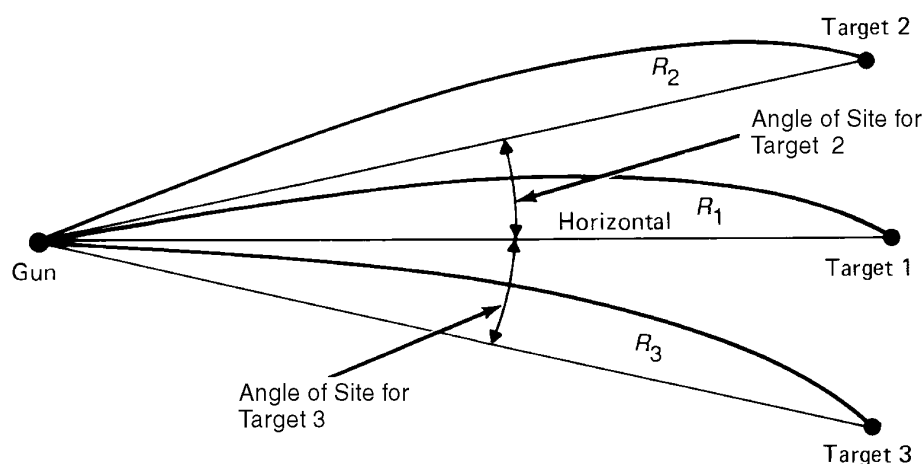
Note: The angles of site are greatly exaggerated here for illustrative purposes.
When they are small, the slant ranges R_1, R_2, and R_3, can be considered to be equal for the quadrant angles that are normally used.

Figure 2-18. Rigidity of the Trajectory for Small Angles of Site

ment of impact has kinematic characteristics that derive from the integrated effects of target velocity and acceleration during the interval of flight. These effects vary with target velocity, the angles of the space geometry, and target range. When the range to the target is long, the angular velocity of the LOS (the apparent motion of the target to the tracking system) is relatively low; hence target motion has relatively little influence on the angular velocity of the LOS in space. Conversely, when the range to the target is short, a small amount of target motion results in a relatively large angular velocity of the LOS. Because target motion that occurs during the TOF would cause the projectile to miss the target if it were directed along the LOS to the target, it is necessary to provide compensation for target motion. This compensation is directional in nature and is applied to the weapon aiming line before launching or firing so that an angle exists between that line and the LOS. It is generally applied in the form of component corrections in elevation and azimuth. The total angular correction provides a weapon orientation that nullifies the miss-producing effect of target motion and allows projectiles to score hits on the target.

2-2.6 THE PREDICTION ANGLE

After a projectile has been launched, it is acted upon by various forces peculiar to the weapon, to the environment through which it passes, and to the motion along the path of flight. The associated corrections that must be applied as compensation are directional in nature, i.e., each correction takes the form of an angle. Similarly, compensation for the effects of target motion during the TOF of the projectile also takes the form of an angular correction. The total correction angle, made up of the sum of these individual correction angles, forms the required angle between the weapon line and the LOS for hitting a target. This angle is referred to as the prediction angle since it is the overall angle that must be predicted in advance of firing in order to aim the weapon to obtain hits on the target. It is this angle that must be generated by fire control equipment by one means or another to effect the required offset angle of the weapon line from the LOS. The prediction angle for the case of stationary target is depicted in Fig. 1-1, whereas Fig. 2-19 represents the prediction angle for the case of a moving target.
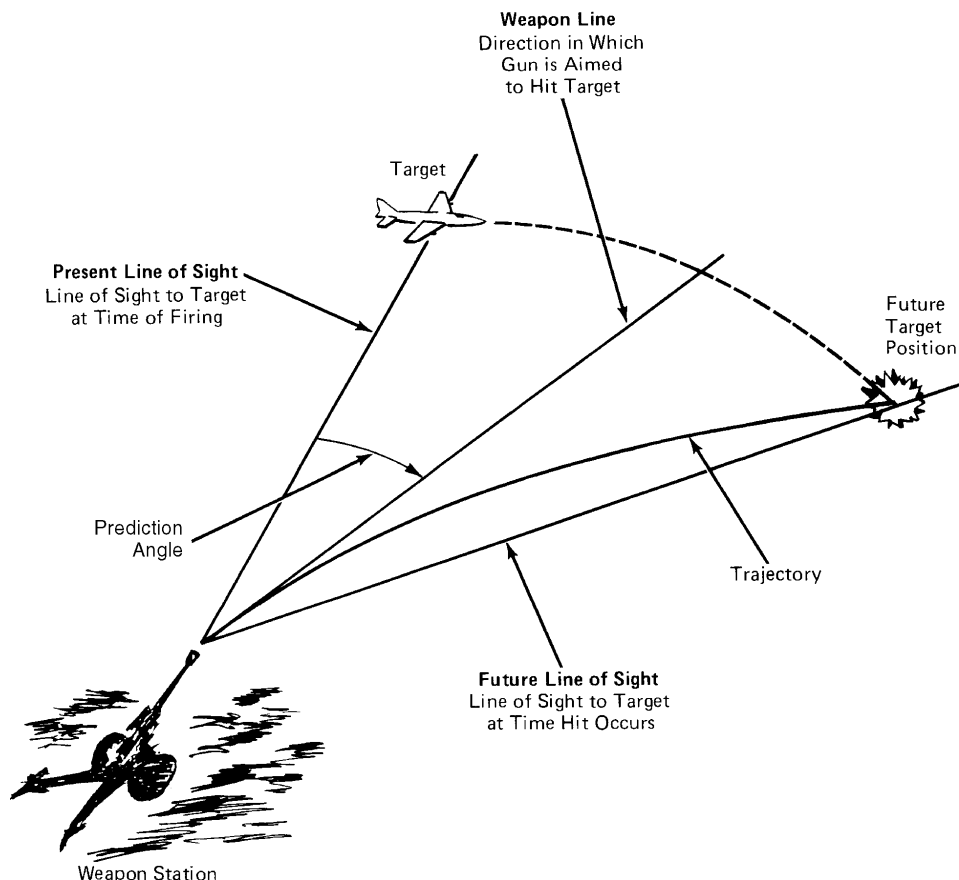
Figure 2-19. Prediction Angle for the Case of a Moving Target (Ref. 1)

The prediction angle is composed of three major components: kinematic lead, ballistic lead, and compensating corrections. Each is discussed in turn in the paragraphs that follow. The geometry associated with these prediction angle components is portrayed in Fig. 2-6 and based on the fire control situation shown in Fig. 2-19.

Kinematic lead is the angular correction required to compensate for target motion during the TOF of the projectile and is a function of that TOF. It is the angle between the LOS to the target at the time of firing and the predicted future LOS to the target at the time a hit occurs. In the case of a stationary weapon and a stationary target, there is no need for the kinematic lead component of the prediction angle. An example of this situation is given by Fig. 2-20, which represents those aspects of field artillery fire control problems that lie in the elevation plane. Here the elevation component of the total prediction angle is the angle of elevation. It is comprised of the quadrant angle of departure, the angle of site, and a correction for any vertical jump. No kinematic lead correction is required.

Ballistic lead, or curvature correction, is an angular correction required to compensate for the effect of the various in-flight forces, such as air resistance and gravity, that act on a projectile during the TOF and result in a curved trajectory. As in the case of the kinematic lead correction, it is also a function of the TOF of the projectile. Geometrically, it is the angle between the predicted future LOS to the target and the projectile line.
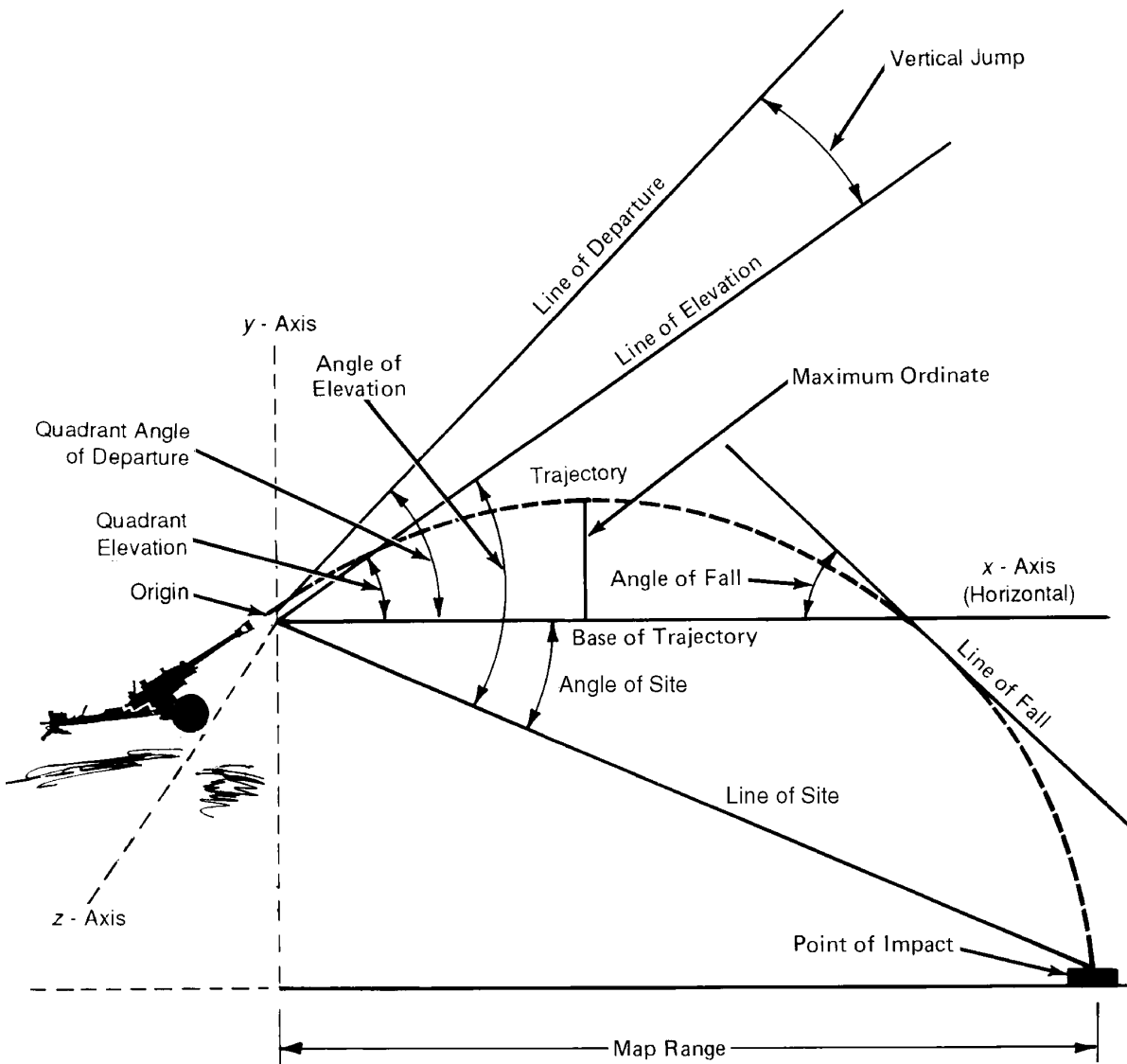
Figure 2-20. Aspects of the Field Artillery Fire Control Problem Associated With the Elevation Plane (Ref. 8)

The compensating corrections account for jump and variations from standard conditions. Jump correction compensates for initial trajectory effects. It may be defined as the correction required to compensate for the nonparallelism of the weapon line and the initial projectile velocity vector in the particular coordinate reference system chosen. Unlike lead corrections, jump correction is not a function of TOF of the projectile. It can be visualized geometrically as the angle between the projectile line and the weapon line, the former being the direction of the initial velocity of the projectile. Corrections for variations from initial conditions are made on the basis of available information concerning propellant temperature, projectile weight, air density, and wind velocity.

2-2.7 DIFFERENCES BETWEEN FIRE CONTROL FOR GUNS AND ROCKETS

It was noted at the start of the discussion of the fire control problem that the term "projectile" is used in its general sense to include bullets, projectiles, and rockets. From the standpoint of the geometrical approach, however, it becomes necessary to delineate the differences that may exist between firing bullets and projectiles on one hand and firing rockets on the other.

Gunfire and rocket fire are similar; the essential difference between them lies in the method of propulsion. In gunfire the propellant and its gases are confined in the gun tube, and the projectile is ejected by the pressure produced by these gases. In rocket fire the propellant and its gases travel with the rocket while the propellant burns. A pseudo or fictitious initial velocity thus must be used to account for the continued propulsion of the rocket after launching.

In general, bullets and projectiles are fired with a relatively high initial (muzzle) velocity; by contrast, the military rocket has a low initial velocity when fired from a static launcher. For a given target range, this low initial velocity increases the TOF and lessens the chances of hitting a moving target. If the rocket is fin-stabilized (in contrast to spin-stabilized bullets or projectiles), the low initial velocity results also in reduced stability during flight and, therefore, in greater dispersion.

Rocket fire tends to be less accurate than gunfire. A gun-fired projectile usually is guided very accurately along the bore during the burning time of the propellant; the turbulent actions of the expanding gases behind the projectile have little effect on the path of flight. In contrast, similar turbulences developed in the rocket exhaust gases are unrestrained and free to produce variations in the direction of flight. For this reason rockets fired from a static launcher are less accurate than gun-fired projectiles. When rockets are fired forward from high-speed aircraft, rocket fire accuracy is greatly increased because of the high initial velocity and the aerodynamic effectiveness of the large protruding fins. This method of aircraft rocket fire approximates long-range artillery equivalence for low-velocity, short-range rockets when used in air-to-surface weapon fire.

Corrections for jump effects apply both to gunfire and rocket fire. In the case of gunfire, however, jump phenomena result from the elasticity of the weapon system, whereas in the case of rocket fire the phenomena known as weathercocking result from the influence of the folded rocket fins on the rocket path as the rocket is fired from the aircraft launching tube into the airstream.

The rocket-assisted projectile (or equivalently a gun-boosted rocket) is a development in which a rocket motor is added to the projectile, and the combination is fired from a gun. The result is either an increase in range, an increase in the payload that can be carried to the same range as that obtained by the projectile alone with its normal payload, or an increase in the projectile velocity at target impact. In each case there is no decrease in the mobility of the gun. The advantages and disadvantages of using the rocket-assisted projectile, particularly from the standpoint of accuracy, are discussed in Ref. 5.

2-3 SOLUTION OF THE FIRE CONTROL PROBLEM

2-3.1 GENERAL

The solution of the fire control problem comprises three distinct phases:
1. Sighting, ranging, and tracking
2. Computation of firing data
3. Application of fire control solution.

Each of these phases is treated in turn in the remainder of this chapter.

2-3.2 SIGHTING, RANGING, AND TRACKING

2-3.2.1 General

The first requirement in solving any fire control problem is to locate the target continually with respect to the weapon. This requirement is satisfied by use of the sighting, ranging, and tracking procedures described in subpars. 2-3.2.2 through 2-3.2.4.

Target location is usually established in spherical polar coordinates in an earth reference frame. Fig. 2-21 shows how the target is located with respect to the weapon by this method in a typical antiaircraft fire control problem. The LOS between weapon and target is established when the target azimuth angle A_o and elevation angle E_o are determined. The next required element of data is the target slant range R_o. When there is relative motion between the weapon and the target, the target must be "tracked" to determine the rates of change of these three basic elements of data, i.e., azimuth, elevation, and range, so that proper leads may be computed.

Fig. 2-21 also indicates two alternate coordinate systems (also in an earth reference frame) that are used to establish the location of a target with respect to a weapon:

　　1. In the rectangular coordinate system the mutual orthogonal distance coordinates x_o, y_o, and h_o fix the target. (Note that the positive directions for the x- and y-axes are east and north, respectively.) The rectangular coordinate system is used in many automatic computers. The raw data are obtained in polar coordinates, and the computer converts the data to rectangular coordinates and then solves for firing data.

　　2. A second alternate system uses the quantities A_o, r_o, and h_o. This system is used when the target position data are measured from maps.

Additional methods used to locate the target for particular fire control applications would be in terms of the other coordinate reference frames discussed in subpar. 2-2.3.

2-3.2.2 Sighting

There are two general ways of sighting on a target:

　　1. The direct laying method associated with direct fire control (described in subpar. 1-1.3.1)

　　2. The indirect laying method associated with indirect fire control (described in subpar. 1-1.3.2).

The direct laying method is used when the target can be sensed directly from the weapon via optics, electro-optics, etc. The simplest means is to mount a sight on the weapon, adjust the alignment so that the sight line is parallel to the axis of the bore (the weapon line), and then move the weapon in elevation and azimuth until the sight is aligned with the target. For rifle fire the range might be estimated and set on the sights before actually sighting on the target. For larger caliber guns, for which various forms of optical sights might be used, the sighting would be maintained during the period the sight is being adjusted for the actual conditions of the fire control situation, i.e., the target range and the angle of site.

The indirect laying method is used when either the target cannot be sensed directly from the weapon or remote control is used. This method requires that the azimuth and elevation of the LOS be determined by some independent means such as map data or a remote observation post. If the weapon is equipped with calibrated and oriented angle-measuring devices similar to those on a surveyor's transit, it can be laid on the azimuth and angular elevation of the target, and the weapon line extended would intersect the target.

Thus direct sighting is the simplest method since it is necessary only that the sight be capable of being aligned with the weapon line. In the indirect sighting method the sights must not only be capable of being aligned with the weapon line, but they must also be capable of being leveled and oriented on the same reference—grid north, magnetic north, an aiming stake, a collimator, the longitudinal axis of an aircraft, etc.—on which the target angle data are based. The indirect sighting system is obviously more complex and subject to more error and time lag in functioning. It is more flexible, however, and capable of engaging unseen as well as visible targets.
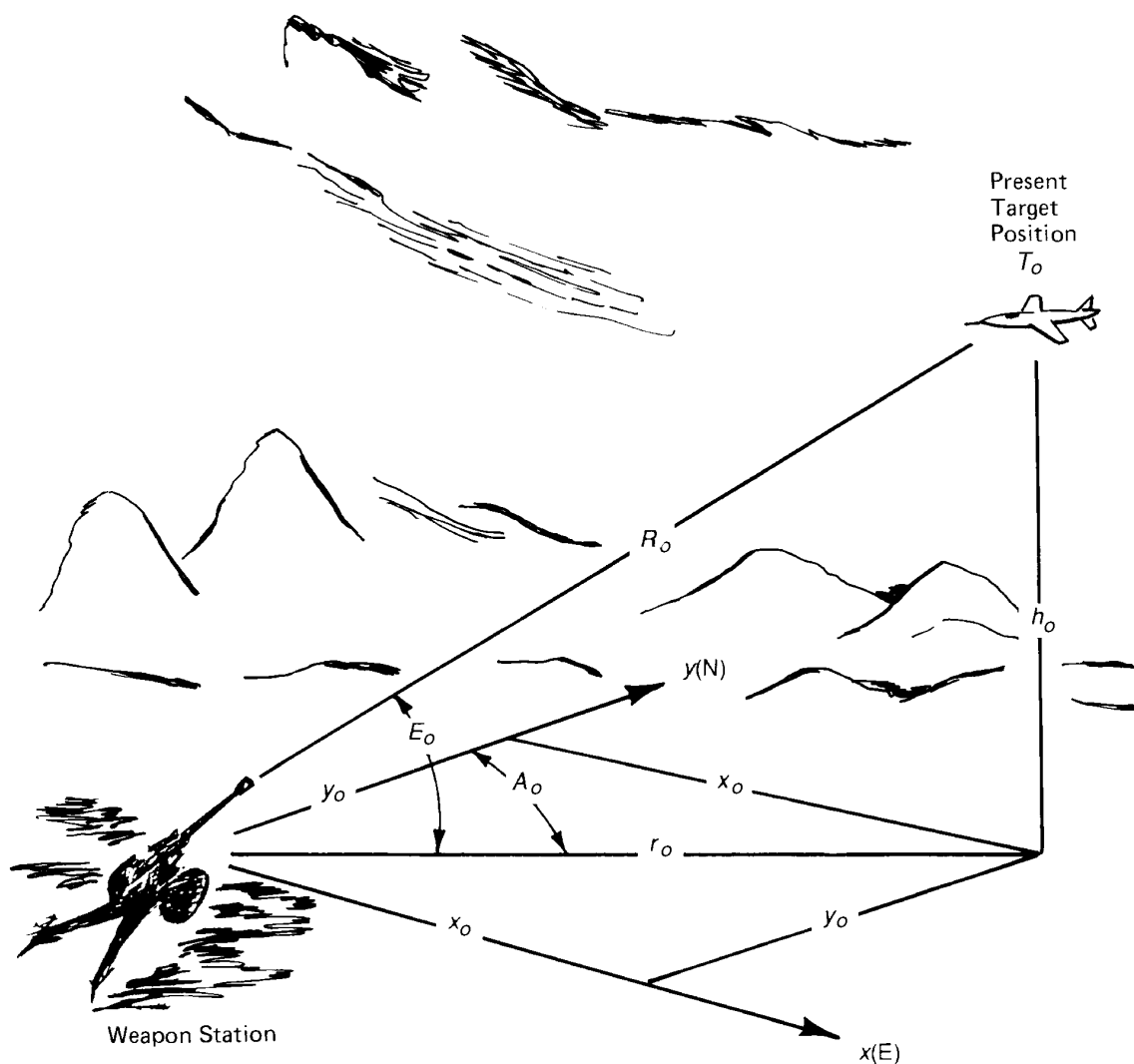
$x(E) = x$-axis of xyz-reference coordinate frame
(directed toward geographic east)

$y(N) = y$-axis of xyz-reference coordinate frame
(directed toward geographic north)

Note: The z-axis which completes this reference coordinate
frame, although not shown in the illustration, is directed upward
from the origin at the weapon station in a vertical orientation.

x_o = target distance coordinate along x-axis $\left.\begin{array}{l} \\ \\ \\ \end{array}\right\}$ for target
y_o = target distance coordinate along y-axis   present
h_o = target height above the horizontal xy-plane   position T_o

A_o = target azimuth angle; measured clockwise from true north,
i.e., from $y(N)$-axis

E_o = target elevation angle with respect to horizontal

R_o = target slant range

r_o = projection of slant range R_o, to present target position T_o,
onto the horizontal xy-plane

Figure 2-21. Reference Coordinate Frames for Locating the Target With Respect to the Weapon Station

2-3.2.3 Ranging

Although target ranges are sometimes estimated visually, as in the case of small arms fire, use of the laser range finder (LRF) and microwave radar are the means commonly used to obtain target range in most modern fire control systems. Techniques dependent upon geometrical considerations, e.g. the optical baseline range finder, have been virtually phased out of operation in all weapon system applications because of complexity, cost implications, and lack of accuracy. Although now widely used, both radar and the laser have their limitations. To obtain range, a pulse of transmitted energy must be reflected from the target, and the duration of the round-trip time must be accurately measured. The narrow beam of the laser assures to a large extent that the return of the received energy is from the target but only if the laser is properly pointed. On the other hand, a radar beam is sufficiently large that returns cannot be attributable to the target alone unless it is spatially isolated. If the target is on or close to the surface of the earth, radar often requires sensing of target motion, if it exists, in order to discriminate the target from ground "clutter". Radar, however, is usually operational under all weather conditions due to the relatively low absorption and scattering of the transmitted energy in the frequencies of the electromagnetic spectrum employed.

All LRFs presently used are pointed by optical or electro-optical sights. Because of the optical or near-infrared (IR) frequencies at which the 1990s lasers operate, they are degraded by adverse weather conditions. The initial developments with a ruby rod were limited to 1 to 3 pulses/s, but more recent developments in neodymium (Nd) provide a 10- to 20-pulse/s rate for target designation. This rate is also commensurate with the data rate range finder requirements of most engagement kinematics.

Development of the carbon dioxide (CO_2) laser offers higher pulse rates at a frequency that is compatible with thermal imaging devices and extends range finder and designation operation into the region of adverse weather operation.

Although both the laser and radar transmit electromagnetic energy, the laser is more acceptable in the battle area because of its narrow beam width and its reduced chance of detection.

2-3.2.4 Tracking

Tracking generally refers to the functions in which the LOS of a targeting sensor is continuously maintained on target by means of manual or automatic control and thereby provides measures of target position and motion. The sighting and ranging functions discussed earlier generally refer to discrete operations during which the weapon system and target are at rest. Tracking implies that the weapon system and/or target are in motion. Range, angle, or three-dimensional tracking is usually used in modern fire control applications. The ranging aspects of tracking were discussed in the previous paragraph with respect to radar and laser operation. A full discussion of radar angular tracking that uses monopulse, conical scan, and phased array techniques is included in most radar texts, such as Ref. 9.

Because of the radar limitations discussed earlier, extensive use of radar has been restricted primarily to the surface-to-air role. In most other fire control applications, pointing of a sight line is accomplished by an operator using manual track controls optimized for the specific kinematics of the typical engagement encountered and the constraints imposed by the operational environment. The requirement for precise angle track from combat vehicles and helicopters has led to the development of inertially stabilized sights and platforms that decouple the sight line from vehicle disturbances and permit smooth and accurate track by an operator viewing with magnification through an optical sight or using a remote display.

Since tracking performance is usually limited by the human element in the control loop, several approaches to providing operator assistance have been introduced over the years. Operator input, formerly introduced by separate handgrip motions in elevation and azimuth, can now be accomplished by displacement of or pressure applied to a single joystick, a ball or a thumb control. A "rate-aided" feature assures that the control displacement or pressure results in a change in sight line position as well as a change in sight line rate. "Motion compensation" refers to an implementation in which a measure of the weapon system velocity is used in conjunction with an estimate of target range to generate an angular rate that is introduced into the tracking network and thereby relieves the operator of the need to provide this input. "Regenerative track" involves generation of target motion data from the solution of differential equations

chosen to represent target behavior; prior track information provides initial conditions for solution. The data are used in an attempt to replace most of the operator's required manual tracking input and leave him only the need to provide a "trim" input to compensate for deviations from the predicted track. "Aided" track signals derived from a Kalman filter implementation offer a similar solution. That is, the predicted target states, obtained from the system equations, are corrected to track commands and are introduced into the manual track network.

In recent years the use of video and IR imaging systems as fire control targeting elements has provided video signals that contain the scene information regarding target and background after the manual system has been used to acquire the target initially. Processing algorithms that attempt to differentiate between target and background characteristics have been developed to generate tracking signals that drive the sensor gimbals automatically. The most successful have been those based upon target edge or contrast, target centroid determination, and frame-to-frame correlation. Often different processing techniques are used simultaneously to overcome the shortcomings of each. When conditions are favorable, passive video autotrackers can provide an order of magnitude improvement over manual tracking.

To date, laser angle trackers have not been adapted for fire control use, although they are extensively used by the test and evaluation community for target measurement in field instrumentation.

2-3.3 COMPUTATION OF FIRE CONTROL SOLUTION

With the target position data known or with tracking data available in the case of amoving target, the next step is to solve the complete fire control problem by using the known ballistic performance data of the weapon and correcting the standard ballistic data to allow nonstandard meterological, ammunition, or weapon conditions. The objectives are firing azimuth and firing elevation (or their equivalents in whatever coordinate system is used as described in subpar. 2-3.2.1), and when applicable, TOF. Four general cases exist:

1. Weapon and target both stationary
2. Weapon stationary and target moving
3. Weapon moving and target stationary
4. Weapon and target both moving.

Each case is described in the subparagraphs that follow.

2-3.3.1 Weapon and Target Both Stationary

In the direct fire situation only the relative positional data are required. The fire control problem has been reduced to one of ballistics. The factors considered in computing the trajectory depend upon the system accuracy required. Usually the flat portion of trajectory is used, and the TOF is relatively small. A ballistic curve fit can usually satisfy the accuracy needed for a computer solution.

2-3.3.2 Weapon Stationary and Target Moving

Here it is necessary to "lead" the target. The future position of the target is determined based upon the rates of change of present-position data. In short-range, direct fire weapons kinematic lead is frequently estimated as a function of range and hence TOF and target speed.

For more accurate weapon fire there are three general types of prediction processes that can be used by computers to determine kinematic lead:

1. The angular rate of travel method
2. The linear speed method
3. The nonlinear method.

The angular rate of travel method gives the fastest solution. Fig. 2-22 shows that if the weapon is fired when the target is at point T_o, by the time the projectile arrives at T_o, the target will be located at the predicted future target position T_p. Consider azimuth only; if the TOF t_p to the predicted future target position T_p is known, the approximate kinetic lead correction C_A is

$$C_A \approx t_p \dot{A}_o, \text{ rad} \qquad (2\text{-}1)$$
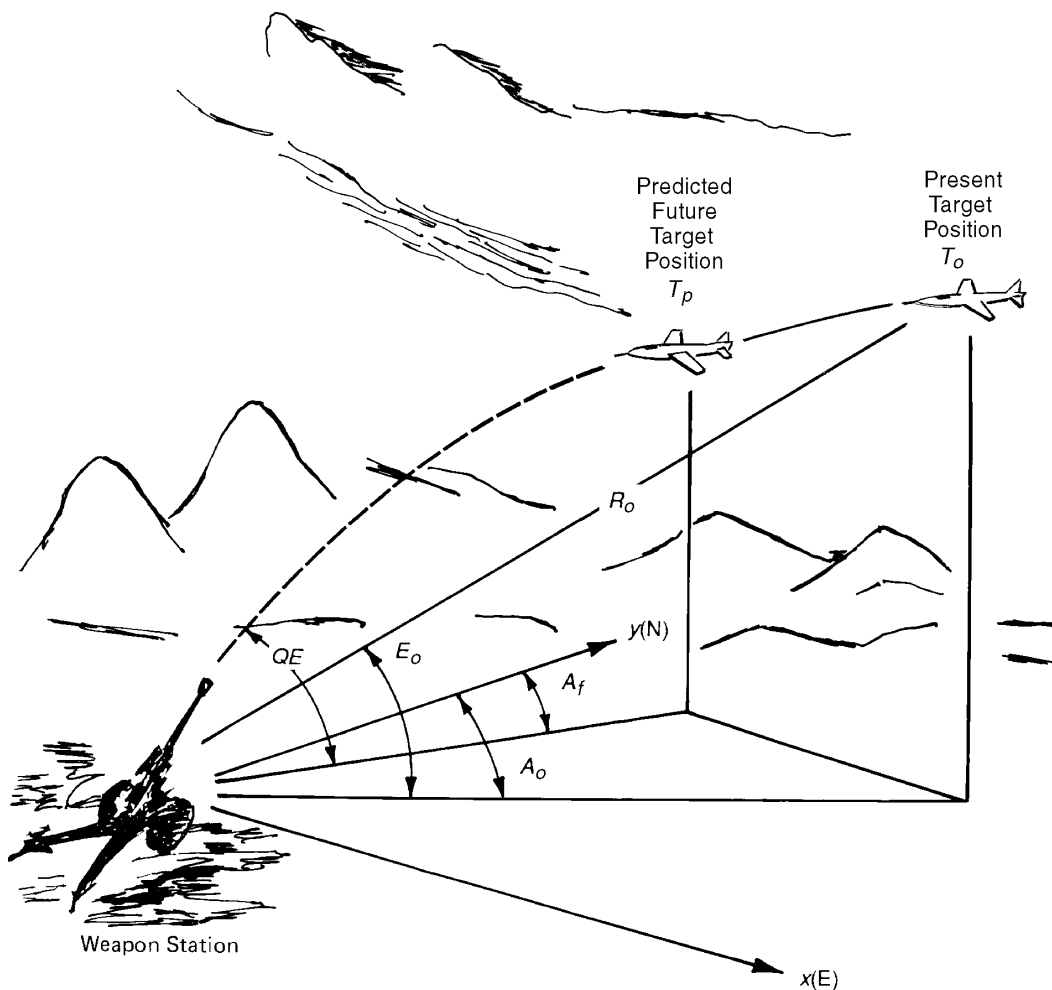
Note: The z-axis that completes this reference coordinate frame, although not shown in the illustration, is directed upward from the origin at the weapon station in a vertical orientation.

A_f = firing azimuth; measured clockwise from true north
QE = quadrant elevation

Figure 2-22. Stationary Weapon Firing at a Moving Target by Using the Angular Rate of Travel Method of Prediction

where

C_A = approximate kinetic azimuth lead correction, rad
t_p = projectile time of flight to predicted future target position, s
$\dot{A}_O$ = time rate of change of A_O, or azimuth angular rate of target, rad/s.

The computer obtains t_p as a function of present-position data (i.e., A_O, R_O, and E_O) and measures the rate of change of A_O by measuring the angular rate of tracking in azimuth. To store ballistic data the computer adds the necessary drift and windage corrections, and arrives at the firing azimuth A_f. A similar process uses elevation tracking rate data and adds a correction of gravity to obtain the quadrant elevation QE. Inasmuch as $\dot{A}_O$ and $\dot{E}_O$, the elevation angular rate of the target, are seldom constant and t_p is not equal to the projectile time of flight to present target position t_O, the TOF to the present target position is only an approximation. It is suitable, however, for short-range fire with automatic weapons against high-speed targets because its mechanization is rapid and relatively simple. The volume and dispersion pattern of automatic weapon fire compensate for the errors that result from approximation of angular rates.

The linear speed method is more exact in its solution. In the linear speed method the computer converts A_o, E_o, and R_o, which are supplied as input data from the tracking system, to x_o, y_o, and h_o as shown in Fig. 2-23. The computer then takes the derivatives of these values with respect to time, i.e., $\dot{x}_o$, $\dot{y}_o$, and $\dot{h}_o$, and multiplies them by the TOF of the projectile to obtain future position data x_p, y_p, and h_p. The TOF t_p used, which the computer obtains by a successive approximation method, is the actual TOF to the future target position T_p. Next the computer corrects stored ballistic data for gravity, drift, wind, and other meteorological and ballistic factors; then it delivers A_f, QE and, if necessary, fuze setting. The accuracy of the linear speed method is dependent upon the target maintaining a constant course and speed; this method finds application with antiaircraft guns.

Figure 2-23. Stationary Weapon Firing at a Moving Target by Using the Linear-Speed Method of Prediction

The nonlinear method of prediction requires higher order time derivatives of target motion in addition to velocity. However, measurements of acceleration, jerk, etc., that provide estimates sufficiently accurate to warrant inclusion in the prediction process are not as straightforward as those of velocity. Nevertheless, nonlinear prediction is presently being investigated for use in helicopter air-to-air and tank ground-to-ground applications. Again, the difficulty is obtaining sufficiently accurate position and rate track data which, when filtered, will provide acceleration estimates that do not degrade the solution when included. Usually, means are provided by the computer to detect unrealistic acceleration estimates and to replace the predictions with the linear solution to eliminate the acceleration terms. Although the use of the Kalman filter has introduced the possibility of using a target motion estimate advanced by the projectile time of flight for prediction, the computations involved have discouraged designers. The penalty paid for accurate acceleration estimates is sometimes an increase in the time required for the filter to settle, which results in an extension of the overall system reaction time. As in the linear prediction method, the ballistic corrections are applied to the predicted position.

In more recent years the computing flexibility of digital equipment and improved communications have encouraged investigation of target prediction for the field artillery indirect fire application. Although the projectile TOF is generally very long, target speeds are relatively slow and often predictable since targets usually follow roads or other surface characteristics of the earth. Once again the curvature, jump, and nonstandard conditions for trajectory computation are applied to the target predicted position.

2-3.3.3 Weapon Moving and Target Stationary

When the target is known to be stationary, the velocity of the weapon referenced to earth, if measured, can be added to the gun muzzle velocity. The result is a projectile velocity with respect to earth that is used to solve the ballistic equations. There is no kinematic lead involved, only the ballistic lead. If, however, the problem is to be solved in the weapon system reference frame, the target must be assumed to be moving relative to the weapon system. Onboard fire control can be used to measure the relative motion and compute pseudokinematic leads in the conventional manner, and thus derive the ballistics with the gun muzzle velocity. The trajectory must be compensated for the air mass flow over the weapon (vehicle air velocity). This case is typical for helicopter fire control. However, since the fire control must also treat the moving target situation, the fire control is designed for Case 4, and Case 3 becomes a subset.

2-3.3.4 Weapon and Target Both Moving

Obviously, this is the most complex of the four general cases. The possibility of the conditions existing in the other cases must be considered a subset in the solution. As discussed previously, there are several alternatives for the reference and computational frames that can be used for the fire control solution. Tank fire control tends to express the solution in a weapon-system-centered reference by using the earth inertial coordinate system to perform computation. Relative values of range rate and angle rates are filtered and used directly for kinematic lead angle solutions, by using the product of angle rate and TOF approximation in the azimuth plane only. Because a single round is fired at a time, tolerances are tight and all known contributing ballistic error sources are considered in the solution. This case is also considered in helicopter fire control. The solution is generally expressed in an earth reference coordinate frame, and the computation is conducted in a stabilized sight coordinate system. Both weapon and target motion are referenced to the earth where models predicting ballistic behavior can be better expressed. Weapon velocity is added to the weapon muzzle velocity to generate the ballistic solution. Kinematic leads are computed based on target ground speed and accelerations, not relative velocity.

To date, field artillery requirements have not included a need to fire on the move. Air defense gun requirements have included such a need but permit "degraded" accuracy. Here the problem has been formulated in a weapon system frame, and the computations performed in sight line and earth-referenced inertial coordinate systems. Sight line angle data or sight line angle and angle rate data along with range have been filtered to provide estimates of target relative range, velocity, and acceleration for nonlinear prediction. The weapon muzzle velocity drives the vehicle-referenced ballistic solution. As discussed in earlier cases in which engagement motion exists, a tradeoff between accuracy and reaction time

must always be made, which requires a full understanding of the factors involved to achieve proper resolution.

2-3.4 SENSOR NOISE COMPENSATION

If it were not for the fact that all input data to the fire control system is contaminated with noise, the solution to the fire control problem would be relatively simple and straightforward, i.e., expressible in terms of the geometry of deterministic parameters. However, the fact is that this is not the case, and since the inception of modern fire control, many designers have sought methods whereby the truth could be extracted from this input data to optimize the fire control solution. Discussion of the solution of the input data noise problem is not intended at this stage; it is intended only to alert the reader to its existence since its implications are far-reaching in regard to all aspects of the problem. Obviously, the level of noise in all input sensors should be kept to a minimum consistent with cost and effectiveness implications. Before the data are used to obtain a solution, appropriate filters must be conceived and developed to condition the data insofar as is possible to obtain the best estimates of the pertinent state variables. Prediction algorithms conditioned by using these estimates require development. The choice of computational coordinate frames is often determined by the noise implications. In short, the treatment of noise in the system is a formidable and challenging aspect of the fire control system design. This subject is discussed in some depth in par. 4-3.

2-3.5 APPLICATION OF FIRE CONTROL SOLUTION

Once the target has been located and the firing parameters computed, it is necessary to aim the weapon accordingly. For some weapons this function is performed by the weapon sighting system. Sights are essentially angle-measuring devices, calibrated for the ballistics of the weapon and ammunition with which they are used. Sights are classified generally as either optical (glass sights), electro-optical (infrared), or mechanical (iron sights). Fig. 2-24 shows a simple elevation sighting arrangement and its application to laying a weapon in elevation. The parallax can be ignored in most weapons since it is merely a matter of a few inches, but it can be reduced by having the sight axis depressed to converge with the gun
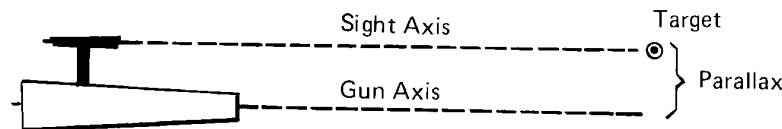
(A) Sight Setting for Zero Range
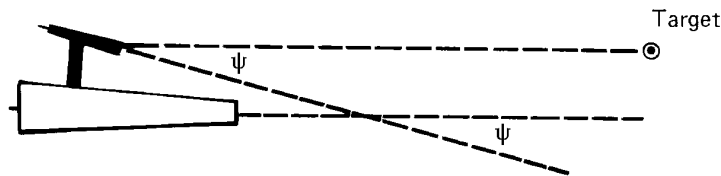
(B) Sight Setting for a Range of "x" Meters
(required superelevation of ψ mils)
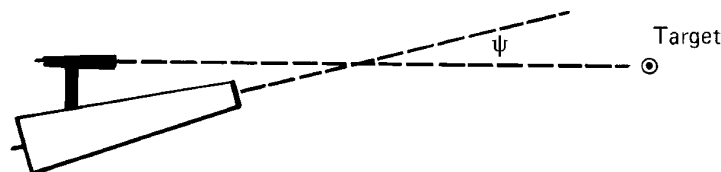
(C) Gun Laid in Elevation for a Range of "x" Meters

Figure 2-24. Use of a Simple Sighting Arrangement for Laying a Weapon in Elevation

axis at some convenient range. In the case of tanks, for example, this convergence is done frequently in the field, and the converging range is referred to as "boresight range". (For a complete discussion of the parallax problem and its solution, see Ref. 10.)

Assume that it is desired to hit a target at a range of "x" meters and that the firing table shows that a superelevation angle of ψ mils is required to compensate for the effect of gravity on the projectile during its TOF. If the sight axis is depressed ψ mils below the gun axis, then elevating the gun until the sight is back on the target will place the gun axis on the proper superelevation angle with respect to the horizontal plane. By properly calibrating the elevation sighting controls in terms of meters of range rather than mils, it is possible to eliminate the firing table steps, as is done in the cases of some modern rifles, tank guns, etc. This is the procedure usually used with direct fire weapons. On the other hand, sights for indirect fire weapons, such as mortars and howitzers, are usually calibrated in angular units, and reference is made to some arbitrary aiming point instead of to the line of sight to the target. However, when artillery pieces are laid in the indirect fire mode, use is made of the gravity vector and special sights and quadrants for referencing gun orders to surveyed positions. See subpars. 1-2.4 and 1-2.5 for an overall summary of sighting equipment that has been developed during the twentieth century.

Many weapons, particularly helicopter and antiaircraft guns, are positioned by remote control. Their sighting and computing equipment is located remotely from the weapon, and the firing data are transmitted, usually electrically, to the guns. Synchro electrical systems are most commonly used for this purpose. At the gun servomechanisms use these electrically transmitted firing commands to position the gun. Remote control systems offer the advantage of smoother, more accurate tracking rates against high-speed targets. They also permit mounting weapons where optimum fields of fire may be obtained but could not be used because of either space or vulnerability considerations if the gunner had to be located there.

Most antiaircraft guns, like modern tank main weapons, are mounted in the vehicle turret with the operator or gunner and the fire control equipment. Rotation of the turret provides azimuth freedom while the gun is driven around the trunnion axis to impart elevation motion. The sight mounted in the turret also rotates with the gun in azimuth. To introduce the azimuth lead, the sight must be gimballed so that the sight line can be offset from the gun line. Therefore, to maintain the sight line on target while introducing the required lead between sight and gun lines, the turret with gun must be rotated forward by the lead angle while the sight line is set back from the gun line via the gimbal by the lead angle. If these two motions are not synchronously introduced in time and space (as is the usual case), the gunner observes motion between sight reticle and target, i.e., the reticle is "disturbed". If the sight line is inertially stabilized so that it is isolated from turreted motion, this phenomenon does not occur. The sight is then designated as a "director"-type sight because it has the same sight characteristics as the off-carriage fire control of the remote weapons previously discussed. Modifications of the vulcan air defense system (VADS) sight to a "director" type was essential in that product improvement program. When tanks engaged moving targets, the disturbed reticle characteristics of some tank sights became evident. This problem led to efforts to provide computer-generated signals for synchronization of lead inputs to weapon and sight.

REFERENCES

1. W. Wrigley and J. Hovorka, *Fire Control Principles*, McGraw-Hill Book Company, Inc., New York, NY, 1959.

2. J. M. Norwood, *Exterior Ballistics for Airborne Applications*, Technical Report No. AFAL-TR-73-196, Texas University, Austin, TX, June 1973.

3. R. Lieske and R. McCoy, *Equations of Motion of a Rigid Projectile*, BRL Report No. 1244, US Army Ballistics Research Laboratories, Aberdeen Proving Ground, MD, March 1964.

4. T. J. Hayes, *Elements of Ordnance*, John Wiley & Sons, Inc., New York, NY, 1938.

5. AMCP 706-107, Engineering Design Handbook, *Elements of Armament Engineering, Part Two, Ballistics*, September 1963.

6. AMCP 706-242, **Engineering Design Handbook**, *Design for Control of Projectile Flight Characteristics*, **September 1966.**

7. AMCP 706-140, **Engineering Design Handbook**, *Trajectories, Differential Effects, and Data for Projectiles*, **August 1963.**

8. **Special Text ST 9-153**, *Fundamentals of Ballistics*, **US Army Ordnance Center and School, Aberdeen Proving Ground, MD, 1964.**

9. **M. Skolnik**, *Introduction to Radar Systems*, **McGraw-Hill Book Company, Inc., New York, NY, 1962.**

10. **AMCP 706-331, Engineering Design Handbook**, *Compensating Elements*, **September 1963.**

BIBLIOGRAPHY

AMCP 706-283, Engineering Design Handbook, *Aerodynamics*, **April 1965.**

B. Barnet, *Trajectory Equations for a Six-Degree-of-Freedom Missile Using a Fixed Plane Coordinate System*, **Technical Report No. 3391, Picatinny Arsenal, Dover, NJ, June 1966.**

G. A. Bliss, *Mathematics for Exterior Ballistics*, **John Wiley & Sons, Inc., New York, NY, 1944.**

Firing Tables FT8-J-2, Cannon, 8-inch, Howitzer M3, M2A1, and M47; Firing Shell, HE, M106, **Headquarters, Department of the Army, Washington, DC, 1958.**

Davis, Follin, and Blitzer, *The Exterior Ballistics of Rockets*, **D. Van Nostrand Co., New York, NY, 1958.**

W. Dziwak, *Solution to the Ballistic Point Mass Equation Including Rigid Body Effects*, **Technical Report No. ARSLD-TR-85015, Picatinny Arsenal, Dover, NJ, October 1985.**

Firing Tables FT 155-AS-1, 155-mm Cannons, Howitzers, and Copperhead Projectile, **Headquarters, Department of the Army, Washington, DC, December 1990.**

H. P. Hitchcock, *Computation of Firing Tables for the US Army*, **Report No. X-102, US Army Ballistics Research Laboratory, Aberdeen Proving Ground, MD, 1934.**

Kelley, McShane, and Reno, *Exterior Ballistics*, **The University of Denver Press, Denver, CO, 1953.**

R. Lieske and M. Reiter, *Equations of Motion for a Modified Point Mass Trajectory*, **BRL Report No. 1314, US Army Ballistics Research Laboratories, Aberdeen Proving Ground, MD, March 1966.**

A. S. Locke, *Guidance*, **D. Van Nostrand Company, Inc., Princeton, NJ, 1955 (part of the series titled "Principles of Guided Missile Design" and edited by G. Merrill).**

R. McCoy, *Aerodynamic Characteristics of the 30 mm-XM78 Projectile*, **BRL Report No. ARBRL-MR-03019, US Army Ballistics Research Laboratory, Aberdeen Proving Ground, MD, May 1980.**

F. R. Moulton, *New Methods in Exterior Ballistics*, **University of Chicago Press, Chicago, IL, 1926.**

C. Murphy, *Measurement of Nonlinear Forces and Moments by Means of Free Flight Tests*, **BRL Report No. 974, US Army Ballistics Research Laboratory, Aberdeen Proving Ground, MD, February 1956.**

Rocket Fundamentals, **Chapters 4 and 5, Office of Scientific Research and Development, George Washington University, Washington, DC, 1944.**

Weapon Systems Engineering, Vol I, Tools of Analysis and Elements of Armament Engineering, **Department of Engineering, US Military Academy, West Point, NY, 1980.**

AMCP 706-286, Engineering Design Handbook, *Structures*, **September 1963.**

AMCP 706-284, Engineering Design Handbook, *Trajectories*, **March 1960.**

AMCP 706-281, Engineering Design Handbook, *Weapon System Effectiveness* **(U), August 1963 (THIS DOCUMENT IS CLASSIFIED SECRET RESTRICTED DATA.).**

CHAPTER 3
FUNCTIONAL ELEMENTS OF FIRE CONTROL EQUIPMENT

This chapter considers the functions that must be performed to accomplish the goals of fire control. Thus it considers the acquisition and tracking, computing, and weapon pointing functions, and each of these is the subject of another volume in the Fire Control Series of handbooks. In addition, the importance of command, control, and communication; data transmitting; and fuze setting is discussed. Examples of how these functions are implemented in real systems are given and include combat vehicles, air defense, field artillery, aircraft, and small arms. Finally, there is a discussion of the compatibility requirements of the various elements of fire control systems.

3-1 INTRODUCTION

Fire control equipment is any equipment used to assist in fire control operations, i.e., operations concerned with the solution of fire control problems. As discussed in Chapter 1, such equipment is sometimes classified according to its physical location with respect to the weapon as "on-carriage" or "off-carriage" equipment. (The word "carriage" refers to the weapon and its mount.) Some weapons have sufficient on-carriage fire control equipment to aim them, but the position-finding and data computation phases of fire control operations are performed by off-carriage equipment. When such a fire control system is considered in its entirety, however, it is referred to as an off-carriage fire control system. On the other hand, some weapons have all (or substantially all) their fire control equipment on-carriage. This is the case for some aircraft guns, certain medium caliber antiaircraft weapons (as shown in Fig. 3-1, for example), and direct fire weapons such as tank and antitank weapons. On-carriage fire control equipment is usually specialized in construction, i.e., any one item of fire control equipment can usually be used only with a particular weapon. Off-carriage fire control equipment, however, can generally be used with several different weapons.
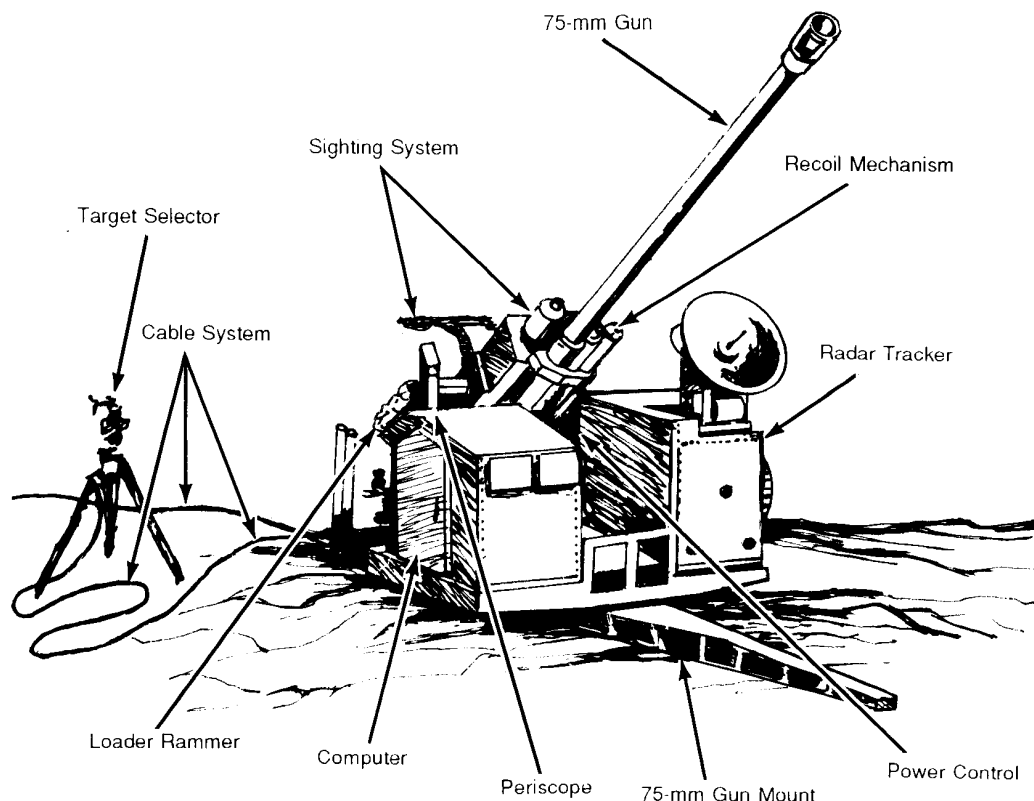
Figure 3-1.   Antiaircraft Weapon as an Example of an On-Carriage Fire Control System

Fire control equipment can also be classified according to the particular function it is designed to perform in the overall fire control system. It is with this classification of fire control equipment that Chapter 3 is primarily concerned.

The discussion uses so-called functional diagrams. These diagrams, which are also known as block diagrams or data flow diagrams, can be used to represent in graphic form an operating system of any complexity. They have the advantage of readily indicating (1) the major subsystems and components of the system or equipment under consideration and (2) the signal flow paths. By convention, the main direction of signal flow through the system from input to output is usually drawn from left to right. A detailed discussion of the various types of functional diagrams is included in Ref. 1.

This chapter first describes and illustrates the various types of functional elements found in fire control equipment. Next, there are discussions of the following related topics:

    1. Factors associated with the integration of functional elements into fire control systems

    2. Compatibility problems associated with various operating elements.

The chapter concludes with examples of how the various functional elements combine to form particular types of fire control systems.

The information presented in this chapter is of a background nature. Details of particular aspects of fire control equipment are not presented.

3-2 FIRE CONTROL FUNCTIONS

The functional elements into which the most complex fire control system conceivable can be divided follow:

    1. Acquisition element
    2. Tracking element
    3. Ballistic data element
    4. Predicting element
    5. Ballistic correction element
    6. Compensating element
    7. Pointing element
    8. Data-transmitting elements
    9. Fuze-setting element
    10. Command, control, and communication element
    11. Navigational element.

As the complexity of fire control systems decreases, the number of functional elements usually does also. In the simple case of small arms, e.g., the functional elements have all but disappeared. Typically, fire control equipment consists of sights that can be reasonably conceived—from the functional viewpoint—as a combined tracking and pointing element. All of the other functional elements required are incorporated in the human being who is firing the weapon.

The arrangement of the various types of functional elements that form a complete fire control system is shown in Fig. 3-2. As indicated by this figure, certain functional elements can be logically grouped together to form three functional subsystems of the complete fire control system, other functional elements serve as connecting elements for these subsystems. The three functional subsystems are

    1. The acquisition and tracking system
    2. The fire control computing system
    3. The weapon pointing system.

The acquisition and tracking system encompasses all of the equipment used to observe and determine the position of the target and to track the target if either it or the weapon is in motion. The second system includes all of the data computation equipment. In the third system is all of the equipment used in the application of firing data to the weapon. The three functional subsystems are discussed in the subparagraphs that follow.
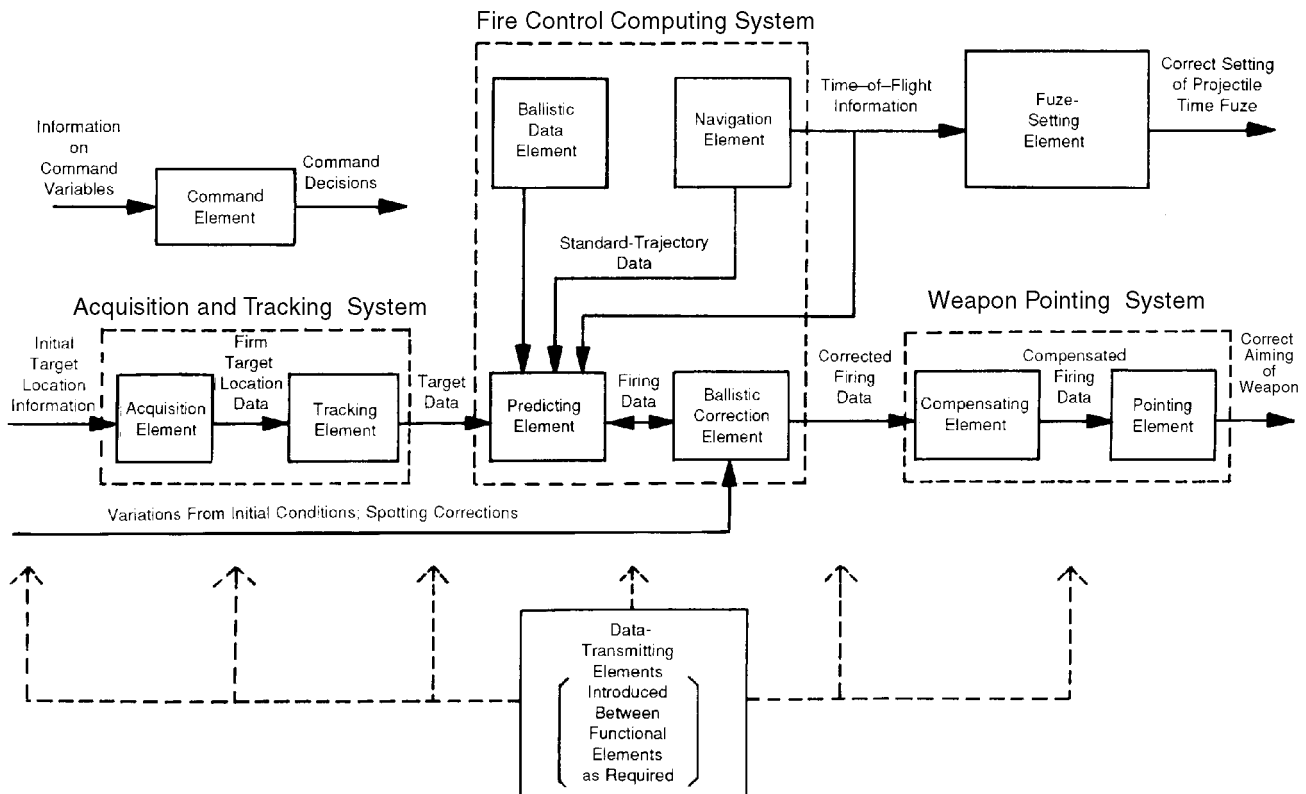
Figure 3-2. **Functional Diagram of a Hypothetical Fire Control System That Contains All of the Functional Elements Associated With Fire Control Equipment**

3-2.1 ACQUISITION AND TRACKING SYSTEM

3-2.1.1 Acquisition Element

The basic function of this element of a fire control system is to acquire the target, i.e., to detect its presence by various means and maintain the capability of continued observation, and provide initial information on its position. Related functions are to identify the nature of the target, e.g., size, shape, and type, and whether it is hostile or friendly by using identification friend or foe equipment.

An example of an acquisition element is the acquisition radar used in the type of fire control system that forms an integral part of certain antiaircraft artillery weapon systems. This acquisition radar might operate in conjunction with a surveillance radar that is considered to lie outside the bounds of the weapon system proper and hence does not comprise an element of the fire control system. Surveillance radar maintains a continuous air watch over an area of land or water of primary significance to the antiaircraft defenses. It supplies pertinent information on all aerial targets to the antiaircraft artillery defense with sufficient accuracy to localize them to a degree that will permit transfer to more accurate radars of the antiaircraft defenses and at a sufficiently long range to enable the outermost firing elements to engage the targets at maximum range. The acquisition radar is of shorter range but greater accuracy than the surveillance radar. Its normal function is to acquire targets on direction from a surveillance radar (or by independent search under certain circumstances) and to transfer these targets to the tracking radar.

The acquisition element is usually mechanized in a fire control system as part of the acquisition and tracking system as shown in Fig. 3-2.

3-2.1.2 Tracking Element

The basic functions of this element of a fire control system are to track the target continuously once it has been acquired and the tracking equipment has been locked onto the target and to generate tracking data that represent the position of the target, i.e. range, elevation, and azimuth, and allow computation of the relative speed and the direction of relative motion of the target with respect to the weapon.

If there is no significant relative motion between target and weapon, the term "sighting and ranging" is more applicable than the term "tracking". Tracking denotes the action of keeping target-locating equipment, e.g., radar and optics, continuously pointed at a moving target. Sighting and ranging, on the other hand, denotes the actions of determining (1) the position of a stationary target in terms of the direction of the line between weapon and target and (2) the range between weapon and target (See also subpar. 2-3.2.).

A typical example of a tracking element is the tracking radar that would be used in conjunction with the acquisition radar, whose function in an antiaircraft artillery weapon system is described in subpar. 3-2.1.1. The tracking radar used in such a weapon system has a higher order of accuracy than either the surveillance radar or the acquisition radar. It has the function of supplying accurate position data on aerial targets so that the required range and angle data can be obtained for gun-laying purposes. For some applications the acquisition and tracking functions can be performed by the same piece of equipment. An example is an acquisition and tracking radar, which is a radar set capable of locking onto a target and then tracking the target.

The tracking element is usually mechanized in a fire control system as part of the acquisition and tracking system, as shown in Fig. 3-2.

3-2.2   FIRE CONTROL COMPUTING SYSTEM

The current discussion is concerned with fire control functions rather than with the manner in which a function is implemented. Some weapon systems may have a central computer which performs many functions such as navigation, fuel management, and crew interface with different systems. The fire control computations may be performed by such a central computer rather than by a dedicated fire control computer. Regardless, the computational functions discussed in the subparagraphs that follow are in fact fulfilled.

3-2.2.1   Ballistic Data Element

The basic function of this element of a fire control system is to supply data to other functional elements of the system regarding the trajectory of the particular projectile and weapon. (See Chapter 2 and its references for source information relating to projectile trajectories.)

An example of a ballistic data element is that portion of a fire control computer which stores trajectory data for the particular weapon system of interest. This may take the form of tabular data, curve fit, or ballistic differential equations, but it must be expressed in a reference frame consistent with that in which the overall fire control problem is expressed.

The ballistic data element is usually mechanized in a fire control system as part of the computing system, as shown in Fig. 3-2.

3-2.2.2   Predicting Element

The basic function of this element of a fire control system is to compute continuously—based on data provided by the tracking and ballistic data elements—the direction in which the weapon must be aimed to hit the target.

For a target that is stationary with respect to the weapon, the computation must consider the various forces acting on the projectile during its flight to the target position and the jump effects that can cause the initial projectile velocity direction to differ from the direction in which the weapon is fired. For a target that is moving, a future target position must be calculated that includes target motion during the period in which the projectile is in flight. Such calculation also establishes the future line of sight (LOS) to that position. The computations associated with weapon fire on a stationary target must then be modified to fire against the future target position.

As discussed in subpar. 2-3.4, sensor data providing information to the prediction process must be filtered to reduce the effect of noise. In this way it is possible to extract estimates of the essential parameter states for predicting target and projectile future behavior. Because of its importance, the filtering function is often considered to be accomplished as a distinct and separate element, but because of its close coupling with prediction, it is considered here to be part of that element. For the Kalman filter the plant equation assumed in its development can be used directly to predict target motion.

A typical example of a predicting element is that component of a fire control computer which takes the information supplied by the tracking element and the ballistic data element and derives the data necessary to position the weapon.

The predicting element is usually mechanized in fire control systems as part of the computing system, as shown in Fig. 3-2.

3-2.2.3 Ballistic Correction Element

The basic function of this element of a fire control system is to introduce into the output of the predicting element either or both of the following types of corrections:

1. Corrections required because the actual conditions present at the time of firing depart from the conditions on which the data supplied from the ballistic data element are based

2. Spotting corrections based on observation of actual weapon fire.

A typical example of a ballistic correction element used for the first type of correction is the means by which changes in initial projectile velocity are determined and introduced into the fire control system. The miss distance corrections provided by the forward observer in connection with artillery fire exemplify the second type of correction element.

The ballistic correction element is usually mechanized in a fire control system as part of the computing system, as shown in Fig. 3-2.

3-2.2.4 Navigational Element

The basic function of this element is to provide the fire control system with data regarding the states of its reference platform. These may include position, velocity, acceleration, attitude, attitude rates, attitude accelerations, heading, heading rates, and heading accelerations. The requirements for fire-on-the-move and autonomous operation have made the need for measurement of these states critical to a timely response to external engagement information and to the solution to the on-board fire control problem. Use of these data is discussed in par. 3-3 and Chapter 4. The navigational element is considered to be part of the computing system. The hardware itself, however, quite often is not integral to fire control, and only the data are available from the computer.

3-2.3 WEAPON POINTING SYSTEM

3-2.3.1 Compensating Element

The basic function of this element of the fire control system is to correct for any motion of the system mechanical reference frames from the basic coordinate frame used for computing purposes. Such a compensating element would be required, e.g., between the computing system and the weapon pointing system, if the coordinate system used by the computing system to derive the firing data required to aim the weapon differed from the mechanical reference frame associated with weapon orientation. An auxiliary function would be in connection with parallax correction.

The compensating element is considered to be mechanized in the fire control system as part of the weapon pointing system, as shown in Fig. 3-2.

The compensating element could just as logically be considered part of the computing system. Further, a compensating element may also be needed between the acquisition and tracking system and the computing system if the mechanical reference frame associated with tracking the target differs from the coordinate frame used by the computing system.

Detailed information on compensating elements is given in Ref. 2.

3-2.3.2 Pointing Element

The basic function of this element of a fire control system is to aim the weapon in accordance with the firing data, e.g., azimuth and elevation commands, generated by the prediction and ballistic elements.

A typical example of a pointing element is a rocket launcher and the associated positioning drive mechanisms. This element is considered to be mechanized in a fire control system as the main element of the weapon pointing system, as shown in Fig. 3-2.

3-2.4 COMMAND, CONTROL, AND COMMUNICATING ELEMENT

The basic function of this element of a fire control system is to provide opportunity for the command function to enter into operation of the fire control system and in some cases provide direct control over particular functions. The command level is presumed to have access to intelligence regarding enemy operations. It can therefore direct fire to locations and at times be effective. This capability is a result of advanced communication networks and high-speed processing. See subpar. 3-3.3 for an example of how this type of functional element is used.

3-2.5 DATA-TRANSMITTING ELEMENTS

The basic function of these elements of a fire control system is to transmit data between other elements of the fire control system located at some distance from one another. The fact that data-transmitting elements often are used at various points in a fire control system is the basis for the method chosen to represent these elements in Fig. 3-2.

Various types of equipment are used to accomplish the data-transmitting function. An accurate and reliable analog implementation is the well-known synchro system. With the recent advent of digital processing, digital transmission buses are featured.

It is in the acquisition and tracking systems that data transmission is first needed to pass information among the several elements of a fire control system.

3-2.6 FUZE SETTING ELEMENT

The basic function of this element of a fire control system is to set the time fuze of a projectile. Use of time fuzes had at one time become quite uncommon; instead proximity fuzes were usually used. The deployment of guided and unguided submunitions from rockets and projectiles, however, reestablished the need for time fuzes.

3-3 FACTORS ASSOCIATED WITH THE INTEGRATION OF FUNCTIONAL ELEMENTS INTO FIRE CONTROL SYSTEMS

As noted, all of the various functional elements represented in Fig. 3-2 usually are not found in a given fire control system. The factors that determine which elements comprise a particular fire control system and the complexity of the functional arrangement include these:

1. The function of the weapon
2. The kind and size of weapon
3. The manner in which the weapons are to be used, e.g., single-purpose or multipurpose
4. The degree of desired mobility
5. The degree to which human participation supplies some of the functional elements of a given fire control system
6. The speed and accuracy requirements of the weapon system.

Generally, these factors are stated in the weapon system performance specification, which in turn is driven to a large extent by the perception of the threat. The paragraphs that follow give examples of how these factors have influenced selection of the elements of systems developed for various types of weapon systems. A revision of the generalized functional diagram of the hypothetical fire control system, Fig. 3-2, is given with each system example. The revisions represent more specifically the data flow of the respective examples.

3-3.1 COMBAT VEHICLE

The fire control for the M1 main battle tank (MBT) has been selected to illustrate the impact that the functional factors have on the determination of the elements used in the system. The principal function of the system is to destroy enemy armor with the main gun either from a stationary position or on the move. The 105-mm rounds on the M1 and the 120-mm rounds on the M1A1 offer the means to defeat heavy armor. These rounds have a relatively short time of flight (TOF) to extended ranges and a low round-to-round dispersion; however, the rate of fire is low. Full azimuth and modest (30-deg) elevation

coverages are required along with an effective range that extends to 3 km or more. Both the tank commander and the gunner must be capable of laying the weapon by using the full fire control system. The commander is expected to provide the lead in acquiring and prioritizing targets. Extremely high first-round kill probability is expected when the weapon is stationary; there is little degradation under moving conditions. The high accuracy of tank fire places much importance on getting off the first round, particularly in a one-on-one tank duel situation. Performance is required under day, night, and degraded visibility conditions. Active sensors, which might reveal tank positions, are not acceptable. Most of the functional factors of the type discussed are generally cited in the performance requirements of the operational requirements document.

The size, weight, and recoil of the main gun dictate the use of a heavy, rugged turret. Azimuth and elevation servo controls must be capable of driving the turret and gun at rates and accelerations compatible with the slew time requirements for initial target acquisition and track requirements consistent with engagement geometry. The need for fire-on-the-move capability imposes additional demands on the servo response of the weapon pointing element to isolate the gun and sighting system from vehicle pitch, roll, and yaw disturbances. Stabilization gyros on the vehicle hull, turret, and sighting system, along with associated electronics, generate compensating signals for the control system input to effect this capability. To meet the severe dynamic requirements of the turret and gun drives, an electrohydraulic approach was taken by the developer.

The commander and gunner, who are completely enclosed in the armored turret, require magnified periscopic sights that offer the capability to locate, acquire, identify, and track targets at extended ranges. Stabilization of the sight line and image is required to permit accurate tracking and to maintain resolution despite vehicle motion and vibration. Electro-optical devices, i.e., forward-looking infrared (FLIR) and laser, are aligned with the visual sight line and provide the means to perform night viewing and target ranging. (Because of the submil tracking requirement, the need for high-resolution viewing, and passive operation requirements, the radar alternative, which conceivably could provide all-weather operation, is not acceptable for this application.) In order to implement this optical/electro-optical approach, the developer provided the gunner a stabilized, periscopic-type optical sight with integrated electro-optical sensors. An optical relay extension to the commander permits him to share the targeting features of the gunner's primary sight. (The M1A2 features a commander's independent thermal viewer.) Dual sensor fields of view (FOVs) are used to optimize target acquisition and track functions. The commander is also provided a wide FOV, fixed focus sight at his station in order to provide for general surveillance, target acquisition, and firing the .50 caliber machine gun. In this tank example both the target acquisition and track functions are performed in the same element.

The computing system, which is a digital implementation in the M1 MBT, generates the fire control solution in near real time. The ballistic element stores a curve fit representation of the flat trajectory with added corrections for nonstandard ballistic and environmental conditions. In addition to exercising the curve fit relationship with initial conditions, the prediction element computes an azimuth kinematic lead based on the product of the corresponding sight line rate and the projectile TOF. The TOF is computed on the basis of ammunition type and a filtered value of laser range. This approximation to the full fire control solution is justified by the existence of only a modest relative motion—generally constrained to a plane—between target and weapon. Additionally, the projectile TOF to intercept ranges of interest is short as a result of high muzzle velocity.

The autonomous operation of the system and the direct fire nature of its mission preclude the need for a complex navigational system for ballistic computations. (The M1A2 has a position navigation system primarily for battlefield control and navigation.) Only the sensor that provides the cross component of airspeed and the pendulous cant sensor could possibly qualify as belonging to the navigational element. The other ballistic and environmental sensors provide inputs to the computing element by means of data-transmitting elements.

Provisions are made to introduce manual input of ballistic corrections for variation of air temperature, ammunition type and temperature, barometric pressure, tube wear, tube bending, and boresight. A manual override is available to introduce estimates of cant, crosswind, lead, and range.

Command, control, and communications (C^3) are limited to verbal discussion over a radio link (and digital transmission of position information in the M1A2).

For use against ground targets, fuzes are generally impact detonating. For tank fire against helicopters, proximity fuzes will probably be used.

The elements previously discussed evolved over a period of many years in response to quite similar functional factors. For this example of fire control, the generalized functional diagram of Fig. 3-2 would reduce to Fig. 3-3.

3-3.2 AIR DEFENSE

For this example it is assumed that the air defense weapon system is configured around twin 40-mm automatic weapons (See the division air defense system discussion in subpar. 1-2.5.4.9.). The function of the system is to defeat fixed and rotary wing aircraft within the useful range of the weapon under day, night, and adverse weather conditions. Several bursts of about 30 rounds each are considered possible, if required, during engagement of a single aircraft. A secondary function of the system is deployment against stationary and moving ground targets. Full operation is required of the system when in motion, and some degradation in accuracy is permitted.

A two-man turret provides both the gunner and squad leader the means to execute required fire control functions. The high speed of fixed wing targets imposes stringent requirements on the time line associated with the sequence of fire control targeting functions. The accuracy of the system is primarily dependent upon the ability to predict the target future position at the projectile time of flight to intercept. Performance is stated in terms of burst or engagement kill probability on targets that exhibit realistic flight profiles. For this example of fire control, the generalized functional diagrams shown in Fig. 3-2 would reduce to the diagram shown in Fig. 3-4.

The selection of a high-rate-of-fire automatic weapon for this application offers the opportunity to place many rounds on the target during a short exposure time. Furthermore, the weapon dispersion provides the means to compensate for system errors that are beyond the designers' control as discussed in subpar. 2-2.4.5. In addition to being receptive to automatic feed, the smaller caliber weapon has lower moments of inertia and thereby significantly eases the dynamic demands of the weapon servos in order to meet the required angular rates and accelerations. In this example the electrically controlled hydraulic
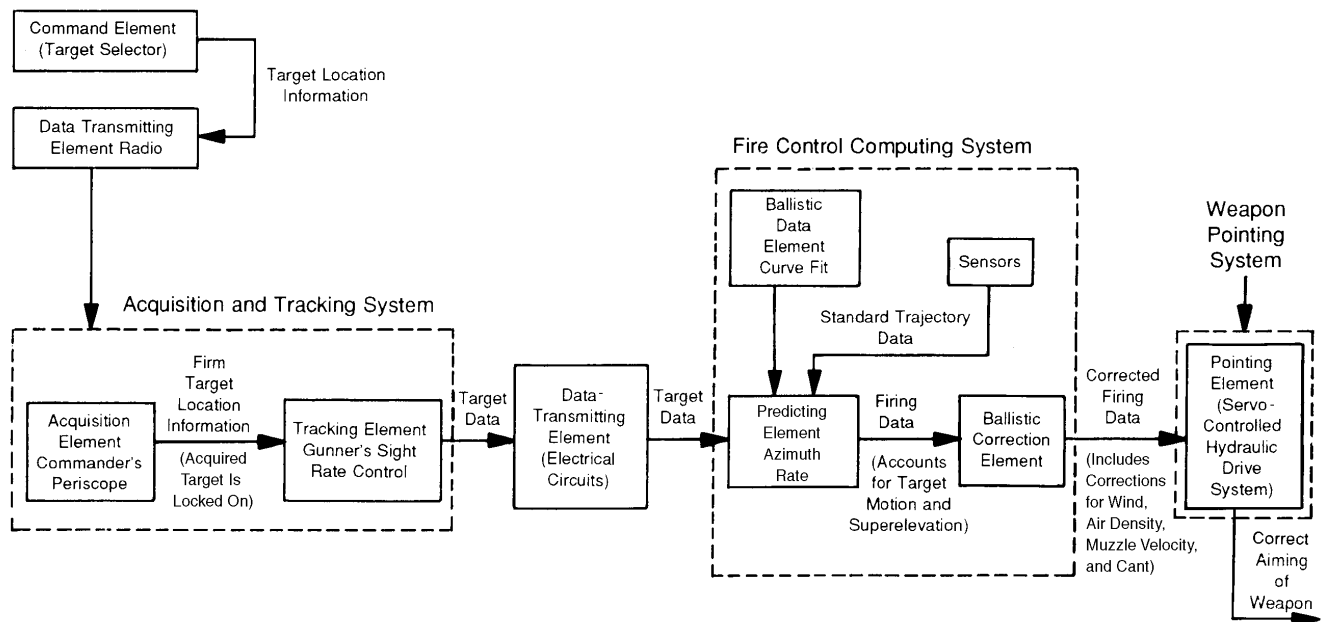
Figure 3-3.   Functional Diagram of a Typical Fire Control System Used With Main Battle Tanks
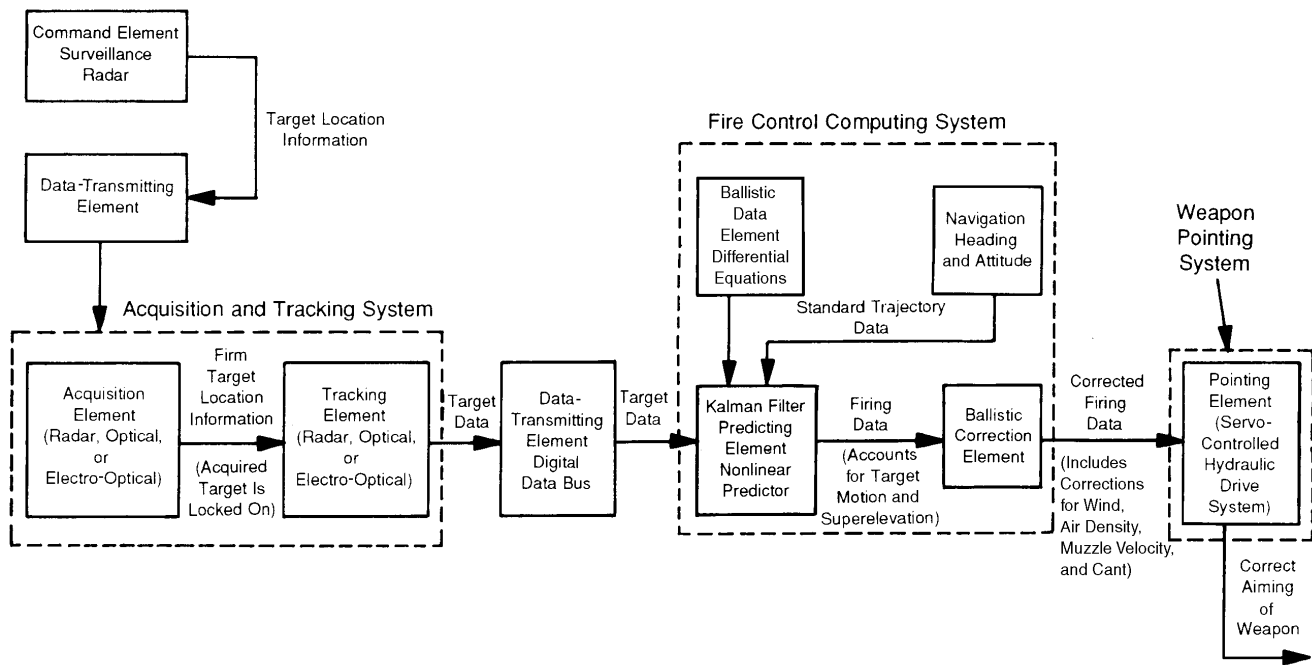
Figure 3-4. **Functional Diagram of a Typical Fire Control System Used With an Air Defense Gun System**

drive system constitutes the weapon pointing element. The servo components compare values of gun azimuth and elevation with the corresponding commands generated by the computer and strive to drive the difference to zero. The commands include the corrections necessary to stabilize the weapon against vehicle disturbance. No cant compensation element is required since turret cant is measured and included in the computer solution.

The digital computing system determines the firing commands by means of

1.   A ballistic element that stores and solves a set of three-degree-of-freedom differential equations to generate projectile TOF and curvature for target prediction and ballistic lead computation

2.   A prediction element that generates kinematic leads by using Kalman filtered target states and the projectile TOF

3.   A navigation element that consists of an attitude and heading reference system (AHARS) and a vortex-type wind sensor. The AHARS provides measurement of the turret attitude and heading and respective rates for critical coordinate transformations. The wind sensor measures the wind velocity (speed and direction).

4.   Automatic input of air pressure and temperature from appropriate environmental sensors and a measure of muzzle velocity by the system radar. This method eliminates the need for manual input.

The acquisition element in this example consists of a pulse Doppler radar that searches to ranges that allow target closure during computer setting time and the projectile TOF to intercept. Full hemispherical, all-weather coverage is accomplished by the scanning in azimuth of a search antenna. The scanning pattern is formed by three overlapping beams in elevation. The scan rate and pulse repetition frequency are consistent with the expected target velocity and the required false alarm rate. The range and angle data are sufficiently accurate to prioritize and transfer targets to the track radar subsystem. The radar is capable of monopulse target tracking while conducting a continuous search by time-sharing the radar electronics between search and track antennas. The radar displays are monitored by both operators.

The track mode provides accurate measurement of target slant range, radial velocity, and target orientation (via antenna directional cosines) to the computer for the fire control solution. In this example the radar satisfies the functional requirements of the acquisition and track elements. However, there is an alternate optical and electro-optical acquisition and track mode of operation for use when the radar is ineffectual or inoperative. In this mode the squad leader controls the stabilized optics of a search peri-

scope to acquire targets for handoff to the gunner's sight. This gunsight with stabilized optics and an integrated laser range finder (LRF) is the counterpart of the track radar. Integration of an image intensifier tube in both periscope and gunsight further enhance their use for night air and ground engagements. The periscope and gunsight are included in the acquisition and track elements, respectively.

The (1) attitude reference unit and the computer subsystem and the (2) displays and controls offer the means to fire the weapons in an indirect fire mode upon receipt of external targeting information. They can also be used to keep track of the locations of other fire units to aid in coordination of fire.

A proximity fuze development was initiated for the 40-mm projectile to enhance hit probability at longer ranges. Therefore, the time fuze setting element is not required.

The data-transmitting element can best be expressed in terms of a number of data paths between system elements. The principal path is a serial digital data bus that transmits all the measurements, control signals, and commands between the radar, the fire control computer, and other elements of the system through the system controller. The communication paths from the system controller to the other elements of the fire control subsystems are (1) slower serial digital buses, (2) parallel digital, analog signals, and (3) discrete signals on individual wires for critical control signals. The system controller is in fact a digital processor that coordinates and directs the activities of all other system elements.

3-3.3 FIELD ARTILLERY

The field artillery example considered features the indirect fire mission. The target is acquired, and its position determined by a source remote from the weapon and weapon control center. This position, referred to a common grid, is transmitted by means of a C^3 system to the control center where target, priority, weapon assignment, target type, time, and duration of fire are assigned to each weapon. Required data are then forwarded to the gun battery where gun orders are computed and provided to gun crews and/or automated traversing and elevating systems for weapon pointing. In addition to target position, the position of the weapon is necessary for the computation. An azimuth reference is also required to lay the weapon. A survey or navigation system provides values of weapon position and the azimuth reference. Measurement of meteorological conditions and stored ballistic data is also required for gun order solution. Obviously, the accuracy of fire and time to deliver fire is dependent upon the execution of the individual functions involved.

Development of field artillery fire control differs significantly from that in other types of weapons, because the subsystems that provide these functions are often developed independently by one of several agencies with mission responsibility in the area. Specification of subsystem performance must be firmly established based upon accuracy and time allocations generated by analysis of full system requirements. However, it should be recognized that the subsystems, particularly target acquisition and location, are often multifunctional; they have more than the demands of field artillery to satisfy. For example, the control center may call for an air strike rather than use field artillery to engage a target. The generalized fire control functional flow, given in Fig. 3-2, becomes that of Fig. 3-5 for this example.

A number of different systems can be used to locate targets not only at or near the forward line of own troops (FLOT) but also deep to the enemy's rear. The Joint Air Force/Army Surveillance and Target Attack Radar System (J-STARS) provides commanders with complete information to attack both moving and stationary targets far forward of the FLOT. In addition, all of the targeting information developed by the Air Force TR-1 system is routinely supplied to Army intelligence elements to be transmitted to the Army command organization as appropriate.

More conventional target location techniques have also been upgraded. To enhance visual performance and extend target location range, optical and electro-optical aides are provided. Conventional optical instruments, LRFs, and thermal viewers are available to the ground forward observer; observation helicopters and the unmanned aerial vehicle (UAV) carry video and FLIR sensors. Laser target designators are provided to forward troops for use with artillery guided weapons. Efforts are underway to combine electro-optical, acoustic, and passive radio frequency sensors at a single station where advanced processing techniques optimize the combined output. The acquisition element in this example therefore includes equipment that makes use of many technologies in both ground and airborne applications.
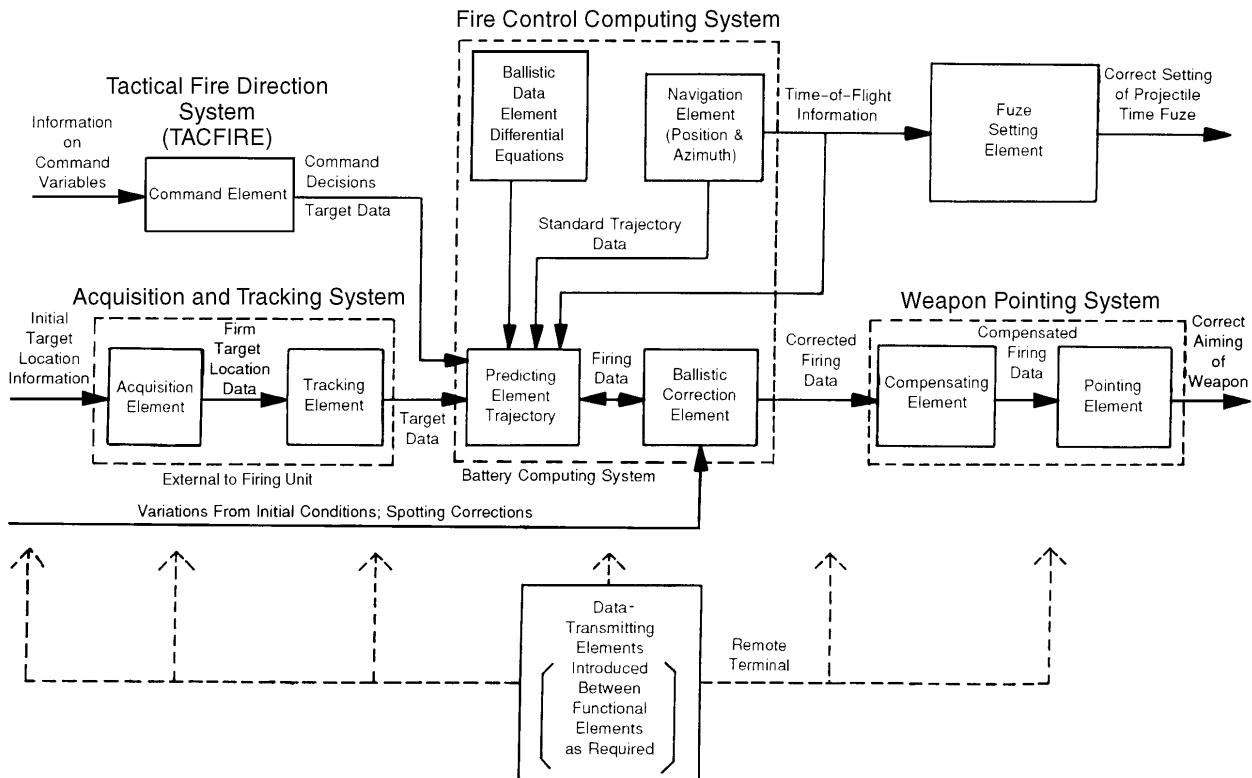
Figure 3-5. Functional Diagram of a Field Artillery Fire Control System

For the most part, the target acquisition element is used for target track, or more properly termed in this application, sighting and ranging, since the target is usually stationary. An integrated LRF measures target range. When measured with respect to geographical north and local gravity, the sight angles establish the target position relative to the observer. This target position, combined with the observer position referenced to geographical north and local gravity reference, is forwarded by a communication link to the control center. Equipment used to locate targets for field artillery is discussed in subpar. 1-2.5.2.2.

The artillery communication, command, and control element in this example is the tactical fire direction system (TACFIRE). It provides computerized digital communication, automated processing of normal fire support functions (e.g., fire planning, conduct of fire, and target data), and rapid dissemination of the results of processing and positive feedback. The data collection and summary features of TACFIRE relieve the fire support personnel of many tedious, routine, and often error-prone tasks. This reduced burden allows them to concentrate on analyzing alternatives, allocating resources, and determining the best combination of weapon system, munition, and volume of fire for targets. TACFIRE equipment consists of two types of central computers and three types of remote terminals. The division artillery computer is used only for "tactical fire control"; it has more components and a larger memory than the battalion computer and is programmed to perform more functions. The remote terminals are issued to the elements of the field artillery system that require access to computers. The chief of each fire support team (FIST) uses a digital message device to communicate digitally with other subscribers. Other remote terminal users have a variable format message entry device to transmit and receive digital traffic from the computer. The battery computer system (BCS) is found at each firing battery and provides the means to perform battery mission control and technical fire control.

The ballistic element is located in the software of the BCS or the battalion TACFIRE computer. The element includes a three-degree-of-freedom representation of the ballistic differential equation and the numerical procedure to effect its integration. Ballistic data that define the in-flight characteristics for each

type of round to be used are stored for use in the trajectory solution. Air density and temperature and wind magnitude and direction—as functions of altitude—are appropriately considered in equation representation. The equations generate a trajectory based upon initial conditions, i.e., the initial velocity. The target and flight path coordinates are compared for miss distance assessment. Gun pointing initial conditions, i.e., gun azimuth and elevation angle, are modified in this manner until the miss distance is nulled. The corresponding gun azimuth and elevation angle are the desired firing commands.

The methods used to compensate weapon firing orders for target motion during the time elapsed between target location and projectile impact have been investigated in field experiments. However, they have not yet been implemented in production systems for prediction.

Provisions have been made to introduce ballistic inputs to the computer to account for air temperature and pressure, wind, muzzle velocity, and gun droop. The firing data generated in the computer are referenced to a level coordinate system. Compensation for the cant of each weapon is, therefore, necessary in the weapon pointing process.

As previously mentioned in the target location discussion, the position of the forward observer or his counterpart may be required in a geographical reference frame. Use of maps, optical triangulation, self-contained navigators, and netting procedures using land or global positioning systems (GPSs) can satisfy this need. The location of the weapon must also be known. The AN/USQ-70 position and azimuth determining system (PADS) permits the artillery to conduct surveys eight to 10 times faster with less chance of error than previous methods. The M109A6 has an integral position navigation system. The satellite-based GPS is in full operation. This system, either alone or combined with a tactical communications network, is capable of providing positioning location with the needed accuracy. The navigational element includes the necessary references and all of the equipment required to determine observer and weapon positions.

In the past the weapon pointing element included the panoramic telescope and compensating mount, the aiming circle, the elevation quadrant, and the manual elevation and azimuth weapon drives. This function is automated in the M109A6 by using hydraulic drives commanded by computer.

The data-transmitting element is represented here primarily by the digital communication network discussed under the C^3 element.

3-3.4 AIRCRAFT

An attack helicopter, such as the AH-64 Apache, has been chosen as an example of how functional factors impact the selection of system elements. The example differs from the others previously discussed in that a single weapon system fire control is used to direct delivery of free rockets, gun projectiles, and guided missiles. The antitank Hellfire missile is not discussed per se; however, the commonality of certain fire control elements is discussed.

The Apache carries a 30-mm automatic weapon capable of firing 725 rounds per minute to an effective range of 3 km. User requirements are a specific 50-round burst hit probability on a stationary or moving point target at 1 km and a particular burst hit probability on a ground area target at 2 and 3 km. Similar area-type target accuracy requirements are specified for rocket fire out to 6 km. As might be expected, performance is required over a range of helicopter operational velocities (forward and transverse) and altitudes under limited maneuver conditions. The gun turret is limited to excursions of ±120 deg in azimuth and −45 to +30 deg in elevation. The rocket pods, each containing 19 rockets, may be mounted on the inner and outboard wing pylons, which are flexible in elevation from −15 to +5 deg. The presence of the rotor blades limits the elevation excursion of all weapons. A stores management subsystem controls the sequencing and the firing rate of the rockets. Uncertainties caused by the relatively large dispersion of the rockets, particularly when launched at low aircraft velocity, and the rocket response to rotor downwash limit the angular accuracy achievable.

The gunner is seated forward of the pilot in the tandem cockpit, i.e., in the better position to carry out the fire control functions. Both, however, have functions to perform for the efficient firing of all weapons. Survivability is highly dependent upon helicopter mobility in nap-of-the-earth (NOE) operations. Targets must be engaged under these conditions at distances consistent with weapon ranges and in a time

frame that minimizes aircraft exposure. These requirements are the major functional factors that influence design of the fire control and the associated elements.

An optical and electro-optical sensor subsystem, the target acquisition and designation system (TADS), was selected as the means to accomplish the target detection, acquisition, recognition, and track functions under day and night visual conditions. The TADS includes a FLIR, television, direct view optics, and a laser designator. By trading off FOV for magnification, the range requirements for the targeting functions could be met. To maintain the quality of sensor imagery and establish a stable LOS under disturbances caused by helicopter vibration and flight instabilities, high-quality inertial stabilization is necessary. The gunner normally views the visual, television, and FLIR imagery through an eyepiece and an optical relay tube and directs the orientation of the sensor or LOS by supplying signals to torque motors on the gimballed sensor platform via a pressure thumb control. The specified Hellfire requirement to point the LOS and the boresighted laser designator and rangefinder dictated the need to use a video autotracker to augment the manual track mode. During the track process, resolvers on the TADS sensor gimbals provide a measure of the sight line orientation, stabilization gyros output a measure of sight line rates, and the laser, operating in the range finder mode, measures target range. These measurements are supplied to the fire control digital computer where they are used in the fire control solution. Miniature-cathode-ray tube (CRT) display units mounted on the pilot and gunner helmets offer both crew members the option of viewing the television or FLIR imagery in a heads-up mode. As shown in Fig. 3-6, the same hardware elements are used for both target acquisition and track functions.

The ballistic data element of the fire control computer is a software representation of a set of algebraic equations containing arbitrary constants that take on predetermined values for either the gun or the rocket solution. The mathematical form of the equations was determined by the use of simplifying assumptions and approximations applied to the three-degree-of-freedom trajectory differential equation. The equations were then generalized by inclusion of terms that involve the arbitrary constants. The values of the constants were then determined for both the gun and rocket ballistic representation through use of a least-square curve fit to data generated by a full six-degree-of-freedom trajectory solution. The equations express the desired elevation and traverse components of the gun and rocket unit pointing vector, as well as the projectile time of flight, in a sight-referenced coordinate frame. These are functions of the target position and all variables that significantly influence projectile flight.
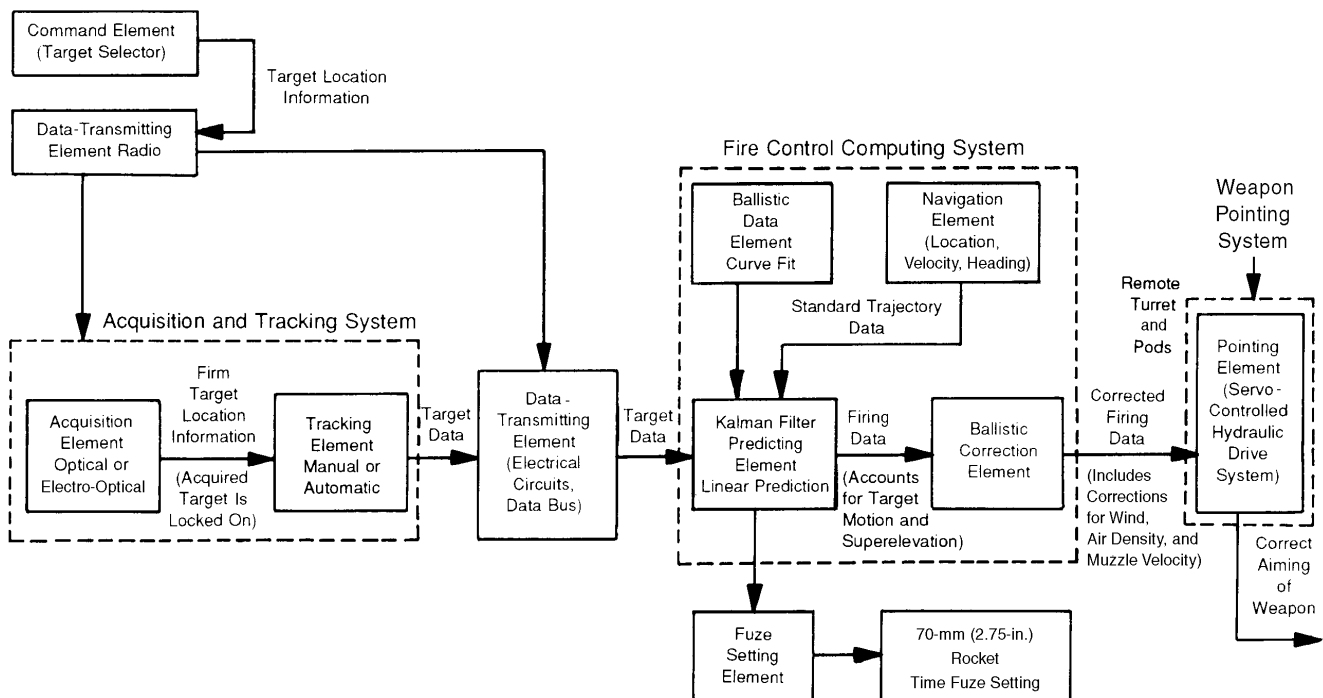
Figure 3-6.   Functional Diagram of Fire Control for Attack Helicopter

Estimates of the helicopter state, i.e., position, velocity, acceleration, and attitude, are continuously provided by the high-quality navigational subsystem, which consists primarily of an integrated Doppler ground speed radar and an inertial heading and attitude reference system (HARS). Navigation performance is assessed in terms of the accuracy of the position data generated in an earth reference frame as a function of distance traveled. Data obtained from the TADS during tracking of known ground checkpoints may be used to update the navigational estimates. Conversely, the navigational system may provide the TADS with pointing commands for timely acquisition of targets with known coordinates. The helicopter state estimates—the navigator has its own filter—are used by the fire control computer for the ballistic solution and target prediction. It also appears appropriate to include as part of the navigational element the mast-mounted airspeed sensor that measures the forward and side components of helicopter velocity with respect to the air mass; these are used to determine the relative wind velocity.

For the most part, input of all of the required variables for the fire control solution is accomplished automatically. Provisions for the manual input of muzzle velocity and range, however, are considered to be representative of the manual correction element.

In this particular fire control implementation, the mathematical relationship that predicts target travel in the earth reference frame during the flight time of the projectile is included in the ballistic equations. Normally, this relationship stands apart and may be readily identified. Because of the relatively slow speed of the ground targets considered for engagement and the rather simple linear relationship used for prediction, the implementation has been found to be acceptable, although not the generally preferred approach. A Kalman filter, the form of which was modified several times during system development, provides the estimates that are used in conjunction with helicopter navigational data to compute target future position. The prediction terms embedded in the ballistic equations and the Kalman filter representation are considered to make up the prediction element.

In this application the pointing element included provisions for driving the gun turret in elevation and azimuth and for the rocket launchers in elevation. Because of the stringent requirements on the pointing accuracy of the turreted weapon, satisfactory performance has been most difficult to achieve. Factors that influenced design of the hydraulic servo control include the effect of gun recoil, particularly with the gun offset from the turret azimuth axis; the flexing of the airframe due to g-loading under maneuver flight conditions; and the demands on servo response due to airframe instability and maneuver conditions. Modifications were made to the original design to address these factors more fully. They include the introduction of feedback sensors to increase servo response, the introduction of body bending compensation terms in the gun orders based on the National Aeronautics and Space Administration (NASA) advanced finite element structural analysis system (NASTRAN) modeling, and the inclusion of feed forward terms to the servo to anticipate the turret motion necessary to compensate for helicopter base motion. NASTRAN is described in Ref. 3. Although many of the same factors influenced the pointing in elevation of the rocket launchers, the larger tolerance imposed due to a softer accuracy requirement was more easily satisfied.

No compensating element exists in this application. All of the transformations required to convert firing data from one coordinate frame to another are embedded in the software.

The weapon system has been developed to perform the weapon delivery function in a completely autonomous mode. Tactics, however, call for close coordination with ground controllers and scout helicopters to direct the aircraft where fire support is needed. The navigational system, which can readily generate a flight heading to reach a desired position, is particularly helpful in this regard. If the Hellfire missile is to be used with an alternate laser designator, close radio contact with the ground or airborne observer performing the designation must be maintained to effect proper coordination.

Transmission of digital data throughout the weapon system is accomplished by use of a multiplex bus subsystem (Ref. 4). It features a megabit per second transmission rate with a 20-ms basic frame time and a 5-µs gap between frames. Thirteen remote terminals are located at key subsystem locations that bring them into the data flow. Input/output capability permits handling of discrete, dc and ac analog, serial digital, and synchro signals. The bus controller resides in the fire control computer. A backup bus controller with degraded performance is available for emergency situations.

One of the few present-day applications for a time fuze setting element exists in the deployment of the 70-mm (2.75-in.) rocket with the submunition warhead from the attack helicopter. The fuze setter programs the warhead timer so that detonation and submunition release take place at a time in the rocket flight that corresponds to an activation point predetermined by a computer. The individual submunitions are carried along a high-drag secondary trajectory to the desired ground impact point. This delivery mode essentially eliminates the negative effect of the large angular dispersion of the rocket. It also brings the submunitions in on a high angle of fall. The higher vulnerability of the target vehicle top surface can then be fully exploited.

3-3.5 SMALL ARMS

As previously stated, in most small arms weapon systems almost all of the fire control functions are assigned to the shooter. In some cases some simple hardware is provided to assist the shooter in carrying out the function. For example, the rifle sling is intended to assist in stabilizing the rifle for weapon pointing.

The reason for the lack of technical fire control with small arms is the individual soldier must be mobile and unencumbered of all but absolutely necessary equipment. In addition, the costs of providing equipment, which would be almost perfectly reliable in the environments in which infantrymen are required to operate, might be quite high.

For rifle fire all functions are performed by the shooter. Traditionally, iron sights have been provided. Optical sights are provided to snipers. Night sights are provided on a selective basis.

In addition to iron sights, machine gunners often have a bipod or a tripod with a traversing and elevating mechanism on which to mount the gun. This is intended to provide stabilization and thus assist the gunner in the weapon pointing function.

There are some members of the small arms community who believe that firing rifles in the traditional manner is too difficult. If the performance standards are high, e.g., high probability of a first-round hit on a soldier-sized target at long range, the task can indeed be difficult.

An often-repeated proposal is to equip the infantryman with a fragmenting (airburst) or flechette round which needs only to be delivered to the area in which a target or targets is located. A fire control system for such a weapon has been demonstrated using a rifle grenade weapon. The fire control consisted of an LRF and the equivalent of an elevation quadrant. After the range to the target is determined, the rifle is pointed to cause the grenade to fly to that range.

The US Army Materiel Command is exploring the use of advanced technology to improve fire control for the individual soldier equipped with an individual weapon. The program recognizes that the soldier and the small arm is the weapon system. To improve target acquisition, the soldier may be equipped with a long-range hearing device; helmet-mounted displays to view computer, sensor, and sight imagery; and an integrated sight with a thermal imager. The small arm may be an improved individual weapon that

Figure 3-7. Generation II Advanced Technology Demonstration Soldier

fires airburst and kinetic energy rounds. As shown in Fig. 3-7, the soldier will have the use of a digital compass and a mini laser range finder and aiming light to improve the weapon pointing subsystem.

The small arms common module fire control system (SACMFCS) is a prototype of a full solution, day/night fire control system intended for use on the M60 (7.62-mm) and M2 (caliber .50) machine guns and the MK 19 (40-mm) grenade machine gun. The SACMFCS is also applicable to a wide range of other direct view weapons systems with development of additional weapons interface adapters and insertion of appropriate ballistics tables.

The SACMFCS is comprised of six modules integrated into a single 9-lb. unit. The day/night sight module mounts and maintains alignment of all optical components, a third generation image intensifier, a laser receive channel and a 2.2× to 9× zoom eyepiece. The ballistics computer module is a 386-based microprocessor that processes environmental sensor inputs, target range, and ammunition ballistics to establish a corrected aiming point, monitors and controls system operation, and conducts a self-test during power-up and operation. The sensor suite module measures and calculates crosswind, air temperature, air pressure, target rate, and cant, and it houses all operator controls and displays. The laser range finder includes an eye-safe laser that uses one pulse to measure ranges from 90 to 3000 m plus or minus 10 m. The aiming point display module is a set of x- and y-stepper motors, which drive a reticle to the corrected aiming point as computed and commanded by the ballistic computer. The power supply module provides all system voltages from replaceable lithium or nickel-cadmium batteries or via an external connection to vehicle power.

The basic SACMFCS unit is augmented by three interface adapters. The M60 and M2 adapters are mechanical devices that provide interface to the weapon and zeroing and boresighting adjustment capability. For the MK 19 these capabilities are provided by an electromechanical superelevation mechanism. This device offsets the line of sight in azimuth and drives the sight in elevation so that the weapon can be used to its maximum effective range while keeping the target within the gunner's field of view. Switch and cable sets allow the gunner to initiate an engagement and lase the target without removing his hands from the spade grips of the weapon.

Systems similar to the SACMFCS are being developed for existing and new weapons.

3-4 COMPATIBILITY PROBLEMS OF VARIOUS TYPES OF OPERATING ELEMENTS

3-4.1 GENERAL PRINCIPLES

It is well known to system designers that for effective design the operating elements of a system must be compatible with one another. This means, for example, that a particular operating element—regardless of how excellent its performance may be as an individual entity or in other applications—should not be allowed to remain in a system design if its use is detrimental to the overall functioning of the system. Frequently there is the questionable case of just how adversely one element affects the operation of its companion elements. In such instances, the tradeoff of performance between individual components must be carefully evaluated to determine the net effect on overall system performance, which is the ultimate criterion.

It is also generally considered inadvisable to use operating elements whose individual performances are so high in comparison with system needs and the performance of other elements of the system that their full potential will never come close to being used. Therefore, their inclusion under these conditions would usually be economically unsound.

3-4.2 FACTORS REQUIRING PARTICULAR ATTENTION

The following factors affect the compatibility of one operating component with another:
1. Relative accuracies
2. Relative speeds of operation
3. Relative ranges of operation
4. Types of associated equipment
5. Interconnecting devices used between system elements.

The effect of each of these factors is illustrated by general examples in the paragraphs that follow.

3-4.2.1 Relative Accuracies

The relative accuracies of the operating elements in a system represent a factor of prime importance since the accuracy of the least-accurate element in a chain generally establishes the overall accuracy of the chain. As an example of the importance of this factor, a fire control computing system is considered that supplies firing data to a weapon pointing system whose accuracy for positioning the weapon is only one-tenth the accuracy of the firing data. Obviously, the two subsystems of the fire control system are mismatched and hence incompatible. The situation should be corrected by improving the accuracy of the weapon pointing system, if the overall accuracy specified for the complete weapon system requires improved accuracy. Otherwise, the computing system should probably be simplified—with attendant economies—until the output accuracy of the firing data closely matches the accuracy of the weapon pointing system.

3-4.2.2 Relative Speeds of Operation

The relative speeds of operating elements in a fire control system frequently comprise a significant factor, particularly for systems used where the target is within the firing range of the weapon for only a brief period of time. An example is a hypothetical antiaircraft fire control system whose speed of determining firing data is such that the weapon cannot be used during the initial phase of an incoming air attack, even though the target is within firing range of the weapon. If the rest of the fire control system—aside from the computing elements—can operate at the required speed, the computing elements are incompatible with the other elements of the system and with the overall requirements of the weapon system.

3-4.2.3 Relative Ranges of Operation

An example of how the factor of relative ranges of operation affects the compatibility of operating components in a system is an acquisition and tracking radar whose range capability for locking onto the target and commencing the tracking operation is only slightly greater than the effective range of the weapon. Inasmuch as a certain amount of accurate tracking is required before usable target data can be generated by the tracking element for use by the computing system, it is clear that the range limitation of the radar makes this operating element incompatible with the remaining elements of the fire control system. On the other hand, a radar whose lock-on range is about 1.5 times the effective range of the weapon would probably be quite compatible with the system.

3-4.2.4 Types of Associated Equipment

Certain fire control situations require fixed types of equipment for one or more parts of the system, but the equipment used in the remainder of the system may be of various types. The essential requirement here is that this latter equipment must be compatible with the equipment that is incapable of modification.

3-4.2.5 Interconnecting Devices

An example of interconnecting devices in the compatibility of system design is a complex fire control system that has been set up with a particular type of data transmission equipment, e.g., synchro-type equipment. No matter how well a particular element in the system that receives synchro signals might perform in isolation, it would be incompatible with the overall system if it were not adapted to use these signals efficiently.

REFERENCES

1. Draper, McKay, and Lees, *Instrument Engineering, Vol 1, Methods for Describing the Situations of Instrument Engineering*, McGraw-Hill Book Company, Inc., New York, NY, 1952.

2. AMCP 706-331, Engineering Design Handbook, *Compensating Elements*, September 1963.

3. *NASA Advanced Finite Element Structural Analysis System (NASTRAN)*, Computer Software Management Information Center, University of Georgia, Athens, GA, 1992.

4. MIL-HDBK-1553A, *Multiple Application Handbook*, 31 January 1993.

CHAPTER 4
DESIGN PHILOSOPHY

The procedures to be followed in the design of a fire control system are given in this chapter. The use of mathematical models to characterize system behavior is introduced, and some examples of fire control models are described. The concept of hit probability is developed in conjunction with weapon system accuracy requirements. By using probability theory, it is shown how error analysis techniques can be used to determine allowable errors for system elements. Some system design highlights are presented, and a brief discussion of fire control system testing concludes the chapter.

4-0   LIST OF SYMBOLS

"U" is used to represent the fact that there are units of measure associated with the function or variable when actual values are used. A "U" with a subscript, e.g., U_x, indicates that the unit is that of the variable denoted by the subscript.

A = **position of the stimulus as a function of time, m**

$[A]$ = **Jacobian matrix of the output state variables, U**

$A(s)$ = **position of the stimulus (the visible spot), m**

$[A(t)],[B(t)],[C(t)]$ = **ordinary matrices used to linearize the state of a system, U**

$A_o(t)$ = **current measurement of target bearing, rad**

$A_p(t)$ = **predicted target bearing, rad**

A_T = **projected target area, m^2**

$\dot{A}_o$ = **constant target slew rate, rad/s**

$\dot{A}_o(t)$ = **rate of change of measured target bearing, rad/s**

$\dot{A}_p(t)$ = **time derivative of predicted target bearing, rad/s**

a = **arbitrary constant in Eq. 4-217, U_v/U_{v1}**

a = **constant determined for the particular experiment, s**

a = **general arbitrary value of z about which a Taylor series is evaluated, U**

a = **known lower limit for unknown constant, dimensionless**

$a^i(t)$ = **acceleration in the ith direction at time t, m/s^2**

a_n^i = **ith component of aircraft kinematic acceleration at time step n, m/s^2**

a_1 = **constant in Eq. 4-97, U_{y1}/U_{x1}**

a_2 = **constant in Eq. 4-99, U_{y2}**

$\dot{a}$ = **symbol denoting a time derivative of a, U_a/s**

$\mathbf{a}'$ = **transpose of $\mathbf{a}$**

$[B]$ = **Jacobian matrix of the input vectors, U**

b = **arbitrary constant in Eq. 4-217, U_v/U_{v2}**

b = **constant determined for the particular experiment, dimensionless**

b = **known upper limit for the unknown constant, dimensionless**

b_{is} = **elements of the system error matrix, units depend on matrix element**

b_x,b_y = **errors in x- and y-coordinate directions caused by burst-to-burst variations, m**

b_{xi},b_{yi} = **manifestation of the total bias in the x- and y-directions in the ith burst, m**

b_2 = **constant in Eq. 4-99, U_{y2}/U_{x1}^2**

C = **constant value of $\Phi_{\varepsilon A_o}(j\omega)$, rad^2·s**

C = **unknown constant, dimensionless**

$C_{e_{im}}$ = **scaling coefficient between the mth internally generated error and the ith element output, U_{yi}/U_{ym}**

$C_{x_{il}}$ = **scaling coefficient between the lth input and the ith output, U_{yi}/U_{xl}**

c = **constant determined for the particular experiment, $1/s$**

d = **constant, dimensionless**

$d(x,y)$ = **two-dimensional target damage function, U^{-1}**

$d(x,y,z)$ = **three-dimensional target damage function, U^{-1}**

$E(j\omega)$ = **Fourier transform of continuous time signal $e(t)$, $U \cdot s$**

E_N = **expected number of hits in an N round burst, dimensionless**

$E_S(j\omega)$ = **Fourier transform of sampled data series $e_S(t)$, $U \cdot s$**

$E[w(i)w(j)]$ = **covariance of the function $w(n)$, $(m/s^2)^2$**

$E[w(n)]$ = **expectation value, or mean, of $w(n)$, m/s^2**

e_i = **error term associated with the output of the ith system element, U**

e_{io} = **reference value of e_i, U_{yi}**

$e_{yi}(t)$ = **error generated within the ith element, U_{yi}**

$F_n(j\omega)$ = **Fourier transform of linear operator $f_n[x_n(t)]$, $U \cdot s$**

$F(z)$ = **arbitrary Taylor series function of the single dependent variable, U_F**

F_m = **nonlinear function associated with the mth state equation, U**

$[F_n]$ = **$m \times m$ state transition matrix at time step n, U**

$[F_0]$ = **initial state transition matrix, U**

$\mathsf{F}(\theta|\mathbf{z})$ = **joint likelihood function of θ given the observed $\mathbf{z}$ values, $(z_1,\cdots,z_n)$, m^{-n}**

$F(\theta|\mathbf{z})$ = **a posteriori distribution for θ given the observed $\mathbf{z}$ values, dimensionless**

$f(b_x,b_y|v_x,v_y)$ = **conditional probability density function (pdf) for the distribution of errors b_x and b_y caused by burst-to-burst variations, $U^{-1} \cdot m^{-2}$**

$f(\mathbf{x},t)$ = **function of a known nonlinear function of the system state, U**

$f(\mathbf{Z}|\theta)$ = **joint probability distribution (coproduct) of $\mathbf{Z}$ for an arbitrary value of θ, m^{-n}**

f_i = **conditional probability density function (pdf) for the bias errors in the ith burst, $U^{-1} \cdot m^{-2}$**

$f_i(\cdots)$ = **homogenous functional operator for the ith ideal element, U_{yi}**

$f_n[x_n(t)]$ = **function that defines a set of arbitrary linear operations on the input variable $x_n(t)$, U**

$f_V(\cdots)$ = **pdf for the random noise variable, m^{-1}**

f_x = **fixed bias in the x-direction, m**

f_y = **fixed bias in the y-direction, m**

$G(j\omega)$ = **Fourier transform of linear operator $g[y(t)]$, $U \cdot s$**

$G(x,y)$ = **joint probability distribution function in the rectangular x,y coordinate system, U**

$[G_n]$ = **$m \times r$ input parameter matrix at time step n, U**

$[G_0]$ = **initial input parameter matrix, U**

$G_1(z),\cdots$ = **pulse transfer function relating inputs and outputs, $U_1,U_2,\cdots$**

$g(v_x,v_y)$ = **pdf for the distribution of errors v_x and v_y caused by the fixed and occasion-to-occasion biases, per unit$/m^2$**

$g[y(t)]$ = **function that defines a set of arbitrary linear operations on the output variable $y(t)$, U_{gy}**

$g_i(\cdots)$ = **functional operator of the ith system element, U_{yi}**

$g_\theta(u)$ = **pdf of θ with dummy variable of integration u, U**

$g_\theta(\theta)$ = **assumed probability density function (pdf) for θ, U**

H = height of the projected target area, m

$H(s)$ = operator's hand position, m

$H(u,v)$ = bivariate normal pdf for the u,v coordinate system, dimensionless

$H(-\mu_x,-\mu_y)$ = bivariate normal pdf evaluated at point $(-\mu_x,-\mu_y)$, $U^{-1}\cdot m^{-2}$

$[H_k]$ = $s \times m$ measurement matrix, U

$h(r_x,r_y\,|\,v_x,v_y,b_x,b_y)$ = conditional pdf for the distribution of errors r_x and r_y caused by round-to-round variations, $U^{-1}\cdot m^{-2}$

$h(t)$ = operator's hand position as a function of time, m

h_i = conditional probability density function (pdf) for the round-to-round errors in the ith burst, $U^{-1}\cdot m^{-2}$

$h_k(\mathbf{x}_k)$ = known nonlinear function of the system state, U

$[I]$ = identity matrix, dimensionless

i = index number, dimensionless

j = $(-1)^{1/2}$, dimensionless

K = constant related to the projectile muzzle velocity, s/m

K = required number of successes or hits, dimensionless

K_a = acceleration error constant, $1/s^2$

$[K_n]$ = Kalman gain matrix, U

$[\hat{K}_n]$ = estimated Kalman gain matrix, U

K_p = position error constant, $1/m$

K_v = velocity error constant, $1/s$

k = index number and time step integer, dimensionless

k = integer identifier for the qth system element with $k \neq i$, dimensionless

$k,|$ = transformed coordinates of the x- and y-directions, m

L = a number of hits, dimensionless

$L(\theta,\delta^*)$ = loss function for the estimation error $(\delta^* - \theta)$, U

$[M_0]$ = initial state covariance matrix, U

$[M_1]$ = system state covariance at $n = 1$, U

m = integer, dimensionless

$\max\limits_{\theta \in \Omega} r(\theta,\delta^*)$ = maximum expected risk for $\theta \in \Omega$ of all the other estimators, U^{-1}

$\max\limits_{\theta \in \Omega} r(\theta,\theta^*)$ = maximum expected risk for $\theta \in \Omega$ using θ^* as an estimator, U^{-1}

N = total number of trials or rounds fired, dimensionless

$\binom{N}{K}$ = symbol defining the binomial coefficient $\dfrac{N!}{N!\,(N-K)!}$, dimensionless

n = integers from 1 to p that define individual inputs to the element, dimensionless

n = time step number, dimensionless

$P(H\,|\,v_x,v_y)$ = conditional single-shot hit probability for a given manifestation of the occasion-to-occasion biases v_x and v_y, U^{-1}

$P(H_i)$ = conditional single-shot hit probability for the ith burst, U^{-1}

$P(jk\omega_s)$ = Fourier coefficients, dimensionless

$P(K\,|\,H)$ = conditional probability of a kill given that a hit has occurred, U^{-1}

$P(K/N)$ = absolute probability of K hits in an N round burst, U^{-1}

$P(K/N\,|\,v_x,v_y)$ = conditional probability of achieving exactly K hits in a burst of N rounds for a given manifestation of the occasion-to-occasion biases v_x and v_y, U^{-1}

$P(K_1/N_1,K_2/N_2)$ = absolute probability of achieving exactly K_1 hits in the first burst of N_1 rounds and exactly K_2 hits in a second burst of N_2 rounds, U^{-1}

$[P_n]$ = covariance matrix of the error in the prediction for the state vector at time step n, U

P_r = probability

P_{SSH} = single-shot hit probability, U^{-1}

P_{SSK} = single-shot kill probability U^{-1}

p = probability of a success in any one of the independent trials, U^{-1}

$p(t)$ = unit pulse function, 1/s

$p(t_k)$ = unit pulse function at time t_k, 1/s

$p(x)$ = pdf for the input variable x, dimensionless

$p(x,y)$ = two-dimensional pdf of the impact point of the projectile trajectory with the normal plane at the target range, $U^{-1} \cdot m^{-2}$

$p(x,y,z)$ = three-dimensional pdf for the location of the points of detonation of rounds fired at a target, $U^{-1} \cdot m^{-3}$

p_o = multidimensional reference point $(x_{1o}, \cdots, x_{ro}, y_{1o}, \cdots, y_{qo})$, U

$[Q_n]$ = $r \times r$ covariance matrix of $\mathbf{w}_n$, U

$[Q_0]$ = initial covariance of the input function vector, U

q = known variance of $\mathbf{w}(n)$, $(m/s^2)^2$

q = the number of inputs to an element originating from within the system, dimensionless

q^i = variance of the random variable μ_n^i, m^2/s^4

R = radius of two-dimensional circular target, m

$[R]$ = observation noise covariance matrix, U

$R(j\omega)$ = element transfer function, i.e., complex ratio of $Y(j\omega)/X(j\omega)$, which is also the Fourier transform of $r(\tau)$, U_y/U_x

$|R(j\omega)|^2 = R(j\omega)R^*(j\omega)$, U_y^2/U_x^2

$R^*(j\omega)$ = complex conjugate of $R(j\omega)$, U_y/U_x

$R(0)$ = transfer function evaluated at $\omega = 0$, U_y/U_x

$R(\delta^*,g_\theta)$ = expected risk, U

$R_{ik}(j\omega)$ = transfer function of the ith element associated with the internal input y_k and output y_i, U_{yi}/U_{yk}

$R_{in}(j\omega)$ = transfer function of the ith element associated with the input x_n and the output y_i, U_{yi}/U_{xn}

$[R_k]$ = $s \times s$ covariance matrix of the random vector $\mathbf{v}_k$, U

$R_n(j\omega)$ = transfer function associated with the nth input and the element output, U_y/U_{xn}

R_o = constant target range, m

$R_o(t)$ = current measurement of target range, m

$R_p(t)$ = predicted target range, m

r = measurement noise variance, m^2

r = number of inputs to an element originating outside the system, dimensionless

r = radial coordinate direction, m

$r(\theta,\delta^*)$ = risk or expected loss, U

$r(\tau)$ = response function of system element to an input function, $U_y/(U_x \cdot s)$

$r_{ii}(t-\tau)$ = response function of the ith element to a unit impulse of direct feedback, 1/s

r_n = discrete response of the element to an impulse x_n, U_y/U_x

r_x, r_y = error in the x- and y-directions caused by round-to-round variations, m

r_{xi}, r_{yi} = random variable representing the round-to-round error in the x- and y-directions in the ith burst, m

$r_0(t_1 - t_k)$ = weighting function, or response function, at time $t_1 - t_k$ to a unit impulse function applied at time $t = 0$, $U_y/(U_x \cdot s)$

$r_1(\eta)$ = discrete impulse response relating perturbation in A_p to the perturbation in A_o, dimensionless

$r_2(\eta)$ = discrete impulse response relating perturbation in A_p to the perturbation in R_o, rad/m

$[S_n]$ = system noise covariance matrix at time step n, U

s = Laplace variable, 1/s

T = time interval of integration, s

t = time, s

t_n = absolute time at the nth step, s

t_0 = absolute time at beginning of a step sequence, s

t_1, t_k = arbitrary points in time, s

U = representation of any unit

u = dummy variable of integration m

u = transformation equal to $x - \mu_x$, m

$u(t)$ = unit impulse function, 1/s

V_i = additive measurement noise range variable associated with the ith observation, m

v = transformation equal to $y - \mu_y$, m

$v(n)$ = nth element of the data sequence $\{v_n\}$, U_v

$v(t)$ = response to unit pulse, U

$v(0)$ = initial value of the series $\{v_n\}$, U_v

v_k = response to a unit pulse occurring at some arbitrary time $t = t_k$, 1/s

$\mathbf{v}_k$ = s-dimensional vector of additive observation noise, U

$v_k(t_1)$ = unit pulse response function, $U_y/(U_x \cdot s)$

$\{v_n\}$ = discrete data sequence, U_v

$\{v_{n1}\}$ = arbitrary data sequence, U_{v1}

$\{v_{n2}\}$ = arbitrary data sequence, U_{v2}

$\{v_{n+v}\}$ = discrete time series shifted by $+v$ time steps from $\{v_n\}$, U_v

$\{v_{n-v}\}$ = discrete time series shifted by $-v$ time steps from $\{v_n\}$, U_v

$\{v_{n+1}\}$ = discrete time series shifted by $+1$ time step from $\{v_n\}$, U_v

$\{v_{n-1}\}$ = discrete time series shifted by -1 time step from $\{v_n\}$, U_v

v_x = error in x-direction caused by fixed and occasion-to-occasion variations, m

v_y = error in y-direction caused by fixed and occasion-to-occasion variations, m

v_0 = response to a unit pulse occurring at time t_0, U

W = width of the projected target area, m

$\mathbf{w}_0$ = initial value of the input function vector, U

$w(n)$ = time series function that characterizes the random time-varying inputs to the target, m/s^2

$\mathbf{w}(t)$ = stochastic input function, U

$w^i(t)$ = wideband stationary white noise, m/s^3

$\mathbf{w}_n$ = r-dimensional random input function vector at time step n, U

$X(j\omega)$ = Fourier transform of input $x(t)$, $\mathbf{U_x \cdot s}$

$X_n(j\omega)$ = Fourier transform in the nth input variable $x_n(t)$, $\mathbf{U_{xn} \cdot s}$

$\mathbf{x}$ = input variable vector, $\mathbf{U}$

x,y,x = three-dimensional coordinates, $\mathbf{U}$

$x(k)$ = discrete time representation of a function, $\mathbf{U}$

$x(t)$ = continuous input time function, $\mathbf{U_x}$

$x(t)$ = input signal in Eq. 4-230, m

$\mathbf{x}(t),\mathbf{y}(t),\boldsymbol{\mu}(t)$ = vector denoting system input, output, and state, respectively, $\mathbf{U_1,U_2,U_3}$

$x(t_k)$ = value of $x(t)$ at time t_k, $\mathbf{U_x}$

x_i = input variable of ith system element, $\mathbf{U}$

x_k = value of observed data at time step k, $\mathbf{U}$

x_n = dynamic quantity at time step n, $\mathbf{U}$

$\{x_n\}$ = input data sequence, $\mathbf{U_x}$

$\mathbf{x}_n$ = true value of the m-dimensional system state vector at time step n, $\mathbf{U}$

$\mathbf{x}(n)$ = true value of the state variable at time step n, $\mathbf{U}$

$\hat{\mathbf{x}}(n)$ = other linear predictors, $\mathbf{U}$

$\hat{\mathbf{x}}*(n)$ = optimum robust linear predictor at time step n, $\mathbf{U}$

$x_n(t)$ = element input, $\mathbf{U_{xn}}$

x_p = pth input variable, $\mathbf{U_{xp}}$

$\mathbf{x_0}$ = initial system state vector, $\mathbf{U}$

$x_1(n)$ = horizontal target position at time step n, m

$x_2(n)$ = horizontal target velocity at time step n, m/s

$x_3(n)$ = horizontal target acceleration at time step n, m/s^2

$\overline{x(t)}$ = time average of the random variable $x(t)$, $\mathbf{U}$

$\overline{x^2(t)}$ = mean square value of the random variable $x(t)$, $\mathbf{U_x^2}$

$Y(j\omega)$ = Fourier transform of output variable $y(t)$, $\mathbf{U_y \cdot s}$

$\mathbf{y}$ = output state variable vector, $\mathbf{U}$

$\dot{\mathbf{y}}$ = first time derivative of the output state variable vector, $\mathbf{U/s}$

$y(t)$ = continuous output time function, $\mathbf{U_y}$

$y(t)$ = element output, $\mathbf{U_y}$

y_i = output variable of ith system element, $\mathbf{U}$

$y_i{}^*$ = output of the ith nonideal system element, $\mathbf{U_{yi}}$

y_m = mth output state variable, $\mathbf{U_{ym}}$

$\{y_n\}$ = output data sequence, $\mathbf{U_y}$

y_n = variable at time step n, $\mathbf{U}$

y_{n+1} = variable at time step $n+1$, $\mathbf{U}$

$\overline{y(t)}$ = time average of the random variable $y(t)$, $\mathbf{U_y}$

$\overline{y^2(t)}$ = mean square value of the random variable $y(t)$, $\mathbf{U_y^2}$

$\mathbf{Z}$ = vector of an independent random variable of target range, m

Z = ZT operation on the discrete data sequence, $\mathbf{U_v}$

$Z\{r_n\}$ = PTF of an element, $\mathbf{U}$

$Z[x(k)]$ = z-transform of $x(k)$, $\mathbf{U}$

$Z\{\delta A_{o_n}\}$ = ZT of the discrete time series of bearing measurement errors, rad

$Z\{\delta A_{p_n}\}$ = ZT of the discrete time series of predicted target bearing errors, rad

$Z\{\delta R_{o_n}\}$ = **ZT of the discrete time series of range measurement errors, m**

Z_i = **random variable representing ith target range measurement, m**

z = **vector of observed values of target range, m**

$\mathbf{z}_k$ = **set of s-dimensional observations of the system state at time step k, U**

z = **independent variable of the Taylor series function $F(z)$, $\mathbf{U_z}$**

z = **complex parameter used in z-transform ($z = \mu + j\omega$), U**

z = **complex transform variable, dimensionless**

z_i = **value of ith observation of target range, m**

α = **ratio of the sampling pulse width to the sampling period, dimensionless**

α^i = **positive real number, 1/s**

β = **constant state transition coefficient, dimensionless**

β_n^i = **(possibly uncertain) parameter at time step n, dimensionless**

Γ_0 = **discrete time index set $(0,\cdots,N)$, dimensionless**

Γ_1 = **discrete time index set $(1,\cdots,N)$, dimensionless**

γ_p = **AR time series coefficient, dimensionless**

γ_x,γ_y = **standard deviation of the occasion-to-occasion biases in the x- and y-directions, U**

Δt = **sampling interval, s**

Δt = **time interval between steps, s**

Δy_n = **first-order difference operator, U**

δ^* = **estimator of the parameter θ expressed as a function of the random variable Z, m**

$\delta A_o(j\omega)$ = **Fourier transform of the perturbed target bearing measurement, rad**

$\delta A_o(n)$ = **discrete input time series of errors in measured target bearing angle, rad**

$\delta\{A_o(n)\}$ = **nth element in the bearing error time series, rad**

$\delta A_o(n - \eta)$ = **discrete input time series of sampled target bearing errors, rad**

$\delta A_o(t)$ = **perturbation on the measured target bearing, rad**

$\delta \dot{A}_o(t)$ = **perturbation on the rate of change of the measured target bearing, rad/s**

$\delta A_p(j\omega)$ = **Fourier transform of the perturbed target bearing prediction, rad**

$\delta A_p(n)$ = **discrete input time series of errors in predicted target bearing angle, rad**

$\delta\{A_p(n)\}$ = **nth element in the bearing prediction error time series, rad**

$\delta A_p(t)$ = **perturbation on the predicted target bearing, rad**

$\delta R_o(j\omega)$ = **Fourier transform of the perturbed target range measurement, m**

$\delta\{R_o(n)\}$ = **nth element in the range error time series, m**

$\delta R_o(t)$ = **perturbation on the measured target range, m**

$\delta R_p(j\omega)$ = **Fourier transform of the perturbed target range prediction, m**

δ_{ij} = **Kronecker delta function, dimensionless**

δ_x = **perturbation on the input state vector, U**

δ_y = **perturbation on the output state vector, U**

$\varepsilon(t)$ = **servo error, m**

$\varepsilon_{xn}(\tau)$ = **error in the nth input of the system element, $\mathbf{U_{xn}}$**

$\varepsilon_x(\tau)$ = **error in $x(\tau)$, the single input to the system element under consideration, $\mathbf{U_x}$**

$\varepsilon_{x|}$ = **error in the $|$th external input to a system element, $\mathbf{U_{x|}}$**

$\varepsilon_{x\tau_n}$ = **magnitude of the discrete impulse at time τ_n, $\mathbf{U_{xn}}$**

ε_{yi} = **perturbation in the output y_i due to the nonideal characteristics of the element, $\mathbf{U_{yi}}$**

ε_{yio} = **reference value of ε_{yi}, $\mathbf{U_{yi}}$**

ε_{yk} = **error in output y_k, of the kth internal system element, $\mathbf{U_{yk}}$**

$\varepsilon_\mu(t), \varepsilon_x(t), \varepsilon_y(t)$ = errors in the system state, input, and output, respectively, U

$\overline{\varepsilon_x^2}$ = mean square value of the error in the input signal, U_x^2

$\overline{\varepsilon_y^2}$ = mean square value of the error in the output signal, U_y^2

η = discrete time step different from n, dimensionless

η^i = intensity of the constant power spectral density function of the wideband white noise, m^2/s^5

η_{e_y} = mean value of the element error, U_y

$\eta_{e_{yi}}$ = mean value of the error generated in the ith element, U_{yi}

η_{ε_x} = mean value of the input error, U_x

$\eta_{\varepsilon_{xn}}$ = mean value of the nth system input error, U_{xn}

η_{ε_y} = mean value of the output error, U_y

$\eta_{\varepsilon_{yk}}$ = mean value of the error associated with the output y_k, U_{yk}

θ = true (unknown) range to target, m

θ = circumferential coordinate direction, rad

θ^* = maximum likelihood estimator of θ, m

λ_1, λ_2 = worst-case probabilities for the uncertain system parameter, U^{-1}

μ_k = sequence of independent random variables with zero mean and common variances, U

μ_n = sequence of independent random variables with zero mean and common variance, U

μ_n^i = sequence of independent random variables with zero mean, m/s^2

μ_x, μ_y, μ_z = location of the distribution mean in the x-, y-, and z-coordinate directions, m

ν = constant integer > 0, dimensionless

ν = substitute variable of time integration, s

ν, μ, ρ, λ = substitute variables of time integration, s

$\nu^i(t)$ = sequence of independent random variables with zero mean and variance $\eta^i \Delta t$, U

ν_x, ν_y = standard deviation of the round-to-round errors in the x- and y-directions, m

ξ = arbitrary variable of time integration, s

ρ = correlation coefficient between the distributions in the x- and y-directions, dimensionless

σ^2 = variance of a distribution, U^2

σ_d = standard deviation for which $\sigma_x = \sigma_y = \sigma_d$, m

$\sigma_{e_m}^2$ = variance in the random component of the internally generated error in the mth element, U_{ym}^2

σ_i^2 = variance of the ith random variable, U^2

σ_S^2 = variance of the sum of the N independent random variables, U^2

σ_x, σ_y = standard deviation of the distribution in the x- and y-directions, U

$\sigma_x, \sigma_y, \sigma_z$ = standard deviation of the detonation points about the mean in x-, y-, and z-directions, m

$\sigma_{x_l}^2$ = variance of the random component of the output error in the lth element input, $U_{x_l}^2$

σ_{yi}^2 = variance of the random component of the output error in the ith element, U_{yi}^2

$\sigma_{\varepsilon_x}^2$ = variance of the input error, U_x^2

$\sigma_{\varepsilon_y}^2$ = variance of the output error, U_y^2

$\sigma_{\varepsilon_{yi}}^2$ = total variance of the error ε_y associated with output y_i, U_{yi}^2

$\sigma_{\varepsilon_y}^2(x)$ = variance of the output error as a function of the input x, U_y^2

τ = first-order time constant of the prediction lag, s

τ = generalized time variable, s

τ = reaction time in Eq. 4-228, s

τ' = generalized time variable for t_k, s

$\Phi_{e_y}(j\omega)$ = PSD of the internally generated element error, U_y^2

$\Phi_{e_{yi}}(j\omega)$ = PSD of the error generated in the ith element, $U_{yi}^2 \cdot s$

$\Phi_{xx}(j\omega)$ = PSD function of the random variable $x(t)$, $U_x^2 s$

$\Phi_{yy}(j\omega)$ = PSD function of the random variable $y(t)$, $U_y^2 s$

$\Phi_{\varepsilon_x}(j\omega)$ = PSD of the error in the input signal $x(t)$, $U_x^2 s$

$\Phi_{\varepsilon_{xn}}(j\omega)$ = PSD of the error associated with the nth system input, $U_{xn}^2 \cdot s$

$\Phi_{\varepsilon_y}(j\omega)$ = PSD of the error in the output signal $y(t)$, $U_y^2 s$

$\Phi_{\varepsilon_{yk}}(j\omega)$ = PSD of the error ε_y associated with output y_k, U_{yk}^2

$\phi_{xx}(\tau)$ = autocorrelation function of the input variable $x(t)$, U_x^2

$\phi_{yy}(\tau)$ = autocorrelation function of the output variable $y(t)$, U_y^2

ω = angular frequency, rad/s

ω_b = highest frequency in the continuous data spectrum, 1/s

ω_m = maximum frequency limit, 1/s

ω_s = constant sampling frequency, 1/s

ψ_x, ψ_y = standard deviation of the burst-to-burst biases in the x- and y-directions, m

Ω = set of all possible values of a range, m

$[\cdots]$ = symbol denoting a matrix, U_a

$[\cdots]^{-1}$ = inverse of $[\cdots]$

$[\cdots]'$ = transpose of $[\cdots]$

4-1 INTRODUCTION

A successful design for a fire control system is likely to result from the satisfaction of two fundamental technical requirements:

1. The system designer (or team of system designers) must obtain a clear understanding of the objectives of the system and a good concept of the functional breakdown of the system into subsystems and of the characteristics required for each of these subsystems. In other words, the design team must become completely familiar with the fire control problem being addressed.

2. To achieve an optimum solution to the problem, the system designer must use a unified design approach or philosophy. Therefore, the designer's attention must be directed toward the development of a system that is optimum. Achievement of an overall optimum solution frequently means that the performances of some of the subsystems will not be as good as they might have been if attention were focused specifically on achieving maximum performance from each subsystem individually.

Realistic performance specifications for subsystems can be established only within a system framework in which the functional interrelationships among the subsystems and the role each subsystem plays within the overall system are taken into account. For example, the use of a very precise servo control system in a fire control system in which the basic information-gathering equipment introduces large errors may increase system cost without providing any improvement in overall system accuracy and may reduce system reliability.

The first requirement is met automatically if the system designer is completely familiar with the type of system being considered. This situation occurs only if the system to be designed represents only a small change from systems that have been built previously. If, however, the system under consideration represents a significant advance over existing systems or is intended to perform a completely new function, the designer must become familiar with the broad aspects of the problem by making a preliminary study of the system requirements. When such a study is necessary, it should lead to a very clear understanding of (1) the basic functions to be performed by the fire control system, (2) the basic physical phenomena in-

volved in the operation of the system, and (3) the form of the system that will be acceptable to the user and compatible with the conditions imposed by such factors as environment and economics. Every effort should be made to differentiate between essential and nonessential system characteristics.

The remainder of this chapter describes the elements of a unified design approach that can be useful in meeting the second requirement. The discussion should be viewed more as an example of the manner in which the design problem should be addressed than as a rigorous set of design procedures.

With the rapid advance of technology, military systems have become more complex, and system designers have found it increasingly more difficult to apply their specific experience directly to the solution of the system design problem. It is only through the use of a unified design approach which uses mathematics to the fullest extent that the designer can develop an optimum design efficiently and cost effectively.

The basis for a fire control system design is usually a performance specification that defines the performance requirements. The particular form of this specification varies depending on the originator and the particular type of fire control system concerned.

4-2 DEVELOPMENT OF MATHEMATICAL MODELS AND SIMULATIONS

This handbook is concerned primarily with models. In this handbook the term "mathematical model" is used to identify a set of abstract mathematical relationships, or algorithms, which define static, dynamic, deterministic, stochastic, or logical interactions among physical factors that represent specific attributes of a system and its subsystems. The term "simulation" refers to the numerical results obtained when the abstract mathematical symbols representing the independent factors are assigned numerical values and the corresponding numerical values for the dependent factors are determined. Development of the mathematical models used during the process of designing a complex fire control system are discussed in the following subparagraphs.

4-2.1 GENERAL CONSIDERATIONS

Once the overall aspects of a fire control system are thoroughly understood (either through experience gained on similar systems or as the result of a preliminary study) the system designer can begin a quantitative mathematical analysis of the system, the ultimate objective of which is the development of the mathematical model that best satisfies all system requirements.

The designer begins the model development process by defining the performances required of the various subdivisions of the system in rigorous mathematical terms and develops models for each of the subdivisions and joins them together to form a complete model for the entire system. The models take the form of a set of equations that describe the system with sufficient accuracy to permit the designer to (1) evaluate such factors as dynamic response and accuracy and (2) select appropriate system parameters to be used in the final design. The mathematical model provides a basis for the study of the simulated system using a digital computer. Such computer studies are usually required at one or more points in the design process and with complex systems, must be introduced at an early stage in the design. However, although the designer must have the accuracy requirements well in mind during the early stages of the formulation of the model, it is only with the completion of a realistic mathematical model that the errors of the projected system can be effectively analyzed.

While studying a complex system, the designer will probably make use of a variety of models, which will iteratively evolve as the design progresses. These models can be classified into the following three groups:

1. Models for idealized systems
2. Models for optimum systems
3. Models for practical systems.

Each of these models is discussed in turn in subpars. 4-2.2 through 4-2.4.

4-2.2 MODELS FOR IDEALIZED SYSTEMS

Mathematical models for idealized systems are representations of system configurations that define the characteristics and interrelationships among the system elements on a functional basis and indepen-

dently of specific hardware realizations. These models should be simple, yet they must include sufficient detail to enable the designer to demonstrate concept feasibility based on fundamental mathematical and physical laws. For example, a model used to study system accuracy must include the effects of target position measurement errors on the accuracy of predictions of future target position and the overall effects of nonzero computation times.

There may be several design configurations for complex systems that look promising, at least in the early stages of a program. Initially, the designer should not limit himself too severely but should look at as many alternative concepts as he can create. Each concept should be evaluated on an idealized basis to determine its capabilities, limitations, and risks. System concepts appearing to have no immutable restrictions that prevent realization of the design goal are then selected for optimization.

4-2.3   MODELS FOR OPTIMUM SYSTEMS

Selection of the optimum system from a family of approximately ideal systems that do not violate physical limitations is termed the optimization procedure. An obvious but essential step in this procedure is the choice of appropriate criteria with which to compare the different systems. Although mathematically precise criteria, such as least-mean-square error, may be used, it should be clearly understood that the final selection of the optimum system will probably not be based not upon a single criterion but upon the designer's application of his engineering judgment to a number of criteria ranging from those that are purely mathematical to those involving economics, procurement schedules, size, reliability, etc.

4-2.4   MODELS FOR PRACTICAL SYSTEMS

As a result of the analytic and computer studies, the system designer should be able to arrive at a mathematical model for the system that is optimum in some sense. As more of the practical aspects of realizing the physical system are defined, additional information must be gathered to indicate the manner in which deviations from the idealized system, as defined by the optimum mathematical model, will affect the performance of the final system. This phase of the work usually involves formulation of another model incorporating these nonideal system characteristics. The performance of the optimum system model (The selection of which has been determined by simulation studies.) then becomes a kind of yardstick against which the performance of the model for the practical system can be measured. The evaluation is usually obtained by computer simulation and governed by the same criteria discussed in connection with models for optimum systems. If this evaluation shows that the performance of the practical system will be essentially as good as that of the optimum system, the job of mathematical formulation is essentially complete. Detailed drawings can now be completed, and fabrication of the physical system can be undertaken. If the idealized system performance is severely degraded by physical realities, however, it may be necessary to retrace the design steps and look at other idealized models and their optimum and practical counterparts.

4-2.5   APPLICATION OF COMPUTERS TO THE STUDY OF MATHEMATICAL MODELS

In the early days of computer modeling of fire control systems, analog computers were widely used. These were especially valuable in areas such as the simulation of servo systems. Now, however, the small size and high speed of digital computers has made them the tool of choice. One important exception remains in hardware-in-the-loop simulation where analog devices are sometimes required to interface with system hardware, such as gun drives.

A model of the complete fire control system is now studied by using digital processing, in which the accuracy achieved for a given computer model is limited only by the programmer's ability to represent the system in a mathematical form. The flexibility of digital computers also offers the opportunity to use statistical processes in addition to deterministic solutions.

A number of factors must be considered during development of a mathematical model for simulation on a computer. Some of the more important factors follow:
   1. Information to be computed
   2. Degree of sophistication necessary
   3. Accuracy required

4. Solution time
5. Memory requirements.

Each of these five factors is discussed briefly in the subparagraphs that follow.

4-2.5.1 Information to be Computed

The first step is to define clearly the type of information being sought. A clear definition of what is to be computed determines the complexity of the computer study and the number of different computer setups that may be required. In addition, it may dictate particular quantities that should be recorded or computed to minimize the problem of analyzing the computer results and arriving at engineering design decisions.

4-2.5.2 Degree of Sophistication Necessary

Much is to be gained by using the simplest model that still retains the essential characteristics of the particular aspect of the system under study. For example, to compute the trajectory of a projectile, it may be perfectly adequate in the case of relatively short-range fire to consider the projectile a single point mass moving in space, but for a longer range projectile it may be necessary to simulate the dynamic response of the projectile as an aerodynamic body to determine its trajectory with sufficient accuracy.

4-2.5.3 Accuracy Required

As a minimum, the computer model must produce solutions that are reproducible to a precision greater than the variations to be attributed to parameter changes. For example, if a computer program is capable of reproducing a miss-distance solution to within a dispersion error of ± 1.0 m, it is of no value to use this particular computer program to evaluate the effect of parameter changes that cause only ± 0.1-m changes in the result.

4-2.5.4 Solution Time

The time required to run a solution on a computer may be greater than, equal to, or less than the time required for the event to take place in the actual physical system. If the entire physical system is simulated on the computer, the choice of solution time, or time scale, is arbitrary. The only case in which no choice of time scale exists is when it is desired to include some of the physical components from the actual system in the simulation. In this case meaningful results can be obtained only if the solutions are run in real time.

4-2.5.5 Memory Requirements

The model sophistication, the number of simulation runs, the execution time, and the data precision are all constrained by the computer memory size and configuration. Current personal computer (PC) systems typically contain several megabytes of random access memory (RAM) and have storage devices, e.g., floppy disks, hard drives, removable hard drives, compact discs (CD), mass storage cassette tapes, and personal computer memory card international association (PCMCIA) cards, with up to several hundred megabytes of memory. Thus large mathematical models can be studied with relatively little concern for the availability of computer memory unless real-time or near-real-time simulations are required.

4-2.6 MODEL VERIFICATION AND VALIDATION

Model verification refers to the process used to assure that the algorithms which comprise the model have been implemented correctly. The process used to determine whether the simulation that results from the model corresponds to the actual behavior of the physical system is referred to as model validation.

Verification is generally a mathematical exercise not requiring knowledge of or data from the physical system. In this process, sets of input/output test data are developed off-line to exercise all of the possible modes and computational paths through the model. The input test data are then loaded into the model, and the model outputs and responses are compared with those in the test data sets. If the test data sets are comprehensive and the model passes the validation process, the designer has reasonable assurance that the logical relationships and software programming have been correctly implemented.

Validation of the model requires data on system or subsystem behavior under the full range of expected system operating conditions. For fire control these data are generally defined in terms of the range of the input variables, e.g., target and own vehicle kinematics, environmental parameters, and ballistic parameters. The behavior of system elements is usually representative of that expected on an ensemble basis since the performance prediction of the entire weapon system fleet is of interest. Element specifications and laboratory and field test results are sources of data on system behavior.

Validation of the model in terms of major system criteria, such as miss distance or reaction time, is often the easiest to consider because the field test is structured primarily for measurement of these data. However, the validation of individual element behavior, which becomes much more critical when system validation cannot be achieved, is sometimes far more difficult. Most modern weapon system designs now provide the means to sample the status of the system without impacting normal operation.

The basic idea underlying the validation techniques is to generate sufficient data with the model to allow determination of the model output frequency distribution. The field test data are then compared with this distribution to determine whether the the data can be designated to belong to the distribution.

4-2.7 EXAMPLES OF MODELS

4-2.7.1 HITPRO (Derived from Hit Probability)

The HITPRO model (Ref. 1) illustrated in Fig. 4-1 contains mathematical descriptions of the major subsystems of a tank: suspension (including springs, dampers, road wheels, and tracks); fire control (including computer, sensors, ballistics, gyros, and internal control system elements); gun stabilization, gun drives, and hydraulics; electrical and electronic subsystems (as they affect weapon operation); gun recoil
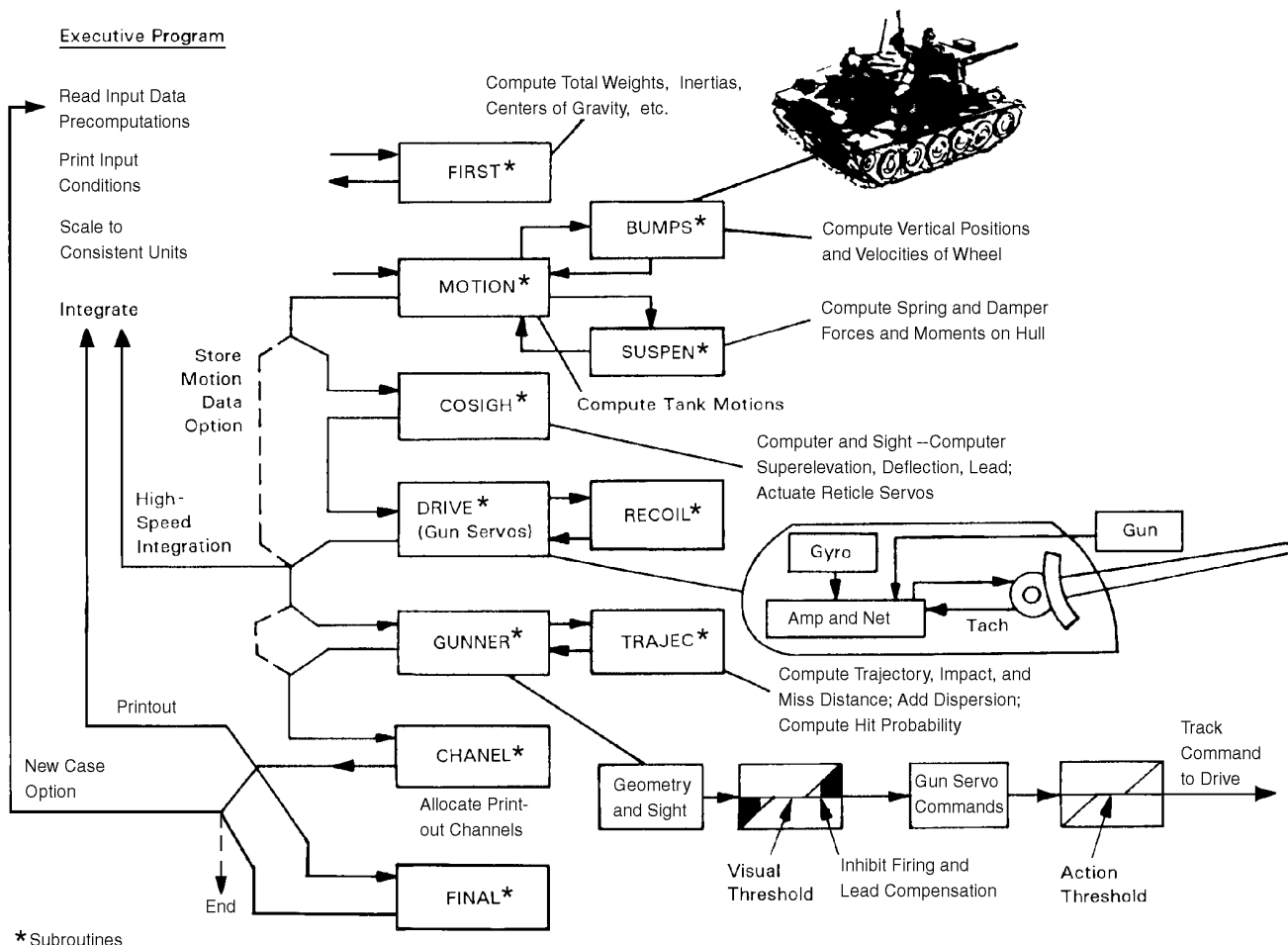
Figure 4-1. Functional Block Diagram of HITPRO (Ref. 1)

system and kinematics; and mathematical model representation(s) of the gunner or tracker. HITPRO was developed in the early 1970s as an engineering design aid for system development.

To keep track of the gun pointing errors and their components, HITPRO simulations were merged with a statistical bookkeeper and firing event manager called DELACC (delivery accuracy (statistical bookkeeper software)). DELACC provides the analyst with the capability to simulate trigger-pull events by monitoring the HITPRO output and comparing it to certain constraints believed to govern actual firing events. DELACC checks whether tracking errors and tracking rate mismatches are within predetermined bounds. If so, DELACC causes HITPRO to initiate a ranging operation. DELACC then selects a time delay from ranging to simulated trigger pull from empirically determined firing time distributions. When the trigger-pull time comes, DELACC queries HITPRO to check whether the actual gun-to-sight pointing angle agrees with the commanded angle according to the control system constraints designed into the tank. DELACC also checks whether the tracking-related errors are still within acceptable bounds. If all criteria for the firing event are satisfied, DELACC records the tracking errors and gun pointing angles, and HITPRO simulates trigger pull. DELACC then looks ahead one time of flight (TOF) and computes the total weapon pointing error for that bullet. The fire-on-the-move engagement then continues with HITPRO and DELACC working together to build up a number of firing events and associated errors for later statistical analysis by DELACC. The results of the statistical analysis are the biases and random errors for fire-on-the-move.

4-2.7.2 The Air Defense Modern Gun Effectiveness Model (MGEM)

When it became clear in the mid-1970s that the US Army would embark on a program to develop a new air defense gun that would take advantage of some of the latest results in the field of modern control theory, it was decided to create a computerized model capable of quantifying the advantages, if any, of such an approach. The result of that decision was the modern gun effectiveness model (MGEM), which is described in Ref. 2.

The MGEM is a digital computer program that simulates the engagement of one aircraft by one ground-based, air-defense gun. The aircraft is passive; it neither reacts to fire from the gun nor attempts to destroy the gun by delivering ordnance on it. The model is time driven and relies on random number generation to realize stochastic processes. The model is generic in the sense that it represents no specific system; it represents a whole class of guns that rely on techniques derived from modern control theory. The basic flow of the model is shown in Fig. 4-2.
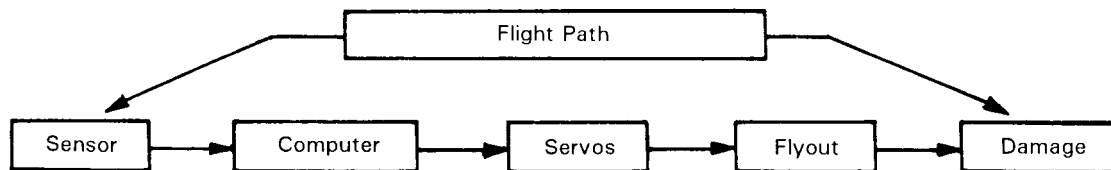
Figure 4-2. MGEM Flow (Ref. 2)

The flight path simulator drives a sensor or tracker model that feeds noisy target position data to the fire control computer. The computer filters, or smooths, the target position data in an attempt to reconstruct the true target position, velocity, and acceleration. Based upon this reconstruction and the ballistic characteristics of the ammunition to be fired, the model of the fire control computer also predicts where the target will be one TOF into the future. The computer model then uses this prediction to issue aiming commands to the gun drive servos. The computer simulation may also issue firing orders to the guns (in which case bullets are fired) based upon the computer-programmed firing doctrine. This decision is made with consideration of the errors related to target intercept. At this point, a lethality submodel is invoked, and the damage to the target is calculated. The process is continued (from sensor to target damage) until either the target is killed or is out of range.

4-2.7.3 ARTOAR (Derived from Air-to-Air)

Modern helicopter weapons systems employ sophisticated avionics as well as powerful fire control computers to solve complex target tracking and ballistic problems. Optimum system performance in these applications is obtained in part by proper use of algorithms based upon modern control and estimation theory. Of particular note is the effectiveness of using a turret-mounted gun in a US helicopter against an accelerating enemy aircraft, either a helicopter or a fixed wing aircraft.

To evaluate the overall performance of the attack helicopter fire control and associated weapon system effectiveness, a comprehensive, general-purpose computer simulation, ARTOAR, has been developed and is described in Ref. 3. The simulation, shown in Fig. 4-3, is highly modular and incorporates features that permit the system designer to evaluate the relative merits of alternative avionics suites, weap-
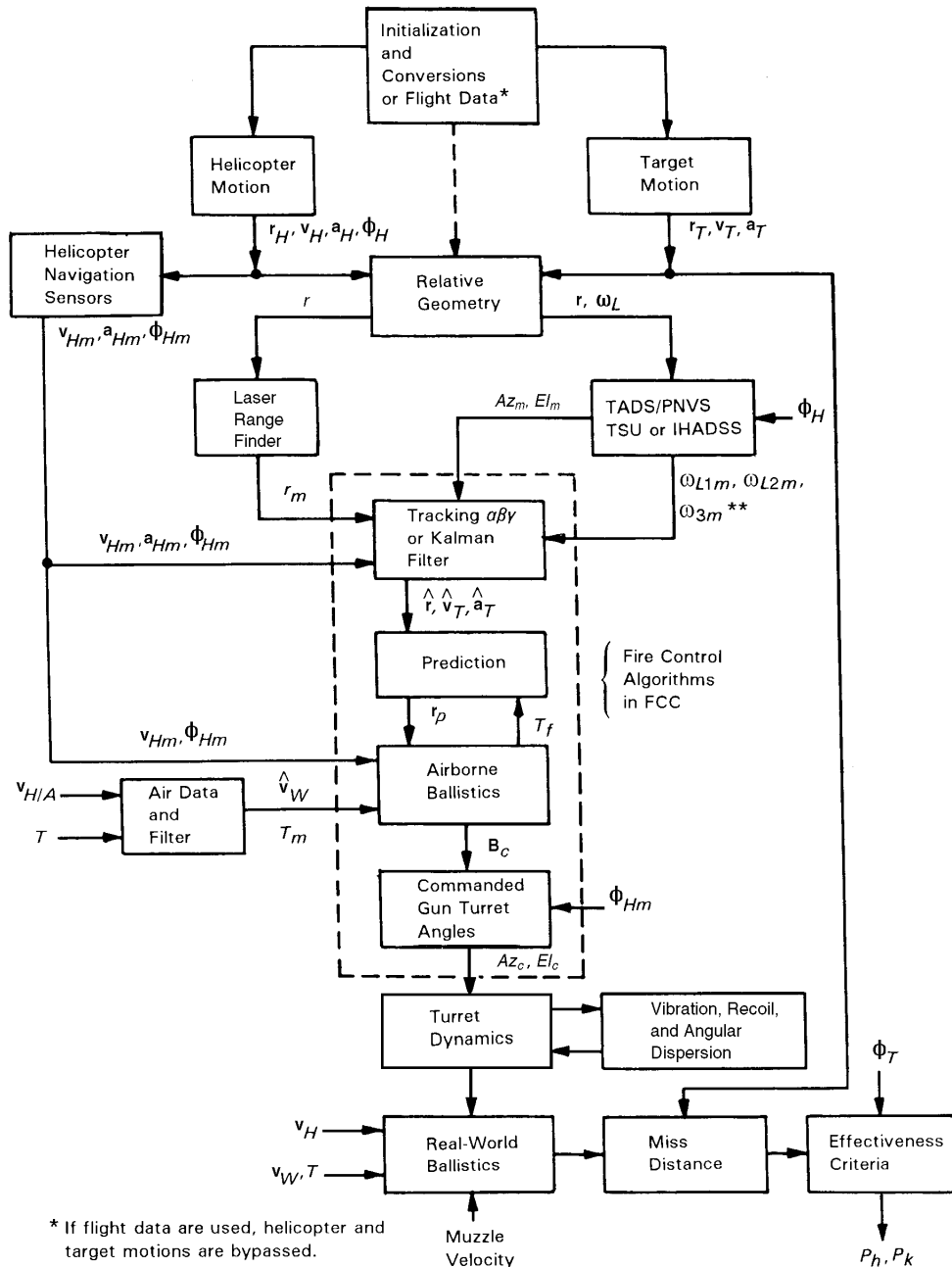
Figure 4-3. ARTOAR Flow Diagram (Ref. 3)

ons, engagement geometry, target characteristics, and fire control computer algorithms. Computational modules for the principal system elements and airborne algorithms are included, as well as models for real-world effects. The simulation measures the results of helicopter engagements by use of the bullet miss distance and by incorporation of a statistical model of the target vulnerability.

The topmost block in Fig. 4-3 contains all of the initializations and conversions from input units, e.g., knots and g's, to internal units, e.g., meters, seconds, and radians.

The block labeled "Helicopter Motion" determines the helicopter vector position, velocity, acceleration, and attitude (represented by a generalized vector angle ϕ_H) with respect to an inertial reference frame, which is earth fixed. Helicopter control variables, such as lift acceleration and lift bank angle, are either fixed constants or determined by a closed-loop steering law. However, a net thrust (or drag) acceleration profile, which varies the speed, can be specified.

The block labeled "Target Motion" determines target vector position, velocity, and acceleration with respect to the same inertial frame. Unlike helicopter attitude, target attitude is not formally required, and a simplified approach used to determine target attitude and effective area is described in conjunction with determining hit and kill probabilities. Desired target maneuvers are also achieved by choice of the control variables for the target, i.e., lift and net thrust (or drag) acceleration and lift bank angle.

The true helicopter and target motions are combined in the block "Relative Geometry" to produce various helicopter-to-target kinematic variables, such as vector range $\mathbf{r}$, its magnitude scalar range r, range rate $\dot{r}$, range acceleration $\ddot{r}$, vector line-of-sight rate $\boldsymbol{\omega}_L$, line-of-sight rate magnitude ω_L, its derivative $\dot{\omega}_L$, kinematic roll rate ω_r, relative velocity and relative acceleration of the target with respect to the helicopter, unit vectors $\mathbf{i} = \mathbf{r}/r$, $\mathbf{k} = \boldsymbol{\omega}_L/\omega_L$, $\mathbf{j} = \mathbf{k} \times \mathbf{i}$ and components of relative acceleration, and target and helicopter total velocity and acceleration along $\mathbf{i}$, $\mathbf{j}$, and $\mathbf{k}$.

The true helicopter motion is also measured by Doppler radar, the attitude and heading reference system (AHARS) platform for the Apache, and the vertical gyro and magnetic compass for the Cobra. These sensors are modeled in the block "Helicopter Navigation Sensors", the outputs of which are the measured helicopter velocity, acceleration, and attitude $\mathbf{v}_{Hm}$, $\mathbf{a}_{Hm}$, and ϕ_{Hm}, respectively.

The true scalar range r is input to the block "Laser Range Finder", which then outputs the measured range r_m. Similarly, the true vector range $\mathbf{r}$ and line-of-sight rate $\boldsymbol{\omega}_L$ are input to the block labeled "TADS/PNVS" (target acquisition and designation system/pilot night vision system) for the Apache and "TSU" (telescopic sight unit) for the Cobra. The sight line attitude combined with the helicopter attitude determines the sight line angles azimuth Az and elevation El relative to the helicopter. These angles are then corrupted by measurement noise to produce angles Az_m and El_m. Similarly, the vector line-of-sight rate is converted to components ω_{L1} and ω_{L2} and then noise corrupted to simulate the measurements ω_{L1m}, ω_{L2m}. "TADS/PNVS" also has a roll-rate gyro; the measured roll rate is ω_{3m}.

"Tracking" contains several variable coefficient α, β, λ filters or a Kalman filter. Both types are mechanized, and one or the other is used on a specific flight. In particular, $\alpha\beta\lambda$ is used on Cobra missions, and Kalman, on Apache missions. These filters estimate target range, velocity, and acceleration.

The block "Prediction" predicts target vector position one bullet time of flight T_f into the future. It is closely related to the tracking block. The variable T_f enters this block from "Airborne Ballistics", which is an approximate solution to the inverse ballistics problem, i.e., where to point the gun barrel to achieve a hit on the target T_f seconds from the present time. Inputs to "Airborne Ballistics" are predicted position $\mathbf{r}_p$, helicopter velocity $\mathbf{v}_{Hm}$, helicopter measured attitude ϕ_{Hm}, filtered wind velocity $\hat{\mathbf{v}}_W$, and measured temperature T_m. The output of this block is the unit vector $\mathbf{B}_c$ that defines the commanded gun barrel direction.

The block "Commanded Gun Turret Angles" converts $\mathbf{B}_c$ to commanded gun azimuth and elevation relative to the helicopter.

"Turret Dynamics" generates the response of the gun turret servo system to the angular commands. Related to this is the block "Vibration, Recoil, and Angular Dispersion', which simulates a statistical error in gun pointing due to these effects. The net output is the actual gun barrel direction B.

"Real-World Ballistics" computes the exact bullet trajectory (after a conceptual firing) for approximately one T_f using a step-by-step integration procedure. Helicopter true velocity, true winds, tempera-

ture, and muzzle velocity are also inputs here. The target motion is also extrapolated approximately one T_f into the future by continuing its control variable history.

The extrapolated bullet and target motions are combined into the block "Miss Distance" to determine the closest approach of the bullet to the target.

The miss distance and target aspect are then input to the block "Effectiveness Criteria", which computes the kill probability P_k.

The simulation terminates after a prescribed running time.

The air-to-air simulation software provided by ARTOAR allows a fire control systems designer to examine the individual contribution of each of the error sources, to decide which errors are significant, and finally to decide what steps, if any, can be taken to minimize their influence. The Monte Carlo approach enables each of the error sources to be modeled (as in the case of MGEM) with considerable freedom to choose from a wide variety of engagement conditions.

4-2.8   CONCLUSIONS

For the development of mathematical models and simulations, the following are generally true:

1. Mathematical analysis of a system does not lead to a unique solution for any particular problem.

2. The real test of good engineering is whether the result is development of the particular approach that will meet the established specifications most economically and with a reliability sufficient to meet the system requirements.

3. Early in the system analysis, hardware alternatives should be examined, and the advantages and limitations of each should be carefully weighed.

4. Under some conditions the wise approach to system design may be to refine proven designs to meet new requirements, whereas in other cases it may be better to attempt a totally new approach.

5. At the initiation of the design of a complex system, it is important that the system designer be given the freedom necessary to examine the alternatives and an opportunity to present his findings to those who ultimately will decide what approach should be taken.

4-3   FILTERING AND PREDICTION

Filtering and prediction play a fundamental role in virtually all fire control systems. Filtering refers to the process of extracting time-varying information on the state of the vehicle from incomplete observations of the state of the vehicle. Prediction refers to the process of inferring the future value of the state of a vehicle system based on a finite record (finite time series) of partial observations of the state of the vehicle. For example, to employ a gun against an evasive target, it is necessary to be able to infer accurately the future values of the position of the target over a time interval characterized by the TOF of the projectile.

Filtering and prediction are two important processes in which dynamic systems and probabilistic models are combined to study the motion of uncertain dynamic systems. Further, filtering and prediction are part of a larger body of knowledge known as "decision making under uncertainty".

In fire control the engineer is faced with the need to design and implement recursive algorithms that will efficiently estimate and/or predict the motion of generally nonlinear dynamic systems. The primary algorithm technology that forms the basis for these filters and predictors is the extended Kalman filter (EKF). The EKF represents a nonlinear extension of the Kalman filter. The standard Kalman filter is a linear procedure that provides a minimum mean square error (MMSE) estimate when (1) the dynamic system has a known linear finite dimensional state representation (including first- and second-order statistics) and (2) the observation relations are representable by a known linear transformation of the system state vector in additive noise, with known first- and second-order statistics. It is assumed that the stochastic input to the dynamic system and the observation noise are either white noise processes or can be made to look like white noise by finite dimensional shaping filters. A major consideration in the application of Kalman filter techniques is the effect of uncertainties in the model, which characterizes the true behavior of the underlying stochastic dynamic system. This model is called the truth model and should be distinguished from a generally much simpler model that is implemented in the filter. These underlying mod-

eling errors can seriously degrade filter and predictor performance. Appendix B includes an introduction to the Kalman filter.

Algorithms designed for recursive state estimation must be able to contend with both known and unknown mismatches between the dynamic stochastic model used for filter implementation and a generally more complex truth model. Two basic approaches are used to deal with uncertain truth models: (1) robust techniques and (2) adaptive techniques. Robust techniques use estimation algorithms that are designed to work in spite of uncertainties in the truth model dynamics and in the statistical characterization of the underlying stochastic processes, whereas, adaptive techniques use methods that reduce the effects of truth model uncertainty by simultaneously estimating unknown truth model parameters during the state estimation process. Adaptive techniques may be applicable when the system information structure allows a successful learning process to occur and the decision interval is long enough to allow adequate estimation of the truth model parameters. Hence, if the uncertain truth model parameters are stationary, then adaptive techniques can provide superior steady state statistical performance. Stationary stochastic processes are discussed in subpar. C-4.2 of Appendix C. On the other hand, adaptive techniques are not preferred when estimator requirements include good transient performance, reliable convergence, and minimal complexity. By comparison, properly designed robust techniques can provide good transient performance and statistical accuracy, with protection against uncertain truth models, at affordable complexity.

The design of filters and predictors begins with delineation of a plausible initial model that characterizes the family of possible truth models for the filtering and prediction problem. This initial family of models is called the uncertainty class. The design of the candidate filter and predictor may be based on the initial uncertainty class or a proper subclass of the initial uncertainty class. The option choice is usually based on

1. The complexity of the initial uncertainty class
2. Given design restrictions on the complexity of the candidate filter
3. Prior practical experience with similar dynamic systems
4. Simulation results based on validated mathematical models and/or suitable empirical (test) data.

To delineate a plausible initial uncertainty class, the natures of the underlying dynamic system and observation noise processes that describe the given filtering problem are broadly specified. These specifications include a choice of a filter coordinate system and the salient system state variables relevant to the given problem statement. For example, in an air-defense fire control problem, the engineer might choose to model the motion of an attack aircraft (target) in an inertial XYZ-coordinate system. Based on this selection, a minimal set of relevant state variables would include the XYZ-components of aircraft position, velocity, and acceleration. Further analysis would then be necessary to evaluate the utility of adding additional state variables to model the motion of the target in this fire control application. This iterative modeling process could be based on the analysis of flight-test data that characterize the evasive motion of the attack aircraft during weapon delivery passes against a defended ground target.

4-3.1 DECISION MAKING UNDER UNCERTAINTY

Methodologies used for decision making under uncertainty that are relevant in fire control applications include maximum likelihood estimation (ML), maximum a posteriori probability estimation (MAP), Bayesian statistical decision theory, and game-theoretic techniques. These concepts are summarized in this subparagraph. A more comprehensive discussion is included in Refs. 4 and 5. To simplify the presentation, a single example is used to demonstrate each methodology.

Let $\mathbf{Z} = (Z_1, Z_2, \cdots, Z_n)'$ denote a vector of n independent random variables, each of which represents a measurement of target range and follows the same probability density distribution. These variables are then defined as being independent identically distributed. It is assumed that each variable is characterized by a model of the form

$$Z_i = \theta + V_i, \mathbf{m} \tag{4-1}$$

where

Z_i = random variable representing the ith target range measurement, m

θ = true (unknown) range to the target, m

V_i = additive measurement noise range variable associated with the ith observation, m.

With the model of Eq. 4-1 the additive noise also consists of a set of independent identically distributed variables.

Let Ω denote the set of all possible range values. Specification of Ω constitutes a priori knowledge about the true value of the unknown range θ prior to the observation of **Z**.

4-3.1.1 The Method of Maximum Likelihood Estimation

The method of ML is a parameter estimation technique in which the chosen value of the unknown parameter maximizes the joint probability of obtaining the observed set of measurements. In the range measurement example the additive noise has been assumed to be independent identically distributed. The joint probability distribution for n observations of the random variable V, or equivalently $(Z - \theta)$, is simply the product of n similar probability density distributions. If the symbol $f_V(...)$ is used to represent the form of the pdf for the additive noise, the coproduct of the pdf is given by

$$f(\mathbf{Z} \mid \theta) \;=\; \prod_{i=1}^{n} f_V(V_i) \;=\; \prod_{i=1}^{n} f_V(Z_i - \theta), \;\; \mathbf{m}^{-n} \tag{4-2}$$

where

$f(\mathbf{Z}|\theta)$ = joint probability distribution (coproduct) of **Z** for an arbitrary value of θ, m^{-n}

$f_V(\cdots)$ = pdf for the random noise variable, m^{-1}.

When $(Z_i - \theta)$ is used as the random variable in the joint distribution function and the n variables $(Z_1, \cdots, Z_n)$ are replaced by the numerical values of the n observations, the expression for the joint distribution becomes a function of the unknown parameter θ. In this form the coproduct is called the joint likelihood function of the unknown parameter for the known fixed values of the observations. It can be written as

$$\mathsf{F}(\theta \mid \mathbf{z}) \;=\; \prod_{i=1}^{n} f_V(z_i - \theta), \;\; \mathbf{m}^{-n} \tag{4-3}$$

where

$\mathsf{F}(\theta|\mathbf{z})$ = joint likelihood function of θ given the observed **z** values, $(z_1, \cdots, z_n)$, m^{-n}

z = vector of observed values, m

z_i = value of observed ith value of target range, m.

The maximum likelihood estimator for the parameter θ is that value of θ which falls within the set Ω and which maximizes the likelihood function. This estimator must therefore satisfy the set of equations:

$$\left.\frac{\partial \mathsf{F}(\theta \mid \mathbf{z})}{\partial \theta}\right|_{\theta = \theta^*} = \mathbf{0}, \;\; \mathbf{m}^{-(n+1)}$$

$$\left.\frac{\partial^2 \mathsf{F}(\theta \mid \mathbf{z})}{\partial \theta^2}\right|_{\theta = \theta^*} < \mathbf{0}, \;\; \mathbf{m}^{-(n+2)} \tag{4-4}$$

$$\theta^* \in \Omega, \;\; \mathbf{m}$$

where

θ^* = maximum likelihood estimator of θ, m

Ω = set of all possible values of a range, m.

4-3.1.2   The Method of Maximum A Posteriori Probability Estimation

The maximum a posteriori estimation technique uses a priori knowledge of the unknown parameter to improve the estimate. Specifically, if the unknown parameter can be modeled as a random variable and a pdf for this variable assumed, a conditional joint distribution function can be formed and the estimator chosen as that value which maximizes this function. The conditional distribution function is derived by using Bayes' Theorem (Ref. 4). When the random variables of the function are replaced by the observed values, the distribution becomes a function of the parameter θ and is called the a posteriori distribution for the parameter θ. The a posteriori distribution function for the range measurement example is

$$F(\theta \mid \mathbf{z}) = \frac{g_\theta(\theta) \prod_{i=1}^{n} f_V(z_i - \theta)}{\int_{-\infty}^{\infty} \left[g_\theta(u) \prod_{i=1}^{n} f_V(z_i - u) \, du \right]}, \text{ dimensionless} \qquad (4\text{-}5)$$

where

$F(\theta|\mathbf{z})$ = a posteriori distribution for θ given the observed values of z, dimensionless

$g_\theta(\theta)$ = assumed probability density function for θ, m^{-1}

$g_\theta(u)$ = pdf of θ with dummy variable of integration u, m^{-1}

u = dummy variable of integration, m.

The maximum a posteriori estimator for θ is defined as the value of θ that maximizes the function $F(\theta|\mathbf{z})$ in Eq. 4-5. This estimator θ^* must therefore satisfy Eq. 4-4 but with the function $\mathsf{F}(\theta|\mathbf{z})$ replaced by $F(\theta|\mathbf{z})$.

If the a priori density distribution for θ is constant on Ω, then the ML and MAP rules coincide. Distributions on Ω that are constant, or very nearly so, are referred to as uniform a priori distributions.

4-3.1.3   Statistical Decision Theory

The ML and MAP methods provide the means by which to estimate the unknown parameter θ. These methods, however, do not provide a direct approach to modeling the cost or loss incurred by the user of the fire control system as a consequence of the error $\theta^* - \theta$. Statistical decision theory (SDT) provides a means by which to incorporate such costs.

The approach is first to formulate a loss function that defines the cost to fire control system performance of an error in the estimation of θ. In most situations the true value of the estimated parameter is not known; thus a specific value cannot be assigned to the loss function. The estimator of the unknown parameter is therefore treated as a random variable, and an expression for the expected value of the loss function is derived. The expected value of the loss function is called the risk and is computed from

$$r(\theta, \delta^*) = \int_{-\infty}^{\infty} \cdots \int_{-\infty}^{\infty} L(\theta, \delta^*) f(\mathbf{z} \mid \theta) \, dZ_1 \, dZ_2 \cdots dZ_n, \ \mathbf{U}^* \qquad (4\text{-}6)$$

where

$r(\theta, \delta^*)$ = risk or expected loss, U

δ^* = estimator of the parameter θ expressed as a function of the random variable $\mathbf{Z}$, m

$L(\theta, \delta^*)$ = loss function for the estimation error $(\delta^* - \theta)$, U.

---

*"U" is used to represent the fact that there are units of measure associated with the function or variable when actual values are used.

If the distribution of θ is known, the expected risk can be computed from

$$R(\delta^*, g_\theta) = \int_{-\infty}^{\infty} r(\theta, \delta^*) g_\theta(\theta) \, d\theta, \ \mathbf{U} \tag{4-7}$$

where

$R(\delta^*, g_\theta)$ = **expected risk, U.**

The Bayesian approach to SDT seeks an estimator that minimizes the expected risk.

4-3.1.4 Statistical Decision Theory: A Game-Theoretic Approach

The methodologies of SDT are also applicable when there is no a priori probability distribution for θ. In this situation the fire control system designer can consider a worst-case design philosophy and thus seek a solution based on game theory. Such a solution, referred to as the minimax rule, is expressed as

$$\max_{\theta \in \Omega} r(\theta, \theta^*) \leq \max_{\theta \in \Omega} r(\theta, \delta^*), \ \mathbf{U}^{-1} \tag{4-8}$$

where

$\displaystyle\max_{\theta \in \Omega} r(\theta, \theta^*)$ = **maximum expected risk for $\theta \in \Omega$ using θ^* as an estimator, U^{-1}**

$\displaystyle\max_{\theta \in \Omega} r(\theta, \delta^*)$ = **maximum expected risk for $\theta \in \Omega$ for all other estimators, U^{-1}.**

In essence, Eq. 4-8 states that the minimax estimator θ^* is the one for which the maximum expected value of the loss is less than or equal to the maximum expected loss resulting from the use of any other estimator δ^*.

4-3.2 DYNAMIC MODELS FOR UNCERTAIN DYNAMIC SYSTEMS

The mathematical models of the uncertain dynamic systems most often encountered in fire control filtering and prediction applications are (1) stochastic ordinary differential equations and (2) stochastic difference equations. In this text "stochastic" refers to the existence of (1) random inputs or forcing functions that describe these uncertain dynamic systems and (2) the random (probabilistic) character of the unforced dynamic systems. For example, it is common to model the kinematic acceleration of a fixed wing aircraft target in a Cartesian reference frame by

$$a_{n+1}^i = \beta_n^i a_n^i + \mu_n^i, \ \mathbf{m/s}^2 \tag{4-9}$$

where

a_{n+1}^i = i**th component of aircraft kinematic acceleration at time step $n+1$, m/s^2**

a_n^i = i**th component of aircraft kinematic acceleration at time step n, m/s^2**

β_n^i = **(possibly uncertain) parameter at time step n, dimensionless**

μ_n^i = **sequence of independent random variables with zero mean, m/s^2**

n = **time step defined by Eq. 4-10, dimensionless**

$$n = \frac{t_n - t_0}{\Delta t}, \ \mathbf{dimensionless} \tag{4-10}$$

where

t_n = **absolute time at the nth step, s**

t_0 = **absolute time at beginning of the step sequence, s**

Δt = **time interval between steps, s.**

Eq. 4-9 is referred to as a stochastic difference equation because of its random forcing function μ_n^i and the possibly random coefficient β_n^i. This model is a special case of a general class of time invariant linear systems, which are referred to as autoregressive (AR) time series models. A pth order autoregressive model [AR(p)] has the form

$$X_n = \gamma_1 X_{n-1} + \gamma_2 X_{n-2} + \cdots + \gamma_p X_{n-p} + \mu_n, \ \mathbf{U} \tag{4-11}$$

where

X_n = dynamic quantity at time step n, **U**

μ_n = sequence of independent random variables with zero mean and common variance, **U**

γ_p = AR time series coefficient, dimensionless.

Stochastic difference equation models of this type are obtained by forming a discrete representation of the corresponding linear ordinary differential equation. The relationship between continuous linear differential equations and their corresponding difference equations can be shown by considering the case of a first-order linear differential equation. The results derived for this particular case, however, will be applicable to systems of any order because any higher order differential equation can be formulated as a set of first-order differential equations. Such a set of equations is called a state variable model and is discussed in subsequent paragraphs.

The difference equations corresponding to the following first-order linear differential equation are derived:

$$\frac{da^i(t)}{dt} = -\alpha^i a^i(t) + w^i(t), \ \mathbf{m/s^3} \tag{4-12}$$

where

$a^i(t)$ = acceleration in the ith direction at time t, m/s²

α^i = positive real number, 1/s

$w^i(t)$ = wideband stationary white noise, m/s³

t = time, s.

The white noise $w^i(t)$ is assumed to have a zero mean and a constant power spectral density.

Eq. 4-12 can be solved by ordinary methods of differential equations. The acceleration at time $t + \Delta t$ based on an initial condition for acceleration at time t is given by

$$a^i(t+\Delta t) = \mathbf{exp}\ (-\alpha^i \Delta t)\ a^i(t)\ + \int_t^{t+\Delta t} \mathbf{exp}\ [-\alpha^i(t+\Delta t - \xi)]\ w^i(\xi)\ d\xi, \ \mathbf{m/s^2} \tag{4-13}$$

where

ξ = arbitrary variable of time integration, s.

The first term on the right side of Eq. 4-13 is the complementary solution to the homogeneous differential equation. The integral in the second term is the particular solution for the random white noise forcing function $w^i(\xi)$. It is the convolution integral based on the impulse response of a first-order system. Impulse response techniques are described in subpar. 4-4.3.4.1. If Δt is small, Eq. 4-13 can be approximated by

$$a^i(t+\Delta t) = (1 - \alpha^i \Delta t)\ a^i(t) + v^i(t), \ \mathbf{m/s^2} \tag{4-14}$$

where

$v^i(t)$ = sequence of independent random variables with zero mean and variance $\eta^i \Delta t$, m/s².

For small time steps the first-order difference equation in Eq. 4-9 can be made equivalent to the continuous first-order differential equation in Eq. 4-12 by use of the following equalities:

$$\beta^i = 1 - \alpha^i \Delta t, \ \mathbf{dimensionless}$$
$$q^i = \eta^i \Delta t, \ \mathbf{m^2/s^4} \tag{4-15}$$

where

η^i = intensity of the constant power spectral density function of the wideband white noise, m^2/s^5

q^i = variance of the random variable μ_n^i in Eq. 4-9, m^2/s^4.

The identical result is obtained by replacing the derivative in Eq. 4-12 by the first-order difference operator Δa_n^i, and the variable $a^i(t)$ by a_n^i. In general, the difference operator is defined as

$$\Delta y_n = y_{n+1} - y_n, \; \mathbf{U}$$ (4-16)

where

Δy_n = first-order difference operator, **U**

y_n = variable at time step n, **U**

y_{n+1} = variable at time step $n + 1$, **U**.

Ref. 6 discusses the characteristics and use of difference equations.

Differential equation models of continuous-time systems are important for theoretical considerations. Algorithms for filtering and prediction, however, are always expressed in terms of discrete difference equations.

To design an effective fire control system, it is essential that the model building process be guided by real kinematic data, i.e., target motion data. To justify first-order AR models for target acceleration in a given reference frame, it is necessary that the designer have real target motion data available in sufficient quantities to allow a careful model validation process.

Identification and estimation of parameters in AR(p) models are parts of a subject referred to as time series analysis. Determination of appropriate time series models is a fundamental issue in the formulation of filters and predictors for fire control applications.

The least squares method is one technique used to estimate the value of unknown parameters in discrete autoregressive models. As an example, consider the first-order AR(1) model

$$x_k = \gamma_1 x_{k-1} + \mu_k, \; \mathbf{U}$$ (4-17)

where

x_k = value of observed data at time step k, **U**

γ_1 = time series coefficient, dimensionless

μ_k = sequence of independent random variables with zero mean and common variances, **U**.

An estimate of the coefficient γ_1 is sought based on a set of observed states $\{x_k: 1 \le k \le N\}$ where N is the total number of trials. The method of least squares selects the parameter value γ_1 that minimizes the sum of squares function:

$$\sum_{k=2}^{N} (x_k - \gamma_1 x_{k-1})^2, \; \mathbf{U}^2.$$ (4-18)

The minimizing value of γ_1 is $\hat{\gamma}_1$ and is shown in Ref. 4 to be

$$\hat{\gamma}_1 = \frac{\displaystyle\sum_{k=2}^{N} x_{k-1} x_k}{\displaystyle\sum_{k=2}^{N} x_{k-1}^2}, \; \text{dimensionless.}$$ (4-19)

The standard least squares algorithm is known to be nonrobust to outliers in the data. Thus, to be cautious, other techniques should be used where possible. Robust techniques for estimating the parameters of an AR model of any order are discussed in Ref. 7.

4-3.3 STATE VARIABLE MODELS AND ALGORITHMS USED FOR FILTERING AND PREDICTION IN FIRE CONTROL SYSTEMS

The design of computationally efficient algorithms used for filtering and prediction in fire control applications is generally based on state variable models of the underlying dynamic systems. For mathematical simplicity these dynamic systems are often modeled as finite-dimensional linear systems. State variable models of target dynamics that come under this description are modeled in discrete time by equations of the form

$$\mathbf{x}_{n+1} = [F_n]\,\mathbf{x}_n + [G_n]\,\mathbf{w}_n, \quad \mathbf{U}$$
$$n \in \Gamma_0, \quad \text{dimensionless} \tag{4-20}$$

where

$\mathbf{x}_{n+1}$ = true value of the m-dimensional state vector at time step $n+1$, U

$\mathbf{x}_n$ = true value of the m-dimensional state vector at time step n, U

$[F_n]$ = $m \times m$ state transition matrix at time step n, U

$[G_n]$ = $m \times r$ input parameter matrix at time step n, U

$\mathbf{w}_n$ = r-dimensional random input function vector at time step n, U

Γ_0 = discrete time index set $(0, \cdots, N)$, dimensionless.

The units of each of the terms in Eq. 4-20 depend on the variables in the state vector. The units of each of the elements in the state transition matrix and the input function vector must be consistent with the state vector definition.

The vector $\mathbf{w}_n$ is a sequence of random forcing functions that drive the system being observed. The input matrix $[G_n]$ defines how the forcing functions are coupled into the system dynamics.

The filtering and prediction problem for fire control is to determine a best estimate for the state variable $\mathbf{x}_{n+1}$ based on sampled measurements of the system state at times prior to and including time step n.

It is assumed that the measurements of the system state are not perfect and that each observation has a random noise component associated with it. The set of measurements is represented by

$$\mathbf{z}_k = [H_k]\,\mathbf{x}_k + \mathbf{v}_k, \quad \mathbf{U}$$
$$k \in \Gamma_1, \quad \text{dimensionless} \tag{4-21}$$

where

$\mathbf{z}_k$ = set of s-dimensional observations of the system state at time step k, U

$[H_k]$ = $s \times m$ measurement matrix, U

$\mathbf{v}_k$ = s-dimensional vector of additive observation noise, U

Γ_1 = discrete time index set $(1, \cdots, N)$, dimensionless.

Again units for the terms in Eq. 4-21 must be consistent with the variables selected in the state vector.

The random components within vectors $\mathbf{w}_n$ and $\mathbf{v}_k$ are assumed to be statistically independent. In addition, each vector is assumed to have a zero mean and a known covariance. The covariance of $\mathbf{w}_n$ is defined by an $r \times r$ covariance matrix $[Q_n]$, and the covariance of $\mathbf{v}_k$ is defined by an $s \times s$ covariance matrix $[R_k]$. The diagonal terms in the covariance matrix represent the values of the variance for each of the vector components. The off-diagonal terms are measures of the degree of cross-correlation between each of the vector components. Appendices B and C and Ref. 5 contain reviews of the underlying statistical principles used in this subparagraph.

Ref. 5 explains that the covariance matrix for the uncorrelated sequence of random system inputs is represented by

$$[S_n] = [G_n][Q_n][G_n]', \quad \text{U} \tag{4-22}$$

where

$[S_n]$ = system noise covariance matrix at time step n, U

$[Q_n]$ = covariance matrix of the random forcing function w, U

$[G_n]'$ = transpose of the matrix $[G_n]$, U.

With Kalman filtering and prediction techniques, the matrices $[F_n]$ and $[G_n]$ in the state model of the system dynamics, the matrix $[H_k]$, which characterizes the model of the measurement process, and the covariance matrices $[Q_n]$ and $[R_k]$ of the random vectors are specified for each time step in the prediction sequence. The prediction techniques then generate a best estimate of the future value of the state vector based on the set of observations.

An example follows of the formulation of a linear time-varying set of state equations for a maneuvering ground-based target.

The target acceleration is modeled as a first-order AR process:

$$x_3(n+1) = \beta x_3(n) + w(n), \quad \text{m/s}^2 \tag{4-23}$$

where

$x_3(n+1)$ = horizontal target acceleration at time step $n+1$, m/s^2

$x_3(n)$ = horizontal target acceleration at time step n, m/s^2

β = constant state transition coefficient, dimensionless

$w(n)$ = time series function that characterizes the random time-varying inputs to the target, m/s^2.

The random forcing function $w(n)$ is assumed to have a zero mean and a known variance q, i.e.,

$$E[\, w(n)\,] = 0, \quad \text{m/s}^2$$

$$E[\, w(i)\; w(j)\,] = q\delta_{ij}, \quad (\text{m/s}^2)^2 \tag{4-24}$$

$$i,\; j \in \Gamma_0, \quad \text{dimensionless}$$

where

$E[w(n)]$ = expectation value , or mean, of $w(n)$, m/s^2

$E[w(i)w(j)]$ = covariance of the function $w(n)$, (m/s^2)^2

δ_{ij} = Kronecker delta function, dimensionless

$$= \begin{cases} 1, & i=j \\ 0, & i \neq j \end{cases}$$

q = known variance of $w(n)$, (m/s^2)^2.

The specification of the target state is completed by formulating difference equations to represent the horizontal target velocity and horizontal target position:

$$x_2(n+1) = x_2(n) + \Delta t x_3(n), \quad \text{m/s} \tag{4-25}$$

where

$x_2(\cdots)$ = horizontal target velocity, m/s

and

$$X_1(n+1) = X_1(n) + \Delta t x_2(n) + \frac{1}{2}\Delta t^2 x_3(n), \quad \text{m} \tag{4-26}$$

where

$x_1(\cdots)$ = horizontal target position, m.

Eqs. 4-25 and 4-26 are derived from the basic principles of rigid body motion.

It is assumed that the prediction filter uses sampled measurements of target position and that these measurements are corrupted by additive, statistically stationary, band-limited white noise, i.e., there is noise in the measurement data received from the equipment monitoring target position. The sequence of position measurements is represented by

$$z(k) = x_1(k) + v(k), \quad \text{m}$$
$$k \in \Gamma_1, \quad \text{dimensionless.} \tag{4-27}$$

The measurement noise is assumed to have zero mean and known variance. Thus

$$E[v(k)] = 0, \quad \text{m/s}$$
$$E[v(i)\,v(j)] = r\delta_{ij}, \quad (\text{m/s})^2$$
$$i,j \in \Gamma_1, \quad \text{dimensionless} \tag{4-28}$$

where

r = measurement noise variance, m².

For this example, the state vector for the target is represented as

$$\mathbf{x}(\cdots) = \begin{bmatrix} x_1(\cdots) \\ x_2(\cdots) \\ x_3(\cdots) \end{bmatrix}, \quad \text{U.} \tag{4-29}$$

The input and measurement noise vectors are

$$\mathbf{w}_n = \begin{bmatrix} 0 \\ 0 \\ W_n \end{bmatrix}, \quad \text{U} \tag{4-30}$$

and

$$\mathbf{v}_k = \begin{bmatrix} V_k \\ 0 \\ 0 \end{bmatrix}, \quad \text{U.} \tag{4-31}$$

The matrices defined in Eqs. 4-20, 4-21, and 4-22 take the form

$$[F] = \begin{bmatrix} 1 & \Delta t & \dfrac{(\Delta t)^2}{2} \\ 0 & 1 & \Delta t \\ 0 & 0 & \beta \end{bmatrix}, \quad \mathbf{U}$$

$$[G] = \begin{bmatrix} 1 & 0 & 0 \\ 0 & 1 & 0 \\ 0 & 0 & 1 \end{bmatrix}, \quad \mathbf{U}$$

$$[H] = \begin{bmatrix} 1 & 0 & 0 \\ 0 & 0 & 0 \\ 0 & 0 & 0 \end{bmatrix}, \quad \mathbf{U}$$

$$[Q] = \begin{bmatrix} 0 & 0 & 0 \\ 0 & 0 & 0 \\ 0 & 0 & q \end{bmatrix}, \quad \mathbf{U}$$

$$[S] = [G][Q][G]' = \begin{bmatrix} 0 & 0 & 0 \\ 0 & 0 & 0 \\ 0 & 0 & q \end{bmatrix}, \quad \mathbf{U}$$

$$[R] = \begin{bmatrix} r & 0 & 0 \\ 0 & 0 & 0 \\ 0 & 0 & 0 \end{bmatrix}, \quad \mathbf{U}$$

(4-32)

where

$[R]$ = the observation noise covariance matrix.

Previous studies of flight-test data (Ref. 8) have investigated the adequacy of first-order models of aircraft acceleration in a Cartesian coordinate system. Although not optimal, these models provide a baseline for filter design and evaluation. The following example provides some numerical results for models based on actual flight-test data.

Following the previous example,

$$x_3(n+1) = \beta x_3(n) + w(n), \quad \mathbf{m/s}^2 \tag{4-33}$$

denotes a first-order Markov process for target acceleration. If the time increment $\Delta t = 0.1$ s, a nominal value for β obtained from the flight-test data studied in Ref. 8 is 0.995. The nominal value of the variance of the input process $w(n)$ is $q = 1.0$ $(m/s^2)^2$.

These nominal values are obtained by applying the least squares techniques, as described previously in this chapter, to the acceleration data in the FACT II database of Ref. 8.

When linear models do not provide adequate representations for target and observation models, the fire control system designer is left with two other options: (1) approximation of the nonlinear state equations over small time intervals by an equivalent set of linear equations and the application of the standard linear Kalman filter theory or (2) application of the EKF, which is an ad hoc technique used to

adopt the nonlinear form of the dynamic system and observation equations to the nominal form of the linear Kalman filter. The resulting EKF is a nonlinear system that seeks to capture the essence of the nonlinear model for state transition and covariance updating without losing the entire benefit of the original linearity and mathematical and computational simplicity of the standard linear Kalman filter.

4-3.3.1 Linear Kalman Filters

The standard Kalman filter is defined in terms of the parameter matrices, which define the structural and statistical behaviors of the linear target model. If the underlying random variables are jointly Gaussian, the Kalman filter obtains the optimal estimate in the sense of minimum mean-square error. When the assumption of joint normality does not apply, the Kalman filter provides the best linear estimate for the state, again in the sense of minimum mean-square error. In the following discussion, it is assumed that the initial system state, the system input noise, and the observation noise represent three statistically independent sets of random vectors.

If the system dynamics and the observation relations can be defined by the linear models presented in Eqs. 4-20, 4-21, and 4-22 and the underlying random variables are jointly normal, a recursive procedure is used to obtain predictions of the future system state and an estimate of the prediction error. The equations defining the procedure are derived in Appendix B and in Ref. 5.

The computation process starts with an assumed initial condition for the system state vector at time step 0. Measurements of the system state start at time step 1. At each subsequent time step, predictions from the prior step are updated based on current measurements of the system state, and a new prediction for the next time step is generated. The computations also include an estimate for the prediction error, and these are also updated by the current measurements.

The update of the prediction from the prior time step is computed by

$$\hat{x}_n | n = \hat{x}_n | n - 1 + [K_n] (\mathbf{z}_n - [H_n] x_n | n - 1), \ \mathbf{U} \qquad \textbf{(4-34)}$$

where

$\hat{x}_n | n$ = updated estimate of the current system state vector at time step n based on new measurements $\mathbf{z}_n$, U

$\hat{x}_n | n - 1$ = predicted value of the current system state vector made in the prior time step $n - 1$, U

$[K_n]$ = Kalman gain matrix defined in Eq. 4-35, U

$\mathbf{z}_n$ = vector containing the measurements of the system state at time step n, U

$[H_n]$ = measurement matrix for time step n, U.

The Kalman gain matrix is defined as

$$[K_n] = [P_n] [H_n]' ([H_n] [P_n] [H_n]' + [R_n])^{-1}, \ \mathbf{U} \qquad \textbf{(4-35)}$$

where

$[P_n]$ = covariance matrix of the error in the prediction for the state vector at time step n, U.

The covariance matrix $[P_n]$ is based on measurements taken at time step $n - 1$ and is defined as

$$[P_n] = E[(\mathbf{x}_n - \hat{x}_n | n - 1) (\mathbf{x}_n - \hat{x}_n | n - 1)'], \ \mathbf{U} \qquad \textbf{(4-36)}$$

where

$\mathbf{x}_n$ = true value of the system state vector at time step n, U.

The new prediction for the state vector at time step $n + 1$ is given by

$$\hat{\mathbf{x}}_{n+1} \big| n = [F_n] \hat{\mathbf{x}}_n \big| n, \ \mathbf{U}. \tag{4-37}$$

The error covariance matrix for the new estimate is

$$[P_{n+1}] = ([F_n] - [\hat{K}_n][H_n])[P_n]([F_n] - [\hat{K}_n][H_n])' + [G_n][Q_n][G_n]'$$
$$+ [\hat{K}][R_n][\hat{K}_n]', \ \mathbf{U} \tag{4-38}$$

$$[\hat{K}_n] = [F_n][K_n], \ \mathbf{U}$$

where

$[P_{n+1}]$ = error covariance matrix for the state vector prediction at time step $n + 1$, U
$[\hat{K}_n]$ = estimated Kalman gain matrix, U.

The computation process begins with an assumed initial state for the system. This state is defined by a Gaussian random vector with zero mean and an assumed covariance matrix. Thus

$$E(\mathbf{x}_0) = \mathbf{0}, \ \mathbf{U}$$
$$E(\mathbf{x}_0 \mathbf{x}_0') = [M_0], \ \mathbf{U} \tag{4-39}$$

where

$\mathbf{x}_0$ = initial system state vector, U
$[M_0]$ = initial state covariance matrix, U.

The system state vector at time step $n = 1$ is determined from the initial values of the state model matrices and system forcing function. From Eq. 4-20 with $n = 0$

$$\mathbf{x}_1 = [F_0]\mathbf{x}_0 + [G_0]\mathbf{w}_0, \ \mathbf{U} \tag{4-40}$$

where

$[F_0]$ = initial state transition matrix, U
$[G_0]$ = initial input parameter matrix, U
$\mathbf{w}_0$ = initial value of the input function vector, U.

The propagation of the system covariance between the initial state and state $n = 1$ is expressed as

$$[M_1] = [F_0][M_0][F_0]' + [G_0][Q_0][G_0]', \ \mathbf{U} \tag{4-41}$$

where

$[M_1]$ = system state covariance at $n = 1$, U
$[Q_0]$ = initial covariance of the input function vector, U.

Eq. 4-41 is derived in Ref. 5 or can be inferred from Eq. 4-38. Eq. 4-38 represents the prediction error at time step $n + 1$ based on measurements of the system state at the previous time step. If n is equal to zero in Eq. 4-38, the equation represents the prediction error at time step 1 based on conditions existing in the initial state. Since no measurements of system state have yet been used, the matrices $[\hat{K}_0]$ and $[R_0]$ in Eq. 4-38 are zero. Thus

$$[P_1] = [F_0][P_0][F_0]' + [G_0][Q_0][G_0]', \ \mathbf{U} \tag{4-42}$$

In accordance with Eq. 4-36 the prediction error matrices $[P_1]$ and $[P_0]$ are equal to the respective covariances of the state vectors because no estimates of the system state have yet been made. Thus

$$[P_0] = E[\mathbf{x}_0\mathbf{x}_0'] = [M_0], \ \mathbf{U}$$
$$[P_1] = E[\mathbf{x}_1\mathbf{x}_1'] = [M_1], \ \mathbf{U}. \tag{4-43}$$

Substituting Eq. 4-43 into Eq. 4-42 yields Eq. 4-41.

The first estimate of the system state based on the initial state is shown in Appendix B, subpar. B-5.3, to be

$$\mathbf{x}_1 \,\big|\, 0 = 0, \ \mathbf{U}. \tag{4-44}$$

The computation process now proceeds using the first set of system state measurements $\mathbf{z}_1$. Letting $n = 1$ in Eq. 4-34 and using the result of Eq. 4-44 yield

$$\hat{\mathbf{x}}_1 \,\big|\, 1 = [K_1]\,\mathbf{z}_1, \ \mathbf{U}. \tag{4-45}$$

If Eq. 4-43 is used in Eq. 4-35, the following expression for the Kalman gain matrix $[K_1]$ results:

$$[K_1] = [M_1]\,[H_1]' \,([H_1]\,[M_1]\,[H_1]' + [R_1])^{-1}, \ \mathbf{U}. \tag{4-46}$$

With $n = 1$ Eqs. 4-37 and 4-38 give a state prediction and error estimate covariance for time step 2:

$$\hat{\mathbf{x}}_2 \,\big|\, 1 = [F_1]\,\hat{\mathbf{x}}_1 \,\big|\, 1, \ \mathbf{U}$$
$$[P_2] = ([F_1] - [\hat{K}_1]\,[H_1])\,[M_1]\,([F_1] - [\hat{K}_1]\,[H_1])' \tag{4-47}$$
$$+ [G_1]\,[Q_1]\,[G_1]' + [\hat{K}_1]\,[R_1]\,[\hat{K}_1]', \ \mathbf{U}.$$

An update of the state estimate at time step 2 is made with Eq. 4-34 and the set of measurements $\mathbf{z}_2$. The prediction process proceeds in time with Eqs. 4-34, 4-37, and 4-38 being used in sequence at each step in time.

4-3.3.2 Extended Kalman Filters

The EKF is an ad hoc technique used to adapt the nonlinear form of the dynamic system and observation equations to the nominal form of the linear Kalman filter. The EKF is a nonlinear formulation designed to capture the essence of the nonlinear model for state transition and covariance updating without losing the entire benefit of the original linearity and the mathematical and computational simplicity of the standard linear Kalman filter.

The EKF is applied to systems whose dynamics are characterized by continuous nonlinear stochastic differential equations and whose state is sampled at discrete time intervals. The equation for the system dynamics has the form

$$\frac{d\mathbf{x}}{dt} = f(\mathbf{x},t) + \mathbf{w}(t), \ \mathbf{U} \tag{4-48}$$

where

$f(\mathbf{x},t)$ = function of a known nonlinear function of the system state, U

$\mathbf{w}(t)$ = stochastic input function, U.

The discrete measurement process is defined by

$$\mathbf{z}_k = h_k(\mathbf{x}_k) + \mathbf{v}_k, \ \mathbf{U} \tag{4-49}$$

where

$h_k(\mathbf{x}_k)$ = known nonlinear function of the system state, U.

It is assumed that the initial system state, the system input noise, and the observation noise represent three statistically independent sets of random vectors.

The EKF yields a minimum variance estimate of the system state. Ref. 5 contains the derivation of the basic recursion relations and differential equations for the EKF.

It is important to emphasize that (1) the derivation of EKF is based on heuristic arguments that are based on local approximations rather than globally applicable approximations and (2) there is no global theory for the statistical behavior or stability of the EKF algorithm. This should be contrasted with the very complete theory for the corresponding linear case, i.e., with a known dynamic system and known measurement relations. A discussion of linear filter design when there is uncertainty in the specification of the linear target model is presented in the following subparagraph on robust linear Kalman filters.

4-3.3.3 Robust Linear Kalman Filters

The robust linear Kalman filter is an estimation technique designed for use when there are uncertainties in the specification of the system model. The principal ingredient in the robust design methodology is the concept of a worst-case probability distribution for the unknown parameters. This concept is illustrated with the following simplified example.

Consider a system whose dynamics are modeled by a discrete first-order AR process and whose state is sampled at discrete time intervals. The system dynamics and measurement are characterized by linear difference equations of the form

$$\mathbf{x}(n+1) = C\mathbf{x}(n) + \mathbf{w}(n), \quad \mathbf{U}$$
$$\mathbf{z}(k) = \mathbf{x}(k) + \mathbf{v}(k), \quad \mathbf{U} \tag{4-50}$$

where

C = unknown constant, dimensionless.

Eq. 4-50 is written in a computer programming, not a theoretical, form, i.e., $\mathbf{v}(k) = \mathbf{v}_k$, $\mathbf{z}(k) = \mathbf{z}_k$, $\mathbf{x}_k = \mathbf{x}_k$, $\mathbf{w}(n) = \mathbf{w}_n$, and $\mathbf{x}(n) = \mathbf{x}_n$.

As in the previous discussions, the variables $\mathbf{w}(n)$ and $\mathbf{v}(n)$ are, assumed to represent zero mean random processes with known variance. The unknown constant C is assumed to be bounded within the limits defined by

$$-1 < a \le C \le b < 1, \quad \text{dimensionless} \tag{4-51}$$

where

b = known upper limit for the unknown constant, dimensionless

a = known lower limit for the unknown constant, dimensionless.

The limits a and b define the uncertainty class for the system model.

The objective is to find a recursive linear filter, or predictor, that satisfies some predefined error criterion based on measurements z_k ($k = 1,2,\cdots, n-1$). One approach is to create a filter, or predictor, whose maximum mean-square prediction error over the possible range of values of the unknown parameter is less than the maximum mean-square prediction errors produced by all other filtering, or prediction, schemes. This criterion of robustness is called the minimax mean-square error criterion, and it protects against worst-case values of the unknown parameter. It is defined mathematically as

$$\max_{C \in [a,b]} E\{[\hat{\mathbf{x}}^*(n) - \mathbf{x}(n)^2]\} \le \max_{C \in [a,b]} E\{[(\hat{\mathbf{x}}(n) - \mathbf{x}(n))^2]\}, \mathbf{U} \tag{4-52}$$

where

$\hat{\mathbf{x}}^*(n)$ = optimum robust linear predictor at time step n, $\mathbf{U}$

$\hat{\mathbf{x}}(n)$ = other linear predictors, $\mathbf{U}$

$\mathbf{x}(n)$ = true value of the state variable at time step n, $\mathbf{U}$.

The required robust filter, or one-step predictor, is obtained by computing the linear Bayes rule with respect to a worst-case probabilistic mixture of unknown values of *C*.

Worst-case probability distributions for the uncertain system parameters always exist and can be realized by finite distributions—even for the most general uncertain *m*th-order time-varying dynamic system. Although it is mathematically possible for a discrete worst-case distribution to have numerous points of support, practical experience gained with this methodology suggests that simple mixture models can almost always be obtained to approximate the desired robust recursive filter. Thus in many practical applications the robust recursive filter can be realized by a Kalman filter with a state vector dimension that is only slightly larger than the minimum value imposed by the reduced-order uncertainty class.

For example, in a typical fire control problem in which target acceleration is modeled as an uncertain first-order AR process, the robust, steady state Kalman filter for each Cartesian coordinate would have a maximum of four state variables. This fact represents at most one more state variable than would be necessary if there were no model uncertainty with which to contend. The system state and measurement models for this example can be represented by Eqs. 4-23 through 4-28. In this case, however, the state transition parameter β and the system input q and measurement noise r variances are assumed to be unknown but bounded quantities:

$$0 < \beta_1 \leq \beta \leq \beta_2 < 1, \ \mathbf{U}$$
$$q_1 \leq q \leq q_2, \ \mathbf{U} \tag{4-53}$$
$$r_1 \leq r \leq r_2, \ \mathbf{U}.$$

Here the intervals $[\beta_1, \beta_2]$, $[q_1, q_2]$, and $[r_1, r_2]$ define the overall reduced-order model uncertainty class.

The robust steady state Kalman filter, or one-step predictor, is completely parameterized by the following matrices:

$$[F] = \begin{bmatrix} 1 & \Delta t & \dfrac{(\lambda_1)^{\frac{1}{2}} \Delta t^2}{2} & \dfrac{(\lambda_2)^{\frac{1}{2}} \Delta t^2}{2} \\ 0 & 1 & (\lambda_1)^{\frac{1}{2}} \Delta t & (\lambda_2)^{\frac{1}{2}} \Delta t \\ 0 & 0 & \beta_1 & 0 \\ 0 & 0 & 0 & \beta_2 \end{bmatrix}, \ \mathbf{U}$$

$$[H] = \begin{bmatrix} 1 & 0 & 0 & 0 \\ 0 & 0 & 0 & 0 \\ 0 & 0 & 0 & 0 \\ 0 & 0 & 0 & 0 \end{bmatrix}, \ \mathbf{U}$$

$$[R] = \begin{bmatrix} r_2 & 0 & 0 & 0 \\ 0 & 0 & 0 & 0 \\ 0 & 0 & 0 & 0 \\ 0 & 0 & 0 & 0 \end{bmatrix}, \ \mathbf{U}$$

$$[S] = \begin{bmatrix} 0 & 0 & 0 & 0 \\ 0 & 0 & 0 & 0 \\ 0 & 0 & q_2 & 0 \\ 0 & 0 & 0 & q_2 \end{bmatrix}, \ \mathbf{U}$$

(4-54)

where

λ_1, λ_2 = worst-case probabilities for the uncertain system parameter, $\mathbf{U}^{-1}$.

The probabilities λ_1 and λ_2 are defined by the following relationships:

$$\lambda_1 = P_r[\beta = \beta_1, \ q = q_1, \ r = r_1], \ \mathbf{U}^{-1}$$
$$\lambda_2 = P_r[\beta = \beta_2, \ q = q_2, \ r = r_2], \ \mathbf{U}^{-1}$$
$$\lambda_1 + \lambda_2 = 1, \ \mathbf{U}^{-1}.$$

(4-55)

The worst-case probability distribution for the uncertain parameters is referred to as a least favorable prior distribution in statistical decision theory.

4-4   ACCURACY CONSIDERATIONS AND ANALYSIS

4-4.1   INTRODUCTION

A weapon system–of which the fire control system is a major part–is designed to have the capability to destroy or disable a hostile target. The task of the fire control portion of the weapon system is to point the gun or projectile launcher in a direction that will cause the projectile to hit or to come sufficiently close to the target to achieve the required terminal ballistic effect. The degree of damage required to defeat any target depends on the characteristics of the target. The projectiles fired are selected to match target characteristics in order to assure such damage. Targets may range from widely distributed troop formations to hard point targets such as incoming missiles or distant aircraft and armored vehicles. Targets might also include buildings and other large structures of military significance. Specialists in operations research and military strategy are generally assigned the problem of identifying the need for a new weapon system and for defining the class of targets the system will be designed to engage. Various types of combat models and combat simulations are then used to establish the military requirements for these systems. These requirements can be expressed in terms of kill rates or probabilities of destroying or disabling the assigned targets in any defined engagement scenario. The requirements that are transmitted to the fire control designer are derived from these probabilities and relate primarily to accuracy of fire. Ref. 9 provides an excellent introduction to the mathematical methods used to study the various aspects of military operations. It also includes discussions of weapon performance, target vulnerability, and combat models.

The destructive effect of a weapon system is determined by (1) the destructive effect of the individual projectile, (2) the accuracy with which the projectile can be delivered to the target, and (3) the number of projectiles delivered, which is determined by the rate of fire and the length of the engagement. The engagement length is primarily determined by target characteristics, the range of the weapon, and user requirements but may be somewhat affected by the fire control system design.

The overall characteristics of the projectile, the projector (gun or launcher), and the fire control system are determined during the preliminary design of the weapon system and are based on a balancing of the factors involved. The main objective is to maximize the destructive power of the weapon system. Secondary objectives may be to maximize the range at which the engagement commences, to minimize the time required to complete the engagement, to minimize the amount of ammunition fired without destructive effect, and to prevent overkill, i.e., expenditure of ammunition beyond the minimum required to disable or destroy the target.

Accuracy is the primary factor under the control of the fire control system designer. In fact, fire control system accuracy is the basic specification from which he must determine subsystem accuracies and speeds of response. This paragraph considers the accuracy specification problem in some detail starting with a discussion of the specification of system accuracy that is followed by a description which shows how the subsystem accuracies are derived from it.

The fire control system determines the direction in which the gun or launcher must point in order for the projectile to destroy the target. Most of the current fire control systems are capable of solving this problem for a stationary target or for targets moving in a straight line or in simple curvilinear paths. Since conclusions drawn for the case of a moving target can readily be reduced to the simpler stationary target case, only moving targets are discussed.

If the target is not taking evasive action, the fire control system can track the target and from this tracking information can determine its speed and direction of motion. The system must then compute the orientation of the gun or launcher that will cause the projectile trajectory to intersect the target path at a common future point in time. Such an intersection defines a hit. In other words, an ideal fire control computer must continuously compute the intersection in space of the predicted target path and a ballistic trajectory. Because of the complexity of the ballistic computation, all practical fire control computers approximate the exact solution. Errors due to the approximations used can be computed by straightforward techniques and would of course be designed to be small compared with the physical errors of the system. If the target is taking evasive action, the tracking process and the process of

extracting the actual target states, e.g., velocity and acceleration, from the data and predicting the future position become more difficult.

In practice, targets are not always treated as simple points in space. They are considered to extend over a finite area or volume, different regions of which are more vulnerable to damage than others. The impact of a projectile on such a target may result in complete destruction, may disable one of the primary missions of the target (such as firepower or mobility), or may only partially disable one of the mission areas. In the last case more than one hit would be required to neutralize the target fully. The probability that a single hit will destroy or neutralize a target is expressed in terms of a conditional probability, i.e., the probability of causing destruction or disablement given that a hit has already occurred. This probability is given the generic name "conditional single-shot kill" probability. More descriptive terms such as "probability of firepower kill" or "mobility kill" can also be used.

The conditional kill probability is not affected by the characteristics of the fire control system. Its magnitude depends, for example, on the specific point of impact with the target, the physical characteristics of the target, the shape of the projectile, its kinetic energy at impact, and on the amount and type of explosive contained within the warhead.

Combat simulations and other military strategy analyses often establish weapon system requirements in terms of kill rates or kill probability for the weapon system in a specified set of engagement scenarios. The kill referred to is not the conditional kill described previously but the unconditional kill, which includes the conditional vulnerability statistics as well as the statistics related to the probability of achieving a hit on the target.

To make use of kill rate and kill probability requirements in the design of the fire control system, it is necessary to remove those factors relating to the conditional target vulnerability and in the case of kill rates also to remove factors relating to the weapon firing rates. These sets of factors are not generally under the control of the fire control designer. The former falls under the mission of the ammunition developers, and the latter, under the responsibility of the armament developer, which includes the gun tube or projectile launcher and the projectile handling and loading equipment.

The specifications of primary interest to the fire control designer relate to the probabilities of hitting the target or of getting sufficiently close to the target in the case of projectiles armed with proximity or timed fuses. These probabilities are functions of the weapon system errors and can be computed from the kill rate and kill probability specifications.

The parameters most commonly used to characterize weapon system accuracy are the single-shot hit probability and the engagement hit probability. As its name implies, the former is the probability that when only one projectile is fired, it will hit or come within some required proximity of the target. The engagement hit probability refers to situations in which more than one round is fired at the target. It is generally expressed as the probability of having at least (or exactly) a specified number of hits during an engagement in which a specified larger number of rounds are fired.

The mathematical relationships among the various kill and hit probabilities that have been discussed are presented in subpar. 4-4.2.1. The equations and procedures used to compute hit probabilities from the system errors are discussed in subpar. 4-4.2.2.

4-4.1.1 Systematic and Random Errors

The various physical errors in a fire control system, as distinguished from the errors inherent in the mathematical model, that are discussed in par. 4-3, may be characterized as either systematic (bias type) or random (dispersion or noise type). Systematic errors are caused by such factors as misalignment, slow drift in components, and slowly varying environmental effects. Random errors are caused by such factors as radar noise, uncertainties in bearings and gearing, vibrations produced when the weapon system is in motion, and ammunition variations. The effect of any error is, of course, a displacement of the burst or impact point relative to the aim point on the target. The burst or impact point is considered to be the center of the destructive effect of the projectile. In the case of random errors, it is often assumed that these points have a circular random distribution centered at the target. This is discussed in greater detail in subpar. 4-4.2.2. If systematic errors are also present, the center of the distribution is displaced

from the target aim point by a distance defined as the bias. Frequently a weapon system incorporates two axes, each with different random errors. Under such conditions the impact points have an elliptical, rather than a circular, distribution.

All practical fire control systems have both dispersion and bias errors. Weapon systems, however, are often provided with the capability to reduce the bias error before or during an engagement by sensing those factors contributing to the error or by sensing miss distance from previous firings and compensating the gun aim accordingly. On the other hand, random errors cannot in general be reduced at the time of firing. Their magnitude is inherent to the system design and to the manufacturing processes used to produce the system and its ammunition.

If the bias cannot be totally eliminated, some degree of dispersion can be helpful in increasing hit probability in weapon systems that fire a salvo or burst of rounds in rapid succession. This is illustrated in Fig. 4-4. For diagrammatic simplicity the target is shown as a circular area and the projectiles as points as would be the case if someone were firing a rifle at a bull's-eye target. Fig. 4-4(B) shows how a dispersion error whose magnitude is approximately equal to that of the bias error increases the probability that at least a few rounds from the salvo will be on target.

It is important to note that cases have been recorded in which the designers of a weapon system have so reduced the dispersion in an attempt to improve the single-shot hit probability that the dispersion was finally significantly less than the bias. In subsequent engagement trials the "improved" system had poorer performance than a less elaborate weapon in which the systematic and random errors, although larger, were better balanced.

When establishing the performance requirements for the various weapon subsystems based on a desired overall system probability of a hit, each of the error sources that affects the system performance must be identified as being either biasing or random. In addition, when analyzing hit probabilities for multiple-round engagements, the random errors must be grouped into categories. These categories are described in the following paragraph. In fact, the category allocation can change depending on the specifics of the engagement scenarios being studied.

(A) Dispersion Less Than the Bias

(B) Dispersion Greater Than the Bias

T = assumed center of target

I = center of dispersion, or mean value, of shots
(also known as center of impact (CI))

h = bias

X = shots

⬜ = cross section of target
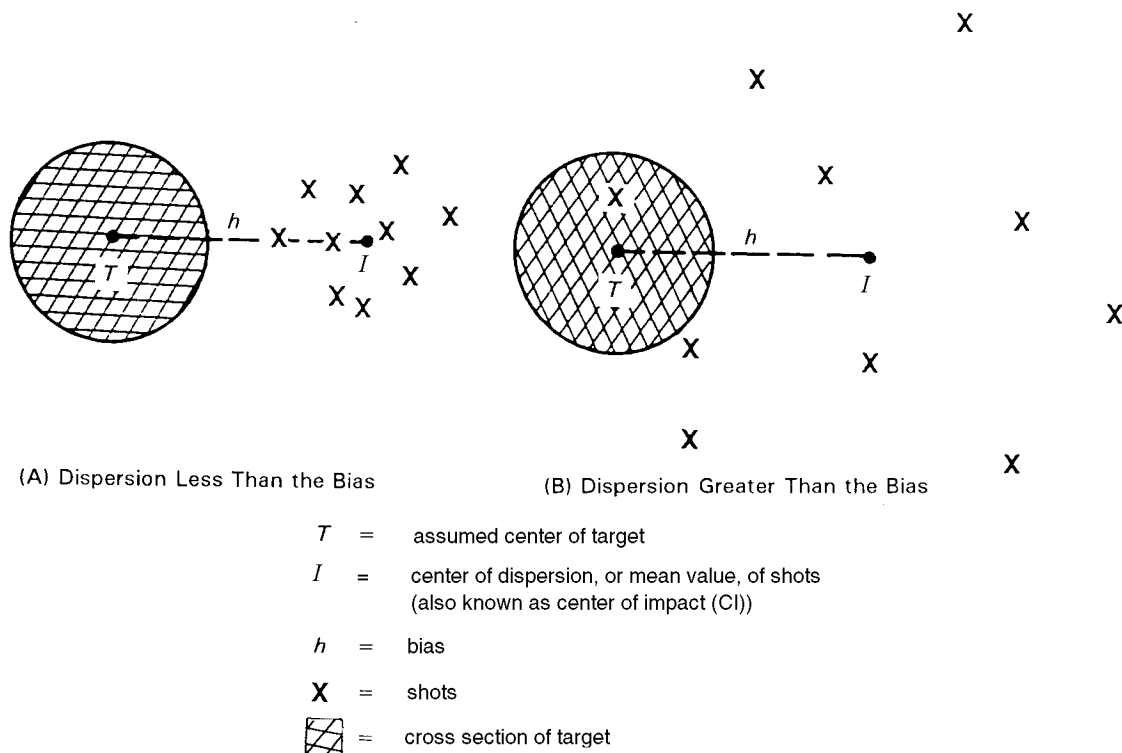
Figure 4-4. Dispersion and Bias in an Engagement

4-4.1.2 Engagement Hit Probability

In many situations a target engagement is not limited to a single shot. The target may be engaged by firing several shots in succession where the gunner re-lays on the target after each shot. Weapons with automatic cannons have the capability to fire a salvo of rounds in rapid succession, and the engagement may consist of firing a single salvo or a series of salvos where the gunner re-lays his aim point only after each salvo.

The engagement hit probabilities for these two cases will not be the same even if each engagement is carried out against the same target with the same weapon system and the same crew. The difference occurs because the firing of each round is not generally an independent statistical event. Statistical dependencies exist because parts of the total system error are shared by the rounds. Some errors are shared by all rounds fired during the engagement. Others are shared by all rounds fired within a burst or salvo. Still others change from round to round. For example, the error associated with the ability of a gunner to place the weapon aim point on a specific target feature is shared by all rounds fired in a salvo. On the other hand, when single rounds are fired and the gunner re-lays his aim point after each firing, the aiming error will have a different realization with each round.

Current practice (Ref. 10) in the design of combat vehicles is to divide the fire control errors into four categories: fixed biases, occasion-to-occasion biases, burst-to-burst biases, and round-to-round errors. An occasion is one tactical engagement between vehicles. A burst is a series of rounds fired in rapid succession with the same point of aim.

As their name implies, fixed biases are constant at a given range. Gravity drop-off, drift of spin-stabilized projectiles, and parallax error (due to sight offset from the weapon) are examples of fixed biases. Another source that may contribute to this type of error is fire control equipment which is damaged or out of adjustment. In a moderately sophisticated, well-maintained fire control system, correction is made for all fixed biases.

Occasion-to-occasion biases are errors that change from time-to-time but so slowly that they can be considered constant over the length of an engagement. Errors due to vehicle cant, wind velocity, air density, and temperature changes are considered to be occasion-to-occasion biases. These biases vary randomly from engagement to engagement. In general, these errors are functions of weapon system parameters (ammunition type, muzzle velocity, etc.), the geometry of the tactical situation (range), and the firing conditions.

Burst-to-burst biases are random and generally have different values for each burst fired during an engagement. If a gunner lays the reticle onto the target before each burst of fire from an automatic cannon, the laying error is a burst-to-burst type of error.

Round-to-round errors are random and take on different values for each round. Ammunition dispersion, due to the number and size of projectile propellant grains, fit of projectile to case, orientation of the round in the chamber, etc., and ground-induced hull disturbances must be treated as round-to-round errors.

4-4.1.3 An Outline of the Procedure Used to Design a Fire Control System of Prescribed Accuracy

The capability to achieve a specified engagement kill probability or kill rate is the fundamental military requirement that is usually imposed on a weapon system. From this military requirement, a requirement for the engagement and single-shot hit probabilities is developed through studies of the effectiveness of the weapon system. The special discipline of operations research plays the major role in this development . The subject of operations research lies outside the scope of this handbook; however, a few examples of its use in arriving at prescribed hit probabilities are discussed. The fire control system designer should be as familiar as possible with the concepts of operation research as well as the concepts of hit and kill probability because development of the required engagement hit probability is most effective when he is in a position to cooperate with the operations research specialist in this development. The problem of the fire control system designer, stated in its simplest terms, is to derive, from the prescribed engagement and single-shot hit probabilities, the accuracy requirements of the fire control

system, then those of its various subsystems, and finally those of the components that make up the subsystems. In actuality the fire control designer may find that a particular component is required to have a better accuracy than the current state of the art permits. Sometimes it is imperative to break through the state of the art for the component concerned if the time schedule permits. In other cases, the designer must lay out the system to minimize the effect of this component on the overall error of the fire control system. Other problems requiring judicious balancing of component and system errors will also arise.

Because the purpose of Chapter 4 is to describe and exemplify design principles, the basic, straightforward procedure is presented. With such a straightforward procedure the task of the fire control system designer to determine accuracy requirements would be carried out in the following steps:

1. Determine the allowable overall error of the weapon system from the required engagement or single-shot hit probability.

2. Identify those errors of the weapon system that are inherently beyond the control of the fire control system designer. (These errors are primarily those associated with the input and output portions of the weapon system.)

3. Establish the allowable error for that portion of the fire control system whose errors are not beyond the control of the designer.

4. Determine the allowable errors of each of the subsystems and components of the fire control system that are under the designer's control in accordance with the contribution of the particular subsystem or component to the total error.

In actual practice the determination of accuracy requirements, like the design process itself, is an iterative process, and the steps listed are repeated as the design converges to its final implementation.

4-4.2   HIT AND KILL PROBABILITY THEORY

It has been previously stated that the fire power requirements for weapon systems can be specified in terms of engagement kill probabilities and kill rates. This paragraph clarifies the concepts of kill probability and kill rate by example and shows how fire control system requirements are derived from them. The concept of target vulnerability is introduced in the course of this discussion.

The kill probabilities and rates are derived by military strategists based on various types of combat models and assumed engagement scenarios. The engagement kill probability specification is used when the target is passive or poses no threat to the weapon system during the engagement. Attacks on buildings and other fixed emplacements or against targets that have an active defense capability but are presently beyond engagement range of the weapons systems are examples. In this case the engagement is one sided, and although the time required to complete it is important, the time would be a secondary consideration. Because of ammunition supply considerations, the expected number of hits vis-à-vis the available number of rounds does, however, enter into the analysis.

When both sides possess effective offensive or active defensive capabilities, time is essential. Here the objective is to disable the enemy before being disabled, and the ability to fire the first round or salvo is as significant as system accuracy and projectile destructive power. Under these conditions the requirement for a kill or target servicing rate would be specified.

Target vulnerability studies are conducted to establish the amount of damage that can be expected to be inflicted against each class of target by each type of ammunition available for use by the weapon system under development. These studies could involve experimental programs with live fire, the use of computer simulations, or simply the application of existing target and component vulnerability data. The results are predictions of conditional kill probability, i.e., the probability of achieving a desired level of damage given that a hit occurs.

In many cases a target is not uniformly vulnerable over its exposed area, so the analyses are performed separately for each region. An example of a computer vulnerability model is the TACOME3 armored vehicle vulnerability analysis model maintained by the US Army Tank-Automotive and Armaments Command (TACOM) (Ref. 11). In this model the user specifies an armor configuration, the characteristics of major internal and external target components, and the kinetic and chemical

characteristics of the ammunition at detonation or impact. The model then predicts the probabilities of occurrence of the various categories of damage. These categories are referred to as K-kill for total damage, M-kill for loss of vehicle mobility, and FP-kill for loss of vehicle firepower.

The vulnerability studies include engagements using ammunition that produces damage upon impact or fused or timed ammunition whose damaging effects are caused by the burst alone, i.e., with or without impact. An example of damage upon impact is the use of high-velocity kinetic energy rounds for antiarmor engagements. The damage occurs in this case when the projectile penetrates the armor and produces spall inside the vehicle. The level of damage inflicted by such kinetic energy rounds is dependent on the distance to the target. Timed or fused rounds are used against dispersed targets such as troop emplacements and against aircraft because the blast energy can throw the aircraft out of control. The use of depth charges against submarines is another example of this type of engagement.

4-4.2.1 Kill Probability

Several examples are presented to demonstrate the relationship between kill rate and kill probability specifications and between hit probabilities and system accuracy.

The first example considers an engagement against a target using a timed explosive round in which an engagement kill probability is specified. The vulnerability of the target can be specified in terms of a damage function $d(x,y,z)$, which represents the probability that the target will be disabled when the point of detonation occurs at the location defined by the coordinates (x,y,z). The origin of the x,y,z coordinate system is assumed to be at the center of the target. Because of the blast effect, the damage function will have nonzero values both within and without the physical boundary of the target. It is important to note that the damage function is a probability assignment function, not a pdf. Appendix C contains a discussion of pdf's.

The probability of achieving a kill by firing one round is expressed by the integral

$$P_{SSK} = \int_{-\infty}^{\infty} \int_{-\infty}^{\infty} \int_{-\infty}^{\infty} d(x,y,z)\, p(x,y,z)\, dx\, dy\, dz, \ \mathbf{U}^{-1} \tag{4-56}$$

where

P_{SSK} = single-shot kill probability, $\mathbf{U}^{-1}$

$d(x,y,z)$ = three-dimensional target damage function, $\mathbf{U}^{-1}$

$p(x,y,z)$ = three-dimensional pdf for the location of the points of detonation of rounds fired at the target, $\mathbf{U}^{-1}\cdot\mathbf{m}^{-3}$

x,y,z = three-dimensional coordinates, $\mathbf{U}$.

If the errors in each of the three coordinate directions are independent and normally distributed, the function $p(x,y,z)$ for an engagement consisting of a single shot can be represented by the joint probability density distribution:

$$p(x,y,z) = \frac{1}{(2\pi)^{3/2}\sigma_x\sigma_y\sigma_z}\exp\left[-\frac{(x-\mu_x)^2}{2\sigma_x^2} - \frac{(y-\mu_y)^2}{2\sigma_y^2} - \frac{(z-\mu_z)^2}{2\sigma_z^2}\right], \ \mathbf{U}^{-1}\cdot\mathbf{m}^{-3} \tag{4-57}$$

where

μ_x = location of the distribution mean in the x-coordinate direction, m

μ_y = location of the distribution mean in the y-coordinate direction, m

μ_z = location of the distribution mean in the z-coordinate direction, m

σ_x = standard deviation of the detonation points about the mean in the x-direction, m

σ_y = standard deviation of the detonation points about the mean in the y-direction, m

σ_z = standard deviation of the detonation points about the mean in the z-direction, m.

The means and variances shown in Eq. 4-57 represent the fixed and random errors that are of interest to the fire control designer. When the analysis is based on an engagement limited to a single shot, the errors, which are classified as occasion-to-occasion, burst-to-burst, and round-to-round, can all be combined into a single standard deviation for each coordinate dimension by simply adding the variances for all of the error sources in that direction.

The integral in Eq. 4-56 can always be solved by numerical techniques. Certain assumptions about the form of the damage function $d(x,y,z)$, however, are sometimes made to simplify the mathematics and to allow an algebraic solution to be used. Examples of such functions are given in Ref. 9 and are not addressed further in this discussion.

The next case considered is a direct fire engagement against a concrete bunker with a high-energy explosive round. A target hit is required to detonate the round. For this case the problem can be formulated in two dimensions by considering the target area to be the projection of the target profile onto a plane normal to the path of the projectile trajectory just before impact. If the single-shot kill probability is the specified requirement, the governing relation is

$$P_{SSK} = \int_{-\infty}^{\infty} \int_{-\infty}^{\infty} d(x,y) \ p(x,y) \ dx \ dy, \ \mathbf{U}^{-1} \tag{4-58}$$

where

$d(x,y)$ = two-dimensional target damage function, $\mathbf{U}^{-1}$

$p(x,y)$ = two-dimensional pdf of the impact point of the projectile trajectory with the normal plane at the target range, $\mathbf{U}^{-1}\cdot\mathbf{m}^{-2}$.

For this example the damage function will have nonzero values for all regions within the projected target area and a zero value outside. Eq. 4-58 can then be written as

$$P_{SSK} = \int_{-H/2}^{H/2} \int_{-W/2}^{W/2} d(x,y) \ p(x,y) \ dx \ dy, \ \mathbf{U}^{-1} \tag{4-59}$$

where

W = width of the projected target area, m

H = height of the projected target area, m.

If the target has a uniform vulnerability over its projected area, the damage function $d(x,y)$ can be treated as a constant within the region of integration, and Eq. 4-59 can be written as

$$P_{SSK} = P(K \mid H) \int_{-H/2}^{H/2} \int_{-W/2}^{W/2} p(x,y) \ dx \ dy, \ \mathbf{U}^{-1} \tag{4-60}$$

where

$P(K \mid H)$ = conditional probability of a kill given that a hit has occurred, $\mathbf{U}^{-1}$.

The integral on the right side of Eq. 4-60 is the single-shot hit probability, which is a function of the fixed and variable errors of the weapon system.

For a third example, it is assumed that vulnerability studies show that on the average four hits are required to destroy the bunker in the previous example. The engagement kill probability for this situation is then equal to the probability that four target hits can be achieved during the engagement. The problem can also be formulated to answer several more specific questions, e.g., the probability of getting four hits by firing exactly four rounds or the probability of getting four hits by firing more than four rounds. Each of these quantities is dependent on the fire control system errors and on the way they are grouped into the four categories defined in subpar. 4-4.1.2. The computation of these quantities, as well as the pdf $p(x,y)$, is discussed in more detail in subpar. 4-4.2.2.

4-4.2.2 Probability of Hit

In field-test evaluations it is the impact of the projectile on the actual target presentation that is measured for conformance to system accuracy specifications. Ideally, not only are hits on the target recorded, but also the miss distance, i.e., distance of closest approach, so that complete probability density distribution can be obtained. Single-shot and engagement hit probabilities are readily calculated from such data. In new systems data are not available to characterize the pdf, so an assumption must be made. For the reasons that follow, the distribution is generally assumed to be normal:

1. It has been empirically observed that most continuous random processes in nature can be described approximately by a normal distribution.

2. Discrete random variables are often described by a binomial distribution, but for a large number of trials the binomial distribution is approximated by the normal.

3. If a random variable is derived from a sum of a number of individual random variables, each of which may have any distribution, the resultant random variable is found to have a distribution approaching normal as the number of variables becomes large.

The single-shot and engagement hit probability relationships developed in this paragraph are based upon the assumption of normality.

The analysis of system accuracy in many direct fire scenarios can be simplified by projecting the three-dimensional target onto a plane normal to the direction of the relative velocity vector between the projectile and the target at the closest point of approach. If the target is stationary, this plane will be normal to a vector that is tangent to the projectile trajectory in the vicinity of the target.

The fixed and random bias errors of the system are usually described in a two-dimensional rectangular coordinate system whose center coincides with the center of the projected target area.

The pdf's derived from the system errors are also formulated in the two-dimensional rectangular coordinate system, and the single-shot and engagement hit probabilities are computed by integrating the appropriate distribution over the two-dimensional projected target area.

The pdf used for two-dimensional fire control problems and formulated in rectangular coordinates is the bivariate normal distribution. In its most general form it is represented by

$$G(x,y) = \frac{1}{2\pi\sigma_x\sigma_y} \exp\left\{-\frac{1}{2(1-\rho^2)}\left[\frac{x-\mu_x^2}{\sigma_x^2}\right.\right.$$

$$\left.\left.- 2\rho\frac{(x-\mu_x)(y-\mu_y)}{\sigma_x\sigma_y} + \frac{(y-\mu_y)^2}{\sigma_y^2}\right]\right\}, \quad U^{-1}\cdot m^{-2}$$

(4-61)

where

$G(x,y)$ = the joint pdf in the rectangular x,y coordinate system, $U^{-1}\cdot m^{-2}$

σ_x = standard deviation of the distribution in the x-direction, m

σ_y = standard deviation of the distribution in the y-direction, m

ρ = correlation coefficient between the distributions in the x- and y-directions, dimensionless.

Discussions of the properties of the bivariate normal distribution are included in most references on statistics. The form shown in Eq. 4-61 and the discussion that follows are based on the presentation in Ref. 12.

An important characteristic of the bivariate normal distribution is that the distributions are normal in each coordinate direction. That is, the distribution of the y-values of all elements in the population is normal, regardless of their values in the x-direction. Similarly, the distribution of all of the x-values is normal regardless of their values in the y-direction. This characteristic is demonstrated in Ref. 12 by

integrating Eq. 4-61 in the *y*-direction from $-\infty$ to $+\infty$ to give the distribution of all of the *x*-values. Integrating from $-\infty$ to $+\infty$ in the *x*-direction gives the distribution of all of the *y*-values. In both cases the resulting expression is the one-dimensional Gaussian distribution.

In many applications the correlation between the effects of the error sources in the *x*- and *y*-directions is small enough to allow the assumption that the correlation coefficient approaches zero. The joint pdf can then be represented as the product of two one-dimensional normal distributions:

$$G(x,y) = \frac{1}{\sqrt{2\pi}\sigma_X} \exp\left[-\frac{1}{2}\left(\frac{x-\mu_x}{\sigma_x}\right)^2\right] \frac{1}{\sqrt{2\pi}\sigma_y} \exp\left[-\frac{1}{2}\left(\frac{y-\mu_y}{\sigma_y}\right)^2\right], \quad \mathbf{U}^{-1} \cdot \mathbf{m}^{-2}. \qquad (4\text{-}62)$$

Fig. 4-5 shows plots of the distribution represented by Eq. 4-62 for the cases in which $\sigma_x \neq \sigma_y$ and $\sigma_x = \sigma_y$.

When a joint pdf is bivariate normal and the correlation coefficient is zero, the distributions in the *x*- and *y*-directions are said to be independent. Subpars. 4-4.2.2.1 and 4-4.2.2.2 show that this independence simplifies the error analysis. Before it is applied, however, the fire control designer must carefully study all of the error sources involved and verify that an assumption of independence is valid. There are always some error sources that have an effect in both coordinate directions, and these will introduce a

(A) Case When $\sigma_x \neq \sigma_y$

(B) Case When $\sigma_x = \sigma_y$
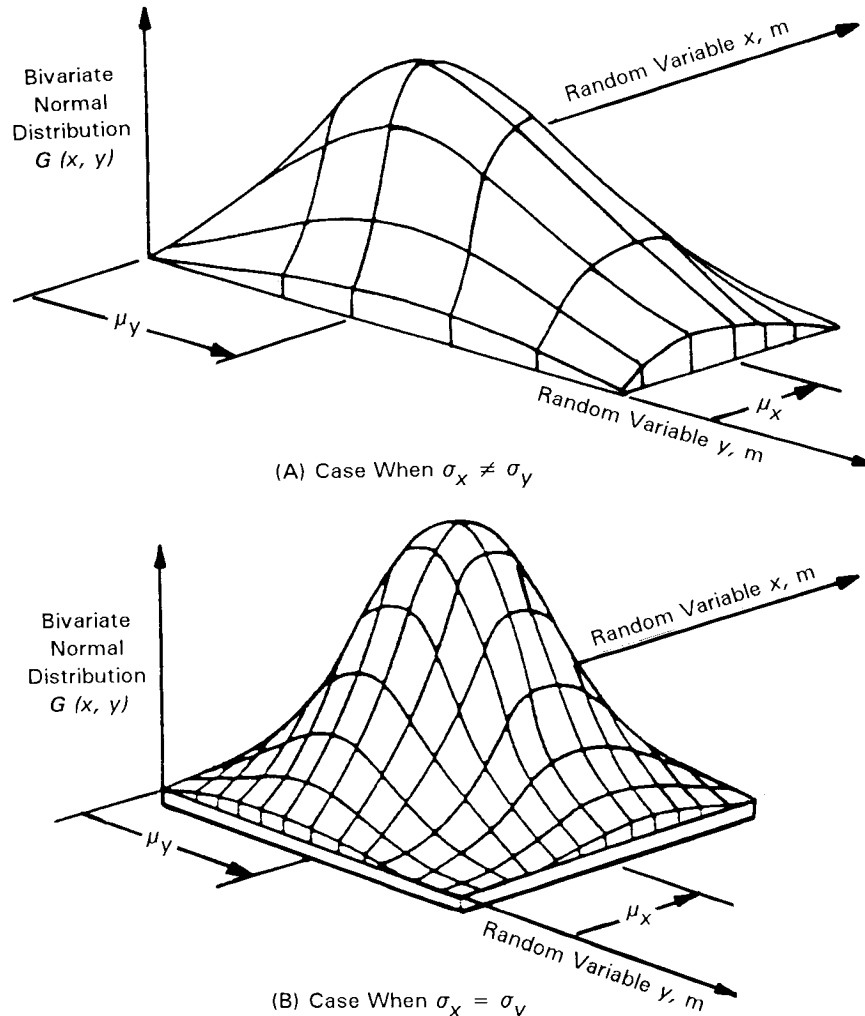
Figure 4-5. Representative Plots of the Bivariate Normal Distribution

correlation. If the covariances due to these effects are much smaller than the combined variances result-ing from the independent error sources, the assumption of independence can be made. The error anal-ysis of the M1 tank presented in Chapter 6 includes examples of both independent and correlated error sources.

4-4.2.2.1   Single-Shot Hit Probability

The single-shot probability of hit is the probability that in the firing of a single projectile, the trajec-tory of the projectile will intersect the target volume. With a two-dimensional target formulation in rect-angular coordinates, the single-shot hit probability can be computed:

$$P_{SSH} = \int\int_{A_T} G(x,y)\ dx\ dy,\ \mathbf{U}^{-1} \tag{4-63}$$

where

P_{SSH} = single-shot hit probability, U^{-1}

A_T = projected target area, m^2

$G(x,y)$ = bivariate normal pdf as defined by Eq. 4-62, $U^{-1} \cdot m^{-2}$.

In general, Eq. 4-63 must be solved by numerical integration techniques. By making certain simplify-ing assumptions, however, the designer can conveniently use tabulated numerical results. In one formu-lation a complete analytical solution can be obtained. Engineers find solutions such as these very useful during the preliminary stages of the design or requirements analysis process. Examples of several spe-cial cases follow.

If the x- and y-distributions are independent and if the target is rectangular with its edges aligned to the coordinate directions x and y, Eq. 4-63 becomes

$$P_{SSH} = \left[\frac{1}{\sqrt{2\pi}\sigma_x}\int_{-W/2}^{W/2} e^{-\frac{1}{2}\left(\frac{x-\mu_x}{\sigma_x}\right)^2} dx\right]\left[\frac{1}{\sqrt{2\pi}\sigma_y}\int_{-H/2}^{H/2} e^{-\frac{1}{2}\left(\frac{y-\mu_y}{\sigma_y}\right)^2} dy\right],\ \mathbf{U}^{-1} \tag{4-64}$$

The values of each of the bracketed terms in Eq. 4-64 can be readily computed from published tables of the Gaussian distribution after shifting and scaling of the coordinate axes in accordance with the following two transformation equations:

$$k = \frac{x-\mu_x}{\sigma_x},\ \text{dimensionless}$$

$$l = \frac{y-\mu_y}{\sigma_y},\ \text{dimensionless} \tag{4-65}$$

where

k = transformed coordinate in the original x-direction, dimensionless

l = transformed coordinate in the original y-direction, dimensionless.

The differentials dk and dl in the transformed coordinates are

$$dk = (dx)/\sigma_x,\ \text{dimensionless}$$

$$dl = (dy)/\sigma_y,\ \text{dimensionless.} \tag{4-66}$$

Eqs. 4-65 and 4-66 are substituted into Eq. 4-64 to yield

$$P_{SSH} = \left(\frac{1}{\sqrt{2\pi}} \int_{z_1}^{z_2} e^{-k^2/2} \, dk \right) \left(\frac{1}{\sqrt{2\pi}} \int_{z_3}^{z_4} e^{-l^2/2} \, dl \right), \ U^{-1} \tag{4-67}$$

where

$$z_1 = \frac{\left(-\dfrac{W}{2} - \mu_x \right)}{\sigma_x}, \ \text{dimensionless}$$

$$z_2 = \frac{\left(\dfrac{W}{2} - \mu_x \right)}{\sigma_x}, \ \text{dimensionless}$$

$$z_3 = \frac{\left(-\dfrac{H}{2} - \mu_y \right)}{\sigma_y}, \ \text{dimensionless}$$

$$z_4 = \frac{\left(\dfrac{H}{2} - \mu_y \right)}{\sigma_y}, \ \text{dimensionless.}$$

The values represented by the integrals in the bracketed terms in Eq. 4-67 can be obtained directly from tables of standardized Gaussian distributions, which have a zero mean and unity variance.

The mean values μ_x and μ_y in Eq. 4-67 are the fixed system biases described in subpar. 4-4.1.2. For the single-shot hit probability there is no sharing of the random biases as in multiple-round firings. The variances associated with the round-to-round, burst-to-burst, and occasion-to-occasion random biases are therefore independent and can be combined by simple addition in each coordinate direction. The standard deviations σ_x and σ_y in Eq. 4-67 are the square roots of these summed variances.

A second set of simplifications can be made if the target is circular and if the x- and y-distributions are independent. In this case it is convenient to transform the double integral of Eq. 4-63 into polar coordinates. As shown in Ref. 13, this is accomplished by making the following substitutions for x and y in the expression for $G(x,y)$:

$$x = r \cos \theta, \ m$$
$$y = r \sin \theta, \ m \tag{4-68}$$

where

r = radial coordinate direction, m

θ = circumferential coordinate direction, rad.

The differential rectangular area $dxdy$ in the double integral of Eq. 4-63 must also be replaced by its equivalent in polar coordinates. In Ref. 13 this is

$$dx \ dy = r \ dr \ d\theta, \ m^2. \tag{4-69}$$

If the origin of the polar coordinate system is placed at the center of the circular target and if the variances in x and y are independent, the equation for the single-shot hit probability in polar coordinates is

$$P_{SSH} = \frac{1}{2\pi\sigma_x\sigma_y}\int_{r=0}^{R}\int_{\theta=0}^{2n}\exp\left[-\frac{1}{2}\left(\frac{r\cos\theta-\mu_x}{\sigma_x}\right)^2 + \left(\frac{r\sin\theta-\mu_y}{\sigma_y}\right)^2\right] r\ dr\ d\theta, \ \mathbf{U}^{-1} \ \text{(4-70)}$$

where

R = radius of two-dimensional circular target, m.

Ref. 14 presents analytical and tabular results for the following three special cases of Eq. 4-70:

Case A: Equal variances in x and y with no fixed bias

Case B: Equal variances in x and y with a fixed bias in the x-direction

Case C: Unequal variances in x and y with no fixed bias.

In Case A, the following special conditions apply:

$$\sigma_x = \sigma_y = \sigma_d, \ \mathbf{m}$$
$$\mu_x = \mu_y = 0, \ \mathbf{m}.$$

where

σ_d = standard deviation for which $\sigma_x = \sigma_y = \sigma_d$, m.

For these conditions the single-shot hit probability is shown in Ref. 14 as

$$P_{SSH} = 1 - \exp\left[\frac{-R^2}{2\sigma_d^2}\right], \ \mathbf{U}^{-1}. \tag{4-71}$$

Tabulated numerical results are given in Ref. 14 for Cases B and C.

As a final special case, if the standard deviations in the x- and y-directions are much greater than any of the dimensions of the target, the single-shot hit probability can be computed directly from the bivariate normal pdf $G(x,y)$. First, a coordinate transformation is made to place the origin of the coordinate system at the center of the distribution. The transformation equations are

$$u = x - \mu_x, \ \mathbf{m}$$
$$v = y - \mu_y, \ \mathbf{m}. \tag{4-72}$$

Upon solving for x and y in Eq. 4-72 and substituting into Eq. 4-61 the bivariate normal pdf in the new (u,v) coordinate system is

$$H(u,v) = \frac{1}{2\pi\sigma_x\sigma_y}\exp\left\{\frac{-1}{2(1-\rho^2)}\left[\frac{u^2}{\sigma_x^2} - \frac{2\rho uv}{\sigma_x\sigma_y} + \frac{v^2}{\sigma_y^2}\right]\right\}, \ \mathbf{U}^{-1}\cdot\mathbf{m}^{-2} \tag{4-73}$$

where

$H(u,v)$ = bivariate normal pdf for the u,v coordinate system, $U^{-1}\cdot m^{-2}$.

The single-shot hit probability for a target of area A_T can now be computed directly from

$$P_{SSH} = A_T H(-\mu_x, -\mu_y), \ \mathbf{U}^{-1} \tag{4-74}$$

where

$H(-\mu_x, -\mu_y)$ = bivariate normal pdf (of Eq. 4-73) evaluated at the point $(-\mu_x, -\mu_y)$, $U^{-1}\cdot m^{-2}$.

4-4.2.2.2 Engagement Hit Probability

The engagement hit probability is defined as the probability of achieving a specified number of hits in the firing of a specified number of rounds. Two associated parameters are the probability of achieving at least a specified number of hits and the number of hits expected in the firing of a specified number of rounds. The equations used to compute these parameters and tabulations of numerical results are derived in Ref. 10. This subparagraph presents the key concepts in the development of the theory of engagement hit probability and shows how the system errors are used to obtain statistically correct estimates for different engagement scenarios. As in the previous discussions, it is assumed that the target is two dimensional and that the random system errors follow Gaussian statistics and are independent in the two coordinate directions.

To perform analyses for engagement hit probability, the system errors must be grouped in accordance with the definitions given in subpar. 4-4.1.2. Each grouping is characterized by a distinct Gaussian pdf in which the variance of the distribution in each coordinate direction is equal to the sum of the variances of the individual independent error sources in the group.

The first group consists of those error sources that remain constant during an engagement but may vary randomly from engagement to engagement. This includes both the fixed biases and the occasion-to-occasion random biases. The pdf for this group has mean values equal to the algebraic sum of the fixed system biases in each direction and variances equal to the sum of the individual variances in the group. This distribution is represented by

$$g(v_x, v_y) \ = \ \frac{1}{2\pi\gamma_x\gamma_y}\exp\left\{-\frac{1}{2}\left[\left(\frac{v_x - f_x}{\gamma_x}\right)^2 + \left(\frac{v_y - f_y}{\gamma_y}\right)^2\right]\right\}, \quad \mathrm{U}^{-1}\cdot\mathrm{m}^{-2}. \tag{4-75}$$

where

$g(v_x, v_y)$ = pdf for the distribution of errors v_x and v_y caused by the fixed and occasion-to-occasion biases, $\mathrm{U}^{-1}\cdot\mathrm{m}^{-2}$

v_x = error in x-direction caused by fixed and occasion-to-occasion variations, m

v_y = error in y-direction caused by fixed and occasion-to-occasion variations, m

γ_x = standard deviation of the occasion-to-occasion biases in the x-direction, m

γ_y = standard deviation of the occasion-to-occasion biases in the y-direction, m

f_x = fixed bias in the x-direction, m

f_y = fixed bias in the y-direction, m.

The second pdf characterizes those error sources that vary from burst to burst but remain constant during any one burst. This distribution is a conditional pdf because it defines the probability of occurrence of the random burst-to-burst errors given that some realization of the fixed and occasion-to-occasion biases v_x and v_y has occurred. The random variable representing the burst-to-burst biases is assumed to have a mean of zero. The conditional pdf for the distribution defined by the burst-to-burst biases is given by

$$f(b_x, b_y \mid v_x, v_y) \ = \ \frac{1}{2\pi\psi_x\psi_y} \ \exp\left\{-\frac{1}{2}\left[\left(\frac{b_x - v_x}{\psi_x}\right)^2 + \left(\frac{b_y - v_y}{\psi_y}\right)^2\right]\right\}, \quad \mathrm{U}^{-1}\cdot\mathrm{m}^{-2} \tag{4-76}$$

where

$f(b_x, b_y \mid v_x, v_y)$ = conditional pdf for the distribution of errors b_x and b_y caused by burst-to-burst variations, $\mathrm{U}^{-1}\cdot\mathrm{m}^{-2}$

ψ_x = standard deviation of the burst-to-burst biases in the x-direction, m

ψ_y = standard deviation of the burst-to-burst biases in the y-direction, m

b_x = error in the x-coordinate direction caused by burst-to-burst variations, m

b_y = error in the y-coordinate direction caused by burst-to-burst variations, m.

The third grouping consists of those errors that vary from round-to-round within a burst. This pdf is also formulated as a conditional pdf since all rounds in the burst share the same realization of the burst-to-burst biases b_x and b_y and the occasion-to-occasion biases v_x and v_y. The random variable that represents the round-to-round errors has a mean of zero. The conditional pdf for the distribution defined by the round-to-round variables is

$$h(r_x, r_y \mid v_x, v_y, b_x, b_y) = \frac{1}{2\pi v_x v_y} \exp\left\{-\frac{1}{2}\left[\left(\frac{r_x - (b_x + v_x)}{v_x}\right)^2 + \left(\frac{r_y - (b_y + v_y)}{v_y}\right)^2\right]\right\}, \ \mathbf{U}^{-1} \cdot \mathbf{m}^{-2} \quad (4\text{-}77)$$

where

$h(r_x, r_y \mid v_x, v_y, b_x, b_y)$ = conditional pdf for the distribution of errors r_x and r_y caused by the round-to-round variations, $\mathbf{U}^{-1} \cdot \mathbf{m}^{-2}$

r_x = error in the x-direction caused by round-to-round variations, m

r_y = error in the y-direction caused by round-to-round variations, m

v_x = standard deviation of the round-to-round errors in the x-direction, m

v_y = standard deviation of the round-to-round errors in the y-direction, m.

The first parameter to be studied is the probability of achieving exactly K hits in the firing of N rounds. This parameter is represented by the symbol $P(K/N)$. The equations for three separate cases are developed; each involves a different application of the variable system biases. Two of the cases are weapon systems with automatic cannons in which a burst of rounds is fired with each trigger pull. The third case is a weapon that fires a single shot with each round. Equations are also presented to compute the probability of achieving at least K hits in N rounds, the average number of rounds that have to be fired to achieve one hit, and the number of hits expected in the firing of N rounds.

The equations for engagement hit probability in all of these cases use a relationship derived from the theory of combinatorial probability, i.e., the probability of achieving exactly K successes out of N trials when each trial is independent.

To achieve exactly K successes, there must also be $(N - K)$ failures. The probability of this occurring in any one sequence is given by

$$p^K(1 - p)^{N-K}, \ \mathbf{U}^{-1} \quad (4\text{-}78)$$

where

p = probability of a success in any one of the independent trials, $\mathbf{U}^{-1}$

$(1 - p)$ = probability of failure in any trial, $\mathbf{U}^{-1}$.

Within the N firings the K hits can occur in a number of different ways (or sequences). From combinatorial theory (See par. C-8 of Appendix C and Ref. 15.) it is known that the number of combinations of N items taken K at a time without regard to order is given by the binomial coefficients that can be computed from

$$\binom{N}{K} = \frac{N!}{K!(N-K)!}, \ \text{dimensionless} \quad (4\text{-}79)$$

where

$\binom{N}{K}$ = symbol defining the binomial coefficients, dimensionless

K = required number of successes, dimensionless

N = total number of trials, dimensionless.

The probability of exactly K successes in N trials without regard to sequence is, therefore, $\binom{N}{K}$ times the probability of the occurrence of any single sequence as given by Eq. 4-78. The final expression, which is known as the binomial pdf, is

$$\binom{N}{K} p^K (1-p)^{N-K}, \quad \mathbf{U}^{-1}. \tag{4-80}$$

In the analyses of engagement hit probability, the relationship of Eq. 4-80 is applied to conditional probabilities.

The first case considered is the probability of achieving exactly K hits with the firing of a single burst of N rounds. Because only one burst is being considered, all of the errors must be classified as either occasion-to-occasion biases or round-to-round errors. The probability of achieving the K hits within this single burst is conditioned by the occasion-to-occasion biases that exist during the firing. Within the burst, however, the round-to-round errors are independent. Ref. 10 therefore defines a conditional probability of achieving K hits in N rounds based on the relationship in Eq. 4-80. For the scenario under consideration this probability is defined by

$$P(K/N \,|\, v_x, v_y) = \binom{N}{K} [P(H \,|\, v_x, v_y)]^K [1 - P(H \,|\, v_x, v_y)]^{N-K}, \quad \mathbf{U}^{-1}. \tag{4-81}$$

where

    $P(K/N \,|\, v_x, v_y)$ = conditional probability of achieving exactly K hits in a burst of N rounds for a given manifestation of the occasion-to-occasion biases v_x and v_y, $\mathbf{U}^{-1}$

    $P(H \,|\, v_x, v_y)$ = conditional single-shot hit probability for a given manifestation of the occasion-to-occasion biases v_x and v_y, $\mathbf{U}^{-1}$.

The distribution of the rounds within the burst were characterized by the conditional pdf of Eq. 4-77. The conditional single-shot hit probability in Eq. 4-81 can be obtained by integrating this function over the projected target area and noting that for the case in question there are no burst-to-burst biases. The resulting expression for the conditional single-shot hit probability is

$$P(H \,|\, v_x, v_y) = \int_{-H/2}^{H/2} \int_{-W/2}^{W/2} h(r_x, r_y \,|\, v_x, v_y) \, dr_x \, dr_y, \quad \mathbf{U}^{-1}. \tag{4-82}$$

The absolute probability for K hits in a single burst of N rounds is obtained by multiplying the conditional probability of Eq. 4-81 by the probability density distribution of the occasion-to-occasion biases as shown in Eq. 4-75 and integrating over all possible values of the random occasion-to-occasion variables v_x and v_y. The resulting expression is

$$P(K/N) = \binom{N}{K} \int_{-\infty}^{\infty} \int_{-\infty}^{\infty} [P(H \,|\, v_x, v_y)]^K$$
$$\times [1 - P(H \,|\, v_x, v_y)]^{N-K} g(v_x, v_y) \, dv_x \, dv_y, \quad \mathbf{U}^{-1} \tag{4-83}$$

where

    $P(K/N)$ = absolute probability of K hits in an N round burst, $\mathbf{U}^{-1}$.

Ref. 10 presents techniques for solving Eq. 4-83.

The probability of getting at least L hits in a single burst of N rounds can be computed from

$$P(\text{at least } L \text{ hits in an } N \text{ round burst}) = \sum_{K=L}^{N} P(K/N), \ \mathbf{U}^{-1}$$

$$= 1 - \sum_{K=0}^{L-1} P(K/N), \ \mathbf{U}^{-1}.$$

(4-84)

Ref. 10 presents tables and plots of numerical solutions to Eq. 4-84 for several values of L and N and for a wide range of values of the occasion-to-occasion biases and round-to-round errors.

Another useful parameter is the expected number of rounds that will hit a target E_n in a single N round burst. This parameter can be computed from

$$E_N = \sum_{K=0}^{N} KP(K/N), \ \textbf{dimensionless}$$

(4-85)

where

E_N = expected number of hits in an N round burst, dimensionless.

Ref. 10 shows that by substituting the expression for $P(K/N)$ as defined in Eq. 4-83 into Eq. 4-85 and performing some manipulations,

$$E_N = N \int_{-\infty}^{\infty} \int_{-\infty}^{\infty} P(H \mid v_x, v_y) \, g(v_x, v_y) \, dv_x \, dv_y, \ \textbf{dimensionless.}$$

(4-86)

The integral in Eq. 4-86 is the unconditional single-shot hit probability. Thus the expected number of hits in a single burst of N rounds is simply N times the single-shot hit probability.

The second example is an engagement in which a tank fires a series of shots in rapid succession against a column of armored vehicles. It is assumed that the tank gunner re-lays the gun and performs a new range measurement and that a new ballistic computation is performed before each firing. The parameter of interest in this example is the probability of getting K hits in the firing of N single shots. As was the case for the example of K hits in a burst of N rounds, the weapon system errors are grouped into the two categories of round-to-round errors and occasion-to-occasion biases. The equation for $P(K/N)$, which was developed for that case, is also applicable here. The only difference is the way in which the errors associated with aiming and tracking the target and the ballistic computations are allocated. For the weapon with an automatic cannon, these errors affect all rounds in the burst in the same way. They are therefore considered part of the occasion-to-occasion bias. In the tank engagement scenario, the random variables that represent these errors take on a different value with each firing. Thus they are considered part of the round-to-round errors. Eqs. 4-82 and 4-83 and the numerical solutions presented in Ref. 10 can be used.

The final case is an engagement consisting of two bursts of fire and the system performance is stated in terms of the probability of achieving a specified minimum number of hits in each burst. The system errors must now be classified into the three groupings, namely, occasion-to-occasion biases, burst-to-burst biases, and round-to-round errors.

The development of the engagement hit probability equations is similar to that for the single-burst

engagement, but the additional level of variability associated with the burst-to-burst biases must be considered. The two bursts share a common manifestation of the occasion-to-occasion biases, but each has its own unique conditional single-shot hit probability and manifestation of the burst-to-burst errors.

To simplify notation in the equations that follow, the following symbols are introduced to represent the error pdf's:

$$f_1 = \frac{1}{2\pi\psi_x\psi_y} \exp\left\{-\frac{1}{2}\left[\left(\frac{b_{x1}-v_x}{\psi_x}\right)^2 + \left(\frac{b_{y1}-v_y}{\psi_y}\right)^2\right]\right\}, \ U^{-1}\cdot m^{-2} \qquad (4\text{-}87)$$

where

f_1 = conditional pdf for the bias errors in the first burst, $U^{-1}\cdot m^{-2}$

b_{x1} = manifestation of the total bias in the x-direction in the first burst, m

b_{y1} = manifestation of the total bias in the y-direction in the first burst, m

and

$$f_2 = \frac{1}{2\pi\psi_x\psi_y} \exp\left\{-\frac{1}{2}\left[\left(\frac{b_{x2}-v_x}{\psi_x}\right)^2 + \left(\frac{b_{y2}-v_y}{\psi_y}\right)^2\right]\right\}, \ U^{-1}\cdot m^{-2} \qquad (4\text{-}88)$$

where

f_2 = conditional pdf for the bias errors in the second burst, $U^{-1}\cdot m^{-2}$

b_{x2} = manifestation of the total bias in the x-direction in the second burst, m

b_{y2} = manifestation of the total bias in the y-direction in the second burst, m

and

$$h_1 = \frac{1}{2\pi v_x v_y} \exp\left\langle -\frac{1}{2}\left\{\left[\frac{r_{x1}-(b_{x1}+v_x)}{v_x}\right]^2 + \left[\frac{r_{y1}-(b_{y1}+v_y)}{v_y}\right]^2\right\}\right\rangle, \ U^{-1}\cdot m^{-2} \qquad (4\text{-}89)$$

where

h_1 = conditional pdf for the round-to-round errors in the first burst, $U^{-1}\cdot m^{-2}$

r_{x1} = random variable representing the round-to-round error in the x-direction in the first burst, m

r_{y1} = random variable representing the round-to-round error in the y-direction in the first burst, m

and

$$h_2 = \frac{1}{2\pi v_x v_y} \exp\left\langle -\frac{1}{2}\left\{\left[\frac{r_{x2}-(b_{x2}+v_x)}{v_x}\right]^2 + \left[\frac{r_{y2}-(b_{y2}+v_y)}{v_y}\right]^2\right\}\right\rangle, \ U^{-1}\cdot m^{-2} \qquad (4\text{-}90)$$

where

h_2 = conditional pdf for the round-to-round errors in the second burst, $U^{-1}\cdot m^{-2}$

r_{x2} = random variable representing the round-to-round error in the x-direction in the second burst, m

r_{y2} = random variable representing the round-to-round error in the y-direction in the second burst, m.

The conditional single-shot hit probabilities for each burst are represented by

$$P(H_1) = \int_{-H/2}^{H/2} \int_{-W/2}^{W/2} h_1 \; dr_{x1} \; dr_{y1}, \; \mathbf{U}^{-1} \tag{4-91}$$

where

$P(H_1)$ = conditional single-shot hit probability for the first burst, $\mathbf{U}^{-1}$

and

$$P(H_2) = \int_{-H/2}^{H/2} \int_{-W/2}^{W/2} h_2 \; dr_{x2} \; dr_{y2}, \; \mathbf{U}^{-1} \tag{4-92}$$

where

$P(H_2)$ = conditional single-shot hit probability for the second burst, $\mathbf{U}^{-1}$.

$P(H_1)$ and $P(H_2)$ are both functions of the burst-to-burst error distributions b_x and b_y and the occasion-to-occasion error distributions v_x and v_y.

The absolute probability of achieving exactly K_1 hits in a first burst of N_1 rounds and exactly K_2 hits in a second burst of N_2 rounds is computed by applying the combinatorial relationship of Eq. 4-80 to each burst, multiplying by the pdf's for the burst-to-burst and occasion-to-occasion biases, and integrating over all values of the six random variables that represent the burst-to-burst and occasion-to-occasion biases. The resulting equation is

$$P(K_1/N_1, K_2/N_2) = \int_{-\infty}^{\infty} \int_{-\infty}^{\infty} \left\{ \binom{N_1}{K_1} [P(H_1)]^{K_1} [1 - P(H_1)]^{N_1 - K_1} \right.$$

$$\times \binom{N_2}{K_2} [P(H_2)]^{K_2} [1 - P(H_2)]^{N_2 - K_2} \tag{4-93}$$

$$\times \left. f_1 \; f_2 \; g(v_x, v_y) db_{x1} \; db_{y1} \; db_{x2} \; db_{y2} \; dv_x \; dv_y \right\}, \; \mathbf{U}^{-1}$$

where

$P(K_1/N_1, K_2/N_2)$ = absolute probability of achieving exactly K_1 hits in the first burst of N_1 rounds and exactly K_2 hits in a second burst of N_2 rounds, $\mathbf{U}^{-1}$.

Ref. 10 presents a simplified form of Eq. 4-93 to reduce the complexity of the numerical calculation.

The probability of achieving at least K_1 hits in the first burst and K_2 hits in the second burst can be computed from

$$P(\text{at least } K_1 \text{ and } K_2) = \sum_{j=K_2}^{N_2} \sum_{i=K_1}^{N_1} P(K_i | N_1, K_j | N_2), \; \mathbf{U}^{-1} \tag{4-94}$$

where

$P(\text{at least } K_1 \text{ and } K_2)$ = probability of achieving at least K_1 hits in the first burst and K_2 hits in the second burst, $\mathbf{U}^{-1}$.

4-4.3 ERROR ANALYSIS IN FIRE CONTROL SYSTEMS

4-4.3.1 Introduction

The material presented in subpar. 4-4.2 describes a means to determine the allowable error in a weapon system if a specified engagement hit probability and the number of shots in an engagement are given. The allowable error is usually expressed in terms of its systematic and random components which are specified, respectively, by the mean error (bias) and the variance of the dispersion about the mean. As noted in the procedural summary in subpar. 4-4.1.3, the next step in the design of a fire control sys-

tem from the accuracy standpoint is the determination of those errors of the weapon system that are inherently beyond the control of the fire control system designer. The sensors and components involved in the processes of target acquisition and tracking and of determining the state, e.g., position, orientation, and motion, of the weapon system platform provide the primary inputs to the fire control system. The errors associated with these sensors are generally beyond the control of the fire control system designer. Similarly, errors associated with the gun, the gun pointing mechanisms, and the projectile may cause errors at the output end of the weapon system; these are also beyond the control of the fire control system designer. A discussion of these input and output weapon system errors is given in subpar. 4-4.4.

Before this topic is addressed, however, the steps involved in an error analysis of a fire control system must be considered and useful error propagation equations must be derived.

The flow of errors through a weapon system is the same as the flow of their associated signals. Input errors enter the weapon system through the acquisition and tracking process, e.g., from a gyroscope in the tracking system or from target locations issued by a command post. The final result of all errors associated with the weapon system is the error in the system output, which is usually expressed in terms of the mean bias error and the variance of the dispersion.

The procedure used to allocate allowable errors in a fire control system follows:

1. First, determine from a functional block diagram of the system and from the sets of error propagation equations, which are developed in the following paragraphs, the apportionment of the total allowable error among the major subsystems.

2. Next, extend this procedure to determine the allowable error in each of the components that make up the subsystems.

An analysis of error propagation in systems that are describable by equations other than differential equations can be carried out relatively straightforwardly. Much greater complexity is introduced if differential equations must be used to describe the system. The analytical procedures for both of these cases are discussed in subpars. 4-4.3.2 and 4-4.3.4.

4-4.3.2 Analysis of Error Propagation in Systems Described by Equations Other Than Differential Equations

An analysis of the propagation of errors in assemblages of devices that can be described by algebraic, trigonometric, or empirical equations (not differential equations) can be made by separating the system into independent operating elements, each of which has an identifiable error that is independent of errors in the other elements. In actual systems this independence generally exists, because, for convenience in design and maintenance, it is desirable to assemble such systems from standard modules, each of which has measurable characteristics that are largely independent of the preceding and following modules.

The simplest type of element has one input and one output. The output is assumed to be a function of the input but is independent of time or any other variable. The functional dependence of the output on the input can be expressed by a generalized equation in the form

$$y = g(x), \ \mathbf{U_y}^* \tag{4-95}$$

where

y = the output variable, $\mathbf{U_y}$

x = the input variable, $\mathbf{U_x}$.

Functions such as $y = a\cos(x)$ and $y = bx^2$ are examples of relationships that can be represented by the generalized form of Eq. 4-95. A generalized designation of units for the input and output variables is maintained throughout this and the other similar discussions. $\mathbf{U_x}$ is the generalized unit designation of x, and $\mathbf{U_y}$, the unit designated for y.

---

* The dimensions will be those of the variable identified by the subscript.

The simplest single input/single output element just described may be expanded to include an operating element that receives multiple inputs and generates a single output, as shown in Fig. 4-6. The system element shown in Fig. 4-6 has r inputs $x_1, x_2, \cdots, x_r$ and a single output y. With this configuration a system element with more than one output would be treated as two or more elements, each with a single output. The complete system is considered to be of many such elements, some of whose outputs are also the inputs to other elements.
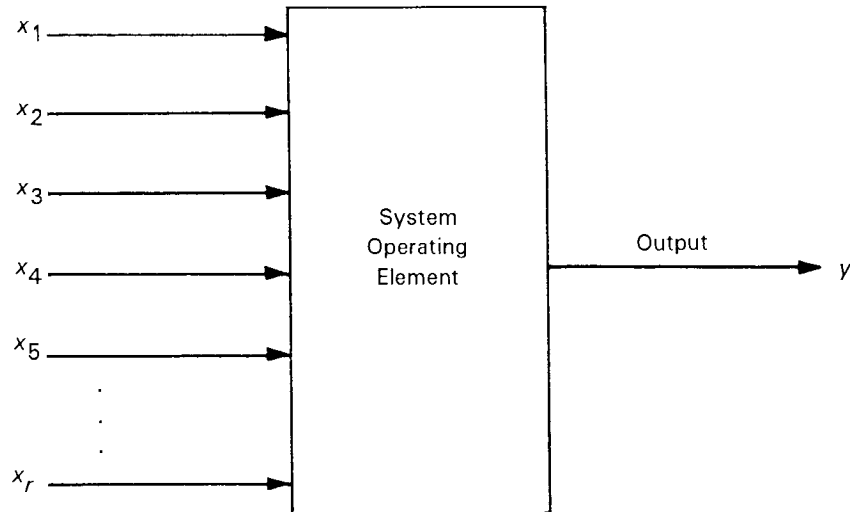
Figure 4-6. Functional Representation of an Element Having Multiple Inputs and a Single Output

In the most general case, each system element has inputs from outside the system and inputs from other elements inside the system. An element of this type is shown in Fig. 4-7. It is designated as the ith element and has r inputs from outside the system and q inputs from inside. The inputs from inside can also include feedback from the actual output of the element, as shown in the illustration. The output

Inputs from the Various Elements of the System, Including the ith System Element
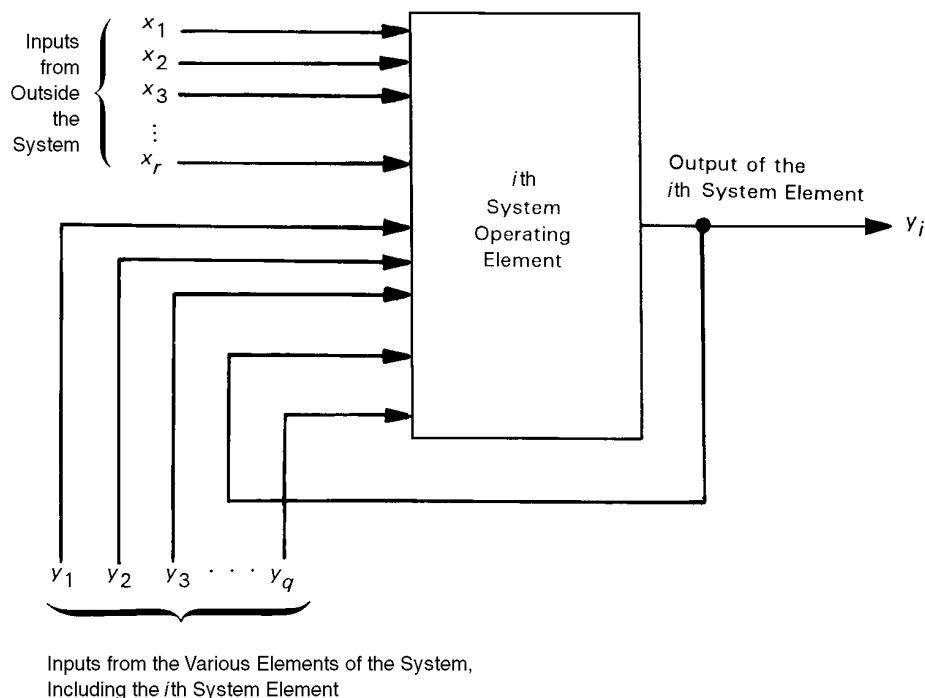
Figure 4-7. Functional Representation of a Generalized Ideal System Element With Multiple Inputs

from the element shown in Fig. 4-7 can be expressed in functional form as

$$y_i = g_i(x_1, \cdots, x_r; y_1, \cdots, y_j, \cdots, y_q) , \ \mathbf{U_{yi}} \tag{4-96}$$

where

$x_1, \cdots, x_r = r$ inputs to the ith element from outside the system, $\mathbf{U_{x1}}, \cdots, \mathbf{U_{xr}}$

$y_1, \cdots, y_j, \cdots, y_q = q$ inputs to the ith element from other elements in the system, $\mathbf{U_{y1}}, \cdots, \mathbf{U_{yi}}, \cdots, \mathbf{U_{yq}}$

$g_i(\cdots) =$ functional operator of the ith system element, $\mathbf{U_{yi}}$.

The functional operator $g_i(\cdots)$ represents the mathematical relationship between each of the element inputs and the output y_i.

Specific examples of some simple multiple input operating elements are shown in Fig. 4-8. Fig. 4-8(A) represents a simple two-input element. An example of an equation appropriate for this configuration is

$$y_1 = a_1 x_1 \cos(x_2) , \ \mathbf{U_{y1}} \tag{4-97}$$

where for Fig 4-8(A) and Eq. 4-97

$y_1 =$ element output, $\mathbf{U_{y1}}$

$a_1 =$ constant, $\mathbf{U_{y1}/U_{x1}}$

$x_1 =$ first input variable, $\mathbf{U_{x1}}$

$x_2 =$ second input variable, rad in this case.

(A) Element With Two
Input Variables

(B) Element With One of Its
Two Inputs Held Constant

(C) Element Employing
Unity Feedback
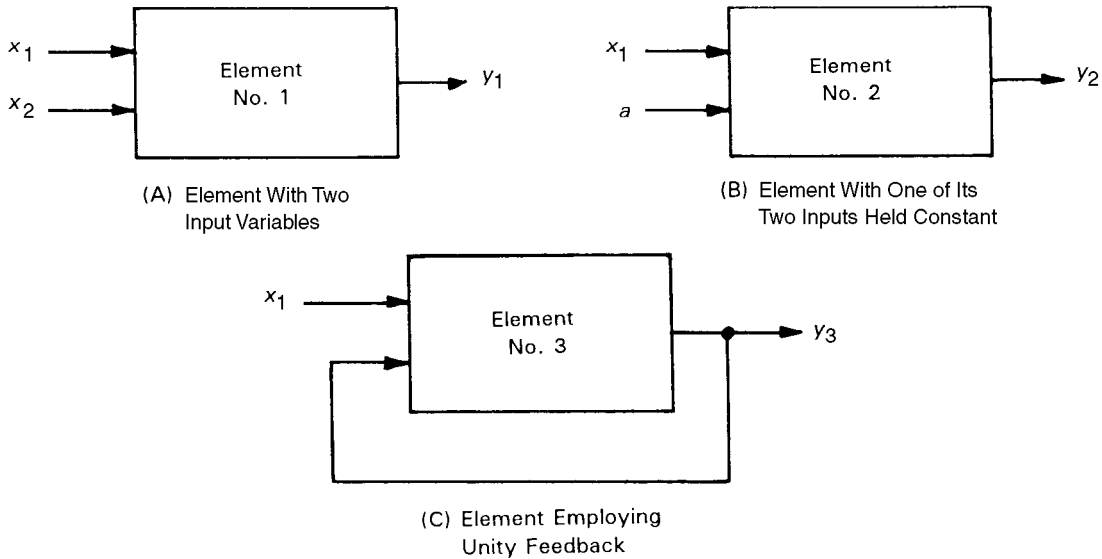
Figure 4-8. Elements of Simple Multiple-Input Operating Elements

Eq. 4-97 can be expressed in general functional form as

$$y_1 = g_1(x_1, x_2), \ \mathbf{U_{y1}}. \tag{4-98}$$

Fig. 4-8(B) illustrates an example of an element with an additive constant. It may be treated as a two-input element with one input held constant. An equation appropriate for this case is

$$y_2 = a_2 + b_2 x_1^2, \ \mathbf{U_{y2}} \tag{4-99}$$

where for Fig 4-8(B) and Eq. 4-99

y_2 = element output variable, U_{y2}
a_2 = constant, U_{y2}
b_2 = constant, U_{y2}/U_{x1}^2
x_1 = input variable, U_{x1}.

In a functional form Eq. 4-99 would be written as

$$y_2 = g_2(x_1), \quad U_{y2}. \tag{4-100}$$

Fig. 4-8(C) shows an element with unity feedback. If, for example, the output variable y_3 is processed as negative feedback within the element, the equation defining element operation would be

$$y_3 = d(x_1 - y_3), \quad U_{y3} \tag{4-101}$$

where for Fig. 4-8(C) and Eq. 4-101

y_3 = output variable, U_{y3}
d = constant, dimensionless
x_1 = input variable, U_{x1}.

In this case $U_{x1} = U_{y3}$.
Eq. 4-101 can be solved explicitly for the output y_3; the result is

$$y_3 = \frac{d}{1+d}x_1, \quad U_{y3}. \tag{4-102}$$

The functional form of Eq. 4-102 is simply

$$y_3 = g_3(x_1), \quad U_{y3}. \tag{4-103}$$

where

$g_3(x_1)$ = scalar function $dx_1/(1 + d)$ in Eq. 4-102, U_{y3}.

A system containing a combination of elements is shown in Fig. 4-9. Application of Eq. 4-96 to element No. 2 in Fig. 4-9 yields the functional relationship

$$y_2 = g_2(x_2, y_5), \quad U_{y2}. \tag{4-104}$$

If, for example, element No. 2 is a resolver, its operation can be represented by

$$y_2 = x_2 \cos y_5, \quad U_{y2} \tag{4-105}$$

where

y_5 = angular output from element No. 5, rad.

Comparison of Eqs. 4-104 and 4-105 shows that

$$g_2(x_2, y_5) = x_2 \cos y_5, \quad U_{y2}. \tag{4-106}$$

In the derivation of the error propagation equations, it is convenient to express the generalized functional equations for the elements in homogeneous form and to define a new functional notation. Eq. 4-104, for example, can be written as

$$y_2 - g_2(x_2, y_5) = 0, \quad U_{y2}. \tag{4-107}$$

This homogeneous expression will be represented by the notation

$$f_2(x_2,y_2,y_5) = 0, \ \mathbf{U_{y2}}. \tag{4-108}$$

where

$f_2(x_2,y_2,y_5)$ = homogeneous functional notation for Eq. 4-107, $\mathbf{U_{y2}}$.

The generalized performance equation given by Eq. 4-96 can be expressed in homogeneous notation as

$$f_i(x_1,\cdots,x_r;y_1,\cdots,y_i,\cdots,y_q) = y_i - g_i(x_1,\cdots,x_r;y_1,\cdots,y_i,\cdots,y_q) = 0, \ \mathbf{U_{yi}}. \tag{4-109}$$

where

$f_i(\cdots)$ = homogeneous functional operator for the ith ideal element, $\mathbf{U_{yi}}$.

Based on the general form of Eq. 4-109, homogeneous performance equations for each of the five elements of Fig. 4-9 are written as

$$\begin{aligned}
f_1(x_1,y_1) &= y_1 - g_1(x_1) = 0, \ \mathbf{U_{y1}} \\
f_2(x_2,y_2,y_5) &= y_2 - g_2(x_2,y_5) = 0, \ \mathbf{U_{y2}} \\
f_3(x_2,x_3,y_3) &= y_3 - g_3(x_2,x_3) = 0, \ \mathbf{U_{y3}} \\
f_4(y_1,y_2,y_4) &= y_4 - g_4(y_1,y_2) = 0, \ \mathbf{U_{y4}} \\
f_5(y_3,y_5) &= y_5 - g_5(y_3) = 0, \ \mathbf{U_{y5}}.
\end{aligned} \tag{4-110}$$
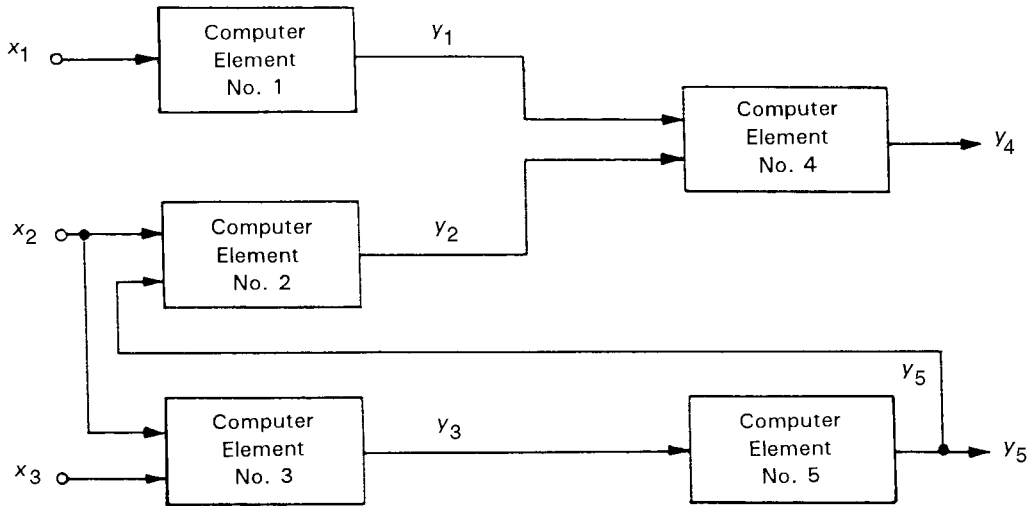
Figure 4-9. Functional Block Diagram of a Typical Analog Computer With Five Elements and Three Inputs

These five simultaneous equations are the performance equations for the system of Fig. 4-9. In general, system performance equations consist of a set of simultaneous equations, and the number of equations is equal to the number of elements in the system.

The generalized functional form of Eq. 4-96 represents the performance equation for an ideal system element. An actual system is not ideal and may have errors associated with the inputs to the elements, as well as errors associated with the elements themselves. A nonideal element produces an error in its output, even in the presence of ideal inputs. This error, which is generated internally within the

element, is treated as an additional signal that is added at the element output, as shown in Fig. 4-10. The element is now considered to include this additive function, as indicated by the dotted border. In this representation the error e_i can be treated mathematically in the same way as all of the other inputs to the element. The output signal is designated by y_i^* to distinguish it from the output of the corresponding ideal element.
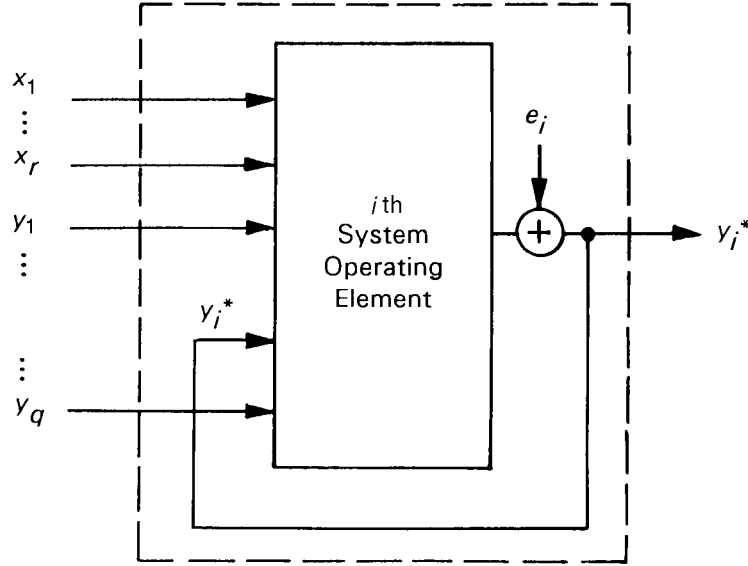
Figure 4-10. Functional Representation of a Generalized Nonideal System Element With Multiple Ideal Inputs

In the analyses that follow it is assumed that all errors are small enough to be represented as small perturbations to the corresponding signals for the ideal case. Based on this assumption, the output of the nonideal element is represented as

$$y_1^* = y_i + \varepsilon_{yi}, \quad \mathbf{U_{yi}} \tag{4-111}$$

where

y_i^* = output of the ith nonideal system element, $\mathbf{U_{yi}}$

ε_{yi} = perturbation in the output y_i due to the nonideal characteristics of the element, $\mathbf{U_{yi}}$.

Error propagation equations are derived first for the case of a nonideal system element with ideal (error-free) inputs. This is followed by the more general case in which the system element and element inputs are nonideal.

The homogeneous form of the performance equations for nonideal elements is designated by the symbol $h_i(\cdots)$. The performance equation for the nonideal element in Fig. 4-10 is written as

$$h_i(\cdots) = h_i(x_1, \cdots, x_r, y_1, \cdots, y_i^*, \cdots, y_q, e_i) = \mathbf{0}, \quad \mathbf{U_{yi}} \tag{4-112}$$

where

e_i = error contribution generated within the ith element, $\mathbf{U_{yi}}$.

Eq. 4-112 can also be expressed as a separate function of y_i and ε_{yi}:

$$h_i(\cdots) = h_i(x_1, \cdots, x_r, y_1, \cdots, y_i, \cdots, y_q, \varepsilon_{yi}, e_i) = \mathbf{0}, \quad \mathbf{U_{yi}}. \tag{4-113}$$

A relationship between the output error ε_{yi} and the error e_i can be obtained by representing the functional equations $f_i(\cdots)$ and $h_i(\cdots)$ as Taylor series expansions, which are described in Ref. 16. This type of series provides a means to approximate the value of any differentiable function in terms of a power series expansion of the function about some reference point.

The basic form for the Taylor series is

$$F(z) = F(a) + \frac{(z-a)}{1!}\frac{dF(a)}{dz}$$

$$+ \frac{(z-a)^2}{2!}\frac{d^2F(a)}{dz^2} + \frac{(z-a)^3}{3!}\frac{d^3F(a)}{dz^3} + \cdots, \ \mathbf{U_F} \qquad (4\text{-}114)$$

where

z = **independent variable of the Taylor series function** $F(z)$, $\mathbf{U_z}$

$F(z)$ = **arbitrary Taylor series function of the single dependent variable,** $\mathbf{U_F}$

a = **general arbitrary value of** z **about which a Taylor series is evaluated,** $\mathbf{U_z}$

$\dfrac{dF(a)}{dz}, \dfrac{d^2F(a)}{dz^2}, \cdots$ = **first, second, … derivative of the function** $F(z)$ **with respect to** z **evaluated at** $z = a$, $\mathbf{U_F/U_z}$, $\mathbf{U_F/U_z^2}, \ldots$.

Multidimensional functions can be similarly expanded in a Taylor series, as shown in Ref. 16. The Taylor expansion for the performance equation Eq. 4-109 is written as

$$f_i(\cdots) = f_i(p_o) + \frac{(x_1-x_{1o})}{1!}\frac{\partial f_i(p_o)}{\partial x_1} + \frac{(x_1-x_{1o})^2}{2!}\frac{\partial^2 f_i(p_o)}{\partial x_1^2} + \cdots$$

$$\vdots$$

$$+ \frac{(x_r-x_{ro})}{1!}\frac{\partial f_i(p_o)}{\partial x_r} + \frac{(x_r-x_{ro})^2}{2!}\frac{\partial^2 f_i(p_o)}{\partial x_r^2} + \cdots$$

$$+ \frac{(y_1-y_{1o})}{1!}\frac{\partial f_i(p_o)}{\partial y_1} + \frac{(y_1-y_{1o})^2}{2!}\frac{\partial^2 f_i(p_o)}{\partial y_1^2} + \cdots \qquad (4\text{-}115)$$

$$\vdots$$

$$+ \frac{(y_q-y_{qo})}{1!}\frac{\partial f_i(p_o)}{\partial y_q} + \frac{(y_q-y_{qo})^2}{2!}\frac{\partial^2 f_i(p_o)}{\partial y_q^2} + \cdots, \ \mathbf{U_{yi}}$$

where

p_o = **multidimensional reference point** $(x_{1o},\cdots,x_{ro},y_{1o},\cdots,y_{qo})$, **U**

$f_i(p_o)$ = **value of** $f_i(\cdots)$ **evaluated at** p_o, $\mathbf{U_{yi}}$

$\dfrac{\partial f_i(p_o)}{\partial x_1}$ = **value of** $\dfrac{\partial f_i(\cdots)}{\partial x_1}$ **evaluated at** p_o, $\mathbf{U_{yi}/U_{x1}}$

$\dfrac{\partial^2 f_i(p_o)}{\partial x_1^2}$ = **value of** $\dfrac{\partial^2 f_i(\cdots)}{\partial x_1^2}$ **evaluated at** p_o, $\mathbf{U_{yi}/U_{x1}^2}$.

Eq. 4-115 represents the expansion of $f_i(\cdots)$ **about the multidimensional reference point** $(x_{1o},\cdots,x_{ro}, y_{1o},\cdots, y_{qo})$. **This reference point defines an operating state for the ideal element and must satisfy the performance equation** $f_i(\cdots) = 0$. **The term** $f_i(p_o)$ **in Eq. 4-115 is, therefore, identically equal to zero. The**

functional equation for the nonideal element is expanded about this same reference point and includes terms for the errors e_i and ε_{yi}.

Expanding Eq. 4-113 in a Taylor series yields

$$
\begin{aligned}
h_i(\cdots) =\ & h_i(p_o) + (x_1 - x_{1o}) \frac{\partial h_i(p_o)}{\partial x_1} + \frac{1}{2}(x_1 - x_{1o})^2 \frac{\partial^2 h_i(p_o)}{\partial x_1^2} + \cdots \\
& \vdots \\
& + (y_i - y_{io}) \frac{\partial h_i(p_o)}{\partial y_i} + \frac{1}{2}(y_i - y_{io})^2 \frac{\partial^2 h_i(p_o)}{\partial y_i^2} + \cdots \\
& \vdots \\
& + (\varepsilon_{yi} - \varepsilon_{yio}) \frac{\partial h_i(p_o)}{\partial \varepsilon_{yi}} + \frac{1}{2}(\varepsilon_{yi} - \varepsilon_{yio})^2 \frac{\partial^2 h_i(p_o)}{\partial \varepsilon_{yi}^2} + \cdots \\
& + (e_i - e_{io}) \frac{\partial h_i(p_o)}{\partial e_i} + \frac{1}{2}(e_i - e_{io})^2 \frac{\partial^2 h_i(p_o)}{\partial e_i^2} + \cdots,\ \mathbf{U_{yi}}
\end{aligned}
\tag{4-116}
$$

where

$h_i(p_o) = h_i(\cdots)$ evaluated at p_o, $\mathbf{U_{yi}}$

$\dfrac{\partial h_i(p_o)}{\partial y_i}$ = first derivative of $h_i(\cdots)$ with respect to y_i evaluated at p_o, dimensionless

ε_{yio} = reference value of ε_{yi}, $\mathbf{U_{yi}}$

e_{io} = reference value of e_i, $\mathbf{U_{yi}}$.

Since $h_i(\cdots)$ has been expanded about the reference point p_o, which represents an ideal, error-free, operating state, the reference values e_{io} and ε_{yio} are equal to zero. In addition, the term $h_i(p_o)$ is by Eq. 4-113 also equal to zero.

All terms on the right side of Eq. 4-116 except those containing ε's and e's are identical to corresponding terms in the Taylor expansion of $f_i(\cdots)$ in Eq. 4-115. Substitutions are made; Eq. 4-116 can then be written as

$$
\begin{aligned}
h_i(\cdots) =\ & f_i(\cdots) + \varepsilon_{yi} \frac{\partial h_i(p_o)}{\partial \varepsilon_{yi}} + \frac{1}{2}\varepsilon_{yi}^2 \frac{\partial^2 h_i(p_o)}{\partial \varepsilon_{yi}^2} + \cdots \\
& + e_i \frac{\partial h_i(p_o)}{\partial e_i} + \frac{1}{2} e_i^2 \frac{\partial^2 h_i(p_o)}{\partial e_i^2} + \cdots,\ \mathbf{U_{yi}}.
\end{aligned}
\tag{4-117}
$$

It is assumed that the errors are small. Therefore all terms in Eq. 4-117 higher than the first order are assumed to be negligible and are dropped. In addition, the terms $h_i(\cdots)$ and $f_i(\cdots)$ in Eq. 4-117 are equal to zero because these functions are homogeneous. Thus Eq. 4-117 reduces to

$$
\varepsilon_{yi} \frac{\partial h_i(p_o)}{\partial \varepsilon_{yi}} + e_i \frac{\partial h_i(p_o)}{\partial e_i} = 0,\ \mathbf{U_{yi}}.
\tag{4-118}
$$

If the chain rule is used, Eq. 4-118 can be rewritten as

$$\varepsilon_{yi} \frac{\partial h_i(p_o)}{\partial y_i^*} \frac{\partial y_i^*}{\partial \varepsilon_{yi}} + e_i \frac{\partial h_i(p_o)}{\partial e_i} = 0, \; \mathbf{U}_{yi}. \tag{4-119}$$

From Eq. 4-111

$$\frac{\partial y_i^*}{\partial \varepsilon_{yi}} = 1, \; \textbf{dimensionless.} \tag{4-120}$$

Therefore, Eq. 4-119 becomes

$$\varepsilon_{yi} \frac{\partial h_i(p_o)}{\partial y_i^*} + e_i \frac{\partial h_i(p_o)}{\partial e_i} = 0, \; \mathbf{U}_{yi}. \tag{4-121}$$

The functional relationship between $h_i(\cdots)$ and y_i^* is identical to the relationship between $f_i(\cdots)$ and y_i. Therefore

$$\frac{\partial h_i(p_o)}{\partial y_i^*} = \frac{\partial f_i(p_o)}{\partial y_i}, \; \textbf{dimensionless.} \tag{4-122}$$

Substituting Eq. 4-122 into Eq. 4-121 yields

$$\varepsilon_{yi} \frac{\partial f_i(p_o)}{\partial y_i} + e_i \frac{\partial h_i(p_o)}{\partial e_i} = 0, \; \mathbf{U}_{yi}. \tag{4-123}$$

The application of Eq. 4-123 is illustrated by use of a simple example. Fig. 4-8(C) depicts an ideal single element with unity feedback. In functional form the governing equation for this element (Eq. 4-102) is

$$f_3(x_1, y_3) = y_3 - \frac{d}{1+d} x_1 = 0, \; \mathbf{U}_{y3}. \tag{4-124}$$

If the element of Fig. 4-8(C) is considered to be nonideal and generates an additive error at its output, the block diagram of this nonideal configuration can be represented as shown in Fig. 4-11. The performance equation for this nonideal element is

$$y_3^* = \frac{d}{1+d} x_1 + \frac{e_3}{1+d}, \; \mathbf{U}_{y3}. \tag{4-125}$$
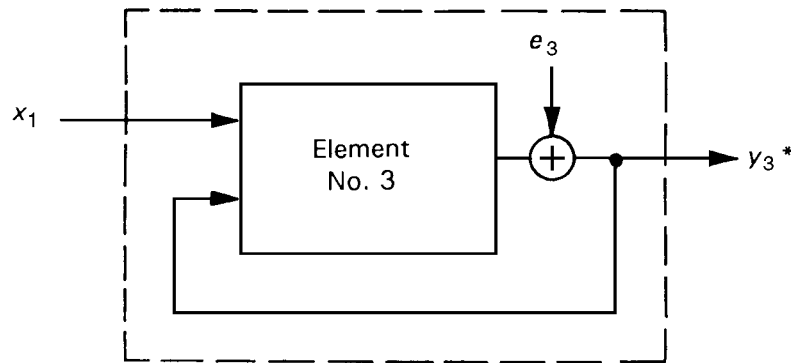
Figure 4-11. Functional Representation of a Nonideal Element Employing Unity Feedback

After Eq. 4-111 with $i = 3$ has been substituted into Eq. 4-125 and the result has been rewritten as a homogeneous equation, the performance equation becomes

$$h_3(x_1, y_3, \varepsilon_{y3}, e_3) = y_3 + \varepsilon_{y3} - \frac{d}{1+d} x_1 - \frac{e_3}{1+d} = 0, \quad \mathbf{U}_{y3} \tag{4-126}$$

Solving Eq. 4-124 for y_3 and substituting the result into Eq. 4-126 yields the following relationship between ε_{y3} and e_3:

$$\varepsilon_{y3} = \frac{e_3}{1+d}, \quad \mathbf{U}_{y3}. \tag{4-127}$$

This same result can also be obtained by using the generalized error equation, Eq. 4-123. The relevant partial derivatives obtained from Eqs. 4-124 and 4-126 are

$$\frac{\partial f_3}{\partial y_3} = 1, \quad \text{dimensionless}$$

$$\frac{\partial h_3}{\partial e_3} = -\frac{1}{1+d}, \quad \text{dimensionless}. \tag{4-128}$$

Substitution of Eq. 4-128 into the general error equation, Eq. 4-123, yields a result that is identical to Eq. 4-127.

The error e_i can be used to represent spurious signals generated within a device, as well as errors in the functional relationships being implemented. This usage is demonstrated in par. C-10 of Appendix C by the error analysis of a simple amplifier that has a gain error and a fixed offset bias.

If the inputs to a nonideal element have error components, the generalized performance equation is

$$h_i(x_i, \cdots, x_l, \cdots, x_r, \varepsilon_{x1}, \cdots, \varepsilon_{xl}, \cdots, \varepsilon_{xr}, \cdots, y_1, \cdots, y_i, \cdots, y_q, \varepsilon_{yi}, e_i) = 0, \quad \mathbf{U}_{yi} \tag{4-129}$$

where

ε_{xl} = error in the lth external input to a system element, $\mathbf{U}_{xl}$.

The error propagation equations for the general case can be shown to be

$$\sum_{k=1}^{q} \varepsilon_{yk} \frac{\partial f_i(p_o)}{\partial y_k} = -\sum_{l=1}^{r} \varepsilon_{xl} \frac{\partial f_i(p_o)}{\partial x_l} - e_i \frac{\partial h_i(p_o)}{\partial e_i}, \quad \mathbf{U}_{yi} \tag{4-130}$$

where

k = index number for all inputs to the ith element originating from within the system, dimensionless

l = index number for all inputs to the ith element originating from outside the system, dimensionless.

Eq. 4-130 is the error equation for the ith element of a system. When all system elements are nonideal, the complete set of system error equations is

$$\sum_{k=1}^{q} \varepsilon_{yk} \frac{\partial f_1(p_o)}{\partial y_k} = -\sum_{l=1}^{r} \varepsilon_{xl} \frac{\partial f_1(p_o)}{\partial x_l} - e_1 \frac{\partial h_1(p_o)}{\partial e_1}, \ \mathbf{U_{y1}}$$

$$\vdots$$

$$\sum_{k=1}^{q} \varepsilon_{yk} \frac{\partial f_i(p_o)}{\partial y_k} = -\sum_{l=1}^{r} \varepsilon_{xl} \frac{\partial f_i(p_o)}{\partial x_l} - e_i \frac{\partial h_i(p_o)}{\partial e_i}, \ \mathbf{U_{yi}} \qquad \textbf{(4-131)}$$

$$\vdots$$

$$\sum_{k=1}^{q} \varepsilon_{yk} \frac{\partial f_q(p_o)}{\partial y_k} = -\sum_{l=1}^{r} \varepsilon_{xl} \frac{\partial f_q(p_o)}{\partial x_l} - e_q \frac{\partial h_q(p_o)}{\partial e_q}, \ \mathbf{U_{yq}}.$$

Eq. 4-131 is a set of q linear equations that are solved simultaneously for the output errors ε_{yk}.

4-4.3.2.1 Analysis of Random Errors

Errors in fire control system elements can be categorized as either systematic or random. A systematic error is the difference between the mean value of a set of observations of an actual variable and the true, or ideal, value of that variable. Systematic errors are often called bias errors. A random error is the deviation of the actual values in the set of observations from the mean value. Because of their noisy nature, random errors are also referred to as uncertainties. Random errors are described in terms of statistical parameters, such as the variance σ^2 or the standard deviation σ. A review of fundamental statistical principles is presented in Appendix C.

To perform an error analysis, it is first necessary to identify and quantify the systematic and random components of each error source. The systematic component of the error in each element output can be obtained from Eq. 4-131 if each of the error terms in the equation is replaced by its corresponding systematic component.

Random errors are treated differently. The basis for the analysis of random errors is the statistical theorem that the variance of the sum of a number of statistically independent random variables is equal to the sum of the variances of the individual variables. This theorem is derived in par. C-9 of Appendix C and is written mathematically as

$$\sigma_S^2 = \sum_{i=1}^{N} \sigma_i^2, \ \mathbf{U}^2 \qquad \textbf{(4-132)}$$

where

σ_S^2 = variance of the sum of the N independent random variables, $\mathbf{U}^2$

σ_i^2 = variance of the ith random variable, $\mathbf{U}^2$.

The requirements for the use of this equation are that the individual random variables be independent and that all of the variables have identical units.

When applied to the error analysis of fire control systems, Eq. 4-132 is written as

$$\sigma_{yi}^2 = \sum_{l=1}^{r} (C_{x_{il}})^2 \sigma_{x_l}^2 + \sum_{m=1}^{q} (C_{e_{im}})^2 \sigma_{e_m}^2, \ \mathbf{U_{yi}^2} \qquad \textbf{(4-133)}$$

where

$\sigma_{y_i}^2$ = variance of the random component of the output error in the ith element, $\mathbf{U_{yi}^2}$

$\sigma_{x_l}^2$ = variance of the random component of the error in the lth element input, $\mathbf{U_{xl}^2}$

$\sigma_{e_m}^2$ = variance in the random component of the internally generated error in the mth element, $\mathbf{U_{ym}^2}$

$C_{x_{il}}$ = scaling coefficient between the lth input and the ith output, $\mathbf{U_{yi}/U_{xl}}$

$C_{e_{im}}$ = scaling coefficient between the mth internally generated error and the ith element output, U_{yi}/U_{ym}.

The scaling coefficients are functions of the partial derivatives in Eq. 4-131, and they define for every operating state p_o the sensitivity of the output errors to each of the input and element errors. These coefficients also provide the required consistency in units. For example, if the output of the element is a voltage, all terms in the summation on the right side of Eq. 4-133 must also be in volts. If one of the inputs is a temperature reading in degrees centigrade, the scaling coefficient for this input will define the effect that temperature has on the voltage output and will have units of V/°C. A summation of the type represented by Eq. 4-133 is called the sum square. The square root of each side of Eq. 4-133 is often used, and the result is known as the root sum square (rss). The rss values are used when system errors are to be expressed in terms of standard deviations.

The scaling coefficients $C_{x_{i|}}$ and $C_{e_{im}}$ are obtained from the solution of Eq. 4-131. This solution can be written in matrix notation as

$$
\begin{bmatrix} \varepsilon_{y1} \\ \vdots \\ \varepsilon_{yi} \\ \vdots \\ \varepsilon_{yq} \end{bmatrix}
=
\begin{bmatrix} b_{11} & \cdots & b_{1\,(r+q)} \\ \vdots & & \\ b_{q1} & \cdots & b_{q\,(r+q)} \end{bmatrix}
\begin{bmatrix} \varepsilon_{x1} \\ \vdots \\ \varepsilon_{x|} \\ \vdots \\ \varepsilon_{xr} \\ e_1 \\ \vdots \\ e_m \\ \vdots \\ e_q \end{bmatrix}
, \ \mathbf{U}
\qquad (4\text{-}134)
$$

where

b_{is} = elements of the system error matrix, U.

The elements of the matrix in Eq. 4-134 are the scaling coefficients required by Eq. 4-133, i.e.,

$$
\begin{aligned}
C_{x_{i|}} &= b_{is} & \text{for } i &= 1,2,\cdots,q \\
& & s &= | = 1,2,\cdots,r \\
C_{e_{im}} &= b_{is} & \text{for } i &= 1,2,\cdots,q \\
& & s &= m = (r+1),\cdots,(r+q) .
\end{aligned}
\qquad (4\text{-}135)
$$

The solution to the set of linear error equations can be determined using matrix algebra, as described in Ref. 17, or by sequential substitution. The latter technique is demonstrated by illustrative examples in pars. C-11 and C-12 of Appendix C.

The derivation of error propagation equations is based on the assumption that the errors are small enough to neglect nonlinear effects. If this assumption is not valid, output errors must be obtained by solving the set of generalized governing equations, as represented by Eq. 4-96. The equations are first solved for the case with no errors and then for the case in which appropriate errors are added; the output errors are obtained by subtracting the two results. The advantage of using the small error approxi-

mation is the computational task is reduced and very often a closed form solution can be obtained. Such solutions give the designer insights into the behavior of the system that are not always obvious when solutions are obtained by numerical techniques.

4-4.3.2.2 Determination of Operating Points

The values for both the systematic and random components of the system output errors depend on partial derivatives, which are evaluated at some nominal system operating state. In addition, the magnitudes of the individual input and element errors are often dependent on the operating state. The designer must therefore select the operating state to be used in his evaluation when performing error analyses on fire control systems.

One approach to the selection of an appropriate operating state is to study the change in each of the system output errors as a function of the input variables. This is called a parametric sensitivity analysis. It is convenient to plot curves of output error versus one of the input variables with all of the other input variables held constant. A two-dimensional sensitivity analysis can be performed by plotting a family of curves. Each curve is a plot for a different value of a second input variable. Fig. 4-12 shows a typical set of sensitivity curves. By generating curves for different combinations of input variables, the designer can determine the operating state that produces a worst-case maximum error.

Whenever a U (with or without a subscript) appears next to the variable, it indicates the use of any appropriate unit.
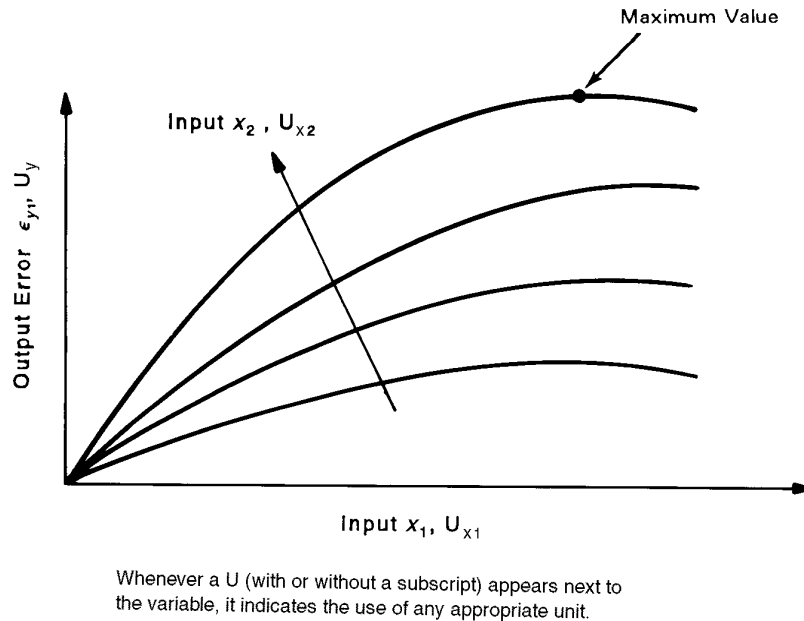
Figure 4-12. Typical Families of Error Sensitivity Curves

Alternatively, the designer may have information on the probable range of values for each of the input variables. He can then compute the error based on a mean value for each of the input parameters and can establish probable limits for the output errors. Limits are often set at plus or minus one standard deviation ($\pm 1\sigma$) about the mean. The output errors are then computed for the mean operating state and for the operating state representing the 1σ conditions. Fig. 4-13 depicts the use of probability density functions in the analysis of errors. Fig. 4-13(A) shows the dependence of the variance of the system output $\sigma^2_{\varepsilon_y}(x)$ on an input variable x. Fig. 4-13(B) shows a Gaussian pdf for x. The mean value of $\sigma^2_{\varepsilon_y}(x)$ is shown as point A, and the 1σ limits, as points B and C. A most probable error (MPE) is obtained by taking a weighted average of the output variance over all possible values of x, as shown in Fig. 4-13(C). The MPE is computed from

$$\text{MPE} = \left[\int_{-\infty}^{\infty} \sigma^2_{\varepsilon_y}(x) \; p(x) \; dx \right]^{1/2} , \; \text{U}_y \tag{4-136}$$

where

$\qquad$ MPE = most probable error, U_y

$\qquad$ $\sigma^2_{\varepsilon_y}(x)$ = variance of the output error as a function of the input x, U_y^2

$\qquad$ $p(x)$ = pdf for the input variable x, dimensionless.
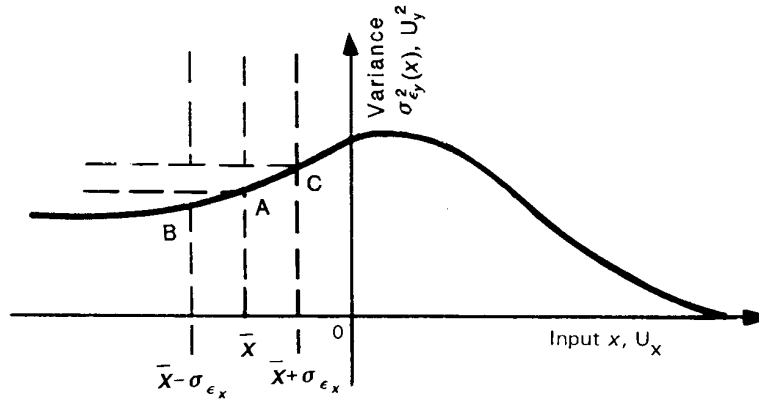
(A) Variance of Output Errors Dependent on an Input x
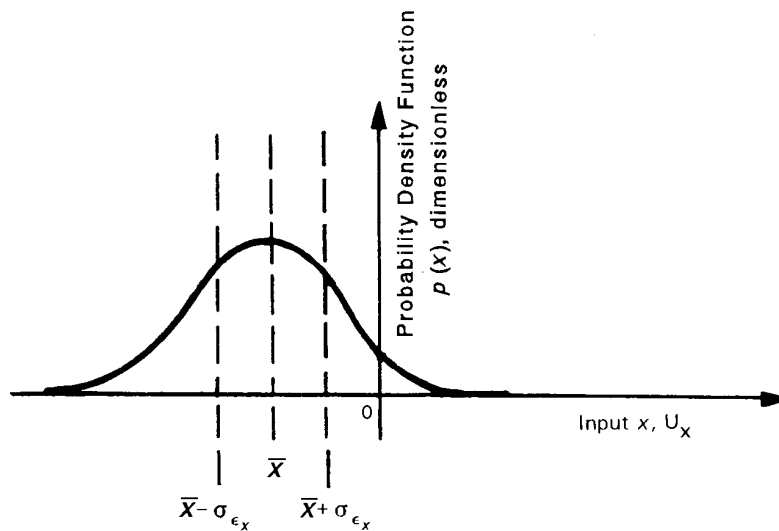
(B) Probability Density Function for the Input x
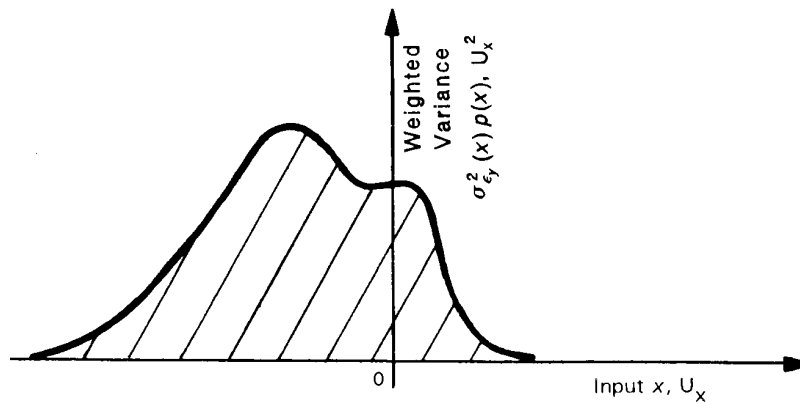
(C) Weighted Variance of the Output Errors Dependent on an Input x

Figure 4-13. Development of the Weighted Average of a Group of Dependent Random Errors

In systems with multidimensional inputs the MPE can be determined by a similar technique. If the errors associated with each of the inputs are statistically independent, the variance in the output error can be obtained by summing the MPE variances with each input taken separately, i.e.,

$$\text{MPE} = \left[\sum_{i=1}^{r} \int_{-\infty}^{\infty} \sigma_{\varepsilon_y}^2 (x_i) \; p(x_i) \; dx_i \right]^{1/2}, \; \text{U}_y. \tag{4-137}$$

In this multidimensional case the function $\sigma_{\varepsilon_y}^2 (x_i)$ would be computed using mean values of all of the other input variables.

If there is significant statistical dependence among input errors, multivariate probability density functions must be used. In many cases, however, only a small fraction of the error variance of one input is statistically correlated to another, and the assumption of statistical independence can be made to simplify the analysis. Par. C-12 in Appendix C is an illustrative example of an error sensitivity analysis.

An additional error analysis technique is the Monte Carlo simulation. In this technique the functional equations for the system are solved numerically for different values of the input variables and error sources. Many runs are made, each of which represents a different operating state. The values of the input variables are selected randomly based on the available knowledge about the nature of the probability distribution for each variable. If little information is known, the distribution is assumed to be uniform over a range of values. In many instances, however, data exist; thus it is possible to be more definitive in specifying the distribution.

4-4.3.3 Illustrative Examples for a System Described by Equations Other Than Differential Equations

Use of the set of error propagation equations shown in Eq. 4-131 is demonstrated in par. C-10 of Appendix C for the error associated with a simple amplifier. Two solutions are presented. The first follows the steps in the derivation of Eq. 4-131 and is presented as Solution A. The second solution (Solution B) is obtained by direct substitution into Eq. 4-131 after computation of the partial derivatives. A more complex example, based on Ref. 18, is given in par. C-11 of Appendix C. This example demonstrates the formulation of the error propagation for an electromagnetic resolver network.

Use of the error propagation equation for systematic and random error components is demonstrated in par. C-12 of Appendix C. This example is a continuation of the resolver circuit example of par. C-11 of Appendix C and illustrates the use of a parametric sensitivity analysis to determine maximum and expected error values.

4-4.3.4 Analysis of Error Propagation in Systems Described by Differential Equations

The technique just described may be used to determine the propagation of errors in certain portions of a fire control system, e.g., the coordinate transformation and ballistic correction elements, but other parts of the system (such as those used in the computation of lead angle) require the solution of differential equations. In this case the input and output variables are time-varying quantities, and the system equations include time derivatives of these quantities. The set of q error equations represented by Eq. 4-131 becomes a set of q differential equations of the form:

$$\sum_{k=1}^{q}\left(\frac{\partial f_1}{\partial y_k}\varepsilon_{yk}+\frac{\partial f_1}{\partial \dot{y}_k}\dot{\varepsilon}_{yk}+\frac{\partial f_1}{\partial \ddot{y}_k}\ddot{\varepsilon}_{yk}+\cdots\right)$$

$$=-\sum_{l=1}^{r}\left(\frac{\partial f_1}{\partial x_l}\varepsilon_{xl}+\frac{\partial f_1}{\partial \dot{x}_l}\dot{\varepsilon}_{xl}+\frac{\partial f_1}{\partial \ddot{x}_l}\ddot{\varepsilon}_{xl}+\cdots\right)-e_1\frac{\partial f_1}{\partial y_1}, \ \mathbf{U_1}$$

$$\sum_{k=1}^{q}\left(\frac{\partial f_i}{\partial y_k}\varepsilon_{yk}+\frac{\partial f_i}{\partial \dot{y}_k}\dot{\varepsilon}_{yk}+\frac{\partial f_i}{\partial \ddot{y}_k}\ddot{\varepsilon}_{yk}+\cdots\right)$$

$$=-\sum_{l=1}^{r}\left(\frac{\partial f_i}{\partial x_l}\varepsilon_{xl}+\frac{\partial f_i}{\partial \dot{x}_l}\dot{\varepsilon}_{xl}+\frac{\partial f_i}{\partial \ddot{x}_l}\ddot{\varepsilon}_{xl}+\cdots\right)-e_i\frac{\partial f_i}{\partial y_i}, \ \mathbf{U_i} \quad\quad \text{(4-138)}$$

$$\sum_{k=1}^{q}\left(\frac{\partial f_q}{\partial y_k}\varepsilon_{yk}+\frac{\partial f_q}{\partial \dot{y}_k}\dot{\varepsilon}_{yk}+\frac{\partial f_q}{\partial \ddot{y}_k}\ddot{\varepsilon}_{yk}+\cdots\right)$$

$$=-\sum_{l=1}^{r}\left(\frac{\partial f_q}{\partial x_l}\varepsilon_{xl}+\frac{\partial f_q}{\partial \dot{x}_l}\dot{\varepsilon}_{xl}+\frac{\partial f_q}{\partial \ddot{x}_l}\ddot{\varepsilon}_{xl}+\cdots\right)-e_q\frac{\partial f_q}{\partial y_q}, \ \mathbf{U_q}$$

where

      $(\dot{})$ = first derivative with respect to time, U/s

      $(\ddot{})$ = second derivative with respect to time, U/s^2.

Two approaches can be used to solve the set of error equations in Eq. 4-138:
1. The impulse-response approach in the time domain
2. The transfer-function approach in the frequency domain.

Both approaches require that the system performance equations be linear or at least linearized representations of nonlinear system equations.

Methods of error analysis using the time domain (impulse-response approach) and methods using the frequency domain (transfer-function approach) are described in subpars. 4-4.3.4.1 and 4-4.3.4.2, respectively. Means of transforming from one domain to the other by means of direct and inverse Fourier transforms are given in subpar. 4-4.3.4.2.

4-4.3.4.1 Impulse-Response Approach

As noted in subpar. 4-4.3.2, a fire control system can be considered to consist of an assemblage of elements, such as the system depicted in Fig. 4-7. As indicated in Fig. 4-7, the output of each such element can be expressed as a function of the inputs by

$$y_i = g_i(x_1,\cdots,x_r;y_1,\cdots,y_i,\cdots,y_q), \ \mathbf{U_{yi}} \quad\quad \text{(4-96 repeated)}$$

In the impulse-response approach the first step toward the solution of Eq. 4-138 is to derive a particular form of the performance operator $g_i(\ldots)$ that relates an output time-dependent function to an input time-dependent function. This form of the performance operator is known as the weighting function and is the response of the system element to a unit impulse function.

These functions are defined first and then derived for a simple system element having one input and one output, as represented in Fig. 4-14. A unit impulse function is the limiting case of a unit pulse function $p(t)$ shown in Fig. 4-15(A). The unit pulse function has an amplitude of $1/\Delta t$ between $t = 0$ and $t = \Delta t$ and has zero amplitude everywhere else. As Δt approaches zero, the unit pulse function becomes a unit impulse function $u(t)$ which has infinite amplitude at $t = 0$ and zero amplitude everywhere else, as shown in Fig. 4-15(B). Note that the area under the unit pulse function is unity and remains at unity in the limit as Δt approaches zero. Therefore, the area under the unit impulse function is always unity.
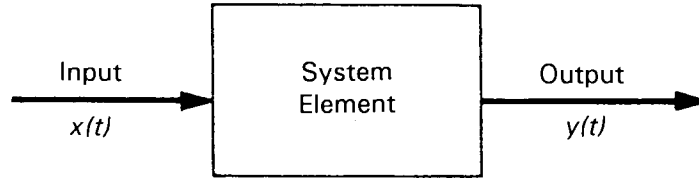
Figure 4-14. Functional Representation of a System Element With a Single Time-Varying Input and a Single Time-Varying Output

(A) Unit Pulse Function $p(t)$

(B) Unit Impulse Function $u(t)$
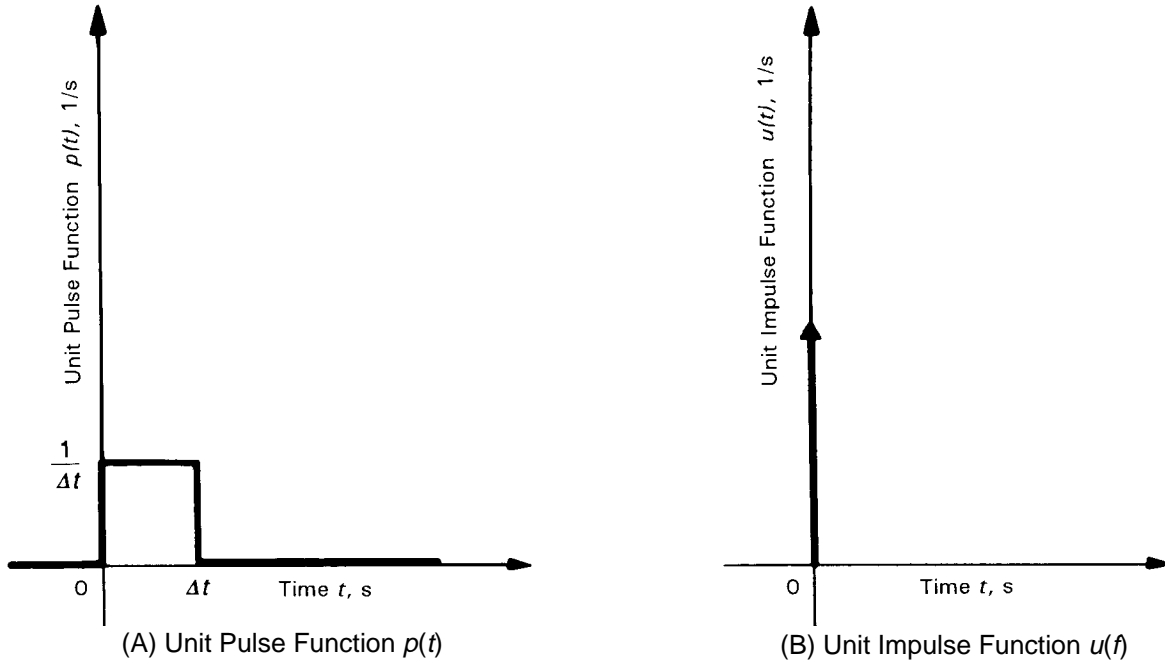
Figure 4-15. Graphical Representation of the Unit Pulse Function and the Unit Impulse Function

When the unit pulse function is applied to the system element at $t = 0$, there is a time response $v(t)$ that typically might have a form similar to the solid curve shown in Fig. 4-16. This curve is identified by the symbol $v_0(t)$ to indicate that it is the response to a unit pulse function applied at time $t = 0$. If the pulse width is sufficiently narrow, the unit pulse response will approach the unit impulse response. For reasons discussed subsequently, the unit impulse response is called the weighting function $r(t)$.

The dashed curve shown in Fig. 4-16 is the response to a pulse applied at time $t = t_k$. Accordingly, this response is identified by the symbol $v_k(t)$. For a linear system element, the response $v_0(t)$ and the response $v_k(t)$ have the same shape and are separated by a time interval t_k. In mathematical terms the constancy of shape of the responses is expressed by

$$v_k(t_1) = v_0(t_1 - t_k), \ \mathbf{U} \tag{4-139}$$

where

v_k = response to a unit pulse occurring at some arbitrary time $t = t_k$, U

4-68

v_0 = response to a unit pulse occurring at time t_0, U

t_1, t_k = arbitrary points in time, s.
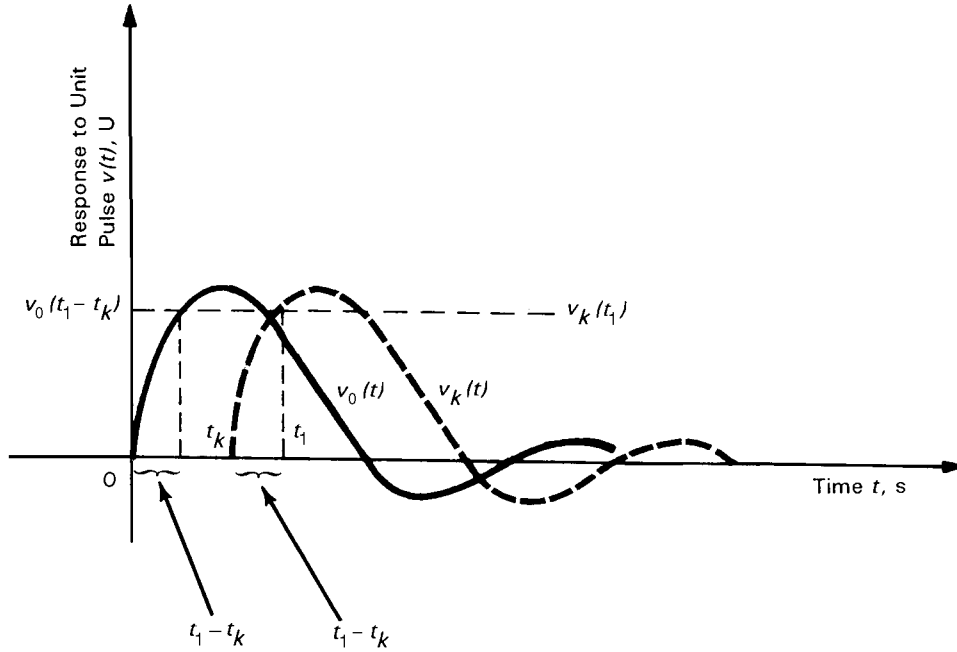
Figure 4-16. Typical Pulse Responses $v(t)$

Any random input function $x(t)$ can be approximated by a series of pulse functions. To begin, a unit pulse function occurring at time $t = t_k$ is denoted $p(t_k)$ and is illustrated in Fig. 4-17(A). When the unit pulse function $p(t_k)$ is multiplied by Δt, a pulse of unit amplitude at time t_k is obtained, as shown in Fig. 4-17(B). As shown in Fig. 4-17(C), the amplitude of the random input function $x(t)$, is $x(t_k)$ at $t = t_k$. Accordingly, a pulse function of width Δt and amplitude $x(t_k)$ will approximate the plot for $x(t)$ at that point. This pulse function is obtained by multiplying the unit amplitude pulse $p(t_k)\Delta t$ by the amplitude $x(t_k)$ to give $x(t_k)p(t_k)\Delta t$, as shown in Fig. 4-17(C). Extending this concept, the function $x(t)$ can be approximated by a series of such pulse functions, as shown in Fig. 4-17(D). The approximation is given in mathematical terms by

$$x(t) \cong \sum_{k=-\infty}^{\infty} x(t_k)\, p(t_k)\, \Delta t, \;\; \mathbf{U_x} \qquad (4\text{-}140)$$

where

$x(t)$ = continuous input time function, $\mathbf{U_x}$

k = time step integer, dimensionless

$x(t_k)$ = value of $x(t)$ at time t_k, $\mathbf{U_x}$

$p(t_k)$ = unit pulse function at time $(t)_k$, 1/s.
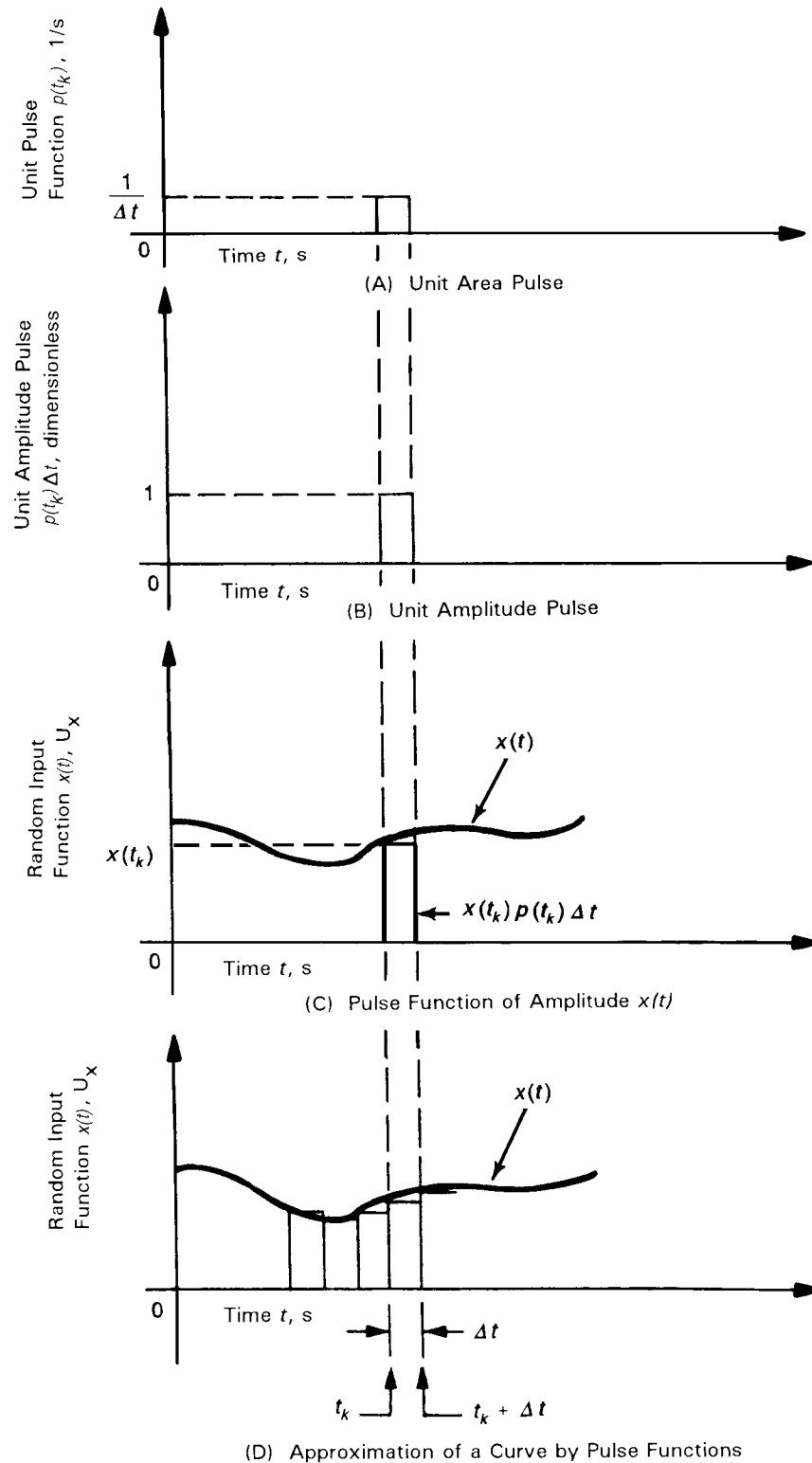
Figure 4-17. Approximation of a Random Input Function by a Series of Pulse Functions

The response of a system element to a unit pulse function at time $t = t_k$ has been defined as $v_k(t)$, as shown in Fig. 4-16. Therefore, for a linear system element the response to a unit amplitude pulse is Δt times as great, or $v_k(t)\Delta t$, and the response to a pulse of amplitude $x(t_k)$ is $v_k(t)x(t_k)\Delta t$. If the output of the system element is denoted $y(t)$, at time t_1 the output resulting from a single pulse of amplitude $x(t_k)$ at time t_k is

$$y(t_1) \;=\; v_k(t_1)\, x(t_k)\, \Delta t, \;\; \mathbf{U_y} \tag{4-141}$$

where

$y(t_1)$ = continuous output time function, $\mathbf{U_y}$

$v_k(t_1)$ = unit pulse response function, $\mathbf{U_y}/(\mathbf{U_x \cdot s})$.

The substitution from Eq. 4-139 into Eq. 4-141 shows that

$$y(t_1) \;=\; v_0(t_1 - t_k)\, x(t_k)\, \Delta t, \;\; \mathbf{U_y}. \tag{4-142}$$

Therefore, the response of the system element at time t_1 to the summation of pulses represented by Eq. 4-140 is given by

$$y(t_1) \;=\; \sum_{k=-\infty}^{\infty} v_0(t_1 - t_k)\, x(t_k)\, \Delta t, \;\; \mathbf{U_y}. \tag{4-143}$$

Since $v_0(t_1 - t_k)$ and $x(t_k)$ are continuous functions, the resulting function becomes an integral in the limit as $\Delta t \to 0$ and is given mathematically by

$$y(t_1) \;=\; \int_{-\infty}^{\infty} r_0(t_1 - t_k)\, x(t_k)\, dt_k, \;\; \mathbf{U_y} \tag{4-144}$$

where

$r_0(t_1 - t_k)$ = weighting function, or response function, at time $t_1 - t_k$ to a unit impulse function applied at time $t = 0$, $\mathbf{U_y}/(\mathbf{U_x \cdot s})$.

The substitution of a new time variable τ for $t_1 - t_k$ in Eq. 4-144 yields the relationship

$$y(t_1) \;=\; -\int_{\infty}^{-\infty} r_0(\tau)\, x(t_1 - \tau)\, d\tau = \int_{-\infty}^{\infty} r_0(\tau)\, x(t_1 - \tau)\, d\tau, \;\; \mathbf{U_y} \tag{4-145}$$

where

τ = generalized time variable, $t_1 - t_k$, s.

The integral on the right side of Eq. 4-145 is known as a convolution integral. General convolution integrals and theorems are discussed in Refs. 16, 17, and 19. Inasmuch as t_1 is any arbitrary point in time, it can be replaced by the general symbol for time t. In addition, for simplification the subscript zero is dropped from $r_0(\tau)$ because the impulse function is conventionally applied at time $t = 0$. When applied to Eq. 4-145, these steps result in the most general form for the convolution integral:

$$y(t) \;=\; \int_{-\infty}^{\infty} r(\tau)\, x(t - \tau)\, d\tau, \;\; \mathbf{U_y} \tag{4-146}$$

where

$r(\tau)$ = response function of system element to an input function, $\mathbf{U_y}/(\mathbf{U_x \cdot s})$.

Since t_k is also arbitrary, Eq. 4-144 can be generalized by replacing t_1 with t and t_k with τ' to give an alternative form of the convolution integral:

$$y(t) \;=\; \int_{-\infty}^{\infty} r(t - \tau')\, x(\tau')\, d\tau', \;\; \mathbf{U_y} \tag{4-147}$$

where

τ' = generalized time variable for t_k, s.

The convolution process represented by the right side of Eq. 4-146 can be visualized with the aid of Fig. 4-18. The curve in Fig. 4-18(A) represents $x(t)$. The function $x(t - \tau)$ shown in Fig. 4-18(B) is generated from $x(t)$ in Fig. 4-18(A) by sweeping to the left an amount τ from the initial value at t. When τ is zero, $x(t - \tau)$ is equal to $x(t)$, and when $\tau = t$, $x(t - \tau)$ is equal to $x(0)$. In Fig. 4-18(C) the impulse response $r(\tau)$ is swept out as τ increases by a line moving to the right. Thus the convolution process involves the integration of the product of two time functions: $r(\tau)$, which is being swept out in the direction of increasing τ, and $x(t - \tau)$, which is being swept out in the direction of decreasing t. In the second form of the convolution integral, which is given by Eq. 4-147, each value of the input variable $x(\tau')$ is weighted by the impulse response $r(t - \tau')$ at time $t - \tau'$, and the output $y(t)$ is then obtained as the infinite sum of these weighted values of the inputs. This is the origin of the alternate term, weighting function, for the impulse response.

By convention only positive values of time t are considered. Since τ must also be a positive value less than or equal to t, it follows that Eq. 4-146 takes the form

$$y(t) \ = \ \int_{0}^{t} r(\tau) \, x(t - \tau) \, d\tau, \ \ \mathbf{U_y}. \tag{4-148}$$

and $y(t)$ is the output of the system element at time t.
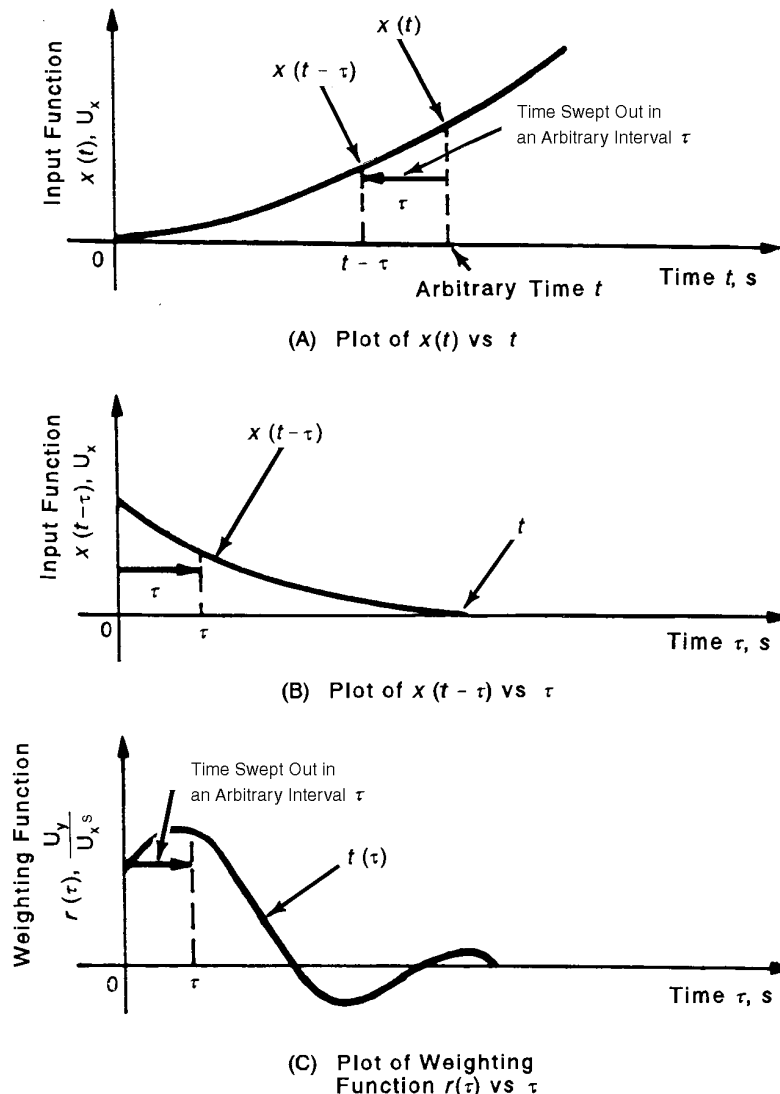
Figure 4-18. Pictorial Representation of the Convolution Process

Since the impulse response of a linear element is a fixed property of that element, Eq. 4-148 can be considered a particular form of performance equation, Eq. 4-96, for the case of a linear system element with a time-varying input.

Based on Eq. 4-147, $y(t)$ can also be expressed in the alternative form

$$y(t) = \int_0^t r(t-\tau)\, x(\tau)\, d\tau, \quad \mathbf{U_y}. \tag{4-149}$$

The corresponding error equation that relates an error $\varepsilon_x(\tau)$ in the input to the resulting error $\varepsilon_y(t)$ in the output can be written from Eq. 4-149 by inspection and using the fact that for a linear system element an input error is acted upon in the same way as an input. The result is

$$\varepsilon_y(t) = \int_0^t r(t-\tau)\, \varepsilon_x(\tau)\, d\tau, \quad \mathbf{U_y} \tag{4-150}$$

where

$\varepsilon_x(\tau)$ = error in $x(\tau)$, the single input to the system element under consideration, $\mathbf{U_x}$

$\varepsilon_y(t)$ = error in the output $y(t)$, $\mathbf{U_y}$.

For those situations in which the functions in Eq. 4-150 are not readily integrable, an approximate method can be used. In this case the error in the input to the system element can be approximated by a summation of discrete impulse functions, i.e.,

$$\varepsilon_x(\tau) = \varepsilon_{x\tau_1} + \varepsilon_{x\tau_2} + \cdots + \varepsilon_{x\tau_n}, \quad \mathbf{U_x} \tag{4-151}$$

where

$\varepsilon_{x\tau_1}, \varepsilon_{x\tau_2}, \cdots, \varepsilon_{x\tau_n}$ = magnitudes of the discrete impulses at times $\tau_1, \tau_2, \cdots, \tau_n$, respectively, $\mathbf{U_{x1}}, \cdots, \mathbf{U_{xn}}$.

Eq. 4-142 shows that after a time interval t

$$\varepsilon_{y\tau_1}(t) = v_0(t-\tau_1)\, \varepsilon_{x\tau_1} \Delta t, \quad \mathbf{U_y} \tag{4-152}$$

where

$\varepsilon_{y\tau_1}(t)$ = output error contribution at time t from an input pulse $\varepsilon_{x\tau_1}$ applied at time τ_1, $\mathbf{U_y}$.

Therefore, for the current example the total output error $\varepsilon_y(t)$ is the sum of the contributions from the total of n separate error impulses used:

$$\varepsilon_y(t) = \varepsilon_{y\tau_1}(t) + \varepsilon_{y\tau_2}(t) + \cdots + \varepsilon_{y\tau_n}(t), \quad \mathbf{U_y}. \tag{4-153}$$

The following procedure illustrates the development of a more generalized set of equations for a multielement system:

1. Eq. 4-150 is an expression that relates a single time-varying input error to a single time-varying output error for a single system element. For an ideal system element that has p multiple inputs, the output error has the form of a summation of expressions like that of Eq. 4-150:

$$\varepsilon_y(t) = \sum_{n=1}^{p} \int_0^t r_n(t-\tau)\, \varepsilon_{xn}(\tau)\, d\tau, \quad \mathbf{U_y} \tag{4-154}$$

where

$\varepsilon_{xn}(\tau)$ = error in the nth input of the system element, $\mathbf{U_{xn}}$

$r_n(t-\tau)$ = response function of the single element to a unit impulse of the nth input, $\mathbf{U_y}/(\mathbf{U_y}/\mathbf{U_{xn}} \cdot \mathbf{s})$.

$\varepsilon_y(t)$ = error in the output of the system element, $\mathbf{U_y}$

n = integers from 1 to p that define individual inputs to the element, dimensionless.

If the element is not ideal, the element error must be added to Eq. 4-154, and the error has the form

$$\varepsilon_y(t) = \sum_{n=1}^{p} \int_0^t r_n(t-\tau) \, \varepsilon_{xn}(\tau) \, d\tau + e_y(t), \quad \mathbf{U_y} \qquad (4\text{-}155)$$

where

$e_y(t)$ = error generated within the element, $\mathbf{U_y}$.

2. In a multielement system each element has as inputs some of the outputs of other system elements. When the response is added to these inputs, Eq. 4-155 yields an expression for the error in the output of the ith of q system elements:

$$\varepsilon_{yi}(t) = \sum_{n=1}^{p} \int_0^t r_{in}(t-\tau) \, \varepsilon_{xn}(\tau) \, d\tau$$

$$+ \sum_{k=1 \neq i}^{q} \int_0^t r_{ik}(t-\tau) \, \varepsilon_{yk}(\tau) \, d\tau + e_{yi}(t), \quad \mathbf{U_{yi}} \qquad (4\text{-}156)$$

where

$r_{in}(t-\tau)$ = response function of the ith element to a unit impulse of the nth input, $\mathbf{U_{yi}}/(\mathbf{U_{xn} \cdot s})$
$r_{ik}(t-\tau)$ = response function of the ith element to a unit impulse of the kth input, $\mathbf{U_{yk}}/(\mathbf{U_{yi} \cdot s})$
ε_{yk} = error in an output y_k of the kth internal system element, $\mathbf{U_{yk}}$
k = integer identifier for the qth system element with $k \neq i$, dimensionless
$e_{yi}(t)$ = error generated within the ith element, $\mathbf{U_{yi}}$.

Eq. 4-156 represents the ith equation of a set of q equations that define the output errors of a system containing q elements. Eq. 4-156 is a particular solution of Eq. 4-138 that applies to a system that has linear elements with time-varying inputs and nonideal element errors e_{yi}.

3. If the element under consideration has direct feedback from its own output, the final set of q error equations can be represented by the equation for the ith element, which is

$$\varepsilon_{yi}(t) = \sum_{n=1}^{p} \int_0^t r_{in}(t-\tau) \, \varepsilon_{xn}(\tau) \, d\tau$$

$$+ \sum_{k=1 \neq i}^{q} \int_0^t r_{ik}(t-\tau) \, \varepsilon_{yk}(\tau) \, d\tau \qquad (4\text{-}157)$$

$$+ \int_0^t r_{ii}(t-\tau) \, \varepsilon_{yi}(\tau) \, d\tau + e_{yi}(t), \quad \mathbf{U_{yi}}$$

where

$r_{ii}(t-\tau)$ = response function of the ith element to a unit impulse of direct feedback, $1/s$.

Refs. 20 and 21 contain further development of expressions in the form of Eq. 4-150 and examples of how they can be used in error analyses of systems having time-varying inputs.

4-4.3.4.2 Transfer Function Approach

As noted in subpar. 4-4.3.4, an alternative approach to carrying out an error analysis for systems whose performance is represented by differential equations is to use functions of frequency. As shown in the paragraphs that follow, an error analysis performed in the frequency domain has the advantage of requiring only the multiplication of functions, in contrast with the convolution operation required for time functions. Also the frequency response of a system element, i.e., the amplitude and phase angle

of the output response to a sinusoidal input forcing function, is quite commonly available for many elements, including servo elements and other components of fire control systems. This frequency domain technique of error analysis has been extensively applied and is described in terms that are most useful for fire control calculations. Extensive applications of this technique are illustrated in Ref. 22. (The remaining material of subpar. 4-4.3.5 is based directly on the analyses developed by Dr. J. G. Tappert and presented in Ref. 18.)

The transfer function approach to error analysis is demonstrated first for the single input, single output system element depicted in Fig. 4-14. The element performance is characterized in the frequency domain by the transfer function $R(j\omega)$. This is a complex ratio defined as

$$R(j\omega) = \frac{Y(j\omega)}{X(j\omega)}, \ \mathbf{U_y/U_x} \tag{4-158}$$

where

$R(j\omega)$ = element transfer function, $\mathbf{U_y/U_x}$
$X(j\omega)$ = Fourier transform of input variable $x(t)$, $\mathbf{U_x \cdot s}$
$Y(j\omega)$ = Fourier transform of output variable $y(t)$, $\mathbf{U_y \cdot s}$
ω = angular frequency rad/s
$j = \sqrt{-1}$, dimensionless.

The Fourier transform of the input and output functions $x(t)$ and $y(t)$, respectively, are defined by

$$X(j\omega) = \int_{-\infty}^{\infty} x(t) \ \mathbf{exp}(-j\omega t) \ dt, \ \mathbf{U_x \cdot s}$$

$$Y(j\omega) = \int_{-\infty}^{\infty} y(t) \ \mathbf{exp}(-j\omega t) \ dt, \ \mathbf{U_y \cdot s}. \tag{4-159}$$

This transform process can be reversed by the inverse Fourier transforms:

$$x(t) = \frac{1}{2\pi} \int_{-\infty}^{\infty} X(j\omega) \ \mathbf{exp}(j\omega t) \ d\omega, \ \mathbf{U_x}$$

$$y(t) = \frac{1}{2\pi} \int_{-\infty}^{\infty} Y(j\omega) \ \mathbf{exp}(j\omega t) \ d\omega, \ \mathbf{U_y}. \tag{4-160}$$

The assumption that the element is linear implies that $R(j\omega)$ is not a function of the input. For the frequency domain approach the functional representation of a system element shown in Fig. 4-14 becomes modified to the form shown in Fig. 4-19. In Fig. 4-19 the time dependency has been replaced by the frequency dependency through the term $j\omega$.
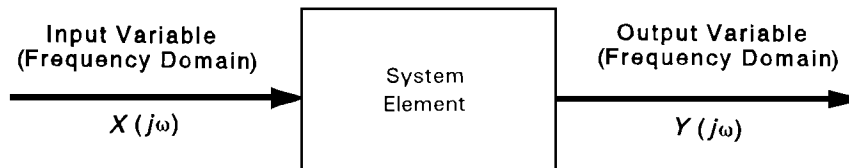
Figure 4-19. Functional Representation of a System Element in the Frequency Domain

A formal relationship exists between the transfer function $R(j\omega)$ and the impulse response function $r(\tau)$. The relationship is derived in the equations that follow. The time domain input-output relationship given by Eq. 4-146 can be substituted into the definition of $Y(j\omega)$ given by Eq. 4-159:

$$Y(j\omega) = \int_{-\infty}^{\infty} \exp(-j\omega t) \left[\int_{-\infty}^{\infty} r(\tau) \, x(t-\tau) \, d\tau \right] dt, \ \mathbf{U_y \cdot s.} \tag{4-161}$$

A change in the variable of integration of Eq. 4-161 yields

$$Y(j\omega) = \int_{-\infty}^{\infty} \exp[-j\omega(\tau+\nu)] \left[\int_{-\infty}^{\infty} r(\tau) \, x(\nu) \, d\tau \right] d\nu, \ \mathbf{U_y \cdot s} \tag{4-162}$$

where

ν = substitute variable of time integration $t - \tau$, s.

The variables τ and ν may be separated, and Eq. 4-162, rewritten as

$$Y(j\omega) = \int_{-\infty}^{\infty} x(\nu) \, \exp(-j\omega\nu) \, d\nu \int_{-\infty}^{\infty} r(\tau) \, \exp(-j\omega\tau) \, d\tau, \ \mathbf{U_y \cdot s.} \tag{4-163}$$

The double integral of Eq. 4-163 may be integrated as the product of two single integrals. The first integral of Eq. 4-163 is the Fourier transform of $x(\nu)$, i.e., $X(j\omega)$. Eq. 4-163 can therefore be written as

$$Y(j\omega) = X(j\omega) \int_{-\infty}^{\infty} r(\tau) \, \exp(-j\omega\tau) \, d\tau, \ \mathbf{U_y \cdot s.} \tag{4-164}$$

A comparison of Eq. 4-164 with Eq. 4-158 shows that

$$\int_{-\infty}^{\infty} r(\tau) \, \exp(-j\omega\tau) \, d\tau = R(j\omega), \ \mathbf{U_y / U_x.} \tag{4-165}$$

Eq. 4-165 states that the element transfer function $R(j\omega)$ is the Fourier transform of $r(\tau)$, the unit impulse response function of the system element. This simplification can be directly obtained by invoking the convolution theorem discussed in Ref. 19.

In the frequency domain the relationship among the input $X(j\omega)$, the output $Y(j\omega)$, and the transfer function $R(j\omega)$ is one of simple multiplication. This process is in contrast with the time domain representation, which requires the evaluation of a convolution integral.

Use of the frequency domain in the analysis of random errors necessitates the introduction of two additional statistical functions: the autocorrelation function and the power spectral density (PSD) function.

The autocorrelation functions of the input and output variables are defined as

$$\phi_{xx}(\tau) = \lim_{T \to \infty} \frac{1}{2T} \int_{-T}^{T} x(t) \, x(t+\tau) \, dt, \ \mathbf{U_x^2}$$

$$\phi_{yy}(\tau) = \lim_{T \to \infty} \frac{1}{2T} \int_{-T}^{T} y(t) \, y(t+\tau) \, dt, \ \mathbf{U_y^2} \tag{4-166}$$

where

$\phi_{xx}(\tau)$ = autocorrelation function of the input variable $x(t)$, $\mathbf{U_x^2}$

$\phi_{yy}(\tau)$ = autocorrelation function of the output variable $y(t)$, $\mathbf{U_y^2}$

$x(t+\tau)$ = value for the random variable $x(t)$ at time $t+\tau$, $\mathbf{U_x}$

$y(t+\tau)$ = value of the random variable $y(t)$ at time $t+\tau$, $\mathbf{U_y}$

T = time interval of integration, s.

Eq. 4-166 is the time average of the product of two values of a random variable that are measured at times separated by a time interval τ. The autocorrelation function therefore characterizes the temporal aspect of the random variable. The limiting process $T \to \infty$ imposes the requirement that T be large enough to ensure that the functions remain constant with further increases in T.

The PSD is defined as the Fourier transform of the autocorrelation function. Thus

$$\Phi_{xx}(j\omega) = \int_{-\infty}^{\infty} \phi_{xx}(\tau) \, \mathbf{exp}(-j\omega\tau) \, d\tau, \ \ \mathbf{U_x^2 \cdot s}$$

$$\Phi_{yy}(j\omega) = \int_{-\infty}^{\infty} \phi_{yy}(\tau) \, \mathbf{exp}(-j\omega\tau) \, d\tau, \ \ \mathbf{U_y^2 \cdot s}$$

(4-167)

where

$\Phi_{xx}(j\omega)$ = PSD function of the random variable $x(t)$, $U_x^2 \cdot s$

$\Phi_{yy}(j\omega)$ = PSD function of the random variable $y(t)$, $U_y^2 \cdot s$.

The integral defined in Eq. 4-167 extends over both positive and negative frequencies. Although they have no physical existence, negative frequencies are retained since this double-sided mathematical form simplifies the analysis. For the real signals, which are the subject of this analysis, the left half of the spectrum is a mirror image of the right half, as discussed in Ref. 19. It is important to note that the PSD defines the distribution of signal energy over the frequency spectrum. It is measured in units of the square of the unit of the random variable divided by the frequency unit. The total energy is obtainable by integrating $\Phi_{xx}(j\omega)$ over all frequencies.

The PSD is uniquely related to the second statistical moment where the random process can be assumed to be stationary and ergodic. A stationary ergodic random process is defined as a process whose statistical properties do not vary with time. A more in-depth discussion of stationary random variables appears in Ref. 23 and in subpar. C-4.2 of Appendix C.

For a stationary ergodic random process it is permissible to equate the statistical moments to the corresponding time averages. The first statistical moment is the time average of the random variable and is defined as

$$\overline{x(t)} = \lim_{T\to\infty} \frac{1}{2T} \int_{-T}^{T} x(t) \, dt, \ \ \mathbf{U_x}$$

$$\overline{y(t)} = \lim_{T\to\infty} \frac{1}{2T} \int_{-T}^{T} y(t) \, dt, \ \ \mathbf{U_y}$$

(4-168)

where

$\overline{x(t)}$ = time average of the random variable $x(t)$, U_x

$\overline{y(t)}$ = time average of the random variable $y(t)$, U_y.

The second moment is the time average of the variable squared and is called the mean-square value:

$$\overline{x^2(t)} = \lim_{T\to\infty} \frac{1}{2T} \int_{-T}^{T} x^2(t) \, dt, \ \ \mathbf{U_x^2}$$

$$\overline{y^2(t)} = \lim_{T\to\infty} \frac{1}{2T} \int_{-T}^{T} y^2(t) \, dt, \ \ \mathbf{U_y^2}$$

(4-169)

where

$\overline{x^2(t)}$ = mean square value of the random variable $x(t)$, U_x^2

$\overline{y^2(t)}$ = mean square value of the random variable $y(t)$, U_y^2.

Both $\overline{x(t)}$ and $\overline{x^2(t)}$ are numbers, not time functions.

The derivation of the relationship between the mean-square value and the PSD function is straightforward. If τ is set equal to zero in the definition of the autocorrelation function, Eq. 4-166 becomes

$$\phi_{xx}(0) = \lim_{T \to \infty} \frac{1}{2T} \int_{-T}^{T} x^2(t)\, dt, \quad U_x^2$$

$$\phi_{yy}(0) = \lim_{T \to \infty} \frac{1}{2T} \int_{-T}^{T} y^2(t)\, dt, \quad U_y^2$$

(4-170)

Since the right sides of Eq. 4-170 are identical with the corresponding right sides of Eq. 4-169, it is evident that

$$\overline{x^2(t)} = \phi_{xx}(0), \quad U_x^2$$

$$\overline{y^2(t)} = \phi_{yy}(0), \quad U_y^2.$$

(4-171)

The right sides of Eq. 4-171 can be expressed in terms of the inverse Fourier transformation of Eq. 4-160. For any value of τ

$$\phi_{xx}(\tau) = \frac{1}{2\pi} \int_{-\infty}^{\infty} \Phi_{xx}(j\omega) \exp(j\omega\tau)\, d\omega, \quad U_x^2$$

$$\phi_{yy}(\tau) = \frac{1}{2\pi} \int_{-\infty}^{\infty} \Phi_{yy}(j\omega) \exp(j\omega\tau)\, d\omega, \quad U_y^2.$$

(4-172)

With $\tau = 0$

$$\phi_{xx}(0) = \frac{1}{2\pi} \int_{-\infty}^{\infty} \Phi_{xx}(j\omega)\, d\omega = \overline{x^2(t)}, \quad U_x^2$$

$$\phi_{yy}(0) = \frac{1}{2\pi} \int_{-\infty}^{\infty} \Phi_{yy}(j\omega)\, d\omega = \overline{y^2(t)}, \quad U_y^2.$$

(4-173)

Eq. 4-173 is the desired relationship between the PSD and the second statistical moment, or mean-square value.

It is shown in Ref. 24 that $\Phi_{xx}(j\omega)$ and $\Phi_{yy}(j\omega)$ are related through the element transfer function as follows:

$$\Phi_{yy}(j\omega) = |R(j\omega)|^2 \Phi_{xx}(j\omega), \quad U_y^2 \cdot s$$

(4-174)

where

$$|R(j\omega)|^2 = R(j\omega)R^*(j\omega), \quad U_y^2/U_x^2$$

and

$$R^*(j\omega) = \text{complex conjugate of } R(j\omega), \quad U_y/U_x.$$

The relationship described by Eq. 4-174 can be applied directly to the PSD of the errors associated with the input and output signals. Therefore,

$$\Phi_{\varepsilon_y}(j\omega) = |R(j\omega)|^2 \Phi_{\varepsilon_x}(j\omega), \quad U_y^2 \cdot s$$

(4-175)

where

$\Phi_{\varepsilon_x}(j\omega)$ = PSD of the error in the input signal $x(t)$, $U_x^2 \cdot s$

$\Phi_{\varepsilon_y}(j\omega)$ = PSD of the error in the output signal $y(t)$, $U_y^2 \cdot s$.

The relationships between the mean-square values and the PSDs of the input and output signals, as given in Eq. 4-173, also apply to the associated errors. Therefore,

$$\overline{\varepsilon}_x^2 = \frac{1}{2\pi} \int_{-\infty}^{\infty} \Phi_{\varepsilon_x}(j\omega) \, d\omega, \quad \mathbf{U_x^2}$$

$$\overline{\varepsilon}_y^2 = \frac{1}{2\pi} \int_{-\infty}^{\infty} \Phi_{\varepsilon_y}(j\omega) \, d\omega, \quad \mathbf{U_y^2}$$

(4-176)

where

$\overline{\varepsilon}_x^2$ = mean-square value of the error in the input signal, $\mathbf{U_x^2}$

$\overline{\varepsilon}_y^2$ = mean-square value of the error in the output signal, $\mathbf{U_y^2}$.

The mean-square error $\overline{\varepsilon}_y^2$ in the output signal can now be expressed as a function of the PSD of the input error by substituting Eq. 4-175 into Eq. 4-176:

$$\overline{\varepsilon}_y^2 = \frac{1}{2\pi} \int_{-\infty}^{\infty} |R(j\omega)|^2 \, \Phi_{\varepsilon_x}(j\omega) \, d\omega, \quad \mathbf{U_y^2}.$$

(4-177)

Fire control error analyses are generally formulated in terms of the mean and the variance of the individual error components. An additional equation is therefore required to relate the error variance in a signal to its mean-square value. It is shown in Ref. 12 and in subpar. C-5.4.3 of Appendix C that

$$\sigma_{\varepsilon_x}^2 = \overline{\varepsilon}_x^2 - \eta_{\varepsilon_x}^2, \quad \mathbf{U_x^2}$$

$$\sigma_{\varepsilon_y}^2 = \overline{\varepsilon}_y^2 - \eta_{\varepsilon_y}^2, \quad \mathbf{U_y^2}$$

(4-178)

where

$\sigma_{\varepsilon_x}^2$ = variance of the input error, $\mathbf{U_x^2}$
$\sigma_{\varepsilon_y}^2$ = variance of the output error, $\mathbf{U_y^2}$
η_{ε_x} = mean value of the input error, $\mathbf{U_x}$
η_{ε_y} = mean value of the output error, $\mathbf{U_y}$.

If Eq. 4-177 is substituted into Eq. 4-178, the variance in the error at the output is given by

$$\sigma_{\varepsilon_y}^2 = \frac{1}{2\pi} \int_{-\infty}^{\infty} |R(j\omega)|^2 \, \Phi_{\varepsilon_x}(j\omega) \, d\omega - \eta_{\varepsilon_y}^2, \quad \mathbf{U_y^2}.$$

(4-179)

It is shown in Ref. 24 that the mean error η_{ε_y} in the output is related to the mean error η_{ε_x} in the input through the transfer function

$$\eta_{\varepsilon_y} = R(0) \, \eta_{\varepsilon_x}, \quad \mathbf{U_y}$$

(4-180)

where

$R(0)$ = transfer function evaluated at $\omega = 0$, $\mathbf{U_y}/\mathbf{U_x}$.

Substituting Eq. 4-180 into Eq. 4-179 yields

$$\sigma_{\varepsilon_y}^2 = \frac{1}{2\pi} \int_{-\infty}^{\infty} |R(j\omega)|^2 \, \Phi_{\varepsilon_x}(j\omega) \, d\omega - [\, \eta_{\varepsilon_x} R(0) \,]^2, \quad \mathbf{U_y^2}.$$

(4-181)

Eq. 4-181 expresses the variance of the output error due to a single input error in terms of the power spectral density and mean of the input error.

If the element is not ideal, the error generated within the element must be added to Eq. 4-181. Thus

$$\sigma^2_{\varepsilon_y} = \frac{1}{2\pi} \int_{-\infty}^{\infty} |R(j\omega)|^2 \Phi_{\varepsilon_x}(j\omega)\, d\omega - [\ \eta_{\varepsilon_y} R(0)\ ]^2$$

$$+ \frac{1}{2\pi} \int_{-\infty}^{\infty} \Phi_{e_y}(j\omega)\, d\omega - \eta^2_{e_y},\ \ \mathbf{U_y^2}$$

(4-182)

where

$\Phi_{e_y}(j\omega)$ = PSD of the internally generated element error, $\mathbf{U_y^2}$

η_{e_y} = mean value of the element error, $\mathbf{U_y}$.

The mathematical development can be expanded to include multiple-input, multiple-element systems by following a procedure that is directly analogous to that described for the time domain in Eqs. 4-154, 4-156, and 4-157. Use of the concept of a transfer function implies that the equations defining element performances are linear. Thus, in an element with multiple inputs, the principle of superposition can be applied, and the element output can be represented by a linear, perhaps differential, equation of the form

$$g[y(t)] = \sum_{n=1}^{p} f_n[x_n(t)]\,, \ \ \mathbf{U_{gy}}$$

(4-183)

where

$g[y(t)]$ = function that defines a set of arbitrary linear operations on the output variable $y(t)$, $\mathbf{U_{gy}}$

$f_n[x_n(t)]$ = function that defines a set of arbitrary linear operations on the input variable $x_n(t)$, $\mathbf{U_{f_n x_n}}$

$x_n(t)$ = element input, $\mathbf{U_{x_n}}$

$y(t)$ = element output, $\mathbf{U_y}$.

If a Fourier transform is performed on both sides of Eq. 4-183, the additive property of the Fourier transform as discussed in Ref. 19 yields

$$G(j\omega)\, Y(j\omega) = \sum_{n=1}^{p} F_n(j\omega)\, X_n(j\omega)\,, \ \ \mathbf{U_y}$$

(4-184)

where

$G(j\omega)$ = Fourier transform of linear operator $g[y(t)]$, $\mathbf{U_{gy} \cdot s}$

$F_n(j\omega)$ = Fourier transform of linear operator $f_n[x_n(t)]$, $\mathbf{U \cdot s}$.

Eq. 4-184 can be rewritten as

$$Y(j\omega) = \sum_{n=1}^{p} \frac{F_n(j\omega)}{G(j\omega)} X_n(j\omega)\,, \ \ \mathbf{U_y \cdot s}$$

(4-185)

where

$X_n(j\omega)$ = Fourier transform of the nth input variable $x_n(t)$, $\mathbf{U_{xn} \cdot s}$.

The factors $\dfrac{F_n(j\omega)}{G(j\omega)}$ are the transfer functions of the element output associated with each of the n input variables. In the presentation that follows these transfer functions are designated by $R_n(j\omega)$.

The illustrative example in subpar. 4-4.3.4.3 shows how these transfer functions are derived when the performance equations for the elements are nonlinear.

The output error for an element having p inputs from outside the system is obtained by superposition. Using Eq. 4-181 yields

$$
\begin{aligned}
\sigma_{\varepsilon_y}^2 = \ & \frac{1}{2\pi} \sum_{n=1}^{p} \int_{-\infty}^{\infty} \left| R_n(j\omega) \right|^2 \Phi_{\varepsilon_{xn}}(j\omega)\, d\omega \\
& - \sum_{n=1}^{p} \left[R_n(0)\ \eta_{\varepsilon_{xn}} \right]^2 \\
& + \frac{1}{2\pi} \int_{-\infty}^{\infty} \Phi_{e_y}(j\omega)\, d\omega - \eta_{e_y}^2, \quad \mathbf{U_y^2}
\end{aligned}
\tag{4-186}
$$

where

$R_n(j\omega)$ = transfer function associated with the nth input and the element output, $\mathbf{U_y/U_{xn}}$

$\Phi_{\varepsilon_{xn}}(j\omega)$ = PSD of the error associated with the nth system input, $\mathbf{U_{xn}^2 \cdot s}$

$\eta_{\varepsilon_{xn}}$ = mean value of the nth system input error, $\mathbf{U_{xn}}$.

In a system having q elements but no direct feedback, the variance of the output error of the ith element is given by an expression that is analogous to Eq. 4-156 for the output error in the time domain:

$$
\begin{aligned}
\sigma_{\varepsilon_{yi}}^2 = \ & \frac{1}{2\pi} \sum_{n=1}^{p} \int_{-\infty}^{\infty} \left| R_{in}(j\omega) \right|^2 \Phi_{\varepsilon_{xn}}(j\omega)\, d\omega \\
& + \frac{1}{2\pi} \sum_{\substack{k=1 \\ k \neq i}}^{q} \int_{-\infty}^{\infty} \left| R_{in}(j\omega) \right|^2 \Phi_{\varepsilon_{yk}}(j\omega)\, d\omega \\
& - \sum_{n=1}^{p} \left[R_n(0)\ \eta_{\varepsilon_{xn}} \right]^2 - \sum_{\substack{k=1 \\ k \neq i}}^{q} \left[R_k(0)\ \eta_{\varepsilon_{yk}} \right]^2 \\
& + \frac{1}{2\pi} \int_{-\infty}^{\infty} \Phi_{e_{yi}}(j\omega)\, d\omega - \eta_{e_{yi}}^2, \quad \mathbf{U_{yi}^2}
\end{aligned}
\tag{4-187}
$$

where

$\sigma_{\varepsilon_{yi}}^2$ = total variance of the error ε_y associated with output y_i, $\mathbf{U_{yi}^2}$

$R_{in}(j\omega)$ = transfer function of the ith element associated with the input x_n and output y_i, $\mathbf{U_{yi}/U_{xn}}$

$R_{ik}(j\omega)$ = transfer function of the ith element associated with the internal input y_k and the output y_i, $\mathbf{U_{yi}/U_{yk}}$

$\Phi_{\varepsilon_{yk}}(j\omega)$ = PSD of the error ε_y that is associated with an output y_k, $\mathbf{U_{yk}^2}$

$\eta_{\varepsilon_{yk}}$ = mean value of the error associated with the output y_k, $\mathbf{U_{yk}}$

$\eta_{e_{yi}}$ = mean value of the error generated in the ith element, $\mathbf{U_{yi}}$

$\Phi_{e_{yi}}(j\omega)$ = PSD of the error generated in the ith element, $\mathbf{U_{yi}^2 \cdot s}$.

The set of error equations in the frequency domain for a system having q elements and feedback is represented by the following equation for the ith element:

$$\sigma^2_{\varepsilon_{yi}} = \frac{1}{2\pi} \sum_{n=1}^{p} \int_{-\infty}^{\infty} |R_{in}(j\omega)|^2 \Phi_{\varepsilon_{xn}}(j\omega)\ d\omega$$

$$+ \frac{1}{2\pi} \sum_{k=1}^{q} \int_{-\infty}^{\infty} |R_{ik}(j\omega)|^2 \Phi_{\varepsilon_{yk}}(j\omega)\ d\omega$$

$$- \sum_{n=1}^{p} [\ R_{in}(0)\ \eta_{\varepsilon_{xn}}]^2 - \sum_{\substack{k=1 \\ k \neq i}}^{q} [R_{ik}(0)\ \eta_{\varepsilon_{yk}}]^2 \qquad \text{(4-188)}$$

$$+ \frac{1}{2\pi} \int_{-\infty}^{\infty} |R_{ii}(j\omega)|^2 \Phi_{\varepsilon_{yi}}(j\omega)\ d\omega$$

$$+ \frac{1}{2\pi} \int_{-\infty}^{\infty} \Phi_{e_{yi}}(j\omega)\ d\omega - \eta^2_{e_{yi}}, \quad \mathbf{U^2_{yi}}.$$

Eq. 4-188 is analogous to Eq. 4-157 in the time domain, and it is not an explicit expression for the unknown output variance since the term $\Phi_{\varepsilon_{yi}}(j\omega)$ appears on the right-hand side of the equation. If, however, the known error PSDs $\Phi_{\varepsilon_{xn}}(j\omega)$ and $\Phi_{\varepsilon_{yk}}(j\omega)$ are computed from data or signals that have been filtered to remove the mean values, the equation takes the following form:

$$\int_{-\infty}^{\infty} [1 - |R_{ii}(j\omega)|^2]\ \Phi_{\varepsilon_{yi}}(j\omega)\ d\omega = \sum_{n=1}^{p} \int_{-\infty}^{\infty} |R_{in}(j\omega)|^2 \Phi_{\varepsilon_{xn}}(j\omega)\ d\omega$$

$$+ \sum_{\substack{k=1 \\ k \neq i}}^{q} \int_{-\infty}^{\infty} |R_{ik}(j\omega)|^2 \Phi_{\varepsilon_{yk}}(j\omega)\ d\omega \qquad \text{(4-189)}$$

$$+ \int_{-\infty}^{\infty} \Phi_{e_{yi}}(j\omega)\ d\omega, \quad \mathbf{U^2_{yi}}$$

where the term $\sigma^2_{\varepsilon_{yi}}$ in Eq. 4-188 has been replaced by the integral of its PSD as defined in Eq. 4-179.

The integrands on both sides of Eq. 4-189 can be equated and the equation solved explicitly for the output error PSD function:

$$[1 + |R_{ii}(j\omega)|^2]\ \Phi_{\varepsilon_{yi}}(j\omega) = \sum_{n=1}^{p} |R_{in}(j\omega)|^2 \Phi_{\varepsilon_{xn}}(j\omega)$$

$$+ \sum_{\substack{k=1 \\ k \neq i}}^{q} |R_{ik}(j\omega)|^2 \Phi_{\varepsilon_{yk}}(j\omega) \qquad \text{(4-190)}$$

$$+ \Phi_{e_{yi}}(j\omega), \quad \mathbf{U^2_{yi}}.$$

The output error PSD function $\Phi_{e_{yi}}(j\omega)$ can be determined from Eq. 4-190 at every appropriate frequency across the spectrum.

The mean or systematic error $\eta_{\varepsilon_{yi}}$ in the output is computed from

$$[1 - R_{ii}(0)]\ \eta_{\varepsilon_{yi}} = \sum_{n=1}^{p} R_{in}(0)\ \eta_{\varepsilon_{xn}} + \sum_{k=1}^{q} R_{ik}(0)\ \eta_{\varepsilon_{yk}} + \eta_{e_{yi}}, \quad \mathbf{U_{yi}}. \qquad \text{(4-191)}$$

The $R(j\omega)$ functions, i.e., the transfer functions of the system elements, are, in general, known frequency responses of the system elements. Thus a means is available to determine the variance and bias of the output error of a system that is describable by differential equations and is subjected to random time-varying input errors. In combination with the techniques developed in subpar. 4-4.3.2 for systems describable by other than differential equations, this technique provides the fire control system designer with the means to analyze the errors of many of the systems with which he is likely to be confronted. The calculations require considerable effort for a complex system. Therefore, it is common practice to approximate the smaller errors and reserve detailed treatment for the larger errors. Such approximations do not appreciably affect the accuracy of the analysis because one of the characteristics of an rss analysis, such as that used in the error-summation relationships, is that the large errors tend to be emphasized over the smaller ones.

In many instances the error equations have to be solved by numerical techniques. This requirement arises because the element performance equations may not be integrable or differentiable in closed form or because the data characterizing the element transfer functions or the error spectra have been obtained experimentally and are in a discrete form. Subpar. 4-4.3.4.4 provides a brief introduction to the mathematics of discrete signal and discrete time system analysis.

4-4.3.4.3 Illustrative Example of an Error Analysis for a System Described by Nonlinear Differential Equations

This example is presented to illustrate the procedures defined in subpar. 4-4.3.4 and to show how they can be applied to systems with nonlinear performance equations.

The example is a simple target prediction device that has a first-order lag in its prediction mechanism. The predictor is designed for a scenario in which the target is assumed to move in a plane along the arc of a circle at constant speed. The weapon is located at the center of the circle, and the element predicts the future position of the target based on measurements of the angular bearing to the target and the target range.

The analysis that follows shows how errors in the prediction of the future target bearing and range are related to the errors in the measurement of the current bearing and range.

The performance equations for this element are assumed to be

$$\tau \dot{A}_p(t) + A_p(t) = A_o(t) + \dot{A}_o(t) KR_o(t), \ \textbf{rad}$$
$$R_p(t) = R_o(t), \ \textbf{m}$$

(4-192)

where

τ = first-order time constant of the prediction lag, s

$A_p(t)$ = predicted target bearing, rad

$\dot{A}_p(t)$ = time derivative of predicted target bearing, rad/s

$A_o(t)$ = current measurement of target bearing, rad

$\dot{A}_o(t)$ = rate of change of measured target bearing, rad/s

K = constant related to the projectile muzzle velocity, s/m

$R_p(t)$ = predicted target range, m

$R_o(t)$ = current measurement of target range, m.

The factor $KR_o(t)$ in Eq. 4-192 is a simplified representation for the projectile time of flight to a range $R_o(t)$. The term $\dot{A}_o(t)$ is often called the target slew rate.

It is clear that the performance equation for $A_p(t)$ is nonlinear. Since the errors are assumed to be small compared with the measured quantities, however, it is appropriate to seek a linearized form of Eq. 4-192 to represent these errors. The linearized equations can then be used to define the transfer functions that are required by Eq. 4-187. A common technique for linearization is to use the Taylor expan-

sion to define deviations in the time-varying states of the element outputs as small perturbations about the states that represent the ideal performance of the element.

A description of this technique is presented in Ref. 25. Element performance can be represented by a set of first-order state equations of the form

$$\dot{\mathbf{y}} = [f(\mathbf{y},\mathbf{x})], \ \mathbf{U} \tag{4-193}$$

where

$\dot{\mathbf{y}}$ = first time derivative of the output state variable vector, U/s

$[f]$ = nonlinear function matrix, U/s

$\mathbf{y}$ = output state variable vector, U

$\mathbf{x}$ = input variable vector, U.

The linearized form of Eq. 4-193 is represented by

$$\frac{d(\delta\mathbf{y})}{dt} = [A]\,\delta\mathbf{y} + [B]\,\delta\mathbf{x}, \ \mathbf{U} \tag{4-194}$$

where

$[A]$ = Jacobian matrix of the output state variables, U

$\delta\mathbf{y}$ = perturbation on the output state vector, U

$[B]$ = Jacobian matrix of the input vectors, U

$\delta\mathbf{x}$ = perturbation on the input state vector, U.

The Jacobian matrices are defined as

$$[A] \triangleq \begin{bmatrix} \dfrac{\partial F_1}{\partial y_1} & \cdots & \dfrac{\partial F_1}{\partial y_m} \\ \vdots & & \vdots \\ \dfrac{\partial F_m}{\partial y_1} & \cdots & \dfrac{\partial F_m}{\partial y_m} \end{bmatrix}, \ 1/s$$

$$\tag{4-195}$$

$$[B] \triangleq \begin{bmatrix} \dfrac{\partial F_1}{\partial x_1} & \cdots & \dfrac{\partial F_1}{\partial x_p} \\ \vdots & & \vdots \\ \dfrac{\partial F_m}{\partial x_1} & \cdots & \dfrac{\partial F_m}{\partial x_p} \end{bmatrix}, \ \mathbf{U_y}/\mathbf{U_x}/s$$

where

F_m = nonlinear function associated with the mth state equation, U

y_m = mth output state variable, U_{ym}

x_p = pth input variable, U_{xp}.

To use Eqs. 4-194 and 4-195, Eq. 4-192 is rewritten in the normal state variable form:

$$\frac{d(A_p(t))}{dt} = \frac{1}{\tau}[-A_p(t) + A_o(t) + \dot{A}_o(t)KR_o(t)]$$

$$= F_1[A_p(t), A_o(t), \dot{A}_o(t), R_o(t)], \text{ rad/s}$$

$$0 = -R_p(t) + R_o(t) = F_2[R_p(t), R_o(t)], \text{ m.}$$

(4-196)

The terms in the Jacobian matrices associated with Eq. 4-196 are

$$\frac{\partial F_1}{\partial A_p(t)} = -\frac{1}{\tau}, 1/s \qquad \frac{\partial F_1}{\partial \dot{A}_o(t)} = \frac{KR_o(t)}{\tau}, \text{ dimensionless}$$

$$\frac{\partial F_1}{\partial A_o(t)} = \frac{1}{\tau}, 1/s \qquad \frac{\partial F_1}{\partial R_o(t)} = \frac{\dot{A}_o(t)K}{\tau}, \text{ rad/m/s}$$

(4-197)

$$\frac{\partial F_2}{\partial R_p(t)} = -1, \text{ dimensionless} \qquad \frac{\partial F_2}{\partial R_o(t)} = 1, \text{ dimensionless.}$$

Eq. 4-197 is applied to Eq. 4-194 to yield the following linearized perturbation equations:

$$\frac{d[\delta A_p(t)]}{dt} = -\frac{1}{\tau}\delta A_p(t) + \frac{1}{\tau}\delta A_o(t) + \frac{KR_o}{\tau}\frac{d[\delta A_o(t)]}{dt} + \frac{\dot{A}_oK}{\tau}\delta R_o(t), \text{ rad/s}$$

(4-198)

$$0 = -\delta R_p(t) + \delta R_o(t), \text{ m}$$

where

$\delta A_p(t)$ = perturbation on the predicted target bearing, rad
$\delta A_o(t)$ = perturbation on the measured target bearing, rad
$\delta \dot{A}_o(t)$ = perturbation on the rate of change of the measured target bearing, rad/s
$\delta R_o(t)$ = perturbation on the measured target range, m
R_o = constant target range, m
$\dot{A}_o$ = constant target slew rate, rad/s.

In the formulation of this illustrative example, it has been assumed that the true target range and slew rate are constant. Eq. 4-198 is, therefore, a linear differential equation with constant coefficients, and the Fourier transform can be taken directly. If the range and slew rate were not constant, Eq. 4-198 would still be valid as long as it could be assumed that the changes in these variables are slow enough that over a time interval T, as defined in Eqs. 4-166 and 4-169, they could be considered constants. In such a case, however, the perturbation dynamics changes throughout the scenario, and the error variances should be evaluated where their value is maximum.

The Fourier transform of Eq. 4-198 yields

$$j\omega\delta A_p(j\omega) = -\frac{1}{\tau}\delta A_p(j\omega) + \frac{1}{\tau}\delta A_o(j\omega) + \frac{KR_o}{\tau}j\omega\,\delta A_p(j\omega)$$

$$+ \frac{\dot{A}_oK}{\tau}\delta R_o(j\omega), \text{ rad/s}$$

(4-199)

$$\delta R_p(j\omega) = \delta R_o(j\omega), \text{ m}$$

where

$\delta A_p(j\omega)$ = Fourier transform of the perturbed target bearing prediction, rad

$\delta A_o(j\omega)$ = Fourier transform of the perturbed target bearing measurement, rad

$\delta R_p(j\omega)$ = Fourier transform of the perturbed target range prediction, m

$\delta R_o(j\omega)$ = Fourier transform of the perturbed target range measurement, m.

The Fourier transform of the time derivative of a function is $j\omega$ times the Fourier transform of the function.

After combining terms and multiplying through by τ, Eq. 4-199 becomes

$$(1 + j\omega\tau)\,\delta A_p(j\omega) \;=\; (1 + j\omega K R_o)\,\delta A_o(j\omega) \;+\; \dot{A}_o K\,\delta R_o(j\omega)\;,\;\; \textbf{rad}$$

$$\delta R_p(j\omega) \;=\; \delta R_o(j\omega)\;,\;\; \textbf{m.}$$

(4-200)

With reference to Eq. 4-185 and using the $R_n(j\omega)$ notation, it can be seen that the transfer functions associated with the perturbed element inputs and outputs are

$$R_1(j\omega) \;=\; \frac{1 + j\omega K R_o}{1 + j\omega\tau},\;\; \textbf{dimensionless}$$

$$R_2(j\omega) \;=\; \frac{\dot{A}_o K}{1 + j\omega\tau},\;\; \textbf{rad/m}$$

$$R_3(j\omega) \;=\; 1,\;\; \textbf{dimensionless}$$

(4-201)

where

$R_1(j\omega)$ = transfer function relating the perturbation in A_p to the perturbation in A_o, dimensionless

$R_2(j\omega)$ = transfer function relating the perturbation in A_p to the perturbation in R_o, rad/m

$R_3(j\omega)$ = transfer function relating the perturbation in R_p to the perturbation in R_o, dimensionless.

If it can be assumed that the errors in the measured quantities do not have any systematic components and that there is no noise or bias introduced by the element, the variances in the predicted quantities can be expressed in the form of Eq. 4-187:

$$\sigma^2_{\varepsilon_{Ap}} = \frac{1}{2\pi}\int_{-\infty}^{\infty}\left|R_1(j\omega)\right|^2 \Phi_{\varepsilon_{Ao}}(j\omega)\,d\omega$$

$$+\; \frac{1}{2\pi}\int_{-\infty}^{\infty}\left|R_2(j\omega)\right|^2 \Phi_{\varepsilon_{Ro}}(j\omega)\,d\omega,\;\; \textbf{rad}^2$$

$$\sigma^2_{\varepsilon_{Rp}} = \frac{1}{2\pi}\int_{-\infty}^{\infty}\left|R_3(j\omega)\right|^2 \Phi_{\varepsilon_{Ro}}(j\omega)\,d\omega,\;\; \textbf{m}^2$$

(4-202)

where

$\sigma^2_{\varepsilon_{Ap}}$ = variance in the predicted target bearing , rad²

$\Phi_{\varepsilon_{Ao}}(j\omega)$ = PSD of the target bearing measurement error, rad²·s

$\Phi_{\varepsilon_{Ro}}(j\omega)$ = PSD of the target range measurement error, m²·s

$\sigma^2_{\varepsilon_{Rp}}$ = variance in the predicted target range, m².

The squares of the transfer function magnitudes in Eq. 4-202 are computed as follows:

$$|R_1(j\omega)|^2 = \left(\frac{1 + j\omega K R_o}{1 + j\omega\tau}\right)\left(\frac{1 - j\omega K R_o}{1 - j\omega\tau}\right)$$

$$= \frac{1 + \omega^2 K^2 R_o^2}{1 + \omega^2 \tau^2}, \text{ dimensionless}$$

$$|R_2(j\omega)|^2 = \left(\frac{\dot{A}_o K}{1 + j\omega\tau}\right)\left(\frac{\dot{A}_o K}{1 - j\omega\tau}\right) \qquad (4\text{-}203)$$

$$= \frac{\dot{A}_o^2 K^2}{1 + \omega^2 \tau^2}, \text{ rad}^2/\text{m}^2$$

$$|R_3(j\omega)|^2 = 1, \text{ dimensionless}.$$

Substituting Eq. 4-203 into Eq. 4-202 yields

$$\sigma_{\varepsilon_{Ap}}^2 = \frac{1}{2\pi} \int_{-\infty}^{\infty} \frac{1 + K^2 R_o^2 \omega^2}{1 + \tau^2 \omega^2} \Phi_{\varepsilon_{Ao}}(j\omega)\, d\omega$$

$$+ \frac{1}{2\pi} \int_{-\infty}^{\infty} \frac{\dot{A}_o^2 K^2}{1 + \tau^2 \omega^2} \Phi_{\varepsilon_{Ro}}(j\omega)\, d\omega, \text{ rad}^2 \qquad (4\text{-}204)$$

$$\sigma_{\varepsilon_{Rp}}^2 = \frac{1}{2\pi} \int_{-\infty}^{\infty} \Phi_{\varepsilon_{Ro}}(j\omega)\, d\omega, \text{ m}^2.$$

If it can be assumed that the error spectra exist over a limited frequency band with a maximum frequency limit ω_m and that the product $\tau\omega_m \ll 1$ over this band, Eq. 4-204 can be rewritten as

$$\sigma_{\varepsilon_{Ap}}^2 = \frac{1}{2\pi} \int_{-\omega_m}^{\omega_m} [1 + K^2 R_o^2 \omega^2] \, \Phi_{\varepsilon_{Ao}}(j\omega)\, d\omega$$

$$+ \frac{1}{2\pi} \int_{-\omega_m}^{\omega_m} \dot{A}_o^2 K^2 \, \Phi_{\varepsilon_{Ro}}(j\omega)\, d\omega, \text{ rad}^2 \qquad (4\text{-}205)$$

$$\sigma_{\varepsilon_{Rp}}^2 = \frac{1}{2\pi} \int_{-\omega_m}^{\omega_m} \Phi_{\varepsilon_{Ro}}(j\omega)\, d\omega, \text{ m}^2$$

where

ω_m = maximum frequency limit in the error spectrum, 1/s.

Using the definition of variance in Eq. 4-179 with a zero mean, Eq. 4-205 becomes

$$\sigma_{\varepsilon_{Ap}}^2 = \sigma_{\varepsilon_{Ao}}^2 \frac{K^2 R_o^2}{2\pi} + \int_{-\omega_m}^{\omega_m} \Phi_{\varepsilon_{Ao}}(j\omega) \ d\omega$$

$$+ \ \dot{A}_o^2 K^2 \sigma_{\varepsilon_{Ro}}^2, \ \textbf{rad}^2$$

$$\sigma_{\varepsilon_{Rp}}^2 = \sigma_{\varepsilon_{Ro}}^2 \ , \ \textbf{m}^2.$$

$$(4\text{-}206)$$

Further insight into Eq. 4-206 is gained by assuming that the PSD of the bearing measurement error is a constant over the frequency band. Then

$$\sigma_{\varepsilon_{Ap}}^2 = \sigma_{\varepsilon_{Ao}}^2 + \frac{K^2 R_o^2}{\pi} \frac{C\omega_m^3}{3} + \dot{A}_o^2 K^2 \sigma_{\varepsilon_{Ro}}^2, \ \textbf{rad}^2$$

$$\sigma_{\varepsilon_{Rp}}^2 = \sigma_{\varepsilon_{Ro}}^2 \ , \ \textbf{m}^2$$

$$(4\text{-}207)$$

where

C = **constant value of** $\Phi_{\varepsilon_{Ao}}(j\omega)$, **rad**^{2}**·s.**

C **can be expressed in terms of** $\sigma_{\varepsilon_{Ao}}^2$ **by observing that**

$$\sigma_{\varepsilon_{Ao}}^2 = \frac{1}{2\pi} \int_{-\omega_m}^{\omega_m} C d\omega = \frac{1}{\pi} \ C\omega_m, \ \textbf{rad}^2.$$

$$(4\text{-}208)$$

Therefore,

$$C = \frac{\pi}{\omega_m} \sigma_{\varepsilon_{Ao}}^2, \ \textbf{rad}^2\textbf{·s.}$$

$$(4\text{-}209)$$

Substituting Eq. 4-209 into Eq. 4-207 results in the final expression:

$$\sigma_{\varepsilon_{Ap}}^2 = \left(1 + \frac{K^2 R_o^2 \omega_m^2}{3} \right) \sigma_{\varepsilon_{Ao}}^2 + \dot{A}_o^2 K^2 \sigma_{\varepsilon_{Ro}}^2, \ \textbf{rad}^2$$

$$\sigma_{\varepsilon_{Rp}}^2 = \sigma_{\varepsilon_{Ro}}^2 \ , \ \textbf{m}^2.$$

$$(4\text{-}210)$$

For the example given, the effect of an error in A_o is amplified by the square of the width of the error frequency band. This noise or error amplification is an inherent characteristic of target predictors and represents an ongoing challenge to the fire control designer.

The military forces seek to acquire weapon systems with increased probabilities of kill and require that these improvements be achieved at longer engagement ranges and, in many situations, while the vehicle is on the move. The designer therefore has to increase system accuracy in an operational environment in which hull motion disturbances introduce increased tracking errors. This task is especially challenging in current armored vehicle systems in which the tracking function is performed manually by

the gunner. In this case the hull vibrations from the moving vehicle make it very difficult for him to maintain a steady and uniform track on the target.

One of the solutions being investigated is automation of the tracking function by use of automatic video target trackers. With these devices each frame of video imagery is digitized and processed to segment the target image from its background. The target position relative to the background is then determined on a frame-by-frame basis and used to generate target position and rate information. These devices have the potential to generate accurate tracking data even in the presence of hull-induced jitter in the video imagery.

4-4.3.4.4 Discrete Time and Sampled Data Systems

The analyses of error propagation that have been presented to this point in subpar. 4-4.3.4 have assumed that the input and output signals to and from the system element are continuous in time. With modern advances in digital technology, however, many of the commercial and military systems engineers encounter are generated or driven by signals that consist of discrete time sequences.

For example, digital controllers are devices that receive sampled data on the state of the system under control and issue the appropriate corrective commands in order to drive the system to a desired state. At its most fundamental level the controller would generate the control commands as a discrete time sequence in binary format. This digital controller is, therefore, an example of a device with discrete inputs and outputs, that computes its control commands at discrete intervals of time. At some point in the system to control a nondigital device, the digital control command must be converted to its analog equivalent and then processed to produce a stepped, piecewise linear or smoothed analog signal. This subsequent digital-to-analog process, called the data hold, is an example of a function with a digital input and analog output. This step can be performed either as part of the output processing of the controller or as part of the input processing function of the device under control.

Another example of a system with a discrete input and a continuous output would be a digitally controlled gun-turret drive on a weapon system. The input control commands to the drive could consist of a discrete binary sequence that is generated by a digital controller and transmitted over a high-speed data bus. The drive would then provide the digital-to-analog conversion described in the previous paragraph. The drive output would be the physical gun position and velocity, which would be represented by a set of continuously varying state variables. These variables would then be sampled, converted into a binary format, and transmitted back to the controller. The data sampler is an example of a device with an analog input and a discrete output.

A special set of mathematical functions and operations have been developed to simplify the analysis of discrete data and sampled data systems. Although it is beyond the scope of this handbook to present the details of discrete time system analysis, the discussion that follows shows that these functions and operations have a direct correspondence to those used previously in this paragraph to study continuous systems. In addition, it is shown that the discrete forms of the mathematical equations can be solved directly on digital computers by using simple arithmetic operations. With these numerical solutions, the limitations of linearity and time invariance of differential equation coefficients imposed on the closed-form error propagation equations in both the time and frequency domains no longer apply. The discussion that follows focuses on elements having discrete inputs and outputs. Ref. 25 explains how these approaches can be extended to elements functioning as discrete-to-continuous or continuous-to-discrete processors.

In subpar. 4-4.3.4.1 the time-varying response of an element to a generalized, continuous forcing function was studied in the time domain by the use of the impulse response and convolution functions. The impulse response represented the general solution of the governing differential equations for a unit impulse input.

The first step in the analysis of a discrete data system in the time domain is to convert the ordinary differential equations or set of normal differential state equations that characterize the element behavior into an equivalent set of difference equations. The discrete impulse response to the difference equations can be determined and a discrete convolution function used to generate the discrete time series that represents the system response to the discrete time series input.

For example, Eq. 4-198 is the linearized differential error equation for the predictor described in the illustrative example of subpar. 4-4.3.4.3. The corresponding difference equation is

$$\delta A_p(n+1) \ = \ \left(1 - \frac{\Delta t}{\tau}\right)\delta A_p(n) \ + \left(\frac{KR_o + \Delta t}{\tau}\right)\delta A_o(n)$$

$$+ \ \frac{\dot{A}_o K\Delta t}{\tau}\ \delta R_o(n)\ - \frac{KR_o}{\tau}\ \delta A_o(n-1),\ \textbf{rad} \qquad \textbf{(4-211)}$$

where

$n = 0,1,2,\cdots$, discrete time step defined in Eq. 4-10, dimensionless

Δt = sampling interval, s

$\delta A_p(n)$ = discrete input time series of errors in predicted target bearing angle, rad

$\delta A_o(n)$ = discrete input time series of errors in measured target bearing angle, rad.

The difference equation is solved analogously to the differential equation in order to obtain the discrete impulse response. This response is then convolved with the input data sequence to yield the output data sequence. The solution is analogous to Eq. 4-154, which is the convolution equation. In discrete time this procedure can be applied to the example problem presented in subpar. 4-4.3.4.3 and is expressed by

$$\delta A_p(n) \ = \ \sum_{\eta=0}^{N-1} [\ r_1(\eta)\,\delta A_o(n-\eta)\ +\ r_2(\eta)\,\delta R_o(n-\eta)\ ],\ \textbf{rad} \qquad \textbf{(4-212)}$$

where

$\eta = 0,1,2,\cdots,N$, discrete time step different from n, dimensionless

$\delta A_o(n-\eta)$ = discrete input time series of sampled target bearing errors, rad

$r_1(\eta)$ = discrete impulse response relating perturbation in A_p to the perturbation in A_o, dimensionless

$r_2(\eta)$ = discrete impulse response relating perturbation in A_p to the perturbation in R_o, rad/m.

The solution of Eq. 4-212 is valid since the governing equation, Eq. 4-198, is linear and has constant coefficients. If it were necessary to study the behavior of the full, nonlinearized model of Eq. 4-192, the impulse response technique could not be applied. However, the equivalent difference equation for Eq. 4-192 could be solved directly by repeated use of the difference equation with increasing values of the time step parameter n.

The difference equation for Eq. 4-192 is

$$A_p(n+1) \ = \left(1 - \frac{\Delta t}{\tau}\right)A_p(n) + \frac{\Delta t}{\tau}\ A_o(n)\ + \ \frac{KR_o(n)}{\tau}\ [\ A_o(n) - A_o(n-1)\ ],\ \textbf{rad.} \ \textbf{(4-213)}$$

Given an arbitrary set of data samples $A_o(n)$ and $R_o(n)$ for the target range and bearing, the data sequence for the predicted target bearing angle is determined by solving each of the following equations in sequence:

$$A_p(1) = \left(1 - \frac{\Delta t}{\tau}\right) A_p(0) + \frac{\Delta t}{\tau} A_o(0) + \frac{KR_o(0)}{\tau} [\, A_o(0) - A_o(-1)\,]\,, \text{rad}$$

$$A_p(2) = \left(1 - \frac{\Delta t}{\tau}\right) A_p(1) + \frac{\Delta t}{\tau} A_o(1) + \frac{KR_o(1)}{\tau} [\, A_o(1) - A_o(0)\,]\,, \text{rad} \qquad \text{(4-214)}$$

$$A_p(3) = \left(1 - \frac{\Delta t}{\tau}\right) A_p(2) + \frac{\Delta t}{\tau} A_o(2) + \frac{KR_o(2)}{\tau} [\, A_o(2) - A_o(1)\,]\,, \text{rad}.$$

$$\cdots$$

It is possible to study error propagation with the technique of Eq. 4-214 by solving the equations by using ideal data and then comparing this result with the solution obtained with added error.

If the predictor in the illustrative example of subpar. 4-4.3.4.3 had been implemented in digital form, Eq. 4-213 with $\tau = 0$ would be the algorithm incorporated into the computer. In this case Eqs. 4-211 and 4-213 represent a valid model of the prediction process. If, as initially postulated, the predictor is an analog device with a continuous output, Eq. 4-212 represents an approximation to the true device response, and the designer has to select carefully a proper time step interval Δt for the numerical solution. For example, if the data sampling rate is much slower than the system response, the solution step interval may have to be smaller than the data update step to yield a valid response curve.

The error analyses can also be performed by using difference equations. For example, Eq. 4-194 is the generalized state variable form of a linearized error equation developed in subpar. 4-4.3.4.3. The equivalent error difference equation is

$$\delta\mathbf{y}(n+1) \; = \; (\,[I] + \Delta t[A]\,)\, \delta\mathbf{y}(n) \; + \Delta t[B]\, \delta\mathbf{x}(n)\,, \quad \mathbf{U_y} \qquad \text{(4-215)}$$

where

     $[I]$ = identity matrix, dimensionless.

4-4.3.4.4.1 Use of z-Transform

The power and convenience of transform calculus can be extended to the study of discrete data systems by use of the z-transform (ZT). The ZT is formulated specifically for data sequences and is the discrete analog of the Fourier and Laplace transforms. The concept can be applied simply and directly to systems or elements in which the mathematical model can be formulated by using a discrete input and a discrete output and in which the data rate for both are the same and synchronized. This concept can also be applied to elements with a discrete input and a continuous output. In this case the technique gives only the value of the output response at discrete time intervals corresponding to the input data rate.

The ZT technique requires that the performance equations be formulated as difference equations and produces a solution to these equations that is valid at each of the discrete time steps. However, it neglects the element response between the intervals and, for example, would not be able to detect the existence of a high-frequency signal component between sampling points in the actual analog device. A technique known as the modified ZT can be used to obtain the element response for intermediate data points, as shown in Ref. 26.

The ZT of a data sequence is defined by

$$Z\{v_n\} \triangleq \sum_{n=0}^{\infty} v(n)\, z^{-n}, \quad \mathbf{U_v} \qquad \text{(4-216)}$$

$$n = 0, 1, 2, 3, \cdots$$

where

     Z = ZT operation on the discrete data sequence, $\mathbf{U_v}$

    $\{v_n\}$ = discrete data sequence, $\mathbf{U_v}$

$v(n) = n$th element of the data sequence $\{v_n\}$, $\mathbf{U_v}$

$z =$ complex transform variable, dimensionless.

The following properties of the ZT are useful in performing system analysis:
1. *Theorem 1*: **Linearity**

$$Z\left(a\{v_{n1}\} + b\{v_{n2}\} \right) = aZ\{v_{n1}\} + bZ\{v_{n2}\}, \ \mathbf{U_v} \qquad (4\text{-}217)$$

where

$\{v_{n1}\}$ = arbitrary data sequence, $\mathbf{U_{v1}}$

$\{v_{n2}\}$ = arbitrary data sequence, $\mathbf{U_{v2}}$

a = arbitrary constant, $\mathbf{U_v/U_{v1}}$

b = arbitrary constant, $\mathbf{U_v/U_{v2}}$.

2. *Theorem 2*: **Real Translation**

$$Z\{v_{n-\nu}\} = z^{-\nu} Z\{v_n\}, \ \mathbf{U_v}$$

$$Z\{v_{n-\nu}\} = z^\nu \left[Zv_n - \sum_{m=0}^{\nu-1} v_m z^{-m} \right], \ \mathbf{U_v} \qquad (4\text{-}218)$$

where

$\{v_{n-\nu}\}$ = discrete time series shifted by $-\nu$ time steps from $\{v_n\}$, $\mathbf{U_v}$

ν = constant integer > 0, dimensionless

$\{v_{n+\nu}\}$ = discrete time series shifted by $+\nu$ time steps from $\{v_n\}$, $\mathbf{U_v}$

m = integer, dimensionless.

3. *Theorem 3:* **Positive and Negative Time Shifts of 1**

$$Z\{v_{n+1}\} = zZ\{v_n\} - zv(\mathbf{0}), \ \mathbf{U_v}$$

$$Z\{v_{n-1}\} = z^{-1} Z\{v_n\}, \ \mathbf{U_v} \qquad (4\text{-}219)$$

where

$v(\mathbf{0})$ = initial value of the series $\{v_n\}$, $\mathbf{U_v}$

$\{v_{n+1}\}$ = discrete time series shifted by +1 time step from $\{v_n\}$, $\mathbf{U_v}$

$\{v_{n-1}\}$ = discrete time series shifted by -1 time step from $\{v_n\}$, $\mathbf{U_v}$.

If an element or its error propagation are modeled using linear, time-invariant equations with discrete inputs and outputs, Ref. 25 shows that the ZT of the output sequence is related to the ZT of the input sequence by

$$Z\{y_n\} = Z\{r_n\} \, Z\{x_n\}, \ \mathbf{U_y} \qquad (4\text{-}220)$$

where

$\{y_n\}$ = output data sequence, $\mathbf{U_y}$

$\{x_n\}$ = input data sequence, $\mathbf{U_x}$

r_n = discrete response of the element to an impulse x_n, $\mathbf{U_y/U_x}$

$Z\{r_n\}$ = pulse transfer function, i.e., ZT of impulse response function of an element, $\mathbf{U_y/U_x}$.

These results are analogous to those presented in subpar. 4-4.3.4.2 for the analysis of continuous systems. The pulse transfer function (PTF) now replaces the transfer function.

The use of the ZT is demonstrated with the linearized error equation for the target predictor in the illustrative problem of subpar. 4-4.3.4.3. The difference equation for the error propagation is given in Eq. 4-211.

It is assumed that discrete time series representing sampled values of the present target bearing and range are the predictor inputs and that each measurement has an associated additive error. The ZT operating on Eq. 4-211 is used to determine the values of the errors in the predictor outputs at discrete time intervals synchronized with the input data.

Applying Eqs. 4-216, 4-217, 4-218, and 4-219 to Eq. 4-211 yields

$$zZ\{\delta A_{p_n}\} - z\delta A_p(0) = \left(1 - \frac{\Delta t}{\tau}\right) Z\{\delta A_{p_n}\} + \frac{K\dot{A}_o \Delta t}{\tau} Z\{\delta R_{o_n}\}$$

$$+ \left(\frac{KR_o + \Delta t}{\tau}\right) Z\{\delta A_{o_n}\} \qquad \text{(4-221)}$$

$$- \frac{KR_o}{\tau}\left[z^{-1} Z\{\delta A_{o_n}\}\right], \ \text{rad}$$

where

$Z\{\delta R_{o_n}\}$ = ZT of the discrete time series of range measurement errors, m
$Z\{\delta A_{o_n}\}$ = ZT of the discrete time series of bearing measurement errors, rad
$Z\{\delta A_{p_n}\}$ = ZT of the discrete time series of predicted target bearing errors, rad.

After combining terms and letting $\delta A_p(0) = 0$, Eq. 4-221 becomes

$$\left[z - \left(1 - \frac{\Delta t}{\tau}\right)\right] Z\{\delta A_{p_n}\} = \frac{K\dot{A}_o \Delta t}{\tau} Z\{\delta R_{o_n}\}$$

$$\text{(4-222)}$$

$$+ \left(\frac{KR_o + \Delta t}{\tau} - \frac{KR_o}{\tau}z^{-1}\right) Z\{\delta A_{o_n}\}, \ \text{rad.}$$

On application of Eq. 4-216 the ZT of the three time series are given by

$$Z\{\delta R_{o_n}\} = \delta R_o(0) + z^{-1}\delta R_o(1) + \cdots + z^{-n}\delta R_o(n) + \cdots, \ \text{m}$$

$$Z\{\delta A_{o_n}\} = \delta A_o(0) + z^{-1}\delta A_o(1) + \cdots + z^{-n}\delta A_o(n) + \cdots, \ \text{rad} \qquad \text{(4--223)}$$

$$Z\{\delta A_{p_n}\} = \delta A_p(0) + z^{-1}\delta A_p(1) + \cdots + z^{-n}\delta A_p(n) + \cdots, \ \text{rad}$$

where

$\delta\{A_o(n)\}$ = nth element in the bearing error time series, rad
$\delta\{R_o(n)\}$ = nth element in the range error time series, m
$\delta\{A_p(n)\}$ = nth element in the bearing prediction error time series, rad.

Since Eq. 4-212 represents a process with two inputs, there are two PTFs. These are obtained directly by inspection of Eq. 4-222:

$$G_1(z) = \frac{(KR_o + \Delta t - KR_o z^{-1})}{\tau\left[z - \left(1 - \dfrac{\Delta t}{\tau}\right)\right]}, \quad \text{dimensionless}$$

$$G_2(z) = \frac{K\dot{A}_o \Delta t}{\tau\left[z - \left(1 - \dfrac{\Delta t}{\tau}\right)\right]}, \quad \text{rad/m}$$

(4-224)

where

$G_1(z)$ = PTF relating the perturbation in A_p to the perturbation in A_o, dimensionless

$G_2(z)$ = PFT relating the perturbation in A_p to the perturbation in R_o, rad/m.

Eq. 4-222 can be solved for each of the unknown elements in the prediction error time series by using the definition of the inverse ZT and tables of ZT pairs. Techniques for obtaining solutions and tables of transform pairs are presented in Refs. 25, 26, and 27.

4-4.3.4.4.2 PSD of Sampled Data Systems

Error propagation equations expressed in terms of the statistical properties of the error were developed in subpar. 4-4.3.4.2. The same equations and techniques can also be applied to sampled data systems. The only difference is that the frequency spectrum, and, therefore, the PSD, of sampled data differs from that of the continuous signal from which it is taken. It is fortuitous, however, that the spectrum of the sampled data can be obtained directly from the spectrum of the continuous data signal.

Ref. 25 shows that the Fourier transform of a sampled data signal is related to the Fourier transform of the continuous signal by

$$E_s(j\omega) = \sum_{k=-\infty}^{+\infty} P(jk\omega_s)\, E[\,j(\omega - k\omega_s)\,], \quad \text{U·s}$$

(4-225)

where

$E(j\omega)$ = Fourier transform of continuous time signal $e(t)$, U·s

$E_s(j\omega)$ = Fourier transform of sampled data series $e_s(t)$, U·s

$P(jk\omega_s)$ = Fourier coefficients, dimensionless

ω_s = constant sampling frequency, 1/s.

The terms $E[j(\omega - k\omega_s)]$ represent the spectrum of the unsampled data signal translated to the frequencies $\pm k\omega_s$.

The Fourier coefficients $P(jk\omega_s)$ are given by

$$P(jk\omega_s) = \frac{1}{\pi k}\sin(k\alpha\pi), \quad \text{dimensionless}$$

(4-226)

where

α = ratio of the sampling pulse width to the sampling period, i.e., the sampling duty cycle, dimensionless.

If the width of the sampled pulse is much less than the sampling period, Eq. 4-226 can be written as

$$P(jk\omega) = \frac{1}{\pi k}k\alpha\pi = \alpha, \quad \text{dimensionless.}$$

(4-227)

Fig. 4-20 shows the effect of sampling on the spectra of a band-limited data signal. Fig. 4-20(A) shows the spectrum of the continuous data signal, whereas Fig. 4-20(B) is the spectrum of the sampled data where the sampling frequency is greater than twice the highest frequency ω_b in the continuous data spectrum. For this case the spectrum of the sampled signal is simply replicated about each integer multiple of the sampling frequency and scaled by the factor $P(jk\omega_s)$. If the sampling frequency is less than twice the highest frequency in the unsampled signal, the spectra run together and distort the PSD, as shown in Fig. 4-20(C). This distortion is called aliasing, and the criterion of sampling at a frequency of at least twice the maximum signal frequency is called the Nyquist interval.
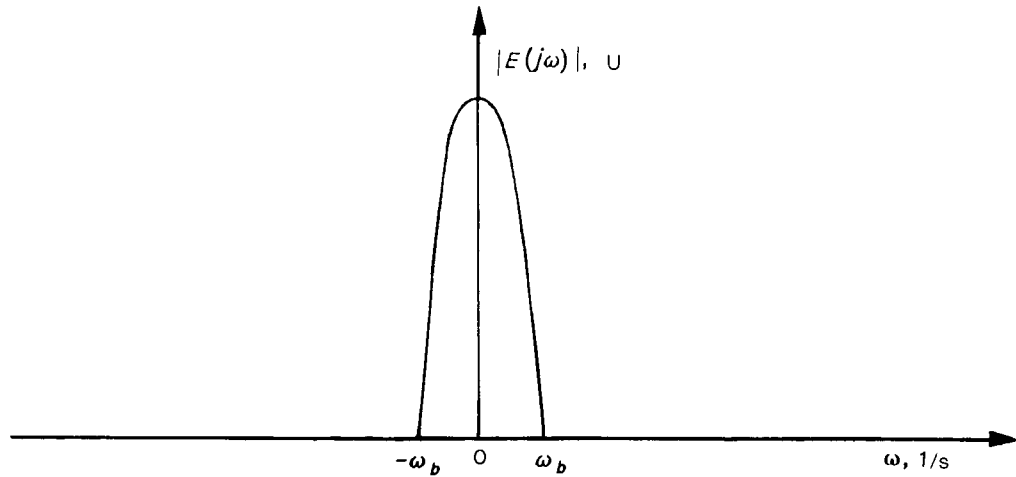
(A) Spectrum of the Continuous Data Signal
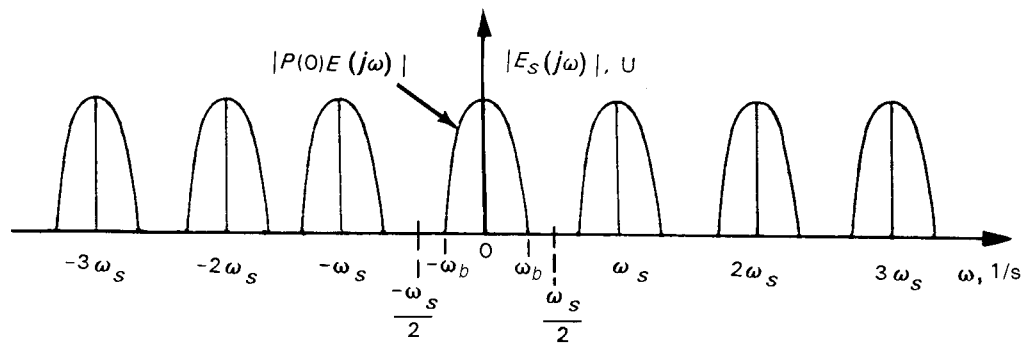
(B) Frequency Spectrum of Sampled Data With $\omega_s > 2\omega_b$
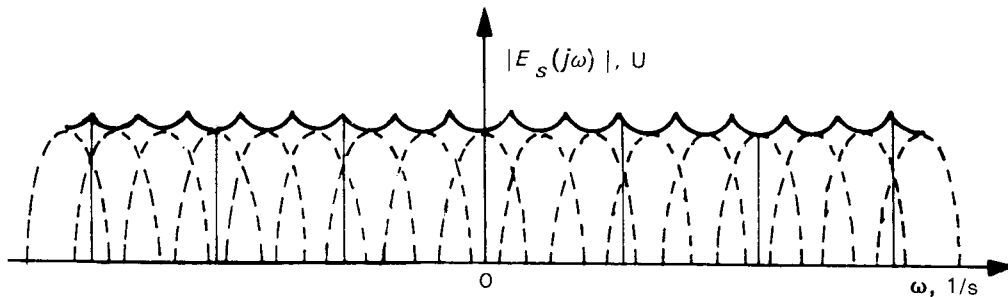
(C) Frequency Spectrum of Sampled Data When $\omega_s < 2\omega_b$

Figure 4-20. Effect of Sampling on the Spectra of Continuous Data Signals

When performing spectral analyses of continuous signals with digital spectrum analyzers, the signal must be sampled at least twice the signal bandwidth to avoid spectral distortion in the analysis. When dealing with the control of data sampled systems, however, the sampling frequency is selected using stability criteria and may often be much less the noise bandwidth in the system.

The propagation of the signal noise through the system can be studied by use of Eqs. 4-181, 4-182, and 4-186 to 4-188. The PSD of the sampled noise spectra is obtained by multiplying $E_s(j\omega)$ in Eq. 4-225 by its complex conjugate.

The digital spectrum analyzers mentioned compute the Fourier transforms of the sampled data stream by use of a discrete Fourier transform (DFT) algorithm and a rapid computational technique called the "fast Fourier transform" (FFT). A discussion of these techniques is contained in Refs. 27 and 28.

4-4.4 WEAPON SYSTEM ERRORS THAT ARE BEYOND THE CONTROL OF THE FIRE CONTROL SYSTEM DESIGNER

In practice, the errors in certain parts of the weapon system are usually beyond the control of the fire control system designer. Such circumstances might occur for some parts of the weapon system because their performance characteristics are dictated by natural phenomena or because there is a requirement to use existing components or subsystems in the weapon system design. Those parts of a weapon system whose errors are not under the control of the fire control system designer are usually associated with the input portion of the weapon system (the fire control acquisition and tracking subsystem) and the output portion of the weapon system (the weapon pointing system and the weapon itself). The errors associated with the input portion of the weapon system are considered first in subpar. 4-4.4.l, and the errors associated with the output portion of the weapon system are considered in subpar. 4-4.4.2. On the other hand, the errors associated with the fire control computing system are considered to be under the control of the fire control system designer. These errors are discussed in subpar. 4-4.5.

4-4.4.1 Errors Associated With the Input Portion of a Weapon System

The input portion of a weapon system, which comprises the target acquisition and tracking devices, may use radar, direct view optical sights, laser range finders, infrared sensors, or video imaging sensors. In addition, gyroscopes or pendulous elements may also be used to stabilize the input portion of a weapon system especially if the fire control system is mounted on a moving base, e.g., in a tank or helicopter fire control system. This subparagraph qualitatively describes the physical sources of errors for a variety of fire control input devices.

The target acquisition device detects the presence and approximate position coordinates of a target to allow the tracking device to initiate tracking of the target when it is so commanded. The acquisition and tracking devices may be combined or left as separate subsystems. The tracking device generates signals that describe the target motion and serve as inputs to the fire control computing system.

In general, bias errors can be considered to be under the control of the fire control system designer and can be handled by previously described techniques except for wind loading and other atmospheric effects . Tracking systems, however, are also subject to random input errors that are associated with the real or apparent motion of the target about the tracking line and cannot be controlled by the fire control system designer. By analogy with communication systems these random errors are called "noise". The noise of concern for tracking systems consists of relatively low frequencies since high-frequency components are effectively filtered by the fire control system. Such filtering action can be accomplished, for example, by smoothing in the fire control computing system or by filtering directly in the tracking servos. This noise should be distinguished from atmospheric and resistance noise that determines the maximum range of an acquisition radar or from the atmospheric effects that limit the range of a telescopic acquisition device. Once the target has been acquired and transferred to the tracking device, the signal strength is usually well above the atmospheric noise level. The atmospheric noise level then principally affects the resolution of the tracking device.

The input noise of prime importance to the fire control system designer is the real or apparent ran-

dom motion of the target about the tracking line. This noise may arise due to motion of the target, which is caused either by evasive action or by unintentional motions, or it may be caused by shifts in the apparent center of reflection of the radiation that is providing the tracking intelligence (the so-called "glint effect" in radar systems). Another source of noise is the imperfection of the tracking device, which may be controlled automatically or by a human operator.

4-4.4.1.1 Radar Glint Noise

The angular accuracy of tracking radar is influenced by such factors as the mechanical properties of the radar antenna and pedestal, the method by which the angular position of the antenna is measured, the quality of the servo system, the stability of the electronic circuits, the noise level of the receiver, the antenna beam width, atmospheric fluctuations, and the reflection characteristics of the target. These factors can degrade the tracking accuracy by causing the antenna beam to fluctuate in a random manner about the true target path. These noise-like fluctuations are sometimes referred to as tracking noise, or jitter. In many cases the two factors that ultimately limit the angular accuracy of practical tracking radars are the mechanical errors and the target-reflectivity characteristics.

A simple radar target such as a smooth sphere does not cause degradation of the angular tracking accuracy since the radar cross section of a sphere is independent of the aspect at which it is viewed. Consequently, its echo does not fluctuate with time. The same is true, in general, of a radar beacon if its antenna pattern is omnidirectional. Most radar targets, however, are of a more complex nature than a simple sphere. The amplitude of the echo signal from a complex target may vary over wide limits as the aspect changes with respect to the radar. In addition, the effective center of radar reflection may also change. Both of these effects—amplitude fluctuations and wandering of the radar center of reflection—can limit the tracking accuracy.

Changes in the target aspect with respect to the radar can cause the apparent center of radar reflections to wander from one point to another. The apparent center of radar reflection is defined by the direction of the antenna when the error signal is zero. In general, the apparent center of reflection might not correspond to the geometric center of the target. In fact, it need not be confined to the physical extent of the target and may be off the target a significant fraction of the time. The random wandering of the apparent radar-reflecting center induces tracking noise. This form of tracking noise is called angle noise, angle scintillations, angle fluctuations, or target glint. The angular fluctuations produced by small targets at long range may be of little consequence in most instances. At short range or for relatively large targets (as might be seen by a radar seeker on a homing missile), however, angular fluctuations may be the chief factor limiting tracking accuracy. Angle fluctuations affect all tracking radars whether conical scan, sequential lobing, or monopulse.

4-4.4.1.2 Radar Amplitude Noise

A complex target such as an aircraft or ship may be considered a number of independent scattering elements. The echo signal can be represented as the vector addition of the contributions from the individual scatters. If the target aspect changes with respect to the radar—as might occur because of target motion or turbulence in the case of aircraft targets—the relative phase and amplitude relationships of the contributions from the individual scatterers also change. Consequently, the vector sum and the amplitude change with changing target aspect.

Amplitude fluctuations of the echo signal are important in the design of the lobe-switching radar and the conical-scan radar but are of little consequence to the monopulse tracker. Both the conical-scan tracker and the lobe-switching tracker require a finite time to obtain a measurement of the angle error. For the conical-scan tracker this time corresponds to at least one revolution of the antenna beam. With lobe switching the minimum time is that necessary to obtain echoes at the four successive angular positions. In either case a minimum of four pulse repetition periods is required to make a measurement, but in practice many more than four are often used. If the target cross section were to vary during this observation time, the change might be erroneously interpreted as an angular error signal. On the other hand, the monopulse radar determines the angular error on the basis of a single pulse; therefore, its accuracy will not be affected by changes in amplitude with time.

4-4.4.1.3 Video Trackers

The advent of video and forward-looking infrared (FLIR) imaging sensors for target viewing also introduced the possibility of automatic passive tracking. Error signals representing the difference between the sensor boresight axis and the target center can be generated and used to drive a servo for control of the sensor gimbal. The difficulty lies in determination of the target position based on the video signals in the presence of the background. Processing logic that discriminates the target from the background based upon the shape or contrast of man-made structures has been used successfully. However, early trackers that relied only upon the contrast of a target edge to the background were replaced by those using more sophisticated logic. These early versions tended to drift along the target edge and often jumped to a background feature of similar contrast. The centroid-type trackers generally overcome target-edge-based shortcomings by averaging the signal levels within variable gates established around the target on a contrast basis. In this manner a point generally close to the physical center of the target is established to generate the servo error signal.

The correlation-type tracker, as the name implies, attempts to maintain the point of track at the same reference in the scene by maximizing frame-to-frame correlation. The correlation and centroid trackers can be quite sensitive to changes in target aspect, signal-to-noise ratio, target-to-background contrast, etc. For these reasons developers have resorted to including several redundant logic designs in a single tracker and thereby reducing the susceptibility of any one logic design to particular tracking scenario conditions.

Virtually all of the trackers developed to the late 1980s require an operator to acquire the target and establish a level of initial track. The automatic tracker is then engaged, and the performance monitored by the operator. When functioning properly, the tracker can often perform to an order of magnitude faster than a human tracker because of its ability to respond to more rapid changes in target movements, i.e., higher frequency response. When such auto trackers lose track, however, system recovery can be difficult. More recent developments have led to logic algorithms that greatly enhance the ability of auto trackers to "coast" and reestablish a track (based on prior position data) after the target has been obscured (lost) by scene objects (such as trees, boulders, buildings, etc.) in the field of view. Considerable development effort has been expended to refine video-processing algorithms to the point at which automatic target detection can be performed. The follow-on track process is then readily accomplished by using the target signature, on which detection is based.

Although the processing data rate may be sufficiently high to continue generation of a representative error signal, the response time of the servo drive may not be sufficiently fast to close the control loop properly. Accordingly, the sight gimbal angles do not necessarily represent the true target orientation but have inherent errors that are represented by the magnitude of the error signal. The availability of the error signal then permits correction of the gimbal angle measurement in order to give correct target orientation.

4-4.4.1.4 Laser Range Finder

When analyzing the errors for even the most basic fire control system, inaccuracies in range are generally among the largest contributors to the error budget. Errors in range estimation yield errors in gun elevation angle. Optical range finders, such as stadia and stereoscopic instruments, provide errors that are at best proportional to the true range. For example, a 15% range measurement error (representative of a stadia reticle) at 2000 m, i.e., 300-m error in range estimation, can result in an elevation error, which will cause the projectile to miss the target by several hundred meters.

When it is compared with its optical predecessors, one of the most attractive features of the laser range finder is that the inherent errors are independent of target range. If properly pointed, only the error made in measuring the round trip-travel time of the light pulse is significant. Generally, the timing networks are designed to keep this error to within 5 m (corresponding to a timing error of ~20 ns), which is acceptable in any fire control system.

The proper pointing of the laser can, however, be difficult under certain conditions. First, it is desirable that virtually all of the laser energy fall on the target alone. In actual practice this is seldom real-

ized due to the divergence of the laser beam, the limited size of military targets, the extent of the misalignment between the laser and the tracking sensor, and the sensor tracking error. If the laser beam strikes objects in addition to the target, multiple returns from a single transmitted pulse are often sensed by the laser receiver. These may represent objects at various ranges. Processing logic, designed into all receivers, permits the operator the option of selecting the first or last of the multiple returns for the range measurement. The selection is usually made based on a particular scenario. Although this logic is helpful, quite often measured returns do not represent the exact target range, and the data must be filtered. The relatively low laser pulse rate (compared to radar) limits the information available for processing and can be detrimental, especially for a large relative velocity between the gun and the target. Another problem that can occur, and one that the conventional filter cannot resolve, is the receipt of a consistent set of initial returns from a false target. In applications in which this situation occurs, a prefilter is often introduced in an attempt to recognize the phenomenon and to keep the main filter from reacting to it.

In a fire control system the range data are usually the last of the input data available for solution because an acceptable angle track must be accomplished before ranging can commence. Therefore, the accuracy and data rates of the ranging device are particularly critical to determination of the system reaction time.

4-4.4.1.5 Target Motions

Motions of slowly moving targets are not of great significance in most cases because the prediction of future target positions is relatively easy. In the case of aircraft, however, both unintentional motion caused by wind gusts and thermal currents and intentional evasive actions make prediction more difficult by adding to the noise input. There is little the fire control system designer can do to counter the effects of unpredictable evasive action other than to keep the computer settling time as short as possible. Guided missiles can correct for evasive maneuvers by the target inasmuch as their trajectories can be continually modified. This fact is one of their major advantages over unguided projectiles. However, there are also circumstances in which unguided projectiles have advantages over guided missiles due to their higher muzzle velocities. For example, an aircraft about to approach and attack a target can no longer take evasive actions. In this case, the approaching enemy aircraft can be effectively engaged by an unguided projectile because the higher speed of such a projectile has the advantage of reaching the approaching aircraft more quickly, i.e., before the enemy can release its weaponry.

4-4.4.1.6 Tracking Noise

The positioning of the sight line may be accomplished manually, automatically by servos, or by a combined system. Noise is introduced into the tracking system by such nonideal mechanical factors as Coulomb friction, backlash, gear irregularities, and vibration. If the positioning is accomplished automatically, the design of the servos and the mechanical components should minimize these effects. Viscous friction and inertia of the tracking head are helpful in attaining smooth tracking by acting as mechanical, low-pass filters but detract from rapid, accurate positioning. If the tracking system must be capable of both smooth tracking and rapid positioning, some compromise in the design must be made.

Most tracking systems use a human operator at some point in the tracking loop. Human operators are also used in other parts of the fire control system to make decisions, to serve as communications links, and to perform computations that do not have to be made rapidly. Modern fire control systems are designed to make the task of the human operator as simple as possible to improve his speed and accuracy, to reduce the effects of fatigue, and to reduce the amount of required training. This portion of the design process, which combines the disciplines of psychology, physiology, and engineering, is known as human engineering. A knowledge of the principles of human engineering is valuable to the designer of audible and visual data presentations, hand and foot controls, seats, and enclosures for human operators. Human engineering is discussed briefly in Chapter 5 of this handbook. A full treatment of the topic is included in Ref. 29. The discussion that follows covers those facets of the subject which contribute to tracking error.

Human operators are used in tracking systems (1) because a suitable detector is lacking, (2) to distin-

guish signals from noise (a function a trained operator can perform better in most respects than a filter circuit), or (3) because an operator is still required to make decisions and the designer wishes to economize by using him for the tracking function as well.

The simplest form of tracking is accomplished by pointing a tracking head mounted on a pivot; however, this approach requires the operator to provide the torque needed to rotate the head. Thus it necessitates use of muscles that are not particularly suited for fine operations. Also any undesirable angular motion introduced by the operator is transmitted to sight line motion. These shortcomings can be lessened if a tracking servo is used to drive the sight line in order to permit use of manual input devices such as a joystick, ball, or thumb control which utilize the more sensitive tactile capabilities of the fingers and thumb. Such devices also offer the means to isolate the track input from vehicle motion that is normally transmitted to the operator's body. Additionally, the servo permits scale factor change between the input device and sight line so that the sensitivity to extraneous inputs can be reduced. The use of a servo in the control loop does not completely remedy the shortcomings of a manual tracking system since a human operator is still involved in the process with his limited "built-in" response time.

Many measurements of human operators in both positioning and tracking systems indicate that there is an average delay time of 0.5 s and that this time is substantially independent of the extent of the motion required. Measured responses of humans to a sinusoidal input show good tracking ability to about 3 or 4 Hz.

Efforts to develop a linear mathematical model of the human operator in tracking tasks have been made by Raggazini, who measured the response of a subject using a hand control (Ref. 30). The subject was asked to maintain the position of a moving dot in the center of a cathode-ray tube. Tustin (Ref. 31) used a gun carriage where the subject could control the angular rate. The mathematical model in both experiments was shown to be the algebraic equation

$$H(s) = \left[\left(as + b + \frac{c}{s}\right)e^{-\tau s}\right]A(s), \ \mathbf{m} \tag{4-228}$$

where

$A(s)$ = position of the stimulus (the visible spot), m

$H(s)$ = operator's hand position, m

a,b,c = constants determined for the particular experiment, (s, dimensionless, and 1/s, respectively)

s = Laplace variable, 1/s

τ = reaction time, s.

Eq. 4-228 is the Laplace transform of the operational differential equation

$$h(t) = \left(a\frac{dA}{dt} + bA + c\int A dt\right) \tag{4-229}$$

where

t = time, s

$h(t)$ = operator's hand position as a function of time, m

$A = A(t)$ position of the stimulus as a function of time, m.

Thus the operator's response is made up of motions proportional to the stimulus, its derivative, and its integral and delayed by the reaction time τ, which was determined to be about 0.3 s. It appears that this mathematical model can be used with considerable confidence.

The tracking of rapidly moving targets can be greatly facilitated by the provision of controls that provide, by means of servos or gyro precession, a tracking rate that is proportional to the motion of the control. Further improvement is secured by aided tracking, in which both a position and rate response are obtained for a given control movement.

4-4.4.2 Errors Associated With the Output Portion of a Weapon System

The output portion of a weapon system includes the weapon, i.e., the projectile and its launching system, and the associated weapon pointing system. To a large degree, the errors associated with this portion of the fire control system have been considered to be outside the control of the fire control system designer. This thinking has been true principally because of the nature of the weapon system development process. Traditionally, the fire control system of a weapon system has been designed to match either an existing weapon or one that is already under development. Thus the fire control system designer has been forced to adapt his designs to match already existing components, even though it has frequently been apparent that some modification of these components would result in worthwhile improvements in the overall performance of the weapon system. The modern weapon system design concept, however, has considerably modified this traditional approach.

The new approach incorporates a system planning stage in which the individual designs of the acquisition and tracking system, the computing system, the weapon pointing system, and the weapon are adjusted to obtain an optimum overall weapon system design within the available time and funds.

Both systematic and random errors are associated with the output portion of a weapon system. The systematic errors are largely the boresight errors of the weapon. In order to keep these systematic errors to a minimum, provision is made for the accurate alignment of the weapon and the tracking system. Methods have been incorporated to make on-line compensations for tube bending due to environmental conditions. In addition, since gun tubes may wear unevenly and gun carriages may settle unevenly, provision can be incorporated somewhere in a fire control system for corrections to be made from time to time based on observations of actual projectile trajectories or impact points.

Projectile muzzle velocity may shift over the life of a gun tube due to tube wear, or it may vary from round to round or from engagement to engagement due to changes in projectile temperature and variations in projectile and propellant lots. The effect is the introduction of angular dispersion about the target in the prediction plane. Computation is often provided by sensing the error prediction factors or by measuring the muzzle velocity directly.

4-4.5 WEAPON SYSTEM ERRORS THAT ARE UNDER THE CONTROL OF THE FIRE CONTROL SYSTEM DESIGNER

The portion of a weapon system that is most under the control of the fire control system designer is the fire control computing system. At the input end of the weapon system, the design of the acquisition and tracking system is limited by the nature of the problem (as discussed in subpar. 4-4.4.1). At the output end of the weapon system, on the other hand, the fire control system designer is limited by the fact that he does not have any control over the design of the weapon itself and in some instances has no control over the weapon pointing system. The computing system, by virtue of its central position in the weapon system is in effect isolated from these two limitations.

Although in the 1990s, there are fielded weapon systems that still use fire control analog computers, e.g., the M-60 series main battle tank, all major systems now take advantage of the accuracy and flexibility afforded by digital processing. Thus no longer must the fire control designer be completely knowledgeable in the detail of computer design, as was the case with analog devices. For such systems it was necessary that the fire control designer be fully aware of the potential of components to generate arbitrary functions and perform analog mathematical operations of interest. In addition, it was necessary that he be capable of expressing the fire control solution in a mathematical form conducive to implementation with these components. Considerable experience and imagination were required to master this implementation art. Such experience is not the case for the implementation of digital computers. The designer selects a computer with the overall required characteristics (e.g., word length, processing time, storage capacity, input-output features, etc.) with little regard to the detailed design of the logic. The equations selected for implementation are not constrained by limitations of computer circuitry. The required algorithms can be implemented by programming specialists who make use of a vast library of conventional mathematical relationships and numerical methods developed over many years. The system designer is of course responsible for verification and validation, but those functions are also carried out by software specialists.

Although the analog techniques used in the development of fire control computers have been phased out of Army operations with few exceptions, they still play a prominent role in the development of servo control systems. Most weapon systems currently use analog techniques to control the pointing of targeting sensors and the weapons. The analog components and their errors are discussed in subpar. 4-4.5.2 and are considered primarily because of this type of application.

Attempts have been made to employ digital servo systems to control weapon pointing. Attempts to reduce weapon pointing errors have also led to investigation of the application of adaptive control techniques based upon modern control theory, microcomputer technology, and fast algorithms. The objective has been to maintain peak operating performance in the presence of variations in the structural and dynamic characteristics of the weapon system over the disturbance frequency spectrum. In 1993 there was considerable interest in all electric gun drive systems because they are less sensitive to environmental and operational conditions.

Precision aiming techniques have also been considered to improve weapon pointing and have achieved some level of acceptance for tank application. For these techniques, when the weapon orientation passes through an acceptable firing window, firing circuits are initiated. Servo control must assure that the weapon passes through the window, possibly in two dimensions, in a reasonable time and that delays in the firing chain are anticipated.

4-4.5.1 Errors in Digital Computers

Digital computing elements are not subject to error in the same sense analog computing elements are. The fundamental digital computing elements are either storage elements or logical elements, and all such elements can assume only two states, 0 or 1. Consequently, the only error that can occur in such an element is the loss of a bit, and depending on the significance of the digit in question, such an error can be either negligible or catastrophic. Therefore, much effort has gone into development of error-detecting and -correcting codes and circuits and of redundant circuitry, all of which are more fully described in Ref. 32.

Error checking is so essential and so highly developed that the errors existing in the fundamental digital computing elements do not merit further discussion here. The error sources discussed in connection with digital computing elements involve (1) problems of providing inputs to, and of obtaining outputs from, an element, which cause sampling errors in time-varying data, and (2) problems arising from the approximation of continuous functions by discrete elements, which thereby introduce truncation errors. These error sources are found in both simple and complex digital computing elements. They are discussed in subpars. 4-4.5.1.1 and 4-4.5.1.2, titled "Dynamic Errors" and "Static Errors", respectively.

4-4.5.1.1 Dynamic Errors

The use of digital computing elements in fire control systems often requires that the input signals, initially in analog form, be converted to digital form. This analog-to-digital conversion is performed by sampling the electrical (or mechanical) signal at regular time intervals and then quantizing the samples to provide a digital representation. For example, a mechanical shaft angle can be digitized by coupling a brush that rides over a fixed commutator to it. At regular intervals a voltage pulse is applied to the brush, and the pulse then appears at a particular commutator bar, which is determined by the shaft angle at that instant. Since each commutator bar is assigned a numerical value, the device described produces a digital representation of the shaft angle.

The fact that the sampling process introduces dynamic errors is evident because for a fixed sampling rate the amount of information lost between sampling intervals is a function of the frequency of the input signal. If the sampling frequency is less than twice the maximum frequency of importance in the system (the Nyquist criterion), serious alias distortion results. On the other hand, the computer must complete a set of calculations on one sample before the end of the sampling interval so that the registers can be cleared to accept the next sample. At higher sampling rates this procedure requires the designer to use either higher speed computer components or more parallel components to reduce the amount of time-sharing. In the analytical work associated with this design problem, the digital computer

can be represented by a simple system composed of an impulse modulator (representing the sampling process) and a pure time delay.

Another error due to sampling procedures has been termed the transportation lag. A bit of information available for processing may be delayed to such an extent within the sampling system that it is not sufficiently current to provide a real-time solution. If a system check is available and the bit is time tagged, it may be possible to compensate the solution for the known delay.

4-4.5.1.2 Static Errors

In contrast to analog elements digital elements can be designed to have any accuracy desired subject only to the limitations of computation speed and circuit complexity. In reality, however, it makes no sense to digitize a signal to a level beyond the resolving power of the (analog) sensor, or to provide a level of digitization beyond that required for the purpose at hand. The task of the system designer is, therefore, to achieve a compromise among accuracy, speed, and complexity.

The digital computation is also subject to round-off errors, which occur at every stage of the computation because of the limited capacity of the registers. Depending on the equipment design, individual round-off errors are at most the value of the least significant digit, but successive roundings may build up the error. If the difference between two large numbers is taken, the round-off error may be excessive. These difficulties can be corrected by improvements in software.

A continuous function can be represented in a digital computer by the storage of a series of stepwise values or more efficiently by the computation of a series approximation to the function. Differential equations are solved in a digital computer by programming one of several methods of numerical integration. These methods involve computation of small increments in the function, using series expansions, and in some cases a knowledge of the preceding increments. Naturally, as few terms as possible are retained in the series; therefore, the errors caused by truncation of the series must be given serious consideration. Truncation errors are minimized by reducing the interval in the input variable or by increasing the number of terms in the series.

The variation in the truncation error achieved by adjusting the interval in the input variable is explained with the aid of Fig. 4-21, which illustrates a continuous function $f(x)$ plotted as a function of the variable x. In the simplest digital scheme this continuous function is represented in a stepwise manner; the value of $f(x)$ occurs at the beginning of any interval Δx and is held constant throughout the interval. The difference between the continuous curve and the approximation (the small semitriangular regions shown in Fig. 4-21) is the truncation error. It is evident from the figure that a reduction in Δx will decrease the truncation error, whereas an increase in Δx will increase the error.
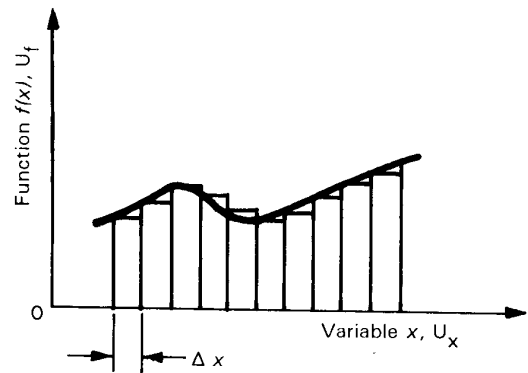
Figure 4-21. A Simple Example of a Truncation Error

4-4.5.2 Errors in Analog Components

The reduction of uncertainties and nonlinearities in analog devices can be accomplished by refining the design and reducing manufacturing tolerances or by the ingenious application of new methods. The attainment of higher levels of accuracy is, therefore, a slow process. At the present state of development maximum error can be held to the order of magnitude of ±0.01% under laboratory conditions. The designer must consider not only the initial error but also the error at the end of the useful life of the component.

4-4.5.2.1 Mechanical Elements

Eccentricities in shafts, bearings, cams, gearing, etc., introduce nonlinearity errors and may also contribute to backlash in gearing. Inaccurate gear cutting also produces both backlash and nonlinearity errors. Inaccuracies in high-speed gears may be treated as noise since the variations are generated at high frequencies.

Distortion of mechanical parts under load may contribute to errors in those parts of the system, such as the weapon pointing servos, that undergo heavy loading. The weapon pointing system may also have dynamic errors caused by vibrations induced by the rapid motion of heavy masses.

4-4.5.2.2 Servos

Servos are used to convert signals from electrical to mechanical form. Sensor platform and weapon pointing are performed by hydraulic or electric servos. The servo performance may be specified by the permissible static error and the required bandwidth. Alternatively, the position, velocity, and acceleration error constants may also be specified. For the latter set of specifications the servo error can be expressed by

$$\varepsilon(t) = \frac{1}{1 + K_p} + \frac{1}{K_v}\,\dot{x}(t) + \frac{1}{K_a}\ddot{x}(t)\,,\ \ \mathbf{m} \tag{4-230}$$

where

$\varepsilon(t)$ = servo error, m

$x(t)$ = input signal, m

K_p = position error constant, 1/m

K_v = velocity error constant, 1/s

K_a = acceleration error constant, $1/s^2$.

Servo position response may be measured by a potentiometer or synchro-type device. Output rate can be measured by a tachometer. Shaft encoders are digital alternatives to any of these devices. Information on servo design techniques is included in Refs. 33, 34, and 35.

4-4.5.2.3 Potentiometers

Wire-wound potentiometers are limited in their accuracy by the number of turns in the winding, which determines the resolution (or conversely, the uncertainty level). The development of helical winding techniques makes it possible to compress a very long winding into a small volume and thus provide practical potentiometers with high resolution and excellent linearity. Improved housings have reduced the eccentricity errors, and improved contact materials have increased the life to several million revolutions.

Nonlinear functions can be generated by (1) potentiometers with shaped windings, (2) tapped linear potentiometers with resistive loads connected to the taps, or (3) tapped linear potentiometers with voltage sources connected to the taps. In addition to the errors inherent in any potentiometer, nonlinear potentiometers have errors introduced by inaccuracies in the shaping of the winding. In the case of tapped potentiometers, errors are introduced by inaccuracies in the location of the taps and by the approximation of the function by straight-line or parabolic segments.

4-4.5.2.4 Resolvers and Synchros

A resolver is a device that generates voltages proportional to the sine and cosine of its shaft angle. When shaped potentiometers are used as resolvers, the considerations given in the preceding subparagraph apply. Electromagnetic resolvers and synchros are quite similar; they differ only in the arrangement of the windings. Both have errors that are invariant with shaft angle and caused by transformer coupling, in which such errors may be compensated for by summing the error with a voltage having the same magnitude but opposite phase angle. Errors that cannot be so compensated are those that vary with shaft angle, e.g., those caused by magnetic anomalies and winding inaccuracies. In addition, the magnetic circuit induces odd harmonic voltages, and an error voltage proportional to shaft speed is generated.

4-4.5.2.5 Tachometers

Tachometers used in analog circuits are either permanent magnet field dc generators or drag-cup-type ac generators. The dc type suffers from voltage fluctuations at low speeds caused by commutation. The ac types also have low-speed fluctuations but at lower levels. Fixed errors are produced by transformer coupling, and small voltages proportional to shaft acceleration are generated.

4-4.5.2.6 Operational Amplifiers

High-gain dc feedback amplifiers are used for summation, integration, isolation, and other functions in analog circuits. The major source of error in such amplifiers is drift of the output when the input voltage is zero. Zero drift is minimized by the use of chopper stabilization, by good regulation of supply voltages, and by temperature control of critical components.

4-4.5.2.7 Gyroscopes

Gyroscopes (usually referred to simply as gyros) are used in fire control systems to measure the angular rate of a tracking device or to provide a stable reference or sight picture on a moving base. Mechanical gyros must be classified as analog devices, although a digital encoder may be used to provide a digital output signal.

Two types of gyros have been used in fire control systems. The first is the two-degree-of-freedom type, which serves either as a vertical reference or as a directional reference, depending on the orientation of its axes. The second is the single-degree-of-freedom rate-integrating type of gyro. This type can be used to measure the angular rate about a tracking axis, or three units can be arranged on a platform with accompanying platform servos to form a stable reference. Gyros with an attached pendulous mass have been used also as accelerometers.

The principal sources of error in gyros are mass unbalance, friction in pivots, vibration, and problems in the electrical pickoffs. In addition, all types of gyros sense the component of the angular velocity of the earth that is directed along an input axis. Usually, however, this resulting error is insignificant in fire control systems.

Mass unbalance introduces disturbing torques whenever the unbalanced mass is accelerated, by motion of the gyro base or by gravity. Balancing two-degree-of-freedom gyros is much more difficult than balancing single-degree-of-freedom gyros. At constant temperature the unbalance can be adjusted to a minimum value, which is determined by the precision of measurement available. A major source of mass unbalance is the shifting of the rotor position that arises chiefly from end play in the rotor bearings. Even with preloaded bearings, the rotor position may shift somewhat under acceleration loading against the elasticity of the bearings. Gyro balance also shifts with temperature because of the unequal temperature coefficients of expansion of the various gyro parts. Thus many precision gyros are accordingly temperature compensated.

The other major source of disturbing torques is the frictional or elastic coupling arising from the gimbal pivots and the electrical connections to the gimbals. Of these, the frictional torque of the gimbal pivots has the greatest magnitude of error. Conventional ball bearings are inexpensive but have poor frictional characteristics for this application. Pivot bearings are better, but they are easily damaged. Flotation of the gimbal has been used with pivot bearings and has achieved both protection of the bearing and a reduction of the load on the bearing to reduce the friction level farther. A large reduction in the error due to pivot friction can be achieved if fluid bearings are introduced where either air or a hydraulic fluid is used. Developments in the application of magnetic supports in which an electromagnetic field is arranged to provide a uniform radial force on the gimbal directed toward the support axis are also in use. Electrostatic fields are also used. The only error-producing torques then remaining are the residual tangential magnetic fields of the support coils and of any magnetic pickoffs, friction torques from slip rings or potentiometer pickoffs, and elastic torques that might arise from pigtail leads and from the non-Newtonian behavior of damping and flotation fluids.

Vibration, due principally to unbalance and bearing defects in the rotor, introduces noise errors. Roughness of potentiometer windings and magnetic anomalies in magnetic pickoffs are also sources of noise errors. A major effect of all of these noise errors is masking of the small gyro output signal near a null. This null error is the limit of resolution for the gyro. Pickoff nonlinearities can produce large errors, although many applications use the gyro in a null-seeking system, e.g., the stable platform system. In such systems nonlinearity of the pickoff is of minor significance.

State-of-the-art sensors such as ring lasers and fiber-optic gyros do exist and are being considered by the US Army for fire control applications. However, a detailed discussion of such technology is beyond the scope of this handbook.

4-4.5.2.8 Voltage Supplies for Analog Components

If the reference voltage (the source of the analog signal voltages in an electrical analog circuit) varies, errors may be introduced. In addition, power supplies that provide operating voltages for electronic components must be well regulated in order to avoid the generation of drift errors.

4-5 IMPLEMENTATION OF THE MODEL

4-5.1 GENERAL CONSIDERATIONS

In the broad sense, the implementation of the mathematical model of the fire control system involves the embodiment in physical hardware of the equations that describe the system. Presumably, previous study of this mathematical model (par. 4-2) has shown the system designer that the proposed system is capable of meeting the specified requirements. Actual implementation includes the following steps:

1. Selecting suitable standard components
2. Preparing detailed drawings and the parts list
3. Fabricating the necessary nonstandard components
4. Assembling the complete system
5. Testing the complete system.

If the fire control system of interest involves any significant research or development effort, it is seldom possible to implement it into its final form in one step. Instead, those concerned with the physical design should work closely with the system designers (particularly the mathematical analysts) to examine those portions of the system that may present difficulties or at least need to be verified because they incorporate new techniques or are pushing the state of the art in some respect.

4-5.2 DEPARTURE FROM NOMINAL PROCEDURE

In many systems major elements in the mathematical model are dictated by the selection of major physical components. This situation results when the use of particular components is spelled out in the specifications or the number of existing alternatives is so small the selection narrows to a few possibilities and essentially no control of the relevant parameters is permitted. Typical examples are the requirement that a fire control system be built around a certain gun with a particular power drive and the requirement that a fire control system derive tracking data from a particular radar. If one or more major physical components are specified and their performance characteristics are well understood, the mathematical analyst may be able to formulate a suitable ideal mathematical model based upon existing data. Then the analyst can proceed with development of the mathematical model to optimize the overall system and leave the specified elements of the fire control system unchanged. Frequently, additional data must be obtained before an adequate mathematical model can be completely established, particularly if the performance of the overall fire control system is highly dependent upon the characteristics of the particular element involved. Thus the testing of the components to be included in a system frequently becomes a necessary phase of the implementation of a mathematical model because components may be used in an unconventional manner or may be so new that their characteristics are not well documented. In such cases, the problems of formulating and mechanizing the mathematical model become completely intertwined.

4-5.3 SYNTHESIS PROBLEMS

The overall task of implementing a fire control system may be subdivided into the mechanization of its three subsystems: (1) the acquisition and tracking system, (2) the computing system, and (3) the weapon pointing system. However, since the overall implementation is a systems problem, the interactions among these three subsystems must be considered. Accordingly, system modifications that might be affected by combining into a single unit function or components that might normally be thought of as belonging to different subsystems should be examined. This is a synthesis problem, and like many synthesis problems, no unique relationship exists that leads from the mathematical description of a system to the physical embodiment of that system. It is exactly this problem of nonuniqueness that makes

this portion of the system design problem difficult and that places such a premium on engineering know-how. On the other hand, the inverse problem of developing a mathematical description for an existing physical system is purely an analytic problem and is completely deterministic.

A typical synthesis problem that might arise in connection with the realization of a fire control system is determination of the most appropriate means of obtaining tracking rate data. Such a problem would involve judicious consideration of the following questions:

1. Should tachometers be installed on each axis of the tracking system to derive relative rate information?

2. Should rate gyros be installed to measure rates with respect to an inertial frame of reference?

3. Should only angular position transducers be provided and tracking rate data be generated by suitable arrangements within the computer?

Each of these alternatives uses different instrumentation, and each imposes different requirements on the computing system. Therefore, only by carefully appraising the accuracies of the available instruments, the overall demands upon the computing system, and the economics involved can the analysts and those responsible for implementation of the system arrive at a truly optimum system.

In many fire control systems relatively little interaction occurs among the tracking, computing, and weapon pointing systems. Therefore, except for the immediate interface problems associated with ensuring that the signals supplied by the tracking system are acceptable for use by the computing system and that the computer output is satisfactory for activating the weapon pointing equipment, the design of each of these major subsystems can be separated to a large degree. Division of responsibility along these major system subdivision lines expedites execution of the overall job but imposes a responsibility on the manager of the project to ensure that changes introduced by one team do not alter the requirements on the work of other teams.

4-6 FIRE CONTROL TESTING

4-6.1 INTRODUCTION

All Army acquisition programs must be supported by a comprehensive test and evaluation (T&E) program, as presented in Ref. 36. T&E is used to assess acquisition risks, verify performance in accordance with specifications, evaluate operational effectiveness, verify defect corrections, and determine MANPRINT requirements. All testing planned during the development and acquisition of a system is identified in a test and evaluation master plan (TEMP).

Testing of all Army materiel, including fire control, takes different forms depending, in part, on the purpose of the test. During the development phase, engineering tests may be required. The purpose of such tests might be to test whether or not an approach is feasible or to obtain engineering measurements of the accuracy, resolution, or response time of components or subsystems. Engineering development tests are normally performed in a laboratory with instrumentation suitable for the environment, but such tests can also be conducted in factory and proving ground environments.

The paragraphs that follow are mainly devoted to a discussion of system tests referred to as development tests (DT) and operational tests (OT). These tests are often mandated by acquisition boards and other high-level Department of the Army or Department of Defense activities. Decisions may be made, in part, based upon the outcome of these tests. Such decisions would include whether or not to continue a system development program or whether or not to proceed with production. At times a combined DT and OT can save time and other resources.

As stated in par. 4-1, fire control is usually embedded in and is an integral part of the system being tested. In the case of most weapon systems, however, the criteria used to formulate decisions have to do with the accuracy and timeliness of fire. Therefore, for weapon systems the fire control designers must be members of the Test Integration Working Group.

There is an inherent logic used in testing, which is shown schematically in Fig. 4-22. Testing of the hypothesis is accomplished using statistical procedures. For the assumptions underlying the statistical procedures to be valid, the test must be properly designed as an experiment, and the observations must be valid and use appropriate instrumentation. The Army has agencies whose sole responsibility is to

conduct tests. However, the materiel developer and, in this instance, the fire control developer must support the conduct of the test.
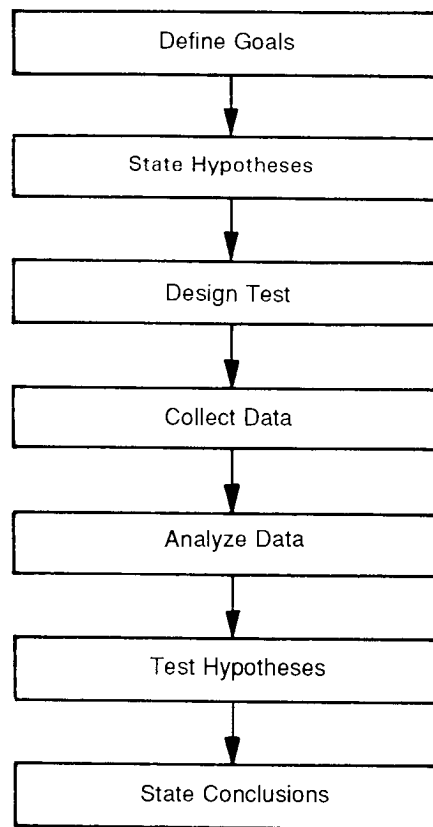
Figure 4-22. Test Program Logic

4-6.2 DEVELOPMENT TESTING

Development testing is conducted for systems of varying complexity, as stated in Ref. 36. These systems can range in complexity from the development of a main battle tank to a component of a main battle tank, such as a fire control system, to even a subcomponent of a fire control system, such as an optical filter. Such testing is usually performed at various levels using a development item or prototype of the system since the timing of the test is such that a production model is not generally available. At the appropriate level, however, development testing of production models must also be performed. The general purpose of this testing is to provide confidence that the production item will meet specifications so that further development and eventual production will be allowed to continue. As part of this testing, the system is stressed to a level representative of the operational environment. Follow-on production testing of production models is also performed at the appropriate time and at the appropriate level of technology.

Although much of the DT of developmental systems is conducted in a laboratory environment, many such tests are also conducted in the field or factory. For fire control equipment this usually requires live firing, and the weapon system crew for such tests is usually made up of contractor personnel. Instrumentation to record the actual trajectories of shells, to count the number of "hits" on target, and to obtain estimates of the bias and dispersion of bursts of rounds is used. Instrumentation on the fire control computer (FCC) collects data used to evaluate what is occurring in the system, and these are the most important data collected. It is necessary for the fire control designer to provide guidance with respect to the instrumentation necessary for such tests. Records of reliability must also be kept. The designer should also be present during testing to observe and, if need be, to provide insight into anomalies. Often, it is helpful if the designer's human engineering specialists and reliability and maintainability people also observe.

4-6.3 OPERATIONAL TESTING

At some level of system development a decision must be made as to whether or not to proceed with full-scale production. To make such a decision on a rational basis, DT (subpar. 4-6.2) must be combined with OT. OT is an important input to this decision, which considers the degree to which the system fills the Army's needs. For systems such as armored vehicles or aircraft, many factors need to be considered such as agility, speed, range, survivability, training requirements, and cost. With respect to fire control, however, the speed and accuracy of delivered rounds and the support requirements are of prime concern.

For OT a complete preproduction model of the system is required. This model should represent the production version and be equipped with the elements planned for the baseline system. The test is conducted at a Government facility to enable simulation of the mission conditions of the system, and in some cases testing at more than one location may be required.

The system will be tested by representative Army crews, so prior training of the crews is necessary. The personnel are normally provided by the proponent school within the US Army Training and Doctrine Command, e.g., infantry, air defense, etc. The physical setting must allow the system to be used under simulated mission conditions. For example, the test range must accommodate live fire of all round types, suitable target maneuvers must be possible (including terrain shielding), and the weapon platform must be free to maneuver.

The instrumentation used to measure weapon system parameters must be more accurate than the weapon elements that control the parameters. The instrumentation must include the timing of simulated engagements and the deviation of the projectile from the aim point, not just a hit/miss tally. In addition, records of reliability and availability must be maintained, and an attempt must be made to assess the training requirements and evaluate the implications on logistics.

4-6.4 TEST ENVIRONMENTS

As previously stated, the test environment is usually chosen to allow high-fidelity simulation of the engagement scenario. It is important that the environmental conditions that affect elements in the system are provided in the actual test engagements. For example, if the system includes a laser range finder, the atmospheric conditions must include dust, rain, smoke, etc., because the laser range finder will be used by soldiers on the battlefield under such conditions.

4-6.4.1 Armored Vehicle

Tests involving the main gun of tanks, such as the M-1 Abrams, can be conducted only at selected sites due to safety limitations. Tank projectiles, especially high-muzzle-velocity discarding sabot rounds, are capable of traveling long distances. Since there are only a few locations at which such firing is allowed, these test ranges are generally well-equipped. As required by the system specification, it should be possible to provide moving targets and maneuvering tank capabilities. Thus terrain suitable for targets and tanks to take fully or partially hidden positions must be available. In addition, controllable atmospheric obscurants and other effects specific to the system must also be available.

4-6.4.2 Air Defense

When live fire is used, drones or remotely piloted aircraft are employed as targets. There is the possibility that the target aircraft might have to be destroyed, and again there are few locations at which such tests can be conducted. These sites are generally well-equipped. It must be possible to fly the aircraft targets at the speeds and altitudes and with appropriate maneuvering ability to simulate the likely tactics of enemy aircraft and to verify specified system performance. Suitable terrain must be available for helicopter targets to find masked positions. Tracking facilities must be provided to keep a record of target locations. If a FLIR is used for target acquisition and/or tracking, testing must be performed under a variety of atmospheric conditions.

Because of the limitations of drone targets and the expense involved in using these flying targets, some of the testing may be performed without drone targets. For such tests, rounds are not actually

fired, and the trajectories are theoretical. Tracking performance of a weapon is often tested in this manner. (See subpar. 4-6.8 for a more complete discussion of an example air defense weapon system.)

4-6.4.3 Artillery

For indirect firing tests of artillery weapons, the impact or burst area of projectiles can be surveyed, and the termination point can be known quite accurately. A similar survey procedure supplemented by onboard navigation instrumentation or a system tracking the weapon can be used to locate the weapon accurately. For such tests the weapon is normally stationary during firing. Instrumentation is also required to measure the attitude of the weapon and the true azimuth of the gun barrel. The measurement precision and accuracy of the atmospheric temperature, pressure, and wind data over the altitude range of the projectile are generally assumed to be the same as they are for the weapon in combat since both test and combat data are obtained from the same type of meteorological equipment.

4-6.4.4 Aircraft

The two generic uses of Army airborne weapons are air-to-air and air-to-ground engagements. In both cases the weapon may be moving or stationary (hovering), and the target may be moving or stationary. The most difficult case is the air-to-air engagement in which both the aircraft and target are moving. In this case suitable instrumentation to measure the three-dimensional position and three-degree-of-freedom attitudes of the weapon and target systems must be provided. Ground-based tracking systems, both radar and optical, can be used to measure position. Attitude is more difficult to measure. For the weapon system the position of the gun barrel or rocket launcher has to be known. For the target, especially if it is a scaled down model, the attitude is required in order to calculate the vulnerable area. As with air defense weapons, dry-fire testing is also used. Environmental considerations for aircraft weapons testing are similar to those for ground weapons. However, additional criteria must be included to consider higher operational speeds, maneuvering capabilities, and conditions relevant to altitude such as turbulence, icing, and temperature.

4-6.4.5 Small Arms

Although there are many sites at which live-fire small arms testing can be conducted, there are few at this time that are adequately instrumented. The quest for "realism" is essential to evaluate the tests, and the Army has tended to favor firing conditions that attempt to simulate what shooters might face in combat. To achieve such realism, the firing range must have both fixed and moving targets and a terrain that provides for masking. "Pop-up" targets are used to simulate the brief appearances of firing opportunities. Means must be provided to control the selection of targets and the timing of their appearances. Instrumentation to measure the location of rounds as they pass through the target plane must be provided in order to measure miss distance.

4-6.5 TEST DESIGN

Generally, fire control systems are affected by many factors such as weather, target motion, equipment variations, etc. For this reason factorial experimental designs are frequently used. Under this design approach every combination of factors (those believed to be important) constitutes a cell, and a number of trials must be carried out for each cell. Clearly, as the number of factors increases, so does the cost of the test. Thus the design of tests is limited by practical considerations.

Tests are designed as experiments with stated hypotheses. The objective of a particular test must be clearly stated because it will directly impact the formulation of the hypothesis. For example, bursts of a given number of a specific round type are required to fall within a certain range of dispersion. This statement is an objective. The results of testing for this objective will indicate that the round type being tested will have or will not have a dispersion equal to or less than a given value of variance at a given confidence level. Technically, only the negative or null hypothesis is tested, but its rejection allows acceptance of the positive alternative. This is an example of one type of factor. However, in addition, the environmental conditions under which such performance is to be tested must be determined. The combination of these environmental factors and the dispersion test constitutes a cell.

The statistician will have selected the appropriate statistical tests that will be used to test the hypothesis after data collection is complete. These statistical tests of differences relate only to the error that arises from testing only a sample. One question to be asked, for example, is what is the probability that a given (large) difference arises by chance?

Because a decision, such as whether or not to start full-scale production of the system, must be made, evaluative inquiry must be undertaken. This is usually performed by personnel at management levels within the Army. The appropriate question now is "If the dispersion of this new weapon is a given number of meters less than that of the older weapon, is it worth the expense to develop the new weapon to achieve this improved accuracy?".

In addition, the test instrumentation must be selected to be consistent with the required objectives. In the previous example, if a dispersion of 1 m at a given range is required, an instrument providing a ± 2-m resolution is clearly unacceptable. Extending this same concept to data analyses implies that a minimum round off of 0.1 m is required.

These same criteria can be used for time parameters. For example, if the example gun is required to fire at a rate of 60 rounds per minute, the data acquisition system must also be capable of at least 60 acquisitions per minute. If off-line processing is used, there are no speed requirements. However, if real-time processing is used, the combined data acquisition and data processing must also be capable of handling at least 60 events per minute.

Finally, the overall cost of testing can be substantial in terms of manpower and equipment. Therefore, it is important that backup equipment be available in the event of a component breakdown.

Everything discussed in this subparagraph must be documented in a test design report, which is distributed to everyone involved in the test.

4-6.6   TEST EXECUTION

At the start of system development a TEMP is prepared. Generally, the fire control design team supplies one or more individuals to support the test. As early as possible, this person must become familiar with the TEMP, the goals of the test, the test design, and the test plan. The test plan is usually prepared by the organization to conduct the test. Typically, when such a test plan is developed, a draft is prepared and distributed for comment to those involved with the system or test. The test plan takes the requirements of the test design and translates them into the specific, day-by-day activities of the test. The test plan also documents the resources required to conduct the test. Fire control personnel must be certain that the test scenarios are adequate to evaluate the software as well as the hardware and crew performance levels.

The fire control support personnel should review the forms to be used to document the conduct of the test in order to ensure that all possible contingencies are adequately covered. Similarly, the fire control expert must interact with the instrumentation people to ensure that the proper measurements are being made and to assure that the fire control equipment is not affected by the instrumentation used to measure its performance.

The fire control representative must be on-site during the test in order to deal with irregularities that affect the fire control or the data related to the fire control. He must continually satisfy himself that the test is being conducted in a manner which will provide valid data for hypothesis testing and that the test is being properly documented.

4-6.7   TEST DATA ANALYSIS

The test design document states the objectives of the test, the hypotheses derived from the objectives, and the statistical tests selected to test the hypotheses. The test plan specifies the form of the data (e.g., 9 track, 6250 bpi tape), any special software requirements (e.g., reformatting data), and the computer. The data processing site and the software to be used to calculate the statistical results are also specified.
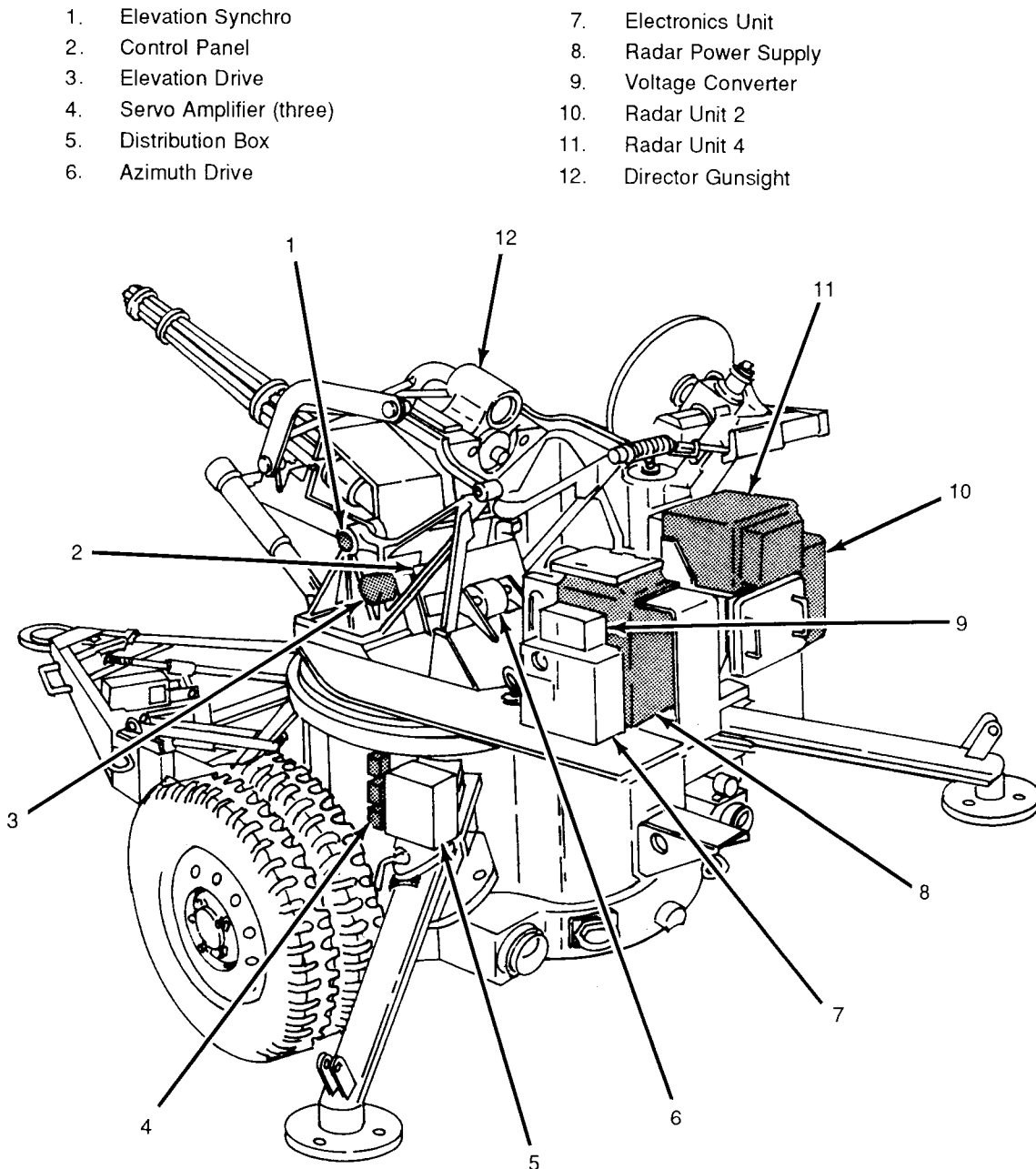
The fire control design representative to the test may want to conduct early reviews of the data to ensure the procedures and instrumentation are adequate.

4-6.8 SYSTEM EVALUATION EXAMPLE

The Product-Improved Vulcan Air Defense System (PIVADS) has undergone system tests for hardware, software, and overall weapon performance. This example illustrates the testing performed on the system for introduction of the 20-mm M940 MPT-SD ammunition. It is a test of the ballistics computation software implemented in EPROM.

4-6.8.1 Test Setup

The vehicle used for testing was the M167A2 PIVADS, Serial Number 418, illustrated in Fig. 4-23. The system baseline was established using Revision B software (currently fielded) by running off-line built-in test (BIT). The software integration test used three test circuit card assemblies. The test circuit card assemblies replaced the production configuration cards in the fire control processor (FCP). The

1. Elevation Synchro	7. Electronics Unit
2. Control Panel	8. Radar Power Supply
3. Elevation Drive	9. Voltage Converter
4. Servo Amplifier (three)	10. Radar Unit 2
5. Distribution Box	11. Radar Unit 4
6. Azimuth Drive	12. Director Gunsight

Figure 4-23. Product-Improved Vulcan Air Defense System (PIVADS) (Ref. 37)

circuit cards were a socketed computer memory board (CMB), a socketed servo controller board (SCB), and a test data transmission board (DTB). The socketed CMB and SCB were the same as a production card with the exception of sockets on the circuit card for the EPROMs. The test DTB was the primary tool used to evaluate software modifications. It provided the capability to collect all of the required data variables from the FCP data bus (Link 2) to evaluate software changes. Fig. 4-24 depicts the data collection setup that was used.
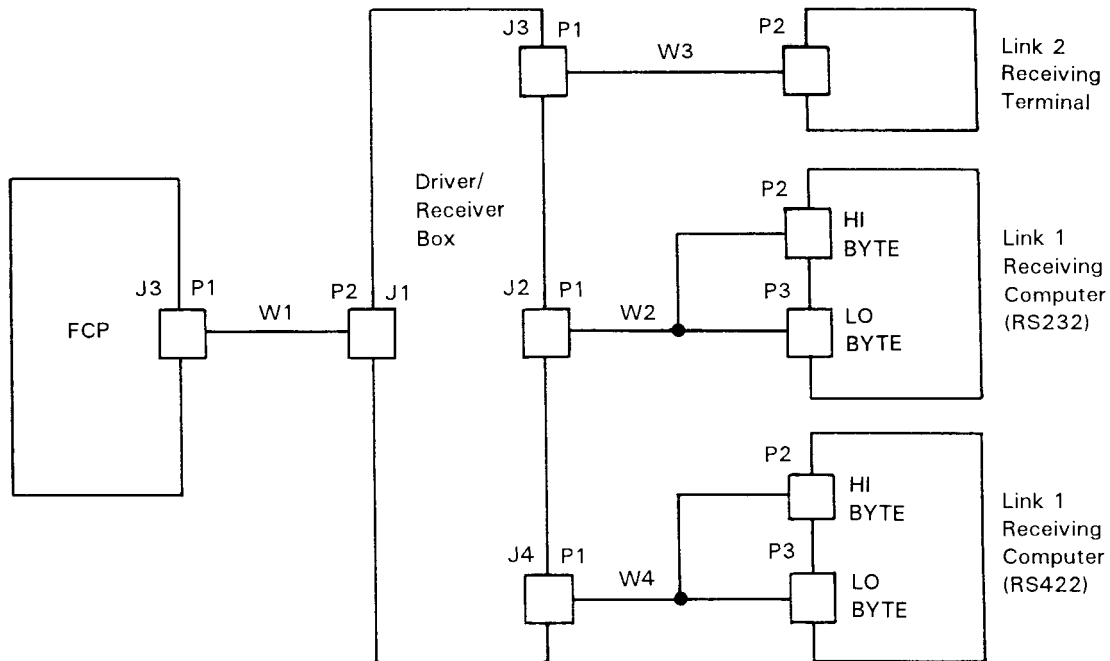
Figure 4-24. Data Link Hookup (Ref. 38)

4-6.8.2 Test Procedures

All testing was performed with Revision C software, except where noted. A baseline series of tests was performed to verify that the system was operational. This was performed by executing off-line BIT (setup E001-E065) with Revision B software and then repeated with Revision C software (test load). Testing would not continue unless an "A2" message was displayed on the ballistics/BIT panel shown in Fig. 4-25. Off-line BIT performed the RAM, read-only memory (ROM), and arithmetic logic unit (ALU)
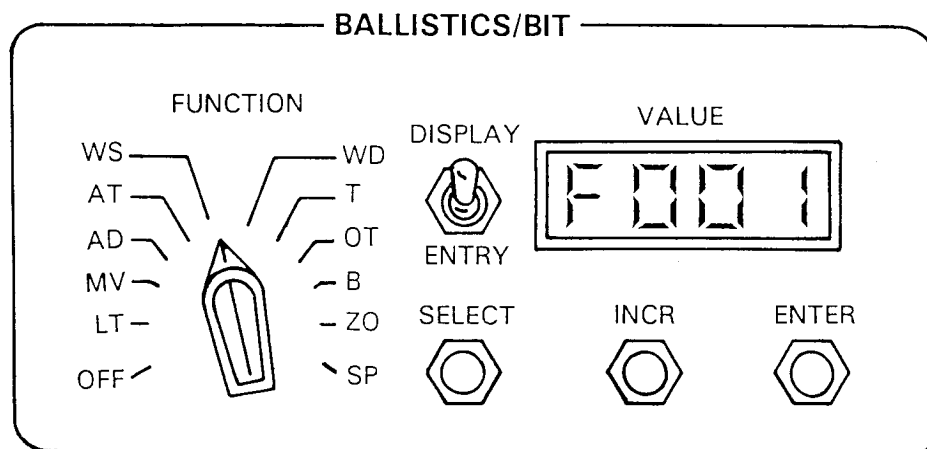
Figure 4-25. Ballistics BIT Control Panel (Ref. 39)

checks on the CMB and SCB. Prior to the start of each test day, off-line BIT was performed with the Revision C software load.

The functional description of the M940 ballistics test is included in the PIVADS Program Performance Specification (Ref. 39).

The ballistics verification test validated implementation of the M940 MPT-SD ballistics coefficients. Table 4-1 identifies the input variables used to generate the ballistic solutions and the critical outputs. The ballistic output data were compared to the ballistic simulation model to verify that the solution was correct. The test cases run were identified in Test Matrix 1.a.1 (Table 4-2) and Test Matrix 1.a.2 (Table 4-3). Test Matrix 1.a.1 was run when Revision B software was being used as a baseline (production CMB). Test Matrix 1.a.2 was run to test/verify Revision C software. The only differences between Matrix 1 and Matrix 2 are modifications made to the muzzle velocity setting step increment/decrement. The testing was performed with the PIVADS in manual mode under static conditions.

1. *Test Matrix 1.a.1, Revision B Software.* To establish a baseline, a wide range of test cases were run with the M246 HEIT (high-explosive incendiary tracer) Selection, Ammo Type 1. The nominal and off-nominal conditions for the input parameters tested in Table 4-1 were entered through the ballistics/BIT panel. Ballistic Test Matrix 1.a.1 (Table 4-2) outlines the specific off-nominal conditions, target ranges, target elevation, and ammunition types. Table 4-4 delineates the output data collected from the system data bus, Link 2 of the FCP. Data were collected when the ready-to-fire (RTF) flag was set, and the flag signified that the ballistic solution was closed. The output data collection was compared to the ballistic simulation model.

TABLE 4-1. BALLISTIC VERIFICATION TEST INPUTS AND OUTPUTS (Ref. 38)

INPUTS	ABBREVIATION OR ACRONYM	LOCATION
Quadrant Elevation	QE	Gunner's Quadrant
Target Range	CR	Control Panel
Ammo Type	AT	Ballistics/BIT Panel
Muzzle Velocity	MV	Ballistics/BIT Panel
Air Density	AD	Ballistics/BIT Panel
Wind Speed	WS	Ballistics/BIT Panel
Wind Direction	WD	Ballistics/BIT Panel
OUTPUTS	ABBREVIATION OR ACRONYM	LOCATION
Predicted Impact Range	R3	Link 2
Predicted Impact Elevation	E3	Link 2
Time of Flight	T2	Link 2
Superelevation	V2	Link 2
Drift	ORLS	Link 2
Range Wind Effect, Superelevation	EWR	Link 2
Crosswind Effect, Drift	WRLS	Link 2
Ready to Fire	RFT	Link 2

TABLE 4-2. BALLISTIC VERIFICATION FOR TEST MATRIX 1.a.1 (Ref. 38)

REVISION B PRODUCTION

CASE	MV	AD	WS	WD
1	5	100	0	
2	5	110	0	
3	5	80	0	
4	3	100	0	
5	7	100	0	
6	5	100	10	3200
7	3	90	0	
8	7	120	0	
9	–	80	0	
10	5	100	10	4800

Target Range: 500 and 1500 m
Quadrant Elevation: 0.10 and 0.90 rad

TABLE 4-3. BALLISTIC VERIFICATION FOR TEST MATRIX 1.a.2 (Ref. 38)

REVISION C

CASE	MV	AD	WS	WD
1	5	100	0	
2	5	110	0	
3	5	80	0	
4	2	100	0	
5	8	100	0	
6	5	100	10	3200
7	2	90	0	
8	8	120	0	
9	1	80	0	
10	5	100	10	4800

M246:

    Target Range: 500 and 1500 m
    Quadrant Elevation: 0.10 and 0.90 rad

M940:

    Target Range: 500 and 1700 m
    Quadrant Elevation: 0.10 and 0.90 rad

TABLE 4-4. BALLISTIC VERIFICATION TEST (Ref. 38)

LINK 2 OUTPUT

VARIABLE	ABBREVIATION OR ACRONYM	INDEX	OFFSET
Ammo Type	ATI	02	10C
Air Density	ADI	02	108
Muzzle Velocity	MVI	02	104
Wind Speed	WSI	02	110
Wind Direction	WDI	02	114
Range, Control Panel	CR	02	02A
Range, Predicted	R3	07	030
Elevation, Predicted	E3	07	03A
Time of Flight	T2	07	006
Superelevation	V2	07	01E
Drift	ORLS	07	022
Range Wind Effect, Superelevation	EWR	07	054
Crosswind Effect, Drift	WRLS	07	01C
Closure Criteria	IR3	07	00C
Ready to Fire	RTF	02	052

2. *Test Matrix 1.a.2, Revision C Software.* **Test matrix 1.a.2 was run with the M246 HEIT Selection, Ammo Type 1, to verify that the M940 ballistic implementation did not impact existing ammunition coefficients. The output (specified in Table 4-3) was compared to the Revision B software output. The outputs for each test case between the two software loads (Revision B and Revision C) should have been the same.**

Test Matrix 1.a.2 was repeated with the M940 MPT-SD Selection, Ammo Type 6. The output data (specified in Table 4-4) were collected and compared to the ballistic simulation model. In addition to verifying the M940 ballistics, the test was to verify the modifications made to the muzzle velocity step increment/decrement.

4-6.8.3 Test Results

The ballistic verification testing performed was to validate all of the software modifications made due to the M940 ballistics implementation. The critical issues of the test were as follows:

1. Did implementation of the modifications impact other ammo type coefficients?

2. Does the system compute the correct TOF, superelevation, and drift under nominal and off-nominal conditions?

3. Does the RTF flag set at the correct range (1900 m)?

4. Does the ballistic solution remain closed (IR3 < 5 m)?

5. Are lead angle commands generated from the ballistic solution?

To verify that existing ammunition coefficients were not impacted, test cases outlined in Test Matrix 1.a.1 were performed with Ammo Type 1, M246 HEIT. The test was performed using a production CMB containing Revision B software. Critical ballistic parameters (TOF, superelevation, and drift) were

collected. Using the Revision C software upgrade, test cases outlined in Test Matrix 1.a.2 were per-formed. This text matrix was performed with Ammo Type 1 (M246) and Ammo Type 6 (M940). The off-nominal conditions, namely, air density, muzzle velocity, wind speed, and wind direction, were the same between Test Matrices 1.a.1 and 1.a.2. Although the muzzle velocity setting values may be different in Cases 4, 5, 7, and 8, the change in off-nominal muzzle velocity is the same between the two test matri-ces, i.e., ± 30 m/s. Making a comparison between the Revision B and Revision C M246 ballistic output sampled in Table 4-5 verifies that implementation of the M940 ballistics did not impact other ammuni-tion types.

TABLE 4-5. TEST MATRIX 1, AMMO M246 (Ref. 38)

CASE	TOF REV B, s	TOF REV C, s	TOF SIMULATION, s
1	0.577	0.577	0.576
2	0.585	0.585	0.585
3	0.557	0.557	0.557
4	0.558	0.558	0.558
5	0.596	0.596	0.596
6	0.576	0.576	0.576
7	0.548	0.548	0.549
8	0.617	0.616	0.616
9	–	0.534	0.535
10	0.577	0.577	0.576

CASE	SUPER-ELEVATION, mrad		DRIFT, m		EWR, mrad		CROSSWIND EFFECT, DRIFT, m	
	REV B	REV C	REV B	REV C	REV B	REV C	REV B	REV C
1	2.875	2.875	0.031	0.031	0	0	0	0
2	2.910	2.918	0.031	0.031	0	0	0	0
3	2.770	2.781	0.031	0.031	0	0	0	0
4	2.770	2.781	0.031	0.031	0	0	0	0
5	2.965	2.973	0.047	0.047	0	0	0	0
6	2.863	2.875	0.031	0.031	0.117	0.121	0	0
7	2.723	2.730	0.031	0.031	0	0	0	0
8	3.074	3.078	0.047	0.047	0	0	0	0
9	–	2.656	–	0.031	0	0	0	0
10	2.875	2.875	0.031	0.031	0	0	0.484	0.484

Range: 500 m
QE: 0.10 rad

The comparison also verified the modification made to the muzzle velocity setting step change, i.e., changing muzzle velocity values from 15 m/s to 10 m/s per muzzle velocity step increment/decrement. In addition, the output ballistic value for the M246 was compared favorably to the simulation model output. Having this very close comparison validates the model used to verify the M940 ballistic outputs. To summarize, there was no significant difference in the M246 ballistic outputs of Revision B software,

Revision C software, and the ballistic simulation model.

   The ballistic verification test outlined in Test Matrix 1.a.2 was performed for the M940 round. All of the test cases met the acceptance criteria for TOF, superelevation, and drift except cases 4, 5, 8, and 9 at a 1700-m slant range and 0.90-rad quadrant elevation angle, as shown in Table 4-6. In these four test cases the TOF error (and the accompanying muzzle velocity (MV) and/or air density (AD) errors) was

   1. Case 4: +7 ms (+30 m/s MV)
   2. Case 5: −7 ms (−30 m/s MV)
   3. Case 8: −8 ms (−30 m/s MV, 120% AD)
   4. Case 9: +6 ms (+40 m/s MV, 80% AD).

   Acceptance criterion was ±5 ms.

TABLE 4-6. TEST MATRIX 1.a.2, AMMO M940 (Ref. 38)

CASE	SECONDS OF ARC		ERROR, ms
	BALL SIM TOF, s	PIVADS TOF, s	
1	2.672	2.672	0
2	2.841	2.841	0
3	2.416	2.417	+1
4	2.592	2.599	+7
5	2.756	2.749	−7
6	2.656	2.655	−1
7	2.464	2.469	+5
8	3.146	3.138	−8
9	2.334	2.340	+6
10	2.672	2.672	0

CASE	SUPER-ELEVATION, mrad		DRIFT, m		EWR, mrad		WRLS, m	
	BALLISTIC SIMULATION	PIVADS	BALLISTIC SIMULATION	PIVADS	BALLISTIC SIMULATION	PIVADS	BALLISTIC SIMULATION	PIVADS
1	9.515	9.539	0.402	0.406	0	0	0	0
2	10.231	10.277	0.452	0.453	0	0	0	0
3	8.456	8.531	0.332	0.328	0	0	0	0
4	9.178	9.234	0.380	0.375	0	0	0	0
5	9.871	9.871	0.427	0.422	0	0	0	0
6	9.515	9.484	0.402	0.406	2.315	2.293	0	0
7	8.648	8.672	0.344	0.344	0	0	0	0
8	11.574	11.582	0.548	0.547	0	0	0	0
9	8.122	8.164	0.310	0.313	0	0	0	0
10	9.515	9.555	0.402	0.406	0	0	5.26	5.2

Range: 1700 m
QE: 0.90 rad

Tolerances:
TOF ±5m
Superelevation ±1 mrad
Drift ±0.5 m
TGT Altitude of 1331 m

The TOF error was traced to the range input for the TOF equation "T2". The incorrect range input was caused by the off-nominal muzzle velocity range effect equation. Truncation errors within this four-term polynomial equation cause a 1-m error in computation per each 10 m/s range in muzzle velocity. This error, however, was magnified by a factor of three due to the test conditions of 30 m/s off-nominal muzzle velocity. A 3-m error in range input into the T2 equation resulted in TOF errors noted under the four test conditions.

The truncation errors are caused by using fixed point calculations within the system software. Fixed point calculations are used in order to compute the fire control solution in real time. At the extreme off-nominal conditions of slant range and quadrant elevation, the TOF errors noted are not considered significant.

The range in which the RTF flag is set for the M940 round is shown in Test Matrix 1.b (Table 4-7). Simulated incoming tracks were performed to verify that the flag was set at a 1900-m predicted impact range. In all cases this condition was met.

TABLE 4-7. RFT/BALLISTIC CLOSURE, TEST MATRIX 1.b, AMMO M940 (Ref. 38)

CASE	RANGE, m	RTF
1	1903 1892	Predicted RTF
2	1910 1899	Predicted RTF
3	1920 1894	Predicted RTF
4	1909 1880	Predicted RTF

The M940 ballistic closure loop was tested to verify that the ballistic solution remained closed throughout a target track. Test Matrix 1.b was performed to simulate incoming tracks. The ballistic closure (IR3) was monitored to verify that IR3 remains less than 5 m (IR3 < 5) throughout the target track. For all tracks the ballistic solution remained closed.

REFERENCES

1. P. G. Cushman, *HITPRO, Volume II (User's Manual)*, RE-TR-71-63, US Army Weapons Command, Rock Island, IL, 15 November 1971.

2. B. M. Lufkin, *The Air Defense Modern Gun Effectiveness Model (MGEM)*, AMSAA Technical Report No. 360, US Army Materiel Systems Analysis Activity, Aberdeen Proving Ground, MD, June 1982.

3. *Attack Helicopter Air-to-Air Fire Control System Simulation*, prepared by Teledyne Systems Company, Northridge, CA, for US Army Armament Research and Development Command, Dover, NJ, August 1983.

4. J. V. Beck and K. J. Arnold, *Parameter Estimation in Engineering and Science*, John Wiley & Sons, Inc., New York, NY, 1977.

5. A. Gelb et al, *Applied Optimal Estimation*, The MIT Press, Cambridge, MA, 1992.

6. R. W. Hamming, *Numerical Methods for Scientists and Engineers*, Second Edition, McGraw-Hill Book Company, New York, NY, 1973.

7. P. J. Rousseeuw and A. M. Leroy, *Robust Regression and Outlier Detection*, John Wiley and Sons, Inc., New York, NY, 1987.

8. S. F. Huling, M. Mintz, and W. Dziwak, *Enhanced Filtering and Prediction for AAA Fire Control: An Ap-*

plication of Game Theory and Time Series Analysis, **Algorithm and Paradigm Technology Co., Philadelphia, PA, for US Air Armament Research and Development Command, Dover, NJ, November 1980.**

9. **J. S. Przemieniecki,** *Introduction to Mathematical Methods in Defense Analysis*, **American Institute of Aeronautics and Astronautics, Inc., Washington, DC, 1990.**

10. **L. R. Cerrato and K. R. Pfleger,** *Multiple Round Hit Probabilities Associated With Combat Vehicle Fire Control Gun Systems*, **Report R-3011, US Army Armament Command, Frankford Arsenal, Philadelphia, PA, May 1974.**

11. **R. R. Beck and D. A. Croke,** *TACOM Simulation Catalog*, **US Army Tank-Automotive Command, Warren, MI, May 1991.**

12. **S. L. Meyer,** *Data Analysis for Scientists and Engineers*, **John Wiley & Sons, Inc., New York, NY, 1975.**

13. **E. Kreyszig,** *Advanced Engineering Mathematics*, **John Wiley & Sons, Inc., New York, NY, 1979.**

14. **A. D. Groves,** *Handbook on the Use of the Bivariate Normal Distribution in Describing Weapon Accuracy*, **Memorandum Report No. 1372, US Army Ballistic Research Laboratory, Aberdeen Proving Ground, MD, 1961.**

15. **M. Abramowitz and I. A. Stegun,** *Handbook of Mathematical Functions*, **Dover Press, New York, NY, 1984.**

16. **I. S. Sokolnifoff and R. M. Redheffer,** *Mathematics of Physics and Modern Engineering*, **McGraw-Hill Book Company, New York, NY, 1958.**

17. **G. Arfken,** *Mathematical Methods for Physicists*, **Academic Press, New York, NY, 1968.**

18. **J. G. Tappert,** *General Theory of the Propagation of Errors in Analog Computers*, **Technical Note No. TN-1106, Frankford Arsenal, Philadelphia, PA, 15 September 1968.**

19. **K. R. Castleman,** *Digital Image Processing*, **Prentice-Hall, Inc., Englewood Cliffs, NJ, 1979.**

20. **K. S. Miller and F. J. Murray, "A Mathematical Basis for an Error Analysis of Differential Analyzers", J. Math. Phys. 32 (1953).**

21. **T. F. Jones, Jr.,** *The Propagation of Errors in Analog Computers*, **Thesis, Massachusetts Institute of Technology, Cambridge, MA, 1952.**

22. **J. C. Glynn and R. C. Pfeilsticker,** *Hit Probability of the Vigilante System*, **Vol. 1, Frankford Arsenal, Philadelphia, PA, 1959.**

23. **E. O. Doebelin,** *Measurement System: Application and Design*, **McGraw-Hill Book Company, New York, NY, 1966.**

24. **A. Papoulis,** *Probability, Random Variables, and Stochastic Processes*, **McGraw-Hill Book Company, New York, NY, 1965.**

25. **O. I. Elgerd,** *Control Systems Theory*, **McGraw-Hill Book Company, New York, NY, 1967.**

26. **B. C. Kuo,** *Analysis and Synthesis of Sampled-Data Control Systems*, **Prentice-Hall, Inc., Englewood Cliffs, NJ, 1963.**

27. **S. S. Soliman and M. D. Srinath,** *Continuous and Discrete Signals and Systems*, **Prentice-Hall, Inc., Englewood Cliffs, NJ, 1990.**

28. **E. O. Brigham,** *The Fast Fourier Transform and Its Application*, **Prentice Hall, Inc., Englewood Cliffs, NJ, 1988.**

29. **MIL-HDBK-759A,** *Human Factors Engineering Design for Army Materiel*, **31 December 1985.**

30. **P. M. Fitts, "Engineering Psychology and Equipment Design",** *Handbook of Experimental Psychology*, **S. S. Stevens, Ed., John Wiley & Sons, Inc., New York, NY, 1951, pp. 1329-30.**

31. **A. Tustin, "The Nature of the Operator's Response in Manual Control and Its Implications for Controller Design", Journal of the Institute of Electrical Engineers, 94, 190-202 (1947).**

32. **D. P. Siewiorek and R. S. Swarz,** *The Theory and Practice of Reliable System Design*, **Digital Press, Bedford, MA, 1982.**

33. **B. A. Chubb,** *Modern Analytical Design of Instrument Servomechanisms*, **Addison-Wesley, Reading, MA, 1967.**

34. **J. W. Brewer,** *Control Systems: Analysis, Design and Simulation*, **Prentice-Hall, Inc., Englewood Cliffs, NJ, 1974.**

35. **G. J. Thaler and R. G. Brown,** *Servomechanism Analysis*, **McGraw-Hill Book Company, New York, NY, 1953.**

36. **AR 70-10,** *Test and Evaluation During Development and Acquisition of Materiel*, **1986.**

37. **T. Cullen and C. F. Foss, Eds.,** *Jane's Land-Based Air Defense 1992-1993*, **Jane's Publishing Company Limited, London, UK, 1992.**

38. **S. Haas,** *Product-Improved Vulcan Air Defense System (PIVADS) Software Integration/ Test Plan*, **US Army Armaments Research, Development, and Engineering Center, Picatinny Arsenal, NJ, October 1990.**

39. *PIVADS Program Performance Specification*, **SW 125 63296, Revision. B, Lockheed Electronics, Inc., Piscataway, NJ, May 1987.**

CHAPTER 5
DESIGNING FOR RELIABILITY, MAINTAINABILITY, EASE OF OPERATION, AND SAFETY

This chapter presents design factors that must be considered during development of fire control systems. It defines and considers reliability and maintainability testing, presents operational environment requirements/testing, and discusses maintenance concepts. The man-machine interface requirements, training strategies, and system safety are presented.

5-1 INTRODUCTION

Most Army fire control equipment must be able to perform in any climate and over all terrain. Components and systems are either installed on vehicles, such as tanks and self-propelled or towed guns, or intended for temporary ground installation. They must be designed for transportability by soldiers, ground vehicles, and aircraft and for quick assembly and disassembly. Much of the equipment may also be air-dropped for immediate use.

Equipment designed to be 100% effective will clearly be ineffective under battle conditions if it is inoperative half the time because of low reliability or maintenance difficulty in the field. Similarly, the accuracy and effectiveness of the equipment are diminished in proportion to the soldier's inability to operate the system under the conditions at hand. Therefore, the design, must include (1) maximum reliability under all foreseeable conditions, (2) ease of maintenance, (3) human engineering to ensure effective operation, and (4) in most cases, transportability. To the extent the designer fails in any of these respects, he or she reduces any other advantages in the design.

Both reliability and maintainability affect the time the equipment is available, and availability is the important parameter of interest. Reliability can be expressed as the mean (or average) time between failures (MTBF). Similarly, maintainability can be expressed as the mean time to repair (MTTR) (given that a failure has occurred). Thus quantitatively availability is

$$Availability = \frac{MTBF - MTTR}{MTBF + MTTR}.$$ **(5-1)**

This relationship shows how both reliability and maintainability critically affect the mission performance of fire control equipment. Given the required system availability and one of the "mean times", it is possible to derive the other.

It is worth emphasizing that most of the resources available to industry for operating and maintaining complex and difficult equipment are simply not available to the Army in the field. For example, industry can hire and take the time to develop skilled mechanics. One major corporation employs only persons with high school diplomas or better as mechanics for electronic controls, trains them for at least two years in practical and theoretical postgraduate work, and continues to train them for at least two more years on the job before they are considered "qualified craftsmen". The requirements of many other companies are equally rigorous. On the other hand, the Army has nonhigh school graduates among its recruits, and the total term of initial enlistment is often shorter than the education and training period of industry. Accordingly, Army fire control equipment must be designed to be operated and maintained by personnel with perhaps minimal education and training, i.e., men and women with perhaps a general equivalency diploma, some specialized schooling, and a limited amount of in-service training. When times of national emergency occur, civilians from all walks of life enter the service and even less time is available for training, so the proportion of trained, experienced personnel declines.

Because it operates from fixed facilities, industry can control the environment in which much of its equipment operates. Humidity and temperature are controlled in many plants, and it is common practice to perform delicate assembly, test, and repair operations in special "clean rooms" with nearly all dust

eliminated, with humidity and temperature maintained within narrow ranges, and with vibration and sound drastically attenuated. At the other extreme, most Army fire control equipment must operate out-doors in a mobile mode, in all types of weather, and usually in an environment of intensive shock and vibration. Also any repair and maintenance at the organizational level are performed under these field conditions.

5-2 RELIABILITY

A fire control system that does not operate to its standards in combat is a most serious liability. Not only does it prevent the crew from bringing timely, effective fire on the enemy, but it also places friendly forces in jeopardy. Although modern fire control systems are complex, the designer must achieve reliability.

Reliability requirements must be met for fire control systems that will be used in field environments. These include extremes in climate and the actions of mechanical and electrical forces. The designer must be aware of these environmental conditions and use components, packaging, and protective devices to assure proper operation.

The paragraphs that follow discuss steps the designer can take. Appropriate standards and specifications, which must be adhered to, are mentioned to create awareness of some of the available aids.

5-2.1 ENVIRONMENTAL FACTORS

Most types of Army fire control equipment should normally be designed for any ground environment anywhere in the world. (By contrast, much Navy equipment is designed for specific environments that may be violent or extreme but are much more narrowly defined. For example, with underwater ordnance equipment the designer may be able to plan for a relatively narrow temperature range extending over about 35 deg C, water of fairly constant salinity, predictable pressures, and a certain amount of shock and vibration.)

For today's mobile Army it is also vital to plan in the design and packaging of the equipment for air transportation at high altitudes and speeds and for airdrop.

It is usually impossible to design optical, electronic, or mechanical equipment so that it can simply be picked up in one extreme, e.g., the tropics, and used without alteration in an opposite extreme, e.g., the arctic regions. Accordingly, the designer must design adaptability into the equipment to permit accommodation of differing environments. For example, a device might contain either elements that can compensate for temperature differentials or elements that can be adjusted in the field. The optimum solution would be a function of the kind of equipment and the environmental extremes involved. A few examples are adjustable heating and cooling elements; knob adjustments to compensate for optical changes due to thermal contraction and expansion or variations in electrical characteristics with temperature; easily installed protective coverings against various environments; and if the equipment must be altered, modular construction to permit quick replacement of the parts affected by the environmental change.

Designing for environmental extremes must be considered from the points of view of (1) designing against the destructive or distorting effects of the environment and (2) designing for ease of maintenance and operation in extreme environments.

The environments considered in detail are climatic extremes, mechanical forces, and interferences from various sources, man-made and natural:

1. *Climatic Extremes*. These conditions include thermal and humidity stress, precipitation, wind, and penetration and abrasion by blowing sand, dust, or snow. An indirect product of climate is fungus, which can be devastating to improperly chosen or protected materials in the tropics. Atmospheric pressure is an increasingly important consideration, particularly in air transport since fire control equipment must be airborne at times.

2. *Mechanical Forces*. These conditions include shock, vibration, and acceleration. These forces may be transmitted from the vehicle in which the equipment is mounted, from explosions caused by enemy fire or fire from the vehicle, from an aircraft or other vehicle in which the equipment is being transported, and from landing on hard ground during an airdrop.

3. Interferences. **These conditions include radio frequency (RF) and other emissions from adjacent equipment and deliberate jamming by the enemy; emissions due to nuclear explosions are also grouped in this category.**

For the purposes of Army weapons the climatic data in such documents as AR 70-38, *Research, Development, Test, and Evaluation for Materiel for Extreme Climatic Conditions,* **(Ref. 1) will suffice for most purposes. This Army regulation divides climatic conditions into five classifications for design purposes:**

1. **Hot-dry (temperature to 50°C)**
2. **Warm-wet (temperatures to 35°C, precipitation to about 2.0 m/yr average)**
3. **Intermediate (temperatures 40°C to –32°C, moderate rainfall)**
4. **Cold (temperatures to –45°C)**
5. **Extreme cold (temperatures to –60°C).**

Each of these conditions is defined in terms of extreme air temperatures and solar radiation as a function of altitude, water temperatures, maximum precipitation over short periods, snow loads, icing phenomena, winds, atmospheric pressures, and blowing snow, sand, and dust. Charts show where and in which season each condition occurs.

AR 705-15 recommends that all combat and support equipment be designed to operate under intermediate conditions and that modification kits be supplied wherever possible to adapt equipment to cold, hot-dry, and warm-wet conditions. Only in the extremely cold areas is it expected that operations may require a preponderance of equipment specially designed for an extremely cold climate.

Nearly everywhere, conditions change a great deal with the season. For example, parts of India experience hot-dry, warm-wet, and intermediate weather, depending on the time of year, and in Greenland the weather varies from intermediate to extreme cold.

MIL-STD-210, *Climatic Information to Determine Design and Test Requirements for Military Systems and Equipment,* **(Ref. 2) gives a breakdown of extreme ground conditions in terms of extremes of heat, cold, humidity, precipitation, wind, snow, dust, and atmospheric pressure. Additional details include the range of infrared (IR), ultraviolet (UV), and visible radiation intensities and the duration of maximum temperatures during 24-h cycles.**

MIL-STD-210 further specifies the extremes that are encountered in the following categories of operations: (1) operation ground, worldwide, (2) operation ground, arctic winter, (3) operation ground, moist tropics, (4) operation ground, hot desert, (5) operation shipboard, worldwide, and (6) storage and transit, short-term, worldwide. Fire control equipment should be designed for the extremes in Categories 1 and 6, where possible.

MIL-STD-210 also includes a detailed tabulation of various atmospheric extremes up to 30,480 m. This information is chiefly of interest to aircraft and missile designers but is also of concern to designers of ground equipment that may be transported by high-altitude aircraft. For example, embrittlement of cold steels can cause devastating damage under conditions of shock and vibration. It may be necessary, therefore, to specify that equipment made of cold steel be transported in a heated, pressurized cabin.

Components, assemblies, and even systems must be subjected to environmental testing to assure suitability. MIL-STD-810, *Environmental Test Methods,* **(Ref. 3) prescribes the procedures that must be followed and discusses acceptance criteria. Strict adherence to this standard is essential.**

Fire control equipment is subject to mechanical vibrations, shock, and high-acceleration forces as a result of the following:

1. **Transport by air, sea, or land**
2. **Motion of the vehicle on which the equipment is mounted (Vibration and shock arise from rough terrain, wheel shimmy, engine and tire vibrations, structural vibrations, and on tracked vehicles, the track striking the ground.)**
3. **Firing guns or other weapons on or near which the equipment is mounted**
4. **Detonations of bombs, projectiles, and related explosive ordnance.**

Damage during transportation can be guarded against by proper packaging and handling procedures. Damage due to vehicular motions, weapons, and explosions can be eliminated only by proper design of the equipment and its mounting.

With ground equipment high g-forces are of concern primarily as a part of the vibration and shock

problem; higher forces are not likely to be encountered that are due, e.g, to the acceleration of the vehicle in which they are mounted or carried. Vibration is a continuing periodic motion induced by an oscillating force that results from an unbalanced mass, mechanically, or from a fluctuating magnetic force, electrically. On the other hand, shock is the effect of a suddenly applied force on a structure or a sudden change in the motion of the structure. On-carriage fire control equipment, for example, experiences shock effects when the weapon is fired or when nonpenetrating ballistic impacts are achieved nearby. Transient vibrations that may be high frequency and high amplitude are produced. The amplitude may become so high that brittle materials fracture and ductile materials yield, and high-frequency vibrations may occur at the resonant frequency of an optical element within an optical sight and cause it to fail or shatter. Another characteristic of shock resulting from abrupt changes in motion is the presence of large accelerations that can be transmitted to components and cause physical damage or loss of accuracy under extreme conditions. The destructive frequencies induced by shock or vehicular motion are generally high frequencies of 10 to 25 Hz. Therefore, an important goal of designing and mounting is to ensure that the equipment will not have natural frequencies in that range (or its harmonics), i.e., natural frequencies should be higher than the destructive range. Low frequencies, such as those induced by the natural frequency of vehicle suspension, are not normally damaging provided that either the amplitude is not excessive or adequate damping is designed into the suspension.

RF interference is a major problem in designing fire control equipment for the Army. In many other types of installations of electronic equipment, the sources, frequencies, and amplitudes of interference can be predicted quite accurately, and proper shielding can be provided. However, because it is portable and subject to use almost anywhere—near radio and radar stations, high-kilovolt generating and transmission systems, and military electronic equipment of various types, most Army fire control equipment must be designed against interference over a broad spectrum of RF energy.

The fire control system designer must be especially sensitive to the normal expansion and contraction of materials. The range of temperatures over which fire control must meet its functional specifications may be from –55˚ to +50˚C. Since many tolerances are necessarily tight, it is vital that the materials used be able to maintain these tolerances. For example, the alignment between a sighting element, such as a tank periscope, and the gun tube must be maintained precisely. Failure to achieve this alignment under all temperature conditions results in failure of the mission.

In hot-wet tropical conditions moisture is inevitably present. In the case of optical sighting equipment, moisture can condense and thereby render the sight useless. Similarly, fungous spores can cause growths that limit visibility. Optical systems are generally sealed to eliminate these problems, and it should be evident that other elements also require sealing. Desiccants within sealed elements are also used sometimes.

When designing active radar equipment and communications systems, the designer must anticipate that the enemy will use electronic countermeasures (ECM). ECM techniques are many and varied, and the specialist designer must be aware of how these techniques function. Some equipment can be made resistant to ECM, or electronic counter-countermeasures (ECCM) can be used to achieve continual functioning of the equipment despite the ECM. The ECM threat is so great that in some instances passive detection and tracking systems, e.g., IR, have been substituted for active systems such as radar.

Nuclear weapons can produce electromagnetic pulses. When severe, these pulses can affect electronic components, such as integrated circuits, and render them useless if they are not properly protected. Shielding, bypassing, and using hardened components are required. The designer should contact an expert in electromagnetic interference (EMI).

The following Engineering Design Handbooks contain detailed discussions of the operational environments of Army equipment: AMCP 706-115, *Environmental Series, Part One, Basic Environmental Concepts*; AMCP 706-116, *Environmental Series, Part Two, Natural Environmental Factors*; AMCP 706-117, *Environmental Series, Part Three, Induced Environmental Factors*; and AMCP 706-118, *Environmental Series, Part Four, Life Cycle Environments* (Refs. 4 through 7, respectively).

5-2.2   DESIGNING FOR RELIABILITY

Reliability and maintainability are discussed under different headings in this chapter because different aspects of design are involved in each. However, by producing reliable equipment, manufacturers have done much to solve the problems of maintainability; equipment that is 100% reliable for its intended life is always available and requires no corrective maintenance. Reliability depends to a large extent on proper manufacturing procedures and quality control, but the design engineer can make major contributions in this field. Reliability must be designed into the equipment; it cannot be built into it.

Reliability has become a major issue. In fact, reliability engineering has become a specialty in its own right. The reasons for this are

1. Increased complexity of equipment

2. Short transition time between the theoretical laboratory stage and engineering design and production in many fields. (Consequently, engineers are working increasingly close to "the limits of experience".)

3. Close tolerances and accurate alignments and consequent careful process controls required in many technologies

4. Increased complexity of industrial and military organizations

5. Increased chance of human error resulting from the foregoing reasons

6. Assurance that reliability will be considered and demonstrated at each step of the development process.

Modern reliability methodology is derived from the mathematics of probability and statistics and, when effectively applied, demands the close cooperation of all engaged in the design, production, and testing of an item. Although detailed discussion cannot be presented here; there are numerous books on this subject. The various means of achieving reliability are summarized in the paragraphs that follow. The following handbooks comprise a complete treatment of reliability:

1. AMCP 706-196, *Development Guide for Reliability, Part Two, Design for Reliability* (**Ref. 8**)

2. AMCP 706-197, *Development Guide for Reliability, Part Three, Reliability Prediction* (**Ref. 9**)

3. AMCP 706-198, *Development Guide for Reliability, Part Four, Reliability Measurement* (**Ref. 10**).

Reliability must be considered in the practical context of the equipment being designed, i.e., the concern is with the reliability of fire control equipment in the actual environments described in par. 5-2 rather than in any abstract or theoretical context. When designing a reliable fire control system, the engineer must always keep in mind the main purpose of the equipment: to ensure first-round target hits. There are also secondary goals, such as light weight, low silhouette, transportability, and ease of maintenance and operation. MIL-HDBK-217, *Reliability Prediction of Electronic Equipment*, (**Ref. 11**) contains detailed information on reliability. MIL-STD-785, *Reliability Program for Systems and Equipment Development and Production*, (**Ref. 12**) contains program requirements to assure reliability of systems.

If other things are equal, the more complex a system, the greater the chance of failure. Reliability can be expressed as the probability of successful operation: therefore the reliability of the system is equal to the product of the probabilities of successful operation of its parts if they are statistically independent. Thus it is possible to increase the reliability of a fire control system directly by making it as simple as its performance requirements permit, e.g., by using as few subsystems and components as possible that must function to carry out the end function of the system as a whole. (This rule, however, does not apply to parallel or backup subsystems; see the discussion of redundancy that follows.)

Redundancy—overdesigning, or providing backup or alternate systems—often provides a direct counter to the product rule of reliability, i.e., the more alternate subsystems there are, the greater the probability that one of them—and, therefore, the system as a whole—will operate satisfactorily. At first glance redundancy seems to be incompatible with the ideals of light weight and compact construction, but it should not be dismissed without careful consideration. In many areas of technology such lightweight and compact components have been achieved that alternate subsystems can be added without any significant increase in total weight and size. This fact is not only true in integrated circuits but also in laser ring gyroscope technology, hydraulics, and other fields. The increase in reliability and the increase in weight, size, and complexity caused by adding backup systems and the extent to which the equipment itself is critical should all be analyzed to determine whether redundancy should be designed into the system.

In computer applications, redundant hardware is routinely used to assure continuous operation and to avoid loss of data in the event of hardware failure. The design of the software is key in these cases since it must allow for continued performance of mission-essential functions while it allows for degraded operation or failure of other functions.

The word "design" implies that something new is being developed. If a new system is made up largely of relatively untried components and subsystems, it is likely that little is known about their behavior in many environments. When two or more such items are combined, their interaction with one another may be ascertained only after extensive testing.

A standard item may be defined generally as any commercially available item or any item in the federal stock system, i.e., an item that does not have to be specially designed for some particular use. In this context "standard" also implies conformity to military or other federal specifications and industrial standards, such as those of the National Electrical Manufacturers Association (NEMA).

Use of components, subsystems, and materials that have been proven in many types of operation greatly increases reliability. The engineer should therefore operate "at the limit of experience" only when necessary to achieve a specific requirement. If new components, such as integrated circuits, are to be embedded into existing designs, these components should have been subjected previously to a thorough reliability testing program.

5-2.3 RELIABILITY TESTING

For major systems, reliability testing may be made a formal component of the development program or the reliability program. (See Ref. 12.) The purpose of these tests is to provide assurance that the equipment will operate in its battlefield environment without failure for the length of time specified.

It is important that reliability test plans be reviewed carefully to be certain they are cost-effective. Reliability testing must be appropriate to the type of equipment and must be tailored to enhance the reliability of the equipment without having a serious effect on cost or schedule. Generally, there are four types of reliability tests to consider for inclusion in the various phases of a development program:

1. *Environmental Testing*. During development, environmental stress testing is conducted on components and assemblies to determine whether or not there are any weak elements. The item being tested is subjected to stress to stimulate failures. The environmental stress need not simulate the actual environment in which the item is to function, but it must cause any weak items to be detected.

Early in the development program an environmental stress plan is prepared and submitted to the program manager (PM) for approval. It usually includes a description of the types and duration of stress, identification of the items to be tested, identification of the failure-free duration of the test by item, and a description of how the performance of the item will be monitored.

Any items that fail the environmental stress testing are subject to a report. The report indicates recommended corrective action whenever possible, which might include substitution of an alternate item, changes in material, or improved workmanship techniques.

2. *Reliability Growth Testing*. A reliability growth testing program is undertaken to detect and correct reliability deficiencies and to verify the effectiveness of the corrective actions taken. Prototypes of a system or subsystems may be used as the test items since this testing should take place as soon as possible during development.

The criterion used to evaluate reliability may be mission reliability or basic reliability or a combination of both. Mission reliability refers to failures that render the system incapable of performing its mission, wheras basic reliability refers to any failure that allows the system to continue to function, albeit with some degradation.

Growth testing emphasizes performance monitoring, failure detection, failure analysis, and the incorporation and verification of design changes.

A test plan is prepared for submission to the PM for approval. The plan addresses test objectives; equipment to be tested; test conditions, duty cycle, and duration; test facility, equipment, and instrumentation; and rationale and procedures for corrective action.

3. *Reliability Qualification*. A reliability qualification test is conducted to determine whether or not the specified reliability requirements have been achieved. Test items must be representative of the pro-

duction configuration. Reliability testing may be integrated with other system tests. (See par. 4-6 for further discussion.)

The test plan must be prepared in accordance with the requirements of MIL-STD-781, *Reliability Testing for Engineering Development, Qualification and Production* (Ref. 13). The plan is submitted to the PM for approval and includes identification of the equipment to be tested, description of the test environment and duration, test procedures and setup, test schedule, and discussion and justification of the criteria to be used.

4. *Production Reliability Testing.* Production reliability acceptance tests are performed to determine whether or not and to what extent reliability is degraded as a result of design changes or changes in production techniques or processes. This testing is of course performed on production equipment. A test plan is prepared and submitted to the PM. Its contents are the same as those of the reliability qualification test. If the system is being developed by a contractor, the government development agent specifies the required reliability testing and reporting in the statement of work.

5-3 MAINTAINABILITY

The previous paragraphs discuss the subject of reliability. This paragraph considers maintainability: a characteristic designed into the equipment that is a measure of the ability of an item to be retained in or restored to a specified condition when maintenance is performed by personnel having specified skill levels and using prescribed procedures and resources of each prescribed level of repair. Maintainability is not to be confused with maintenance, which is essentially the response to the maintainability program, i.e., the series of actions necessary to retain material in or restore it to a serviceable condition. A detailed discussion of maintainability and the techniques used to achieve it is included in DOD-HDBK-791 (AM), *Maintainability Design Techniques* (Ref. 14).

Both reliability and maintainability are components of availability, which is the characteristic ultimately desired. Availability can be expressed as the percentage of total time the equipment is ready to perform its function to the established standards.

5-3.1 DESIGNING FOR MAINTAINABILITY

Designing for maintainability requires understanding of what kinds of maintenance and repair can be performed at each maintenance level. The design engineer should examine the following documents for the equipment being designed or for similar equipment:

1. The appropriate Department of the Army supply catalog, which lists the spare parts assigned to each maintenance level

2. The maintenance allocation chart

3. The specifications or instructions for preparation of technical manuals for the equipment, the actual technical manuals for the equipment, and the actual technical manuals for similar equipment. These publications describe in detail the maintenance procedures to be performed at each level.

The situation differs for different types of equipment and operation. At a large, fixed installation, depot-level repair facilities for fire control materiel may be established on the premises. For fast, mobile combat units, however, maintenance may be limited over long periods to what the operator can perform. In general, the Army carries out maintenance as follows:

1. *Organizational Maintenance.* This maintenance is performed by the using organization. This level is limited to such tasks as preventive maintenance inspections (largely of a simple, visual nature), cleaning, servicing, lubricating, adjusting, and replacing certain easily disassembled parts. This level also includes operator maintenance and that performed by organization maintenance personnel in small unit shops.

2. *Intermediate maintenance.* This maintenance is performed by units organized to support one or more using groups. This level includes the mobile or easily moved shops in close forward support of combat units (direct support) and the more elaborately equipped semifixed shops (general support). Intermediate maintenance is generally limited to troubleshooting, testing, and repairing or replacing unserviceable parts, subassemblies, and assemblies.

3. *Depot Maintenance.* This level operates in fixed installations and is normally capable of major overhauls. It can be considered equivalent to returning equipment to the factory.

5-3.2 FACTORS THAT AFFECT MAINTAINABILITY

Maintenance functions analysis is a key step in the development of a maintainability program. It involves defining what maintenance will be required and what method will be used. This step allows definition of the technical performance requirements and the nature of support equipment that will be required. The functions analysis should

1. Identify maintenance functions down to the level required to make decisions about man-machine tradeoffs

2. Organize and classify these functions for efficient and effective decision making.

During performance of a maintenance function analysis, the following functions should be considered:

1. *Adjusting and Servicing*. Periodic adjustments and required servicing should be identified. These tasks should include only those preventive maintenance actions requiring minimum downtime. Removal of any major component should be included under recycle and overhaul analysis. Identification of the required preventive maintenance actions can be accomplished by reviewing the reliability figures for each component. Equipment redesign should be considered to eliminate any excessive preventive maintenance needs identified.

2. *Verification*. Identification of functions that verify the system is operational requires a detailed functional breakdown of the system. Analysis should begin with the maintenance area most closely in support of mission performance or operational readiness and then proceed to functions in rearward areas.

3. *Troubleshooting*. A troubleshooting function is used when alternative sources of a malfunction produce the same symptom during verification. Analysis should include identification of symptoms that indicate which alternative is malfunctioning. The level of detail required for this analysis depends on the level of maintenance that will be performed to return the equipment to an operational state. For example, a "go, no-go" result may be caused by a malfunction in any one of dozens of parts. If these parts are all located in a single replaceable module, further troubleshooting may not be required. The malfunctioning module is removed and replaced by a functioning module. However, if the parts are not located in a replaceable module, troubleshooting may have to be performed to the piece part level. If identification of the problem involves excessive troubleshooting, equipment redesign should be considered.

4. *Fault Correction*. For each cause of a malfunction indication, the appropriate corrective function should be identified. These functions indicate the action(s) required to ensure that a malfunction has been eliminated. Corrective actions may include adjustments, removal and replacement of the malfunctioning units, cable repair, alignment, etc. These actions should be specified to the level necessary to determine skill, space, access, and support requirements.

5. *Recycle and Overhaul*. Recycle and overhaul are needed because regular preventive and corrective maintenance actions are usually insufficient to restore full operational capability. In some systems, such as aircraft engines, it is necessary to remove components for overhaul in order to restore acceptable reliability.

5-3.2.1 Built-In Test Equipment

Much modern fire control equipment requires test equipment to aid the rapid and accurate diagnosis of problems. Such test equipment generally provides stimulus signals to the unit being tested and instrumentation to measure the response of the unit. The nature of the response provides information to localize the source of trouble. Ref. 14 contains further discussion of how and when built-in test equipment (BITE) and automatic test equipment (ATE) are used.

The Army has developed both general- and special-purpose test equipment to fill various needs. Testing equipment that is embedded in the unit to be tested is called BITE. Even before the widespread use of digital computers in fire control equipment, sensors were placed in the equipment that provided signals to indicators, such as dials or warning lights, but true diagnostic testing of complicated equipment awaited the computer.

In the earliest phases of fire control design, it is essential that decisions be made regarding the testing philosophy. Only in this way can computer resources be allocated to be adequate for all functions. In addition to solving the fire control problem, the computer (or computers) performs diagnostic testing.

At the organizational level, diagnostics of only those failures the crew can repair are required. At in-

termediate and depot levels more detailed fault location is required. Thus the software that is resident in the equipment, needs to provide only organizational diagnostics. Therefore, connectors must be provided for field and depot test equipment. This approach is analogous to a 1990s automobile in which the real-time system tells the driver that, e.g, the battery is not being charged, and the shop tester tells the mechanic which component(s) is responsible.

5-3.2.2 Special-Purpose Test Equipment

Special-purpose test equipment (sometimes called peculiar test equipment) is designed to test a particular piece of equipment. An example is test equipment for the M-5 grenade launcher. It is special-purpose test equipment because it is intended to support only one particular equipment. This specificity results in test equipment that is relatively simple and inexpensive.

As the number of equipment types that form a fire control system increases and as the number of models of an equipment type increases, the number of different special-purpose test equipment items also increases. It soon becomes a very difficult logistic task merely to keep all this test equipment stocked. This serious disadvantage led to the development of generalized ATE.

5-3.2.3 Automatic Test Equipment

ATE diagnoses equipment to the lowest level replaceable part by using some computational capability and appropriate software. ATE can provide stimulus signals that exercise the unit under test and monitor its performance. Based on the stored failure mode symptoms, it may prompt the technician with what corrective action should be taken.

The major advantage of this type of test equipment is that it relieves the maintenance technician of the troubleshooting task. As is the case with BITE, since the intelligence is in the software (test program set) and database (Expert systems are applicable here.), less skilled technicians are required, and less time may be required. Furthermore, by including all of the required instrumentation, such ATE can be generalized to test, for example, M1 fire control equipment or all fire control equipment or, in theory at least, all equipment.

Strictly speaking, ATE is not applicable at the organizational level. The Army has developed ATE for fire control equipment at the depot level that has been in use since the mid-1980s. A field-support-level ATE that should have fire control equipment applications is being developed.

5-3.3 MAINTAINABILITY TESTING

Partial test plans to evaluate achieved maintainability are included in MIL-STD-471, *Maintainability Demonstration* (Ref. 15). All maintainability measures provided for by MIL-STD-471 involve maintenance time, preventive or corrective or both. MIL-STD-471 specifies sampling procedures that are to be used to assure that the maintenance tasks selected for demonstration purposes are representative. Comparable instructions, however, are not provided for sampling the performance of maintenance personnel. The standard merely states that personnel used in the demonstration "...shall be of the type, number, and skill level representative of the personnel who will perform the maintenance during the operational phase.". Nevertheless, care should be exercised to assure that personnel performance is appropriately sampled. Performance can be expected to vary between individuals even when their designated skill levels are the same, and the same individual will not perform even the simplest task with the same accuracy and speed every time.

Although it is difficult to generalize beyond the specific context in which maintainability demonstration data are obtained because there are so many uncontrolled variables and the number of observations is so small, maintainability assurance personnel typically rely upon insights gained from demonstration data as the basis for possible design improvements.

5-4 MANPRINT

Manpower and personnel integration (MANPRINT) is a comprehensive management and technical program to improve total system (soldier and equipment) performance by focusing on soldier performance and reliability. The MANPRINT objectives are achieved by continuous integration of human factors engineering, manpower, personnel, training, system safety, and health hazard considerations throughout the materiel development and acquisition process.

MANPRINT policy, procedures, and organization responsibilities are defined in Army Regulation 602-2, *Manpower and Personnel Integration (MANPRINT) in the Materiel Acquisition Process* (**Ref. 16**).

The philosophy of the MANPRINT program is to have the Army and industry take the actions necessary to answer the question, "Can this soldier, with this training, perform these tasks, to these standards, under these conditions, and using this equipment?". MANPRINT includes

1. Integrating all of the actions in the materiel acquisition process that affect human performance and reliability. This step includes human factors engineering, determination of manpower levels, personnel requirements, training requirements and methods (including training devices), system safety, and health hazards.

2. Developing equipment that will permit effective soldier-materiel interaction within the established performance limits, training time, soldier aptitudes and skills, physical capabilities, and physiological tolerance limits.

As an example, human visual perception capabilities must be considered in the design of sights. These capabilities include acuity, contrast detection, shape discrimination, etc., and must be considered for the conditions under which the soldier must perform. A tank crew member, e.g., experiences motion and vibration, which affect visual performance. Visual performance, in turn, affects target acquisition time and the time required to fire the first round. The degradation of detection probability (one of the elements of target acquisition) as a function of stabilization error and range for the problem of a moving tank is discussed in Chapter 6 of this handbook.

As the performance of forward-looking infrared (FLIR) systems has become increasingly better, there has been a tendency to use the FLIR as the primary sight. Therefore, visual performance must be determined for the FLIR display rather than the direct view optics. At the present time, the user has available the brightness, contrast, and size of target elements as displayed on a cathode-ray tube. In this case the sensor may be the limiting factor in visibility rather than human vision.*

3. Determining and evaluating requirements for overall system performance based upon capabilities and limitations of soldier performance. Limitations on human performance, coupled with the advanced technology available for fire control systems, can have a great impact on system design. For example, limited human performance in tracking targets could result in assigning the tracking function to a system element, i.e., an autotracker. Similarly, limited crew performance in multiple target detection might prompt system designers to include a cuer, which could direct the crew's attention to prioritized targets.

4. Developing and applying methodologies in order to analyze human factors engineering, manpower levels, personnel, training, system safety, and health hazard issues in an integrated manner. To evaluate advanced technology in self-propelled artillery systems, the Human Engineering Laboratory at Aberdeen Proving Ground has configured a number of demonstration systems. The human factors howitzer test bed (HFHTB), for example, is used to study the operation of a howitzer with a reduced crew and improved technology for fire support functions and survivability. The impact of different configurations on crew selection, training and system performance is evaluated to provide a database for definition of new artillery systems.

5. Developing, maintaining, and using databases containing human factors, human performance, manpower, personnel, training, system safety, and health hazard information

———

*During Operation Desert Storm in 1991 thermal sights were used almost exclusively for the detection, acquisition, identification, and engagement of targets because of their night and range capabilities. Most incidents of friendly fire casualties (amicicide) caused by tanks and attack helicopters were due to a gunner's capability to detect, acquire, and engage a target at long range and incapability to identify the target visually through the sight (or by any other means).

6. Selecting, defining, and developing soldier-materiel interface characteristics such as work space layout, work environment, and effective transfer of operator and maintainer skills for similar tasks on similar equipment. Developing and defining a work environment include detailed analyses of the effects of the proposed environment on the health and safety of operator and support personnel. Analyses of the work environment also include consideration of the physical and cognitive demands on personnel based on the operating tempo of the unit in both training and combat environments.

7. Determining human performance requirements for new systems and product-improved systems and matching available human aptitudes with training concepts (including training devices and publications) to produce required skills.

Because of the relationship between the skill of the crew of an armored vehicle and hit probability, for example, much attention has been given to providing crew training so that skills can be practiced by crew members without the expense of using live rounds. For the M1 tank a conduct of fire trainer (COFT) and a tank weapon gunnery simulation system (TWGSS) were developed. These simulators provide the tank commander and gunner with views of simulated tactical situations. The crew is thus able to practice each of the steps required to engage and fire on a target. The simulator also provides feedback of the results of the engagement to the crew.

A networked approach to tactical simulation and training, referred to as SIMNET, was also developed. This system stores a number of complex and detailed tactical scenes in a large, centrally based computer system and provides force-on-force engagements. Users in locations all over the U.S. and overseas are able to call up tactical scenarios from the central location and conduct training exercises with other units at distant locations. Again, knowledge of results is provided.

8. Providing basic soldier-materiel system task sequence data to describe, develop, and assess the human performance required in a soldier-materiel system

9. Determining the numbers and types of soldiers and civilians needed to man a system in order to provide for subsequent personnel planning and training; providing data needed to establish a new military occupational specialty (MOS), additional skill identifier (ASI), or special qualification identifier (SQI) for new or improved materiel systems, doctrine, and force or unit structure, where required. In an attempt to keep levels of tactical capability high in the face of decreasing force levels, it may be desirable to install an autoloader in tanks. This addition would result in a 25% reduction in the number of crew members required per tank. Also computer capabilities can be cost effectively provided to assist crew functions, such as target servicing, ammunition selection, communication maintenance, and embedded training. This assitance can relieve the crew's workload and can enhance crew performance.

10. Assessing the manpower, personnel, and training burden that materiel design or development concepts may impose on the Army

11. Confirming the effectiveness of MANPRINT by evaluating the soldier-materiel systems and unit performance

12. Applying, as appropriate, MANPRINT methodologies to development items, nondevelopment items, and product-improved Army materiel systems throughout each phase of the acquisition cycle

13. Integrating personnel assignment policies to ensure that specifically trained soldiers are assigned to the units and positions for which they are trained.

The objectives of the MANPRINT program follow:

1. To influence soldier-materiel system design for optimum total system performance by considering human performance and reliability issues related to human factors engineering, manpower, personnel, training, system safety, and health hazards

2. To ensure that Army materiel systems and concepts for their employment conform to the capabilities and limitations of the fully equipped soldier to operate, maintain, supply, and transport the materiel in its operational environment consistent with tactical requirements and logistic capabilities

3. To assist the Army trainer determining, designing, developing, and conducting sufficient, necessary, and integrated Army and joint service training

4. To improve control of the total life cycle costs of soldier-materiel systems by ensuring consideration of the costs of personnel resources and training for alternative systems during the conceptual stages and for the selected system during subsequent stages of acquisition

5. To ensure—through studies, analyses, and basic and applied research in human factors engineering, and through soldier-materiel system analysis—that equipment designs and operational concepts are compatible with the limits of operators and maintenance personnel defined in the target audience description

6. To develop a unified, integrated MANPRINT database defining ranges of human performance and to compare these ranges against system performance and provide for the timely development of trained personnel

7. To provide MANPRINT data for the development of technical manuals, training manuals, field manuals, and other training media and technical publications and ensure that use of these publications does not require aptitudes, education, or training beyond the requirements set to perform the tasks the publications describe

8. To apply MANPRINT concepts and current educational technology to analysis, design, and development of training devices

9. To influence the manpower, personnel, and training (MPT)-related objectives of the integrated logistics support (ILS) process

10. To integrate combat development and technology base information systems with long-range personnel planning

11. To ensure that personnel trained for specific force modernization systems (by MOS and ASI) are assigned to the units and positions for which they are trained.

5-4.1 HUMAN FACTORS ENGINEERING

In the design of Army equipment, the human factors engineering program was institutionalized and executed successfully long before the advent of MANPRINT. The basic purpose of human factors engineering is to design equipment and systems to be operated and maintained by soldiers in the intended environment to the required time and accuracy requirements. Since the MANPRINT program integrates all of the areas affecting human performance, human factors engineering has been included.

5-4.1.1 Basic Principles of the Man-Machine Relationship

Military equipment has become so complex, precise, and fast acting that it threatens to exceed the abilities of humans to operate it. Human factors engineers, who are psychologists specializing in man-machine relationships, have become increasingly involved in designing equipment that can be operated effectively. Human factors engineering relies on basic and applied psychological research, i.e., basic research in the capabilities and limitations of human faculties and applied research in the behavior of these faculties in specific situations.

Psychological research differs from research in other fields because it is dependent on the subjective reactions of humans. For example, one can determine the wavelength and energy of light from a source by objective investigation, but the related properties of color and brightness are subjective and exist only in the eye (and brain) of the beholder. Similar relationships exist between the wavelength of sound (objective) and its pitch (subjective), the energy of sound and its loudness, the thermal energy of a material and the sense of its hotness or coldness, etc. Establishing the relationship between the subjective (psychological) and the objective (physical) is the business of psychophysics.

It must not be thought, however, that in the end psychological research is subjective and opinionated. For example, a scale of brightness has been established by recording the observations of a cross section of humans large enough to be statistically valid. Since each point on the scale can be defined by purely physical values, the same brightness can be recreated at any time, and the scale becomes a permanent objective research tool. The same techniques have been applied to other visual functions, to hearing, muscular capabilities, etc. Once the basic scales have been established, more refined research can be carried out. For example, the ability of individuals or special groups of people to discriminate between small changes in brightness can be measured under various conditions or preadaptation.

The branches of human engineering that follow are of chief interest to the designer of mechanical, electrical, and optical equipment:

1. *Vision:*
    a. Light Discriminations:
        (1) Brightness sensitivity (the ability to detect a dim light)
        (2) Brightness discrimination
        (3) Color discrimination
    b. Spatial Discriminations:
        (1) Visual acuity, i.e., the ability to see small objects or distinguish details or changes in contour
        (2) Distance judgment, particularly depth perception, which is the ability to distinguish differences in distance
        (3) Movement discrimination
    c. Temporal Discriminations: For example, the ability to distinguish individual flashes of flickering lights
    d. Dark Adaptation: The ability of the eye to perform at night after various periods of adaptation. This field of investigation cuts across 1a, 1b, and 1c by measuring various discriminations under the special conditions of dim light.
    2. *Audition:*
    a. Pitch Discriminations
    b. Loudness Discrimination
    3. *Motor Performance*: **The ability to perform tasks involving bodily movements, including:**
    a. Speed
    b. Accuracy
    c. Force, e.g., the force the operator can exert to push a lever
    4. *Proprioception:* **The ability to sense the position of the body and its movements in space and time through certain bodily receptors (muscles, tendons, semicircular canals, etc.)**
    5. *Skin Sensitivity:* **The sense of touch, of particular importance to the engineer designing fire control equipment that must be operated effectively during blackouts.**

The interrelationships of these five branches of human factors engineering are also critical. For example, tracking may involve vision, motor performance, and proprioception. In addition to the data available on the foregoing and their interrelationships, the engineer has at his or her disposal considerable information on how these branches are affected by learning, intelligence, and special conditions such as fatigue.

There are three possible ways to overcome the human problems in operating equipment:

1. *Choose Operators Who Are Peculiarly Suited for the Equipment.* **The Army is, of course, selective in its recruiting—men and women with gross visual, auditory, or other defects are not accepted, but it does not normally give highly refined tests nor can it be ultraselective in assigning the ideal man or woman to the task. This problem is multiplied in time of war. Thus although the designer does not have to consider the physically handicapped, he or she must still design for operators whose faculties may be somewhat below average.**

2. *Train Operators for Their Specific Tasks.* **Training can be an effective way to overcome human engineering problems, but as already explained (See par. 5-1 for a discussion.), the Army depends largely on relatively inexperienced recruits who are trained at specialized schools established by various Army commands.**

3. *Design the Equipment for Ease of Operation (The Best Solution).* **The design engineer cannot expect to become a human factors engineer, a graduate psychologist with considerable postgraduate training, but he or she has resources that can help to solve many of the problems of designing for the human operator. These include common sense, publications presenting psychological data for use by design engineers, and the skills of human engineers.**

Common sense is often neglected in design. A familiar example of the lack of it is the automobile designer's use of identical knobs for lights, windshield wipers, ventilator, etc., and the positions of the knobs vary from one model of car to another. By using radically different shapes of knobs (particularly for critical operations) and keeping them in the same relative position they occupied on other, similar equip-

ment, the designer can contribute quite simply to ease of operation. A few other examples of this kind of thinking follow:

1. *Design for Visibility.*

a. Place gages where they can be read by the operator in his or her usual position while he or she is operating associated controls.

b. Provide adjustable lighting for easy reading throughout the ambient light range (including desert sunshine), and luminous dials as necessary for reading in the dark.

c. Make dials, gages, etc., as uncluttered as possible. If operations require a gage to be read to the nearest milliampere, do not clutter it with gradations to the tenths or hundredths of a milliampere.

d. Use logical gradations. A dial marked off in fourths can be extremely hard to interpret if readings must be estimated in tenths.

2. *Locate Controls Logically.* The controls used most often and those used for the most critical operations should be within easy reach and should be grouped so that the operator is required to move in only one direction to perform a sequence of operations.

3. *Design for the Normal Range of Human Faculties.* A common error is to design for the average man, but good human factors engineering practice (and common sense) dictates that designs should include all operators whose body measurements fall within the limits set for Army personnel. Such operations as keeping optical sights or radar antennas aligned on a target, for example, may be performed by men or women who are tall or short, or have long or short arms, as well as men or women falling close to the average. Adjustments should be provided for so that the individual can position the equipment for maximum ease and comfort.

5-4.1.2   Database for Human Factors Engineering

MIL-HDBK-759, *Human Factors Engineering Design for Army Materiel*, **(Ref. 17)** provides fundamental information on human factors engineering design for Army materiel. MIL-STD-1472, *Human Engineering Design Criteria for Military Systems, Equipment and Facilities*, **(Ref. 18)** establishes general human engineering criteria for design and development of military systems, equipment, and facilities. Both publications are recommended to the fire control system and equipment designers.

The Human Research and Engineering Directorate of the US Army Research Laboratory, which has its headquarters at Aberdeen Proving Ground, MD, is responsible for maintaining a database on human factors. When the fire control equipment designer is in doubt regarding the best design choice to assure human performance, it would be prudent to contact HEL. The sources of information that follow can be useful, however, in resolving many day-to-day design decisions.

Common sense can help the design engineer avoid the more obvious pitfalls. The design engineer can go much further toward providing ease of operation by consulting one of several texts prepared by human engineering specialists for practical use by equipment designers. The *Handbook of Human Engineering Data* **(Ref. 19)** contains introductory explanations of the basic principles, plus a great deal of tabular data on most aspects of human engineering, presented so that the "layman" can interpret and use them. In its early chapters *Vision in Military Aviation* **(Ref. 20)** expounds on the principles of vision and instructs design engineers how to apply the basic visual curves to practical problems. The later chapters contain many examples of visual performance as related to specific equipments and situations; much of this information is useful to the fire control designer as well as the aircraft designer. The *Human Engineering Guide to Equipment Design* **(Ref. 21)** is useful for introducing the design engineer to the field of human factors engineering.

In addition, many articles and research reports have been written that apply directly to human factors in military equipment. The fire control equipment designer may be able to obtain data of a very practical nature that apply directly to his problem.

5-4.2   MANPOWER

Manpower management focuses on the determination of essential human resource requirements, which requirements will be supported with authorizations, i.e., are affordable, and what the personnel demands associated with these authorizations will be by grade and skill. The manpower and personnel domains interface and overlap at many points. The difference is that manpower deals with defining the

human resource demand (quantitative) whereas personnel focuses on supporting this demand through the acquisition, training, and assignment of people (qualitative).

During system development the concern in the manpower domain is to determine the impact of the system on Army manpower resources and to assure that the system is optimized from a manpower viewpoint. The force structure implications of the system must be identified. Appropriate goals and constraints regarding the human resource demand of the system should be established in terms of affordability and supportability. Early in the development process and based on force structure and organizational design guidance provided, a manpower "footprint" into which the prospective system must fit is determined.

If a contractor is used, this force structure "footprint" in terms of manpower goals and constraints is furnished. The contractor is required to demonstrate that these stipulated goals and constraints have not been breached by the system design. He must also demonstrate that the desired total system performance can be achieved with the desired manpower requirement. This demonstration requires the contractor to consider (1) manpower in the basic design decisions that will impact on the task, (2) the workload function allocation between the man and the man-machine, and (3) the operational environment projected for the system. The tasks considered must include not only those directly related to the equipment but also the off-equipment tasks the soldier performs. The operational environment, possibly requiring continuous operations, stress, or extreme weather conditions, must also be included. The resulting manpower requirements are measured in terms of soldier performance, which allows total system performance, to meet the required criteria.

The manpower requirement for the system is defined during the development process in the basis of issue plan feeder data (BOIPFD) initiated by the materiel developer. The BOIPFD is accompanied by the quantitative and qualitative personnel requirements information (QQPRI), which defines proposed military occupational specialty (MOS) and workload. The materiel developer uses this information as input for concept studies, life cycle cost estimates, and tradeoff analyses during the research and development process. These are forwarded to the Training and Doctrine Command (TRADOC) for formal development of the basis of issue plan (BOIP) and update of the QQPRI, during which training impacts and any proposed MOS decisions are developed. When approved, the BOIP and QQPRI are the basis for any modification to existing organizational structure and are reflected in a new table of organization and equipment (TOE).

Maintaining manpower requirements within the force structure guidance provided is critical to system development. If increases beyond guidance are required, the affordability of these increases is determined through the total army analysis (TAA) and programming functions to ensure overall Army end-strength constraints are met. This constraint could create a situation in which the manpower requirements for the system are not fully supported by authorizations. This decreased level of manning may degrade actual system performance achieved after fielding to below the level desired. Since early system design decisions dictate the resulting manpower requirement, manpower analyses and tradeoffs done early on are necessary to prevent unanticipated or unsupportable demands being made at the time of system fielding.

Other manpower issues to be considered in design include continuous and/or sustained operations, casualty estimation, anticipated levels of authorization and manning, and the resiliency required on the battlefield to maintain performance.

5-4.3   PERSONNEL

As indicated in subpar. 5-4.2, the manpower process identifies the number of soldiers required and authorized. These authorizations are defined in terms of MOS and skill level (grade) in The Army Authorization Documents System (TAADS). The personnel community must then acquire and assign properly trained, qualified people to fill these established authorizations.

During system development an objective of MANPRINT is to obtain a match between the system requirements and the characteristics of the individual soldiers and crews who will operate and maintain the system. It must be recognized that individuals vary across many dimensions that include their cognitive, physical, and psychomotor skills, reading and writing abilities, and their background and experience.

The primary measurement tool used by the Army to quantify soldier characteristics is the Armed Services Vocational Aptitude Battery (ASVAB) from which Armed Forces Qualification Test (AFQT) scores and aptitude area (AA) scores are derived. These scores are used to establish recruiting quality goals and minimum MOS entrance requirements.

The Military Entrance Physical Strength Capacity Test (MEPSCAT) is used to assess an applicant's physical strength capacity in order to match this capacity with an enlistment MOS for which the individual is qualified. The physical profile PULHES matches physical capabilities with others required to perform in the MOS. Most of the entrance requirements for an MOS are documented in AR 611-201, *Enlisted Career Management Field in Military Occupational Specialty* (Ref. 22).

Since the Army almost exclusively relies on initial entry accessions to man the force, the type of individual available for a system can be described by accessing the current force and projected recruiting information. It is important that the Army provide contractors with information relative to its soldiers so that they may be considered in the system design process. The vehicle in which the range of all appropriate individual characteristics is defined is the target audience description (TAD). By using input from the TAD, the designer can design equipment to achieve the required performance criteria with the type of soldier who will be available to operate or maintain the system when it is fielded. This approach would reverse the existing trend toward equipment that demands higher than existing soldier ability (especially cognitive ability) to produce satisfactory system performance. The current quality requirement already exceeds the current personnel inventory. The projected requirement may further increase this mismatch of requirement to inventory.

The personnel domain must be concerned with the quality of individuals required by a new system. The Army is in recruiting competition with the other uniformed services, private institutions, and higher education facilities. The number of quality individuals that can be recruited each year is limited. These quality individuals, as defined by AFQT, AA scores, and education, must be distributed across all of the MOSs that make up the Army's force to ensure combat effectiveness in all areas. The aggregate demand for quality, however, must stay in line with what is available. Each new system must be kept within established quality requirement constraints. If it is not, either a disproportionate distribution of quality or a shortfall to man the system will result.

In addition to quality demands, other personnel aspects should be considered with regard to the system, namely,

1. Certain MOSs are historically hard to recruit people into, hard to retain people in, difficult to train people for, and difficult to distribute people in. Increasing requirements in these problem MOSs should be avoided if at all possible.

2. Part of the allowable end strength is always in the trainee, transient, holdee, and student (TTHS) account. Soldiers in this overhead account are not available for assignment against force structure authorizations. The biggest factor in the size of the TTHS is length of initial entry training. Increases in the amount of training for an MOS directly increase the number of soldiers in the TTHS, which increases the number that must be recruited to fill existing authorizations. Thus even though no increased manpower authorizations occur, an increased personnel burden is created. With a fixed overall end strength, an increase in one MOS causes an equal decrease to occur in another MOS. For this reason any increases in training requirements should be minimized if possible.

3. Promotion within an MOS is directly affected by the grade structure of the MOS. Changes in a MOS that skew its standards of grade authorizations (SGA) may have a significant impact on promotion opportunities. Unconstrained demands for higher grade personnel cannot be allowed.

4. The new manning system (NMS) has a goal of unit replacement rather than individual replacement. This new system, including regimental affiliation and cohort training and personnel fill, has the potential to enhance unit performance and reduce workload through cohesive bonding of the unit. Fielding by the NMS should be considered.

5-4.4 TRAINING

In the most basic terms training is the process that prepares soldiers to do jobs. The soldier is given a series of tasks, aptly named "soldier tasks", which describe what the Army wants the soldier to do. Per-

formance standards are established to measure how well the Army wants the soldier to do the task, and finally, performance reflects the soldier's ability to accomplish the desired tasks.

When the Army acquires a system, it acquires a training system with it. From a MANPRINT concern training goals and constraints must affect system design in a positive way. Traditionally, the system designer was not initially constrained by the fact that the Army's training resources were taxed. The training community generally faced a completed system design and was asked to structure a training concept that would accommodate the operational and maintenance needs of that design.

The starting point for training is to develop a training strategy that is who, where, what, and when. The "who" is defined in the target audience description, "where" is governed by considerations of training transfer and impact on the operating strength of the MOS, "what" should include all equipment-related tasks and other soldier tasks, and "when" is governed by consideration of timing and training decay. The training concept then defines how the training will be accomplished by considering training delivery options such as embedded training, training devices, and training resources.

The training strategy and concept, which include resource consideration, become the basis for developing training goals and constraints. The training system design process proceeds in parallel with the equipment design process. Because they provide training goals and constraints at the start, the training strategy and concept are considered during function allocation. During tradeoff analysis, cost, performance, and supportability also are considered. In the process, design decisions are affected by training considerations. The following items are some of the important training issues and concerns:

    1. Training time is finite.

    2. Decreased time spent in school increases the number of troops in a unit, i.e., operating strength.

    3. Training time lost to units—because of more time in schools—results in decreased readiness.

    4. Training in schools should adequately prepare soldiers to do their jobs, i.e., the most critical tasks should be covered in school.

    5. The system training strategy must meet the widely varying needs of the Army National Guard and reserve units.

    6. The results of training are not everlasting. The knowledge and skills acquired through training decline over time and with disuse. Therefore, design actions should be taken to design out, if possible, tasks that may have inordinately high skill decay rates because they increase the requirements for sustainment training.

    7. A soldier can learn only so many things.

    8. Training generally cannot overcome poor design.

    9. Training cannot always make up for soldier aptitude differences.

    10. Factors that shape training needs flow from the early function analyses conducted by designers to allocate weapon system function either for performance by the hardware and/or software system or by the soldier. The ability to extrapolate future training demands among the alternative system design approaches is critical to a cost-effective strategy.

5-4.4.1 Embedded Training

Embedded training is an increasingly important consideration because of the tremendous capabilities of microcomputers. Embedded training is training that is provided by capabilities designed to be built into or added onto operational systems to enhance and maintain the skill proficiency necessary to operate and maintain that equipment end item. Early in training, concept development decisions are made regarding whether specific training should be conducted on actual equipment through embedded training, through training devices, or through combinations of both.

An embedded training capability should be thoroughly evaluated and considered the preferred alternative among other approaches to incorporation of training subsystems of all materiel systems. Embedded training has the advantage of permitting training on the weapon system itself. Moreover, it should not adversely impact the operational requirements and/or capabilities of the system, and it should be identified early enough to be incorporated into initial prototype designs. It also avoids delays in receipt of training materials and offers the opportunity for more efficient and frequent training. Embedded training devices encompass four training categories:

   1. *Category A, Individual/Operator.* **Training objective: To attain and sustain individual maintenance and system operation skills**

   2. *Category B, Crew.* **Training objective: To sustain combat-ready crews/teams. This category builds on skills acquired from Category A.**

   3. *Category C, Functional.* **Training objective: To train or sustain commanders, staff, and crews/ teams within each functional area to be used in their operational role**

   4. *Category D, Force Level (Combined Arms Command and Battle Staff).* **Training objective: To train or sustain combat-ready commanders and battle staff by use of the operational system in its combat operational role.**

   The requirements and resources for training must be considered by the proponent of the system in concept formulation of the end item and/or system and pursued throughout the materiel acquisition process. A training strategy that includes consideration of embedded training must be included in the Operational Requirements Document (ORD) (Refs. 23 and 24).

   ILS and MANPRINT are the catalysts for including embedded training starting with the Concept Exploration and Definition Phase of the acquisition process. Embedded training is addressed at all acquisition process reviews and at each milestone for all system acquisition programs through the ILS Plan and Systems MANPRINT Management Plan. During the reviews, system proponents provide a definitive training strategy with associated analysis and rationale supporting use or nonuse of embedded training.

5-4.4.2   Training Devices Development

   There has been enormous growth in the need for and use of training devices and simulators to substitute for the extreme costs associated with the use of actual weapons systems and equipment for training purposes. Training devices are either (1) system devices, i.e., those acquired to support a specific weapon system, or (2) nonsystem devices, such as individual weapons, training on more than one system or several different types of equipment. Training device requirements may be presented as a part of the ORD, a Training Device Needs Statement (TDNS), a Commercial Training Device Requirement (CTDR), or a Nonsystem Training Device Requirement (NSTDR).

   The development of nonsystem devices is usually assigned to the PM Training Devices. System devices are developed by the weapon system PM.

5-4.5   SYSTEM SAFETY

   The Army has the responsibility to ensure that hazards to the soldier are enemy induced, not system induced. As systems become more complex and the battlefield reflects the doctrine of continuous and sustained operations, the soldier's exposure to system hazards increases. The system safety program is designed to identify and measure safety hazards with the following objectives:

   1. To maximize operational readiness and mission performance through accident prevention

   2. To ensure that safety and health risks are eliminated and that residual hazards are formally accepted and documented

   3. To minimize the need for safety retrofits

   4. To ensure that equipment modifications and doctrinal changes do not reduce the safety and health aspects of a system

   5. To apply system safety engineering and management principles to developing technology for new systems.

   The goal of system safety is to design equipment so that safety considerations do not adversely affect soldier performance or increase demands on manpower, personnel, or training resources. No safety hazards are accepted by the Army without formal documentation of the associated risks.

   The materiel developer is responsible for conducting a tailored system safety program for all developed systems. Each PM office establishes a System Safety Working Group (SSWG) to track hazards and document corrective actions. Prior to each milestone decision review, the SSWG prepares a System Safety Risk Assessment that documents the materiel developer's position on those safety hazards that have not been eliminated by system design.

   Industry conducts its own safety program which parallels that of the Army. DoD Instruction 5000.2

(Ref. 23) requires the use of MIL-STD-882, *System Safety Program Requirements*, (Ref. 25) which details the tasks and activities to be performed by the contractor to identify, evaluate, and eliminate the safety hazards of a system or to reduce their associated risks to a level acceptable to the Army. Prior to the start of operational or developmental testing, industry produces a safety assessment report that summarizes the hazard potential of a system and recommends procedures to reduce the risks to test personnel to an acceptable level.

System safety impacts all other domains. For example, the System Safety Risk Assessment is used to prepare the human factors engineering analysis (HFEA) required by AR 602-1, *Human Factors Engineering Program* (Ref. 26). Additionally, training programs may be required for those safety hazards that have been accepted by the Army as a result of constraints imposed by operational effectiveness, time, or cost.

5-4.6 HEALTH HAZARDS AND ENVIRONMENTAL IMPACT

Advanced technologies and sophisticated, complex systems have brought with them greater potential for harm due to greater noise, overpressure, shock and vibration, higher levels of toxic fumes, gases, radiation and chemicals, and a myriad of other conditions. These increases in the degree and intensity of hazardous conditions provide major reasons for concern. The origination of health hazards from technologies such as lasers and ionizing and nonionizing radiation gives reason for even greater concern, particularly in fire control. DoD Instruction 5000.2 (Ref. 23) requires that scientific and engineering principles be applied during design and development to identify and reduce the hazards associated with system operation and support in order to design the safest system possible consistent with mission requirements and cost-effectiveness.

The Health Hazard Assessment (HHA) Program combines with the system safety program in an effort to accomplish the following objectives:

    1. To preserve and protect the health of the individual soldier and other personnel

    2. To enhance soldier performance and system effectiveness

    3. To reduce the requirements for system design retrofits needed to eliminate or control health hazards

    4. To reduce readiness deficiencies attributable to health hazards that bring about restrictions in training or operation

    5. To reduce personnel compensation by eliminating or reducing injuries attributable to health hazards associated with the use of Army systems.

The basic goal of HHA is to identify health hazards as early as possible and to eliminate or control them. It is desired that the optimum degree of health features be integrated into a system design within the bounds of cost, operational effectiveness, and time. As expressed in AR 40-10, *Health Hazard Assessment Program in Support of the Army Materiel Acquisition Decision Process*, (Ref. 27), there will be no compromise of health protection criteria and standards without formal documentation of the accepted risks.

The mental as well as the physical hazards must be considered in order to minimize potential psychiatric casualties. Such casualties can result from lack of a confidence in equipment, organizational or doctrinal isolation, and/or a nonsupportive social environment. For example, in World War II, the French employed their tanks individually rather than in mass (doctrinal isolation). Inside the tank the crew was physically isolated (social isolation). This method of operation had a negative impact on the effectiveness and sustainability of French tank crews. Training is often the solution to these types of casualties, but a result is a greater training burden.

Assessment of health hazards must be conducted by competent Army medical department professionals to determine the overall impact. HHAs are not automatically triggered by some activity or event in the materiel acquisition process; these assessments are initiated only upon formal request through the Surgeon General's Office. The formal HHA reports usually become part of the human factors engineering assessment, which covers all of the MANPRINT domains. The HHA is updated based on new or more mature data prior to each milestone review.

HHA procedures are integrated throughout the materiel acquisition process. In the design process health hazard analyses are conducted to evaluate hazard severity and probability, to assess risk, and to determine operational constraints. This effort also identifies the required precautions, protective devices,

and training requirements to minimize potential hazards. Later in the materiel acquisition life cycle, the HHA is used to assess contractor performance and to ensure that health hazard recommendations are incorporated in doctrinal, maintenance, and training publications.

Industry has the responsibility to design a system that eliminates or controls soldier and crew exposure to hazards. MIL-STD-882, *System Safety Program Requirements*, **(Ref. 25)** provides a means by which the Army can request contractor-supplied data that detail the efforts taken to identify the hazards of a system and to impose design requirements and management controls. The task descriptions should be selectively tailored and based on system complexity and technology and program cost.

The health hazard environmental impact domain interfaces directly with the other domains. For example, if a particular health hazard cannot be eliminated through redesign, it may be necessary to reduce the risk by specialized training or by limiting the personnel selected to operate and maintain the equipment. This is a particularly important area for nondevelopmental items for which system design is firm when the procurement decision is made. Finally, as with system safety, the HHA report is used to prepare the human factors engineering assessment.

Defense systems are to be designed, developed, tested, fielded, and disposed of in compliance with the applicable environmental protection laws and regulations, treaties, and agreements. DoD 5000.2 (Ref. 23) states these requirements during the acquisition process to ensure DoD compliance with environmental protection laws.

REFERENCES

1. AR 70-38, *Research, Development, Test and Evaluation of Materiel for Extreme Climatic Conditions*, 1 August 1979.

2. MIL-STD-210C, *Climatic Information to Determine Design and Test Requirements for Military Systems and Equipment*, 9 January 1987.

3. MIL-STD-810E, *Environmental Test Methods*, 9 February 1990.

4. AMCP 706-115, *Environmental Series, Part One, Basic Environmental Concepts*, July 1974.

5. AMCP 706-116, *Environmental Series, Part Two, Natural Environmental Factors*, April 1975.

6. AMCP 706-117, *Environmental Series, Part Three, Induced Environmental Factors*, January 1976.

7. AMCP 706-118, *Environmental Series, Part Four, Life Cycle Environments*, March 1975.

8. AMCP 706-196, *Development Guide for Reliability, Part Two, Design for Reliability*, January 1976.

9. AMCP 706-197, *Development Guide for Reliability, Part Three, Reliability Prediction*, January 1976.

10. AMCP 706-198, *Development Guide for Reliability, Part Four, Reliability Measurement*, January 1976.

11. MIL-HDBK-217, *Reliability Prediction of Electronic Equipment*, 2 January 1990.

12. MIL-STD-785B, *Reliability Program for Systems and Equipment Development and Production*, 3 July 1986.

13. MIL-STD-781D, *Reliability Testing for Engineering Development, Qualification and Production*, 17 October 1986.

14. DOD-HDBK-791, *Maintainability Design Techniques*, 17 March 1988.

15. MIL-STD-471A, *Maintainability Demonstration*, 10 January 1975.

16. AR 602-2, *Manpower and Personnel Integration (MANPRINT) in the Materiel Acquisition Process*, 19 April 1990.

17. MIL-HDBK-759B, *Human Factors Engineering Design for Army Materiel*, 10 January 1993.

18. MIL-STD-1472D, *Human Engineering Design Criteria for Military Systems, Equipment and Facilities*, 10 February 1994.

19. *Handbook of Human Engineering Data for Design Engineers*, Technical Report SDC 199-1-1, prepared by Tufts University, Medford, MA, Office of Naval Research, Washington, DC, 1949.

20. Wulfeck, Weisz, and Raben, *Vision in Military Aviation*, WADC TR 58-399, Wright Air Development Center, Dayton, OH, 1958.

21. H. P. Van Cott and R.G. Kinkade, Eds., *Human Engineering Guide to Equipment Design*, US Government Printing Office, Washington, DC, 1972.

22. AR 611-201, *Enlisted Career Management Field in Military Occupational Specialty*, October 1990.

23. DoD Instruction 5000.2, *Defense Acquisition Management Policies and Procedures*, 23 February 1991.

24. DoD Manual 5000.2-M, *Defense Acquisition Management Documentation and Reports*, 23 February 1991.

25. MIL-STD-882C, *System Safety Program Requirements*, 19 January 1993.

26. AR 602-1, *Human Factors Engineering Program*, 8 February 1991.

27. AR 40-10, *Health Hazard Assessment Program in Support of the Army Materiel Acquisition Decision Process*, 1 October 1991.

CHAPTER 6
FIRE CONTROL SYSTEM DESIGN

The principles of analysis, modeling, design, and test as considered previously in this handbook are discussed with regard to the system and major subsystems of two examples, the M1 Abrams tank and the AH-64 Apache attack helicopter. The major subsystems discussed are acquisition and tracking, computing, and weapon pointing.

6-0 LIST OF SYMBOLS

The number of symbols used in this chapter is so large that some have more than one definition. To avoid confusion, unique lists of symbols were prepared for the two paragraphs of the chapter in which symbols are used.

6-0.1 LIST OF SYMBOLS FOR PAR. 6-2, "M1 ABRAMS TANK FIRE CONTROL DESIGN"

A = total gun offset in azimuth, mil

A_{BR} = azimuth boresight correction, mil

A_D = magnitude of the angular cross-range deflection, mil

A_{HOR} = horizontal offset, mil

A_{MRS} = azimuth muzzle reference sensor (MRS) correction, mil

A_{PR} = parallax correction in azimuth, mil

A_{TR} = transformed azimuth offset due to A_{HOR} and E_{VER}, mil

A_V = projectile angular component due to cross-range velocity, mil

A_{ZO} = horizontal zeroing correction pertinent to round type, mil

A_{ZW} = horizontal angular shift in impact point due to a unit crosswind, mil/m/s

a_d = 100%

a_{H_i} = range coefficient for standard drift, mil/m^i

a_m = nominal muzzle velocity for specific round, m/s

a_{v_i} = range coefficient for superelevation, mil/m^i

B_w = measured tube wear, m

b_d = conversion factor, 1733.447%•°R/in.–Hg

b_{H_i} = scaling coefficient for nonstandard conditions, m^{1-i}/mil

b_m = linear temperature coefficient for specific round, m/(s•°F)

b_{v_i} = range coefficients for nonstandard air density, m^{1-i}/%

C = turret cant angle, deg

c = experimental coefficient specific to each round type, s^{-1}

c_d = 459.67°R (corresponds to 0°F)

c_{H_i} = range coefficient for crosswind, s/m^i

c_m = quadratic temperature coefficient for specific round, m/(s•°F^2)

c_{V_i} = range coefficient for nonstandard muzzle velocity, s/m^i

D = density of gas, kg/m^3

D_o = air density at standard atmospheric conditions, kg/m^3

d_{V_i} = range coefficient for nonstandard air temperature, m^{1-i}/%

E = total gun offset in elevation, mil

E_{BR} = elevation boresight correction, mil

E_{MRS} = elevation MRS correction, mil

E_{PR} = parallax correction in elevation, mil

E_{TR} = transformed offset in elevation due to A_{HOR} and E_{VER}, mil

E_{VER} = vertical offset, mil

E_{ZO} = vertical zeroing correction pertinent to round type, mil

H = horizontal drift compensation, mil

K = 1018.59, conversion constant, mil/rad

L_{AZ} = horizontal offset of crosswind and lead, mil

n_1 = 5, constant dimensionless

n_2 = 4, constant dimensionless

n_3 = 3, constant dimensionless

n_4 = 3, constant dimensionless

n_{F1} = 5, constant dimensionless

n_{F2} = 3, constant dimensionless

n_{F3} = 2, constant dimensionless

n_{F4} = 2, constant dimensionless

n_{F5} = 4, constant dimensionless

n_{H1} = 3, constant dimensionless

n_{H2} = 3, constant dimensionless

n_{H3} = 3, constant dimensionless

P = pressure of gas, Pa

P_A = actual air pressure, in.-Hg

P_o = air pressure at standard atmospheric conditions, Pa

P_{ss} = probability of achieving a first-round hit against the standard 2.3 m × 2.3 m target, dimensionless per unit

QE_o = standard superelevation, mil

R = measured target range, m

R_a = gas constant of air, 285.9 m²/(s²•K)

R_o = boresight distance, m

R_{PH} = horizontal distance (parallel to the cannon trunnion axis) between the optical axis of the gunner's primary sight at the head mirror and the cannon axis at the trunnions, m

R_{PV} = vertical distance (perpendicular to the cannon trunnion axis) between the optical axis of the GPS at the head mirror and the cannon axis at the trunnions, m

T = absolute temperature of gas, K

T_A = actual temperature, °F

T_{AZ} = horizontal component of target tracking rate, mil/s

T_F = predicted time of flight under actual conditions, s

T_{FO} = standard time of flight, s

T_g = propellant grain temperature, °F

T_{go} = standard propellant grain temperature, °F

T_o = air absolute temperature at standard atmospheric conditions, K

V = muzzle velocity, m/s

V_o = muzzle velocity with respect to the gun tube, m/s

V_R = range component of the vehicle ground velocity, m/s

V_T = target velocity, m/s

$V(T_g)$ = muzzle velocity at grain temperature T_g, m/s

$V(T_{go})$ = muzzle velocity at standard grain temperature T_{go}, m/s

V_W = weapon velocity, m/s

V_{XW} = cross-range component of the vehicle ground velocity V_W, m/s

W = actual wind velocity, m/s

W_X = crosswind velocity, m/s

α_i = range coefficient for standard time of flight, s/m^i

β_i = range coefficient for nonstandard density, s/(m^i•%)

γ_i = range coefficient for nonstandard muzzle velocity, s^2/m^i

ΔD = percentage deviation in air density from standard atmospheric conditions, %

Δh_D = shift in height of projectile impact point due to a unit deviation in air density, m/%

ΔQE = total compensation to quadrant elevation, mil

ΔQE_D = angular quadrant elevation compensation in vertical direction for air density deviation, mil

ΔT = percentage deviation in absolute temperature from standard atmospheric conditions, %

ΔT_{FO} = standard time of flight deviation, s

ΔT_g = deviation in propellant grain temperature from the standard temperature, °F

ΔV = total deviation in muzzle velocity, m/s

ΔV_b = loss in muzzle deviation due to tube wear, m/s

ΔV_g = muzzle velocity deviation due to nonstandard grain temperature, m/s

δ_i = range coefficient for nonstandard propellant temperature, s/(m^i•%)

ε_i = range coefficient for adjustment in quadrant elevation, s/(m^{i-1}•mil)

σ = standard deviation, unit depends on application

$\dot{\phi}$ = filtered azimuth tracking rate in the canted turret plane, mil/s

6-0.2 LIST OF SYMBOLS FOR PAR. 6-3, "AH-64 APACHE ATTACK HELICOPTER FIRE CONTROL DESIGN"

A = helicopter altitude in earth coordinate system, m

A_j = lumped jump parameter, dimensionless

$A_{l_S}, A_{l_L}, A_{l_M}$ = helicopter linear acceleration components in the SLM coordinate system, m/s^2

A_S, A_L, A_M = Kalman filter kinematic helicopter acceleration components in the SLM coordinate system, m/s^2

$\hat{A}_S, \hat{A}_L, \hat{A}_M$ = estimates of the helicopter components in the SLM coordinate system, m/s^2

$\mathbf{A}^T$ = three-dimensional, time-correlated random target vector in inertial reference frame, m/s^2

A_S^T, A_L^T, A_M^T = components of the three-dimensional target acceleration vector in the SLM coordinate system, m/s^2

A_Z = azimuth gimbal angle of the TADS, rad

b_S, b_L, B_m = total lead angle direction cosines in SLM reference frame, dimensionless

C_{D0} = zero yaw drag coefficient, dimensionless

C_U, C_V, C_W = sight line direction cosines relative to aircraft coordinate frame, dimensionless

C_5 through C_{11} = constants, dimensionless

C_{13} = constant, s/m

C_{14} and C_{15} = constants, dimensionless

C_{16} and C_{17} = constants, s^{-3}

D = local air density, kg/m^3

$[D]$ = **XYZ to UVW 3×3 transformation matrix, dimensionless**

D_S = **standard air density, kg/m^3**

d = **projectile diameter, m**

E = **sight line elevation angle, rad**

$[E]$ = **UVW to SLM 3×3 transformation matrix, dimensionless**

E_G = **gun turret elevation angle, rad**

$\dot{E}_G$ = **gun servo lag elevation compensation rate, rad/s**

E_{G_L} = **gun servo elevation command, rad**

El = **elevation gimbal angle of the TADS, rad**

$[F_T]$ = **7×7 state transition matrix (See Eq. 6-43.), units depend on elements**

G = **control logic constant** = $\left\{ \begin{array}{l} \textbf{0, GOODTRACK not active} \\ \textbf{1, GOODTRACK active} \end{array} \right\}$, **dimensionless**

$[G_T]$ = **7×7 noise vector effect matrix (See Eq. 6-43), dimensionless**

$\mathbf{g}$ = **local gravity vector, m/s^2**

g_S, g_L, g_M = **components of gravity in the SLM reference system, m/s^2**

g_X, g_Y, g_Z = **gravity components in earth reference system (Note $g_X = 0$, $g_Y = 0$, $g_Z = g$), m/s^2**

h = **$\pi d^2 \rho C_{D0} M_s / (8 m_p)$, m^{-1}**

$[I]$ = **3×3 identity matrix (See Eq. 6-43.), dimensionless**

J = **control logic constant** = $\left\{ \begin{array}{l} \textbf{0, LMC not active} \\ \textbf{1, LMC active} \end{array} \right\}$, **dimensionless**

K_S^T, K_L^T, K_M^T = **components of white measurement noise along the SLM axes, m, m/s, m/s**

$\mathbf{L}$ = **L-direction unit vector of the SLM coordinate system, dimensionless**

$\mathbf{M}$ = **M-direction unit vector of the SLM coordinate system, dimensionless**

M_a = **local Mach number, dimensionless**

M_s = **standard Mach number at firing, dimensionless**

m_p = **projectile mass, kg**

P_a = **ambient air pressure, Pa**

R = **range between helicopter and target, m**

$\hat{R}$ = **range estimate along S-axis, m**

$\dot{R}$ = **time derivative of target range, m/s**

$\dot{R}, V_e, V_f$ = **velocity components of aircraft relative to the ground expressed in inner platform coordinates, m/s**

R_a = **gas constant for air = 285.9, m^2/(s$^2 \cdot$K)**

r_S, r_L, r_M = **components of target range in the SLM coordinate system, m**

$\mathbf{S}$ = **LOS unit vector of the SLM coordinate system dimensionless**

T = **sight line azimuth angle, rad**

T_a = **ambient air temperature, K**

$[T_A], [T_E], [T_\phi], [T_\psi]$ = **3×3 Euler transformation matrices about the Az, El, ϕ, and ψ axes of the TADS gimbals, dimensionless**

T_G = **gun turret traverse angle, rad**

$\dot{T}_G$ = gun servo lag azimuth compensation rate, rad/s

T_{G_L} = gun servo traverse command, rad

T_M = bullet temperature, K

t = time, s

t_f = TOF of bullet, s

t_p = time of flight of projectile along a trajectory, s

t_0 = time at which prediction is made, s

U_B = muzzle velocity (initial projectile velocity with respect to gun), m/s

U_{B_U} = standard muzzle velocity for given type of ammunition, m/s

V = three-dimensional helicopter velocity vector in initial reference frame, m/s

$\mathbf{V}_B^0$ = three-dimensional helicopter velocity vector in body coordinates, m/s

V_e, V_f = aircraft velocity components relative to ground in inner platform coordinates (See $\dot{R}$, V_e, V_f), m/s

V_{HS}, V_{HL}, V_{HM} = sight velocity components in the SLM coordinate system, m/s

$\hat{V}_{HS}, \hat{V}_{HL}, \hat{V}_{HM}$ = estimates of the sight velocity components in the SLM coordinate system, m/s

$V_{H_U}, V_{H_V}, V_{H_W}$ = helicopter ground speed components in the UVW coordinate system, m/s

$\hat{V}_L, \hat{V}_M$ = estimates of the L- and M-components of helicopter velocity in the SLM coordinate system, m/s

V_S, V_L, V_M = helicopter velocity components in the SLM coordinate system, m/s

V_S^T, V_L^T, V_M^T = components of target velocity vector in the SLM coordinate system with respect to helicopter, m/s

$\mathbf{V}^T$ = three-dimensional target velocity vector in inertial reference system, m/s

$\hat{V}_{TS}, \hat{V}_{TL}, \hat{V}_{TM}$ = estimates of target velocity components in the SLM coordinate system, m/s

V_X, V_Y, V_Z = components of helicopter ground speed in XYZ coordinate system, m/s

W = three-dimensional white noise process vector, m/s³

W_e = pitch rate resulting from thumb controller, rad/s

W_f = yaw rate resulting from thumb controller, rad/s

$W_{R_U}, W_{R_V}, W_{R_W}$ = helicopter airspeed components in the UVW coordinate system, m/s

W_S, W_L, W_M = components of the difference between helicopter ground speed and airspeed transformed into SLM coordinate system, m/s

W_U, W_V, W_W = components of the difference between the helicopter ground speed and airspeed in the UVW coordinate system, m/s

$\mathbf{X}(\cdots)$ = target range vector function, m

$\mathbf{X}_p$ = predicted target random vector one TOF into future, m

X_S = range in the S-axis direction, m

$\hat{X}_S$ = estimate of range in the S-axis direction, m

X^T = X-component of target location in earth coordinates, m

$\mathbf{X}^T$ = three-dimensional target range vector in inertial reference frame, m

$\mathbf{X}^{*T}$ = seven-dimensional state vector $\left[X_S^T,\ V_S^T,\ V_L^T,\ V_M^T,\ A_S^T,\ A_L^T,\ A_M^T \right]'$ in rotating LOS coordinates, m, m/s, m/s, m/s, m/s², m/s², m/s²

X_S^T = S-component of target range in inertial reference frame, m

Y^T = Y-component of target location in earth coordinate system, m

Z^T = Z-component of target location in earth coordinate system, m

Z_1^T = laser range, m

$\mathbf{Z}_2^T$ = two-dimensional relative target velocity vector, m/s

α = projectile total angle of attack, rad

β = angle of sideslip, rad

Γ = inverse correlation time of target acceleration, s^{-1}

γ_L = $\mu_{ff}^{-1}[(V_S - W_S)b_M - (V_L - W_L)b_S]$, dimensionless

γ_M = $\mu_{ff}^{-1}[(V_L - W_L)b_S - (V_S - W_S)b_L]$, dimensionless

ΔE_1 = lead angle elevation correction, rad

ΔT_1 = lead angle azimuth correction, rad

Δt = time interval, s

$\varepsilon_e, \varepsilon_f$ = pitch and yaw IAT errors, rad

ε_ϕ = pitch angle offset, rad

ζ = $r_S - W_S t + V_S^T t_r$, m

η = bias standard deviation, mil

η = $\pi d^2 D C_{D0} M_s/(8 m_p)$, m^{-1}

θ = aircraft roll angle, rad

λ = $g_S/(\eta \mu_S^2)$, dimensionless

μ_{ff} = total initial projectile velocity with respect to air, m/s

μ_S, μ_L, μ_M = components of initial projectile velocity with respect to air in the SLM coordinate system, m/s

ξ = seven-dimensional vector $[-V_S\ 0\ 0\ 0\ 0\ 0\ 0]'$, m/s

ρ = local air density, kg/m^3

ρ^T = drag constant, m^{-1}

$\rho^T \mathbf{V}^T |\mathbf{V}^T|$ = three-dimensional target acceleration due to drag vector, m/s^2

σ = standard deviation, unit depends on variable

τ = time constant, 0.5, s

ϕ = pitch angle, rad

$\dot{\phi}_{LMC}$ = pitch rate generated by LMC, rad/s

ϕ_{LOS} = LOS pitch angle, rad

$\dot{\phi}_{TC}$ = pitch rate command to TADS servo, rad/s

ψ = yaw angle, rad

$\dot{\psi}_{LMC}$ = yaw rate generated by LMC, rad/s

$\dot{\psi}_{TC}$ = yaw rate command to TADS servo, rad/s

$[\Omega]$ = 3 × 3 dyadic matrix of LOS rate vector elements, $\begin{bmatrix} 0 & \omega_M & -\omega_L \\ -\omega_M & 0 & \omega_S \\ \omega_L & -\omega_S & 0 \end{bmatrix}$, s^{-1}

ω = LOS rate vector $[\omega_S, \omega_L, \omega_M]'$ as measured in the inertial reference frame, rad/s

$\omega_{H_U}, \omega_{H_V}, \omega_{H_W}$ = aircraft roll, pitch, and yaw angular rates, rad/s

$\omega_S, \omega_L, \omega_M$ = components of the LOS rate vector in the SLM coordinate system, rad/s

$$[0] = 3 \times 3 \text{ null matrix}, \begin{bmatrix} 0 & 0 & 0 \\ 0 & 0 & 0 \\ 0 & 0 & 0 \end{bmatrix}, \text{dimensionless}$$

6-1 INTRODUCTION

This chapter presents two examples of fire control system design: the M1 Abrams tank and the AH-64 Apache helicopter. The M1 Abrams main battle tank is representative of direct fire control where a high premium is placed on putting the first round on target with the main gun. Relative motion between the weapon system and an enemy combat vehicle is considered in the design, although the short time of flight (TOF) of the high-velocity projectile at typical tank engagement ranges tends to lessen the impact of target motion. The fire control of the AH-64 Apache attack helicopter has been selected as a more complex example. The Apache is armed with the Hellfire missile in addition to a turreted gun and rockets. As presently configured, the Apache can successfully engage stationary and moving ground targets while in modest maneuver.

6-1.1 DESIGN CONSIDERATIONS ASSOCIATED WITH ACQUISITION AND TRACKING SUBSYSTEMS AND WITH WEAPON POINTING SUBSYSTEMS

Acquisition and tracking subsystems and weapon pointing subsystems have the common feature that both are following devices. That is, they respond to signal commands that may be generated by an operator, by the fire control computer, or by an acquisition and tracking sensor. Accordingly, these systems are designed using the principles of automatic control theory, the design of servomechanisms, and the theory associated with the control of man-machine systems. There is detailed coverage of these areas in Refs. 1 through 4.

Additional design considerations relate to the fact that acquisition, tracking, and weapon control may have to be performed on weapon platforms that are moving. In such cases these subsystems are provided with a second set of control signals that attempt to stabilize their relative positions with respect to an inertial frame of reference. Design of the stabilization control is also governed by the general principles of servomechanisms. For many weapon systems, however, primary control and stabilization are considered two distinct control functions because the nature of the system response required is significantly different in each case. In target tracking and weapon control, the speed of response is dictated by the relative speed and dynamics of the target and can often be performed at a much lower frequency bandwidth than is required for stabilization.

Acquisition and tracking subsystems must be able to sense the presence of a target, locate its position within the sensor field of view (FOV), estimate its relative velocity, and in some cases estimate its acceleration. Design considerations for the target-sensing function relate to the resolution, magnification, and FOV of the target sensor; the strength of the signal generated by the presence of the target relative to the signal generated by the surrounding background; and other noise-producing phenomena. An application of these design considerations is given in subpar. 6-2.3.1.1.

Estimation of target velocity and acceleration presents a separate design challenge due to measurements made in the presence of noise, inaccuracies in the acquisition and tracking system, and the presence of disturbances induced by movement of the weapon platform. The principles of signal filtering and prediction, as presented in Chapter 4 of this handbook, can be applied in the development of software and hardware, which can optimize prediction performance.

6-1.2   DESIGN CONSIDERATIONS ASSOCIATED WITH COMPUTING SUBSYSTEMS

6-1.2.1   General Considerations

The design principles of the acquisition and tracking and weapon control subsystems are reasonably straightforward and well documented, but the same cannot be said of computing systems. Therefore, although detailed consideration of the circuitry and operation of computers is covered in Ref. 5, it is appropriate to point out some of the major considerations that influence the implementation of the computing system for any particular fire control system.

It is assumed that whatever other characteristics the computing system has, it is capable of performing the mathematical operations described by the mathematical model. Three major considerations arise, and these can be classified broadly as follows:

1. Accuracy considerations
2. Speed considerations
3. Logical arrangement considerations.

6-1.2.2   Accuracy Considerations

It is obvious that unless the computing system is capable of calculating data required by the weapon pointing subsystem to achieve hits with sufficient accuracy, the overall fire control system will not be satisfactory. The numerical solutions implemented on a digital computer are, however, subject to round-off and truncation errors, and some attempt to appraise these effects should be made before any design is accepted because these effects can become substantial. "Round-off" refers to the fact that the number of bits or digits that can be carried in any digital computer is limited; hence errors are introduced whenever it is necessary to round off a number to the machine word length. When the difference of two nearly equal, very precise numbers is obtained or when many calculations are involved, round-off errors can propagate to a serious level, even in machines having long word lengths, 32 to 36 binary bits. Truncation errors result from the fact that digital computations are performed in a step-by-step manner over intervals in time or spatial direction that are of finite size. Many of the mathematical operations used in fire control, however, use continuous, nonlinear functions, such as the trigonometric relationships and continuous mathematical operations, such as integration and differentiation. Subpar. 4-4.5.1.2 describes how digital computation results in the continuous function or operation being approximated by a truncated infinite series. The resulting truncation errors are affected by both the number of terms retained in the series and the length of the interval.

6-1.2.3   Speed Considerations

When employing a digital computer, the system designer must consider the unavoidable tradeoff between processing time and accuracy. In the laboratory, time can be sacrificed to achieve high levels of computational accuracy, but in a fire control system where real-time operation is essential, accuracy may have to be sacrificed. The extent of the reduction in accuracy that must be accepted is determined by the inherent processing speed of the computer and by the efficiency of the software design. Such a compromise means that the computing interval and the integration or extrapolation rules must be selected to permit real-time operation with the selected computing circuitry. If it is suspected that the computing delays may seriously compromise system accuracy, a proper analysis of these delays should be included in the mathematical model of the system. If the effect cannot be tolerated, appropriate steps must be taken to rectify the situation. Restructuring the data rate time budget to account for individual algorithm demands may be possible.

The speed at which the fire control computer processes data (whether from vehicle-mounted sensors, vehicle crew, or databases) is dependent on both the throughput capacity of the computer and on the capacity of the data bus(ses). Processing time associated with obtaining information from a database, such as the characteristics of a particular ammunition, is primarily related to the throughput capacity of the computer and the acquisition time of the mass storage device (if the data are stored). The processing of data from sensors and from crew stations is dependent not only on the capacity of the computer but also on the capacity of the data bus(ses) and its integrity, i.e., transfer error rate.

The speed of the actual algorithm may vary depending on the structure of the computer software. Fire control computer software is optimized for both speed and size constraints. High-order languages such as Ada may produce smaller modules, but they may not execute as quickly as lower order assembly languages.

6-1.2.4 Logical Arrangement Considerations

Mathematical functions can be mechanized in a fire control system in several ways. The variety of logical arrangements that can be used to carry out coordinate transformations is a particularly good example of this type of problem. Transformations may be instrumented by any one of the following methods:

1. Direct mechanical analogy
2. Computations using Euler angles
3. Computations using direction cosines.

The first means, use of a direct mechanical analogy, uses a stable platform, which is suitably gimbaled and instrumented. Basically, this device would be analog, even though analog-to-digital conversion would be used. The second method, computations based upon Euler angles, is well suited to mechanization by means of instrument servos and resolvers. The third method, direct digital computations using direction cosines, is a method most suitable for a particular application. The use of this approach is determined only in the light of the specific type of equipment, along with the speed, accuracy, and cost requirements associated with the application.

The introduction of ballistic correction data illustrates another situation in which several alternatives may exist. Since nonlinear functions are involved, some method of approximation may be introduced to permit direct analytical approximations of the functions in some simple form. Examples of such approximations include a power series and piecewise linear approximation (based upon storage of information concerning the function and possibly its derivative at particular points). Selection of the more advantageous of these two methods in an actual computing system would depend on the characteristics of the particular nonlinear function to be represented and on the characteristics of the computer.

6-1.3 OPERATIONAL CONSIDERATIONS

In the preceding discussion an attempt was made to develop the ideas that several alternative approaches may exist to mechanize many of the operations called for in the mathematical model of a system and that the choice of the best possible alternative depends upon the characteristics of the specific system being developed and on the characteristics of the specific physical components that might be used in the mechanization of the system. Thus far, attention has been directed primarily at those aspects of the mechanization that influence the mathematical performance of the system. However, the ultimate system must meet the operational field requirements. Frequently it is advantageous to relax the operational requirements on the preliminary model for a fire control system in order to concentrate on demonstrating the basic feasibility of the system. Thus it is likely that the first complete system may not be a system acceptable for actual operational field use. This preliminary model, or prototype, might include some components that would not meet all of the environmental requirements that would be imposed on the final system, might lack some of the test or checkout features that would be essential to its satisfactory performance in combat use, or might not meet all of the accuracy requirements because the technology is not yet available. However, such a prototype could be evaluated before incurring the expense of meeting the broader requirements. Once the changes necessary for the system to meet these broader requirements are designed, the next step may involve production of a limited number of units for field evaluation by service personnel. Only after these units have been pronounced satisfactory and suitable design changes have been incorporated would production of the final operational system be implemented and the mathematical model brought to its ultimate conclusion.

6-2 M1 ABRAMS TANK FIRE CONTROL DESIGN

6-2.1 BACKGROUND

Historically, the primary mission of main battle tanks has been to provide a mobile, high-shock-capability weapons system. In many wars subsequent to World War II (WWII) when both sides in the various conflicts possessed many heavily armored vehicles, the tank vs. tank engagement became primary. In such engagements the key to success is to kill the target before it kills you.

The M60 series tanks, developed in the 1950s and 1960s, were refined to speed the process of acquiring targets and firing accurate first rounds. By the 1970s, however, it became apparent that to counter the perceived threat, a new main battle tank was required.

The M1 tank development program was undertaken to provide the Army with a successor to the M60 series of main battle tanks. The M1 was to possess attributes of combat effectiveness that were significantly superior to those of the M60 series but at low enough levels of acquisition and maintenance costs to allow its fielding in the quantities needed to meet the projected enemy threat. The technology used was to ensure fielding of production units less than eight years after program initiation.

A material need document was developed by the Army in 1972 to define the user's requirements for the new vehicle. This document contained rigid constraints for cost, combat weight, vehicle width, and reliability, availability, and maintainability-durability (RAM-D), but the requirements for improvements in vehicle combat effectiveness were stated in more general terms. Specifically, a list of 19 design requirements was specified in descending order of priority with the requirement that the new vehicle demonstrate "significant" improvements in the 19 areas over the baseline M60 series of tanks, which was fielded at that time.

The 19 design requirement areas were (1) crew survivability, (2) surveillance and target acquisition performance, (3) first-round and subsequent-round hit probability, (4) time to acquire and hit, (5) cross-country mobility, (6) complementary armament integration, (7) equipment survivability, (8) environmental durability, (9) low silhouette, (10) acceleration and deceleration, (11) ammunition stowage, (12) human factors, (13) producibility, (14) operating range, (15) speed, (16) diagnostic aids, (17) growth potential, (18) support equipment, and (19) transportability.

It is important to note that before the development of this new system even began, it was decided that the system must meet certain baseline requirements and provide the potential for growth. For example, although initially fitted with a 105-mm main gun, the tank was later to be equipped with a 120-mm gun. This preplanned product improvement approach is discussed more fully in subpar. 6-2.4.5.

6-2.2 REQUIREMENTS

The requirements for the M1 Abrams tank were defined in the system specification for the M1 tank program (Ref. 6). This specification describes the system, its mission, potential targets, and operational concepts, which are reproduced as follows:

"*General Description.* The M1 tank will be a fully tracked, low-profile land combat assault weapon system possessing armor protection, shoot-on-the-move fire power, and a high degree of maneuverability and tactical agility. The four-man crew shall have the capability to engage the full spectrum of enemy ground targets with a variety of accurate point and area fire weapons.

"*Missions.* The classical offensive, defensive, and retrograde missions of tank units remain in being now and into the foreseeable future. To capitalize on the effectiveness of tank units, and to optimize the results of their employment, the traditional factors of mission, enemy, terrain, and troops available (METT) must be considered in organizing the forces for combat. The commander uses the combined arms team concept and will habitually organize his forces by cross-attachment of tank and infantry units. The M1 tank, utilized as the principal element in the combined arms team, will possess in a single system the essential requisites for mounted combat which consist of a high degree of tactical mobility and protected firepower. The M1 tank, complemented by other elements in the combined arms team, will be the decisive element on the battlefield.

"*Potential Targets.* The M1 system shall have the capability to engage and defeat the potential targets defined in [Table 6-1].

TABLE 6-1.   POTENTIAL TARGETS (Ref. 6)

WEAPON	TARGET
Main Armament	Tank, moving and stationary Infantry Combat Vehicles (ICVS), moving and stationary Antitank Guns Antitank Guided Missiles Troops, moving and stationary Bunkers Antiaircraft Guns
Coaxial Weapon	ICVS, moving and stationary Trucks, moving and stationary Antitank Guns Troops, moving and stationary
Commander's Weapon	Troops, moving and stationary
Loader's Weapon	Troops, moving and stationary aircraft

"*Offensive Mission Concept.* In the offense, the tank will retain its classical role, spearheading the assault elements of the field Army. The tank will be employed as a member of a combined arms force which normally includes artillery, mechanized infantry, air defense, and aviation assets. The tank remains central to the combined arms force. The primary ordnance delivery system and the combined arms force exist primarily to support the tank in its role related to destruction of the enemy force.

"In order to dominate the battlefield, the tank must be able to survive. Survival of the tank is predicated on four basic rules of tank employment and design: utilize terrain, cover and concealment to avoid detection; if detected, use mobility and agility to avoid being hit; if hit, armor protection must be adequate to minimize the probability of penetration; if penetrated, the design of the tank must inherently minimize the damage to critical components and explosive stowage areas, thereby increasing the probability of crew survival.

"*Defensive Mission Concept.* In the defense, the tank platoon will organize in depth, employing three or more positions preselected to optimize cover, concealment, and fields of fire. The platoon defense optimizes the mobility and agility of the M1 tank: attriting the enemy by fire from covered positions and moving to and from the battlefield positions by section, as dictated by the enemy situation. Engagement ranges will vary from in excess of 3000 m to less than 1000 m during the conduct of the operation."

The system specification groups the system requirements into the following functional areas:

1. Combat Operations
    a. Mobility
    b. Surveillance
    c. Communication
    d. Firepower
    e. Survivability
2. Training
3. Maintenance
4. Deployment
5. Storage
6. Verification
7. Logistics
8. Production.

Figs. 6-1 through 6-4 identify the specific operational and performance characteristics defined in the

specification for the functional areas of mobility, surveillance, firepower, and survivability. The system is required to perform all functions on a 24-hour-a-day basis and in all of the climates of the world.
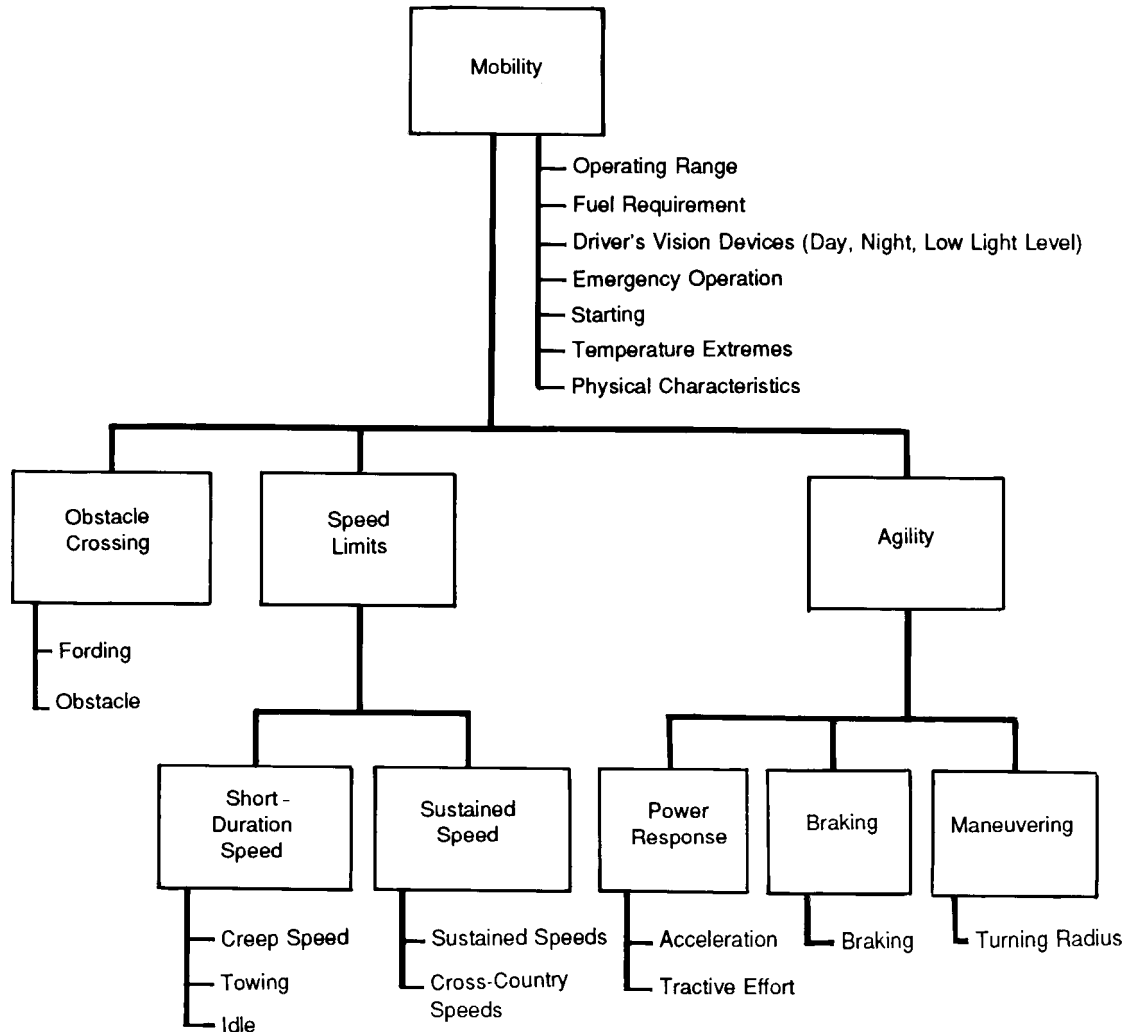
Figure 6-1. Mobility Functional Area Diagram (Ref. 6)

The survivability requirements dictated a short reaction time from target detection to firing and the need for a high probability of a first-round kill while the system is moving. The firepower function required the weapon to be effective at ranges that require the gun to be superelevated. To meet these requirements, it is necessary that the gun be stabilized in space; that the actual range to the target and the target state, i.e., velocity and acceleration, be determined with a high accuracy; that compensation for environmental factors, e.g., temperature, air density, and wind, be achieved; and that the M1 vehicle state, i.e., velocity, cant, and orientation, be known to compensate for relative motion of the target and weapon.

Part of the specification sections are devoted to defining the means by which the weapon system is evaluated to ensure that it conforms to performance requirements. These include not only the engagement scenarios, the environmental conditions, and the firing doctrine under which the system is to be tested but also the methodology and data reduction procedure to be used to evaluate performance. The importance of structuring a test program that is fully representative of the engagement conditions stated in the performance requirements cannot be overstated. Stated requirements are without substance unless backed up with a test procedure that provides the means to demonstrate compliance.

The discussion of the design of the M1 fire control system focuses on the requirements that are directly related to the primary fire control functions, i.e., surveillance, target acquisition, ranging, aiming, track-
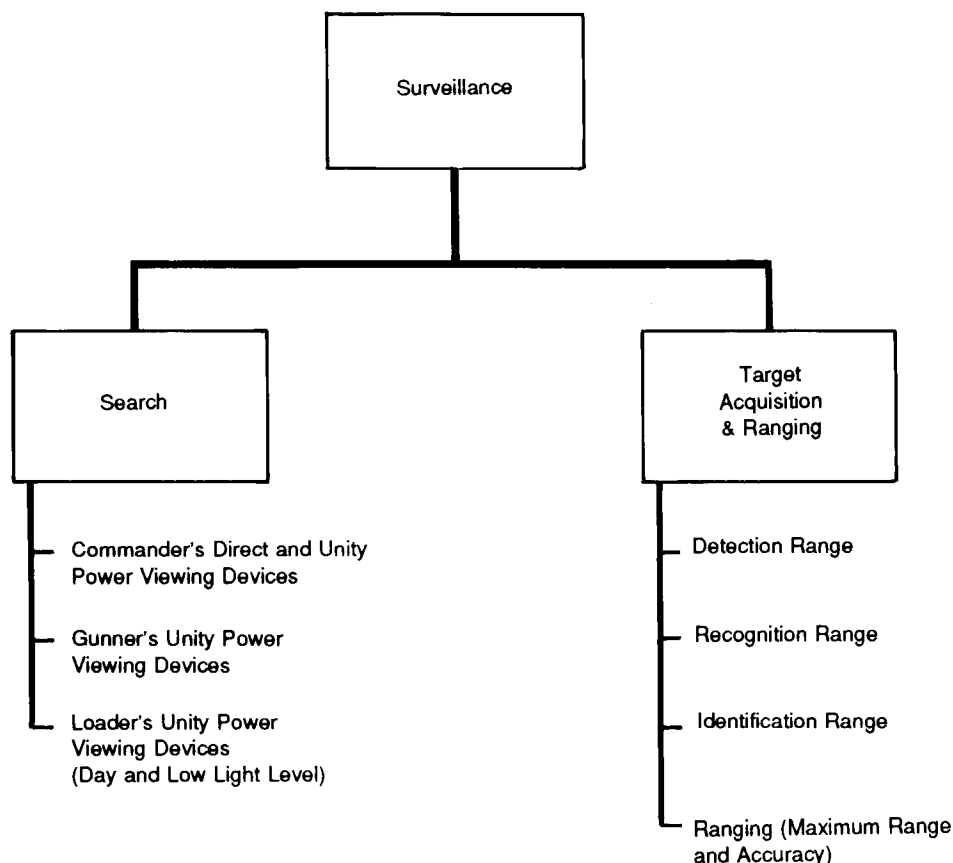
Figure 6-2. Surveillance Functional Area Diagram (Ref. 6)

ing, stabilization, and weapon control, as they apply to the main weapon and to the components that comprise the primary fire control system.

These are the principal elements of the fire control system:
1. Gun and turret drive and stabilization system
2. Ballistic computer
3. Gunner's primary sight (GPS)
4. Commander's extension to the GPS
5. Laser range finder (LRF)
6. Gunner's auxiliary sight
7. Commander's weapon station sight
8. Muzzle reference sensor
9. Sensor suite to provide data for cant, propellant temperature, and wind corrections.
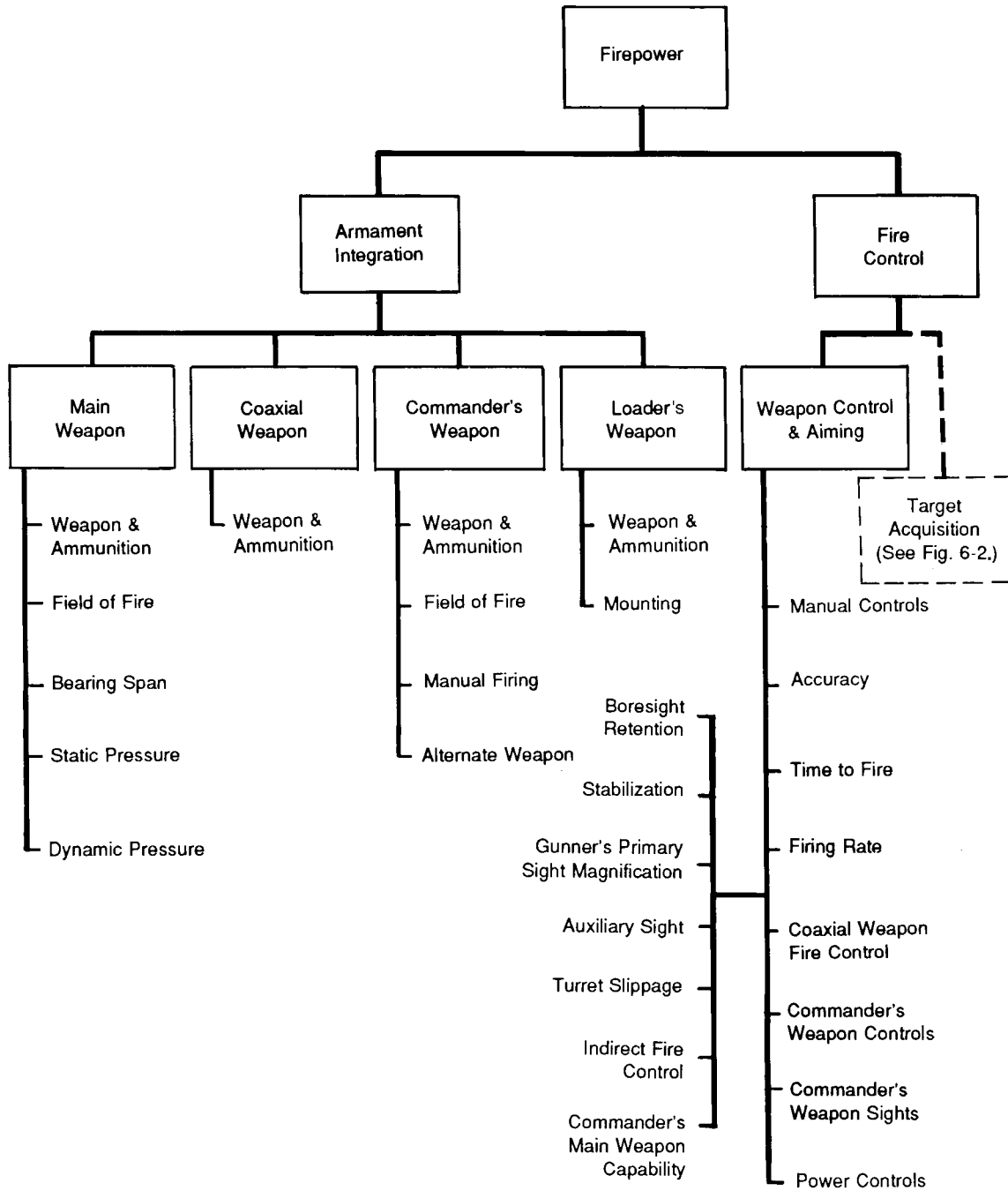
Figure 6-3. Firepower Functional Area Diagram (Ref. 6)
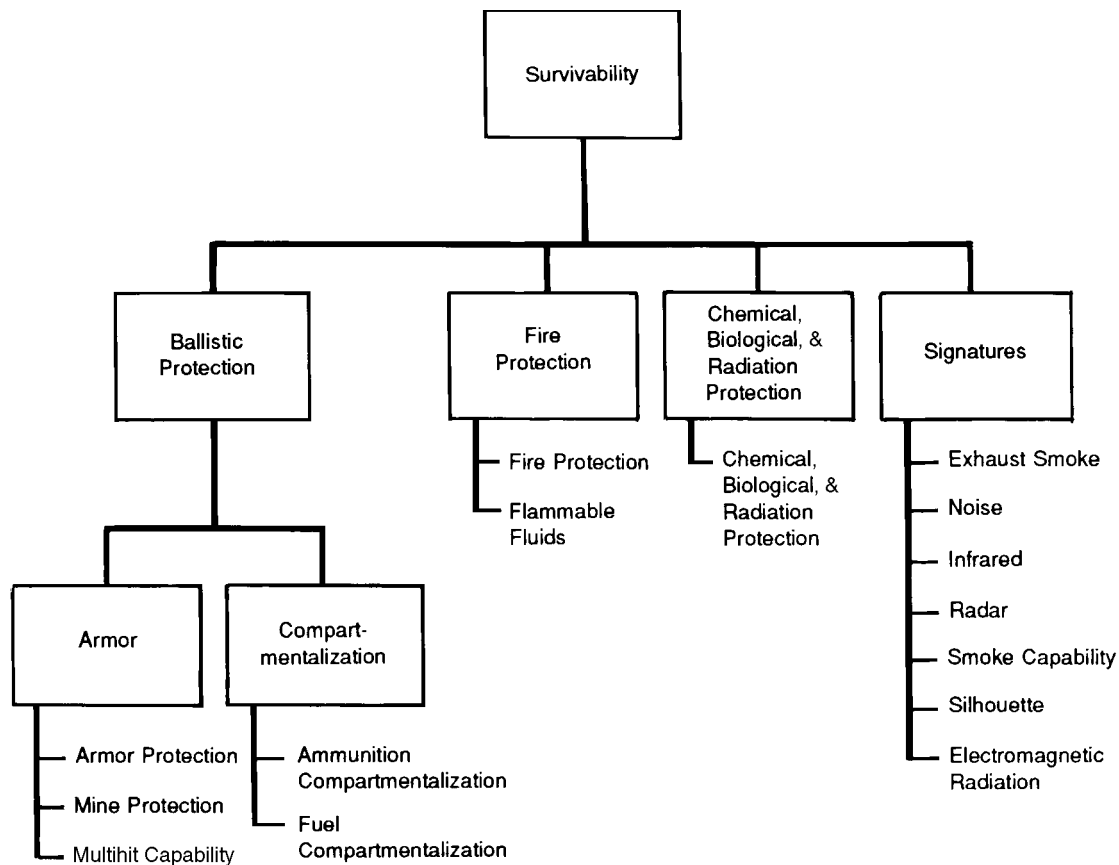
Figure 6-4. Survivability Functional Diagram (Ref. 6)

6-2.3 DEVELOPMENT OF THE SYSTEM CONCEPT

The cost and risk constraints placed on the M1 development program established, a priori, that the new vehicle would represent an evolutionary change and improvement on the existing vehicles rather than a totally new change in the concept for the main battle tank. In addition, changes would have to represent only mature, well-developed technologies.

One obvious improvement to meet these constraints was in the area of gun and sight stabilization. The M60A3 tank incorporated an add-on gun stabilization system that did not provide sufficient isolation of the sighting systems and the gun from the hull motion disturbances to allow either accurate target acquisition or gun firing while on the move. A key objective for the M1 development was to provide the vehicle with a fire-on-the-move capability.

The M60A3 fire control system already included a full solution computer, an LRF, and a thermal imaging sight (TIS). Improvements in system performance could have been attained by increases in the resolution of the thermal imaging system and by the use of radiation wavelengths in the far infrared atmospheric window to reduce the susceptibility of the range finder to battlefield obscurants. The applicable technologies, however, were not sufficiently developed at that time to permit these improvements to be established as either design requirements or objectives.

The LRF and thermal imaging sight in the M60A3 were each product improvements to an earlier version in the M60 series. Thus each of these units was a separate subsystem in the vehicle. The LRF replaced the obsolete and much less accurate optical range finder and, as with the optical system, was operated by the tank commander. The thermal imaging sight replaced the M35E1 image intensifier night sight. The configuration of the thermal sight, however, followed that of the previous passive devices, i.e., separate eyepieces were used for the direct view daylight and for the night imaging channels. As confidence grew in the capability of thermal imaging to enhance target acquisition under conditions of obscuration and

concealment, the thermal sight replaced the direct view optical sight as the primary sighting mode in many scenarios, even in daylight operations. It was desirable, therefore, to have a single eyepiece through which either imaging mode could be viewed. The contractor designed the gunner's sighting system with a single eyepiece for all high-power sighting functions and integrated the LRF into the sight. This approach reduced the commander's task load and also improved maintenance of the alignment between the very narrow range finder beam and the day and thermal sighting optics.

With the shift of the ranging function to the gunner, the commander was free to resume his surveillance of the battlefield for new targets while the gunner completed the engagement with the current target. A logical improvement to the M1 would have been to provide the commander with a separate sighting system that could scan the battlefield independently of the azimuth position of the turret, but cost constraints precluded the inclusion of this option on the M1. Development of an independent commander's viewer did, however, proceed under a separate program with the goal of incorporating it into a future vehicle configuration (M1A2).

The full solution fire control computer on the M60A3 provided corrections to the ballistic solution for nonstandard atmospheric conditions, vehicle cant, target slew rate, and crosswind and for boresight and zeroing offsets. The M1 system concept included all of these and added an onboard capability to sense and compensate for changes in alignment between the gun muzzle and breech. This permitted the gunner to check boresight alignment at any time without the use of special test equipment and without leaving the vehicle. For the M60A3, boresight alignment was at best checked once a day and required that an optical instrument be placed in the gun bore. Without the ability to check the gun alignment periodically, firing errors due to bending of the gun tube from uneven solar heating could exceed a mil.

The ability to provide a fire-on-the move capability within the cost constraints was a significant design challenge. Of the total cost allocated to fire control, 20% was to be consumed by the TIS.

After some analysis, it became obvious that the size of the drives required to stabilize the massive gun and turret adequately is prohibitive in a vehicle with prescribed weight and size constraints. The approach therefore was to employ a so-called director-type system in which the lightweight sight optics are directly stabilized and the gun and turret are stabilized by a servo system that follows the sight. Thus the sight is stabilized to permit target acquisition on the move. The firing errors due to stabilization errors in the gun and turret are then minimized by automatically holding off firing the gun until its position, with respect to the line of sight (LOS), falls within a designated firing window.

Performance and cost tradeoff analyses demonstrated that an acceptable fire-on-the-move capability could be achieved by having the director-type stabilization configuration only for the elevation axis. Only weapon stabilization was retained for the turret, but an azimuth stabilization correction was applied to the reticle in the GPS to improve azimuth tracking performance when the vehicle is maneuvering. The cost savings realized by having a single stabilization axis for the sight head mirror in lieu of a dual-axis gimbal configuration were significant.

6-2.3.1 Accuracy and Time Analysis

The criteria by which the performance of fire-control-related functions in a tank weapon system is evaluated and the factors that influence these criteria are discussed in the subparagraphs that follow. The primary mission areas considered are surveillance and firing effectiveness.

6-2.3.1.1 Surveillance

Surveillance performance is quantized in terms of the probabilities of detecting, recognizing, and identifying potential targets. Each of these is defined and discussed.

Detection is defined as sensing the presence of something in the FOV that may be a potential target. The "something" may be only a portion of the actual target because the target may be partially obscured. Recognition is said to occur when the crew member is able to categorize the sensed object by its type, e.g., bunker, tank, truck, or artillery piece. Identification involves still higher performance; it requires that the object be classified by its specific type, e.g., M1 tank, T-80 tank, or Leopard tank.

Since each progressive level of surveillance requires more perceived detail, it follows that the resolution and magnification requirements for the sighting devices in the tank must be increased appropriately

for each higher level of performance. The level of detail required to perform each surveillance function has been defined in Refs. 7 and 8 in terms of the number of picture elements (alternatively called pixels, resolution elements, or video lines) that must be subtended by the target image in order to detect, recognize, or identify the target. The number of elements required is also dependent on the designer's requirements for the probability of successfully performing these functions. Table 6-2 shows the number of picture elements required to detect, recognize, and identify military-type targets in a battlefield environment with probabilities of approximately 90%.

TABLE 6-2. RESOLUTION REQUIREMENTS

FUNCTION	NUMBER OF LINES OR RESOLUTION ELEMENTS PER CRITICAL TARGET DIMENSION
Detection	3
Recognition	12
Identification	20

In setting the magnification requirements for direct view optical sights, the resolution limiting factor is the observer's eye. In battlefield conditions visual acuity is assumed to be 0.44 mrad (90″). If a direct view optical sight is to be designed to identify a tank-type target at 3000 m, for example, the magnification should be selected so that the tank image at the observer's eye subtends 20×0.44 mrad, or 8.8 mrad.

An offsetting consideration in sight design is the FOV of the sighting device. The final choice of magnification must be made in a tradeoff analysis with the FOV. The tradeoff results from a practical limitation in direct view optical systems that states the apparent FOV should not exceed 60 deg. Thus the product of the magnification and the actual FOV should not exceed 60 deg.

In the example under consideration, a magnification of 11.5 power would be required, and the resulting FOV would be approximately 5.2 deg. Although an FOV of this magnitude is acceptable for target identification and also for target-tracking tasks, it would limit the tank crew's ability to search and scan broad areas of the battlefield rapidly. Two levels of sight magnification were therefore incorporated in the primary sighting systems: a low-magnification, wide FOV mode for general surveillance and a higher magnification, narrow FOV mode for target identification and tracking. A reasonable basis for the choice of the magnification of the low-power mode is to have the theoretical detection performance at low power match the recognition performance at high power. This would establish the ratio of the high- to low-power magnification at about 4:1 based on the data in Table 6-2.

In video imaging systems the resolution limiting factor is the effective number of resolution elements of the sensor. In sighting systems with monocular eyepieces, the optical magnification is selected so that the angle subtended by each video line is just under the limiting resolution of the eye and in addition satisfies the requirements of Table 6-2 for the designated target range. Thus the FOV of such a sight has the same restrictions as the direct view sights described previously.

In the M1 vehicle the high-power and low-power magnifications in both the daylight and thermal channels of the GPS were set at 9.8 power and 3 power, respectively, with the corresponding horizontal subtenses of the FOV at 5 deg and 15 deg, respectively. The 9.8-power magnification gives the gunner's sight an effective resolution of 0.045 mrad, which, as is demonstrated, is sufficient for precision gunnery engagements.

The magnification in the sight for the commander's machine gun was also set at 3 power. Because the effective range of this weapon in direct fire applications was limited to 1800 m (It has been extended.), as described in Ref. 9, the sight did not require a high-magnification mode.

An assessment of the surveillance performance of passive thermal imaging devices-–most commonly referred to as forward-looking infrared (FLIR) devices–can be made with the aid of the data in Table 6-3. This table shows the maximum theoretical range in a perfectly clear atmosphere under which the imaging requirements stated in Table 6-2 would be satisfied in the M1 gunner's sight. The ranges in Table 6-3 are

based on the limiting factor in FLIR performance: the number of detector elements that can be placed into the detector array and hence across the FOV. Due to the technology available at the time of the M1 development, the maximum number of elements was 120. This restriction arose from the fact that signal processing functions, e.g., multiplexing, could not be integrated into the detector chip. Each detector therefore had to be individually wired to the post processing electronics where there was a limit to the number of wires that could be accommodated with adequate reliability. Advanced technology development prgrams involving "focal plane arrays" in which signal processing functions are integrated into the detector chip were under way, but hardware for military systems was not yet available.

It is clear from Table 6-3 that the FLIR image quality would not be as good as that of the visible optical channel under ideal atmospheric conditions. The advantage of the FLIR, however, is that it will provide an image under conditions in which the visible optics are ineffective.

TABLE 6-3. SURVEILLANCE PERFORMANCE FOR M1 FLIR IMAGING SYSTEM

FUNCTION	MAXIMUM RANGE, m	
	Low Power (3)	High Power (9.8)
Detection	986	3067
Recognition	246	767
Identification	148	460

M1 Common Module FLIR: 180 elements

When acquiring targets while on the move is required, the degree of stabilization in the vehicle sighting systems influences the probabilities of detecting, recognizing, and identifying potential targets. Vibration of the sight image blurs fine details and thereby reduces the effective resolution of the sighting system. For a stationary vehicle or a perfectly stabilized image, the limiting resolution in a direct view optical or video-based sight is set by the observer's eye, whereas for image vibration the sight itself becomes the limiting factor. Fig. 6-5 depicts the LOS stabilization requirements for detection and recognition of armored vehicle targets while on the move. The figure shows, for example, that the standard deviation (1 σ) of the stabilization error must be less than 0.1 mrad (0.1 mil) in order to detect a target at 4000 m or to recognize a target at 1000 m. LOS stabilization requirements are generally specified in terms of a frequency response for the disturbance rejection capability of the stabilization system. This is the ratio of the power spectral density of the positional error in the LOS to the power spectral density of the hull disturbance over the expected frequency range of the hull disturbance.

With analog controllers representative of the technology of the 1970s, sight stabilization in a director configuration over the roughest terrain was no better than about 0.2 mrad (0.2 mil). This, however, was

0.50 Probability of Target Detection
(3 elements across target)

0.50 Probability of Target Recognition
(12 elements across target)

Target size: 2.3 m x 2.3 m
Probability without motion: 0.85
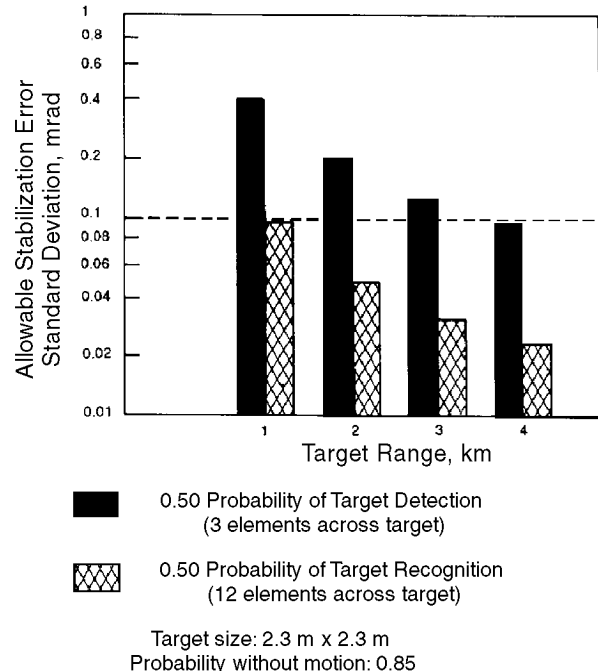
Figure 6-5. Line-of-Sight Stabilization Requirements for Target Aquisition on the Move

a significant improvement over the M60A3, which could achieve a stabilization level of only 1 mrad with its add-on stabilization configuration.

Fig. 6-5 indicates that with a 0.2-mrad (0.2-mil) stabilization error target recognition could not be accomplished at any useful engagement range. It would appear, therefore, that the requirement to acquire and engage targets while on the move could not be satisfied with the technology of the 1970s. If the positions of threat and friendly forces are known, it is possible, however, to allow the engagement of a target to proceed on the basis of detection alone. Under such circumstances engagements out to 1500 m, a range at which a high percentage of tank battles has occurred, would be possible. In general, however, the risk of fratricide is high if targets are engaged at detection before recognition and identification occur. Thus the rules of engagement might preclude firing while on the move in longer range engagements in which friendly force locations are uncertain.

6-2.3.1.2 Firing Effectiveness

Because a main battle tank is to be a highly mobile antiarmor assault weapon, the success of its offensive and defensive missions and its survival in close combat engagements are dependent, among other characteristics, upon the ability of the crew and weapon system to fire first and to fire with a precision that ensures a first-round hit. The size of the standard North Atlantic Treaty Organization (NATO) target used for armored vehicle performance evaluations is 2.3 m × 2.3 m, which is representative of the frontal vulnerable area of a tank-type vehicle. This vulnerable area is the source of the overall system accuracy requirements. The criterion used to evaluate firing accuracy is the probability of achieving a first-round hit P_{ss} against the standard 2.3 m × 2.3 m target. The ability to fire first is assessed by using criteria such as time to fire, rate of fire, and rate of engagement. The considerations of firing accuracy and timing are discussed in the subparagraphs that follow.

6-2.3.1.2.1 Firing Accuracy

Engagement of a target after it has been acquired involves the following steps:

1. Acquisition of appropriate data relating to the state of the weapon platform, the target, and the surrounding environment
2. Development of a ballistic solution using the acquired data
3. Weapon pointing and control to implement the solution.

The factors that influence the solution of the fire control problem in direct fire target engagements are listed in Table 6-4. Each of these has been discussed previously in this handbook. The parameters which characterize the factors that have a significant effect on this solution must be sensed by the fire control system and the resulting data used as input to the computations.

The mission descriptions for the M1 imply that in any specific engagement the vehicle need function only in an autonomous role. Therefore, there was no need, as there is in artillery engagements, for the tank to have an onboard navigation system or inertial platform. Thus data acquisition, computation, and gun control could be accomplished in a simple weapon-centered coordinate system.

Two coordinate systems were used. In both systems one of the coordinate directions is placed along the optical LOS. A second coordinate direction is orthogonal to the sight axis. In one system it is located in the plane of rotation of the turret and in the second system it is located in a horizontal plane, i.e., normal to the local gravity vector. In both systems the third coordinate direction is oriented to form an orthogonal right-hand set. In these systems all data, computations, and gun commands are referenced to the LOS. Computations are made in the system with the horizontal coordinate direction, and data acquisition and gun control are accomplished in the system oriented with the turret plane.

The magnitudes of the compensations required for precision tank gunnery engagements with armor-piercing, high-velocity rounds are listed in Table 6-5. The values shown are typical for engagements at 1200 m and 3000 m and are based on the assumptions listed in the footnotes to the table. Ballistic data used in the computations are taken from 105-mm armor-piercing discarding sabot (APDS) firing tables. The compensations shown would in general be larger for the lower velocity, high-explosive plastic (HEP) and high-explosive antitank (HEAT) rounds.

TABLE 6-4.   FACTORS THAT INFLUENCE THE FIRE CONTROL SOLUTION IN DIRECT FIRE ENGAGEMENTS

Present target position (3-dimensional)

Relative motion (velocity and acceleration) between target and weapon

Direction of local gravity vector with respect to vehicle coordinate reference frame

Sight and weapon parallax

Angular misalignment between weapon and sight axes (boresight misalignment)

Nonstandard conditions related to internal ballistics:
   Charge temperature
   Projectile weight
   Barrel wear

Nonstandard conditions related to external ballistics:
   Muzzle velocity
   Speed of sound in air mass
   Air density
   Crosswind
   Range wind
   Angle of sight
   Coriolis acceleration due to earth rotation
   Vertical and horizontal jump

Own vehicle motion

The required magnitudes of compensation were used to determine which factors required compensation. The significance of the magnitudes of the compensations can be appreciated with the aid of Table 6-6. This table gives the single-shot hit probability as a function of total fire control system error for a 2.3-m × 2.3-m target located at ranges of 1000 m and 3000 m. The table is computed on the assumptions that the system errors in the azimuth and elevation directions are equal and that the round-to-round dispersion is 0.27 mil. This dispersion is reasonable for the 105-mm APDS round on the M1. If each of the factors that contribute to the total system error is statistically independent, the total error can be estimated as the square root of the sum of the squares of the individual error contributions.

The following two observations can be made:

1. For target engagements at 3000 m, all compensations approximately 0.1 mil or greater have a significant influence on the fire control solution. This range includes most of the factors shown in Table 6-4.

2. For target engagements at 1200 m, compensations approximately 0.3 mil or greater have a significant influence on the fire control solution. This range includes the compensations for superelevation, jump, and moving targets. The solution is, however, relatively insensitive to the other compensation factors. This observation provides the basis for the so-called "battlesight" mode of operation, which is discussed later.

The next step in the design process was to perform a tradeoff analysis between cost and the increase in mission effectiveness due to the implementation of each compensation function. The following is a synopsis of the conclusions drawn from this analysis:

1. *Superelevation.* Accurate superelevation compensation for target range must be provided in all precision gunnery engagements. The requirement for accurate range data and the desire to consolidate the ranging function into the GPS were sufficiently important reasons to justify the cost of developing a new range finder. As a result of this effort, a neodymium-YAG laser operating at 1.06 μm was selected over the ruby laser previously used in the M60 tank. A major justification for this change was to reduce the radiation signature of the vehicle in the visible band of the spectrum.

TABLE 6-5.   COMPENSATIONS IN DIRECT FIRE ENGAGEMENTS

FACTOR	COMPENSATION, mil			
	1200 m		3000 m	
	Vertical	Horizontal	Vertical	Horizontal
Superelevation	2.8	na	7.6	na
Traverse Rate[1]	na	14.0	na	15.0
Elevation Rate[2]	0.8	na	0.9	na
Range Rate[3]	0.05	na	0.16	na
Trunnion Cant[4]	0.01	0.25	0.03	0.68
Sight/Weapon Parallax[5]	0	0	0.26	0.35
Tube Bend[6]	2.0	na	2.0	na
Boresight Alignment[7]	0.15	0.15	0.15	0.15
Jump Dispersion[8]	0.25	0.25	0.25	0.25
Earth Rate[9]	0.02	0.02	0.05	0.05
NON-STANDARD CONDITIONS				
Muzzle Velocity[10]	0.06	0	0.16	0
Air Temperature[11]	0	0	0.01	0
Air Density[12]	0	0	0.02	0
Crosswind[13]	0	0.1	0	0.26
Range Wind[14]	0	na	0	na
Angle of Site[15]	0	na	0.01	na
OWN VEHICLE MOTION				
Cross Range[16]	na	13.8	na	13.8
Downrange[16]	0.08	0	0.22	0

na = not applicable
  1. Target velocity : 20 m/s
  2. Target velocity: 4 m/s on 30% grade
  3. Target velocity: 20 m/s approaching
  4. 5-deg cant angle (1σ)
  5. 0.73 m horizontal, 0.55 m vertical parallax distances in M1
  6. Field measurements in direct sunlight
  7. Specification requirement at breech
  8. Ref. 10
  9. Coriolis acceleration resulting from projectile velocity
10. 1% of nominal
11. 1.5% of standard absolute air temperature (288 K) (Ref. 10)
12. 1.5% of standard atmospheric pressure (101.325 kPa) (Ref.10)
13. 3.5 m/s based on worldwide meteorological surveys
14. 3.5 m/s
15. With 2 deg of angle of site
16. Vehicle speed: 20 m/s, no range wind compensation

2. *Azimuth Rate.* The rate gyro required in the azimuth loop of the turret stabilization system could, with additional digital filtering, provide the data input required for target lead compensation in azimuth. This compensation could therefore be provided at no increase in hardware cost.

TABLE 6-6. EFFECT OF SYSTEM ERROR ON SINGLE-SHOT HIT PROBABILITY WITH 0.27-mil AMMO DISPERSION

SYSTEM ERROR, mil	SINGLE-SHOT HIT PROBABILITY P_{SS}, dimensionless	
	1000 m	3000 m
0	0.99	0.74
0.2	0.99	0.57
0.3	0.98	0.45
0.4	0.97	0.34
0.5	0.92	0.26
0.6	0.86	0.20
0.8	0.69	
1.0	0.55	

3. *Elevation Rate.* Data for elevation rate compensation could be provided by the rate gyro that was to be included in the LOS stabilization subsystem. This compensation was not, however, included in the system design. The reasoning behind this decision has been lost with time, but it is suspected that the designers believed that armor targets would not be a primary threat if they were traveling on hilly terrain. Also, if range compensation, as discussed next, could not be implemented at low cost, there was no justification to provide compensation in elevation.

4. *Range Rate.* Range rate compensation would not be provided because the stated primary role of the M1 was to be antiarmor and not, for example, air defense. The ability to track ground targets in range did not provide sufficient justification for the added equipment cost. If range rate compensations had been implemented, an additional, or an entirely new, sensor would have been required. The LRF that was to be installed on the vehicle to provide static range data would not have had sufficient accuracy or pulse repetition frequency to support the range rate function. With the existing state of the art, systems that did require three-dimensional data on target position and rate used radar trackers. These systems were also able to incorporate nonlinear prediction algorithms to enhance performance against maneuvering targets.

5. *Trunnion Cant.* Compensation for trunnion cant would be provided but only for a stationary vehicle. This decision, which required that the vehicle be level when firing on the move, was judged not to have a significant impact on mission effectiveness. A pendulous-type cant sensor had been fielded on previous versions of the M60 series tanks and was to be used in the M1. The problem with this type of sensor when on the move is that the pendulum responds to transverse vehicle accelerations and generates biased data. Thus a new dynamic cant sensor would have to be developed if cant compensation were to be provided on the move.

6. *Parallax.* With the use of a digital fire control computer, the compensation for parallax between the weapon and sight can be implemented with a few additional lines of computer code. This compensation was included in the M1 design.

7. *Boresight.* As discussed earlier, one of the significant development efforts for the M1 was to provide an improved muzzle boresighting system to reduce battlefield-induced alignment errors. This required a muzzle-mounted collimator and additional optics and controls in the gunner's sight. Boresight misalignment is measured by sighting on the collimator with the gunner's sight. Offset data are automatically sensed and stored in the computer.

8. *Jump.* Jump correction data for each type of main gun ammunition are stored in the digital com-

puter, and the appropriate data are automatically input to the ballistic solution. The cost impact of implementing this compensation was minimal. The data are derived by driving a reference reticle in the gunner's sight to the center of the zeroing burst pattern. The offset data are automatically acquired and stored in the computer.

9. *Muzzle Velocity.* At the time of the development of the M1, there was no low-cost, reliable technique to sense muzzle velocity directly. Compensations for muzzle velocity deviations were therefore derived from empirical relations by using actual measurement data on the temperature of the propellant and tube wear.

10. *Air Temperature and Density.* Compensations for nonstandard air temperature and density were to be provided from data derived from meteorological reports. The data were entered manually into the computer.

11. *Crosswind.* Crosswind compensations were to be provided for each of the main gun rounds. Data based on the ballistic firing tables were stored in the form of polynomial coefficients from which angular drift could be computed as a function of target range and filtered wind speed data. Wind sensors based on four different physical principles were available for selection; several of these were already in the Army inventory for use in the M60 vehicles. Each of the sensor types had the capability to provide range and crosswind measurements.

12. *Range Wind.* The designer decided not to implement any compensation for range wind. This decision was based on the fact that the required compensation for the engagement ranges in which the rounds were used was relatively insignificant. For example, the compensation for the APDS round at 3000 m is less than 0.01 mil. For the HEAT round the compensation required at 3000 m is 0.09 mil. The accuracy of this round dictates, however, that it not be used for ranges in excess of 2000 m. At this range the required compensation is only 0.02 mil. Cost savings were realized by not having to provide additional digital filtering of the raw wind data and by having a sensor with only a single measurement axis. Data filtering is needed to remove the effects of vehicle- and ground-induced turbulence.

13. *Angle of Site.* Implementation of this compensation would require an additional sensor to measure the inclination of the line of site with respect to a horizontal reference. Since the level of compensation required is small, the cost to develop a new sensor could not be justified. Therefore, the compensation was not implemented.

14. *Vehicle Motion.* In general, implementation of compensations for the effects of a moving weapon platform on the fire control solution requires knowledge of the ground speed of the vehicle and the orientation of the turret with respect to the hull. If the inertial effects of the rotation of the earth can be neglected, the solution can be implemented in terms of vehicle airspeed and target motion relative to the vehicle. This latter approach was not attractive because sufficiently accurate ground speed sensors had not been used on armored vehicles and the designers wished to avoid the cost of developing and fielding an entirely new sensor. The feasibility of the approach, however, depended on the restriction that the vehicle maintain a relatively constant velocity during the engagement process to avoid measuring or deriving vehicle acceleration data. Such data would have been difficult to extract from the noisy wind speed signal. An accurate measure of steady state airspeed could, however, be extracted after filtering. The constant speed requirement was not a problem since it was consistent with existing doctrine.

If wind speed data are used, the compensation for cross-range velocity is automatically provided by the tracking rate and crosswind compensations that are implemented for a stationary vehicle. This compensation is demonstrated in subpar. 6-2.3.2. Similarly, a compensation for downrange vehicle motion based on measuring range wind would be feasible if range rate data were available. Without this data the error remains and has to be incorporated into the overall system error budget.

6-2.3.1.2.2   Timing

Timing requirements for the M1 system are specified in terms of time to fire and rate of fire. These parameters can be understood by considering the sequence of events that take place in direct fire engagements. An engagement consisting of a single shot is shown in Table 6-7; the events are divided into three distinct phases: acquisition, engagement, and assessment.

TABLE 6-7.   SINGLE-SHOT, DIRECT FIRE ENGAGEMENT SEQUENCE

ACQUISITION:
     Target appears
     Detect
     Recognize
     Identify
     Decision to engage

ENGAGEMENT:
     Issue fire command
     Slew weapon to target
     Aim and/or track
     Range
     Fire control solution:
          Target state estimation
          Vehicle state sensing
          Environmental state sensing or estimation
          Prediction
          Ballistic computation
          Gun order computation
     Firing demand
     Firing delay
     Shot exit

ASSESSMENT:
     Target strike
     Damage assessment

Time to fire includes all of the events in the acquisition phase and the events in the engagement phase up to and including the exit of the projectile from the muzzle of the gun. The sequence shown assumes that a round has already been loaded into the breech of the gun, and this assumption is in accordance with tank gunnery doctrine for a vehicle traveling in hostile territory.

The rate-of-fire parameter implies multiple firings at a single target. In this situation the timing sequence includes events associated with gun recoil and reloading. The modified engagement sequence for multiple-round engagements is shown in Table 6-8. The rate of fire is then the reciprocal of the time it takes the tank crew to cycle repeatedly through all of the events in the engagement and assessment phases shown in Table 6-8. Time of fire and rate of fire both depend on the skill of the tank crew and on the speed of response of the system hardware.

For multiple-target engagements an additional parameter called rate of engagement is used. This parameter represents the time to complete all of the events shown in Table 6-8.

Fig. 6-6 illustrates the relationship between the events in the timeline and the timing parameters.

The requirements specified for the timing parameters can be derived from combat models, which simulate force-on-force engagements and one-on-one tank duels. These simulations can, for example, estimate the probability of destruction of enemy and friendly forces as an engagement progresses in time for assumed values of rate of fire, time to fire, and single-shot hit probability for each of the opposing forces. Ref. 11 describes several combat models that can be used for this type of an analysis. One example in Ref. 11 clearly illustrates the obvious statistical advantage of achieving surprise and of being the first to fire in a one-on-one engagement.

In general, a tank crew can engage in two types of gunnery with the main gun: battlesight and precision. The choice is made by the commander and communicated to the other crew members. Battlesight eliminates the ranging function and therefore is somewhat faster. In battlesight mode a range for each ammunition type is entered into the computer prior to the start of the mission. Then, if the commander

calls "battlesight" while engaging, the gunner depresses a battlesight switch, and the superelevation for the chosen ammo at the preselected range is added to the ballistic solution. For high-speed ammunition, such as armor-piercing, fin-stabilized, discarding sabot (APFSDS) at modest ranges, the trajectory is fairly flat. Thus, if a battlesight range of 1200 m were used, a hit might be assured if the target was actually at any range between, say, 800 m and 1500 m.

TABLE 6-8. MULTIPLE-SHOT FIRE ENGAGEMENT SEQUENCE

ENGAGEMENT:
    Issue fire command
    Relay and track target
    Range
    Fire control solution:
        Target state estimation
        Vehicle state sensing
        Environmental state sensing or estimation
        Prediction
        Ballistic computation
        Gun order computation
    Firing demand
    Firing delay
    Shot exit
    Recoil
    Run out
    Index gun
    Reload
    Reindex

ASSESSMENT:
    Target strike
    Damage assessment
    Decision to reengage
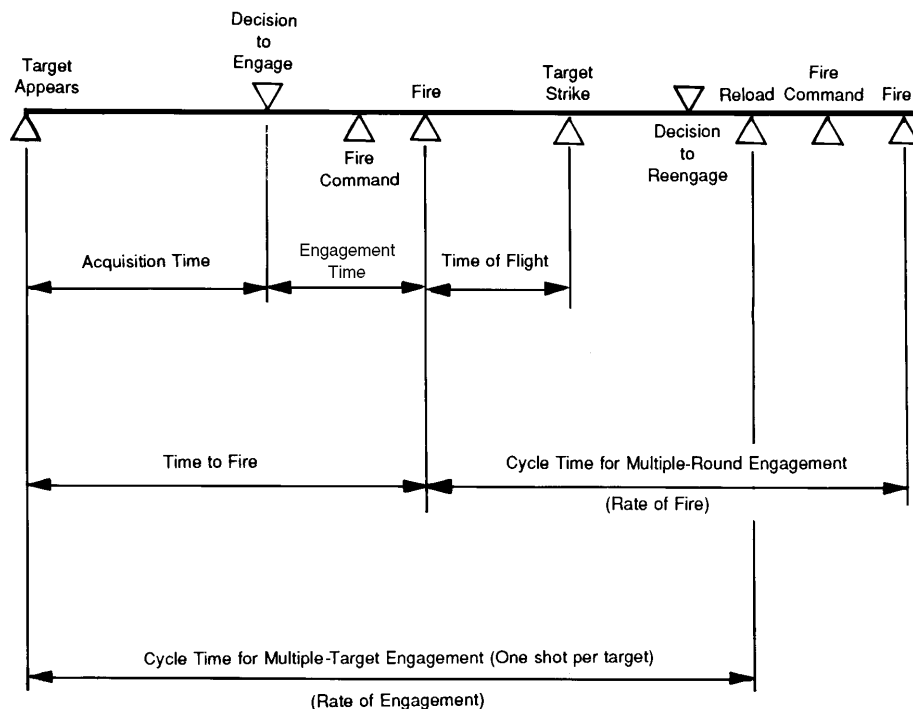
Figure 6-6. Description of Time Line Terms

6-25

For precision gunnery the gunner aims at the target, pushes the "Laser Fire" button, and waits until he reads the measured range. If he believes the range to be correct, he can then fire the gun. The fire control computer adds the superelevation for the measured range to the ballistic solution.

The time needed to perform the acquisition functions is dependent on the target range, the contrast of the target against the background, and the level of background clutter. If the target contrast is low, the scene, as imaged by the sight, must be scanned by moving the retina of the eye across the FOV. This is a slow process as demonstrated by the data in Table 6-9. If the contrast in the target image is high, the target is seen immediately by the less sensitive peripheral portion of the retina. No scanning is required, and detection occurs in a fraction of a second. This potential for significantly reducing acquisition time under low-contrast conditions is, in addition to increasing the probability of detection, another reason to incorporate thermal and low-light sensors into various fire control systems.

TABLE 6-9.   TIME-TO-SEARCH FIELD OF VIEW FOR STATIONARY, LOW-CONTRAST TARGETS (Ref. 8)

TARGET RANGE, m	SCAN TIME, s		
	Scene Clutter		
	High	Moderate	Low
500	7	4	0.7
1000	29	15	3
2000	115	57	12
3000		129	26
4000			46

Field of view: 10 deg (50% scan)
Target size: 2.3 m
Detection probability: 0.5*

*Probability of concentrating foveal vision on specific target position

Table 6-10 illustrates the premium placed on the speed demonstrated by the tank crew. It shows the number of points assigned to a crew in precision gunnery exercises as a function of time to fire when a first-round hit is achieved.

TABLE 6-10.   SCORING OF ENGAGEMENT TIME

Time to fire a first-round hit, s	10	15	20	25	30
Assigned score	100	90	70	40	0

The timing assumes that the gun is preloaded before commencement of the exercise. In battlesight engagements the highest score would be assigned to a 6-s time to fire.

Fig. 6-7 shows a detailed timeline for a multitarget engagement. The appearance of the first target represents the start of the timeline, and the time to fire at this first target is shown to be 9 s. A second target appears 5 s into the engagement but cannot be acquired until the completion of the damage assessment on the first target. This example assumes that there is no independent viewer for the commander, which would allow him to acquire the second target at an earlier time. The engagement cycle time in this example is the 16-s interval between the completion of the assessments for the first and second targets.

Figure 6-7. Multitarget Engagement Time

6-2.3.2 Mathematical Models

The conclusions drawn from the cost benefit analyses simplified the implementation of the fire control computations. The most significant simplification arises from the decision not to implement a correction for target range rate. Without this simplification the ballistic and prediction equations of motion must be solved simultaneously to determine the location of the future point of impact or the empirical ballistic relationships based on the firing tables must be used to identify by an iterative process the specific ballistic trajectory that will intercept the predicted target path of motion. The resulting range and TOF to the point of impact can then be used to determine the offset between the line of fire and line of sight for standard and nonstandard weapon and environmental conditions. With the constant range assumption the distance to the point of impact is known a priori, and the required offsets can be computed directly.

The following equations define the process used to obtain the angular offsets in azimuth and elevation between the gun line and the instantaneous line of sight in the M1 vehicle. The parameters of the standard ballistic trajectories and the effects of the nonstandard conditions are represented by polynomial expansions that are fit to the ballistic and unit effects data contained in firing tables. The coordinate systems used for data acquisition and computations are noted. The equations were later used to determine the sensitivity of the computational accuracy to errors and to set tolerances on the measurement accuracy of input parameters.

The process begins with computation of the deviations in air density and air temperature from standard conditions. The meteorological data available to the forces operating on the battlefield include measurements of local air temperature and pressure but not air density. The determination of air density and

its deviation from standard conditions are therefore derived from these measurements by using the relationships defined by the ideal gas law, which states

$$\frac{P}{D} = R_a T, \ \mathbf{m^2/s^2} \tag{6-1}$$

where

P = pressure of gas, Pa
D = density of gas, kg/m^3
T = absolute temperature of gas, K
R_a = gas constant of air, 285.9, m^2/(s^2·K).

The actual air density based on the measured conditions of temperature and pressure is given by

$$D = \frac{P}{R_a T}, \ \mathbf{kg/m^3}. \tag{6-2}$$

Similarly, the density under standard conditions is given by

$$D_0 = \frac{P_0}{R_a T_0}, \ \mathbf{kg/m^3} \tag{6-3}$$

where

D_0 = air density at standard atmospheric conditions, kg/m^3
P_0 = air pressure at standard atmospheric conditions, Pa
T_0 = air absolute temperature at standard atmospheric conditions, K.

The standard conditions of temperature and pressure are 288.15 K (59°F) and 101,040 Pa (29.9213 in.-Hg), respectively.

The ballistic tables give data that show the effect of unit deviations in nonstandard conditions on ballistic trajectories. These data are called the unit effects. The unit effect for nonstandard air density is expressed in terms of a percentage deviation from standard conditions, i.e.,

$$\Delta D = 100 \frac{D - D_0}{D_0}, \ \% \tag{6-4}$$

where

ΔD = percentage deviation in air density from standard atmospheric conditions, %.

Substituting Eqs. 6-2 and 6-3 into Eq. 6-4 and rearranging yield

$$\Delta D = 100 \left(\frac{T_0 P}{P_0 T} - 1 \right), \ \%. \tag{6-5}$$

The air temperature and pressure data included in the meteorological messages used by U.S. forces are expressed in units of °F and in.-Hg, respectively. These data are entered manually by the gunner into the ballistic computer. The implementation of Eq. 6-5 in the M1 tank is to facilitate the manual entry of the temperature and pressure in the available units. Thus the computation of the air density deviation is put into the form shown in Eq. 6-6 in which the denominator of the second term represents the absolute temperature in °R.

$$\Delta D = -a_d + b_d \frac{P_A}{c_d + T_A}, \ \% \tag{6-6}$$

where

P_A = **actual air pressure, in.-Hg**
T_A = **actual air temperature, °F**
a_d = **100 %**
b_d = **conversion factor, 1733.447, % • °R / in.-Hg**
c_d = **459.67°R (corresponds to 0°F).**

Ballistic trajectories are affected by the actual value of the speed of sound in the air. This influence is characterized by the Mach number, which is proportional to the square root of the absolute temperature for a given humidity. Accordingly, the unit effects data for nonstandard temperatures are given in terms of the percent deviation in absolute temperature, which is expressed as

$$\Delta T = \frac{100(T - T_o)}{T_o}, \ \% \tag{6-7}$$

where

ΔT = **percentage deviation in absolute temperature from standard atmospheric conditions, %.**

To accommodate the manual input of the air temperature in °F, this expression is implemented as

$$\Delta T = \frac{100(T_A - 59)}{518.67} = \frac{T_A - 59}{5.1867}, \ \%. \tag{6-8}$$

The constants 59 and 518.67 in Eq. 6-8 are the standard air temperature expressed in units of °F and °R, respectively.

The next phase of the ballistic computation relates to the effects of nonstandard interior ballistic conditions. The dominant conditions for which compensations are made are the propellant grain temperature and the diameter of the tube bore. Both of these contribute to a deviation in the projectile muzzle velocity from the standard values.

The relationship between muzzle velocity and grain temperature is based on experimental measurements, and an empirical equation derived from the experimental data is generated for each type of ammunition used by the weapon system. The empirical equations are expressed in the form:

$$V = a_m + b_m T_g + c_m T_g^2 \ , \ \mathbf{m/s} \tag{6-9}$$

where

V = **muzzle velocity, m/s**
T_g = **propellant grain temperature, °F**
a_m = **nominal muzzle velocity for specific round, m/s**
b_m = **linear temperature coefficient for specific round, m/(s·°F)**
c_m = **quadratic temperature coefficient for specific round, m/(s·°F²).**

The deviation in muzzle velocity is defined as

$$\Delta V_g = V(T_g) - V(T_{go}), \ \mathbf{m/s} \tag{6-10}$$

where

ΔV_g = **muzzle velocity deviation due to nonstandard grain temperature, m/s**
$V(T_g)$ = **muzzle velocity at grain temperature T_g, m/s**
$V(T_{go})$ = **muzzle velocity at standard grain temperature T_{go}, m/s**
T_{go} = **standard propellant grain temperature, °F.**

The standard temperature used in muzzle velocity measurements is 21°C or 70°F.

Eq. 6-9 is used to obtain expressions for the muzzle velocities at temperatures T_g and T_{go}. Upon substitution of these into Eq. 6-10, the muzzle velocity deviation is

$$\Delta V_g = b_m(T_g - T_{go}) + c_m(T_g^2 - T_{go}^2), \ \ \mathbf{m/s.} \tag{6-11}$$

Eq. 6-11 can be rewritten as

$$\Delta V_g = b_m(T_g - T_{go}) + c_m(T_g + T_{go})(T_g - T_{go}), \ \ \mathbf{m/s.} \tag{6-12}$$

The deviation in grain temperature is defined as

$$\Delta T_g = T_g - T_{go}, \ \ \mathbf{°F} \tag{6-13}$$

where

ΔT_g = deviation in propellant grain temperature from the standard temperature, °F.

Using the definition of Eq. 6-13 and substituting into Eq. 6-12 yield the equation for the muzzle velocity deviation due to a deviation in propellant temperature is implemented in the M1. Thus with some manipulation Eq. 6-11 becomes

$$\Delta V_g = b_m \Delta T_g + 2 c_m \Delta T_g \left(T_{go} + \frac{\Delta T_g}{2} \right), \ \ \mathbf{m/s.} \tag{6-14}$$

Each round that is fired erodes the inner diameter of the gun tube. This wear increases the clearance between the projectile and the tube bore, allows more of the propellant gases to escape around the projectile, and results in a gradual decrease of muzzle velocity over the life of the gun tube. The loss in muzzle velocity due to tube wear is computed by an empirical linear equation whose coefficients are based on experimental data for each type of round. The equation implemented in the M1 is

$$\Delta V_b = c B_W, \ \ \mathbf{m/s} \tag{6-15}$$

where

ΔV_b = loss in muzzle velocity due to tube wear, m/s
c = experimental coefficient specific to each round type, s^{-1}
B_W = measured tube wear, m.

The total deviation in muzzle velocity ΔV from the nominal is obtained by combining the effects of propellant grain temperature and tube wear:

$$\Delta V = \Delta V_g - \Delta V_b, \ \ \mathbf{m/s} \tag{6-16}$$

where

ΔV = total deviation in muzzle velocity, m/s.

The unit effects portion of the ballistic tables for each type of round give data on the changes in the location of the impact point and in the TOF of a projectile due to unit deviations in muzzle velocity, air density, air temperature, wind, and elevation angle. The corrections in the gun pointing angles required to compensate for the actual deviations are derived from these data.

The changes in impact point are given as shifts in the vertical height and horizontal offset of the intersection of the ballistic trajectory with a vertical plane located at the measured target range. The changes are given separately for each type of deviation at 100 m increments of target range. For the M1 implementation, the data on the vertical and horizontal shifts for the impact point are represented as a set of power series in range for each unit deviation. For example, the shift in height of the impact point due to a unit deviation in air density is represented by the series:

$$\Delta h_D = \sum_{i=1}^{n_2} b_{V_i} R^i, \ \ \text{m/percent} \tag{6-17}$$

where

Δh_D = shift in height of projectile impact point due to a unit deviation in air density, m/%

R = measured target range, m

b_{V_i} = range coefficients for nonstandard air density, $\text{m}^{1-i}/\%$

n_2 = 4, constant, dimensionless.

The compensation in mils due to the actual air density deviation is obtained by taking the negative of Eq. 6-17, dividing it by the measured range, multiplying by the actual air density deviation, and applying a factor to convert from radians to mils. The resulting equation is

$$\Delta QE_D = -K\Delta D \sum_{i=1}^{n_2} b_{V_i} R^{i-1}, \ \ \text{mil} \tag{6-18}$$

where

K = 1018.59, conversion constant, mil/rad

ΔQE_D = angular quadrant elevation compensation in vertical direction for air density deviation, mil.

The total angular offset in the vertical plane is called the quadrant elevation and is composed of a superelevation for standard conditions plus a compensation for all of the nonstandard conditions. To compute the total compensation, it is assumed that the principle of superposition can be applied and that the changes in impact point and TOF for the individual deviations can be added algebraically. Therefore, the compensation to the quadrant elevation is

$$\Delta QE = -K\Delta D \sum_{i=1}^{n_2} b_{V_i} R^{i-1} - K\Delta V \sum_{i=1}^{n_3} c_{V_i} R^{i-1} - K\Delta T \sum_{i=1}^{n_4} d_{V_i} R^{i-1}, \ \ \text{mil} \tag{6-19}$$

where

ΔQE = total compensation to quadrant elevation, mil

c_{V_i} = range coefficient for nonstandard muzzle velocity, s/m^i

d_{V_i} = range coefficient for nonstandard air temperature, $\text{m}^{1-i}/\%$

n_3 = 3, constant, dimensionless

n_4 = 3, constant, dimensionless.

The ballistic tables list the superelevation required under standard conditions for each 100 m increment of target range. This relationship is also implemented as a power series in range, as shown by

$$QE_o = \sum_{i=1}^{n_1} a_{V_i} R^i, \ \ \text{mil} \tag{6-20}$$

where

QE_o = **standard superelevation, mil**

a_{V_i} = **range coefficient for superelevation, mil/m^i**

n_1 = **5, constant, dimensionless.**

The elevation offset for superelevation under nonstandard conditions is therefore

$$QE = QE_o + \Delta QE, \text{ mil.} \qquad (6\text{-}21)$$

Note that the values of the range coefficients defined in Eqs. 6-17 through 6-20 are specific for each type of round.

A vertical zeroing correction, unique for each type of round, is added to Eq. 6-21 to yield a vertical offset for those factors defined in the vertical plane of the earth coordinate system. This offset is given by

$$E_{VER} = QE + E_{ZO}, \text{ mil} \qquad (6\text{-}22)$$

where

E_{VER} = **vertical offset, mil**

E_{ZO} = **vertical zeroing correcting pertinent to round type, mil.**

The horizontal offset corresponding to the vertical offset of Eq. 6-22 is comprised of drift compensations for the gyroscopic precession of the spinning projectile under standard and nonstandard conditions, a compensation for crosswind, a lead angle to account for relative angular motion between the target and the weapon, compensation for any cross-range component of weapon motion, and a horizontal zeroing correction.

The effect of drift consists of the standard drift listed in the ballistic tables plus the horizontal shift due to the nonstandard air density, air temperature, and muzzle velocity. Since the horizontal shifts due to nonstandard conditions are much smaller than the corresponding shifts in the vertical direction, the compensation is derived from the total nonstandard compensation in the vertical direction by applying a range-dependent scaling factor. The total horizontal drift compensation is computed from

$$H = \sum_{i=1}^{n_{H1}} a_{H_i} R^i + K \Delta QE \sum_{i=1}^{n_{H2}} b_{H_i} R^{i-1}, \text{ mil} \qquad (6\text{-}23)$$

where

H = **horizontal drift compensation, mil**

a_{H_i} = **range coefficient for standard drift, mil/m^i**

b_{H_i} = **scaling coefficient for nonstandard conditions, m^{l-i}/mil**

n_{H_1} = **3, constant, dimensionless**

n_{H_2} = **3, constant, dimensionless.**

The unit effects for a l m/s crosswind are tabulated in the ballistic tables and are implemented in the M1 by the power series

$$A_{ZW} = K \sum_{i=1}^{n_{H3}} c_{H_i} R^{i-1}, \text{ mil/m/s} \qquad (6\text{-}24)$$

where

A_{ZW} = horizontal angular shift in impact point due to a unit crosswind, mil/m/s
c_{H_i} = range coefficient for crosswind, s/m^i
n_{H3} = 3, constant, dimensionless.

The crosswind compensation and the tracking lead in the horizontal direction are combined into a single offset. This offset is

$$L_{AZ} = T_{AZ} T_F - A_{ZW} W_X, \text{ mil} \tag{6-25}$$

where

L_{AZ} = horizontal offset of crosswind and lead, mil
T_{AZ} = horizontal component of target tracking rate, mil/s
T_F = predicted TOF under actual conditions, s
W_X = crosswind velocity, m/s.

The crosswind velocity W_X is measured by a sensor mounted on top of the turret. On a stationary weapon, it is identical to the absolute crosswind velocity, and the unit effects data in the ballistic tables are directly applicable. If the vehicle is moving and the gun is pointed off the longitudinal axis of the vehicle, the wind sensor measures only the relative crosswind velocity. That the compensation defined by Eq. 6-25 is still accurate for a moving vehicle because the use of the relative wind velocity measurement automatically compensates for a cross-range velocity component imparted to the projectile by the vehicle motion is shown at the end of this paragraph.

The horizontal target tracking rate is obtained by processing the turret azimuth rate signals, which are generated in the gunner's hand control unit. The processing consists of filtering to remove any high-frequency signal components and a transformation of the signal amplitude to account for the fact that the weapon may not be situated on level ground. In such a case the tracking rate would be measured in the canted turret plane and its horizontal component obtained from

$$T_{AZ} = \frac{\dot{\phi}}{\cos C}, \text{ mil/s} \tag{6-26}$$

where

$\dot{\phi}$ = filtered azimuth tracking rate in the canted turret plane, mil/s
C = turret cant angle, deg.

The TOF used in Eq. 6-25 consists of the standard TOF to the target range plus corrections for the nonstandard conditions and for the quadrant elevation adjustment ΔQE defined by Eq. 6-19. All of the values are derived from the ballistic and unit effects tables and implemented as power series expansion in range. The TOF is computed from

$$T_F = \sum_{i=1}^{n_{F1}} \alpha_i R^i + \sum_{i=1}^{n_{F2}} \beta_i R^{i-1} \Delta D \tag{6-27}$$

$$+ \sum_{i=1}^{n_{F3}} \gamma_i R^{i-1} \Delta V$$

$$+ \sum_{i=1}^{n_{F4}} \delta_i R^{i-1} \Delta T_g$$

$$+ \sum_{i=1}^{n_{F5}} \varepsilon_i R^{i-1} \Delta QE, \text{ s}$$

where

α_i = range coefficient for standard TOF, s/m^i

β_i = range coefficient for nonstandard density, s/(m$^{i \cdot}$%)

γ_i = range coefficient for nonstandard muzzle velocity, s^2/m^i

δ_i = range coefficient for nonstandard propellant temperature, s/(m$^{i \cdot}$%)

ε_i = range coefficient for adjustment in quadrant elevation, s/(m$^{i-1} \cdot$ mil)

n_{F1} = 5, constant, dimensionless

n_{F2} = 3, constant, dimensionless

n_{F3} = 2, constant, dimensionless

n_{F4} = 2, constant, dimensionless

n_{F5} = 4, constant, dimensionless.

The first summation on the right-hand side of Eq. 6-27 is the standard time of flight T_{FO}. The sum of the remaining terms is the deviation from the standard time of flight ΔT_{FO}.

A horizontal zeroing correction, unique for each type of round, is added to the results of Eqs. 6-23 and 6-25 to yield the horizontal offset for factors defined in the horizontal plane of the earth coordinate system. The offset is given by

$$A_{HOR} = H + L_{AZ} + A_{ZO}, \ \ \textbf{mil} \tag{6-28}$$

where

A_{HOR} = horizontal offset, mil

A_{ZO} = horizontal zeroing correction pertinent to round type, mil.

The vertical and horizontal offsets, E_{VER} and A_{HOR}, respectively, are transformed into a vehicle coordinate system defined by the canted gun trunnion axis and a vector that is normal to the plane of rotation of the turret. The transformation equations are

$$A_{TR} = A_{HOR}\cos C + E_{VER}\sin C, \ \ \textbf{mil} \tag{6-29}$$

$$E_{TR} = E_{VER}\cos C - A_{HOR}\sin C, \ \ \textbf{mil} \tag{6-30}$$

where

A_{TR} = transformed azimuth offset due to A_{HOR} and E_{VER}, mil

E_{TR} = transformed offset in elevation due to A_{HOR} and E_{VER}, mil.

Compensations for boresight, parallax between the sight and the gun, and muzzle deflection as sensed by the muzzle reference sensor (MRS) are now added to the transformed offsets A_{TR} and E_{TR} to yield the total azimuth and elevation offsets for the gun.

The predetermined boresight corrections A_{BR} and E_{BR} compensate for any misalignment between the axis of the gun and the line of sight of the GPS. The correction factors are established in the field using a target located at a known distance, normally 1200 m. The policy established for the M1 (Ref. 12) mandates that boresight be established using a muzzle boresight device. This aligns the sight with the muzzle end of the gun, whereas previous boresighting techniques established boresight with an axis centered at the breech and muzzle ends.

The parallax correction provides an adjustment to the basic boresight correction when the target is not located at the boresight distance. The parallax corrections in the vehicle coordinate system are

$$A_{PR} = K\frac{R_{PH}}{R} - K\frac{R_{PH}}{R_o}, \ \text{mil}$$

$$\tag{6-31}$$

$$E_{PR} = K\frac{R_{PV}}{R} - K\frac{R_{PV}}{R_o}, \ \text{mil}$$

where

A_{PR} = **parallax correction in azimuth, mil**

E_{PR} = **parallax correction in elevation, mil**

R_{PH} = **horizontal distance (parallel to the cannon trunnion axis) between the optical axis of the gunner's primary sight at the head mirror and the cannon axis at the trunnions, m**

R_{PV} = **vertical distance (perpendicular to the cannon trunnion axis) between the optical axis of the GPS at the head mirror and the cannon axis at the trunnions, m**

R_o = **boresight distance, m.**

The measured MRS corrections A_{MRS} and E_{MRS} adjust the basic boresight correction for any change in gun tube droop between the droop that existed when the basic boresight was established and the droop that exists at the time of fire.

Gun tube droop is defined as the angular difference between the cannon axis at the trunnions and the axis at the muzzle. A change in droop must be accounted for because the cannon position in elevation is measured and controlled at the trunnions, but the initial flight path of the projectile is determined in part by the orientation of the muzzle.

The total gun offset in azimuth is

$$A = A_{TR} + A_{PR} + A_{MRS} + A_{BR}, \ \text{mil} \tag{6-32}$$

where

A = **total gun offset in azimuth, mil**

A_{MRS} = **azimuth MRS correction, mil**

A_{BR} = **azimuth boresight correction, mil.**

The total offset in elevation is

$$E = E_{TR} + E_{PR} + E_{MRS} + E_{BR}, \ \text{mil} \tag{6-33}$$

where

E = **total gun offset in elevation, mil**

E_{MRS} = **elevation MRS correction, mil**

E_{BR} = **elevation boresight correction, mil.**

The elevation offsets are used to displace the gun line from the instantaneous position of the line of sight in elevation. The azimuth offset is implemented by displacing the reticle in the GPS. A flow diagram that gives a concise overview of the ballistic computations is Fig. 6-8.
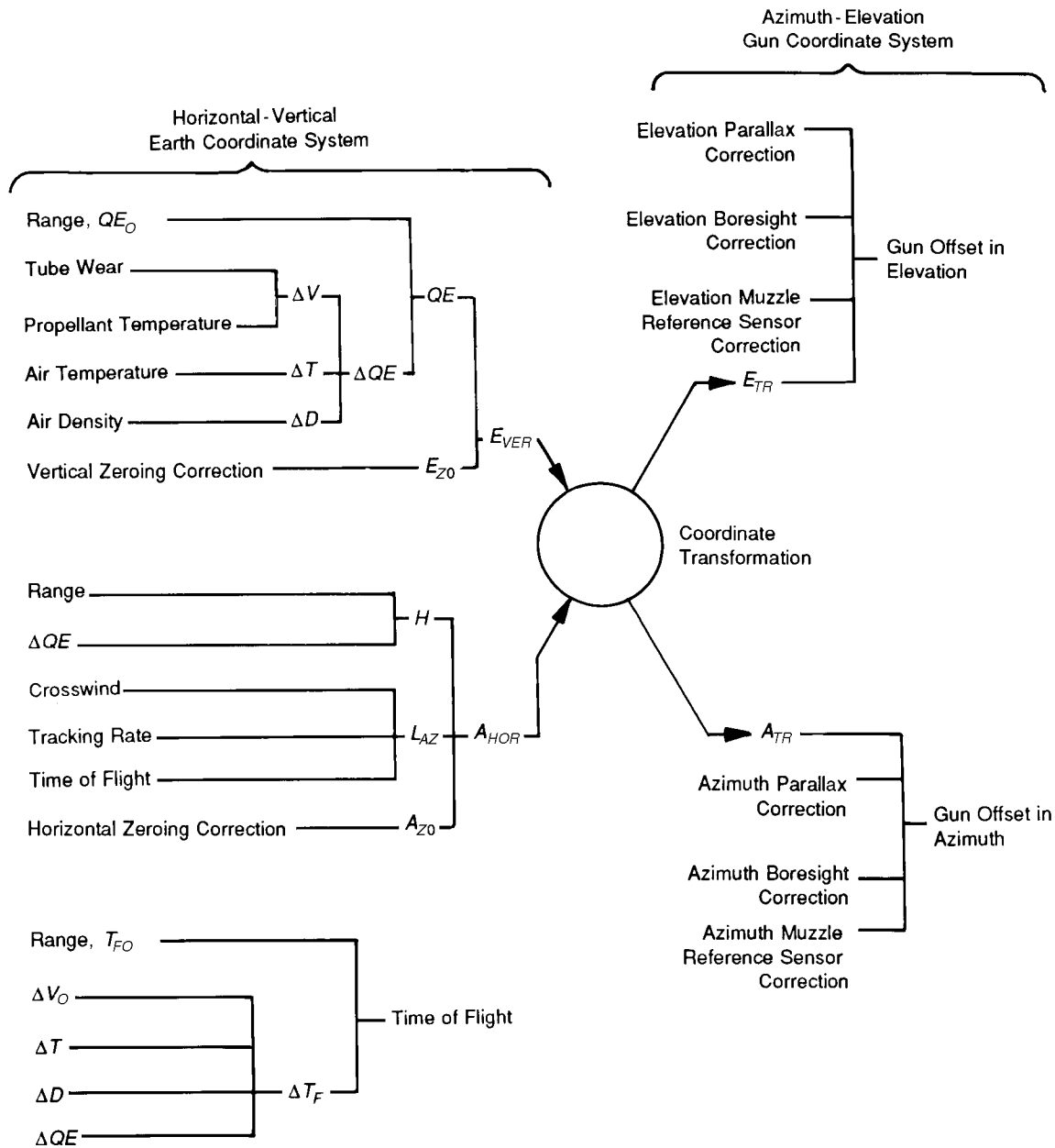
Figure 6-8. Flow Diagram of M1 Gun Order Computation

The offsets for tracking lead and crosswind correction provide an accurate compensation for the cross-range component of weapon platform motion. The engagement scenario depicted in Fig. 6-9 is used as an example. It is assumed that a weapon traveling with a velocity V_W is engaging a target (whose velocity V_T is zero) off its own right flank. The distance to the target is R, and the actual wind velocity W is assumed to be zero. An example with a target moving in a circular path, i.e., constant range about the original weapon location, and with a crosswind would provide the same results as the simplified case.
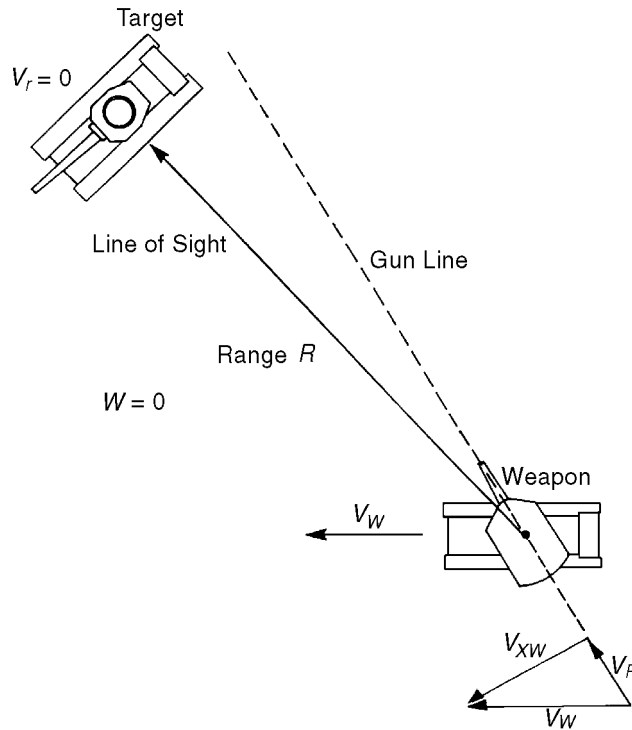
Figure 6-9. Geometry for a Moving Weapon Engagement

With Eq. 6-25 the magnitude of the computed azimuth offset L_{AZ} is equal to

$$L_{AZ} = -KV_{XW}\frac{T_F}{R} - A_{ZW}(-V_{XW}), \text{ mil} \tag{6-34}$$

where

V_{XW} = cross-range component of the vehicle ground velocity V_W, m/s.

The fact that the crosswind sensor, which is mounted on top of the turret, outputs a signal that is the negative of the actual cross-range velocity is manifest in Eq. 6-34. The range component of the vehicle ground velocity V_R has a negligible effect on the fire control solution and is therefore neglected in the analyses.

The criterion necessary for the projectile to hit the target is that its line of departure in azimuth with respect to the ground must be displaced angularly from the instantaneous LOS shown by an amount equal only to the offsets for ballistic drift, parallax, and the boresight and zeroing corrections.

At the time of fire the gun line is displaced from the instantaneous LOS by the amount L_{AZ} plus the offsets for drift, parallax, boresight, and zero. The projectile does, however, acquire an additional angular component A_V due to the cross-range velocity component of the weapon. This component has a magnitude of

$$A_V = K\frac{V_{XW}}{V_o}, \text{ mil} \tag{6-35}$$

where

A_V = projectile angular component due to the cross-range velocity, mil
V_o = muzzle velocity with respect to the gun tube, m/s.

If the criterion stated is to be satisfied, the sum of the L_{AZ} and A_V offsets, as represented by Eqs. 6-34 and 6-35, should be identically equal to zero.

A classical expression exists for the ballistic deflection of a projectile due to crosswind. It states that the magnitude of the angular cross-range deflection A_D can be approximated by

$$A_D = W_X \left[K \left(\frac{T_F}{R} - \frac{1}{V_o} \right) \right], \text{ mil} \qquad (6\text{-}36)$$

where

A_D = magnitude of the angular cross-range deflection, mil.

The US Army Ballistics Research Laboratory, now part of the US Army Research Laboratory at Aberdeen Proving Ground, MD, demonstrated analytically and by comparison with actual ballistic data that the error in these equations is less than 0.5% for projectiles in which the angle of departure with respect to the horizontal is less than 5 deg (Ref. 13). This condition is satisfied for all of the rounds used with the M1, and the error is less than 0.1%.

If the expression in brackets in Eq. 6-36 is now substituted for A_{ZW} in Eq. 6-34, the result in Eq. 6-35 is identically zero. Therefore, the compensation for the effects of vehicle cross-range velocity is automatically applied by the tracking and crosswind corrections.

6-2.3.3 Error Budget

The next step in the design process is to establish an overall allowable system error and to attempt to distribute this error among each of the fire control system functions. The errors that were considered in the design of the M1 are listed in Table 6-11, which has been annotated to reflect the implementation of the various compensating features previously discussed. The errors for those bias factors that the designers choose to leave uncompensated, as indicated by the asterisk, must be left at their full expected value in the error assignment. The errors for those factors for which compensation is being provided, as shown by the double asterisk in Table 6-11, represent instrumentation error and an estimate of the degree to which the measured parameter characterizes the actual condition being sensed. For example, the correction for crosswind is based on a measurement of wind speed at the vehicle. The estimate of the error in this compensation must therefore account for the accuracy with which the wind speed can be measured and for any expected nonuniformity in the crosswind velocity along the flight path of the projectile.

TABLE 6-11. FIRE CONTROL ERROR SOURCES

Manual tracking error
Line of sight stabilization error
Target relative azimuth rate error
Target range error
Target prediction error
Ballistic computation error
Weapon control error
Weapon stabilization error
Uncompensated bias factors*
Errors in measurement or estimation of bias parameters**
Round-to-round ammunition dispersion

BIAS FACTORS:
    Trunnion cant**
    Angle of site*
    Muzzle deflection**
    Crosswind**
    Range wind*
    Nonstandard muzzle velocity**
    Nonstandard air temperature**
    Nonstandard air density**
    Coriolis acceleration*
    Sight/weapon parallax**
    Projectile jump**
    Vehicle transverse velocity component**
    Vehicle gun line velocity component*

  *Error uncompensated by designer choice
**Compensated error

Once the basic functional configuration of the fire control system has been established, the system designers are limited in their ability to minimize the system error. They can control only the accuracy of

the individual hardware and software configuration items that have been identified as comprising the final fire control system. They have no influence over the nonhardware-related factors such as manual tracking, round-to-round dispersion, and the bias factors that were left uncompensated.

The process used to develop accuracy specifications for the hardware and software is an iterative one. It starts with the selection of an allowable total system error based on a desired system hit probability. (Refer to Table 6-6.) The errors associated with those factors not under the control of the designer are then subtracted from the allowable system error to leave a total allowable error for the hardware and software configuration items.

The designer then allocates the hardware and software error among each of the configuration items and by using relationships that define how the error contribution of each item is related to the accuracy specified for it develops a first set of trial accuracy specifications. These specifications are reviewed to see whether they can be satisfied by the existing technology and hardware. If they cannot be satisfied, the trial error allocation is adjusted and, if necessary, readjusted until a match between the requirements and the technology is achieved. In some cases the available technology is not sufficient to satisfy the requirements.

Table 6-12 gives a final error budget allocation for the M1 based on ballistic data for high-velocity kinetic energy rounds, such as APDS. Where appropriate, the notes associated with the table indicate, the performance tolerances for the various sensors used in the system and the bases for the error estimates. Note that an error in range measurement has its effect not only on the computed superelevation and drift in spin-stabilized projectiles but also on the compensations for nonstandard conditions and target motion. The effects on the compensations for nonstandard conditions are, however, extremely small and can be neglected, but the effect of the range measurement error on TOF and, therefore, on the prediction of future target position is more significant.

Table 6-12 lists two error categories for projectile jump. One is the error associated with the estimation of the location of the center of a burst pattern during zeroing, and the second is the error associated with estimating values for the nonstandard conditions that affect the interior and exterior ballistics of the projectile. Inclusion of these error categories implies that zeroing is done individually by each weapon. In fact, however, an Army policy introduced in 1982 replaced the practice of individual zeroing with the use of a fleet average zeroing correction in the M1.

Studies and field tests conducted by the US Army Armor Center demonstrated that the hit probabilities achieved by advanced tank weapon systems, such as the M1 and M60A3, using fleet average zero corrections were just as high as those achieved using corrections based on individual zeroing procedures. These results coupled with the difficulties and limitations associated with individual zeroing led the Army to adopt the fleet average policy in which standardized computer correction factors for each type of round are issued on a fleet-wide basis and are manually inputted into the fire control computer by each tank crew. Ref. 12 presents an overview of the issues related to the development of this gun calibration policy.

For a baseline condition consisting of a stationary weapon and target with the indicated states for the nonstandard conditions, the expected single-shot hit probabilities at 1200 m and 3000 m would theoretically be 0.90 per unit and 0.15 per unit, respectively.

TABLE 6-12.   M1 FIRE CONTROL ERRORS

	EXPECTED ERROR (1σ), mil			
	1200 m		3000 m	
	V	H	V	H
Manual tracking/pointing[1]	0.20	0.20	0.20	0.20
Round-to-round ammunition dispersion[2]	0.27	0.27	0.27	0.27
Line of sight stabilization	0.1	na	0.1	na
Target relative azimuth rate[3]	na	0.05	na	0.05
Target range[4]	0.01	na	0.01	na
Target prediction (constant range)[5]	na	0.000	na	0.001
Target prediction (range error effect)[6]	na	0.04	na	0.018
Ballistic computation	0.023	0.023	0.037	0.037
Reticle offset control in azimuth	na	0.017	na	0.017
Weapon control	0.1	0.5	0.1	0.5
Weapon stabilization[7]	0.35	0.35	0.35	0.35
Trunnion cant measurement (stationary)[8]	0.001	0.03	0.003	0.07
Trunnion cant (moving)[9]	0.01	0.25	0.03	0.68
Angle of site[10]	0.07	na	0.08	na
Muzzle deflection measurement	0.05	0.05	0.05	0.05
Loss of boresight[11]	0.20	0.20	0.20	0.20
Crosswind measurement[12]	na	0.008	na	0.02
Crosswind estimation[13]	na	0.04	na	0.11
Range wind[14]	~0	na	0.004	na
Estimation of muzzle velocity deviation[15]	0.006	na	0.016	na
Air temperature estimation[16]	0.002	na	0.01	na
Air density estimation[16]	0.002	na	0.01	na
Coriolis acceleration[17]	0.02	0.03	0.05	0.08
Sight/weapon parallax estimation	~0	~0	~0	~0
Projectile jump measurement[18]	0.14	0.14	0.14	0.14
Projectile jump estimation (computer correction factor)[19]	>0	>0	>0	>0
Airspeed measurement (cross range)[20]	na	0.6	na	0.6
Airspeed (downrange)[21]	0.12	na	0.2	na

Notes:
V = Vertical
H = Horizontal
na = not applicable
1. Stationary weapon
2. Typical for high-speed kinetic energy round
3. Stationary weapon; target speed: 20 m/s; 1% azimuth rate accuracy
4. Range finder accuracy ±5 m
5. Linear target path normal to line-of-sight; target speed: 20 m/s
6. Error in time-of-flight computation due to error in target range measurement
7. Stabilization error (reduced by use of 0.3-mil firing window)
8. Sensor accuracy: ±0.5 deg
9. Cant angle: 5 deg (1σ)
10. With 5-deg gun elevation
11. Structural deformations excluding bending of barrel
12. Sensory accuracy: ±0.5 m/s ±10%
13. Assumed actual condition: 3.5 m/s crosswind at vehicle decreasing linearly to zero at target
14. Range wind: 3.5 m/s (1σ)
15. 10% error (1σ) in estimating an actual deviation from the standard muzzle velocity of 1%
16. 10% error (1σ) in estimating an actual deviation from standard conditions of 30%
17. Estimates based on expectation values for weapon latitude and firing direction
18. Error in estimating and observing center of burst pattern
19. Second-order effects due to errors in measuring and estimating nonstandard conditions during zeroing, varies with ammunition lot
20. Sensor accuracy: ±0.5 m/s ±10%; Vehicle speed: 20 m/s
21. Vehicle speed: 20 m/s

6-2.4 SYSTEM MECHANIZATION

This subparagraph discusses how the defined fire control system was implemented in hardware. The acquisition and tracking subsystem, computing subsystem, and gun pointing subsystem are discussed.

6-2.4.1 System Description

The fire control system consists of all of the equipment provided for target sighting, aiming, and firing the 105-mm main gun (120 mm on the M1A1), the 7.62-mm coaxial machine gun, the commander's cal 0.50 machine gun, and the loader's 7.62-mm machine gun. This discussion centers on control of the main gun. Fig. 6-10 shows the fire control components.

The night fighting and obscurant penetration requirements led to the inclusion of a FLIR in the acquisition subsystem. The high cost of the FLIR exacerbated cost constraints. This situation led to the adoption of a single-axis director system for gun pointing and an independent stabilization system for the turret in azimuth.

The primary optical sighting instruments are the GPS and the optical relay extension to the commander. This periscope is mounted on the upper turret structure and incorporates servopositioned reticles for complete ballistic solutions with day and night vision imaging. It is linked in the elevation axis with the main armament through resolver follow-up electrical devices. The LRF transceiver, the thermal night vision subsystem, and the gyro-stabilized LOS platform are integrated within the GPS. The sight is ballistically protected with armor steel covers incorporating protective steel doors over the objective opening that are operable from inside the turret. The gunner also has an auxiliary sight in the simple, rugged telescope affixed directly to the main armament mount; the commander has a three-power, fixed focus periscope for general surveillance and for firing the weapon mounted in his station.
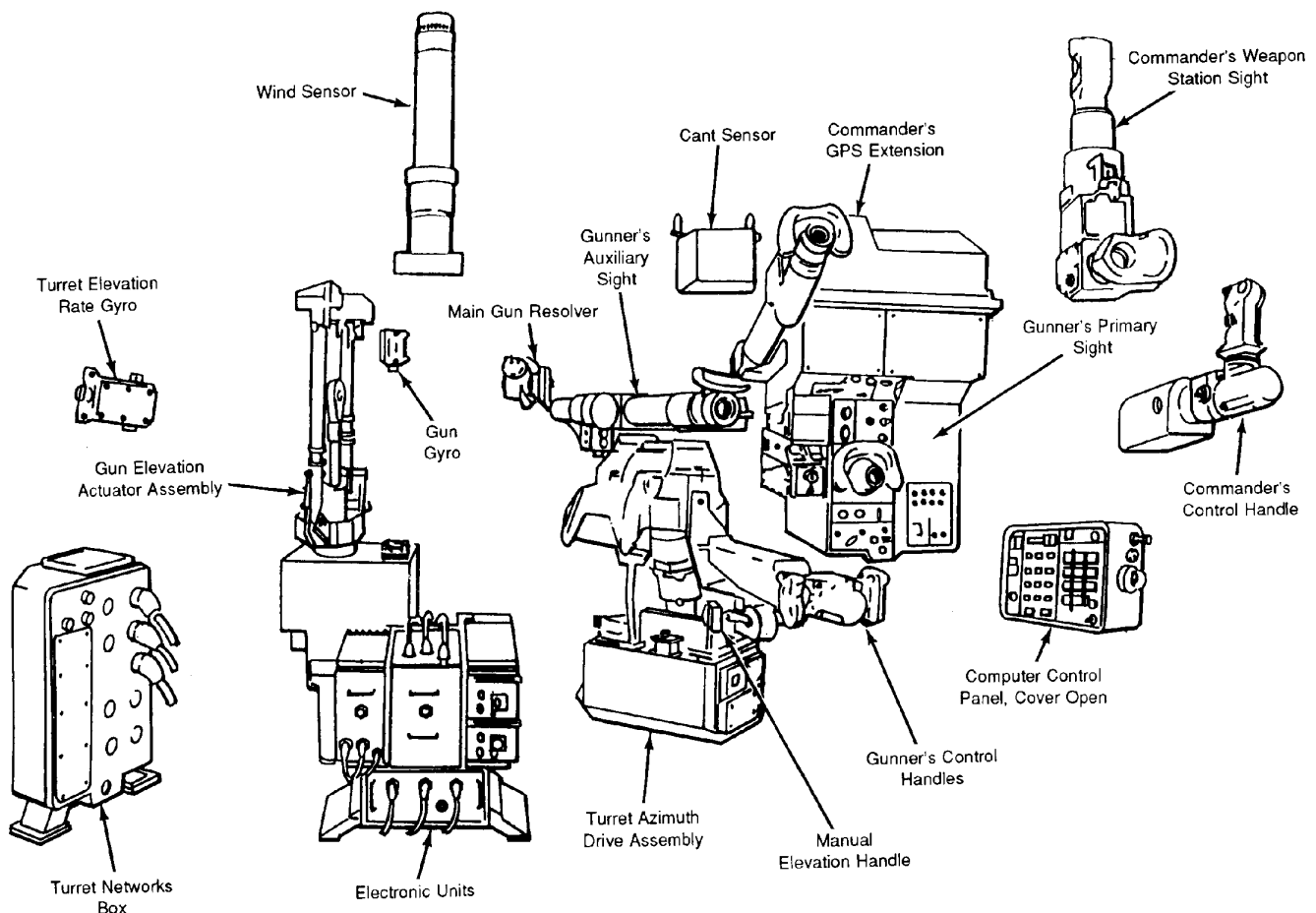
Figure 6-10. M1, M1A1 Tank Fire Control Components (Ref. 14)

The ballistic computation system is an accurate and flexible digital system that continuously controls reticle offsets. The computer is all digital and includes analog-to-digital and digital-to-analog converters, as required by sensors and other vehicle subsystems. Computational accuracy is sufficient to support firing-on-the-move performance. It consists of the digital computer memory and processor and associated input/output devices within an electronic unit mounted under the main armament and a gunner's control panel. An ion-drift wind sensor is mounted at the rear of the turret bustle roof, and a pendulum static cant sensor is located at the turret roof center. The outputs of both of these sensors are automatically fed to the computer.

The gun and turret drive subsystem is electrohydraulic. Its power is provided by an engine-driven pump through a slip ring at the turret/hull interface to a power valve in a manifold beneath the main gun. Engine-off hydraulic power is provided through the slip ring by a hull-mounted, battery-driven hydraulic pump. Space stabilization in the azimuth plane is accomplished through gyroscopic sensors and servo-controlled valving in the azimuth drive gear assembly. The gun and turret drive system consists principally of

1. An azimuth drive assembly located directly in front of the gunner
2. The elevation actuator assembly located left of the main gun
3. An electronic unit located under the main armament.

The primary function of the fire control system is to aim and fire the main gun with sufficient accuracy to attain the specified hit probabilities. Fig. 6-11 depicts the major functional interfaces between components required to accomplish the primary function of main gun control. This figure also provides an overview of the fire control system.

The overall design of the fire control system includes a substantial amount of redundancy to provide survivability and fightability through alternate modes of operation if the primary system becomes damaged during combat. Examples of this redundancy include

1. Availability to the commander of the GPS extension
2. Availability of the gunner's auxiliary sight if the GPS is inoperable
3. Direct slaving of the GPS to the main gun in elevation if the stabilization system fails
4. Manual elevation and traverse if both turret power and auxiliary hydraulic power are lost
5. Design of the computer controls to provide early identification and instant nulling of any malfunctioning inputs
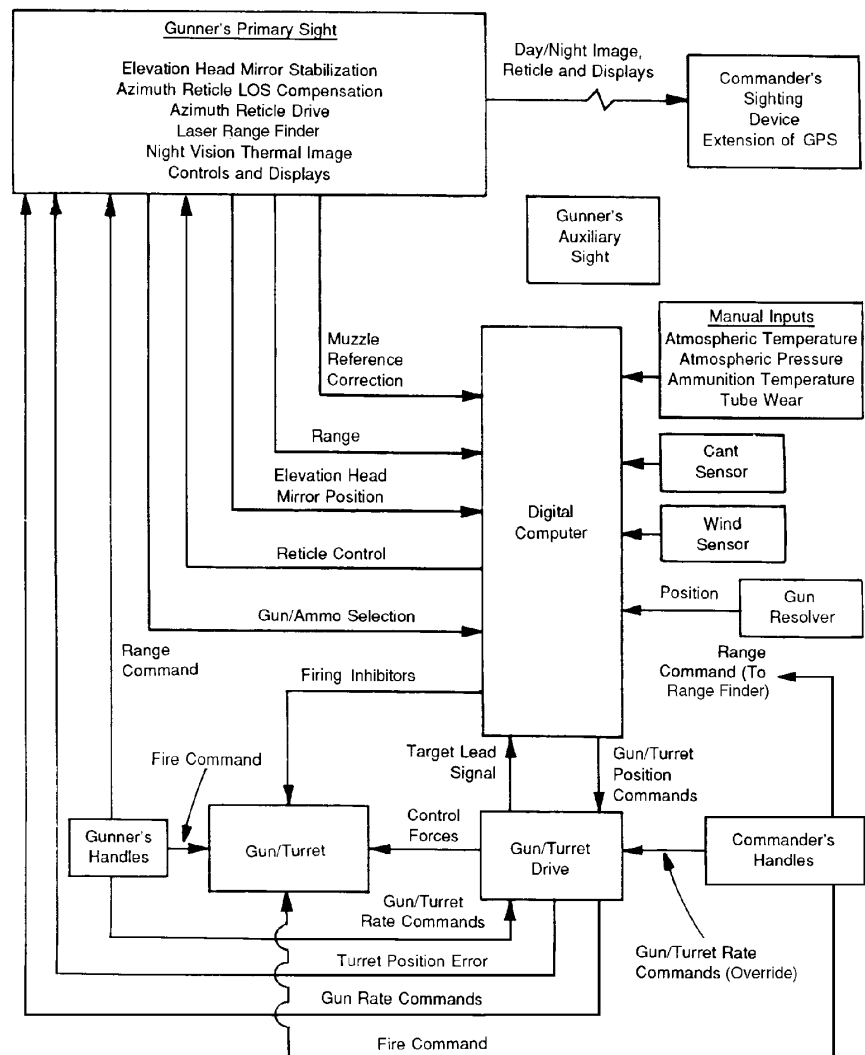
Figure 6-11. Fire Control System Turret Diagram (Ref. 14)

6. Provision in the computer design for manual inputs, if desired, in lieu of automatic sensor inputs

7. Dual controls for the gunner that include two power control handles, two parallel laser buttons, two parallel palm switches, and two parallel weapon triggers

8. An override control handle at the commander's station complete with laser button, palm switch, and weapon trigger

9. A blasting machine to allow main gun firing without vehicle electrical power.

6-2.4.2 Acquisition and Tracking System

The GPS, shown in Fig. 6-12, is comprised of a main housing casting and head assembly cover with the LRF, eyepiece assembly, headrest assembly, and control panel assemblies. There is also an azimuth mirror drive assembly with the servoelectronics for the azimuth mirror drive, the gyro-reticle compensation (GRC) electronics, narrow-field-of-view (NFOV) objective lenses and relay optics with the filter and shutter wheel, LOS cradle assembly, and the parallel-scan thermal system as a separate "bolt-on" modular assembly. The main housing also contains the wide-field-of-view (WFOV) objective lenses and relay optics for the commander's GPS extension (CGPSE). The modular construction of the GPS facilitates both producibility and maintainability. Each module can be separately manufactured and tested to individual specification requirements prior to installation.

The LRF can be replaced in the vehicle without special tools and without destroying the integrity of the pressurized optical system. Conveniently located inlet valves permit easy access for periodic nitrogen purging and charging of the GPS. Removal of the GPS is accomplished from outside the vehicle, and the only prerequisites are the removal of the ballistic cover, mounting bolts, and headrest assembly and the disconnecting of the CGPSE and electrical harnesses. The eyepiece and headrest assemblies are interchangeable with the ones in the CGPSE.

Figure 6-12. Gunner's Primary Sight (Ref. 15)

The GPS provides a wide range of daylight vision alternatives. Unity power vision can be used for close-in surveillance and during slewing operations. The instantaneous FOV is 6 deg vertical and 10 deg horizontal (approximately 17 deg horizontal with head motion). The head mirror is stabilized in elevation and is a common element in all GPS systems. The daylight sight provides a dual-power capability: a wide-angle mode for area surveillance and a high-magnification mode for target identification and gun laying. The high-power sight has a resolution of 50 cycles/mil for high-contrast targets and 30 cycles/mil for

low-contrast targets. A ±4 diopter adjustment is provided. The daylight sight has an exit pupil diameter of 6 mm and a clear eye distance of 22 mm.

The head mirror module, which contains a two-axis gyro, a drive motor, a multispeed resolver, and a unique aluminum head mirror, is a key element in the LOS stabilization system. The two-axis sight gyro senses movement of the sight head mirror, which is input to the LOS electronics unit for stabilization of the mirror, and it senses turret azimuth motion, which is input to the gun/turret drive electronics unit for traverse of the turret.

The two-axis gyro provides inertial-grade, space-referenced signals for the head mirror in elevation. Elevation signals from the gyro are processed in the LOS electronics unit. Drive signals to the head mirror motor provide a movement counter to vehicle motion and thus provide a stable sight pattern in elevation. Vision is accomplished by using a one-piece aluminum mirror with an optical quality replicated surface. This mirror provides a surface large enough and broadband enough to reflect both day and night channels as well as the laser beam. Electrical signals from the resolver provide space-stabilized reference signals to the gun.

Fig. 6-13 shows the overall functional concept of the gunner's reticle projection and azimuth reticle control. This system converts the total azimuth ballistic solution offset generated by the computer into an accurately deflected reticle in the gunner's FOV. The reticle source is located in the LRF where the reticle beam is permanently aligned with the laser beam. A movable dichroic beam splitter reflects the invisible laser light toward the target and partially transmits the red reticle light. The reticle beam is returned along the same path by a retroflector and is partially reflected by the beam splitter into the gunner's day optics. Since the gunner's LOS also passes through the beam splitter, the reticle is superimposed on the gunner's FOV.

The movable beam splitter is controlled by two sequential servo systems. The azimuth reticle drive servo positions photosensors of the azimuth mirror drive servo according to the computer-generated azimuth offset angle. The azimuth mirror drive positions the beam

Figure 6-13. Gunner's Primary Sight Azimuth Drive System (Ref. 14)

splitter according to the position of the photosensors. The rate of the azimuth reticle drive is also supplied to the gun/turret drive (GTD) system to counterrotate the gun in azimuth and maintain the reticle on the target when azimuth offset is applied.

The azimuth reticle drive servo uses a potentiometer for position feedback and a tachometer for stability feedback. These feedback signals are converted to digital signals in the computer and summed with the total azimuth offset position. The resulting error signal is converted to analog, amplified, and applied to the azimuth reticle drive servomotor. The motor drives the carriage holding the photosensors for the azimuth mirror drive.

The azimuth mirror drive servo uses an optical sensor for position feedback and a tachometer for stability feedback. Displacement of the dual-matched photosensors by the reticle drive servo applies a differential error voltage to the servomotor driving the beam splitter until the reflected beam of the light-emitting diode is centered on the photosensors. The total range of angular deflection possible for the reticle is ±50 mil. A direct drive torque motor and tachometer are used to obtain high accuracy and reliable performance.

Gyro-reticle compensation is applied to the azimuth mirror drive to hold the reticle on the target when azimuth disturbance inputs beyond the bandwidth of the turret control system are encountered. The turret stabilization spatial position error is applied to the azimuth mirror drive to counterrotate the reticle and maintain it on the target. The gun is inhibited from firing for azimuth errors exceeding ±0.25 mil.

The LRF used in the M1 fire control system is a neodymium yttrium aluminum garnet (YAG) laser transmitter coupled with a range receiver using a silicon-avalanche diode detector. The LRF is a separate bolt-on module to the gunner's sight. It is hermetically sealed, as is the interface on the GPS, and thus allows easy removal and replacement with the GPS installed in the tank. It is dry nitrogen purged and uses purge valves conveniently located for easy-access purging within the tank without need of special tools. The LRF also serves as the GPS reticle projector. A feature of the M1 LRF integration into the fire control system is the absence of any controls except the lasing button on the handles and an armed-safe, first-last return logic switch on the range finder. All range sensings are entered directly into the computer with a range readout provided in both the commander's and gunner's FOV, along with a multiple-return indicator.

True last-return logic is achieved through the use of a dual counting chain. One counts continuously to maximum range (7990 m), and the other resets to zero for each return received. When the continuous counter reaches maximum range, both counters stop and the time differential or range difference between counting chains indicates "actual last return" range.

The range finder/computer interface consists of the range binary-coded decimal (BCD) lines, the range-ready signal, the continuous monitor signal, and the built-in test equipment (BITE) command and response. When the laser "fire" signal is given, the laser emits a pulse and measures the time from laser fire to received-return, and the LRF logic displays a range-ready signal to the computer, which then accepts the range displayed on the BCD lines.

This range is stored by the computer until a subsequent ranging sequence is completed. The range finder also continuously displays a go or no-go signal to the computer, which indicates that both pulse-forming network and receiver detector bias are present and that counter, logic, and power supplies are operational. In addition, upon receiving the test command from the computer, the LRF runs through its own internal test to verify that the counting chains are functioning, power suppliers are up and within limits, and previously transmitted energy output was within limits as part of the gunner-command sequence test. It then transmits a known range to the computer if the system is functional.

At any time the commander can enter "battle range" and enter any change to battle range by means of the toggle switch and the eyepiece range readout, or the gunner can enter the estimated range similarly on the computer control panel.

The GPS controls and indicators are functionally arranged on the face of the periscope, as shown in Fig. 6-14, to facilitate their use by the gunner. The following is a listing of the controls and displays and a brief description of their functions:

    1. RETICLE CONTROL PANEL (Shown in Fig. 6-14(A))

        a. *Reticle intensity control rheostat.* **Adjusts reticle brightness**

        b. *Defroster ON/OFF toggle switch.* **Energizes the thermostatically controlled defroster and illuminates an indicator light (green) when the defroster is on**

    2. FIRE CONTROL PANEL (Shown in Fig. 6-14(B))

        a. *Panel lights test push-button switch.* **Illuminates all indicator lamps and displays when actuated**

        b. *Indicator lamp intensity control rheostat.* **Adjusts indicator lamp intensity on the GPS**

c. *Fire control mode toggle switch with indicator lamps.* **Selects operating modes of fire control system: "manual", "normal", or "emergency"**

d. *Azimuth and elevation normal mode drift controls.* **Potentiometers used to null out stabilization system drift**

e. *Diopter adjustment.* **Rotary mechanical adjustment of eyepiece used to bring scene and reticle images into sharp focus**

f. *Filter/shutter/clear selector.* **Rotary mechanical knob positions a neutral density filter to reduce scene brightness or a shutter to block out the day scene for thermal system operation or a clear window for normal viewing conditions.**

g. *Gun select MAIN, COAX or TRIGGER-SAFE toggle switch and indicator lamps.* **Switch selects gun (main or coaxial) or trigger safe (deactivates trigger circuits). Switch in coaxial position also selects coax ammunition. Indicator lamps display the selection that has been introduced into the control circuitry by the gunner. "Trigger safe" is always selected when turret power is on.**

h. *Ammunition selector switch and indicator lamps.* **Switch selects main gun ammunition type, and indicator lamps display the selection that has been introduced into the control circuitry by the gunner.**

i. *Magnification selector.* **Lever control selects either three-power or ten-power magnification.**

j. *Laser first/last-return and safe switch.* **(Shown in Fig. 6-12) Selects first or last target range return or allows the gunner to inhibit the laser from accidental firing**

k. *Range and system status display.* **Range data and system status information (READY TO FIRE, MALFUNCTION, MULTIPLE LASER RETURN SYMBOLS) are displayed on the cathode-ray tube (CRT) in the thermal system and superimposed on the FOV seen in front of the eyepiece.**

3. **THERMAL IMAGING CONTROL PANEL (Shown in Fig. 6-14(C))**
   a. *Mode control.* **Off/standby/on, energizes system**
   b. *Polarity switch.* **White-hot/black-hot, selects target polarity**
   c. *Video control.* **Adjusts system receiver sensitivity**
   d. *Brightness control.* **Rheostat adjusts scene brightness.**
   e. *Contrast control.* **Rheostat adjusts level of contrast.**
   f. *TRU status indicator.* **Indicates operating temperature achieved**

Figure 6-14. Gunner's Primary Sight Controls

6-46

g. *Magnification selector.* **Electrically controls electromechanical module to select 3-power or 10-power magnification**

h. *Focus.* **Permits focusing from 50 m to infinity**

i. *Reticle/range.* **Adjusts level of brightness of thermal scene reticle and the range and system status display in the CRT.**

Night vision is provided by a parallel-scan TIS subsystem, which senses heat radiation in the 8- to 14-μm range. The temperature distribution in the scene is displayed as a visible scene from a CRT that can be viewed through the GPS/CGPSE eyepiece. The system relies primarily on emitted rather than reflected radiation and depicts the temperature profile of the scene. A dual-power option provides magnifications of 10 power and 3 power with a rectangular FOV of 2.6 deg by 5 deg and 8 deg by 16 deg, respectively. The effective range of the TIS depends on the temperature contrast of the target and air but is the same for day or night operation. The TIS has been adopted as the GPS in day as well as night conditions.

The MRS provides a means by which the gunner can correct gunnery errors attributable principally to gun tube bend. The system provides for semiautomatic data insertion in the ballistic computer, which allows the gunner to note the magnitude of the errors and take corrective action when gross deviations are detected. To use the MRS, the gunner depresses the MRS button on the computer control panel to extinguish the sighting reticle and illuminate the MRS reticle. Using the toggle switch on the computer, the gunner superimposes the collimated reticle, which is mounted on the gun tube over the reference image. When the two images are superimposed, the gunner depresses the "enter" button, and the muzzle bend correction is automatically entered into the computer, the MRS reticle is extinguished, and the sighting reticle is again illuminated.

The CGPSE, shown in Fig. 6-15, provides the commander with an optical projection of the same scene viewed by the gunner. This scene, including day or night thermal scenes, also provides the commander with the same reticle and range and system status information viewed by the gunner.

The GPS scene is transferred to the CGPSE through a common beam splitter located in the GPS. The image is collimated and projected out of the GPS into the CGPSE where it is reimaged in the commander's eyepiece image plane. Collimated light simplifies the interface and alignment.

The CGPSE has the same dual-power capability as the GPS. The high-power system has a magnification of ten power with an FOV of 6.5 deg; the wide field system has a magnification of three power and an FOV of 21 deg. Resolution of the 10-power system is 40 cycles/mil for high-contrast targets and 25 cycles/mil for low-contrast (20%) targets. The exit pupil diameter is 6 mm, and clear eye distance is 22 mm, which is more than adequate to pick up and track a moving target. A ±4 diopter adjustment capability is also provided.

The gunner's auxiliary sight (GAS), shown in Fig. 6-16, is a simple gun-mounted, articulated telescope that operates independently of the primary fire control system. It is intended as an unsophisticated, reliable backup system with key design emphasis on its capability to survive multiple nonpenetrating ballistic impacts. The GAS has a magnification of 8 power, which results in an FOV of 8 deg and a clear eye distance of 30 mm and an exit pupil diameter
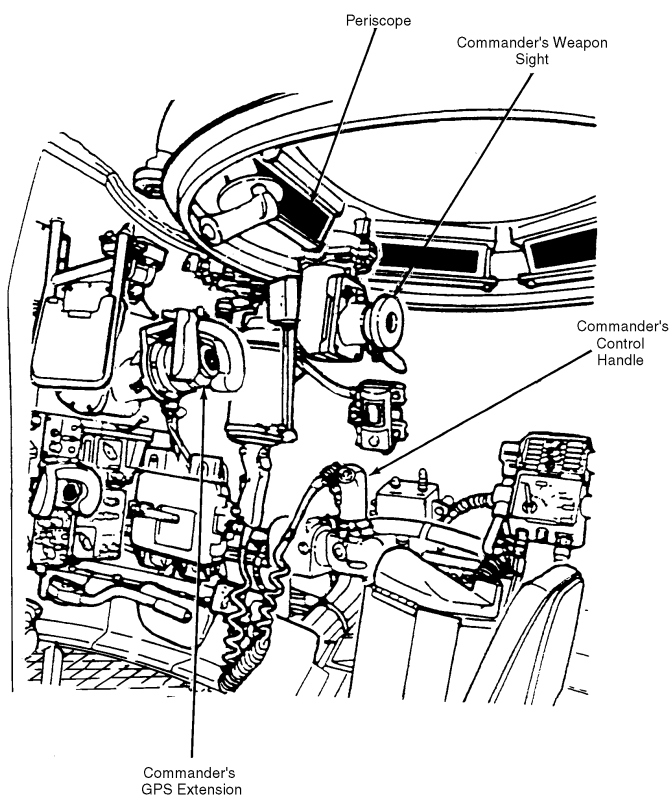
Figure 6-15. Commander's Sights and Controls (Ref. 16)

of 6 mm. A ±4 diopter adjustment capability is also provided. The resolution of the GAS is 25 cycles/ mil, which is sufficient to engage targets to the maximum effective range of the ammunition. Fifty-decibel attenuation of 1.06-μm laser light is provided for the gunner's eye protection along with a neutral density filter to reduce scene brightness. The GAS provides ballistic reticles for sabot and HEAT ammunitions.
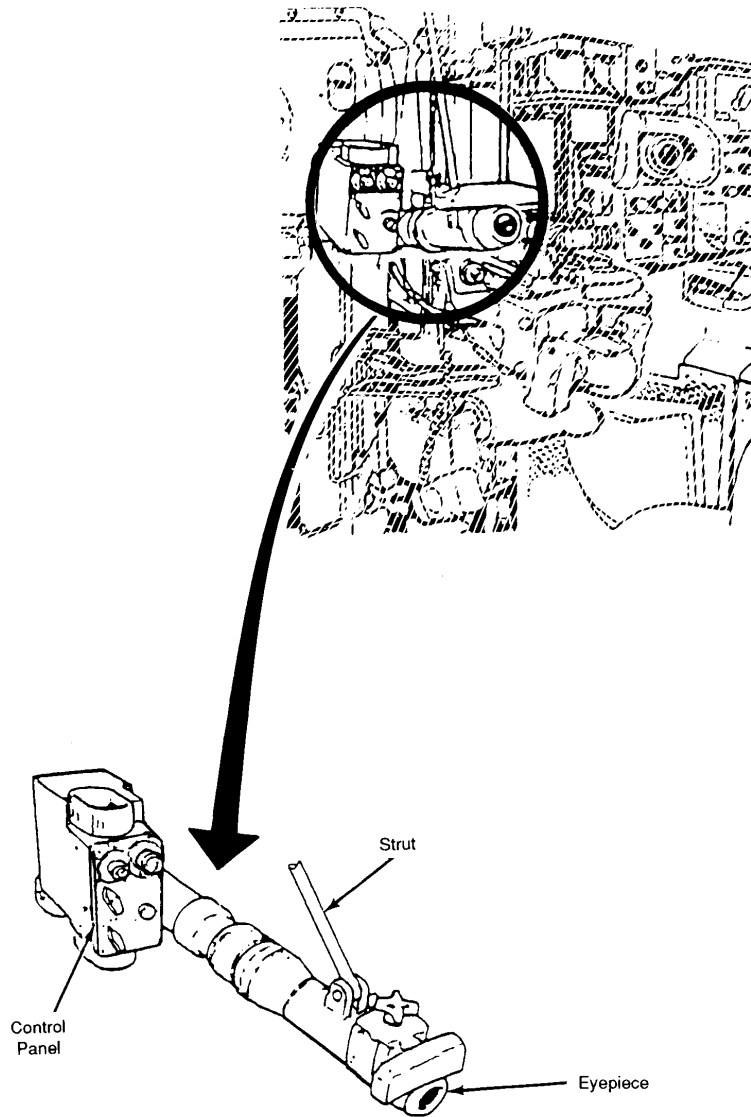
Figure 6-16. Gunner's Auxiliary Sight (Ref. 16)

6.2.4.3 Stabilization System

Rate control is used to drive both the turret in azimuth and the gun in elevation. The gunner's and commander's handles command rates of rotation, which are executed by the drives and in turn sensed by rate gyros in the gun and turret. These gyros also control the servo drives to reduce rate error (command-response) to zero. Use of rate control rather than position control provides smooth motion.

The GTD and stabilization system provides control of the main and coaxial weapons in the stabilized, nonstabilized powered, and manual modes of operation. The stabilized (normal) mode is the mode of operation normally used for all gun and turret control functions. The nonstabilized powered mode (emergency mode) provides backup powered operation independently of stabilization system sensors and circuits. The manual system provides gun and turret control independently of the vehicle electrical and hydraulic power sources.

In the normal mode of operation, the gun is electrically slaved with the stabilized head mirror in the GPS, and the turret is stabilized in azimuth. This approach in conjunction with the gyro-reticle compensation described provides the target acquisition and retention capabilities necessary for both moving and stationary engagements. Infinitely variable and continuous tracking capability from 0.25 to 75 mil/s in azimuth and from 0.25 to 25 mil/s in elevation is provided to the gunner and commander. At least 750 mil/s of slew capability from control handle commands are provided for the turret in azimuth. An elevation handle command slew rate of 400 mil/s and a 750 mil/s rate for azimuth and elevation in response to stabilization system commands are also provided. Stabilization system commands for these rate levels are required to maintain aim retention during vehicle movement over rough terrain or evasive maneuvers.

The electrically controlled emergency mode provides a highly reliable powered backup mode to handle command performance approaching that of the normal mode. During emergency mode operation the GPS head mirror is electrically slaved to the gun. Azimuth and elevation control are provided directly to the turret and gun, so sighting may also be performed using the GAS independently of the operational capabilities of the GPS.

The normal and emergency modes contain logic to prevent the gun from striking the rear deck of the vehicle at gun angles below zero degrees. In the normal mode full control is provided to the GPS head mirror to allow target tracking below zero degrees even though the gun may be elevated to clear the rear deck. Firing is inhibited during this condition until the gun automatically returns to its proper alignment (the head mirror position plus any elevation ballistic correction offset) when the turret or gun moves out of the interference zone. In the normal and emergency modes hydraulic power is normally supplied by an engine-driven pump. For "engine off" conditions hydraulic power is supplied for operation in these modes by an auxiliary electric motor-driven hydraulic supply that enables the GTD system to provide frequent full handle command slew capabilities in azimuth or elevation and sustained tracking capabilities of 35 mil/s in azimuth or 20 mil/s in elevation. The manual controls design concept uses a direct gear drive for azimuth control and a hydraulic fluid hand pump for elevation control.

Mechanical stops in the gun mount limit gun travel in the elevation axis to between 20 deg elevation and 10 deg depression with respect to a horizontal turret plane. A hydraulic cylinder is used to drive the gun in either direction and/or to hold the gun in the proper position.

In the normal mode handle commands and sensor feedback signals are processed in the GTD electronics to provide rate commands to the elevation cylinder under both moving and stationary vehicle conditions. The control system is of the proportional type and incorporates integral and differential control compensation. Velocity lag error is minimized by using an open-loop pitch rate that is sensed by the turret gyro and used to rotate the gun at an equal and opposite rate to provide a stable gun position. Any inaccuracies of this open-loop drive signal cause a spatial position error. This error is sensed by the gun gyro and the gun sight resolver network, both of which provide drive signals to eliminate the error. The computer inhibits gun firing if this error exceeds ±0.25 mil. Differential pressure feedback (torque feedback) is used to provide additional system damping. Automatic bias compensation is provided to eliminate positional errors resulting from hydromechanical component wear, environmental changes, and tolerance variations. Handle commands from the gunner or commander are shaped and summed with normal mode logic to provide smooth tracking capability.

In the emergency mode handle commands are processed through the handle signal-shaping network to control the hydraulic servomechanism directly. Manual control is also provided through the servomechanism from a hydraulic fluid hand pump, accumulator, and shuttle valve system. Manual mode provides 10-mil-per-hand crank revolution at a peak effort of less than 48.9 N (11 lb). The servomechanism contains a hydraulic flow amplifier consisting of an aircraft-type servo valve and output stage spool. The position of the output stage spool is electrically fed back to the input of the servo valve. Bias compensation to eliminate rate offset errors in the emergency mode is provided in this control loop. The servomechanism also contains a low-leakage, four-port, two-position lock valve to prevent drift during "system off" conditions and to provide a 0.1-s engagement time delay to prevent uncommanded transient gun motion when hydraulic power is applied to the drive system. Internal crossover relief valves prevent sys-

tem damage if an external object is struck by the gun, and a manual split lock valve prevents back driving of the manual hand pump when the elevating mechanism is power driven. Oil cleanliness is maintained in the servomechanism by the self-contained, replaceable filters with bypass indicators. The elevating mechanism is attached directly to the servomechanism for low entrapped oil volume. In conjunction with the 58-cm^2 (9-in.^{2}) effective piston area, a double shear zero backlash gun attachment mechanism, and a dual-support strut gimbal mount, this arrangement provides the stiff drive system necessary for the gun to respond to elevation terrain inputs up to 10 Hz.

The azimuth gearbox assembly provides control of the turret throughout 360 deg of travel in the normal, emergency, and manual modes of operation. As in the elevation axis, handle and stabilization sensor commands are processed in the normal mode through a proportional controller incorporating integral and differential control compensation. Open-loop yaw rate is sensed to counterrotate the turret to maintain a spatial position reference. Errors in this counterrotation are sensed by the azimuth portion of the dual-axis gyro mounted on the GPS head mirror drive, and a command signal is generated that is processed to eliminate the error. Differential pressure feedback is used for increased damping. This approach effectively stabilizes the turret for input disturbances of frequencies up to approximately 4 Hz. Uncompensated errors in this range as well as input disturbances of up to 60 Hz are processed through the derived position channel and the GRC circuit to reposition the reticle to maintain target alignment. This essentially stabilizes the reticle and provides the advantages obtained with the stabilized azimuth sight method without the added cost of a two-axis, sight-stabilized system.

Handle commands from the gunner or commander are processed in the normal and emergency modes in a similar manner to the elevation axis. Bias compensation is provided by the derived position channel in the normal mode and by the servomechanism output spool position feedback in the emergency mode.

The azimuth servomechanism houses an aircraft-type servo valve, a flow amplifier, a transient time delay, a strain-gage-type differential pressure transducer, replaceable filters with bypass indicators, a pilot-operated crossover relief valve for motor bypass, and keep-full anticavitators. A bent axis axial piston per rev hydraulic motor (with a displacement of 15.56 cm^3) is coupled directly to the output stage of azimuth servomechanism to provide low entrapped oil volume and establish a high-stiffness hydromechanical coupling. The gearbox design is ruggedized and stiffened and incorporates a single split output pinion. The gearbox assembly, whose ratio is 640:1, houses the turret brake/clutch, which is hydraulically released when the power controls are energized and is spring actuated when the power controls are not in use. The brake/clutch prevents turret slippage during hull maneuvers with the power controls deenergized but allows slippage if the turret is struck by an external object. The mechanical ground for the brake and clutch is provided in the manual traverse section of the gearbox. The slotted detent design prevents back driving of turret motion through to the manual handle. Additional safety is provided in the manual system by a separate slip clutch on the noncrank drive and by a hydraulic power cutoff switch that is actuated by a lever on the hand crank when the hand crank is grasped. The manual drive uses the same ratio as the hydraulic motor to provide a response of 10 mil per hand crank revolution. Because of the low friction of the manual drive and in particular of the hull/turret race assembly, whose driving torque is less than 271 N·m (200 lb·ft), the manual traverse peak effort is less than 48.9 N (11 lb).

The control components used in the GTD system are the gunner's and commander's handles, the gyros, and the electronic control unit. The gunner's and commander's handles provide identical control capabilities for the operator and include palm, trigger, and laser switches. The application of hydraulic power to the control system is provided by energizing one of the system palm switches, which in turn applies power to actuate the turret power valve. On the gunner's dual handles the left or right or both palm switches must be squeezed in order to move the GPS head mirror and gun or turret, to lase, or to fire the main or coaxial weapon. Interlocking the palm switches in this manner prevents inadvertent bumping of the control handles and undesired results. The palm switch on the commander's single-grip joystick-type control handle provides the same function as the gunner's and initiates the override capability for taking control of the main or coaxial weapon. Except for the grip and grip-attaching mechanism, both the commander's and gunner's handle assemblies are identical. Linear variable differential

transformers are cam driven through ±90 deg in azimuth and bell crank driven through ±30 deg in elevation to provide an output voltage proportional to handle position. The mechanisms are self-centered, and spring forces are selected to provide smooth and easy operation. The handle grips are shaped to fit the hand comfortably for easy accomplishment of the required functions and to minimize operator fatigue.

Three identical rate gyros are used specifically for the GTD system to sense gun rate in elevation, vehicle pitch rate, and hull yaw rate. Turret rate is sensed by the azimuth output of the dual-axis gyro, which is located in the GPS.

The modularized electronics unit provides the analog processing logic needed to control the elevation and azimuth axes and the power supply and regulator circuits for the GTD system. The elevation and azimuth control logic is individually contained on two separate printed circuit boards for easy troubleshooting at upper echelon maintenance. The power supply components, except heat-sink-mounted power transistors, are contained on a single printed circuit board. The electronics unit has a test connector on the front face that provides connections to measure pertinent operational conditions throughout the GTD system.

6-2.4.4 Computation System

The ballistic computer system calculates and provides command signals representing ballistic, lead, and parallax offsets for the GPS reticle projector azimuth and the main weapon (MW) elevation. These offsets are dependent upon vehicle environment, static cant, target slant range, tracking rates, ammunition type, tube wear factor, and operational modes. In addition, zeroing values for six types of rounds and GPS to MW azimuth and elevation alignment values are selectively summed to the computed MRS offsets. The system consists of the ballistic computer, which includes the electronics unit and the control panel, the cant sensor, the crosswind sensor, and other vehicle components and systems that provide computer inputs. Fig. 6-17 depicts the functional relationships between the ballistic computer system components and other vehicle systems and components.

The ballistic computer system

Figure 6-17. Ballistic Computer System, Functional Block Diagram (Ref. 14)

automatically senses the cant angle of the vehicle and the crosswind velocity and automatically receives signals representing tracking rate (for lead corrections) and range. These signals are combined with the manual inputs that represent zeroing, boresight, MRS, air temperature, ammunition temperature, barometric pressure, and gun tube wear, and they are used to calculate the required offsets. Electronic signals representing these offsets are automatically fed to the appropriate gun drive system, i.e., azimuth or elevation.

Continuous, automatic malfunction detection capability is incorporated in the fire control system to alert the commander when a gross malfunction has occurred in the ballistic computer system or other major components. A manually initiated built-in test sequence actively exercises the ballistic computer, cant sensor, crosswind sensor, LRF, GTD system, LOS stabilization system, data link, and the GPS reticle drive and compares their individual responses to a predetermined pass/fail criteria. Failure sources are identified by a number code on the computer control panel for appropriate repairs. Manual override capability for the automatic inputs of cant angle, crosswind velocity, lead rate, and range is provided for emergency operation.

The ballistic computer consists of an electronics unit that contains the digital computer, power supply, and other interface circuitry and a covered control panel that contains all of the controls and displays required to provide manual inputs to the computer.

The digital computer contains 6000 words of solid-state read-only memory (ROM). The operating program and the ballistic coefficients for 10 types of rounds are included in this permanent storage area. Four main rounds and one coax round are immediately selectable via the gunner's ammo select control, whereas the remainder are usable by means of manual entry via the computer control panel. Other changes, such as new ammunition, can be accomplished by the exchange of one computer board. A "scratch pad" memory is used to store panel inputs. Required power for this memory is supplied by the vehicle battery when the computer is installed in the tank. When vehicle battery power is lost, an internal battery provides power to maintain the memory. This battery is a low-voltage, rechargeable unit mounted in the computer electronics. When the ballistic computer (BC) is vehicle installed, an internal charging circuit will maintain the battery capacity for longer than five years. Inadvertent loss of both battery power and tank battery power would require only reentry of the manual data using the control panel. Conversion of the computer from accepting manually entered English system units to accepting metric units can be accomplished by removing an internal jumper wire.

The digital control transformer (DCT), located in the LOS electronics unit, and other interface circuitry are organized onto individually removable circuit cards. The DCT is the interface element between the digital computer and the analog gun elevation servo. The signal from the gun trunnion resolver is applied to the DCT, the required ballistic offset is added, and the resultant output is used to position the gun elevation. The computer positions the reticle for the proper offset in azimuth through a closed loop servo. The turret system senses the reticle motion and counter drives to position the gun and turret correctly. These functions occur simultaneously. The MRS correction is used by the ballistic computer to provide automatically the appropriate boresight corrections to accommodate gun tube bending.

Special circuits are provided in both elevation and azimuth to inhibit main weapon firing until the sight-to-gun pointing error is within preestablished limits. In stationary and average cross-country operations, the associated control systems are sufficiently responsive to minimize any firing delays from the inhibit function (The limits are ±0.25 mil in elevation and ±0.30 mil in azimuth.).

The computer control panel, shown in Fig. 6-18, is normally closed during combat operations. It provides the capability to enter manually ballistic parameters and alignments and to override the automatic sensors in the ballistic computer system. The control panel is divided into four major sections: a manual input section, an automatic input self-test section, a boresight and zero section, and a keyboard/display section.

The manual input section contains provisions to enter conditions of air temperature, barometric pressure, ammunition temperature, MRS, battle range, ammunition select, and bore wear. Any of these manual inputs may be used by simply depressing the appropriately labeled key. The computer will acknowledge the addressing of the particular item by illuminating the key that was pressed and by displaying the value currently stored in its memory for that item. The units associated with the display are those in common use, e.g., °F for temperature, and they are listed for convenience on instructions affixed to the control panel cover. After the labeled key has been pushed, the appropriate numerical entries on the keyboard are pressed to change the value of the manual input. These entries are immediately visible in the numeric display. If the new value appears correct, the enter key is depressed, the manual input lamp that was illuminated goes out, and the new value is stored for use in the ballistic solution equations.
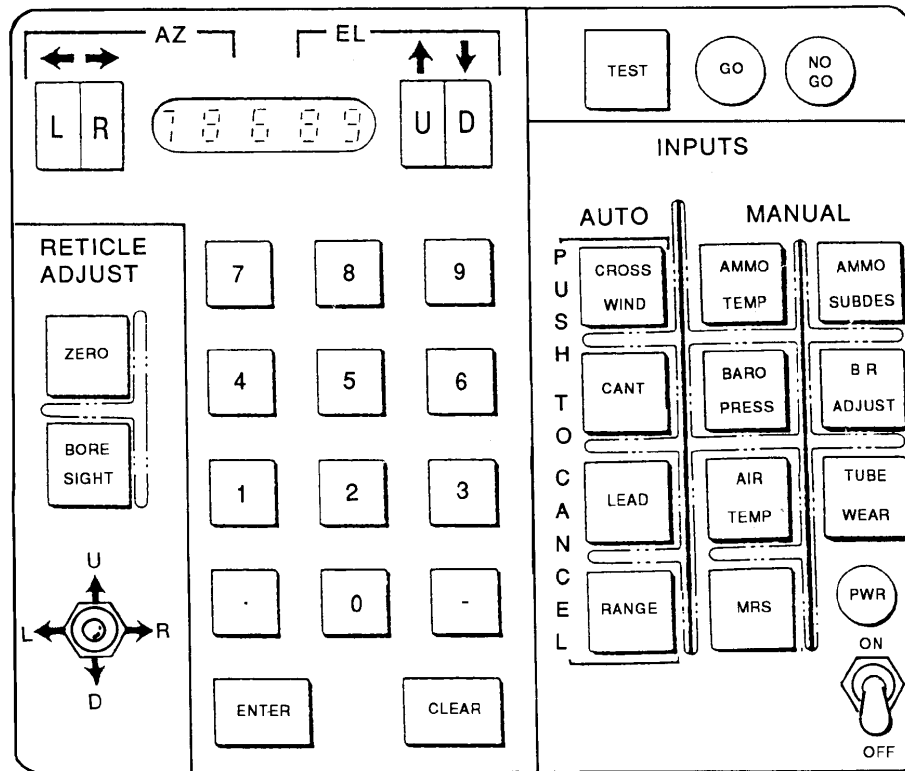
Figure 6-18. Computer Control Panel, Manual Controls (Ref. 14)

Should a totally erroneous entry be made, e.g., 6000°F air temperature, the computer will not accept the input, and the associated manual input key will flash indicating that another input is to be made. It is impossible for any incorrect entry to damage or upset the fire control system. Air temperature and pressure are input from available local data. Ammunition temperature, which is measured from a turret-bustle-mounted sensor, is observed from a thermometer dial located to the commander's right and manually entered in the computer. Tube wear is measured by supporting maintenance personnel with a standard US Army pullover gage and also manually entered. Special provisions are made to enter a separate battle range for each ammunition type and to select a secondary level ammo type, e.g., a particular type of sabot ammunition.

The fire control system self-test is initiated by pressing the test key on the control panel that automatically sequences tests of the fire control subsystem. Should a failure occur, the no-go lamp illuminates, the sensor lamp involved illuminates, and a numeric code is displayed to identify the failure source. Code information is contained on the panel cover. At the completion of a successful test, the go lamp is illuminated. The automatic inputs to the computer, i.e., crosswind, cant, lead, and range, can be displayed and changed in the same manner as the manual inputs. Depressing one of these keys causes the lamp to illuminate, and the associated sensor is ignored by the computer. The value of the sensor output at the time is displayed and may be changed manually. Fixed entries can then be made as they are for manual inputs. This capability allows the fire control system to function properly in a slightly degraded mode in the event of a sensor failure.

Boresighting and zeroing of the GPS in day, night, and MRS modes to the coaxial machine gun and main guns are accomplished by using controls on the GPS and the computer control panel. These modes are set up automatically with selection of "gun", "ammo type", "day", "night", or "MRS". To boresight the GPS, the reticle is moved by use of the up/down/left/right toggle on the computer control panel until it coincides with the aiming point of the gun tube. This would generally be done with a 1200-m target. When a satisfactory lay is obtained, the solution for the sight is entered by depressing the enter button. Zeroing is accomplished in a similar manner except that a round is fired at the target. After depressing the zero button, the GPS reticle is toggled to the center of impact of the zeroing round, and

the enter button is depressed. This zero holds for the particular ammunition selected; it must be repeated for other types of rounds.

The cant sensor is a simple, rugged, and pendulous device derived from the M19 computer subsystem of the M60A3 tank. The ballistic computer contains automatic logic to ignore the cant input when the vehicle is moving. The pendulum is magnetically damped to assure rapid positioning. A rugged potentiometer is used to measure pendulum position.

The cant sensor contains self-test capability that is used in the fire control self-test sequence. Upon command from the ballistic computer, the cant sensor pendulum is magnetically repositioned and released to assume its original angle. The ballistic computer examines the cant sensor output during the test sequence for adherence to prescribed angular deviations and identifies any nonconformance on the computer control panel.

The crosswind sensor determines crosswind velocity by measuring the wind-induced ion stream displacement. Mounted at the center top rear of the turret bustle, the sensor measures the crosswind component of the wind at the vehicle.   This rugged unit and a special rubber shock mount allow high-speed impact and flexure to the horizontal plane on contact with items like tree limbs to occur without damage or permanent orientation shifts to the wind sensor.

The crosswind sensor significantly improves moving vehicle hit performance by measuring any lateral vehicle motion perpendicular to the LOS to the target.   This information is used by the computer to provide trajectory corrections to compensate for the effect of that motion.

The crosswind sensor also provides continuous self-testing of its power supply voltages and analog output stage circuits. Any failures are automatically indicated to the commander by the illumination of the fire control no-go indicator in the sights and on the control panel. In the manual self-test sequence a simulated wind signal is inserted, and the calibration of the wind sensor electronics is verified.

6-2.4.5 Product Improvements

As mentioned previously, the M1 was designed from the beginning to accept upgrades. The first significant set of upgrades was incorporated in the M1A1 version. Production of this version was begun in 1985.

There were significant improvements in mobility and survivability. The most significant change from the standpoint of the fire control system, however, was the increase in firepower provided by replacing the 105-mm main gun with a 120-mm gun. The larger caliber gun is a German-designed smooth bore gun.

This change required that the ballistic data in the fire control computer and the drives of the reticle in the GPS be modified. The ammunition select switch on the gunner's control panel was changed to reflect the fact that only two ammunition types are normally used in the 120-mm gun: HEAT and armor-piercing, fin-stabilized, discarding sabot (APFSDS). The control panel is unchanged, but only two selection codes are used.

Since there is virtually no barrel wear with the smooth bore 120-mm gun, the tube wear input button was no longer used to input a ballistic correction term. That button was then converted to aid in troubleshooting.

From the standpoints of both the fire control system and the fire control hardware, the changes incorporated in the M1A2 growth version were truly extensive. The changes include an improved commander's station, a commander's independent thermal viewer (CITV), a two-axis sight stabilization (full director), a position and navigation indicator, additional armor, and perhaps most significant of all, a high-speed digital data bus.

The commander's independent thermal viewer head is mounted at the top left of the turret. The commander can rotate it through 360 deg continuously. It has been referred to as a "panoramic" sight for this reason. It is equipped with two viewing lenses, a wide angle for surveillance and a narrower field with 10-power magnification.

Unlike the A1 version, the commander does not "share" the GPS. This allows the so-called "hunter-killer" operation. The CITV is independently stabilized in two axes. The commander can use his sight to search for and acquire a target while the crew remains under armor. He is provided with full facilities to

handle the engagement himself, or he can hand the target off to the gunner and immediately start to search for the next target.

Should he decide to hand off, he presses a button on the fire control electronic unit, and the GPS slews to the same azimuth as the CITV to allow the gunner to begin the engagement in a minimum of time. It has been said that typical engagements are completed in 6 to 7 s.

The new commander's station is fitted with a panel called the commander's integrated display (CID), which consists of a visual display unit (VDU) for the CITV, a multirole information display, and a services and armaments control panel. The information display is the VDU, which can show battlefield tactical information including a grid map of the area of operations and a display of the position of the vehicle, arcs of fire, and future moves of the vehicle, and it can provide status reports from the systems and diagnostics.

The single-channel ground and airborne radio system (SINCGARS) tactical radio is fitted with an interface unit to allow the burst transmission of digitally coded map, graphic, and textual information as well as normal frequency modulation (FM) voice communications. All vehicles on a single radio net will automatically rebroadcast data received to overcome interference caused by ground conditions or enemy action. Preformatted messages can be adjusted using menu-driven procedures, and each type of message, e.g., situation reports, fuel demands, or casualty status, has a different signature code. This system allows other vehicles to store the latest of each type of message from every vehicle on the net. In this way a commander can call up the information at his convenience rather than lose it in the chaos of battle.

The position and navigation (POS/NAV) system gives the position and heading of the vehicle to the commander and driver and can significantly speed up movement through difficult country. This information can be used in conjunction with a set of way points, which allow the commander to select a route and then leave the navigation to the driver. Accuracy has been assessed as 2% of the distance traveled per hour.

The heart of the system electronics is a high-speed, military standard 1553 digital data bus. (This is the same data bus used in the Apache helicopter, which is discussed in par. 6-3.) The data bus handles all onboard processed data, automotive as well as fire control, and enables the crew to choose what information is to be displayed at any particular time.

The data bus is regarded as the "backbone of the tank" and has the quality of being "transparent" to the crew. The central processor unit coordinates both the hull and turret functions. Apart from allowing the introduction of specific functions, the Vetronics have improved the crew-vehicle interface by reducing the complexity and number of crew tasks and, in particular, automating the transfer of battlefield information between vehicles and different levels of command using the intervehicular information system.

The next generation fire control system will incorporate some of the following advances. An auto tracker, which would relieve the gunner of the difficult task of tracking moving targets, is planned. Various types of video image processing are being investigated to determine the degree to which they might aid the crew in target detection, recognition, and identification. Many other features, such as maintenance aids, a second-order prediction system for maneuvering targets, and built-in training capabilities, are also under consideration.

Because the service life of a major system is long and technology advances relatively fast, it is prudent to plan for growth and upgrades from the start of system design. This approach has been successful in the case of the Abrams tank and other Army systems.

6-2.5 SYSTEM PERFORMANCE

The numbers that describe the performance of the Abrams tank are classified and cannot be presented in this handbook. This subparagraph discusses some of the testing to which the tank has been subjected, i.e., the extent of the testing, the methods used, the instrumentation involved, and where possible, the general results.

Table 6-13 shows the table of contents of the detailed test plan, initial production test (IPT), for the M1A1 tank (Ref. 17). Since the tank is a weapon system, the testing involves all aspects of its performance. Tests were performed on fuel consumption, mobility, fording, logistic supportability, and other

aspects of the system. Interest here centers on fire control system performance, which is discussed using the main gun as an example.

TABLE 6-13.   TABLE OF CONTENTS OF TEST PLAN (Ref. 17)

In Table 6-13 Sections 2.15, "Gun Control System Performance"; 2.16, "Laying and Tracking"; 2.17, "Sighting System"; 2.18, "Fire Control Performance"; and 2.20, "Gun Stabilizer Performance", can be considered subsystems. These tests are summarized in subpar. 6-2.5.1. Sections 2.21, "Hit Probability", and 2.22, "Time to Fire", can be considered overall system performance measures and are discussed in subpar. 6-2.5.2. The first group is nonfiring tests, whereas those described in subpar. 6-2.5.2 are live-fire tests.

6-2.5.1   Subsystem and Major Component Performance

Major program decisions such as whether or not to proceed with full-rate production of a weapon system are often made in part on how the overall system performs vis-à-vis the requirements. In addition, performance of subsystems must also be evaluated to confirm their contribution to overall system performance. Several M1 subsystem tests are described here.

Gun control system performance was tested to determine the performance of the main gun drive system. The control handle was activated to predetermined deflections, and the gun angular velocity in azimuth and elevation was digitized and recorded. Gun acceleration, overshoot, and undershoot were also measured. The tests were performed in both normal and emergency modes using the gunner's and the commander's control handles.

Laying and tracking performance was tested to determine whether the gun control system is compatible with the crew and the fire control system. To test gun lay, both the azimuth and elevation of the gun were moved from the target. Target size and range were recorded, and the time required for the gunner to lay on the target was measured. Tracking performance was measured using a camera mounted through the commander's GPS extension and a gun-bore-mounted camera and laser. The latter camera recorded the laser spot on or at the target. Targets moved at a constant velocity, and percent time on target was calculated to be compared with the specification requirements.

Sighting system performance (or sight synchronization) was tested to determine whether or not the GPS was maintaining boresight to the main gun. With the fire control computer in the boresight mode, the sight was repeatedly laid at a point on a target grid board. The gun was equipped with a chamber scope, and after each lay of the sight, the gun position on the target board was checked. The deviation from perfect alignment could then be compared with the allowable tolerance.

The test of the fire control system performance checked the system performance in implementing the ballistic corrections, and assessed the accuracy of the muzzle reference system. Ballistic conditions, i.e., ammunition type, range, cant, wind, and environmental conditions, were entered into the computer. The correct elevation angle of the gun for the conditions was known. The gun was then directed to the elevation angle provided by the fire control computer and pointed at a grid board. Any error was recorded. This procedure was repeated for a number of input sets and required both increasing and decreasing elevations of a range of magnitudes and in several tanks. The MRS was checked (under nonfiring conditions) by means of daily boresight checks.

The gun stabilizer performance was tested to determine the accuracy of stabilization while the tank was moving at a range of speeds over a variety of terrains. The data were also used to validate the HITPRO/DELACC model (See Chapter 4 of this handbook.) of the M1. Sight- and gun-tube-mounted video cameras were used to record time on target. The target was tracked by a capable gunner. The tests that were run at each combination of speed and terrain were replicated by three tanks with two repetitions each and using different gunners.

6-2.5.2   System Tests

The live-fire tests of hit probability had several objectives:

1. To develop a final assessment of the system test hit probabilities for comparison with the system specification requirements and for comparison with mission need requirements

2. To measure and verify the accuracy of the main armament system of the M1 tank when firing M829, M865, M830, and M831 ammunition

3. To assess the wear and accuracy characteristics of the M256 cannon tube in order to verify that

the 500-round life is attainable with the production gun tube and to evaluate the possibility of reaching the desired level of 1000 rounds

  4. To develop error magnitudes for the principal error budget elements that drive M1A1 system delivery accuracy.

 All M1 testing was coordinated through the Test Integration Working Group and the Test and Evaluation Master Plan. (See Chapter 4 of this handbook.)

 The live-fire tests were conducted over the same time period as reliability and maintainability (R&M) testing. This timing allowed a sufficient pool of tanks to be available for firing.

 Accuracy testing consisted of main gun firing from eight test vehicles. Seven of the vehicles were R&M tanks, and the eighth was dedicated to fire control testing. All of the rounds scheduled to be fired by the R&M tanks during endurance and reliability testing were evaluated for accuracy. In this subtest the R&M tanks were designated as Tank R-1 through Tank R-7, and the eighth vehicle was designated as Tank A-1.

 The endurance and reliability subtests were broken down into eight 500-mile cycles. Table 6-14 gives the total number of rounds fired by each test vehicle for each mileage cycle. The total number of rounds of each type fired were

  1. M829: 563 rounds (armor-piercing, fin-stabilized, discarding sabot, tracer) (APFSDS-T)
  2. M865: 1511 rounds (training, practice, cone-stabilized, discarding sabot, tracer) (TPCSDS-T)
  3. M830: 145 rounds (high-explosive, antitank, multipurpose, tracer) (HEAT-MP-T)
  4. M831: <u>876 rounds</u> (training, practice, tracer) (TP-T)
    Total 3095 rounds

The following is a breakdown of the 3095 firings:
  Tube zeroing - 160
  Accuracy tests
   Stationary tank/stationary target (S/S) - - - - - - - - - - - - - - - - - - 705
   Stationary tank/moving target (S/M) - 440
   Moving tank/stationary target (M/S) - 315
   Moving tank/moving target (M/M) - 270
   Screening test - 64
  Tube wear testing - 400
  Expenditure rounds - 741.

TABLE 6-14. AMMUNITION REQUIREMENTS FOR R&M/ACCURACY FIRING MILEAGE PHASE (Ref. 17)

TANK	0-500 miles	500-1000 miles	1000-1500 miles	1500-2000 miles	2000-2500 miles	2500-3000 miles	3000-3500 miles	3500-4000 miles	AMMUNITION TOTAL
A-1	130	20	20	0	0	0	0	0	170
R-1	100	100	100	100	100	100	100	100	800
R-2	100	100	100	100	100	100	100	100	800
R-3	100	100	100	100	100	100	100	100	800
R-4	40	20	20	20	20	20	20	20	180
R-5	25	20	20	20	20	20	20	20	165
R-6	20	10	10	10	10	10	10	10	90
R-7	20	10	10	10	10	10	10	10	90
								Grand Total	3095

An initial tube zero was obtained for each gun tube and for the M829, M865, and M831 ammunition types. Upon completion of this firing, each tube was assigned a set of zero numbers for use during accuracy firing for the remainder of the initial production test.

A robust firing matrix was used for evaluation of the M1A1 tank under stationary/stationary conditions. These data were collected during the first three mileage cycles of the test and quantified launch angle errors, curvature errors, jump, quality of implementation of ballistic solution, boresight retention, and consistency of tank accuracy from one firing occasion to another. This test also monitored the structural integrity of the main armament system including gun mating and alignment, MRS alignment, and resistance of the fire control system to alignment changes due to the test environment and operation.

Due to the quantity of variables incorporated into the robust S/S firing matrix, the cause of any accuracy problems encountered would be very difficult to trace. To satisfy this concern, a smaller pretest firing matrix was used as a tool prior to entering the robust firing matrix to identify dominant variables that affect the accuracy of the tank under S/S conditions. The rounds in the screening test were fired with the fire control system of the tank turned off, and aiming was accomplished with the gunner's auxiliary sight at the 1200-m target. Alignment between the muzzle and sight was checked prior to firing each round.

Because of the large quantities of rounds required for endurance and reliability testing, many of the rounds fired were expenditure rounds. These are rounds that did not pass acceptance testing because of dispersion problems. They were fired in large groups and evaluated for center of impact only.

Each round was evaluated at three distances: 800 m, 1500 m, and 3000 m for kinetic energy (KE) rounds (M829 and M865) and 800 m, 1500 m, and 2400 m for high-explosive antitank rounds (M830 and M831).

Firing was conducted at the Trench Warfare II Range at Aberdeen Proving Ground, MD. Fig. 6-19 shows a schematic of the range setup.
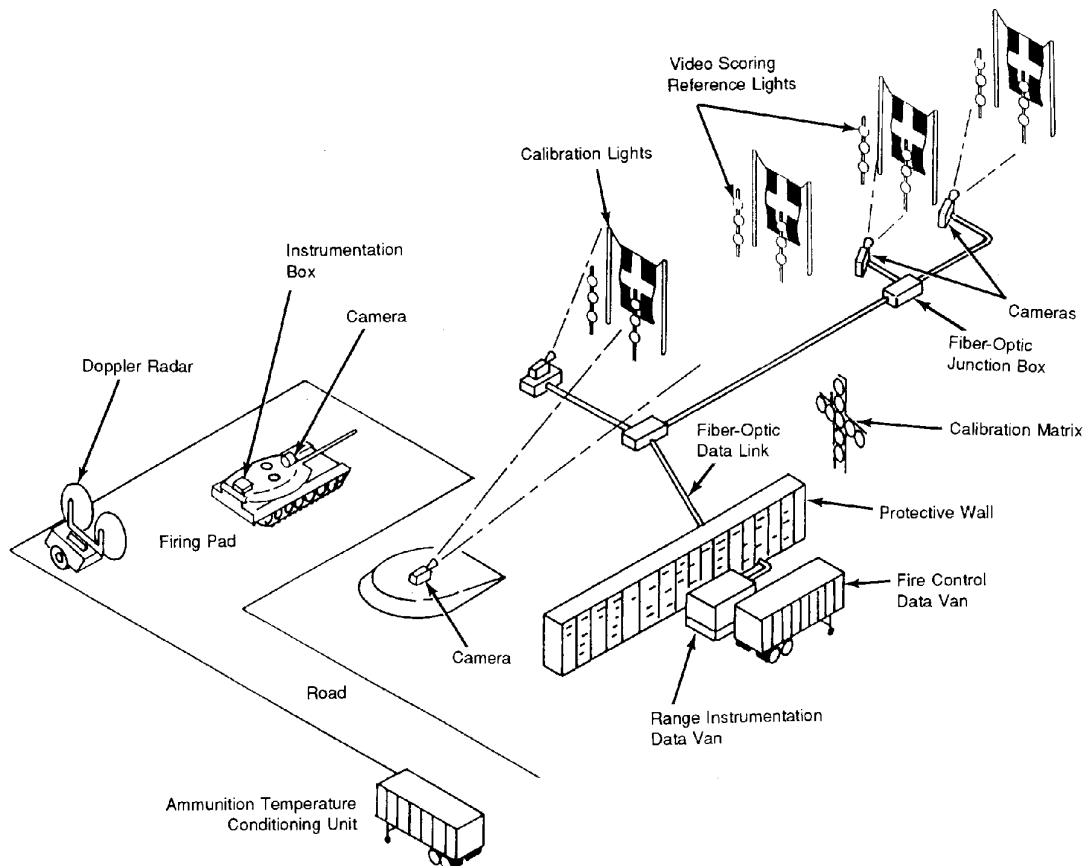
Figure 6-19. Live-Fire Test Setup (Ref. 18)

This firing range includes two separate parallel lines of fire with identical target and range instrumentation. One line of fire is dedicated to testing depleted uranium (DU) KE munitions. A special containment area was built beyond the last target position to contain the DU projectiles. This allows for the recovery and proper disposition of the radioactive metal without affecting personnel or the environment.

There are four target positions located at 800 m, 1500 m, 2400 m, and 3000 m from the test vehicle. The impacts at the 800 m and 1500 m positions are measured by means of the virtual target scoring system (VTSS). The remaining two target positions are cloth targets scored by a video target scoring system. In this scoring process, for each round fired at the 2400-m target (This is the aim point.), two electronically gated video cameras coupled with video recorders capture a section of the trajectory of the round. One camera is used for the 800-m position and one camera for 1500 m. The gate video cameras provide a still image of the rounds tracer at discrete intervals during the trajectory. The TOF of the round is recorded every time the video image is captured and mixed with the video picture by using a video annotator.

In the FOV of each camera is a pair of poles with fiducial marks for angular calibration of the cameras. The recorded video is replayed, and the image of the round and fiducial marks are digitized one frame before and one frame after the round passes the target plane. The time at which the round passes the target plane is determined using a Doppler radar. The angular coordinates of the round are determined relative to a primary fiducial mark by extrapolation. The angular coordinates of the round at 2400 m and 3000 m are measured using a standard video camera and digitizing the tracer, fiducial marks, and aim point as the round passes through the cloth target.

During the first three phases of the test, each tank conducting accuracy firing was instrumented with through-sight and gun tube television cameras. In order to evaluate any tank-to-tank effect on accuracy, the gun tubes were rotated among the eight tanks after every phase of firing. Table 6-15 gives a break-

TABLE 6-15.   BREAKDOWN OF ACCURACY FIRING (Ref. 17)

CONDITION	RANGE, m	REQUIRED NUMBER OF ROUNDS TO BE FIRED			
		M829	M865	M830	M83
S/S	1500	All S/S rounds were fired at the Trench Warfare II Range and scored at various target ranges.			
	2000				
	2500				
	3000	180	210	75	240
S/M	1500	45	50	-	55
	2000	45	50	-	55
	2500	40	45	-	55
M/S	1500	35	30	-	30
	2000	30	30	-	30
	2500	30	30	-	30
M/M	1500	30	30	-	30
	2000	30	30	-	30
	2500	30	30	-	30

down of the number of rounds that were fired for accuracy (Expenditure rounds are not included.) at each test condition for comparison to the system specification requirements.

To assure alignment between the muzzle and the sight, a muzzle reference system update was performed after each group of five rounds fired. Each update was checked by taking grid board readings at 500 m to determine muzzle and sight alignment, and alignment was corrected as required.

All firing that involved a moving tank and/or a moving target was conducted at the Trench Warfare firing range. Courses over which the tank moved included bumps, zigzag, and gravel. The moving target at the Trench Warfare range is a simulated evasive target (a reflected laser dot), which can be programmed to follow a variety of paths.

Although the test program was able to provide insight into subsystem issues, the main purpose was to determine whether or not the M1A1 tank performed as specified in terms of hit probability. For this purpose target impact data derived from the camera systems were analyzed. The variance of the impact points from the target center was calculated for the various ranges, rounds, and engagement conditions. From the variances, estimates of hit probability were made. Although the test result values are classified, the M1A1 Abrams tank system complied with its specifications.

6-3 AH-64 APACHE ATTACK HELICOPTER FIRE CONTROL DESIGN

The design of the AH-64 Apache fire control did not represent a major departure from previous helicopter designs. Personnel involved in the Apache program had the opportunity to study the approach taken in the Cheyenne and Cobra. The nature of the performance requirements imposed on the turreted gun, rocket, and guided missile systems was similar. The use of a gunner-controlled optical/electro-optical targeting sensor, a digital processor, navigation, air and ground speed inputs, pilot head-up displays, and electro-hydraulic gun turret devices remained the same. However, in the decade that followed the Cobra development, the emerging technologies of digital processing, laser transmissions, inertial stabilization, infrared imaging, video, and adaptive control had matured, and significantly improved performance and reliability could be assured. The fire control design concept, which embodies the selection of coordinate reference frames to be used to express the gunnery problem and to compute the solution, was essentially the same as in earlier developments. However, advancements in filter and curve-fit theory provided the means to improve software capabilities. A discussion of the requirements that governed system development follows.

6-3.1 REQUIREMENTS

Apache requirements are given in the *System Specification for the Advanced Attack Helicopter YAH-64* (**Ref. 19**). This document, which directly reflects the user's needs, was the basis for subsequent development of the weapon system. A major portion of the document is devoted to requirements pertaining to development of the airframe, flight controls, and the navigation subsystem. It is an education to scan the requirements section and to note the many considerations involved.

To provide insight into factors that influence fire control design, a few of the more pertinent paragraphs have been excerpted from the text and reproduced in subpar. 6-3.1.1. They are of a general nature and convey an idea of the system and major subsystem objectives.

6-3.1.1 Selected System Specifications from Ref. 19

1. *General description.* "The YAH-64 shall be a twin engine, rotary wing aircraft designed as a stable, manned aerial weapons system to deliver aerial point, area, and rocket target fires."

2. *Missions.* "The YAH-64 shall perform its assigned missions by providing direct aerial fires under day, night, and marginal weather conditions (1/2-mile visibility, 200-foot ceiling)."

    a. *Typical YAH-64 combat missions.* "The YAH-64 shall provide the capability to perform the following missions."

        (1) "Antiarmor (direct aerial fire against armor/mechanized forces)"

        (2) "Air cavalry operations"

        (3) "Airmobile escort and fire support for airmobile operations"

b. *Type YAH-64 peacetime missions.* "The YAH-64 shall be used for aviator and unit training, mobilization, and development of new and improved attack helicopter concepts."

3. *Threat.* "The threat shall be as listed in *Threat to U.S. Army Aviation Systems.*"

4. *Operating conditions.* "The YAH-64 shall have an avionics, visionics, fire control, and armament capability which will allow it to perform its mission by delivering direct aerial fire, day and night, in rotary wing visual meteorological conditions. It will also have the capability of flights to and from the operational area during rotary wing instrument meteorological conditions."

a. *Operations to enhance survivability.* "To enhance survivability, the YAH-64 shall be capable of conducting low level—100 kt, true airspeed (KTAS) at 100 feet, up to 172 KTAS at 200 feet above ground level (AGL)—and nap-of-the earth--0 KTAS to 80 KTAS at 50 feet AGL--flight enroute to and within the operational area. Maximum use will be made of terrain masking, standoff ranges, lateral maneuvering, and protective devices to defeat enemy air defense weapons."

b. *Area of operations.* "The vertical flight performance of the YAH-64 shall permit operations with the payloads specified herein over a maximum portion of the earth's land surface, heavier gross weights with reduced performance and load factor will permit maximum flexibility to meet specific missions or situation demands."

c. *Climatic conditions.* "The YAH-64 shall be capable of operation in environmental conditions specified herein and within atmospheric phenomena that include moderate turbulence and icing. The YAH-64 shall be capable of operation within a range of ambient temperatures from $-25°F$ to $+125°F$ [-31.7 to $51.7°C$] without kits and from $-65°F$ to $+125°F$ [-53.9 to $51.7°C$] with appropriate kits."

5. *Employment and control.* "The YAH-64 shall be employed in teams, platoons, companies, or battalions within divisions and corps of the field Army. It will be controlled by the lowest level ground commander capable of directing and integrating the capabilities of the helicopter into the tactical plan. It shall contain communication, navigation, and fire control equipment necessary to be compatible with the command and control system in the time frame conceived for operation of the YAH-64."

6. *Armament and fire control subsystem characteristics.* "The integrated armament and fire control subsystem shall use modular construction techniques for ease of maintenance and consist of the following subsystems":

a. *Point target subsystem.* "This primary armament shall be utilized to defeat tanks and other hard point-type targets. The Hellfire modular missile system (HMMS) shall be used for this mission and shall be operated primarily by the Copilot/Gunner (CPG) using a Target Acquisition and Designation System (TADS) with day and night operational capability. The pilot shall also have the capability to operate the HMMS. The HMMS shall interface with the fire control and external stores subsystem and shall also operate with laser designation from ground or other airborne laser designators."

b. *Area weapon subsystem.* "The area weapon subsystem shall consist of a gimbaled gun turret mounting a 30-mm automatic weapon, a weapon pointing drive system, an electronic control unit, weapon recoil adapter mount, and a feed and storage system. A linkless ammunition storage and feed system shall be utilized. The area weapon subsystem shall be integrated with the fire control subsystem."

c. *Aerial rocket subsystem.* "This subsystem shall provide rocket fire with the 70-mm (2.75-in.) folding fin aerial rocket (FFAR). The subsystem shall provide capability for in[-]flight selection of various warhead and fuzing options by the pilot. The subsystem shall be integrated with the external stores subsystem and fire control subsystem."

d. *Fire control subsystem.* "The fire control subsystem shall be a totally integrated subsystem consisting of the TADS, air data sensors, aircraft attitude and velocity sensors, a pilot's and CPG's integrated helmet and display sight system (IHADSS), a fire control computer, mux subsystem, symbol generator, and all associated controls and panels."

7. *Weapon Requirements.* The specifications that ultimately establish the design of the fire control are those that state the accuracy required of each of the weapon delivery modes. Although the numerical values associated with accuracy requirements are classified, the following are authors' comments regarding the means by which they are expressed.

a. *Hellfire.* Requirements are specified in terms of single-shot hit probability on a tank-type target as a function of range. Although performance requirements for the autonomous laser designation function

and the missile in-flight guidance loop are stated, the overall hit probability accuracy specification has precedence. Hits on target are counted in field trials, and probabilities are calculated as the ratio of hits to firings, with the number of firings determined by the value necessary to achieve a 0.9 per unit level of significance.

b. *Turreted weapon (30-mm)*. The gun has a dual role in the weapon system concept. At short range it is considered to be a point target weapon firing 50-round bursts at stationary or moving ground targets. Accuracy requirements are specified in terms of burst hit probability, i.e., the probability of at least one round of the burst hitting the designated size target. Beyond one kilometer the gun is considered to be an area weapon. The required accuracy is then specified in terms of the expected number of rounds of a 50-round burst impacting within a rectangular ground target of designated dimensions.

c. *Free rocket 70-mm (2.75-in.)*. The rocket is also considered to be an area weapon and the accuracy requirement is stated in terms of the expected number of rounds per salvo which impact within a rectangular ground target area.

All requirements are expressed not only as functions of target range but also in terms of the weapon system flight conditions when the weapons are fired. Requirements for the point target weapons also include the possibility of limited target motion.

Forming a part of the specification are sections devoted to defining the means whereby the weapon system was to be evaluated for conformance with accuracy requirements. This included not only engagement scenarios, environmental conditions, and firing doctrine under which the system was to be tested but also the methodology and data reduction procedure to be used to evaluate performance. The importance of structuring a test program that is fully representative of the engagement conditions described in the performance requirements cannot be overstated. Specifications alone are meaningless unless backed up with a test procedure that provides the means to demonstrate compliance.

General considerations pertaining to a test program for attack helicopters has been discussed in Chapter 4 of this handbook. There is further discussion concerning the processing of flight-test data to assess system performance of the Apache in subpar. 6-3.3.3. During the test program the evaluator often faces the need to process an overwhelming amount of data in a short period of time on one hand and the availability of sufficient replications to permit valid statistical inference on the other. It is at this point that a proven methodology and data reduction procedure is necessary and appreciated.

6-3.1.2   Element Characteristics

Functional factors determined from system performance requirements were used in Chapter 3 as a basis for selecting examples of suitable elements for various fire control applications. In subpar. 3-3.4 this selection process is applied directly to the Apache fire control. The block diagram in Fig. 3-6 provides an indication of general element characteristics and data flow.

Before discussion of the Apache system concept and implementation including specifics of the evolving elements, a review of the technological characteristics of elements available at the time of development in terms of functional need has been included.

6-3.1.2.1   Acquisition and Track

An optical and electro-optical approach used in the prior development of the Cheyenne and Cobra attack helicopters still afforded the only means to satisfy the acquisition and track functional needs that were driven by Hellfire missile system requirements. Advancements in infrared imaging, video, and optical design offered higher resolution and sensitivity that could extend the night and day viewing range. State-of-the-art lasers could provide 10 to 20 pulses per second data rates with a continuous duty cycle for missile guidance target designation and conventional ranging. However, maintaining the laser energy on target necessitated holding optomechanical alignments and tracking to accuracies not previously achieved. Passive autotrackers, operating on video or infrared imaging with performance that had previously been demonstrated only in experimental prototypes, held the promise of providing the required track accuracy under favorable engagement conditions. The mounting of a CRT on the helmet sight could provide the operator with the added ability to view video or infrared images in a flexible head-up

mode. These technological advancements were exploited by the designers to provide an acquisition and track element that could satisfy system performance requirements.

6-3.1.2.2   Weapon Control

The flexibility of the turreted automatic weapon on the attack helicopter affords the crew the opportunity to engage off-axis targets rapidly and with an accuracy independent of the pilot's ability to point the aircraft. However, the turret drives have to have the dynamics necessary to assure response to computer-generated azimuth and elevation commands derived from target and helicopter engagement kinematics. Although the automatic weapon with a high rate of fire may accumulate large hit probability values over the burst, the disturbance caused by gun recoil may degrade burst accuracy. The turret and turret servo must be designed to reject this disturbance. The turret for the Apache was designed asymmetrically; consequently, the disturbance effect required special attention. The general instability of the helicopter and the requirement to fire during maneuvers introduce base motions that necessitate a high-response servo. A description of the electro-hydraulic servo designed to meet the challenge is included in subpar. 6-3.3.2.4.

6-3.1.2.3   Ballistics

The ballistic equations formulated by the Army for Cobra fire control were available to the designers. These equations expressed the direction cosines of the desired weapon pointing vector in the sight line coordinate reference frame as a function of the variables influencing the trajectory. The TOF as a function of these variables had also been developed for target future position prediction and fuze settings. However, these relationships proved to be inadequate, even with the contractor's attempts to modify them to improve accuracy. A more sophisticated set of equations that represented both the gun and rocket trajectories within the required tolerance was developed by the Army and implemented by the contractor. These equations were represented in the earth inertial reference frame so that the initial projectile velocity included the velocity of the helicopter. The process by which the Army developed these equations is discussed in subpar. 6-3.2.

6-3.1.2.4   Filter

The attack helicopter fire control solution involves the motion of both target and helicopter. Accordingly, estimates of the target motion are required as inputs to the equations discussed in the previous subparagraph. Navigation and tracking subsystems provide measurements of helicopter and target relative motion, but include undesirable noise. Investigations were conducted during the course of the program to develop Kalman filters that would reduce the noise and produce estimates compatible with the system tolerances for accuracy and time. The decision was made early in the program to represent the helicopter and target motion in an earth-based coordinate reference system, which has the advantage that target motion is most readily measured and perceived in this frame. On the other hand, the stabilized sight coordinate system was used as the computing frame. The discussion in subpar. 6-3.2.2 on mathematical models describes the evolution of the filters from those initially proposed to the ones eventually implemented.

6-3.1.2.5   Prediction

Initial studies considering the prediction of target motion during the projectile TOF examined the type of motion attributable to combat vehicles vulnerable to 30-mm ammunition. Evasive target maneuvering was included in these studies. These early studies indicated that the filtering of target data taken under these conditions yielded acceptable estimates of target velocity and accelerations, so nonlinear prediction was productive. However, a three-state filter eventually replaced the original seven-state filter, and the emphasis on engaging a maneuvering target declined. In particular, the system requirements specified performance only for constant-velocity targets. Accordingly, a simple linear predictor was used where the target velocity is multiplied by projectile TOF to the predicted point of impact. In the Apache this linear compensation has been absorbed into the ballistic lead equations so that there is no stand-alone

prediction element. In subsequent studies that considered the Apache turreted weapon in an air-to-air engagement, the seven-state filter and nonlinear prediction were reconsidered.

6-3.1.2.6   Flight Control

A vehicle control element is not generally included as an integral part of a fire control system. It is used only in the airborne application because the vehicle must be oriented precisely to point a weapon, e.g., the rocket launcher. Before the Apache all fielded helicopter systems fired rockets from launchers that were permanently oriented with respect to the longitudinal axis of the aircraft. The launchers on the Apache are independently gimballed and controlled in elevation. The pilot need only orient the helicopter in azimuth in response to a computer-driven reticle displayed in his helmet sight. However, the computed reticle position is a function of the motion of the helicopter that varies as the pilot adjusts yaw orientation. Control of the aircraft in yaw, which can lead to a significant rocket delivery error, is not optimized for this function. The Hellfire launchers, which are also gimballed only in elevation, require aircraft pointing in yaw, but the tolerance needed in this case is large because of the missile guidance. Aircraft pointing is considered to be an error source beyond the control of the fire control designer.

6-3.1.2.7   Navigation

The principal function of an aircraft navigational subsystem is to provide three-dimensional position data in an earth-referenced coordinate system within the required accuracy. Additionally, for the Apache it also provides heading flight data for future rendezvous and TADS prepointing angles for rapid target acquisition and position update. To the fire control designer the primary benefits of this subsystem are its measurements of helicopter motion and attitude. Helicopter motion provides estimates used to establish initial launch velocities for trajectory determination, and helicopter attitude is essential for generation of the transformations between the earth and the airframe coordinate system.

The navigational needs of the Apache are satisfied by integration of the inertial heading and attitude reference system (HARS) and the Doppler ground speed radar. Additionally, an airspeed sensor is required in conjunction with the ground speed measurement to determine wind velocity. Navigational requirements tend to be of a long-term nature and are therefore tolerant of heavy filtering. On the other hand, fire control needs require instantaneous values of kinematic parameters. These opposing requirements created a special filter problem in the use of the available air data sensors during development. Such sensors were susceptible to noise induced by helicopter maneuvering.

6-3.2   SYSTEM CONCEPT DEVELOPMENT

The fire control solution implemented in the Apache assumes, as might be expected, that both the weapon system and the target are in motion. A solution is continuously generated using the weapon system position in the earth-based inertial reference frame. The target position and motion with respect to this reference are required to generate the projectile flight curvature and target kinematic contributions to the total lead angle. The sight gimbal angles and laser range are required during tracking and provide the basis for relative position estimates. However, measurement of the sight line angle obtained by the integrating rate gyros offers a better way to estimate relative target motion. Estimates of target motion with respect to the reference point require that the relative estimates be modified by the motion of the weapon system with respect to earth. Measures of the weapon system motion are obtained from the HARS, the Doppler navigational subsystem, and the TADS mounted linear accelerometers. Estimates of target position and velocity relative to the reference point are used as inputs to the fire control equations (including the projectile TOF function) in order to generate the total lead angle. The weapon is then offset from the sight line by the lead angle.

All filtering of data and computation of lead angles take place in a coordinate system defined by an inertially stabilized orthogonal set of axes along and normal to the LOS. The three components of the sight line rate are measured by the stabilization gyros mounted along those axes. The LOF orientation with respect to the airframe is measured by resolvers mounted on the sight gimbals.

The original Apache filter concept defined a nine-state Kalman filter to provide estimates of the weapon system position and motion and a seven-state Kalman filter to provide estimates of target position and

motion---all relative to earth. Structuring of the two filters in the earth-referenced coordinate frame permits a mathematical definition of the system plant equations that draws upon the database in which vehicle behavior is usually perceived and measured. In contrast, expressing the filter system equations based directly upon motion of a maneuvering target relative to a maneuvering weapon system would be far more difficult. Development of the filter is complicated by the fact that the LOS coordinate system used as the computing reference frame takes on angular motion with respect to the earth. This complication is discussed further when development of the filter model is addressed.

The equations used in an iterative process to compute the ballistic and kinematic contributions to lead angles and the values of projectile TOF are also discussed further when the ballistic model is addressed in subpar. 6-3.2.2.1. For the Apache implementation, equations expressed in the LOS computing frame provide a solution for the total lead as the sum of ballistic and kinematic lead contributions. In addition to the estimates of target and weapon system states provided by the filter, estimates relating to the environmental and ammunition conditions are also required for the solution. Many of the inputs to these equations are expressed initially in coordinate systems other than the system of the LOS; thus appropriate coordinate transformations are required.

Values of the computed total lead angle are ultimately transformed into the coordinate frame for the helicopter and used as commands in conjunction with sight orientation to drive the electrohydraulic turret in azimuth and elevation and thus point the gun. In a sense, the gun is space stabilized since it is referenced to the stabilized sight line. Although both the sight and gun are driven from and referenced to the airframe structure, the fact that there is a physical separation between the two allows sight or gun misalignment to be introduced through airframe flexure. This error is compensated for in the Apache by storing corrections obtained from firing tests in the computer.

For rocket fire the launcher is steerable in only the elevation axis. The pilot must perform a function comparable to the gun turret servo by pointing the aircraft appropriately in this axis. Accordingly, the head-up display provides this azimuth error signal (or equivalent), and the pilot is required to null it out by reorienting the aircraft in heading or yaw. Otherwise, the rocket solutions follow closely those of the gun and are not discussed in detail. The rocket trajectory is, however, more difficult to predict because it has a postlaunch burn phase. Furthermore, it is highly sensitive to wind conditions at launch.

In this earth-referenced implementation, weapon system velocity is vectorially summed with muzzle velocity in order to produce an initial projectile velocity vector with respect to the earth. In a weapon-system-referenced implementation, weapon system velocity with respect to earth would be considered a component of target velocity, and the weapon system velocity with respect to the air mass, a component of the wind. Although the predicted positions in space would differ, the total lead would remain invariant. Also, in the earth-referenced system the stationary ground target solution does not require use of the LOS angle rate. However, since a moving target solution requires the kinematic lead, the provision is necessary.

6-3.2.1 Accuracy and Reaction Time Analysis

The accuracy of the 30-mm turreted weapon is specified at the shorter ranges (below one kilometer) in terms of burst hit probability on a 2.5-m × 2.5-m vertical point-type ground target. A 50-round burst is fired during the engagement at a stationary target or a target moving at a constant velocity of 15 m/s normal to the direction of fire. At longer ranges, on the other hand, the required accuracy is expressed in terms of the expected number of hits from a 50- round burst on an area target with dimensions of 100 m × 500 m. Rocket accuracy is also specified in terms of the area target criterion. Apache flight conditions during engagement are restricted to hover, constant velocity, or a veer maneuver.* The designer's task is to develop a system that meets these (and other) accuracy requirements.

Accuracy analysis is associated primarily with two aspects of development. During design, analysis is used initially to establish accuracy requirements on individual subsystems and components. Thereafter,

---

* A veer maneuver is defined as a coordinated right or left turn to a heading 60 deg from the original heading at a specified bank angle.

the analysis provides the means to predict system performance on a continuing basis as refinements are made to the initial design concept. Once the system has been fabricated and has undergone field evaluation, firing data are analyzed to assess conformance of the system to the stated requirements.

For both applications a relationship must be selected that expresses system accuracy in terms of statistical error parameters. The usual parameters chosen are the mean and the standard deviation of the systematic error (bias) and the standard deviation of the random error (dispersion). In the design phase, estimates of these parameters evolve from the individual contributions of subsystem and component errors that have been established from specification and prior testing. Further discussion of the evaluation for the Apache is given in subpar. 6-3.2.3. In the field evaluation phase the errors are determined directly from the analysis of firing data. This determination for the Apache is discussed more fully in subpar. 6-3.3.3. The estimates of the statistical parameters obtained from the analysis of firing data provide a better measure of system accuracy than is predicted by estimates of subsystem and component performance.

Since the accuracy requirements for ballistic weapons are expressed in terms of burst hit probability and the expected number of hits on target, an accuracy relationship must be selected that best represents these probabilities. In Chapter 4 alternative relationships were developed for engagement hit probability that differed primarily in the assumption of the rate of fire. For the high rate of fire (burst or salvo) assumption, it is assumed that the systematic error (bias) remains constant during the burst. For the low rate of fire assumption, it is assumed that each time a round is fired the bias changes in a random manner. In both cases the dispersion error (round-to-round) is taken to vary with each round fired in a random manner.

The intermediate rate of fire of the Apache 30-mm gun is such that there is some merit to using both expressions, and an investigation of each approach as made during the course of development. However, the eventual data reduction and processing of flight-test firing data tended to support the applicability of the high rate of fire assumption, i.e., the bias remained constant during the burst. As expected, this assumption also proved to be valid with salvo rocket fire.

Either of the two relationships for engagement hit probability can readily be evaluated by numerical methods. Sample curves taken from Ref. 20 indicating representative solutions for both relationships are provided in Figs. 6-20 and 6-21. Not only does the family of such curves provide the means to determine the engagement hit probability given values of the statistical error parameters, but it also offers the op-
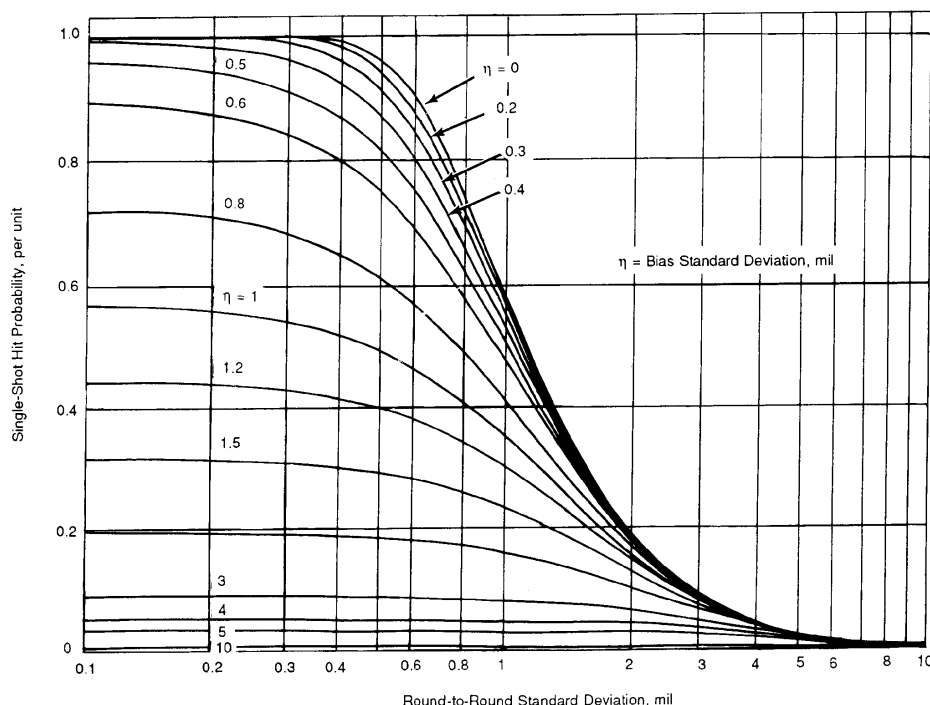
Figure 6-20. Single-Shot Hit Probability (Ref. 20)
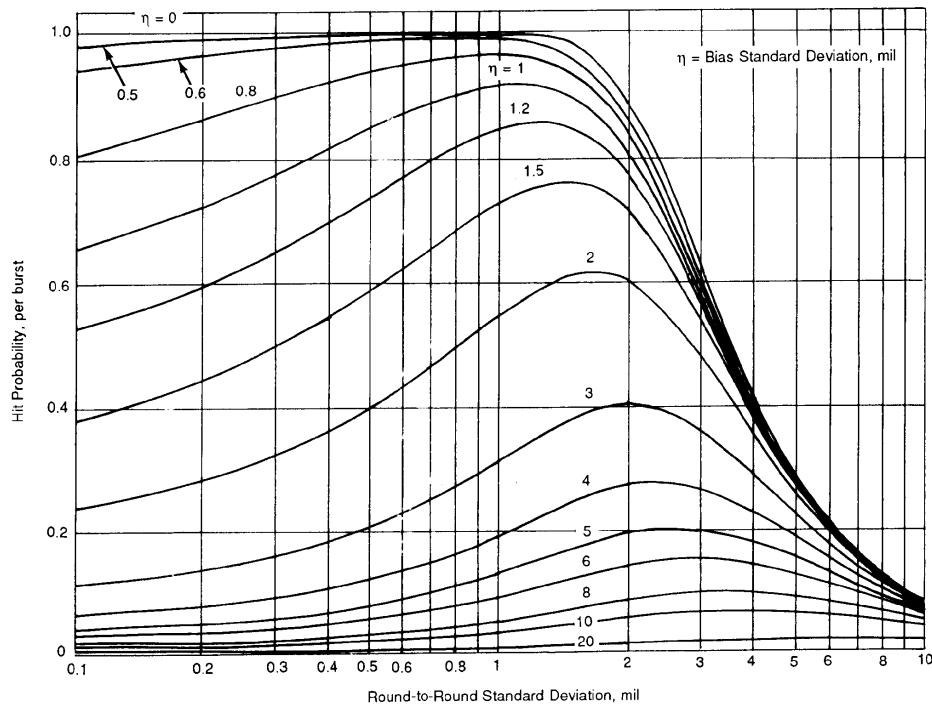
Figure 6-21. Probability of Acquiring at Least One Hit in a 10-Round Burst (Ref.20)

portunity to arrive at an inverse solution. Given a specific value of the engagement hit probability and two of the three statistical parameters, a corresponding value of the third parameter may be determined. This procedure can be used to establish tolerances on the total systematic (bias) error that is compatible with the required burst hit probability. An error budget for each of the subsystems or component bias errors can then be established. In practice, however, this process requires that estimates of the mean of the bias errors and the standard deviation of the dispersion be made. Often the mean value of the bias error is near zero, and the major contribution to the dispersion is the round-to-round gun and ammunition variation. These assumptions along with curves such as those illustrated in Figs. 6-20 and 6-21 can be used to establish the total system tolerance initially on the standard deviation of the bias.

The procedures by which tolerances of the system statistical error parameters are related to the hit probability requirement are addressed in subpar. 4-4.1.3. The Apache error budget was developed using the procedure discussed. Although the burst hit probability criterion is used in this discussion, the same procedure remains valid where the criterion for the expected number of hits on the horizontal area target is considered. However, there is a distinct advantage to expressing this criterion using the slow rate of fire assumptions. The expected number of hits is then the product of the number of rounds in the burst and the single-shot hit probability. The single-shot hit probability is readily expressible in the statistical error parameters for the system. This procedure is not valid using the high rate of fire assumption.

Interest in extending the Apache gun role to include the engagement of aerial targets led to the initiation of additional analyses to assess this capability in both its present configuration and in one optimized for the new task. The error analysis has been expanded to consider the effects of the aerial target kinematics on the filtering and prediction performance as well as the dynamics of sight and gun servos. Monte Carlo techniques have also been used in a model of the Apache gun fire control to evaluate performance in its air-to-air role. The model is driven by input data to the fire control sensors; data that have been generated from appropriate parameters defined by engagement geometry. Sensor errors are expressed in terms of frequency distributions with time-varying statistics that are sampled at rates consistent with actual system functioning. The filtering and prediction equations, represented by the fire control computer software, are reproduced in the model and duly exercised. Projectiles are fired along trajectories determined by gun orientation (resulting from servo response to computer commands) and

the imposition of real-world ballistics. Miss distance between the projectile and the advanced position of the target is used to generate burst hit probability statistics.

The model has the advantage over the error analysis approach of offering flexibility in the representation of error sources through the use of arbitrary frequency distributions. In addition, it provides mathematical rigor by combining the errors in a nonlinear manner. However, to achieve meaningful results, many iterations are necessary.

In addition to accuracy analysis, the response time also needs to be analyzed. To ensure that the fire control can bring fire to bear consistently with engagement needs, a requirement for reaction time is usually included in development specifications. The reaction time is commonly defined as the time elapsed from the moment of target detection to the firing of the first round. It includes the time required to perform the functions of acquisition of the target, initiation of track, generation of a steady state computer solution, slew of the weapon in response to computer commands, and gunner delay in initiation of fire. Since reaction time is highly dependent upon the particular engagement conditions encountered, the requirement is usually developed for a few representative situations. Timelines provide a means of observing the time segments devoted to accomplishing each of these functions and how they relate to the overall reaction time. The Apache specification did not include specific reaction time requirements. Nevertheless, consideration was given to the settling time of the target filter. A follow-on effort to modify the system to engage aerial targets successfully requires further consideration of reaction time.

6-3.2.2 Mathematical Models

The three mathematical models that form the basis for Apache software include ballistics, filtering, and prediction. Their developments are all compatible with the statement of the fire control solution in the earth-referenced coordinate frame; however, computation is performed in the LOS inertial coordinate system. These three models are discussed in the following subparagraphs.

6-3.2.2.1 Ballistics

Subpar. 2-2.4 discusses the development of general ballistic equations that model projectile trajectories to acceptable tolerances. As noted, the general ballistic differential equations, whether they are the six-degree-of-freedom (SDF), the three-degree-of-freedom (TDF), or the modified three-degree-of-freedom (MTDF) representation, are not suited for use in the fire control computer. The fire control computer considers the weapon orientation to be an output rather than an input. Furthermore, the real-time requirement for solution of even the TDF representation in real time is beyond the capacity of the Apache computer. Accordingly, a set of algebraic equations that express the azimuth and elevation gun lead angles in terms of the measurable parameters related to the target, weapon system, environment, and ballistics was developed. This process was accomplished in phases.

The initial phase required development of an SDF model that represents the free flight behavior of the projectile. This representation necessitates obtaining all weights and measures, other physical characteristics, and aerodynamic drag functions peculiar to the munitions of interest.

The next phase required development of a set of equations (or structures) with the potential to represent the projectile trajectories ultimately in the desired form. These equations were obtained by a curve fit to data generated by the SDF model. The basic structure of the equations is obtained by solving the TDF, assuming constant drag, and introducing free-floating parameters whose values are determined by a curve fit procedure. The introduction of arbitrary parameters provided the means to adjust the solution for the constant drag assumption. In Ref. 21 Breaux describes this methodology. The challenge was to provide a structure with the potential to represent the data obtained from the SDF solution over the full range of the engagement geometries while maintaining tight tolerances.

In effect development of the ballistic equations required fitting one model to another, i.e., the structural model to the SDF model. To accomplish this, a database was created by generating a family of trajectories through use of the SDF model. Insofar as the SDF model represented the actual trajectories, the database was considered to be the truth model. Care was taken to ensure that the assumed initial conditions provided trajectories representative of the expected engagement conditions. The trajectory points considered for inclusion in the curve fit database were appropriately weighted to represent the

likelihood of various target and projectile encounters. The true values of the lead angles and the TOF were computed at these points using SDF data.

The values of the parameters of the curve fit were determined by minimizing the sum of the squares of the errors both in position and at the TOF of the projectile. Provisions of the minimization process allowed an automatic extension of the number of arbitrary parameters until the results were within an acceptable tolerance.

Finally, the curve fit models (resulting ballistic equations) for the direction cosines of the lead angles and the TOF were validated. The equations were tested in the exact software program format to be used in the field to assure agreement with the SDF truth model. Comparison of the errors between the software program and the truth model indicated agreement to within a specified tolerance for the lead angles and the TOF over the range of operating variables.

The fire control implementation required the lead angle to be expressed in azimuth and elevation. Therefore, equations were developed to provide these two components. The equations used for the gun solution are Eqs. 6-37 and 6-38. A comparable rocket set of equations that allow for the burn phase is developed in Ref. 21.

The computational coordinate system selected for this application is referred to as SLM and is shown in Fig. 6-22. In the Apache these axes are measured along the axes of the three orthogonal integrating rate gyros of the inner stabilized gimbal of the TAD. Here the S axis points along the LOS, the L axis is normal to S and is constrained to rotate around the line of sight, and the M axis is normal to the SL plane. X, Y, and Z in Fig. 6-22 represent an earth-based inertial reference frame, and A indicates the altitude of the helicopter.
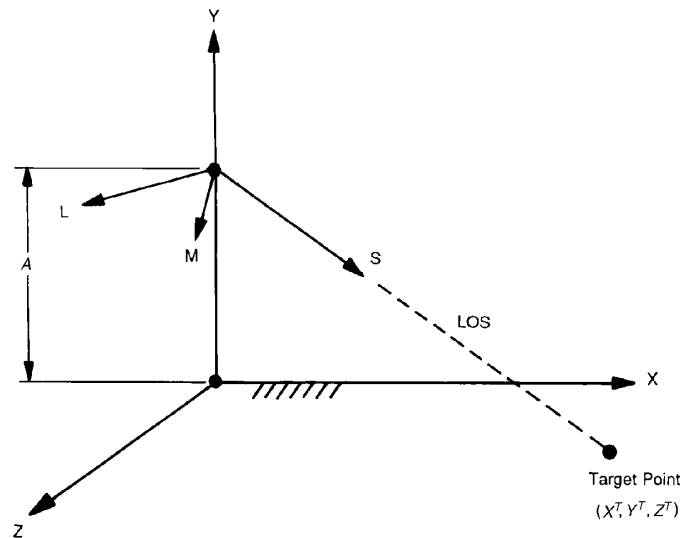
Figure 6-22. SLM Coordinate System Relative to XYZ Earth-Based Inertial Coordinate System

The equation developed for the direction cosines b_M and b_L of the lead angles in the SLM coordinate system is

$$\begin{bmatrix} b_M \\ b_L \end{bmatrix} = -\frac{1}{U_B}\begin{bmatrix} V_M \\ V_L \end{bmatrix} + \frac{\mu_S}{\zeta U_B}\left\{ -\left(t_p - \frac{\zeta}{\mu_S}\right)\begin{bmatrix} W_M \\ W_L \end{bmatrix} + \begin{bmatrix} r_M \\ r_L \end{bmatrix} + t_p\begin{bmatrix} V_M^T \\ V_L^T \end{bmatrix} \right.$$

$$+ C_{13}A_j t_p^2\begin{bmatrix} g_L\mu_S - g_S\mu_L \\ g_S\mu_M - g_M\mu_S \end{bmatrix} + C_{14}A_j\zeta\begin{bmatrix} \gamma_M \\ \gamma_L \end{bmatrix} \qquad\text{(6-37)}$$

$$\left. + \frac{C_{15}\left(t_p - \dfrac{\zeta}{\mu_S}\right)}{(h\mu_S) + C_{16}\,t_p^2 + C_{17}\,\lambda t_p^2}\begin{bmatrix} g_M \\ g_S \end{bmatrix} \right\},\ \textbf{dimensionless}$$

where

b_M = direction cosine for M-component of lead angle for the gun barrel unit vector, dimensionless

b_L = direction cosine for L-component of lead angle for the gun barrel unit vector, dimensionless

U_B = muzzle velocity (initial projectile velocity with respect to gun), m/s

V_S, V_L, V_M = helicopter velocity components in the SLM coordinate system, m/s

μ_S, μ_L, μ_M = components of initial projectile velocity with respect to air in the SLM coordinate system, m/s

t_p = TOF of projectile along trajectory, s

W_S, W_L, W_M = components of the difference between helicopter ground speed and airspeed transformed into SLM coordinate system, m/s

r_S, r_L, r_M = components of target range in the SLM coordinate system, m

V_L^T = L-component of target velocity with respect to helicopter, m/s

V_M^T = M-component of target velocity with respect to helicopter, m/s

V_S^T = S-component of target velocity with respect to helicopter, m/s

A_j = lumped jump parameter, dimensionless

g_S, g_L, g_M = components of gravity in the SLM reference system, m/s²

$\gamma_M = \mu_{ff}^{-1}[(V_L - W_L)b_S - (V_S - W_S)b_L]$, dimensionless

b_S = direction cosine for S-component of lead angle for the gun barrel unit vector, dimensionless

$\gamma_L = \mu_{ff}^{-1}[(V_S - W_S)b_M - (V_L - W_L)b_S]$, dimensionless

μ_{ff} = total initial projectile velocity with respect to air, m/s

C_{13} = constant, s/m

C_{14} = constant, dimensionless

C_{15} = constant, dimensionless

C_{16} = constant, s⁻³

C_{17} = constant, s⁻³

$h = \pi d^2 \rho C_{D0} M_s /(8 m_p)$, m⁻¹

$\zeta = r_S - W_S t + V_S^T t_p$, m

$\lambda = g_S / (\eta \mu_S^2)$, **dimensionless**

d = **projectile diameter, m**

ρ = **local air density, kg/m³**

C_{D0} = **zero yaw drag coefficient, dimensionless**

M_s = **standard Mach number at firing, dimensionless**

m_p = **projectile mass, kg**

$\eta = \pi d^2 D C_{D0} M_s / (8 m_p)$, **m⁻¹.**

The first term on the right side of Eq. 6-37 is the contribution to the lead angle due to the velocity of the helicopter. The second term is the contribution due to wind drift. The third term is the contribution due to the relative positions of the helicopter and the target. The fourth term is the contribution of the velocity of the target relative to the helicopter. The fifth term is the contribution of projectile drift caused by relative air motion. The sixth term is a contribution caused by windage jump. Finally, the seventh term is a contribution due to gravity.

Next, ζ can be interpreted as the distance traveled by the projectile from the helicopter to the target, which is different from the range determined by the LRF. The TOF in Eq. 6-37 can be written as a function of ζ:

$$t_p = \left[C_5 + C_6 \lambda \right] \frac{\zeta}{\mu_S}$$

$$+ \frac{\eta \zeta^2}{\mu_S} \left[C_7 + C_8 \lambda + C_9 C_{D0} \alpha^2 + C_{10}(M_a - M_s) \right] \qquad \textbf{(6-38)}$$

$$+ \frac{C_{11} \eta^2 \zeta^3}{\mu_S}, \ \textbf{s}$$

where

C_5 = **constant, dimensionless**

C_6 = **constant, dimensionless**

C_7 = **constant, dimensionless**

C_8 = **constant, dimensionless**

C_9 = **constant, dimensionless**

C_{10} = **constant, dimensionless**

C_{11} = **constant, dimensionless**

M_a = **local Mach number, dimensionless**

α = **projectile total angle of attack, rad.**

The values for the constants found in Eqs. 6-37 and 6-38, i.e., C_5 through C_{17}, are determined by a least squares fit of data for a given combination of gun and ammunition characteristics. Eqs. 6-37 and 6-38 are coupled, and they must be solved simultaneously.

6-3.2.2.2 Filter

Early helicopter fire control was incapable of generating a full solution for a moving target. Sights and range finders that could supply track data with sufficient accuracy to extract target motion estimates were not available. Although sight data provided a reference for the angular position of the target, only the lead angle due to the velocity and trajectory of the helicopter were computed to generate an offset of the gun line. Pitot tube sensors provided a measure of airspeed, but the target range used for the curvature calculation could only be estimated. Refinements to the solution for such corrections as wind or helicopter maneuver were not considered in light of these more obvious shortcomings.

As shown in Ref. 22, the advent of the stabilized gunner sight and the integrated LRF created the possibility of generating a full solution for both weapon system and target motions. However, the availability

of accurate three-dimensional track data made it necessary to introduce advanced filtering and prediction techniques in order to exploit this capability. Digital computation permitted the required data processing. Although this technology had been addressed for the Cheyenne and Cobra, it was developed to a greater extent for the Apache.

The Apache fire control solution is expressed in an earth-referenced coordinate system. Both the helicopter and target motions are most naturally expressed in this system, as reflected in the Kalman filter system as plant equations. For compatibility the projectile trajectories are also expressed in this earth-based reference frame. The stabilized sight not only supplies accurate track data but also offers a physical orthogonal coordinate system that is used as the basic computational frame, i.e., the SLM coordinate system. This frame is inertially stabilized, and many of the critical input parameters are measured directly in this frame, e.g., target range, angular rates, and helicopter accelerations. Thus the need for their coordinate transformation is precluded. The discussion that follows describes the major effort by the developer to design a filter that would continuously provide estimates of helicopter and target positions, velocities, and accelerations obtained from sensor measurements. Filter performance is ultimately driven by the need to meet the accuracy requirements of the unguided weapon. As a result, a simulation was developed to study the impact of the filter on the performance of these weapons. This model was used to evaluate the many filter versions considered.

A team of experts was tasked by the developer to design a filter for the Apache that would provide estimates of the helicopter and target state variables based on the sensor suite inputs. Accordingly, a nine-state helicopter and a seven-state target filter were designed and evaluated in a simulation representing realistic engagement scenarios of a helicopter and maneuvering ground targets. The nine-state variables of the helicopter expressed in stabilized sight coordinates were the three earth-referenced components of position, their velocities, and their accelerations. The seven-state variables of the target filter were the helicopter-to-target range, the three earth-referenced components of target velocity, and the three earth-referenced components of target acceleration. These target filter variables were also expressed in the SLM coordinate system.

The nine-state filter of the helicopter was eliminated because the HARS and Doppler navigational equipment and the TADS accelerometers provided data that were sufficiently accurate to meet requirements. However, despite the elimination of the nine-state filter, the fire control computer capacity was still being taxed. To reduce computer demands further, prestored gains were empirically generated as a function of time based on filter initiation. However, this effort was not successful because difficulties arose in reaching steady state values in the allotted 1 to 2 s. At this point a three-state target filter was designed to replace the seven-state target filter. This three-state filter was based upon the assumption that the errors in the sight line angular rate measurement were insignificant. Estimates were then made for the relative range, range rate, and range acceleration of the target. Simulation studies indicated that there was little noise in the sight line rate measurements and confirmed the acceptability of the three-state filter, which was then adopted for implementation.

The features of these filters are examined in the text that follows, and a review of the standard Kalman filter formulation is presented in Chapter 4 and Appendix B. Although the seven-state target filter was abandoned in the baseline Apache development, it was later restored for consideration when the weapon system mission requirements were expanded to include air-to-air capability. The discussion that follows is based on the work of Bucy, Asseo, and Weissenberger in Ref. 22, in which the helicopter and target models, the sensor descriptions, and the detailed filter design are given in continuous time and discreet time. However, only the continuous time analysis is presented here. The results and conclusions of these simulation studies are also included in Ref. 22. A key factor in selection of the target filter was the noise level assumed in the LOS rate measurement. The study considered realistic ground target motion, but the Apache specifications required only the consideration of stationary or constant-velocity targets.

Target states are estimated by using helicopter velocity and acceleration measurements as well as range, LOS angle, and LOS rate measurements obtained from the TADS. Filter equations are developed in a rotating, right-hand LOS coordinate system. Time-correlated random acceleration models are used to represent the dynamics of the target. Since the state transition matrices and the observations associ-

ated with this formulation are functions of the LOS rates, the LOS vector of these rates ω was treated as a constant for state transition equations in the sampling interval in order to reduce the problem to one of linear estimation. The LOS vector was also used to obtain target velocity, although it is a somewhat noisy measurement. This technique of treating a variable that affects both the observation and the dynamic model as being quasiconstant was novel and proved to be quite effective. The effectiveness of this formulation was proven through the use of simulations of helicopter and target engagement scenarios. Without this procedure the resulting estimation problem in which the LOS vector is treated as a state becomes extremely complex.

The relative target motion represented in inertial space is modeled in continuous time by

$$\frac{d\mathbf{X}^T}{dt} = \mathbf{V}^T - \mathbf{V}, \ \mathbf{m/s}$$

$$\frac{d\mathbf{V}^T}{dt} = -\rho^T \mathbf{V}^T |\mathbf{V}^T| + \mathbf{A}^T, \ \mathbf{m/s^2}$$ (6-39)

$$\frac{d\mathbf{A}^T}{dt} = -\Gamma \mathbf{A}^T + \mathbf{W}, \ \mathbf{m/s^3}$$

where

$\mathbf{X}^T$ = three-dimensional target range vector in inertial reference frame, m
$\mathbf{V}^T$ = three-dimensional target velocity vector in inertial reference frame, m/s
$\mathbf{V}$ = three-dimensional helicopter velocity vector in inertial reference frame, m/s
$\mathbf{A}^T$ = three-dimensional, time-correlated random target acceleration vector in inertial reference frame, m/s²
$\rho^T \mathbf{V}^T |\mathbf{V}^T|$ = three-dimensional target acceleration due to drag vector, m/s²
ρ^T = drag constant, m⁻¹
Γ = inverse correlation time of target acceleration, s⁻¹
$\mathbf{W}$ = three-dimensional white noise process vector, m/s³.

Consider the vector $\mathbf{X}^T = R\mathbf{S}$, where R is the range between the target and the helicopter. **S, L,** and **M** are the unit vectors of the SLM system shown in Fig. 6-22. Ref. 23 shows that the time derivatives, measured in an inertial set, of rotating unit vectors can be expressed by

$$\frac{d\mathbf{S}}{dt} = \omega \times \mathbf{S}, \ \mathbf{rad/s}$$ (6-40)

where

S = LOS unit vector of the SLM coordinate system, dimensionless

ω = LOS rate vector* $\begin{bmatrix} \omega_S \omega_L \omega_M \end{bmatrix}'$ as measured in the inertial reference coordinate system, rad/s.

In LOS coordinates, target position relative to the helicopter is completely defined by specifying a range R (along **S**). Therefore, only a seven-dimensional target state vector with components $X_S^T \ V_S^T \ V_L^T$, $V_M^T, A_S^T, A_L^T,$ and A_M^T is needed in the LOS coordinate system to define the relative target motion, e.g.,

$$\mathbf{V}^T = V_S^T \mathbf{S} + V_L^T \mathbf{L} + V_M^T \mathbf{M}, \ \mathbf{m/s}$$
$$\mathbf{A}^T = A_S^T \mathbf{S} + A_L^T \mathbf{L} + A_M^T \mathbf{M}, \ \mathbf{m/s^2}$$ (6-41)

---

*The prime denotes transpose, i.e., the vector is a column vector.

where

A_S^T, A_L^T, A_M^T = **components of the three-dimensional target acceleration vector in the SLM coordinate system, m/s².**

   The time derivative of range is given by

$$\dot{R} = V_S^T - V_S, \ \ \mathbf{m/s} \qquad (6\text{-}42)$$

where

R = **range between helicopter and target, m**

$\dot{R}$ = **time derivative of target range,** $\dfrac{d}{dt}R$**, m/s.**

If Eqs. 6-39 and 6-42 are used and the cross products of the angular rates with the position, velocity, and acceleration vectors as represented in Eq. 6-40 are added, the equations of motion for the target state in rotating LOS coordinates can be written as

$$\frac{d\mathbf{X}^{*\,T}}{dt} = \left[F_T\right]\mathbf{X}^{*\,T} + \left[G_T\right]\mathbf{W} + \xi, \ \ (\mathbf{m/s, \ m/s^2, \ m/s^2, \ m/s^2, \ m/s^3, \ m/s^3, \ m/s^3}) \qquad (6\text{-}43)$$

where

   $\mathbf{X}^{*\,T}$ = **seven-dimensional target state vector** $[X_S^T \ V_S^T \ V_L^T \ V_M^T \ A_S^T \ A_L^T \ A_M^T]'$ **in rotating LOS coordinates, (m, m/s, m/s, m/s, m/s², m/s², m/s²), respectively**

   X_S^T = S**-component of target range in inertial reference frame, m**

$\left[F_T\right]$ = **7 × 7 state transition matrix,**

$$\begin{bmatrix} 0 & 1 & 0 & 0 & 0 & 0 & 0 \\ 0 & & & & & & \\ 0 & & -[\Omega] & & & [I] & \\ 0 & & & & & & \\ 0 & & & & & & \\ 0 & & [0] & & -\Gamma[I] - [\Omega] & \\ 0 & & & & & & \end{bmatrix}, \ \ \textbf{units depend on element}$$

$\left[G_T\right]$ = **7 × 7 noise vector effect matrix,**

$$\begin{bmatrix} 0 & 0 & 0 & 0 & 0 & 0 & 0 \\ & & & & & & 0 \\ & [0] & & [0] & & 0 \\ & & & & & & 0 \\ & & & & & & 0 \\ & [I] & & [0] & & 0 \\ & & & & & & 0 \end{bmatrix}, \ \ \textbf{dimensionless}$$

ξ = seven-dimensional vector, $\begin{bmatrix} -V_S & 0 & 0 & 0 & 0 & 0 & 0 \end{bmatrix}'$, m/s

$\begin{bmatrix} \Omega \end{bmatrix}$ = 3 × 3 dyadic matrix of LOS rate vector elements, $\begin{bmatrix} 0 & \omega_M & -\omega_L \\ -\omega_M & 0 & \omega_S \\ \omega_L & -\omega_S & 0 \end{bmatrix}$, s^{-1}

$\begin{bmatrix} I \end{bmatrix}$ = 3 × 3 identity matrix, dimensionless

$\begin{bmatrix} 0 \end{bmatrix}$ = 3 × 3 null matrix, dimensionless.

$[F_T]$ is interpreted as a state transition matrix, which defines the dynamics of a given state. $[G_T]$ is a matrix that defines how the noise vector effects the dynamics of the overall state.

The sensor inputs for the target consist of the laser range and the synthetic measurements of relative target velocity. The observation equations for the target are given by

$$Z_1^T = X_S^T + K_S^T, \qquad \text{m} \tag{6-44}$$

where

Z_1^T = laser range, m

K_S^T = S-component of white measurement noise, m

and

$$\mathbf{Z_2^T} = \hat{R}\begin{bmatrix} -\omega_L \\ \omega_M \end{bmatrix} = \begin{bmatrix} V_L^T \\ V_M^T \end{bmatrix} - \begin{bmatrix} V_L \\ V_M \end{bmatrix} + \begin{bmatrix} K_L^T \\ K_M^T \end{bmatrix}, \qquad \text{m / s} \tag{6-45}$$

where

$\mathbf{Z_2^T}$ = two-dimensional relative target velocity vector, m/s

$\hat{R}$ = range estimate along S-axis, m

K_L^T = L-component of white measurement noise, m/s

K_M^T = M-component of white measurement noise, m/s.

The relative target velocity vector $\mathbf{Z_2^T}$ is a synthetic measurement made up of the range estimate $\hat{R}$ and the LOS rates ω_L and ω_M measured by the Doppler radar perpendicular to the LOS. The measurements of ω_S, ω_L, and ω_M are considered to be exact and will eventually be used in matrices to represent the filter as a discrete time model for digital computation. However, the angular rates multiplied by an estimate of the LOS range are viewed as noisy observations of target velocity.

If the angular rates are assumed to be perfect, the order of the tracking filter can be reduced by eliminating velocities and accelerations perpendicular to the LOS from the target estimation process. The latter can be expressed in terms of angular rates, angular accelerations, and estimates of range, helicopter velocity, and acceleration as follows:

$$V_L^T = \hat{V}_L + \hat{R}\omega_M, \quad \text{m/s} \tag{6-46}$$

$$V_M^T = \hat{V}_M + \hat{R}\omega_L, \quad \text{m/s} \tag{6-47}$$

$$A_L^T = \hat{R}(\dot{\omega}_M + \omega_S\omega_L) + 2\dot{R}\omega_M + \hat{A}_L, \quad \text{m/s}^2 \tag{6-48}$$

$$A_M^T = -\hat{R}(\dot{\omega}_L - \omega_S \omega_M) - 2\dot{R}\omega_L + \hat{A}_M, \ \mathbf{m/s^2} \tag{6-49}$$

where

$\hat{V}_L$ = estimate of L-component of helicopter velocity, m/s

$\hat{V}_M$ = estimate of M-component of helicopter velocity, m/s

$\hat{A}_L$ = estimate of L-component of helicopter acceleration, m/s²

$\hat{A}_M$ = estimate of M-component of helicopter acceleration, m/s².

Essentially, only R, $\dot{R}$, and A_S^T must be estimated; the other states can be found from Eqs. 6-46 through 6-49. The number of states reduces to three, and the plant model may be written as

$$\frac{d}{dt}\begin{bmatrix} R \\ \dot{R} \\ A_S^T \end{bmatrix} = \begin{bmatrix} 0 & 1 & 0 \\ \omega_L^2 + \omega_M^2 & 0 & 1 \\ 0 & 0 & -\Gamma \end{bmatrix}\begin{bmatrix} R \\ \dot{R} \\ A_S^T \end{bmatrix} + \begin{bmatrix} 0 \\ 0 \\ W_S \end{bmatrix} - \begin{bmatrix} 0 \\ \hat{A}_S \\ 0 \end{bmatrix}, \ \begin{bmatrix} \mathbf{m/s} \\ \mathbf{m/s^2} \\ \mathbf{m/s^3} \end{bmatrix} \tag{6-50}$$

where

$\hat{A}_S$ = estimate of S-component of helicopter acceleration, m/s².

Although this design might have advantages due to a reduced computer size and computation time, the three-state filter requires differentiation of the LOS rate measurements. Consequently the estimates are sensitive to small levels of noise in these measurements.

6-3.2.2.3 Prediction

In the filter studies described in subpar. 6-3.2.2.2, the designer used target state estimates in a simulation to predict future target position. The availability of target acceleration estimates permitted use of a nonlinear prediction. To access filter performance, the predicted position for an arbitrary projectile TOF could be compared to the actual target position advanced by the TOF. Although the simulation indicated that the seven-state filter performed better than the three-state filter for the errors presumed in the sensor data and the maneuvering target data, the developer was forced to settle on the three-state filter and the linear prediction due to the constraint of processing time. The estimates of acceleration components were not used, even though estimates of the acceleration were provided by the filter. The three-state filter and linear prediction impacted favorably on computer capacity and could be implemented since the specification required that the software consider only constant-velocity targets.

The standard computational procedure used to generate the predicted linear position of the target in an earth-referenced frame is to multiply target velocity by projectile TOF to obtain the predicted position. Conversion of this linear segment, i.e., vector length from current target position to predicted target position, to angles measured with respect to the sight line provides the two components of the kinematic lead angle. The kinematic and ballistic lead angles are usually derived separately; the latter uses the predicted position as a reference for calculation. However, in the Apache implementation the ballistic lead angle equations have been modified to include a linear compensation term for target motion. Therefore, the expressions for b_L and b_M found in Eq. 6-37 of subpar. 6-3.2.2.1 (ballistics model) include compensation for both target motion and trajectory curvature and are representative of the total lead angle. The expression for the TOF of the ballistic model also includes the prediction term to assure that the TOF is taken at the future, not the present, target position.

In subsequent studies undertaken to update Apache software to meet the air-to-air mission requirements, nonlinear prediction techniques were investigated that considered the availability of target acceleration estimates from the seven-state filter. Second-order prediction has also been employed by using the Taylor expansion:

$$\mathbf{X}_p = \mathbf{X}(t_0 + \Delta t) = \mathbf{X}(t_0 + t_f), \ \ \mathbf{m}$$

$$\cong \mathbf{X}(t_0) + \frac{d\mathbf{X}(t_0)}{dt}t_f + \frac{d^2\mathbf{X}(t_0)}{dt^2}\frac{t_f^2}{2}, \ \ \mathbf{m}$$

(6-51)

where

$\mathbf{X}(\cdots)$ = target range vector function, m
$\mathbf{X}_p$ = predicted target range vector one TOF into future, m
t = time, s
t_0 = time at which prediction is made, s
t_f = TOF of bullet, s
Δt = time interval, s.

Making use of the filter plant equations to predict target position during the projectile TOF has also been considered. However, studies have not progressed to the point at which the value of nonlinear prediction in the air-to-air application has been adequately tested. The filter settling time and noise in the acceleration estimates are major obstacles.

6-3.2.3 Error Budget

Once a system concept(s) is established with the potential to satisfy the performance requirements, it becomes a matter of evaluating its potential through analysis. Of particular interest is the tolerance permitted in the performance of each of the subsystems or components. The usual method used to establish these tolerances involves the generation and use of an error budget. The error budget provides the designer with the means to relate the tolerances for each of the subsystems or components to the tolerance allowable for the entire system.

Subpar. 6-3.2.1 describes the approach taken to establish the allowable total error tolerance of the Apache fire control system. The general error analysis by which the system component errors can be related to the total system error is described in subpars. 4-4.3.1 and 4-4.3.2. For the Apache the designer simplified the error analysis significantly by introducing key assumptions. For example, it was assumed that the sight line always remains on the target center while tracking. This assumption was based upon the premise that the video autotracker, incorporated in the sight sensor, would stay on the target after initial manual acquisition and subsequent lock-on. This assumption is critical to the satisfactory delivery of the Hellfire missile and is considered to be equally applicable for the ballistic weapon.

This target centering assumption eliminates the error and error rate in the track variables found in the usual fire control analysis; it also eliminates the need to deal with the correlation between them. This assumption provides error relationships that are algebraic rather than error relationships that need to be expressed by differential equations. Usually an error analysis is conducted over several representative scenarios, and the error budget considers the variations in error sensitivities. For the Apache the error budget was based upon sensitivities at a few encounter ranges where the weapon system and target were considered to be stationary. This approach was justifiable to a certain extent because dynamic models of subsystem performance were unavailable.

Table 6-16 lists all expected significant error sources associated with each Apache subsystem. In this case the Apache is hovering out of ground effects (HOGE) where the reflection from the earth of rotor downwash does not affect the fire control sensors. Estimates of the 1σ, i.e., one standard deviation, values for the azimuth and elevation are given for three different ranges. The design engineer must determine the relationship between the output errors of each component and its corresponding effect on the pointing error, as indicated in Table 6-16. Also the designer must remember that to a large extent subsystem performance is highly dependent upon flight and gunfire environments. The mean value of each of the errors shown in this table is assumed to be zero for a statistically representative ensemble of components. The tabulated values reflect the tolerance levels considered attainable and acceptable and were provided to the manufacturer as a specification.

TABLE 6-16.   SAMPLE GUNFIRE ERROR BUDGET (Ref. 24)

	ERROR BUDGET 1σ VALUE	1000 m 1σ CONTRI-BUTION, mil		2000 m 1σ CONTRI-BUTION, mil		3000 m 1σ CONTRI-BUTION, mil	
		AZ*	EL*	AZ	EL	AZ	EL
TADS LOS to Digital	0.7 mil	0.7	0.7	0.7	0.7	0.7	0.7
TADS Internal	0.1 mil	0.1	0.1	0.1	0.1	0.1	0.1
LOS D/A Conversion	0.56 mil	0.56	0.56	0.56	0.56	0.56	0.56
LOS Time Delays	10.2 ms	0	0	0	0	0	0
Gun Servo Lag or Overshoot	3.0 mil	3.0	3.0	3.0	3.0	3.0	3.0
Gun Turret Resolver	0.29 mil	0.29	0.29	0.29	0.29	0.29	0.29
Muzzle Velocity Sensor	2.3 m/s	0.11	0.11	0.11	0.23	0.11	0.58
Round-to-Round Muzzle Velocity	6 m/s	0.30	0.30	0.30	0.82	0.30	1.67
HARS Verticality	0.25 deg	0.09	0.01	0.38	0.05	1.00	0.37
Range Finder	5 m	0	0.14	0	0.33	0	0.60
Velocity Estimate (Mixed Velocity)	1.0 m/s	0.1	0.1	0.2	0.2	0.3	0.3
Manual Tracking Error	1.0 mil	1.0	1.0	1.0	1.0	1.0	1.0
Static Bending Calculation Error	0.1 mil	0.1	0.1	0.1	0.1	0.1	0.1
Vibration	0.5 mil	0.5	0.5	0.5	0.5	0.5	0.5
Rate Gyro	0.01 deg/s	0.36	0.36	1.03	1.03	2.07	2.07
Gun Turret Mechanical Tolerance	0.5 mil	0.5	0.5	0.5	0.5	0.5	0.5
Boresight TADS to Reference	0.58 mil	0.58	0.58	0.58	0.58	0.58	0.58
Boresight Gun to Reference	0.58 mil	0.58	0.58	0.58	0.58	0.58	0.58
Ballistics Fit	AZ: 0.12 mil EL: 0.47 mil	0.12	0.47	0.12	0.47	0.12	0.47
Time of Flight	0.043 s	0.58	0.31	0.03	0.39	0.04	0.52
Calculations	0.5 mil	0.5	0.5	0.5	0.5	0.5	0.5
Temperature Sensor	0.5 deg C	0.1	0.1	0.1	0.1	0.1	0.1
Pressure Sensor	69 Pa	0.1	0.1	0.1	0.5	0.1	1.0
Air Data Sensor	1.5 m/s	0.1	0.1	0.5	0.5	2.5	2.5
Doppler Velocity	0.1 m/s	0.1	0.1	0.1	0.1	0.1	0.1
Root-Sum-Square 1σ Error		3.6	3.6	3.74	3.89	4.91	5.30

*AZ = azimuth   EL = elevation

It was anticipated that hardware testing would be conducted to assure conformance with these specifications. Full validation of subsystem performance, however, was not practical due to the influence of flight and gunfire environments. In addition, since only one or two aircraft were instrumented and tested, only one or two samples of each subsystem could be tested under flight conditions.

The design engineer was confident that the system accuracy requirements would be met if the tolerances could be maintained. The influence that each error has on overall system accuracy depends upon the specific aircraft/target scenario under which the engagement takes place. This sensitivity of the total pointing error to each individual error source at the point of engagement was used to evaluate the individual error components. The total pointing error was based on a root-sum-square (rss) analysis. In an rss analysis each individual error must be translated into its corresponding mil units, e.g., a 0.5-deg C error in air temperature produces a 0.1-mil pointing error.

Once the overall Apache fire control system was established, a final version of the pertinent error sources was generated. Once again, the sensitivity of the gun pointing errors to the error sources was obtained by using the ballistic prediction models discussed in subpar. 6-3.2.2. The partial derivative of the lead angle expressions in Eq. 6-37 taken with respect to each error source and when evaluated under engagement conditions provided all of the sensitivities of interest except those due to sight line pointing. The sensitivities of gun pointing and sight line pointing are identical because the gun commands are computed as the sum of sight angle and lead angle. Since the lead angle expressions are dependent on the TOF, the expression for the projectile TOF discussed in subpar. 6-3.2.2 is also involved. Rather than analytically differentiating the lead angle expressions and evaluating them at engagement points of interest, the partial differentiation was approximated by perturbing the input variables around their nominal values one at a time and observing their effect on the lead angles.

The assumed error values of the various components are based upon the knowledge and experience of the design team. Various combinations of the error values can be considered as long as the statistical sum meets the overall system requirements. Generally, there are a few components whose errors predominate the error budget. Special efforts should be made by the design engineer to ensure that the errors of these components are reduced to the level of the remaining components or at least to a minimum level that provides an overall error consistent with system specifications. Obviously, the design concept must be chosen to ensure that the attainable overall system error is consistent with system specifications.

If the error analysis is to be applicable to production weapon systems, the values of the error sources must reflect performance over the component ensemble as well as over time. The tolerance specifications for each subsystem and component therefore need to be well defined and provided to the manufacturers.

In the Apache system the gun turret, airframe flexure, airspeed, and muzzle velocity error sources were among the most difficult to manage. Error sources considered to be beyond the control of the fire control designer are muzzle velocity effects peculiar to Government-furnished ammunition, flight controls critical to fixed weapon pointing, and navigational subsystem outputs that were optimized for functions other than fire control.

6-3.3 SYSTEM MECHANIZATION

After the fire control system concept was established, the prime contractor sought industry participation in the development of major subsystems. Specific performance requirements for each subsystem were generated based on the error budget. These requirements provided the basis for subcontractor proposals and subsequent hardware development subcontracts. The prime contractor performed the function of system integration. Chief among the subsystems planned for subcontract development were the TADS, the fire control computer (FCC), and the turret and turret control system (TCS).

The Army, however, assumed responsibility for development of the TADS, which was to be accomplished under a separate competitive contract and delivered to the prime contractor as Government-furnished equipment (GFE) for system integration. The prime contractor provided specifications to the Army for inclusion in the TADS. The Army evaluated the initial industry proposals and awarded two development contracts for TADS. After evaluation of prototypes, the production contractor was selected.

In addition to TADS, the Hellfire missile and missile launchers, the 30-mm ammunition and gun, and the 70-mm (2.75-in.) rockets and rocket launchers were provided as GFE. Subcontracts were also let be-

tween industry and the prime contractor to furnish an air data system (ADS) and an IHADSS. Software was developed by the prime contractor in accordance with the design concept and functional needs. Such software was verified by modeling and analysis and integrated into the FCC with the support of the FCC developer.

6-3.3.1 System Description

An appreciation of the interaction of the various fire control elements can best be obtained by review of the functional concept block diagram established for the 30-mm gun, as shown in Fig. 6-23. The concept for the rocket, which differs little from that for the gun, is also included following the discussion of the gun. The Hellfire delivery is independent of most of the fire control elements. Only the acquisition, track, and laser designation functions provided by TADS are required to support missile guidance.
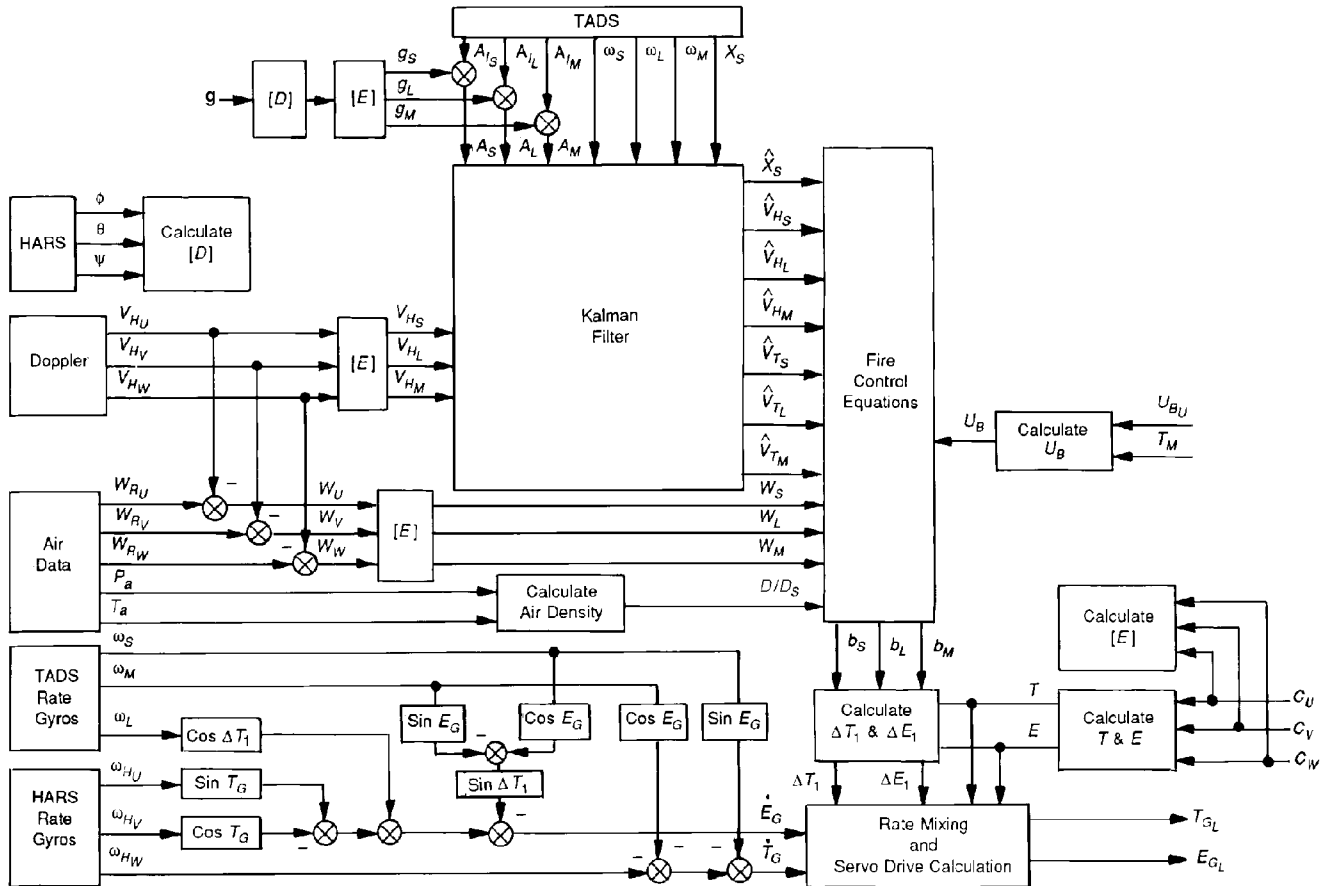
Figure 6-23. Functional Concept Diagram of Fire Control System for 30-mm Gun (Ref. 24)

Fig. 6-23 is discussed on an input-output basis, as described in Chapter 1. Since there is no fuze-setting requirement for the 30-mm projectile, the sole outputs of the subsystem to the turret servo system of the gun are the azimuth and elevation angles, T_{G_L} and E_{G_L}. All subsystem inputs are automatically provided by targeting and navigational sensors. Navigational sensor data are in the form of aircraft pitch, roll, and yaw angles (ϕ, θ, and ψ) and the corresponding angular rates ω_{HU}, ω_{HV}, and ω_{HW} provided by the HARS. The UVW orthogonal coordinate system is shown in Fig. 6-24. U points along the longitudinal axis of the helicopter, V is breadthwise and perpendicular to U and positive to the right side of the helicopter, and W is orthogonal to U and V and is positive down relative to the helicopter. For completeness, the SLM axes of the TADS LOS and the XYZ earth axes are also shown. Helicopter ground speed components in the aircraft UVW reference frame V_{HU}, V_{HV}, V_{HW} are provided by the Doppler radar. Helicopter airspeed components in the aircraft UVW reference frame W_{RU}, W_{RV}, W_{RW}, air pressure P_a, and temperature T_a come from the air data sensor package. Sight line angular rates expressed in the sight reference frame

ω_S, ω_M, ω_L are measured by the TADS rate-integrating gyros. Helicopter linear accelerations A_{I_S}, A_{I_L}, A_{I_M} are sensed by a triad of accelerometers mounted on the TADS stable platform. Sight line direction cosines relative to the aircraft coordinate frame C_U, C_V, C_W are supplied by TADS resolvers.
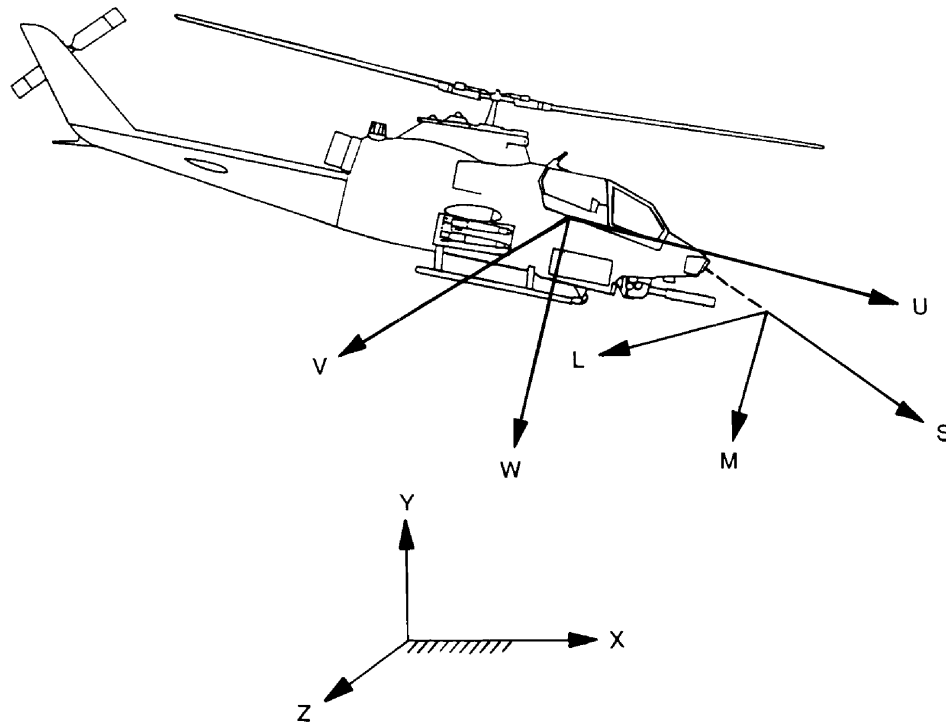
Figure 6-24. UVW Helicopter Coordinate System, SLM Sight Coordinate System, and XYZ Earth-Based Inertial Coordinate System

In order to transform data measured in the earth reference frame (XYZ) to the helicopter reference frame (UVW), the coordinate transformation [D] is generated from HARS roll, pitch, and yaw angles. To transform data expressed in the aircraft set (UVW) to the sight set (SLM), the coordinate transformation [E] is generated from the sight resolver direction cosines. Both the [D] and [E] transformations are applied to the components of **g** in the earth reference set (Note that $g_x = 0$, $g_y = 0$, and $g_z = g$.) to provide their values in the sight set (g_S, g_L, g_M); TADS accelerometer measurements in the sight coordinate system minus the g-components provide the Kalman filter kinematic helicopter accelerations (A_S, A_L, A_M). TADS sight line angular rates and range X_S, as measured by the gyro triad and the LRF in the sight set, are fed directly into the filter. Doppler data are also transformed to the sight coordinates V_{H_S}, V_{H_L}, V_{H_M} before filter processing.

As mentioned in the discussion of the Kalman filter model, component estimates of helicopter velocity $\hat{V}_{H_S}, \hat{V}_{H_L}, \hat{V}_{H_M}$, target velocity $\hat{V}_{T_S}, \hat{V}_{T_L}, \hat{V}_{T_M}$, and range $\hat{X}_S$ are generated for inputs to the fire control equations. The air data sensor with its own filter supplies wind, air pressure, and temperature data directly to the fire control equations. The [E] transformation is used to convert the wind and also the difference between the helicopter airspeed and the ground speed W_U, W_V, W_W from the aircraft coordinates to the sight coordinates W_S, W_L, W_M. The air pressure and temperature are used to calculate the local air density relative to that at standard conditions (D/D_S).

The muzzle velocity U_B is also an input to the fire control equation. U_B is determined from standard values of muzzle velocity for a given type of ammunition U_{B_U} and from propellant temperature T_M. Initial plans called for inclusion of a muzzle velocity measurement sensor in order to measure muzzle velocity variations. Unfortunately, difficulties in the development of such a sensor led to its elimination from the system design.

The fire control equations, as discussed in the ballistic equation model, are solved to provide the direction cosines of the total lead angle in the SLM reference frame b_S, b_L, b_M. (The direction cosine b_S can

be derived from the relationship $b_S{}^2 = 1 - b_L{}^2 - b_M{}^2$.) These are added to the sight line azimuth and elevation angles T and E to obtain the azimuth and elevation lead angle corrections ΔT_1 and ΔE_1. These are referenced to the aircraft coordinates as might be expected since both the sight and gun are driven from this reference.

Along with ΔT_1, ΔE_1, T, and E, $\dot{E}_G$ and $\dot{T}_G$ are used by the rate mixing and servo drive calculation functional block in Fig. 6-23 to compute the traverse and elevation commands T_{G_L} and E_{G_L} to the gun servo. $\dot{E}_G$ and $\dot{T}_G$ are feed-forward terms that have been generated from TADS and HARS rate gyro outputs to compensate for the gun servo lags. The functional flow that produces $\dot{E}_G$ and $\dot{T}_G$ is a representation of equations that express these terms as the difference between TADS and HARS rate components around the turret elevation and traverse axes and by the values of ΔT_1, E_G, and T_G where T_G and E_G are the traverse and elevation angles of the gun turret, respectively. This computation is actually a measure of the sight line rate with respect to the airframe coordinates and an approximation to the desired measure of gun rate, since the time rate of change of lead is not considered to be significant.

Although this functional concept pertains to the deployment of the 30-mm gun, it also expresses the concept of rocket delivery with one major difference. Since the rocket launchers are gimballed only in elevation, no azimuth command is applied to the launcher servo. After additional processing the transverse signal is applied to the IHADSS display where the pilot acts as the servo to point the aircraft (and launcher) in the desired azimuth direction.

6-3.3.2 Subsystem Major Component Description

This subparagraph presents descriptions of the major subsystem components implemented in the fire control solution. Also included are references of their contribution to the error budget.

6-3.3.2.1 TADS Description

The AH-64 TADS is used to detect, recognize, and track targets. Fig. 6-25 provides illustration of how the TADS is physically integrated into the Apache. The target image sensor system consists of direct view optics (DVO), a daytime video (DTV) camera, a pilot night vision system (PNVS), and a FLIR image sensor. The TADS also contains a laser transmitter and receiver system capable of measuring target range, designating a target for another tracker, and detecting the location of a laser spot provided by another laser target designator.

These devices are mounted on an inertially stabilized platform that is attached to the inner gimbal of a

Figure 6-25. TADS Component Locations

four-degree-of-freedom gimbal system. The inner gimbal platform is stabilized with respect to a LOS defined in the inertial reference system. The pointing angle of the TADS inertial platform LOS is controlled by an input signal to the rate-integrating gyros (RIG) attached to the inner platform. There is one RIG for the yaw axis of the inner platform and one RIG for the pitch axis. The displacement of the RIG output axis from its reference position causes a voltage to be generated that drives the torque amplifiers of the servo drives of the yaw and pitch inner gimbals. The outer azimuth and elevation gimbals are driven by servo motors so that a maximum clearance of two degrees is maintained between the yaw and azimuth gimbals, and between the pitch and elevation gimbals. The various electronic units (EU) that interface with TADS are also shown in Fig. 6-25.

The images presented to the DVO eyepiece and the DTV and FLIR sensors are transmitted through a system of interchangeable lenses. These lenses allow the operator to see the scene at several different magnifications and thus control the FOVs. The particular magnification achieved depends on how the scene is displayed to the operator. When viewing the scene using the DVO, the CPG uses the head-down display on the optical relay tube (ORT), and the magnifications are referenced to this viewing position. The WFOV DVO subtends an angle of 18 deg and allows the CPG to view objects at 3.5-power magnification, whereas the NFOV DVO subtends an angle of 4 deg with 16-power magnification. The WFOV DTV subtends 4.0 deg with about 13.5-power magnification, and the NFOV DTV subtends 0.9 deg with 60-power magnification (Both of these magnifications are referenced to the head-down display.). The scene presented by the FLIR subtends 50 deg with 1-power magnification (using IHADSS) for the WFOV, 10 deg with 5.3-power magnification for the medium field of view (MFOV), and 3.1 deg with a 17-power magnification for the NFOV. The latter two magnifications are referenced to the head-down display.

An essential element of successful target engagements is correct operation of the TADS pointing angle control using one of three modes: the manual mode, the external command mode, and the image automatic tracking (IAT) mode. Fig. 6-26 is a block diagram showing how the three pointing command modes are modeled in the pitch axis of the TADS. (Operation of the yaw axis of the TADS is modeled essentially the same way.) This figure illustrates that each of the command modes outputs a line of sight rate command $\dot{\phi}_{TC}$ to the TADS servo. The TADS servo in turn outputs the pitch angle ϕ, which is used as a feedback for the system. ϕ is subtracted from the line of sight pitch angle ϕ_{LOS} and thereby creates an offset in the pitch angle ε_ϕ. A TADS simulation was programmed to include the three control modes and the dynamics of the TADS LOS stabilized gimbal system. This simulation is driven by data from engagement scenario files, which contain aircraft and target variables for various combat situations. This simulation was developed from functional and mathematical models that specify the IAT and TADS data processing logics. The operation of the three TADS LOS control modes and explanations of how they are modeled
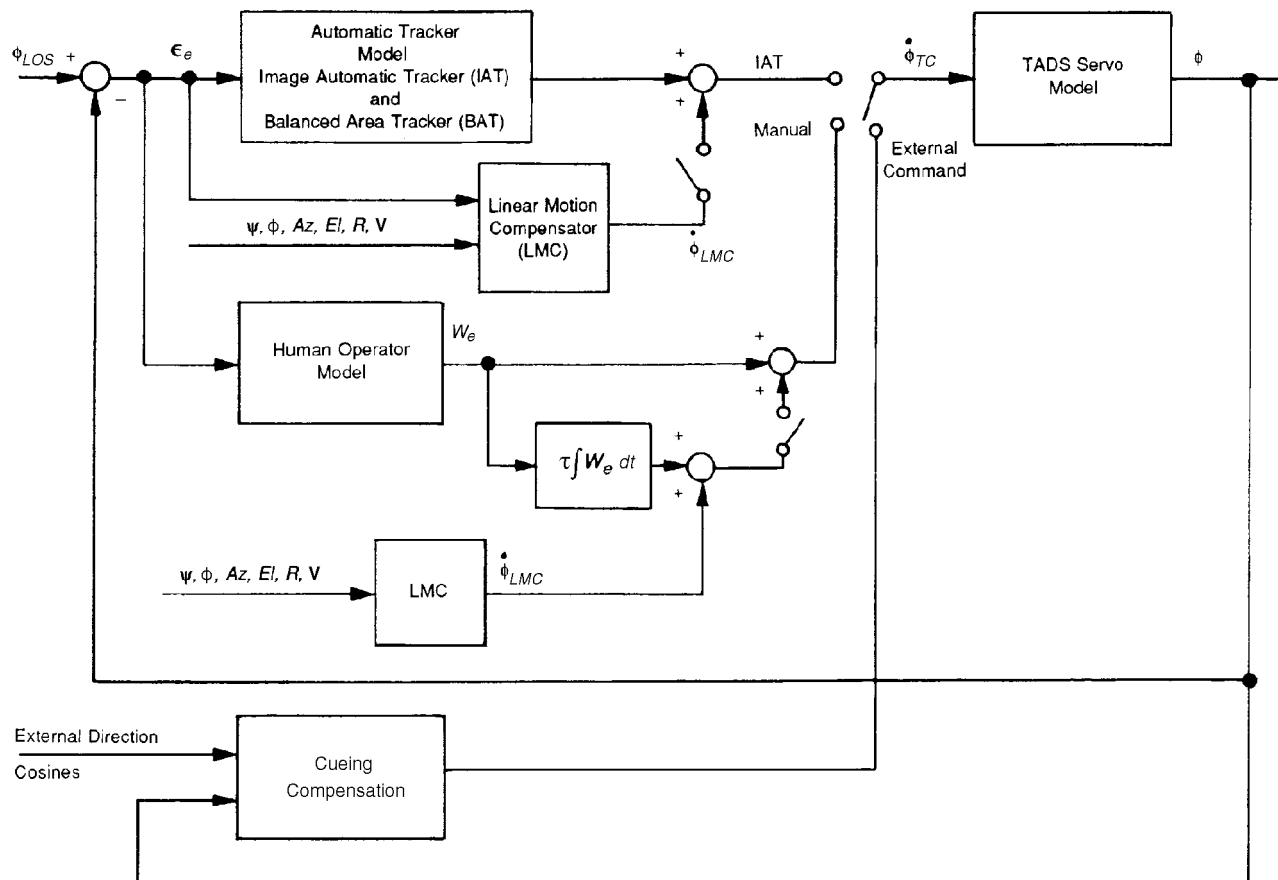
Figure 6-26. TADS Pitch Axis Simulation (Ref. 24)

in the TADS simulation are described in the following subparagraphs, in which each mode refers to Fig. 6-26.

6-3.3.2.1.1   Manual Tracking

Manual tracking allows the CPG to control the TADS LOS using a two-degree-of-freedom thumb force controller located on the right-hand grip of the ORT.   The slew direction is determined by the direction in which the operator applies force to the thumb controller, and the slew rate is determined by the amount of force applied. Manual commands from the thumb controller are translated into the LOS co-ordinate system. The manual tracker is designed to assist in maintaining visual and manual coordination by relating the tracking rate to the selected optical magnification.

The manual control mode outputs pitch and yaw rate commands to the TADS servo mechanism in re-sponse to commands from the thumb force controller and the linear motion compensator (LMC). These inputs are combined according to the following relationship:

$$\dot{\phi}_{TC} = W_e + \tau J \int W_e \, dt + J\dot{\phi}_{LMC}, \ \ \textbf{rad/s}$$

$$\dot{\psi}_{TC} = W_f + \tau J \int W_f dt + J\dot{\psi}_{LMC}, \ \ \textbf{rad/s}$$

(6-52)

where

$\dot{\phi}_{TC}$ = pitch rate command to the TADS servo, rad/s

$\dot{\psi}_{TC}$ = yaw rate command to the TADS servo, rad/s

J = control logic constant = $\left\{ \begin{array}{l} \textbf{0, LMC not active} \\ \textbf{1, LMC active} \end{array} \right\}$, dimensionless

τ = time constant, 0.5, s

W_e = pitch rate resulting from thumb controller, rad/s

W_f = yaw rate resulting from thumb controller, rad/s

$\dot{\phi}_{LMC}$ = pitch rate generated by LMC, rad/s

$\dot{\psi}_{LMC}$ = yaw rate generated by LMC, rad/s.

The purpose the LMC is to compute the pitch and yaw rate commands required to compensate for the tracking (manual and automatic) geometry changes due to aircraft velocity. Inputs to LMC include (1) the four gimballed angles of the TADS ϕ, ψ, Az, and El corresponding to pitch, yaw, azimuth, and eleva-tion, respectively, (2) the target range R, (3) the helicopter velocity vector $\mathbf{V}$, and (4) the pitch and yaw IAT offsets ε_e and ε_f. In the manual mode an integral of the input signal is added to the output command signal when the LMC is active. With the assumption that the target is stationary, the LOS rate is derived from the motion of the helicopter relative to the ground. The equations used in the LMC follow:

$$\begin{bmatrix} \dot{R} \\ V_e \\ V_f \end{bmatrix} = \begin{bmatrix} T_\phi \end{bmatrix} \begin{bmatrix} T_\psi \end{bmatrix} \begin{bmatrix} T_E \end{bmatrix} \begin{bmatrix} T_A \end{bmatrix} \mathbf{V}_B^0, \ \ \textbf{m/s}$$

(6-53)

$$\dot{\theta}_{LMC} = \frac{(- V_f + \dot{R}\varepsilon_e G)}{\hat{R}}, \ \ \textbf{rad/s}$$

$$\dot{\psi}_{LMC} = \frac{(- V_e + \dot{R}\varepsilon_f G)}{\hat{R}}, \ \ \textbf{rad/s}$$

where

$\begin{bmatrix} T_\phi \end{bmatrix}, \begin{bmatrix} T_\psi \end{bmatrix}, \begin{bmatrix} T_E \end{bmatrix}, \begin{bmatrix} T_A \end{bmatrix}$ = three-dimensional Euler transformation matrices about the ϕ, ψ, El, and Az axes of the TADS gimbals, dimensionless

$\dot{R}, V_e, V_f$ = velocity components of aircraft relative to the target expressed in inner platform coordinates, m/s

$\mathbf{V}_B^0$ = three-dimensional helicopter vector in body coordinates, m/s

$\varepsilon_e, \varepsilon_f$ = pitch and yaw IAT errors, rad

$$G = \text{control logic constant} = \left\{ \begin{array}{ll} 0, & \text{GOODTRACK not active} \\ 1, & \text{GOODTRACK active} \end{array} \right\}, \text{dimension-less.}$$

The first line of Eq. 6-53 transforms the velocity vector of the helicopter from the body coordinate system to the LOS coordinate system. The second and third equations calculate the pitch and yaw rate commands of the LMC.

6-3.3.2.1.2 External Command Mode

In the external command mode the TADS LOS orientation relative to the helicopter body axis is controlled by commands coming from other sensors, prestored target locations or other helicopter systems. As seen in Fig. 6-26, the commanded LOS is used in the form of direction cosines relative to the fixed axis coordinate system of the helicopter. The commanded LOS is compared with the existing TADS LOS, and a rate command to the TADS servo is generated, which causes the TADS LOS to be aligned with the commanded LOS.

For the IHADSS on the AH-64, direction cosines of the pilot or CPG helmet LOS relative to the fixed axis coordinate system of the helicopter are generated. In the external command mode the LOS of the TADS can be slaved to the IHADSS line of sight. This mode is useful for commanding the TADS LOS to point quickly in the direction of the target.

The helmet display unit (HDU) in the IHADSS can display the video output of the TADS target sensors—DTV and FLIR—in the operator's helmet. If the IHADSS and the TADS boresighting have been properly harmonized, the IHADSS can be used to point the TADS at targets. However, because of the instability of the human head in a maneuvering vehicle, the visual and manual coordination required to point the TADS accurately at a target is limited. This problem is amplified if the HDU displays the scenes using magnifications greater than 1 power. A small movement of the head can result in a large change in the scene displayed on the HDU and can cause the operator to become disoriented. For this reason the HDU is generally used for rough pointing at low magnification.

6-3.3.2.1.3 Image Automatic Tracker

The IAT mode uses target error information that is derived from processing within the TADS balanced area tracker (BAT). The BAT develops error signals proportional to the displacement of a target image from the center of the video or FLIR FOV. The BAT recognizes target images by comparing video levels in the video output to some predetermined threshold. Video intensity levels above this threshold are considered white, and video intensity levels below this threshold are considered black. A target is defined to be either white on a black background or black on a white background. A contiguous collection of target pixels defines an image for the automatic tracker. Having defined a target image, the BAT defines a rectangle by determining the locations of its extreme upper, lower, and side boundaries. This rectangle is referred to as the target image window, or the tracking window. The BAT derives the vertical and horizontal offsets of the centroid of the target image from the center of the field of view (CFOV) of the video data and outputs these data as the position offsets (ε_e and ε_f) to the TADS IAT.

The BAT processes one frame of video information every 1/60 s. At the end of each frame the BAT executive determines whether the tracker is in the track or cage mode. In the cage mode the IAT moves the tracking window to the CFOV, sets the tracking window size to its minimum, and sets the target position errors to zero. The cage mode is called by the other modes when certain error conditions are exceeded. In the track mode the BAT is either tracking a target or attempting to track a target.

The main criterion for remaining in the track mode is determining whether or not valid video has been detected within the tracking window of the last frame. Absence of valid video causes the BAT to break lock and then enter the search mode. In the search mode the tracking window size is expanded two lines vertically and two pixels horizontally each frame. If the maximum window size is exceeded, the cage function is called. During the search mode, the first frame in which valid video is found within the tracking

window causes the BAT to switch to the seize mode. In the seize mode the center of the tracking window is placed at the location of the valid video, and the tracking window is reduced to its minimum size. After three fields of valid video have been detected within the tracking window, the GOODTRACK flag is set, and the tracking window is expanded until the extreme upper, lower, and side boundaries of the valid video have been included. When the center of the tracking window is displaced from the CFOV, the BAT returns offset commands to the TADS automatic tracking controller.

The BAT continues to hold the valid video image of the target within the tracking gate by expanding or contracting as the target size changes and by commanding the TADS pointing angle by outputting the displacement of the center of the target from the CFOV. This process continues until valid video is lost or until impending break lock conditions are met. The impending break lock criteria are as follows:

1. The farthest edge of the target is within approximately 5% of the allowable good track displacement. The good track displacement limit is approximately 35% of the vertical FOV and 40% of the horizontal FOV.

2. The target height or width is greater than 45% of the FOV.

3. The target width is within three pixels of the minimum width for a good track; the minimum horizontal target size for a good track is 0.72% of the FOV.

4. The target height is within three video lines of the minimum height for a good track; the minimum vertical target size for a good track is 0.74% of the FOV.

5. The target contrast is within 5% of the good track threshold; the good track threshold is greater than 4.5% of the target to background contrast.

When valid video is lost, the break lock mode is entered. While in the break lock mode, the tracking window is expanded at a rate of two lines or pixels per video frame in search of valid target video. If valid video is not found after 1.2 s, the GOODTRACK flag is reset, and the cage mode is entered.

6-3.3.2.1.4 Laser Range Finder and Designator (LRF/D)

The TADS uses return pulses from a high-energy, 1.06-μm, Nd:YAG laser to determine target range. The laser transmits a narrow beam whose energy is concentrated in a very small divergence angle. Because the subtended angle of the transmitted laser beam is quite small, the beam must be aimed very accurately to obtain return pulses from the target. The CPG activates the laser range finder by engaging a trigger on the right side of the ORT. The first detent position of the LRF/D trigger sends a single laser pulse for ranging. The second detent sends a continuous stream of coded pulses for designation. The laser receiver calculates target range based on the reflection return times of the individual pulses.

6-3.3.2.2 Integrated Helmet and Display Sight System (IHADSS)

The IHADSS components are identified in the IHADSS system diagram shown in Fig. 6-27. The IHADSS consists of a single helmet with installed communications equipment (earphones and microphone), electronics and infrared (IR) sensors to establish the head-directed LOS, cables to interconnect with the aircraft installed equipment, and a CRT with optics to provide the pilot (P) or CPG display directly in front of the eyes. A deep-tinted spherical visor assembly is attached to the helmet and is shaped to allow use with the helmet-mounted display (HMD).

The sighting-related equipment consists of the following subcomponents: one sight electronics unit (SEU), four sensor survey units (SSU), two integrated helmet units (IHU), and two boresight reticle units (BRU). The display-related equipment consists of one display electronic unit (DEU), two display adjustment panels (DAPs), and two HMDs. For clarity only one DAP is shown in Fig. 6-27.

The interaction of IHADSS components can be best understood by reference to the IHADSS system diagram, Fig. 6-27. The IHU provides position information to the SEU, where the functions of the system are related either to sighting or to display. In the sight mode the operator is provided a track reticle, which can be maintained on the target by head/helmet rotation. The orientation of the helmet is monitored by two helicopter IR beam SSUs working in conjunction with helmet-mounted sensors. This position information is processed to establish the LOS of the operator (P or CPG) with respect to the aircraft armament datum line (ADL). The BRU and the boresighting equipment help to establish this IHADSS to ADL relationship. In the display mode the operator views video information as presented

for flight control and targeting, so the DEU processes all the video data for the HMD while the sight functions are processed in the SEU. Either the display or sight mode may be used in either cockpit, and the cockpits function independently of one another for IHADSS use. The SEU provides information from either the P or the CPG to the FCC.

Because of the operator's inability to control the pointing of the sight line to better than a few mils and an inherent inaccuracy of the sensor surveying the same magnitude, the primary use of the IHADSS is target acquisition and short-range gunfire.
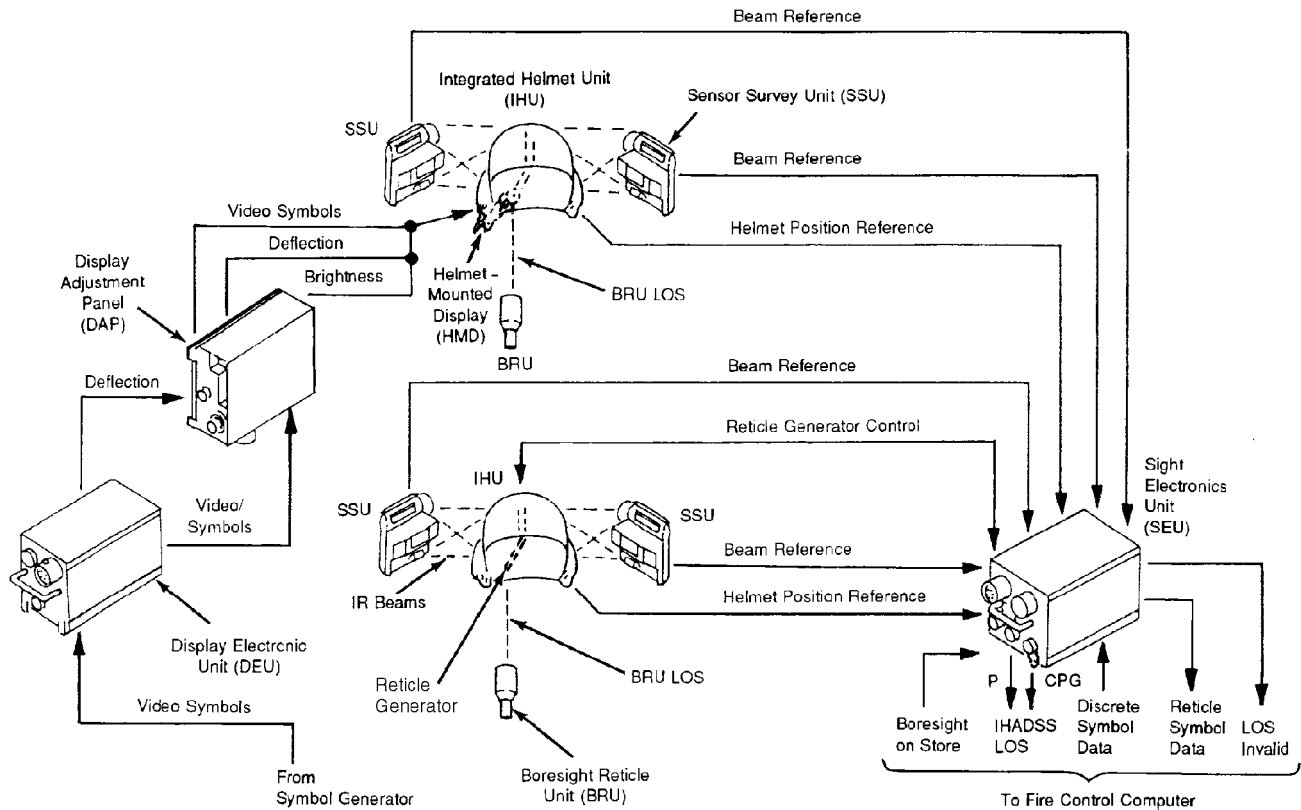
Figure 6-27. IHADSS System Diagram (Ref. 24)

6-3.3.2.3   Fire Control Computer

In the late 1970s a new avionic computer, the TDY-43, was developed. This computer used an architecture referred to as the microprogrammable emulation computer architecture (MECA). At that time it represented state-of-the-art computer architecture. The processor is microprogrammable with a set of 16 general registers. It uses medium-scale integration (MSI) and large-scale integration (LSI), bipolar, low-power Schottky components that are assembled into six hybrid packages. Microelectronics packaging skills were used to produce a reliable, high-performance processor that could satisfy minimal volume and weight constraints.

A summary of TDY-43 features is provided in Table 6-17. Table 6-18 provides a breakdown of the processing speed in terms of the FCC module as estimated during development. The computer top level flowchart is shown in Fig. 6-28. Samples of the computation performed in the FCC follow in terms of the descriptions of the gun processor module (GPM), gun ballistics module (GBM), and the rocket processor module. These module flowcharts are also included.

TABLE 6-17.   MECA COMPUTER FEATURES (Ref. 25)

TYPE
    General-purpose binary
    16, 24, or 32 bit parallel
    2's complement
    16 general registers
    Microprogrammed
    Instruction emulator
    Fixed and floating point

INSTRUCTIONS
    88 basic instructions (TDY-43)
    65k words addressable
       (expandable to 1M)
    Executive control

ADDRESS MODES
    Direct
    Indirect
    Immediate
    Relative
    Indexed (3 registers)
    Register/register
    Stack (LIFO*)

OPERANDS
    Single bit, byte, full word, double word
    32 or 48 bit floating point
    I/O registers

MICROPROGRAMMABLE
    1024 word ROM
    40 bit wide ROM
    Multifunctions per microcycle
    Microcode assembler
    Custom special instructions

HIGH PERFORMANCE
    636k instructions per second
    167-nanosecond microcycle
    Operates with 100 ns ROM
              300 ns RAM (CMOS)
              800 ns core (TDM-1S)

INSTRUCTION TIMES
(Memory Reference)
    <u>Add Instruction Times</u>
    1.625 μs fixed point
    2.531 μs double precision
    7.531 μs floating point

    <u>Multiplication Instruction Times</u>
     4.375 μs fixed point
    11.781 μs double precision
    12.531 μs floating point

INPUT/OUTPUT
    16 vectored interrupts, maskable, expandable
    Discretes, parallel
    Serial standards MIL-STD-1553A
    DMA† (8 channels)
    Analog hybrids

BUILT-IN TEST
    Power fail-safe
    Time-out indicator
    Wraparound I/O
    Microdiagnostics

*LIFO = last in, first out
†DMA = direct memory access

TABLE 6-18.   FCC REAL-TIME USE FOR WORST-CASE ANALYSIS (Ref. 25)

MODULE NAME	WORST-CASE REAL TIME, ms/s
Executive	28.9
Mux (multiplexer)	94.8
Preprocessor	13.7
Mode select	12.0
Waypoint target	4.0
Sight processor	29.4
Range processor	35.5
Missile processor	17.8
Rocket processor	53.5
Gun processor with ballistics	107.2
Keyboard	1.6
Display	67.5
Fault detection location system (FDLS)	5.2
Test	19.3
Miscellaneous (contingency for absolute worst case, mux errors, and DMA)	40.2
Total	530.6 ms/s
% Growth (% of real-time remaining)	46.9 %
% Reserve (% of current program time held in reserve)	88.5 %
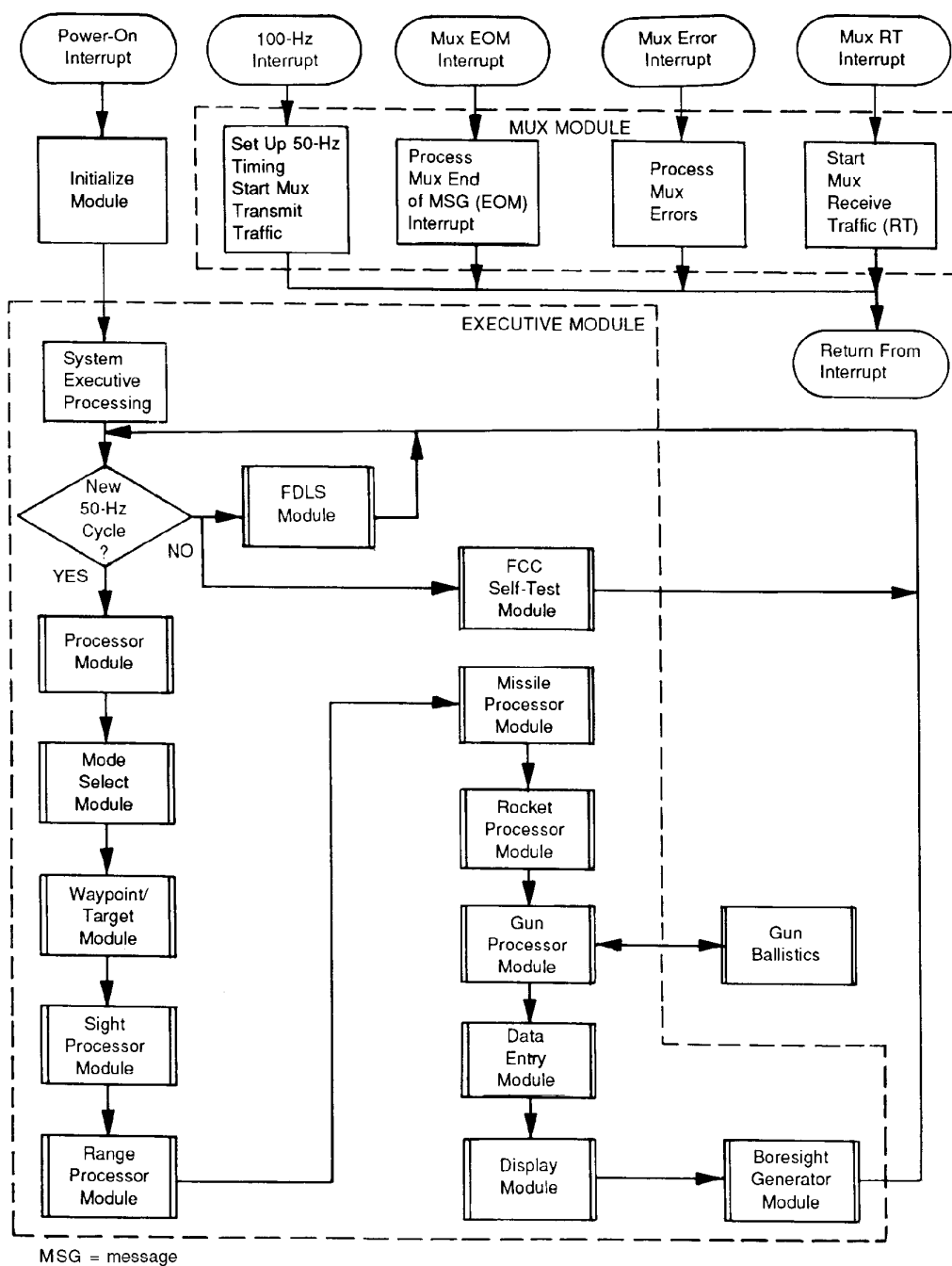
Figure 6-28. FCC Top Level Flowchart (Ref. 24)

6-3.3.2.3.1 Gun Processor Module (GPM)

The GPM provides all of the processing and control necessary for ballistically corrected 30-mm chain gunfire. This module selects and prepares the data required in the ballistic computations and processes the ballistic correction to provide positional control of the gun. The actual ballistic correction computations are performed by the GBM, which is a GPM subroutine. A flowchart of the GPM is shown in Fig. 6-29.
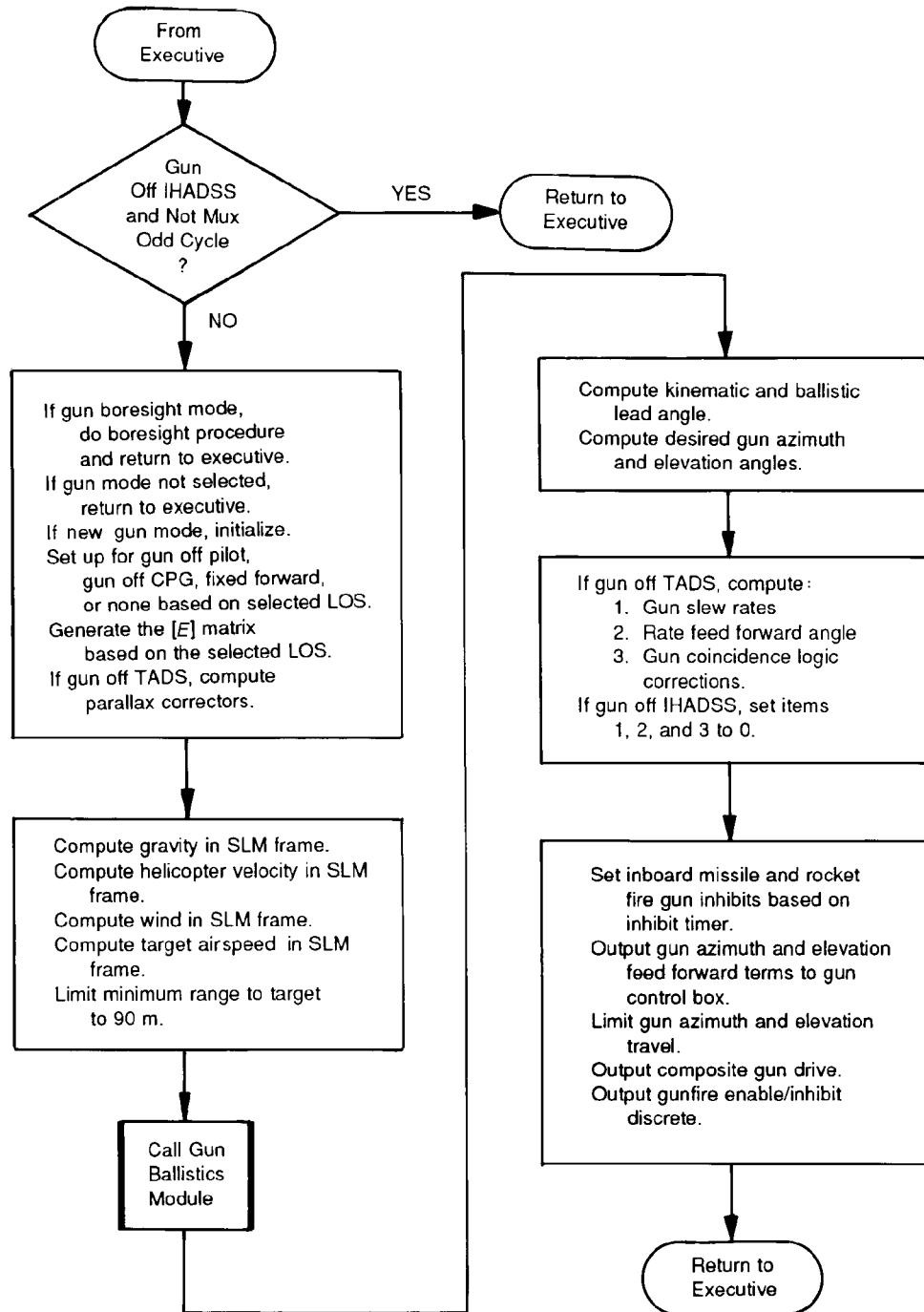
Figure 6-29. Gun Processer Module Flowchart (Ref. 24)

The GPM functions include control of the execution rate and gun processor mode, i.e., sight determination, LOS processing, ballistic computations, preparation and output of gun turret drive, and gunfire inhibit signals.

The GPM is executed at a 50-Hz rate when the LOS is TADS derived and at 25 Hz when either IHADSS derived or during boresighting of the gun. During boresight the GPM simply outputs the gun azimuth and elevation angles developed within the boresight generator module, resets the gun inhibit, and terminates gun processing. In normal operation the gun processor is reinitialized each time the gun is selected as a weapon in order to assure the fastest possible ballistic solution for each new scenario. Further gun processing is terminated if the gun has not been selected by either crew member.

The GPM determines which crew member has selected the gun and whether the fixed forward mode of gunfire has been selected. The LOS is used to generate the aircraft- (UVW) to-sight (SLM) reference coordinate frame conversion matrix [*E*]. Gravity is transformed to the aircraft reference frame and to the sight reference frame and then combined to determine air velocity. Additionally, when the TADS is chosen by the CPG, the resulting TADS and gun parallax is included in the ballistics corrections by the GBM.

Next the ballistic calculations are executed by a call to the GBM, in which a gun line direction cosine change to the LOS is computed in the sight reference frame and upon return to the GPM is transformed to azimuth and elevation angles in the helicopter reference frame.

Following the generation of the basic gun ballistics, the gun slew rates, the rate feed forward angles, and the gun incidence logic corrections are all calculated if the sight source is the TADS. If the LOS is provided by the IHADSS or the fixed forward position, the gun slew rates, the rate feed forward, and the gun coincidence logic corrections are zeroed.

The boresight corrections are computed next and are combined with the basic gun ballistics and gun slew rates to form the composite gun line azimuth and elevation command. The composite gun command is travel limited and outputted to the gun turret control unit. Also outputted are the rate feed forward angles. Based on gunfire lockout following a missile or rocket launch, the gunfire inhibit is computed and outputted to the gun control unit.

6-3.3.2.3.2 Gun Ballistics Module (GBM)

The GBM provides the basic ballistic correction for the 30-mm round, and its flowchart is shown in Fig. 6-30. The ballistic equations, basically those created by the Firing Tables Branch, Fire Control and Software Engineering Division, US Army Research, Development, and Engineering Center, are modified to include target motion compensation and sight to gun parallax corrections.

The GBM is called by the GPM if parallax corrections, gravity, aircraft velocity, and range have been preprocessed for use by the GBM. All computations within the GBM are made in the sight-referenced coordinate system, and the gun line direction cosines of this module are expressed with respect to the LOS. When the TADS and laser are used, target motion compensation is accomplished by generating range values for all three sight reference frame axes based on the TOF and the target velocity. When the TADS sight is not selected or when the range to target is not laser derived, the target is assumed to be stationary, and the range is fully applied along the LOS. The ballistic equations provide compensation for the effects of

     1. Range along the LOS
     2. Gravity
     3. Projectile velocity
     4. Helicopter velocity
     5. Target velocity
     6. Wind velocity and direction
     7. Air density ratio
     8. TADS/gun parallax.
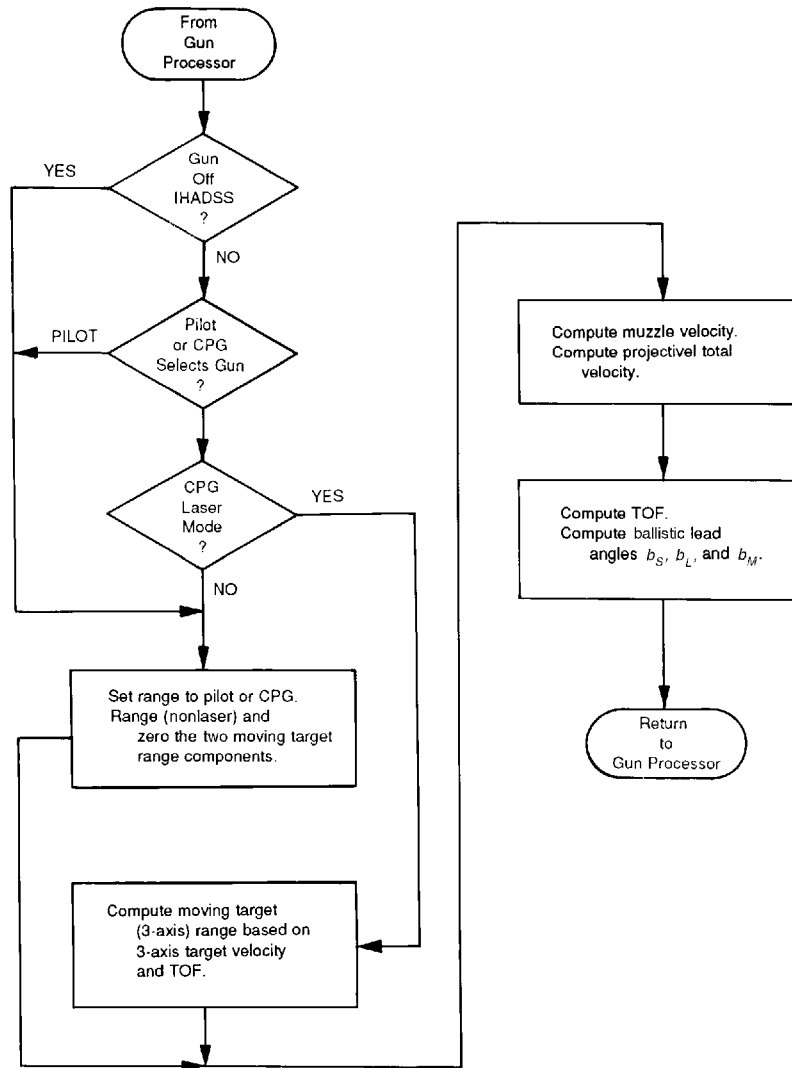
Figure 6-30. Gun Ballistics Module Flowchart (Ref. 24)

6-3.3.2.3.3 Rocket Processor Module (RPM)

The RPM provides all processing and control required for ballistically corrected rocket launch includ-
ing (1) initialization and rocket control panel input processing, (2) LOS processing, (3) ballistic pro-
cessing including downwash correction and boresight compensation, (4) pylon elevation control, (5)
inhibit processing, and (6) processing of output to the rocket control panel.

The RPM is executed at a 50-Hz rate when the LOS is TADS derived and at 25 Hz when IHADSS
derived. For the pylon boresight mode, normal rocket processing and calculations are bypassed, and the
pylon is commanded to the TADS mean elevation angle with the boresight corrector applied only during
the pylon verify mode. When either the P or CPG has selected the missile as a weapon, all rocket pro-
cessing is inhibited to avoid pylon drive conflicts.

When the rocket is selected as a weapon, the RPM determines the sight source (P or CPG, TADS or
IHADSS, or articulated pylon or fixed), determines the range source (laser or not laser range), and limits
the selected range to 6500 m. The rocket type is read from the rocket control panel, and the rocket bal-
listic coefficients are set. The RPM flags and variables are initialized to their starting values each time the
rockets are selected to assure the fastest possible ballistic solution for each new scenario.

Using the selected LOS values, the aircraft-to-earth transformation matrix $[E]$ is generated and used to
transform the aircraft velocities and gravity components from the aircraft to the sight-referenced coordi-

nate system used by the ballistic equations. The target range is converted to its three-axis sight-referenced coordinate system and limited to a 500-m to 6500-m range.

Next the rocket ballistic computations are performed. The results of these computations provide an offset to the LOS in sight-referenced coordinates. These values are then transformed to azimuth and elevation coordinates in the aircraft reference frame for driving the pylon and for display. The elevation command is corrected for rotor downwash, boresight errors, and rate feed forward quickening. The elevation is then limited to the pylon articulation range prior to output.

The rocket fire inhibits are then processed and combined with the pylon out of coincidence and the computed aircraft acceleration inhibits to form a composite inhibit signal. This composite signal is fed to the rocket controller as a rocket fire enable or inhibit control signal. Also outputted to the rocket control panel are the computed time to fuze function, TOF, fuze setting time, and rocket inventory.

6-3.3.2.4 Gun Turret

Figs. 6-31 and 6-32 illustrate the turret assembly and its elevation and azimuth servo actuators. These figures show the two axis-articulated turret supports for the 30-mm, gun, which provide ±110 deg of movement in azimuth and −60 deg to +11 deg of movement in elevation. The azimuth axis of the turret is driven by a rotary hydraulic motor coupled through a speed-reducing gearbox. Hydraulic flow to the motor is controlled by an electrohydraulic servo valve. The elevation axis is controlled by a linear hydraulic actuator with flow controlled by an electrohydraulic servo valve. The electrical signals to both servo valves are generated within the turret control box, which contains an analog computer that provides the signal processing and control laws for to stabilize and maneuver the turret. Both the azimuth and elevation axes are stabilized to angular position references defined by resolvers that measure the angular deviations of the respective gimbals from the commanded positions. The azimuth axis stabilization is augmented with an inertial angular acceleration inner loop that is electronically derived from a rate gyro mounted on the outer gimbal assembly. The elevation axis also uses an angular acceleration-stabilizing inner loop, but it estimates the acceleration from a pressure measurement. The turret control box contains a variety of filters and linear and nonlinear circuitry to mechanize the turret stabilization control laws.

As shown in Fig. 6-32, the gun barrel axis is not symmetrical with the turret suspension. Recoil forces, which are absorbed by the pair of recoil car-

(A) Turret Assembly

(B) Actuator Locations
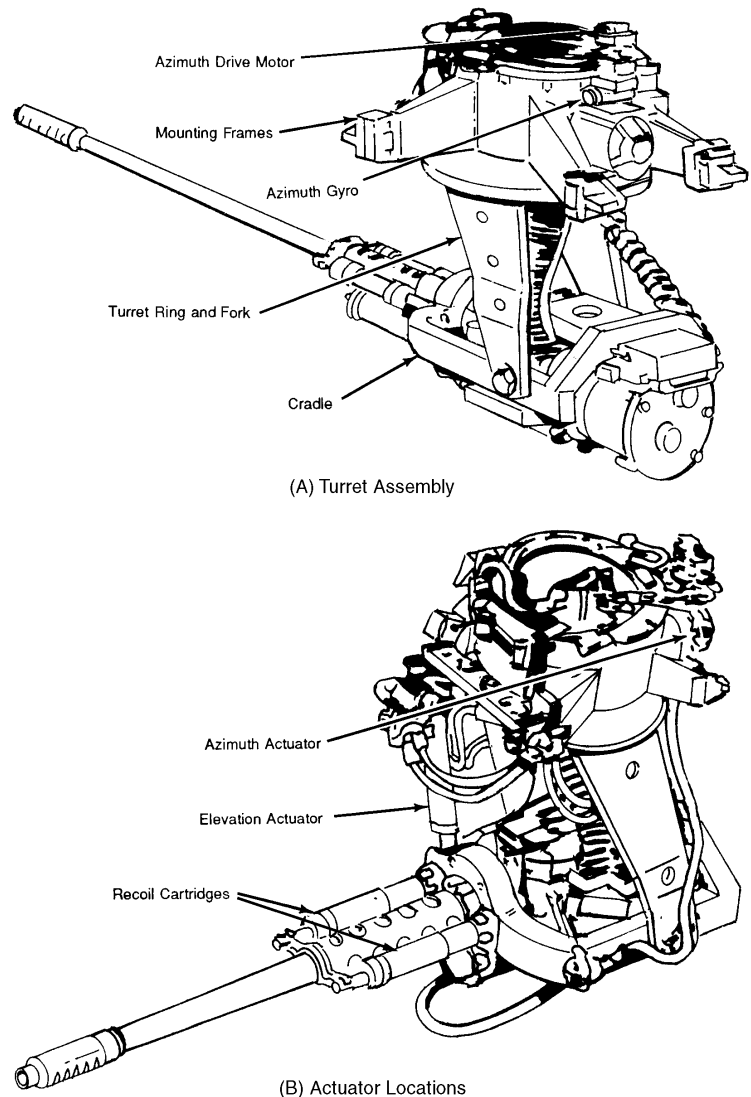
Figure 6-31. Turret Assembly Showing Actuator Locations (Ref. 26)

(A) Turret Side View   (B) Turret Front View
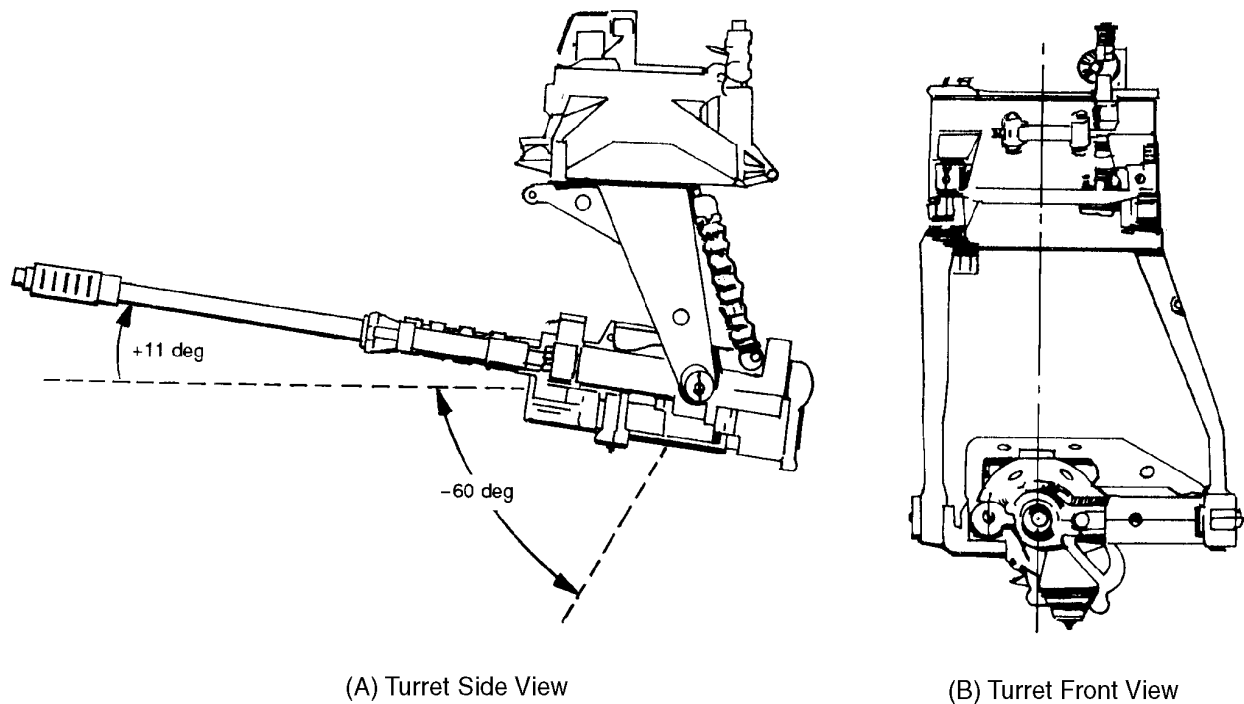
Figure 6-32. Turret Assembly Showing Asymmetric Fork Suspension (Ref. 24)

tridges illustrated in Figs. 6-31 and 6-32, are transmitted to the inner and outer gimbals. These forces result in disturbance moments to the turret servo system. Because of the asymmetric fork suspension, the disturbance moment in azimuth tends to create a bias in addition to a transient effect that correlates with the 10-Hz firing rate of the gun. In the official error budget for the area weapon system of the AH-64, the azimuth and elevation errors, during gun firing disturbances, were represented by a Gauss-Markov process with a correlation time defined by the firing interval and the known resonant frequencies of the dynamic responses of the servo. Subsequent test results support the validity of this model.

The error budget includes a 2.4-mrad random error* associated with the elevation and azimuth servo response plus a 1.0-mrad random error associated with recoil performance. The rss combination of these two random error sources results in a random error of about 2.6 mrad. In addition, there is a 1.0-mrad bias error in the servo response associated with the uncertainty in the recoil bias. The effect of this recoil bias contribution is corrected in the aiming solution. However, this correction must be made separately for each individual turret.

A number of other error sources combine to produce the total turret statistical error. These include a captive boresight harmonization kit accuracy value of 0.346 mrad (bias), a digital-to-analog converter bias error of 0.33 mrad, a boresight procedure bias error of 0.35 mrad, a resolver noise random error of about 0.12 mrad, and a digital-to-analog quantization random error of about 0.5 mrad. All of the bias errors can be taken into account when applying the aiming solutions. Only the random components of the errors are unpredictable.

6-3.3.2.5 Navigation System

The primary function of the navigation system is to provide accurate information on the helicopter position at all times so that its position relative to prestored checkpoints or target locations is precisely known. This information is used to navigate to selected points and to prepoint TADS in order to minimize target engagement times, especially for the launching of Hellfire missiles. Provisions are provided

---

* All specified values are based on one standard deviation (1σ).

to update system accuracy during flight via navigational checkpoints that are either overflown or observed by TADS during flyby. Fig. 6-33 is a schematic of the Apache navigation system.
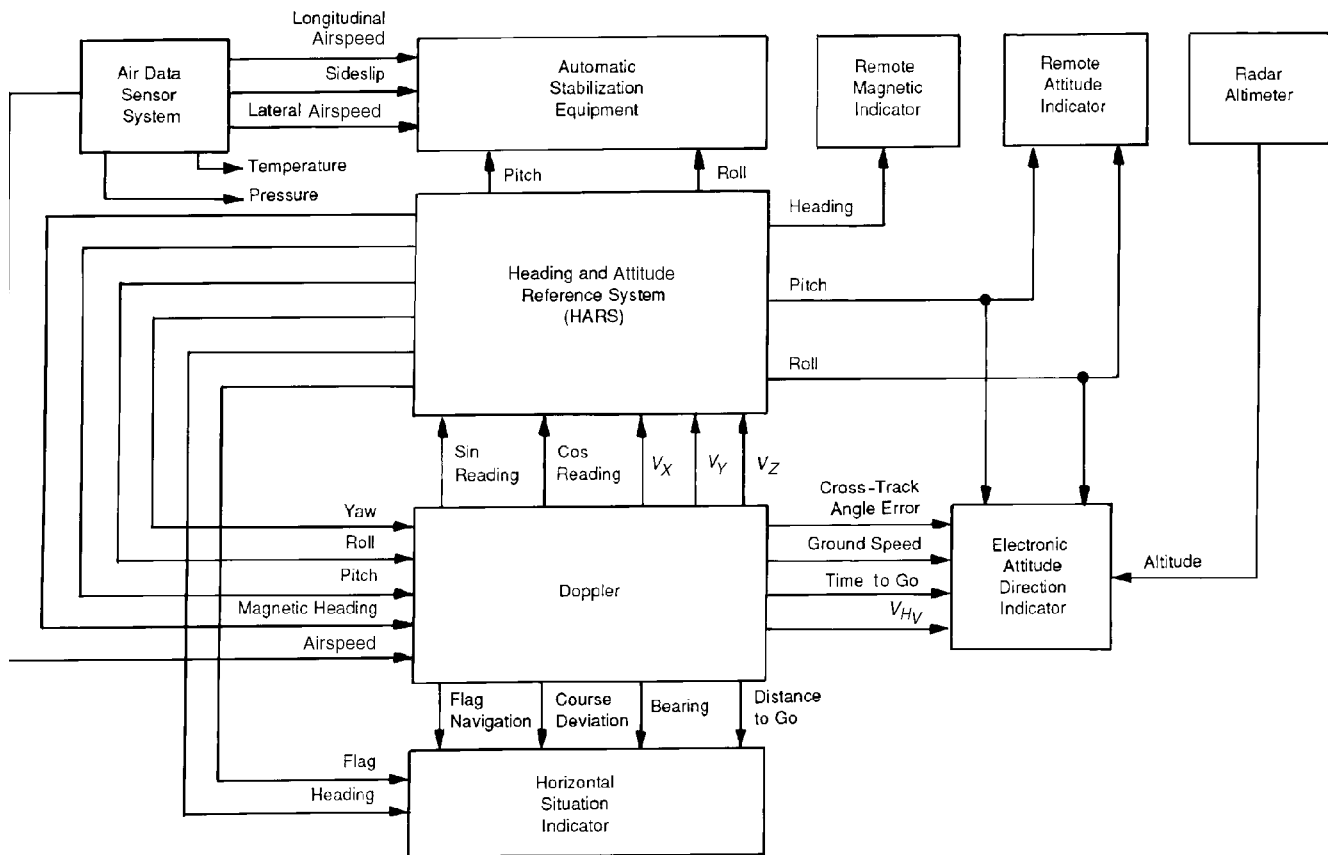
Figure 6-33. AH-64 Navigation System Schematic (Ref. 27)

Additionally, the system provides the fire control computer with several quantities required for conventional weapon system delivery. These quantities include pitch attitude ϕ, rad, roll attitude θ, rad, and body rates ω_{H_U}, ω_{H_V}, ω_{H_W}, rad/s.

Fire control simulation programs were used to determine the azimuth, elevation, and TOF sensitivities to errors in the quantities provided by the navigation system. The effects of these errors are discussed in the following paragraphs.

The primary use of attitude in the aiming solution is to determine the orientation of the gravity vector. Any error in pitch and roll produces corresponding azimuth and elevation errors. The azimuth and elevation errors that result for all conditions are less than 1 mrad. Thus errors from the navigation system measurement of pitch and roll do not significantly effect the fire control solution accuracy.

Fig. 6-34 illustrates a navigation vector diagram showing how errors in track angle affect a planned flight course. The helicopter starts out at its initial location and is required to fly to a final location. At some intermediate location, however, the helicopter has drifted off course by a distance called the cross-track error. At this location the angle between the ground speed vector of the helicopter and the range vector to the final location defines the track angle error. Also defined in Fig. 6-34 are the true heading and track angle measured with respect to true north and the magnetic bearing.

The true heading and other parameters referenced to true or magnetic north and defined in Fig. 6-34 are not used as input to the fire control solution algorithms because for a direct fire system the target is the aiming reference. However, the true headings can be used by the TADS to prepoint the sight in the target direction using target coordinates provided from an external source through use of the automatic target handoff system. Apache navigational data are then used to convert these coordinates to TADS pointing commands. A typical true heading error of 8.7 mrad (0.5 deg) results in an 8.9-mil error in

TADS azimuth pointing. Although such errors cannot be tolerated for purposes of fire control, this limited accuracy is compatible with the TADS prepointing targets acquisition requirements, and it allows the gunner to observe the target readily in the FOV and then to adjust the track reticle for subsequent fire control.

The aircraft body rates are used to make moment arm corrections and to compute an estimate of the angular rate about the LOS for use in the target state estimator. They are also used in conjunction with sight line angle rates to provide an approximation of the gun angle rate with respect to the airframe for feed forward turret control compensation. Sensitivities of the aiming solution to errors in the aircraft body rates have been found to be negligible. Since the moment arm corrections are minor, the resulting body rate errors become insignificant.

The onboard ballistic fire control aiming algorithm was simulated to evaluate the sensitivity of the aiming error to the ground speed velocity error. Although the ground speeds shown by components V_X, V_Y, and V_Z

Figure 6-34. Navigation Vector Diagram (Ref. 27)

are inputs to the onboard ballistic algorithm, along with airspeed, they have no effect on the firing corrections to the 30-mm gun. For the gun system the aiming solution is independent of the HARS ground speed. However, to provide a degree of redundancy, the ground speed input to the aiming solution allows a level of performance (although somewhat degraded) in the event that the air data system of the aircraft becomes inoperable. This ground speed is then used to provide a gross measurement of the airspeed of the helicopter.

6-3.3.2.6 Air Data Servo System

The air data servo system (ADSS) has two major components: the sensor package, which consists of the omnidirectional airspeed sensor (OAS), and the air data converter (ADC). The ADC contains all of the electronic circuitry necessary to process the signals from the sensor package and to provide the desired outputs in the proper format for use in the AH-64 fire control subsystem.

Outputs are generated by the ADSS in the following ways:

1. W_{R_U} and W_{R_V} are the values of airspeed along the U and V axes of the helicopter derived from airspeed measurements made by the OAS.

2. Angle of sideslip β is measured directly by the OAS and corrected in the ADC.

3. Air density ratio D/D_S is computed in the ADC using ambient temperature and pressure values and reference values in the microprocessor memory.

4. Ambient temperature T_a is measured by a dedicated temperature probe mounted on the OAS.

5. Ambient pressure P_a is measured by a pressure transducer mounted in the ADC and vented to a plenum containing ambient atmosphere.

The methods used to measure or derive these values are summarized in the following paragraphs.

Ambient temperature T_a is measured directly via the OAS-mounted temperature probe. This probe is accurate to ±0.28 K (±0.5 deg F) throughout the operating range from 225 K to 325 K ($-55°$F to $+125°$F). The probe is isolated from the body of the OAS, and the signal from the probe is preamplified in the OAS and scaled to 90 mV/K (50 mV/°F). The amplified signal is then buffered and outputted to the AH-64 System.
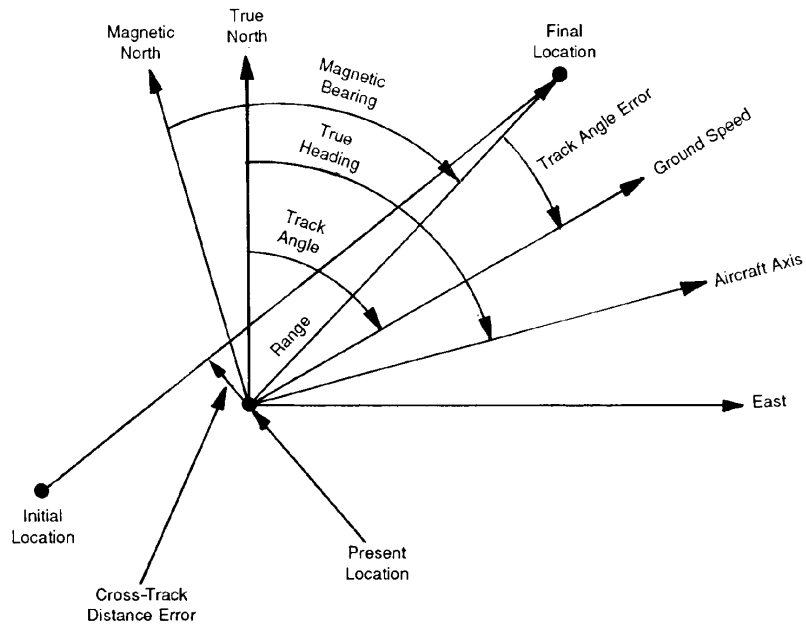
The pressure transducer located in the ADC generates a signal proportional to ambient pressure P_a. Within the range of 34.5 KPa to 116.5 KPa (5 psi to 16.9 psi), this device has an accuracy of 0.69 KPa (0.1 psi). The output analog voltage is scaled, buffered, and outputted to the AH-64 system in analog form in a manner similar to that of T_a.

The air density ratio D/D_S is the measure of air mass density at a given altitude and ambient conditions relative to the air mass density at sea level under standard atmospheric conditions. The local air mass density D is computed using

$$D = \frac{P_a}{R_a T_a}, \ \ \mathbf{kg/m^3} \qquad (6\text{-}54)$$

where

D = local air mass density, kg/m³
R_a = gas constant for air = 285.9 m²/(s²·K)
T_a = ambient air temperature, K
P_a = ambient air pressure, Pa.

As noted previously, the required values of orthogonal airspeed W_{R_U} and W_{R_V} are derived from the capability of the ADSS to measure the true airspeed of the aircraft along its U and V axes. The discussion of orthogonal airspeed centers on the method, or principle, by which the OAS can obtain a signal that is related directly to airspeed.

The OAS has two arms that protrude from opposite sides of a central hub. At the end of each arm a venturi-like tube is mounted normal to the axis of the arm. Inside each venturi there is a small orifice that directly vents into the hollow core of the attached arm. These hollow cores extend into a plenum chamber inside the hub. The two sides of the chamber are separated by a diaphragm that is part of a differential pressure transducer. This hub-arm venturi mechanism is connected to an electrical motor that causes the mechanism to rotate at 720 revolutions per minute (rpm) on the top of the vertical axis of the driveshaft.

During no-wind (or at zero airspeed) operations, the airflow through both venturis is equal. Under this condition the pressures in the two venturi throats, in the arm cores, and within the two plenums are equal. Thus the differential pressure diaphragm is not deflected.

When wind is introduced into the rotational plane of the arms, the air velocity in the advancing venturi is increased, whereas the air velocity in the retreating venturi is decreased. Therefore, there is a decrease in static pressure in the advancing venturi and a corresponding increase in static pressure in the retreating venturi.

Since there is now a pressure difference between the two plenums, the diaphragm of the pressure transducer deflects toward the low-pressure side. The peak magnitude of the deflection (or pressure differential) occurs when the arms are oriented 90 deg to the oncoming airflow and the venturis are oriented with the wind axis.

When the airflow is aligned with the arms, i.e., the venturis are normal to the wind angle, the flow through both venturis is equal, and the diaphragm in the pressure transducer is not deflected. The ADSS measures the angle of the arms with respect to the centerline of the aircraft at this moment. This angle represents the angle of sideslip β and is used to divide the total airflow velocity into its orthogonal components.

Thus the air data system provides the fire control computer with the quantities that follow:
1. Air pressure
2. Ambient air temperature
3. Longitudinal airspeed
4. Lateral airspeed
5. Vertical airspeed.

6-3.3.3   System Performance

The system requirements specify the minimum hit probability to be demonstrated by each of the weapon delivery subsystems before acceptance. Accordingly, the flight tests were structured to obtain firing

data. These data were used as input to the probability equations that express accuracy in the same terms used in the requirements document.

Although similar test programs were conducted for the Hellfire and aerial rocket subsystems, the current discussion emphasizes the procedure used to evaluate the performance of the area weapon system (AWS) using the turreted 30-mm chain gun.

In subpar. 6-3.1.1 the system requirements for a variety of engagement conditions are discussed, and the required accuracy to be demonstrated is also specified for each condition. In addition, the methodology to be used to convert the results of the firing data to a probabilistic evaluation criterion is also stated.

Two methodologies were eventually used to develop data reduction procedures for assessing system performance. Both were predicated upon the firing of a burst and included provisions for estimating the risk associated with accepting or rejecting the system, and both were used in the course of the development program to establish system performance. Additionally, this development is indicative of the variation in results that may be experienced with use of different assumptions and statistical procedures. The first methodology, discussed in subpar. 6-3.1, is given in the Apache system requirements document and uses the "slow rate of fire" assumption. This implies that the time duration between the firing of each round is so large that the systematic error related to each round is independent of all others and can therefore be considered a random error. The alternate assumption used in the second methodology (eventually adopted by the Army to evaluate system performance) considered the rate of fire to be so high that the systematic error remained a constant bias error during the burst. This assumption is known as the "salvo theory".

As discussed in subpar. 4-4.1.1, the results of both approaches tend to converge when the round-to-round dispersion is large compared to the value of the systematic error. The values of the burst hit probability obtained using the slow rate of fire assumption always exceed those of the salvo theory for given values of bias and dispersion. Although the systematic error does vary to some degree during the burst, the magnitude of this drift is difficult to ascertain, and the required mathematical treatment is complex. In the first treatment (contained in the requirements document), approximations are introduced that simplify the procedure to such an extent that the mathematics could be done on a hand calculator. The second methodology and resulting procedure involve the use of statistical sample theory as applied to probability determination and are discussed in subpar. 4-4.2.2. Eventually, the reduction of field data indicated that the variation of the rounds from the mean point of impact in each burst, when considered over all bursts, was low. The round-to-round dispersion indicated that the systematic error was not drifting appreciably during the burst. This result supports use of the salvo theory to estimate performance.

Regardless of the methodology used, performance estimates required the availability of field test firing data. A test plan was developed that defined the flight profiles and firing doctrine of the weapon system and the target and instrumentation needs necessary to evaluate the system conditions for those specified in the system requirements document. Table 6-19 indicates in matrix form the weapon system and target conditions under which the tests were conducted, as well as the replications necessary to achieve statistical validity.

A burst of 20 rounds was considered to be appropriate from a conservation of ammunition point of view. However, this decision resulted in the need to extrapolate the performance estimates to the 50-round burst called out in the specification. An overhead camera was used during the burst firing sequence to record ground impacts with respect to the vertical target position. These impact positions were then transformed to miss distances in the vertical target plane.

For each test, the key statistical parameters necessary to calculate burst hit probability and confidence levels were computed. These were the variation of each round from the mean point of impact of each burst (dispersion), the variation of the mean point of impact of each burst from the target center (bias), and the mean value of the bias over all bursts for the particular engagement conditions tested. Ideally

TABLE 6-19. 30-mm GUN FIRING DEMONSTRATION MATRIX (Ref. 28)

TEST NO.	RANGE, km	SIGHT	AIRSPEED, KIAS	ALTITUDE, ft (m)	TARGET BEARING, deg	TEST ITERATIONS	TARGET	MANEUVER
G1	1.0	DTV	HOV	75 (22.9)	0	20	Static	None
G2	1.0	DTV	HOV	75 (22.9)	45 left or right	8	Static	None
G3	1.0	DTV	HOV	75 (22.9)	90 left or right	8	Static	None
G4	1.0	DTV	HOV	75 (22.9)	110 left or right	8	Static	None
G5	na	DTV	HOV	na	0	8	Static	None
G6	1.0	DTV	35	50 (15)	0 to right	6	Static	Veer left
G7	1.0	DTV	35	50 (15)	0 to left	6	Static	Veer right
G8	1.0	DTV	60	50 (15)	0	6	Static	Rapid ascent
G9	1.0	DTV	80	100 (30)	0 to left	6	Static	Veer right
G10	1.0	DTV	90	1000 (300)	0	6	Static	500 ft/min descent
G11	1.0	DTV	Vh	500 (150)	0 to right	6	Static	Veer left
G12	1.0	DTV	Vh	500 (150)	0 to left	6	Static	Veer right
G13	1.0	DTV	Vh	3000 (900)	0	6	Static	15-deg dive
G14	2.0	DTV	HOV	75 (22.9)	0	8	Horizontal	None
G15	2.0	DTV	35	50 (15)	0 to right	5	Horizontal	Veer left
G16	2.0	DTV	35	50 (15)	0 to left	5	Horizontal	Veer right
G17	2.0	DTV	60	50 (15)	0	5	Horizontal	Rapid ascent
G18	2.0	DTV	80	100 (30)	0 to left	5	Horizontal	Veer right
G19	2.0	DTV	90	1000 (300)	0	5	Horizontal	500 ft/min descent
G20	2.0	DTV	Vh	500 (150)	0 to right	5	Horizontal	Veer left
G21	2.0	DTV	Vh	500 (150)	0 to left	5	Horizontal	Veer right
G22	2.0	DTV	Vh	3000 (900)	0	5	Horizontal	15-deg dive
G23	3.0	DTV	HOV	75 (22.9)	0	8	Horizontal	None
G24	3.0	DTV	35	50 (15)	0 to right	5	Horizontal	Veer left
G25	3.0	DTV	35	50 (15)	0 to left	5	Horizontal	Veer right
G26	3.0	DTV	60	50 (15)	0	5	Horizontal	Rapid ascent
G27	3.0	DTV	80	100 (30)	0 to left	5	Horizontal	Veer right
G28	3.0	DTV	90	1000 (300)	0	5	Horizontal	500 ft/min descent
G29	3.0	DTV	Vh	500 (150)	0 to right	5	Horizontal	Veer left
G30	3.0	DTV	Vh	500 (150)	0 to left	5	Horizontal	Veer right
G31	3.0	DTV	Vh	3000 (900)	0	5	Horizontal	15-deg dive
G32	3.0	DTV	Vmax	na	0	4	Static	2.2-g pull-up
G33	1.0	DTV	HOV	75 (22.9)	0	8	Moving	None
G34	1.0	DTV	HOV	75 (22.9)	45 left or right	5	Moving	None
G35	1.0	DTV	HOV	75 (22.9)	90 left or right	5	Moving	None
G36	2.0	FLIR	HOV	75 (22.9)	0	8	Static	None
G37	3.0	FLIR	HOV	75 (22.9)	0	8	Static	None

na = not available
KIAS = knots indicated airspeed
HOV = hover

Vh = own ship velocity
Vmax = maximum own ship velocity

this burst-to-burst bias should be zero when considered over all engagement conditions. However, this is not usually the case for specific engagement conditions. When values of these statistical parameters were computed for the various engagement scenarios of interest, the system did not meet the specified requirements.

After obtaining this result, the error sources that caused unacceptable impacts were identified. Chief among these were the airframe flexure between gun and TADS, the analog-to-digital conversion in the rate measurement circuits, and the bias in the gun turret drive. After appropriate modifications to system hardware and software were incorporated, the system was retested and was then able to meet the requirements. It was the developer's expectation that although only a single production weapon system was successfully tested, the entire fleet would also meet these requirements.

The expectation of success relies heavily upon the fact that the values of component and subsystem error statistics assumed in the accuracy analysis are taken over the ensemble of systems as well as over time. Unfortunately, the specific values of impact data, statistical parameters, and probability cannot be provided because they are classified. Although this discussion emphasizes the gun mode, the same steps were taken to evaluate the accuracy of the rocket delivery system.

Both vertical and horizontal targets were used for field testing. The vertical target board measured approximately 15.2 m × 15.2 m (50 ft × 50 ft) as shown in Fig. 6-35 and was most often located at a range of 1000 m. Hits were recorded by a combination of still photographs taken after every third burst and high-speed 35-mm motion pictures taken during the firing. The vertical target board was made of plywood sections nailed to a vertical structure. The holes in the board caused by penetrating rounds were repaired or taped over between each flight. IHADSS firings were normally aimed at this target.

The horizontal area target consisted of a field 265 m × 203 m (860 ft × 660 ft) with white markers regularly spaced in a pattern. A white target board with an "X" painted across the face of it was placed in the center of the field as the aim point. A data-recording helicopter hovered above the target and a video camera recorded the dust raised by round impacts. This target was used for ranges of 2000 m and 3000 m. The field was plowed at regular intervals to ensure adequate dust, and the white target markers were kept clean to support accurate round location. Scoring was accomplished by viewing the tapes on a video monitor and scoring round-impact-generated dust clouds.

Testing to determine hit probability was accomplished for 19 flights at a Yuma Proving Ground, AZ, test range for a total of 24.3 h of flight time. A total of 2701 rounds fired in bursts were evaluated.
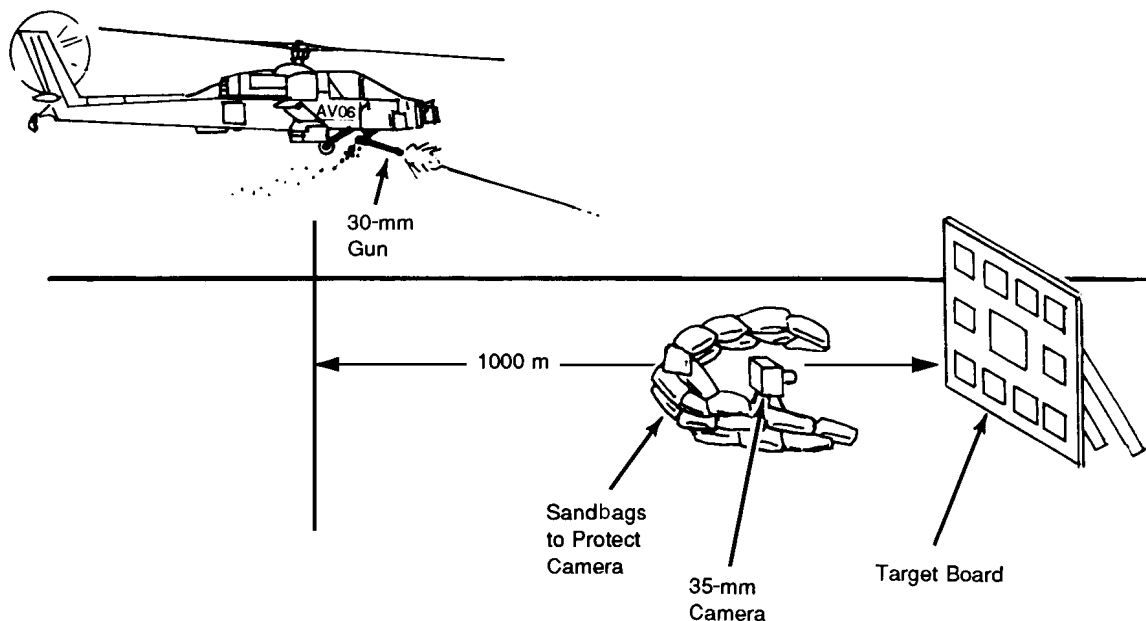
Figure 6-35. AWS Firing at Vertical Target (Ref. 24)

At the beginning of the test program, it was acknowledged that only a limited quantity of rounds could be made available for testing. Because of this limitation, the test plan was amended to reduce the number of bursts and reduce the number of rounds per burst. The burst length was reduced from 50 to 20 rounds by mutual agreement between Army and contractor personnel. This agreement proved to be valid for two reasons:

    1. The dust cloud scoring method suggested and used by Army personnel was enhanced because a smaller percentage of dust patterns could be obscured in a 20-round burst than in a 50-round burst.

    2. More bursts could be fired with the limited available rounds, so a larger sample of test conditions could be provided for analysis.

Although the Apache failed the initial test, it later complied with performance requirements following significant software and hardware modifications.

As mentioned previously, efforts to provide the Apache with an air-to-air capability for its gun, rocket, and missile weaponry have been carried out. These efforts included introduction of improved filter and prediction algorithms, use of flechette rocket warheads, and integration of the Stinger missile. The mast-mounted radar concept has been revived and is being evaluated in conjunction with a modified Hellfire missile to provide the desired fire-and-forget, air-to-ground point target capability. This capability is being implemented as the Longbow Apache.

REFERENCES

1. O. I. Elgerd, *Control System Theory*, McGraw-Hill Book Co., New York, NY, 1967.

2. B. C. Kuo, *Automatic Control Systems*, Prentice-Hall, Inc., Englewood Cliffs, NJ, 1962.

3. D. J. Povejsil, R. S. Raven, and P. Waterman, "Airborne Radar", *Principles of Guided Missile Design*, G. Merrill, Ed., D. Van Nostrand Co., Inc., Princeton, NJ, 1961.

4. G. Frost, "Man-Machine Dynamics", *Human Engineering Guide to Equipment Design*, H. P. Van Cott and R. G. Kinkade, Eds., US Government Printing Office, Washington, DC, 1972.

5. AMCP 706-329, Engineering Design Handbook, *Fire Control Series, Section 3, Fire Control Computing System*, October 1970.

6. *M1 Tank Program: System Specification for Tank, Combat, Full-Tracked, 105-mm Gun, M1, General Abrams*, Volume 1, SA-X00001G, Chrysler Defense, Inc., Warren, MI, for US Army Tank-Automotive Command, Warren, MI, 1981.

7. J. Johnson, "Analytic Description of Night Vision Devices", *Proceedings of The Seminar on Direct-Viewing Electro-Optical Aids to Night Vision*, Report No. S254, L. Biberman, Ed., Institute for Defense Analysis, Alexandria, VA, October 1966.

8. H. H. Bailey, *Target Detection Through Visual Recognition: A Quantitative Model*, Memo RM-6158/1-PR, Rand Corporation, Santa Monica, CA, for Deputy Chief of Staff, Research and Development, Headquarters, US Air Force, Washington, DC, February 1970.

9. FM17-12-1, *Tank Combat Tables M1*, US Armor School, Fort Knox, KY, December 1984.

10. K. R. Pfleger, *Methodology for Tank Delivery Accuracy*, Technical Report ARFSD-TR-92003, US Army Research, Development, and Engineering Center, Picatinny Arsenal, NJ, August 1992.

11. J. S. Przemieniecki, *Introduction to Mathematical Models in Defense Analysis*, American Institute of Aeronautics and Astronautics, Inc., Washington, DC, 1990.

12. D. Brown and R. L. Koecker, "New Tank Gun Calibration Policy", *Armor* (July-August 1982).

13. Robert L. McCoy, *The Effect of Wind on Flat-Fire Trajectories*, BRL Report No. 1900, US Army Ballistics Research Laboratories, Aberdeen Proving Ground, MD, 1976.

14. T. D. Hunter, *M1A1 Tank Characteristics and Description Book*, Systems Technical Support Services for the Abrams Tank Systems, Document No. NL-85-04057-001 (First Edition), General Dynamics Land System Division, Warren, MI, for US Army Tank-Automotive Command, Warren, MI, September 1985.

15. *Gunner's Primary Sight*, **Drawing No. 12282140, US Army Armament Research and Development Command, Dover, NJ, 17 May 1978.**

16. **TM9-2350-264-10-1,** *Operator's Manual Operator Controls and PMCS--Tank, Combat, Full-Tracked 120-mm Gun, M1A1 General Abram*s, **Volume 1, Department of the Army, Washington, DC, December 1985.**

17. **Mark A. Henry and William A. Baetz,** *Detailed Test Plan of Automotive and Weapons Phase of M1A1 Tank System*, **US Army Test and Evaluation Command, Aberdeen Proving Ground, MD, July 1986.**

18. **P. McCall**, *Detailed Test Plan Proof of Principle Demonstration of Advanced Tank Cannon System*, **US Army Test and Evaluation Command, Aberdeen Proving Ground, MD, August 1990.**

19. **AMC-55-AAH-H-1000A,** *System Specification for the Advanced Attack Helicopter YAH-64*, **Hughes Helicopter Company, Culver City, CA, for US Army Aviation and Troop Support Command, St. Louis, MO, 1976.**

20. **P. Pfeilsticker and J. Glynn,** *Hit Probability on a Tank-Type Target*, **Memorandum Report M66-18-1, US Army Frankford Arsenal, Philadelphia, PA, March 1966.**

21. **Harold J. Breaux,** *A Methodology for the Development of Fire Control Equations for Guns and Rockets Fired From Aircraft*, **Memorandum Report No. 872, US Army Ballistic Research Laboratories, Aberdeen Proving Ground, MD, 1982.**

22. **R. S. Bucy, S. J. Asseo, and D. A. Weissenberger,** "Estimation of Helicopter and Target Motion for the Advanced Attack Helicopter Fire Control System", **J. Amer. Helicopter Soc. 11, 16-24 (1982).**

23. **H. Goldstein,** *Classical Mechanics*, **Addison-Wesley Publishing Co., Reading, MA, 1965.**

24. **77FT-8023-2, Hughes Helicopter Company, Culver City, CA, for US Army Aviation and Troop Support Command, St. Louis, MO, 1985.**

25. *MECA-43 AEROSPACE Digital Computer*, **Teledyne System Co., Northridge, CA, for US Army Aviation and Troop Support Command, St. Louis, MO, March 1980.**

26. **77FT-8023-4, Hughes Helicopter Company, Culver City, CA, for US Army Aviation and Troop Support Command, St. Louis, MO, 1985.**

27. **77FT-8023P-2, Hughes Helicopter Company, Culver City, CA, for US Army Aviation and Troop Support Command, St. Louis, MO,1985.**

28. **77FT-8017P-2, Hughes Helicopter Company, Culver City, CA, for US Army Aviation and Troop Support Command, St. Louis, MO, 1985.**

BIBLIOGRAPHY

TM9-2350-264-20-2-1, *Unit Maintenance Manual Vol. 1 of 4 for Tank, Combat, Full-Tracked: 120-mm Gun, M1A1*, **Department of the Army, 30 November 1987.**

CHAPTER 7
NUCLEAR, BIOLOGICAL, AND CHEMICAL
CONTAMINATION SURVIVABILITY

Since a number of potential adversaries have the capability to use nuclear, biological, and chemical (NBC) weapons, the fire control designer must be aware of their potential effects on equipment. The Army regulations concerned with this design aspect are discussed, and guidelines for obtaining expert advice and guidance are provided. To provide survivable and useful equipment, the decontaminability, hardness, and compatibility of the material must be considered. These are discussed against the background of the effects of agents and decontaminants on equipment. The chemical and biological protective equipment and clothing provided for the troops are also discussed.

7-1 INTRODUCTION

This chapter (based in part on Ref. 1) is intended to provide information needed by fire control developers to meet the requirements established for NBC contamination survivability. The requirement for NBC contamination-survivable fire control equipment arises from the capability of potential US adversaries to use NBC weapons and the possibility that contamination of materiel by these weapons may impair or preclude US weapon performance.

In response to the threat the US Army issued Army Regulation (AR) 70-71, *Nuclear, Biological, and Chemical Survivability of Army Materiel*, **(Ref. 2).** This regulation states that all mission-essential items or critical components of one or more mission-essential end-items must be NBC contamination survivable. Mission-essential materiel is that necessary to accomplish the primary or secondary function of a military unit or organization. Fire control equipment is mission essential.

The nuclear hazard addressed by this regulation is limited to the secondary nuclear effects or residual radiological contamination consisting of fallout, rainout, and neutron-induced gamma activity. These residual hazards are distinguished from the primary nuclear effects of blast, thermal radiation, initial nuclear radiation, and electromagnetic pulse (EMP), which are addressed by AR 70-60, *Nuclear Survivability of Army Materiel*, **(Ref. 3).**

The NBC contamination survivability regulation, AR 70-71, establishes the policy and procedures for developing and acquiring NBC-survivable materiel.

The regulation identifies the responsibilities of various agencies involved in materiel development. The US Army Training and Doctrine Command (TRADOC) includes NBC contamination survivability in all materiel requirements documents. The US Army Nuclear and Chemical Agency provides contamination survivability criteria. The US Army Materiel Command (AMC) maintains a technology base in support of survivability, provides test plans to assess survivability, and provides advice and consultation to materiel developers.

AMC has assigned the US Army Chemical and Biological Command at the Edgewood Research, Development, and Engineering Center (ERDEC), MD, as the lead laboratory to support materiel developers. The ERDEC participates in the preparation of procurement documents, source selection boards, and in-process reviews. The designer is urged to contact subject matter experts at the ERDEC for consultation early in the design process.

The basic requirement of protection against NBC is protection of the users of the equipment. Thus fire control materiel, for example, must be able to be decontaminated so that the crew can use it to perform mission-essential functions. Nevertheless, the materiel itself must survive both the contamination and subsequent decontamination to remain usable by the crew.

The characteristics of NBC contamination survivability include decontaminability, hardness, and compatibility. Decontaminability includes the use of materials that minimally absorb NBC contamination and facilitate decontamination; design of equipment to resist contaminant accumulation; devices to control contamination, e.g., positive overpressure and filtering systems; packaging and protective covers; and detection, monitoring, and decontaminating equipment. Hardness is concerned with the ability of material to withstand damage by agents or decontaminants. Compatibility is the capability to operate and main-

tain equipment by personnel wearing the full NBC protective ensemble. These characteristics are discussed in the paragraphs that follow and are discussed in detail in MIL-HDBK-783 (EA), *Chemical and Biological (CB) Contamination Avoidance and Decontamination*, **(Ref. 4).**

7-2 DECONTAMINABILITY

Decontaminability includes design not only to allow equipment to be decontaminated but also to minimize the extent to which decontamination is required. For example, if the designer uses an external finish that does not readily absorb agents, decontamination is easier and more thorough.

Biological agents include anthrax, cholera, plague, Rocky Mountain spotted fever, yellow fever, etc. They are dispersed as liquids, solids (including spores), or vapors that can coat both the internal and external surfaces of equipment.

Chemical agents include nerve agents such as soman, blister agents such as mustard, and blood agents such as hydrogen cyanide, and others. These also can coat the surfaces of equipment.

The Army has available two standard decontaminants, decontaminating solution No. 2 (DS2) and supertropical bleach (STB). Although very effective, STB is highly corrosive, and it is not suitable for use on fire control equipment. DS2 is also an effective paint remover, but produces side effects such as dissolved optical coatings, removal of legends, and degradation of some materials, e.g., rubber and plastics.

7-2.1 MATERIALS

Insofar as is practical, designers should use metal, plastic, and coated materials that do not absorb NBC contaminants. Use of such materials enables the agents to be flushed away during decontamination. Similarly, designers should use nonabsorbing materials that resist the primary (corrosion and loss of strength) and secondary (change of dimensions) effects of decontaminants and decontamination procedures. The equipment must be decontaminated to the point at which the agent poses no hazard to unprotected personnel using the equipment over an indefinite period of time.

The ERDEC (formerly known as the US Army Chemical Research, Development, and Engineering Center) published a handbook entitled *Compatibility of Chemical Agents and Decontaminants With Materials* (Ref. 5). This book should be consulted for guidance regarding the use of materials.

Contamination of materials occurs in various ways. Impermeable materials keep contamination on the surface, other materials may absorb agents into the surface pore structure of the material, and others fully absorb the contaminants.

Agents and decontaminants can affect the properties of materials. The blister agent mustard (HD), for example, has been shown to reduce the tensile strength of various materials such as neoprene, ethylene propylenediene, acrylic rubber, and ethylene acrylic as much as 25 to 40%. Stretched acrylic swells, exhibits hazing, and shows slight crazing when subjected to mustard contamination. HD has also been shown to increase the permeability of materials such as silicones, epoxies, urethanes, and acrylics.

The standard decontaminant, DS2, strips alkyd paints. As the paint absorbs the decontaminant, the surface dissolves away. On the other hand, polyurethane paints are impervious to DS2 and most agents and should be used, if possible.

These are just a few examples of how decontaminability affects the choice of materials.

7-2.2 DESIGN

The designer should incorporate features that reduce or prevent accumulation of NBC contamination and ensure that exposed areas are readily accessible for decontamination.

Within the context of the design guidelines handbook, contamination means that NBC agents adhere to or enter a piece of equipment or some part thereof. Here the broadest interpretation is given enter; it includes not only the penetration of agent into compartment spaces but also the absorption of agent into materials and the infiltration of agent into seams and crevices.

Contamination may result from a direct attack with NBC weapons, or it may result from exposure to a wind-carried agent from another area or from moving over contaminated ground or vegetation. Regardless of the cause, the result is the same: Equipment is contaminated and thus becomes a potential source of contamination to personnel in the area.

Designing to minimize contamination is primarily a matter of eliminating, restructuring, or shielding items that may trap or retain contaminants in areas that can be contacted by personnel or that may create a vapor hazard to personnel. Secondarily, it is a matter of providing good air circulation and exposure to sunlight for items that cannot be shielded from contaminants.

Good design can be accomplished by eliminating surface configurations and crevices that may trap or retain contaminants and by not using materials that absorb contaminants or that react adversely with decontaminants. When contamination cannot be prevented, good decontamination design provides adequate access to areas susceptible to contamination. Unless such access is provided, decontamination will be difficult, and in some cases it will be impossible. Access to areas where dust, dirt, mud, or grime may accumulate is particularly important because some biological agents can survive in such areas for weeks or months.

In general, any feature that can trap or retain a solid, liquid, or gaseous material represents poor design with respect to contamination and decontamination. Such features tend to hold contaminants and are difficult to clean adequately. Crevices where hatches meet deck plates, exposed springs connected to hatch covers, and restricted areas under tie-downs are representative of entrapment and hard-to-clean features. Anything that can be done to eliminate or to reduce the number of such features improves the overall decontamination design of the equipment.

Flexible dust covers, expandable joints, and housings may incorporate canvas, elastomeric materials, and paints that absorb contaminants. If canvas must be used, the item should be designed so that the canvas is easily removable with a minimum of handling. If absorbent elastomers must be used, they should be shielded to the greatest extent possible from contaminants. Alternatively, they should be incorporated as easily replaceable items that can be removed and discarded with a minimum of contact by personnel. If surfaces must be painted, chemical-agent-resistant coatings such as polyurethane should be used. Such paints can also be used to seal small crevices and capillaries under fasteners. In summary, materials that absorb contaminants should not be used. If they must be used, they should be designed as disposable items and made easily removable. If they cannot be made disposable, they should be shielded to the greatest extent possible.

Nonabsorbing seals and sheaths, metal covers, and wider spacing between adjacent parts may be used to improve the overall decontamination design, but they must be used with care to ensure that the intended survivability effect is realized without introducing a problem of equal or greater magnitude either of contamination or of function. For example, eliminating a concave surface may eliminate a contaminant trap, but if the function of the concavity is to deflect bullets, splash, or shell fragments, its elimination is not feasible. The surface must be designed for its functional purpose, and its configuration should be adjusted to the greatest extent feasible to make it less of a contamination trap and to make it easier to clean.

7-2.3 CONTAMINATION CONTROL

The designer should use devices and techniques that reduce the amount of contamination that must be removed from both the outside and inside of the equipment. Barrier packaging for spare parts and supplies and protective and sealing covers on equipment are examples.

Many items of fire control equipment, such as optics and electronics, benefit from being sealed from the environment. The designer should therefore be alert to opportunities to obtain contamination control at little or no added cost. Contamination that is confined to the outside surface of equipment is much more easily eliminated than contamination that reaches interior surfaces as well.

7-2.4 NBC EQUIPMENT

The only widely available chemical decontaminant that is suitable for use on nonrubber or nonplastic fire control equipment is DS2; STB is too corrosive. Decontamination equipment available for use in the field is limited.

US Army fielded decontamination equipment is shown in Table 7-1.

TABLE 7-1. US ARMY FIELDED DECONTAMINATION EQUIPMENT

ITEM	DESCRIPTION AND USE	DIMENSIONS	TECHNICAL DATA REFERENCE
ABC-M11, Decontaminating Apparatus, Portable, DS2, 1 1/2 Quart NSN 4230-00-720-1618	A fire extinguisher-like device used to spray DS2. Comes with mounting bracket for attaching to vehicles. Used to spray DS2 on vehicles and equipment. Comes with spare nitrogen cylinders.	330 mm height 102 mm diameter 2.7 kg (full) 1.4 kg (empty)	TM 3-4230-204-12&P TM 43-0001-26-1
ABC-M12A1, Decontamination Apparatus, Power-Driven, Skid-Mounted (PDDA) NSN 4230-00-926-9488 LIN F81880	Includes pump unit, tank unit, personnel shower assembly, M2 water heater, all mounted on skids. Used to spray water or foam; for deicing, vehicle washing, and personnel showering.	1.42×0.81×1.30 m (pump) 2.13×1.14×1.30 m (1895-L tank) 1.35×0.53×1.09 m (M2 heater)	TM 3-4230-209-34P TM-3-4230-209-ESC TM 3-4410-201-12 TM 3-4410-201-20P TM 43-0001-26-1
M258, Decontamination Kit, Skin NSN 4230-00-123-3180	Kit consists of pads, scrapers, and decontamination solutions in plastic carrying case. Used for skin decontamination.	110×80×60 mm (plastic case) 0.35 kg (full)	TM 3-4230-213-10 TM 43-0001-26-1
NOTE	NOTE: This item is being replaced by the M258A1 Kit and may not be available.		
M258A1, Decontamination Kit, Personal NSN 4230-01-101-3984	Kit consists of foil-packaged towelettes in plastic carrying case. Used for skin decontamination.	110×80×60 mm (plastic case 0.30 kg	TM 3-4230-216-10
M13, Decontamination Apparatus, Portable (DAP) NSN-4230-01-133-4124	Self-contained device used to apply DS2 to metal surfaces. Has a disposable 14-L DS2 container. Can be mounted to standard 19-L fuel can mounts on vehicles and equipment.	14-L capacity 27 kg (filled)	TM 3-4230-214-12&P TM 43-0001-26-1
ABC-M13, Decontaminating and Reimpregnating Kit, Individual NSN 4230-00-907-4828	Decontaminating materials in a plastic case. Used to decontaminate interior of mask and other IPE.	110×80×670 mm (plastic case) 0.40 kg (filled)	TM 3-4230-211-10
NOTE	NOTE: This item is being replaced by the M258A1 Kit and may not be available.		
M17, Transportable, Lightweight Decontamination System [Same item as Air Force A/E32U-8 LDS] NSN 4230-01-153-8660	Designed to draw water from any source and deliver it at pressures up to 689 kPa and temperatures up to 120°C. Includes accessory kit with hoses, cleaning jets, and personnel shower. Includes collapsible, rubberized fabric tank.	1.02×0.59×0.86 m 163 kg (basic unit) 1.06×0.52×0.39 m 65 kg (accessory kit) 32 kg (empty) (5500-L tank)	TM 3-4230-218-14&P
M280, Decontamination Kit, Individual Kit (DKIE)	Kit consists of 20 containers of two towelettes each. Towelettes have same decontaminates as do the M258A1 towelettes. Used on individual weapon and equipment.	77 kg (full)	TM 43-0001-26-1

The 1.5-L decontamination apparatus M-11 is man portable. It contains a nitrogen cartridge that is used as a propelling charge to pressurize the container. The DS2 is then sprayed under pressure on the contaminated surface.

The M-13 decontamination apparatus can be vehicle mounted or man portable. It consists of a pre-filled container of 14 L of DS2 and a manually operated suction pump.

The Army developed, but did not field, a hot-air decontaminating apparatus. The Army is currently developing the XM56 dual-purpose smoke and decontamination system. The system may be used to generate smoke for obscuration purposes as well as high-pressure hot water and hot air for the decontamination of interior surfaces of compartments such as electronics and optics. It uses hot air to evaporate and remove chemical agents. The fire control equipment designer must keep the potential use of hot air in mind when choosing components and materials.

7-3 HARDNESS

The extent to which equipment can withstand the damaging effects of NBC contamination and any decontamination agents and procedures required to decontaminate it is termed "hardness". Although strongly related to decontaminability, hardness is a distinct characteristic. Decontaminability refers to reducing the hazard to personnel as a result of decontamination efforts, whereas hardness refers to the condition of the equipment after it has been subjected to an agent and decontamination. Criteria for hardness were developed by analyzing vulnerabilities of construction materials to agents and decontaminants, considering mission profiles of classes of materials designed to perform mission-essential functions, and determining allowable percentage degradations of quantifiable essential performance characteristics such as reliability, availability, and maintainability (RAM) standards.

Mission-essential equipment such as fire control equipment must perform with no more than 5% degradation of essential characteristics such as detection, tracking accuracy, etc. This degradation level must remain after five exposures over a period of 30 days to NBC contaminates, decontaminates, and decontamination procedures in the field.

Hardness is achieved by designing equipment with materials that are not deteriorated by either the agent or the decontamination process. Not all materials have been tested for their reaction to all agents and decontaminants. However, many have been tested, and the results of the tests are available at the ERDEC. It is necessary to check with ERDEC to assure that exposed materials used in equipment are resistant to known agents and decontaminants.

7-3.1 NUCLEAR

The primary effects of a nuclear detonation (those that occur within one minute of the detonation) are thermal radiation, blast, initial nuclear radiation, and EMP, which are not included in AR 70-71. The secondary effects, referred to as residual radiation, are fallout, rainout, and neutron-induced gamma radiation. Radioactive particulate matter can be flushed from the surface of equipment, and these particles are covered in AR 70-71.

To satisfy operating and transportation environments of Army fire control equipment, the housing and mountings give a large measure of protection from thermal radiation and blast. Components hardened for gamma rays may be specified for use in some circumstances. EMP protection requires consideration of box, structural, and cable electromagnetic shielding; use of conductive coatings on exterior surfaces such as optical windows; ground bonding; surge suppression devices; and bypass filtering. A specialist in this area should be consulted early in the design phase.

The primary results of fallout and rainout are neutron-induced gamma radioactive particles. Although hazardous to the troops, the effects on most fire control materiel are slight.

7-3.2 CHEMICAL AND BIOLOGICAL

Biological agents include bacteria, viruses, fungi, and toxins that cause disease. Generally, these have little affect on equipment. Although fungus may grow on optics and obscure the aperture, it can be removed using appropriate cleaning procedures and solvents. However, if fungi are left on for long periods of time, secretions can cause etching of the surface and eventually failure of any protective coating.

Chemical agents are classified as nerve, blister, blood, choking, and incapacitating. HD is a blister agent. These agents can affect material. Examples of nerve agents include soman (GD) and VX.

HD, for example, has been shown to reduce the tensile strength of various elastomers such as neoprene, ethylene propylenediene, acrylic rubber, and ethylene acrylic as much as 25 to 40%. Stretched acrylic swells, exhibits hazing, and shows slight crazing when subjected to mustard contamination. HD has also been shown to increase the permeability of materials such as silicones, epoxies, urethanes, and acrylics.

Agents affect electronic components. Positive circuit elements generally become corroded (turn black) when exposed to HD, VX, and GD at about 20 V. It has also been shown that exposure of acrylic conformal coatings to HD may reduce their resistivity by 10^5, and they may become more conductive.

7-3.3 DECONTAMINANTS

As discussed in par. 7-2, decontaminants may remove the offending agents but also cause problems by interacting with materials and personnel in a detrimental way. DS2 is combustible, irritating to eyes and skin, and corrosive to silicone rubber and plastics such as polyvinyl chloride (PVC), acrylic, and polycarbonate. DS2, however, is the preferred decontaminant for Teflon®, nylon, polyethylene, and glass-epoxy laminates as well as neoprene rubber.

Thus design options exist, and careful application of MIL-HDBK-783, *Chemical and Biological (CB) Contamination Avoidance and Decontamination*, **(Ref. 4) will assist the designer to achieve appropriate levels of protection.**

7-4 COMPATIBILITY

The ability of a system to be operated, maintained, and resupplied by personnel wearing the full NBC protective ensemble is termed "compatibility". Even if a piece of equipment is completely hardened against NBC contamination and decontaminants and can also be easily decontaminated, it still must have the capability to be operated effectively while the operator is in an NBC-contaminated environment. Thus, in the development of fire control equipment designed to perform mission-essential functions, the combination of the equipment and anticipated NBC protection level of the operator must be considered.

Mission-oriented protective posture (MOPP) levels relate to successively higher protection levels afforded by individual attire. In MOPP 4, the highest level, a soldier is fully clothed in a chemical protective ensemble, including mask, hood, overboots, gloves, and overgarment. Fire control equipment must be completely operable in a contaminated environment by a soldier at MOPP 4 with no degradation in performance greater than 5%.

7-4.1 COLLECTIVE PROTECTION

Collective protection refers to a vehicle, shelter, or building that contains a means for blocking outside, unfiltered air from entering. Frequently, these means are internal overpressure systems with filtering of the recirculated internal air. In such a situation the occupants and their equipment cannot be contaminated with biological or chemical agents as long as they remain inside. The M1 tank features NBC collective protection.

Collective protection enhances compatibility because it provides crew members a clean environment until they must exit to perform some essential task outside the enclosure. Unless individual protective gear is decontaminated or discarded, reentering crewmen will enter contaminated. In some cases, agents may enter collectively protected enclosures before the enclosure is completely sealed. Thus, although collective protection may provide a "shirt sleeve" environment most of the time during a battle, it does not necessarily provide compatibility. However, for those systems for which collective protection does provide a continuously clean environment, the combat developer may elect to fulfill the compatibility requirement by substituting collective protection.

7-4.2 OPERABILITY, MAINTAINABILITY, AND RESUPPLY

Army equipment should be designed to be operated, maintained, and resupplied by personnel wearing the full MOPP 4 attire. There are inherent problems that must be kept in mind, however, when MOPP 4 attire is required. These include visual, tactile, and heat stress limitations. MIL-HDBK-759, *Human Factors Engineering Design for Army Materiel,* (Ref. 6) addresses design features for use in fire control equipment.

The protective mask requires provision for more eye relief at sight eyepieces or the observed field of view is reduced. Also the visual acuity of the operator is degraded, and more magnification may be required to achieve a given detection distance. Mask lens fogging may occur at certain temperature-humidity situations. Obviously, a collective protection system is preferred for most effective use of direct-view optics. Some advanced systems (VETRONICS) prefer electronic sensors and cathode-ray-tube (CRT) displays where magnification can be electronic as well as optical, i.e., the CRT screen is viewed from a distance; thus eye relief problems are eliminated.

Manual dexterity limitations are partly removed by enlarging the size and spacing of keys on data entry and control keyboards.

Heat stress is a function of the external environment and the level of activity. Operation may be affected only by battle stress, but maintenance and resupply can be physically intensive and may be effective only for short time intervals for any one person. Thus backup personnel are needed. Protective shelters may be a viable alternative for tasks too stressful in full protective attire.

REFERENCES

1. *NBC (Nuclear, Biological, Chemical) Contamination Survivability: A Handbook for Development/Management of Materiel Programs*, **Final Report by Battelle Columbus Laboratories, Columbus, OH, for US Army Chemical Research, Development, and Engineering Center, Aberdeen Proving Ground, MD, September 1985.**

2. **AR 70-71,** *Nuclear, Biological, and Chemical Survivability of Army Materiel*, **May 1984.**

3. **AR 70-60,** *Nuclear Survivability of Army Materiel*, **1978.**

4. **MIL-HDBK-783,** *Chemical and Biological (CB) Contamination Avoidance and Decontamination*, **15 October 1990.**

5. *Compatibility of Chemical Agents and Decontaminants With Materials*, **US Army Chemical Research, Development, and Engineering Center, Aberdeen Proving Ground, MD, 1984.**

6. **MIL-HDBK-759,** *Human Factors Engineering Design for Army Materiel*, **1 July 1987**.

Table 7-1: US ARMY FIELDED DECONTAMINATION EQUIPMENT

ITEM	DESCRIPTION AND USE	DIMENSIONS	TECHNICAL DATA REFERENCE
ABC-M11, Decontaminating Apparatus, Portable, DS2, 1 1/2 Quart NSN 4230-00-720-1618	A fire extinguisher-like device used to spray DS2. Comes with mounting bracket for attaching to vehicles. Used to spray DS2 on vehicles and equipment. Comes with spare nitrogen cylinders.	330 mm height 102 mm diameter 2.7 kg (full) 1.4 kg (empty)	TM 3-4230-204-12&P TM 43-0001-26-1
ABC-M12A2, Decontamination Apparatus, Power-Driven, Skid-Mounted (PDDA) NSN 4230-00-926-9488 LIN F81880	Includes pump unit, tank unit, personnel shower assembly, M2 water heater, all mounted on skids. Used to spray water of foam; for deicing, vehicle washing, and personnel showering.	$1.42 \times 0.81 \times 1.30$ m (pump) $3.13 \times 1.14 \times 1.30$ m (1895-dm^3 tank) $1.35 \times 0.53 \times 1.09$ m (M2 heater)	TM 3-4230-209-34P TM-3-4230-209-ESC TM 3-4410-201-12 TM 3-4410-201-20P TM 43-0001-26-1
M258, Decontamination Kit, Skin NSN 4230-00-123-3180	Kit consists of pads, scrapers, and decontamination solutions in plastic carrying case. Used for skin decontamination.	$110 \times 80 \times 60$ mm (plastic case) 0.35 kg (full)	TM 3-4230-213-10 TM 43-0001-26-1
	NOTE: This item is being replaced by the M258A1 Kit and may not be available.		
M258A1, Decontamination Kit, Personal NSN 4230-01-133-4124	Self-contained device used to apply DS2 to metal surfaces,. Has a disposable 14-dm^3 DS2 container. Can be mounted to standard 19×10^{-3} fuel can mounts on vehicles and equipment.	14×10^{-3} capacity 27 kg (filled)	TM 3-4230-214-12&P TM 43-0001-26-1
ABC-M13, Decontaminating and Reimpregnating Kit, Individual NSN 4230-00-907-4828	Decontaminating materials in a plastic case. Used to decontaminate interior of mask and other IPE.	$110 \times 80 \times 670$ mm (plastic case) 0.40 kg (filled)	TM 3-4230-211-10
	NOTE: This item is being replaced by the M258A1 Kit and may not be available.		
M17, Transportable, Lightweight Decontamination System [Same item as Air Force A/E32U-8 LDS] NSN 4230-01-153-8660	Designed to draw water from any source and deliver it at pressures up to 689 kPa and temperatures up to 120C. Includes accessory kit with hoses, cleaning jets, and personnel shower. Includes collapsible, rubberized fabric tank.	$1.02 \times 0.59 \times 0.86$ m 163 kg (basic unit) $1.06 \times 0.52 \times 0.39$ m 65 kg (accessory kit) 32 kg (empty) (5500-dm^3 tank)	TM 3-4230-218-14&P
M280, Decontamination Kit, Individual Kit (DKIE)	Kit consists of 20 containers of two towelettes each. Towelettes have same decontaminates as do the M258A1 towelettes. Used on individual weapon and equipment.	77 kg (full)	TM 43-0001-26-1

APPENDIX A
GENERAL BALLISTIC EQUATIONS

Differential equations of motion and position, a transformation from a ground fixed coordinate system to a spherical earth surface reference frame, equations for projectile yaw and orientation angles, an equation for point mass acceleration, and equations for gravity and rotational accelerations are presented. Equations for aerodynamic forces and moments (drag, spin damping, lift, overturning, Magnus, pitching, and Magnus cross) are derived.

A-0   LIST OF SYMBOLS

A = **axial moment of inertia, kg·m^2**

A_z = **azimuth of fire (clockwise from north), rad (deg)**

B = **transverse moment of inertia, kg·m^2**

d = **reference diameter of projectile, m**

$\mathbf{E}$ = **position vector of projectile with respect to spherical earth surface, m**

e_1 = **horizontal curved component of the position vector E, m**

e_2 = **vertical component of the position vector E, m**

e_3 = **transverse curved component of the position vector E, m**

$\mathbf{F}_D$ = **drag force vector, N**

F_D = **magnitude of $\mathbf{F}_D$, N**

$\mathbf{F}_F$ = **Magnus force vector, N**

F_F = **magnitude of $\mathbf{F}_F$, N**

$\mathbf{F}_L$ = **lift force vector, N**

F_L = **magnitude of $\mathbf{F}_L$, N**

$\mathbf{F}_S$ = **pitching force vector, N**

F_S = **magnitude of $\mathbf{F}_S$, N**

$\mathbf{F}_{XF}$ = **Magnus cross force vector, N**

F_{XF} = **magnitude of $\mathbf{F}_{XF}$, N**

$\mathbf{g}$ = **acceleration vector due to gravity, m/s^2**

g_o = **acceleration due to gravity at point of launch, m/s^2**

$\mathbf{H}$ = **total angular momentum vector, kg·m^2/s**

$\mathbf{h}$ = **total angular momentum vector divided by B, rad/s or s^{-1}**

$\dot{\mathbf{h}}$ = **rate of change of h, rad/s^2 or s^{-2}**

K_A = **spin damping moment coefficient, dimensionless**

K_{D_o} = **drag coefficient, dimensionless**

K_{D_α} = **yaw drag coefficient, dimensionless**

K_E = **fin cant coefficient, dimensionless**

K_F = **Magnus force coefficient, dimensionless**

K_H = **damping moment coefficient, dimensionless**

K_L = **lift force coefficient, dimensionless**

K_M = **overturning moment coefficient, dimensionless**

K_S = **pitching force coefficient, dimensionless**

K_T = **Magnus moment coefficient, dimensionless**

K_{XF} = **Magnus cross force coefficient, dimensionless**

K_{XT} = **Magnus cross moment coefficient, dimensionless**

L = **latitude of launch point, rad (deg)**

$\mathbf{M}_A$ = spin damping moment vector, N·m

M_A = magnitude of $\mathbf{M}_A$, N·m

$\mathbf{M}_H$ = damping moment vector, N·m

M_H = magnitude of $\mathbf{M}_H$, N·m

$\mathbf{M}_M$ = overturning moment vector, N·m

M_M = magnitude of $\mathbf{M}_M$, N·m

$\mathbf{M}_T$ = Magnus moment vector, N·m

M_T = magnitude of $\mathbf{M}_T$, N·m

$\mathbf{M}_{XT}$ = Magnus cross moment vector, N·m

M_{XT} = magnitude of $\mathbf{M}_{XT}$, N·m

m_P = mass of projectile, kg

R = radius of earth at point of launch, m

r = distance between center of earth and projectile, m

t = time, s

$\mathbf{u}$ = velocity vector of projectile with respect to ground, m/s

u_1 = horizontal component of the velocity vector $\mathbf{u}$, m/s

u_2 = vertical component of the velocity vector $\mathbf{u}$, m/s

u_3 = transverse component of the velocity vector $\mathbf{u}$, m/s

$\dot{\mathbf{u}}$ = acceleration vector of projectile with respect to ground, m/s^2

$\mathbf{v}$ = velocity vector of projectile with respect to air, m/s

$v = |\mathbf{v}|$, m/s

v_2 = vertical component of $\mathbf{v}$, m/s

$\mathbf{X}$ = position vector of projectile with respect to ground (at time t), m

X_1 = horizontal component of $\mathbf{X}$ in fixed earth coordinate system, m

X_2 = vertical component of $\mathbf{X}$ in fixed earth coordinate system, m

X_3 = transverse component of $\mathbf{X}$ in fixed earth coordinate system, m

$\mathbf{x}$ = unit vector along longitudinal axis of projectile, dimensionless

x_2 = vertical component of $\mathbf{x}$, dimensionless

$\dot{\mathbf{x}}$ = rate of change (time derivative) of $\mathbf{x}$, s^{-1} or rad/s

$\dot{x}$ = magnitude of $\dot{\mathbf{x}}$, rad/s

$\mathbf{y}$ = unit vector perpendicular to $\mathbf{x}$, dimensionless

$\dot{\mathbf{y}}$ = rate of change (time derivative) of $\mathbf{y}$, s^{-1} or rad/s

$\mathbf{z}$ = unit vector perpendicular to both $\mathbf{x}$ and $\mathbf{y}$, ($\mathbf{z} = \mathbf{x} \times \mathbf{y}$), dimensionless

$\dot{\mathbf{z}}$ = rate of change (time derivative) of $\mathbf{z}$, s^{-1} or rad/s

δ = yaw angle of projectile, rad

ε = angle of elevation of launch, rad

Λ = acceleration vector due to rotation of earth, m/s^2

$\lambda_1, \lambda_2, \lambda_3$ = components of the local earth rotation velocity vector at launch latitude L and firing azimuth A_z, rad/s

ρ = air density (varies with altitude), kg/m^3

ϕ = yaw orientation angle, rad

Ω = angular rotational speed of the earth, rad/s

ω = projectile total rotation vector, rad/s

ω_x = projectile spin rate, rad/s

ω_y = projectile rotation rate about the y-axis, rad/s

ω_z = projectile rotation rate about the x-axis, rad/s

A-1   INTRODUCTION

The two coupled nonlinear vector differential equations that follow are the result of setting all forces acting on the projectile in flight to the vector acceleration of the center of mass and of setting all moments acting on the projectile in flight to the vector angular momentum time derivative. Several supporting relationships that define the parameters involved are also given. Two successive integrations of the three components of projectile vector acceleration yield the position of the center of mass in an earth-oriented reference frame. The two successive integrations in those components of the time derivative of the vector angular momentum yield projectile attitude, which is required in the solution of the force equation. A brief discussion of the forces and moments that drive this differential equation representation of a spinning projectile is also presented. The report (Ref. 1) from which this material has been extracted includes treatment of the finned rocket trajectory equations.

A computer program that provides the solution to the equations, given the appropriate aeroballistic package for the projectile of interest and the governing initial conditions, has been developed by the US Army Research Laboratory, Aberdeen Proving Ground, MD, (formerly the US Army Ballistic Research Laboratory) and has been used extensively and successfully for many years. The application of the program is described in Ref. 2. When the equations are used to generate firing tables, boundary conditions are not required. In the solution of the fire control problem, the point through which the projectile must pass is an additional constraint, which is not treated in this six-degree model. Although the equations given here are expressed as differential equations, the numerical techniques used reduce them to difference equations, and they can then be readily expressed in matrix form.

A-2   GENERAL BALLISTIC EQUATIONS

The following are the vector differential equations of motion:

$$\dot{\mathbf{u}} = -\frac{\rho d^2}{m_P}\left(K_{D_o} + K_{D_\alpha}\delta^2\right)v\mathbf{v} + \frac{\rho d^2}{m_P}K_L\left[v^2\mathbf{x} - (\mathbf{v}\cdot\mathbf{x})\mathbf{v}\right]$$

$$-\frac{\rho d^3}{m_P}K_S v(\mathbf{h}\times\mathbf{x}) + \frac{\rho d^3}{m_P}\frac{B}{A}K_F(\mathbf{h}\cdot\mathbf{x})(\mathbf{x}\times\mathbf{v}) \qquad\text{(A-1)}$$

$$+\frac{\rho d^4}{m_P}\frac{B}{A}K_{XF}(\mathbf{h}\cdot\mathbf{x})\left[\mathbf{h} - (\mathbf{h}\cdot\mathbf{x})\mathbf{x}\right] + \mathbf{g}, \ \text{m/s}^2$$

where

$\mathbf{u}$ = velocity vector of projectile with respect to ground, m/s

$\dot{\mathbf{u}}$ = acceleration vector of projectile with respect to ground (time derivative of $\mathbf{u}$), m/s^2

ρ = air density (varies with altitude), kg/m^3

d = reference diameter of projectile, m

m_P = mass of projectile, kg

K_{D_o} = drag coefficient, dimensionless

K_{D_α} = yaw drag coefficient, dimensionless

δ = yaw angle of projectile, rad

$\mathbf{v}$ = velocity vector of projectile with respect to air, m/s

$v = |\mathbf{v}|$, m/s

K_L = lift force coefficient, dimensionless

$\mathbf{x}$ = unit vector along longitudinal axis of projectile, dimensionless

K_S = pitching force coefficient, dimensionless

h = total angular momentum vector divided by B, **rad/s or s^{-1}**
B = **transverse moment of inertia, kg·m^2**
A = **axial moment of inertia, kg·m^2**
K_F = **Mangus force coefficient, dimensionless**
K_{XF} = **Magnus cross force coefficient, dimensionless**
g = **acceleration vector due to gravity, m/s^2,**

and

$$\dot{\mathbf{h}} = \frac{\rho d^3}{B} K_M v (\mathbf{v} \times \mathbf{x}) - \frac{\rho d^4}{B} K_H v [\mathbf{h} - (\mathbf{h} \cdot \mathbf{x}) \mathbf{x}]$$

$$- \frac{\rho d^4}{A} K_A v (\mathbf{h} \cdot \mathbf{x}) \mathbf{x} + \frac{\rho d^3}{B} K_E \varepsilon v^2 \mathbf{x}$$

$$+ \frac{\rho d^4}{A} K_T (\mathbf{h} \cdot \mathbf{x}) [(\mathbf{v} \cdot \mathbf{x}) \mathbf{x} - \mathbf{v}]$$

$$- \frac{\rho d^5}{A} K_{XT} (\mathbf{h} \cdot \mathbf{x}) (\mathbf{h} \times \mathbf{x}), \ \text{rad/s}^2$$

(A-2)

where
$\dot{\mathbf{h}}$ = **rate of change of h, rad/s^2 or s^{-2}**
K_M = **overturning moment coefficient, dimensionless**
K_H = **damping moment coefficient, dimensionless**
K_A = **spin damping moment coefficient, dimensionless**
K_E = **fin cant coefficient, dimensionless**
ε = **angle of elevation of launch, rad**
K_T = **Magnus moment coefficient, dimensionless**
K_{XT} = **Magnus cross moment coefficient, dimensionless.**

In addition to these two basic differential equations, the equations relating the projectile-centered co-ordinate system to a projectile-centered ground fixed coordinate system denoted by the unit vectors **x, y,** and **z** are needed. By definition

$$\mathbf{H} = A\omega_x \mathbf{x} + B\omega_y \mathbf{y} + B\omega_z \mathbf{z}, \ \text{kg} \cdot \text{m/s}^2 \tag{A-3}$$

where
H = **total angular momentum vector, kg·m/s^2**
ω_x = **projectile spin rate about the x-axis, rad/s**
ω_y = **projectile rotation rate about the y-axis, rad/s**
y = **unit vector perpendicular to x, dimensionless**
ω_z = **projectile rotation rate about the z-axis, rad/s**
z = **unit vector perpendicular to body x and y (z = x $\times$ y), dimensionless.**

By definition

$$\boldsymbol{\omega} = \omega_x \mathbf{x} + \omega_y \mathbf{y} + \omega_z \mathbf{z}, \ \text{rad/s} \tag{A-4}$$

where
ω = **projectile total rotation vector, rad/s.**

Then

$$\mathbf{h} = \frac{\mathbf{H}}{B} = \frac{A}{B}\omega_x\mathbf{x} + \omega_y\,\mathbf{y} + \omega_z\mathbf{z}$$

$$= \omega - \omega_x\mathbf{x} + \frac{A}{B}(\omega_x\mathbf{x}) \tag{A-5}$$

$$= \omega - \frac{B-A}{B}\omega_x\mathbf{x}, \;\; \text{rad/s.}$$

Taking the dot product of h and x and noting that y · x and z · x are both zero yield

$$\mathbf{h} \cdot \mathbf{x} = \frac{A}{B}\omega_x\,(\mathbf{x} \cdot \mathbf{x}) + \omega_y\,(\mathbf{y} \cdot \mathbf{x}) + \omega_z\,(\mathbf{z} \cdot \mathbf{x})$$

$$= \frac{A}{B}\omega_x, \;\; \text{rad/s.} \tag{A-6}$$

From which

$$\omega_x = \frac{B}{A}(\mathbf{h} \cdot \mathbf{x}), \;\; \text{rad/s.} \tag{A-7}$$

Taking the cross product of h and x and noting that x × x is zero and ω × x is $\dot{\mathbf{x}}$ yield

$$\mathbf{h} \times \mathbf{x} = \left(\omega - \frac{B-A}{B}\omega_x\mathbf{x}\right) \times \mathbf{x} \tag{A-8}$$

$$= (\omega \times \mathbf{x}) - 0$$

$$= \dot{\mathbf{x}}, \text{rad/s}$$

where

$\dot{\mathbf{x}}$ = rate of change (time derivative), s^{-1} or rad/s.

Taking the cross product of h and y and noting that x × y is z, ω × y is $\dot{\mathbf{y}}$, and $\omega_x = (\mathbf{h} \cdot \mathbf{x})B/A$ yield

$$\mathbf{h} \times \mathbf{y} = \left(\omega - \frac{B-A}{B}\omega_x\mathbf{x}\right) \times \mathbf{y}$$

$$= (\omega \times \mathbf{y}) - \frac{B-A}{B}\omega_x\,(\mathbf{x} \times \mathbf{y}) \tag{A-9}$$

$$= \dot{\mathbf{y}} - \frac{B-A}{A}(\mathbf{h} \cdot \mathbf{x})\,\mathbf{y}, \;\; \text{rad/s}$$

where

$\dot{\mathbf{y}}$ = rate of change (time derivative) of y, s^{-1} or rad/s.

From which

$$\dot{\mathbf{y}} = (\mathbf{h} \times \mathbf{y}) + \frac{B-A}{A}(\mathbf{h} \cdot \mathbf{x})\,\mathbf{y}, \;\; \text{rad/s.} \tag{A-10}$$

Taking the cross product of h and z and noting that x × z is –y, ω × z is $\dot{z}$, and $\omega_x = \dfrac{B}{A}$ (h · x) yield

$$\mathbf{h} \times \mathbf{z} = \left(\omega - \frac{B - A}{B} \omega_x \mathbf{x} \right) \times \mathbf{z}$$

$$= (\omega \times \mathbf{z}) - \frac{B - A}{B} \omega_x (\mathbf{x} \times \mathbf{z}) \qquad \text{(A-11)}$$

$$= \dot{\mathbf{z}} + \frac{B - A}{A} (\mathbf{h} \times \mathbf{x}) \mathbf{z}, \ \text{rad/s}$$

where

   $\dot{z}$ = rate of change (time derivative) of z, s^{-1} or rad/s.

From which

$$\dot{\mathbf{z}} = (\mathbf{h} \times \mathbf{z}) - \frac{B - A}{A} (\mathbf{h} \cdot \mathbf{x}) \mathbf{z}, \ \text{rad/s.} \qquad \text{(A-12)}$$

   The position of the projectile center of mass in the ground fixed coordinate system is represented by the vector **X** and is given by the integral

$$\mathbf{X} = \int_0^t \mathbf{u} \, dt \qquad \text{(A-13)}$$

where

   X = position vector of projectile with respect to ground (at time t), m

   t = time, s.

   The projectile center of mass position with respect to the spherical earth surface is denoted by **E**. The vector **E** is related to the radius of the earth R and to **X** by

$$\mathbf{E} = \begin{bmatrix} \dfrac{RX_1}{\sqrt{X_1^2 + X_3^2}} \arctan\left(\dfrac{\sqrt{X_1^2 + X_3^2}}{R + X_2} \right) \\[4ex] \sqrt{(R + X_2)^2 + \left(X_1^2 + X_3^2 \right)} - R \\[4ex] \dfrac{RX_3}{\sqrt{X_1^2 + X_3^2}} \arctan\left(\dfrac{\sqrt{X_1^2 + X_3^2}}{R + X_2} \right) \end{bmatrix}, \ \text{m} \qquad \text{(A-14)}$$

where

   E = position vector of projectile with respect to spherical earth surface, m

   R = radius of earth at point of launch, m

   X_1 = horizontal component of **X** in fixed earth coordinate system, m

   X_2 = vertical component of **X** in fixed earth coordinate system, m

   X_3 = transverse component of **X** in fixed earth coordinate system, m.

The relationship between **X** and **E** is shown in Fig. A-1, i.e., e_1, e_2, and e_3 are the respective horizontal curved, vertical, and transverse curved components of the position vector **E** in the spherical earth surface coordinate system.
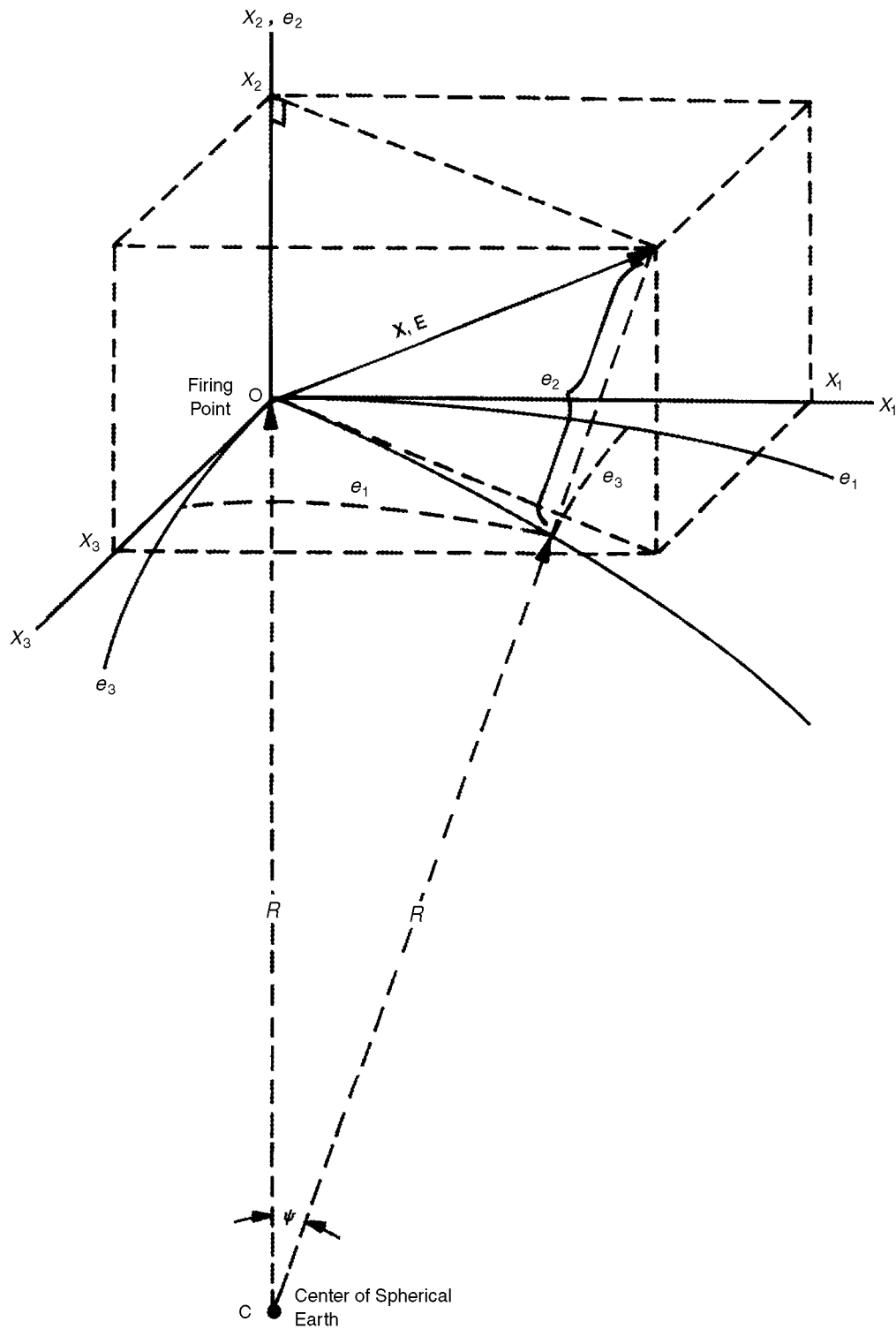
Figure A-1. Relationship Between X and E

A-2.1 YAW AND ORIENTATION OF YAW

The yaw of a projectile δ is the included angle between the vectors $\mathbf{x}$ and $\mathbf{v}$ and is always defined as a positive quantity. Since the dot product of two vectors equals the product of their magnitudes multiplied by the cosine of their included angle, the magnitude of yaw is given by

$$\delta = \cos^{-1}\left(\frac{\mathbf{v} \cdot \mathbf{x}}{|\mathbf{v}|}\right), \text{ rad.} \qquad \text{(A-15)}$$

The orientation of yaw is the angle between the plane containing both $\mathbf{y}$ and $\mathbf{x}$ and a vertical plane containing $\mathbf{v}$ and is measured clockwise from the vertical plane as viewed from the firing point. Yaw orientation ϕ is given by

$$\phi = \begin{Bmatrix} \cos^{-1}\left(\dfrac{vx_2 - v_2\cos\delta}{v\sin\delta}\right), & \delta = 0 \\ 0 & , & \delta = 0 \end{Bmatrix}, \text{ rad} \qquad \text{(A-16)}$$

where

ϕ = yaw orientation angle, rad

v_2 = vertical component of $\mathbf{v}$, m/s

x_2 = vertical component of $\mathbf{x}$, dimensionless.

The angle ϕ becomes indeterminate when δ is zero in Eq. A-16. If ϕ is defined as zero when δ equals zero, Eq. A-16 becomes continuous for all values of δ.

A-2.2 POINT MASS EQUATION

The general six-degree-of-freedom differential equations reduce to the three-degree-of- freedom representation when the projectile takes on the characteristics of a point mass. Since the moments associated with a rigid body theoretically no longer exist, the angular momentum equation is not applicable. Forces derivable from the rigid body treatment are removed from the linear acceleration vector equation resulting in the simplified form that follows:

$$\dot{\mathbf{u}} = -\frac{\rho d^2}{m_P} K_{D_o} v\mathbf{v} + \mathbf{g} + \mathbf{\Lambda}, \text{ m/s}^2 \qquad \text{(A-17)}$$

where

$\mathbf{\Lambda}$ = acceleration vector due to rotation of earth, m/s^2.

The equation is still a nonlinear, nonhomogeneous differential equation that does not have a closed form analytic solution. It is a subset of the more general ballistic six-degree representation, and as such, the numerical techniques used in its solution still apply. However, because of its relative simplicity and solution speed, the equation has been used to solve the fire control boundary problem, i.e., having the projectile pass through a given fixed point.

Since the time of Archimedes, attempts have been made to find an analytical closed form solution to the equation by making assumptions about the form of drag coefficients. These have resulted in approximate solutions that have been useful in certain specialized cases. Today, Newton's solution, i.e., assuming zero drag, has application in outer space. Approximate solutions have also provided forms for structuring curve fit representations.

A-3   AERODYNAMIC FORCES AND MOMENTS

A force or moment is defined to be aerodynamic in origin if it is produced by interaction of a rigid body and its atmospheric medium. The aerodynamic forces and moments presented in this appendix are those considered necessary to form a logically consistent mathematical model for a rigid body possessing rotational symmetry.

A-3.1   DRAG

Drag is historically defined as resistance to the forward motion of a projectile. The magnitude of drag force $\mathbf{F}_D$ is represented in classical exterior ballistics as

$$F_D = \rho d^2 K_{D_o} v^2, \text{ N} \tag{A-18}$$

where

F_D = magnitude of $\mathbf{F}_D$ ($F_D = |\mathbf{F}_D|$), N
$\mathbf{F}_D$ = drag force vector, N.

If the forward velocity with respect to air is represented by the vector **v**, the direction of drag is the direction of –**v**.

Fig. A-2 illustrates the general case of a projectile with the unit vector **x** pointing along the axis of symmetry, and the forward velocity is represented by **v**. The angle between **x** and **v**, denoted by δ, is traditionally called the angle of yaw, or yaw angle.

Yaw increases drag on a projectile by presenting an enlarged cross-sectional area to the airstream. The effect of yaw on drag is accounted for by allowing K_{D_o} to increase with yaw squared. The yaw drag coefficient is denoted by K_{D_α}, and the increase in the drag coefficient due to yaw is then given by $K_{D_\alpha}\delta^2$. Based on these definitions, drag force is represented by the vector equation:

$$\mathbf{F}_D = -\rho d^2 \left(K_{D_o} + K_{D_\alpha}\delta^2 \right) v\mathbf{v}, \text{ N}. \tag{A-19}$$
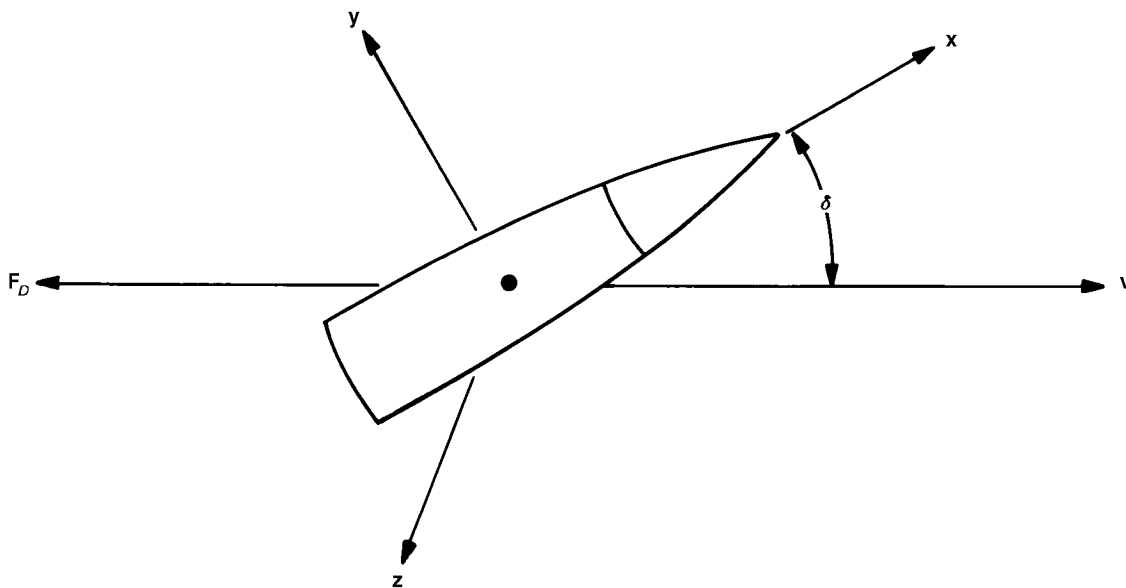
Figure A-2. Drag Force (Ref. 1)

A-3.2 SPIN DAMPING MOMENT

The spin damping moment is an aerodynamic moment produced by viscous friction of the air on the surface of a spinning projectile, and because it acts opposite to spin, it tends to destroy longitudinal axial spin, as shown in Fig. A-3.
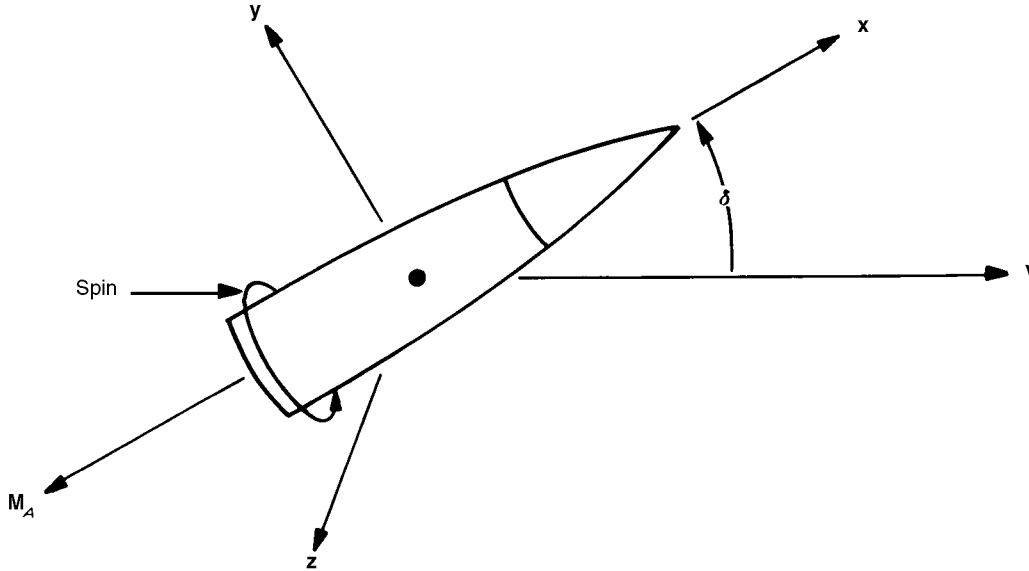
Figure A-3. Spin Damping Moment (Ref. 1)

The magnitude of the spin damping moment is given by

$$M_A = \rho d^4 K_A \omega_x v, \ \mathbf{N \cdot m} \tag{A-20}$$

where

M_A = magnitude of $\mathbf{M}_A$ ($M_A = |\mathbf{M}_A|$), N·m

$\mathbf{M}_A$ = spin damping moment vector, N·m.

Since the spin damping moment opposes axial spin, its direction is the direction of $-\mathbf{x}$. The vector representation of the spin damping moment is given by

$$\mathbf{M}_A = -\rho d^4 K_A \omega_x v \mathbf{x}, \ \ \mathbf{N \cdot m}. \tag{A-21}$$

Replacing ω_x with its equivalent, as obtained in Eq. A-7, yields

$$\mathbf{M}_A = -\frac{\rho d^4 B}{A} K_A v (\mathbf{h} \cdot \mathbf{x}) \, \mathbf{x}, \ \ \mathbf{N \cdot m}. \tag{A-22}$$

A-3.3   LIFT FORCE

Aerodynamic lift is created by an asymmetric airflow over a yawed body. The magnitude of the lift force is given by

$$F_L = \rho d^2 K_L v^2 \sin\delta, \ \text{N} \qquad\qquad \textbf{(A-23)}$$

where

F_L = magnitude of $\mathbf{F}_L$ ($F_L = |\mathbf{F}_L|$), N
$\mathbf{F}_L$ = lift force vector, N.

The lift force acts in the plane of yaw and is perpendicular to the direction of motion of the projectile.

Fig. A-4 illustrates the vector representation of the lift force. Consider the vector [$\mathbf{v} \times (\mathbf{x} \times \mathbf{v})$] . This vector has the magnitude $v^2 \sin\delta$ and is perpendicular to $\mathbf{v}$ in the plane containing $\mathbf{v}$ and $\mathbf{x}$. The vector representation of lift force is then given by

$$\mathbf{F}_L = \rho d^2 K_L [\mathbf{v} \times (\mathbf{x} \times \mathbf{v})], \ \text{N.} \qquad\qquad \textbf{(A-24)}$$

Expanding the triple vector product and rewriting yield

$$\mathbf{F}_L = \rho d^2 K_L \left[v^2 \mathbf{x} - (\mathbf{v} \cdot \mathbf{x}) \mathbf{v} \right], \ \text{N.} \qquad\qquad \textbf{(A-25)}$$

The vector sum of the lift and drag forces can be expressed as a total resistance vector. If the components of vector resistance are resolved parallel and perpendicular to $\mathbf{x}$ instead of $\mathbf{v}$, the axial drag force and normal force result. The normal force is the component of the vector resistance that produces the overturning moment.
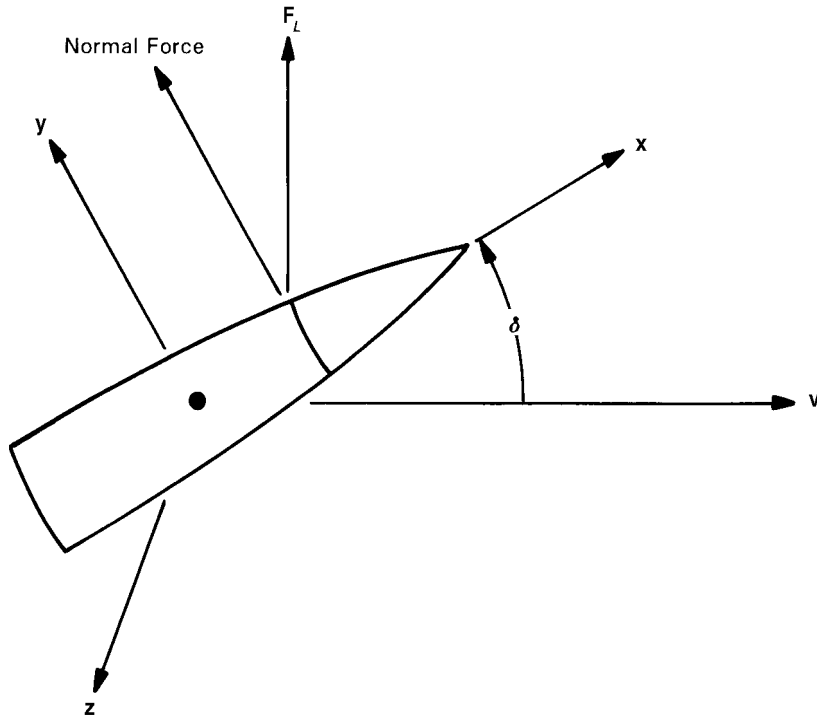
Figure A-4. Lift Force (Ref. 1)

A-3.4 OVERTURNING MOMENT

If the line of action of the aerodynamic normal force does not pass through the center of mass of the projectile, an overturning moment is produced. The magnitude of the overturning moment due to normal force is given by

$$M_M = \rho d^3 K_M v^2 \sin\delta \, , \, \text{N·m} \tag{A-26}$$

where

M_M = magnitude of $\mathbf{M}_M$ ($M_M = |\mathbf{M}_M|$), N·m
$\mathbf{M}_M$ = overturning moment vector, N·m.

The overturning moment is perpendicular to the plane of yaw, or to both **v** and **x**, as illustrated in Fig. A-5. The vector (**v** × **x**) has the proper direction, and in magnitude is equal to $v\sin\delta$. The overturning moment vector is then given by

$$\mathbf{M}_M = \rho d^3 K_M v (\mathbf{v} \times \mathbf{x}), \quad \text{N·m.} \tag{A-27}$$

If the line of action of normal force intersects the axis of symmetry at a point behind the center of mass, the overturning moment acts as a restoring moment. This situation is met by allowing K_M to be negative. The addition of fins at the rear of a body of revolution moves the center of pressure of the normal force to the rear, and usually results in a negative K_M, or restoring moment.
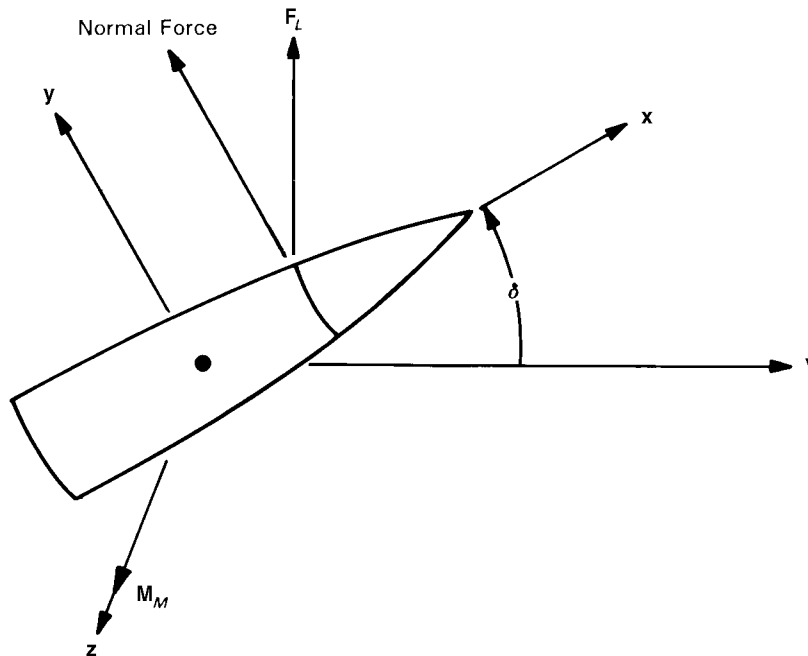
Figure A-5. Overturning Moment (Ref. 1)

A-3.5 MAGNUS FORCE

The Magnus force arises from the interaction of the airstream and the boundary layer of a yawed spinning body. The magnitude of the Magnus force is given by

$$F_F = \rho d^3 K_F \omega_x v \sin\delta, \text{ N}$$
(A-28)

where

F_F = magnitude of $\mathbf{F}_F (F_F = |\mathbf{F}_F|)$, N
$\mathbf{F}_F$ = Mangus force vector, N.

The direction of the Magnus force is perpendicular to the plane of yaw and is represented by the vector $(\mathbf{x} \times \mathbf{v})$ for positive values of ω_x, as illustrated in Fig. A-6. The Magnus force is represented by the vector equation:

$$\mathbf{F}_F = \rho d^3 K_F \omega_x (\mathbf{x} \times \mathbf{v}), \text{ N}.$$
(A-29)

Replacing ω_x with its equivalent, as obtained in Eq. A-7, yields

$$\mathbf{F}_F = \frac{\rho d^3 B}{A} K_F (\mathbf{h} \cdot \mathbf{x}) (\mathbf{x} \times \mathbf{v}), \text{ N}.$$
(A-30)
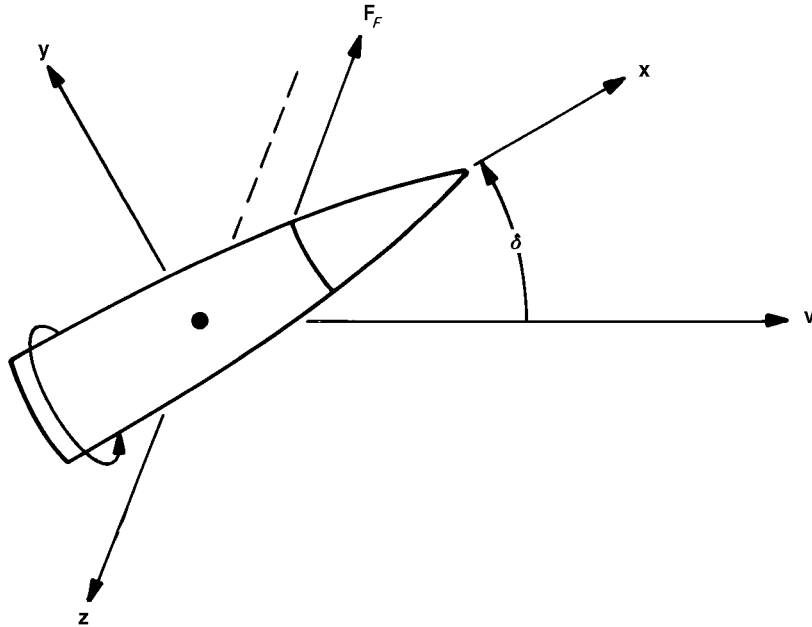
Figure A-6. Magnus Force (Ref. 1)

A-3.6 MAGNUS MOMENT

If the line of action of the Magnus force does not pass through the center of mass of the projectile, a Magnus moment is produced. The magnitude of the Magnus moment is given by

$$M_T \ = \ \rho d^4 K_T \omega_x v \sin\delta \,, \ \text{N·m} \tag{A-31}$$

where

M_T = magnitude of $\mathbf{M}_T (M_T = |\mathbf{M}_T|)$, N·m

$\mathbf{M}_T$ = Magnus moment vector, N·m.

The Magnus moment lies in the plane of yaw and is perpendicular to **x**. The vector [**x** × (**x** × **v**)] has the magnitude $v\sin\delta$ and has the proper direction, as illustrated in Fig. A-7. The Magnus moment is represented by the vector equation:

$$\mathbf{M}_T \ = \ \rho d^4 K_T \omega_x [\mathbf{x} \times (\mathbf{x} \times \mathbf{v})] , \ \text{N·m.} \tag{A-32}$$

Replacing ω_x with its vector equivalent and expanding the vector triple product yield

$$\mathbf{M}_T \ = \ \frac{-\rho d^4 B}{A} K_T (\mathbf{h} \cdot \mathbf{x}) [(\mathbf{v} \cdot \mathbf{x}) \mathbf{x} - \mathbf{v}], \ \text{N·m.} \tag{A-33}$$
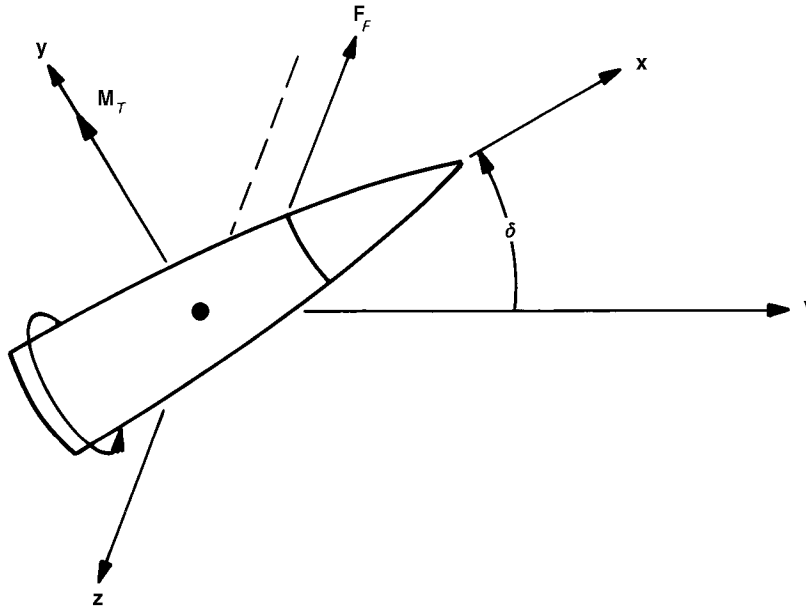
Figure A-7. Magnus Moment (Ref. 1)

A-3.7 PITCHING FORCE

The pitching force is a force opposing any change in the direction of the longitudinal axis of a projectile. If the unit vector $\mathbf{x}$ is in motion, its vector rate of change $\dot{\mathbf{x}}$ is in the plane of motion and is perpendicular to $\mathbf{x}$. If $\dot{x}$ represents the scalar magnitude of $\dot{\mathbf{x}}$, the magnitude of the pitching force is given by

$$F_S = \rho d^3 K_S v\dot{x}, \quad \text{N} \tag{A-34}$$

where

F_S = magnitude of $\mathbf{F}_S$ ($F_S = |\mathbf{F}_S|$), N
$\mathbf{F}_S$ = pitching force vector, N
$\dot{x}$ = magnitude of $\dot{\mathbf{x}}$ ($\dot{x} = |\dot{\mathbf{x}}|$), rad/s.

The direction of the pitching force is parallel to $\dot{\mathbf{x}}$ and oppositely sensed, as illustrated in Fig. A-8. The vector representation of the pitching force is

$$\mathbf{F}_S = -\rho d^3 K_S v\dot{\mathbf{x}}, \quad \text{N.} \tag{A-35}$$

Replacing $\dot{\mathbf{x}}$ with its vector equivalent, as obtained in Eq. A-8, yields

$$\mathbf{F}_S = -\rho d^3 K_S v(\mathbf{h} \times \mathbf{x}), \quad \text{N.} \tag{A-36}$$
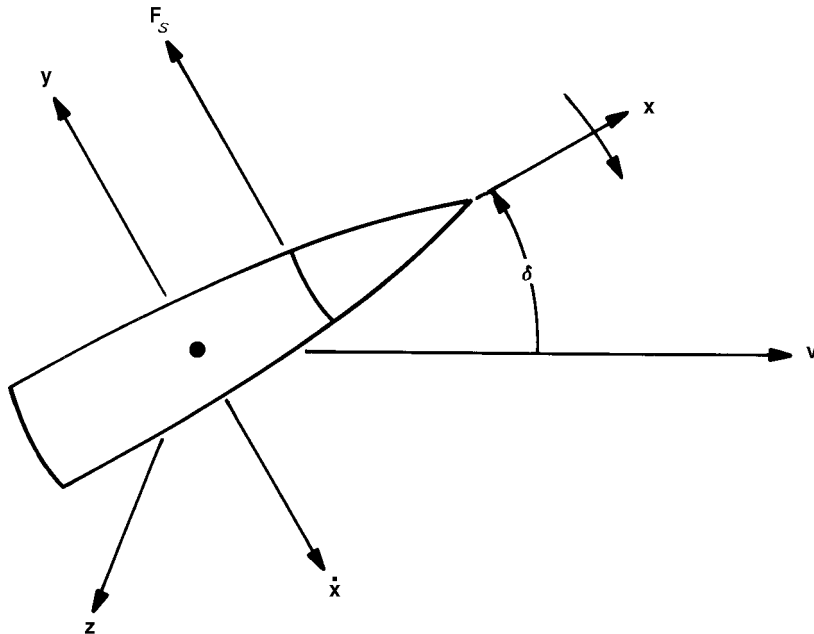
Figure A-8. Pitching Force (Ref. 1)

A-3.8   DAMPING MOMENT

The damping moment is a moment opposing angular velocity of the longitudinal axis of a projectile and is the aerodynamic moment associated with pitching force. If the unit vector **x** is in motion, its vector rate of change is $\dot{\mathbf{x}}$, and the transverse angular velocity vector is (**x** × $\dot{\mathbf{x}}$). The magnitude of the damping moment is given by

$$M_H = \rho d^4 K_H v\dot{x}, \text{ N·m} \tag{A-37}$$

where

M_H = magnitude of $\mathbf{M}_H$ ($M_H = |\mathbf{M}_H|$), N·m

$\mathbf{M}_H$ = damping moment vector, N·m.

The direction of the moment is parallel to (**x** × $\dot{\mathbf{x}}$) and oppositely sensed, as illustrated in Fig. A-9. The damping moment is represented by the vector equation:

$$\mathbf{M}_H = -\rho d^4 K_H v(\mathbf{x} \times \dot{\mathbf{x}}), \text{ N·m.} \tag{A-38}$$

Replacing $\dot{\mathbf{x}}$ with its vector equivalent, as obtained in Eq. A-8 and expanding the resulting triple vector product yield

$$\mathbf{M}_H = -\rho d^4 K_H v[\mathbf{h} - (\mathbf{h} \cdot \mathbf{x})\mathbf{x}], \text{ N·m.} \tag{A-39}$$
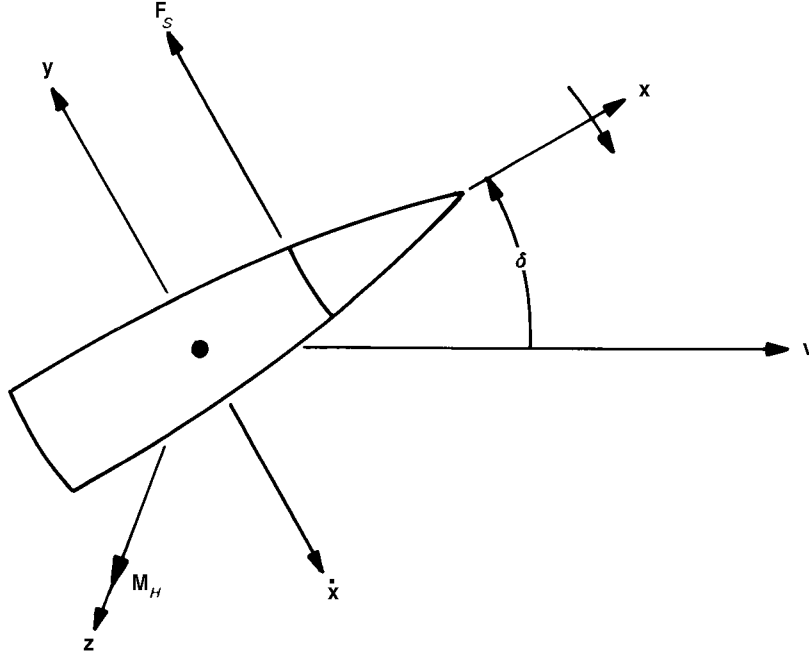
Figure A-9. Damping Moment (Ref. 1)

A-3.9 MAGNUS CROSS FORCE

The Magnus cross force is a Magnus force arising from a transverse angular velocity of the projectile longitudinal axis. The magnitude of the Magnus cross force is given by

$$F_{XF} = \rho d^4 K_{XF} \omega_x \dot{x}, \quad N \tag{A-40}$$

where

F_{XF} = **magnitude of** $\mathbf{F}_{XF} (F_{XF} = |\mathbf{F}_{XF}|)$, N
$\mathbf{F}_{XF}$ = **Magnus cross force vector, N.**

The direction of the Magnus cross force is parallel to the vector $(\mathbf{x} \times \dot{\mathbf{x}})$ and has the same sense for positive values of ω_x, as shown in Fig. A-10. The Magnus cross force is represented by the vector equation:

$$\mathbf{F}_{XF} = \rho d^4 K_{XF} \omega_x (\mathbf{x} \times \dot{\mathbf{x}}), \quad N. \tag{A-41}$$

Replacing ω_x and $\dot{\mathbf{x}}$ with their respective vector equivalents, as obtained in Eqs. A-7 and A-8 and expanding the resulting triple vector product yield

$$\mathbf{F}_{XF} = \frac{\rho d^4 B}{A} K_{XF} (\mathbf{h} \cdot \mathbf{x}) [\mathbf{h} - (\mathbf{h} \cdot \mathbf{x}) \mathbf{x}], \quad N. \tag{A-42}$$
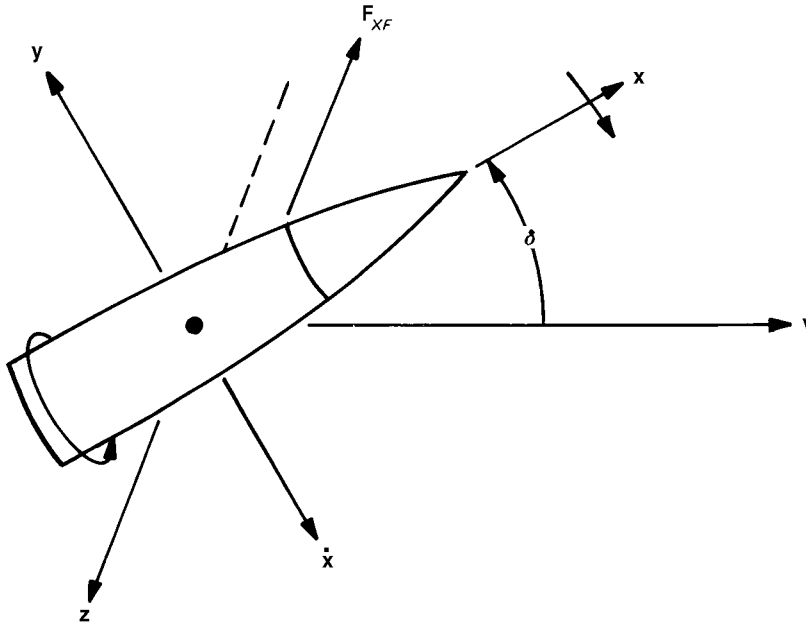
Figure A-10. Magnus Cross Force (Ref. 1)

A-3.10 MAGNUS CROSS MOMENT

The Magnus cross moment is the aerodynamic moment associated with the Magnus cross force. The magnitude of the Magnus cross moment is given by

$$M_{XT} = \rho d^5 K_{XT} \omega_x \dot{x} \text{, N·m} \tag{A-43}$$

where
M_{XT} = magnitude of $\mathbf{M}_{XT}$ (M_{XT} = $|\mathbf{M}_{XT}|$), N·m
$\mathbf{M}_{XT}$ = Magnus cross moment vector, N·m
K_{XT} = Magnus cross moment coefficient, dimensionless.

Since the direction of the Magnus cross moment is parallel to $\dot{x}$ and oppositely sensed, as shown in Fig. A-11, the Magnus cross moment is represented by the vector equation:

$$\mathbf{M}_{XT} = -\rho d^5 K_{XT} \omega_x \dot{\mathbf{x}} \text{, N·m.} \tag{A-44}$$

Replacing ω_x and $\dot{x}$ with their respective vector equivalents, as obtained in Eqs. A-7 and A-8, yields

$$\mathbf{M}_{XT} = -\frac{\rho d^5 B}{A} K_{XT} (\mathbf{h} \cdot \mathbf{x})(\mathbf{h} \times \mathbf{x}) \text{, N·m.} \tag{A-45}$$
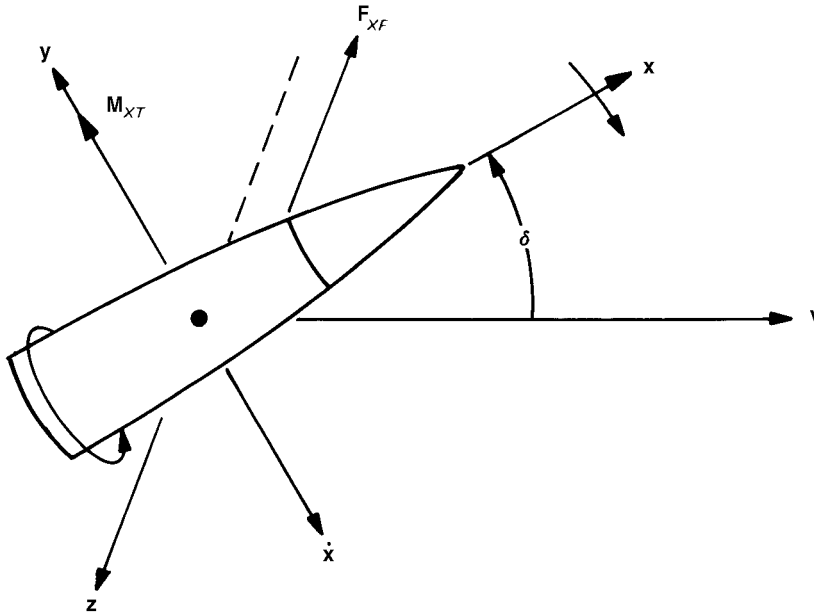
Figure A-11. Magnus Cross Moment (Ref. 1)

The dimensionless aerodynamic coefficients are functions of many dimensionless power products, including the dimensionless shape parameters, Reynolds number, and Mach number. Aerodynamic coefficients are defined with reference to a specific set of shape parameters and may be expressed as functions of Mach number. Additional aerodynamic coefficients may be included to account for the variation of aerodynamic forces and moments with yaw.

A-4 GRAVITY AND ROTATIONAL ACCELERATIONS

The acceleration due to gravity is caused by the force of gravitational attraction between a body and the earth. The magnitude of gravitational force is proportional to the mass of the body and inversely proportional to the squared distance between the centers of mass of the body and of the earth. The line of action is directed from the mass center of the body to the mass center of the earth.

It is assumed that a spherical earth is a sufficiently good approximation for the purpose of trajectory simulation. The position of the projectile center of mass is specified by the vector $\mathbf{X}$ in the ground fixed coordinate system. The force of gravity is approximated by the vector equation:

$$\mathbf{g} = -g_o \frac{R^2}{r^3} \begin{bmatrix} X_1 \\ X_2 + R \\ X_3 \end{bmatrix}, \ \text{m/s}^2 \tag{A-46}$$

where

g_o = acceleration due to gravity at point of launch, m/s^2

r = distance between center of earth and projectile, m

and

$$r = [X_1^2 + (X_2 + R)^2 + X_3^2]^{1/2}, \ \text{m.} \tag{A-47}$$

In the derivation of the force-moment system, all vectors have been referenced to the ground fixed coordinate system. Since the earth is spinning about an axis passing through its center of mass, the acceleration produced by rotation of the earth must be added to the force equation. The acceleration due to rotation of the earth is represented by the vector equation:

$$\mathbf{\Lambda} = \begin{bmatrix} -\lambda_1 u_2 - \lambda_2 u_3 \\ \lambda_1 u_1 + \lambda_3 u_3 \\ \lambda_2 u_1 - \lambda_3 u_2 \end{bmatrix}, \ \text{m/s}^2 \tag{A-48}$$

where

$\lambda_1, \lambda_2, \lambda_3$ = components of local earth rotation velocity vector at launch latitude L and firing azimuth A_z, rad/s

u_1, u_2, u_3 = horizontal, vertical, and transverse velocity $\mathbf{u}$ of the missile with respect to ground, m/s.

The λ's are defined as

$$\lambda_1 = 2\Omega \cos L \sin A_z, \ \text{rad/s}$$
$$\lambda_2 = 2\Omega \sin L, \ \text{rad/s} \tag{A-49}$$
$$\lambda_3 = 2\Omega \cos L \cos A_z, \ \text{rad/s}$$

where

Ω = angular rotational speed of the earth, rad/s

L = latitude of launch point, rad (deg)

A_z = azimuth of fire (clockwise from north), rad (deg).

L is a negative value south of the equator.

REFERENCES

1. **R. F. Lieske and R. L. McCoy,** *Equations of Motion of a Rigid Projectile,* **BRL Report No. 1244, US Army Ballistic Research Laboratory, Aberdeen Proving Ground, MD, March 1964.**
   NOTR:(1) Eq. (5.6) on p. 43 should be

$$\text{``}\quad \vec{E} = \begin{bmatrix} \dfrac{RX_1}{\sqrt{X_1^2 + X_3^2}}\text{Arctan}\left(\dfrac{\sqrt{X_1^2 + X_3^2}}{R + X_2}\right) \\ \sqrt{(R + X_2)^2 + X_1^2 + X_3^2} - R \\ \dfrac{RX_3}{\sqrt{X_1^2 + X_3^2}}\text{Arctan}\left(\dfrac{\sqrt{X_1^2 + X_3^2}}{R + X_2}\right) \end{bmatrix} \quad\text{''}$$

   (2) Eq. (5.15) on p. 45 should be

$$\text{``}\,\psi = \left\{ \begin{array}{ll} \cos^{-1}\left(\dfrac{vx_2 - v_2\cos\alpha}{v \sin \alpha}\right), & \alpha \neq 0 \\ 0, & \alpha = 0 \end{array} \right\}\,\text{''}$$

2. *Equations for Computation of Quadrant Elevation, Deflection, and Fuze Setting for Field Artillery and Mortar Fire Control Computers Using the Point Mass or Modified Point Mass Equations of Motion,* **BRL Document FCI ALL, US Army Ballistic Research Laboratory, Aberdeen Proving Ground, MD, 23 January 1991. (This document, including Appendices 1 through 6, constitutes a complete description of the algorithms required to perform the ballistic computations of technical fire control.)**

BIBLIOGRAPHY

B. Barnet, *Trajectory Equations for a Six-Degree-of-Freedom Missile Using a Fixed Plane Coordinate System,* **Technical Report No. 3391, Picatinny Arsenal, Dover, NJ, June 1966.**

G.A. Bliss, *Mathematics for Exterior Ballistics,* **John Wiley and Sons, Inc., New York, NY, 1944.**

Firing Tables FT8-J-2, "*Cannon, 8-inch; Howitzer M3, M2A1, and M47; Firing Shell, HE, M106***", Department of the Army, Washington, DC, 1958.**

AMCP 706-331, Engineering Design Handbook, *Compensating Elements,* **September 1963.**

Davis, Follin, and Blitzer, *The Exterior Ballistics of Rockets,* **D. Van Nostrand Book Co., Inc., Princeton, NJ, 1958.**

AMCP 706-242, Engineering Design Handbook, *Design for Control of Projectile Flight Characteristics,* **September 1966.**

W. Dziwak, *Solution to the Ballistic Point Mass Equation Including Rigid Body Effects,* **ARSLD-TR-85015, Picatinny Arsenal, Dover, NJ, October 1985.**

AMCP 706-107, Engineering Design Handbook, *Elements of Armament Engineering, Part 2, Ballistics,* **September 1963.**

T. J. Hayes, *Elements of Ordnance,* **John Wiley and Sons, Inc., New York, NY, 1938.**

H. P. Hitchcock, *Computation of Firing Tables for the US Army,* **Report X-102, US Army Ballistic Research Laboratory, Aberdeen Proving Ground, MD, 1934.**

J. Hovorka, and W. Wrigley, *Fire Control Principles,* **McGraw-Hill Book Company, Inc., New York, NY, 1959.**

J. L. Kelley, E. J. McShane, and F. V. Reno, *Exterior Ballistics*, University of Denver Press, Denver, CO, 1953.

R. Lieske and M. Reiter, *Equations of Motion for A Modified Point Mass Trajectory*, BRL Report No. 1314, US Army Ballistic Research Laboratory, Aberdeen Proving Ground, MD, March 1966.

A. S. Locke, *Guidance*, D. Van Nostrand Company, Inc., Princeton, NJ, 1955. (Part of the series titled *Principles of Guided Missile Design* and edited by G. Merrill.)

R. McCoy, *Aerodynamic Characteristics of the 30-mm XM78 Projectile*, BRL Report ARBRL-MR-03019, US Army Ballistic Research Laboratory, Aberdeen Proving Ground, MD, May 1980.

F. R. Moulton, *New Methods in Exterior Ballistics*, University of Chicago Press, Chicago, IL, 1926.

C. Murphy, *Measurement of Nonlinear Forces and Moments by Means of Free Flight Tests*, BRL Report No. 974, US Army Ballistic Research Laboratory, Aberdeen Proving Ground, MD, February 1956.

J. M. Norwood, *Exterior Ballistics for Airborne Applications*, AFAL-TR-73-196, US Air Force Armament Laboratory, Eglin Air Force Base, FL, June 1973.

Rocket Fundamentals, Office of Scientific Research and Development, George Washington University, Washington, DC, 1944.

M. Skelnik, *Introduction to Radar System*, McGraw-Hill Book Company, Inc., New York, NY, 1962.

AMCP 706-140, Engineering Design Handbook, *Trajectories, Differential Effects, and Data for Projectiles*, August 1963.

APPENDIX B
FILTERING AND PREDICTION

This appendix provides an introduction to Kalman filtering for linear systems with discrete representation.

B-0   LIST OF SYMBOLS

$[A]$ = $n \times n$ **nonsingular transpose matrix, dimensionless**

a,b,c = **random variables, U**

$\text{cor}[\mathbf{z},\mathbf{x_2}]$ = **correlation matrix of z and $\mathbf{x_2}$, $\mathbf{U^2}$**

$\text{cov}[E(\mathbf{x_1}|\mathbf{x_2})]$ = **covariance matrix of $E(\mathbf{x_1}|\mathbf{x_2})$, $\mathbf{U^2}$**

d = **any known function of c, U**

$\det[\ ]$ = **determinant of matrix [ ]**

$[D]$ = **arbitrary $k \times (n-k)$ matrix, dimensionless**

$E(\ )$ = **mathematical expectation of quantity in parentheses (or brackets), U**

$E(\mathbf{x_1}|\mathbf{x_2})$ = **expectation of $\mathbf{x_1}$ given $\mathbf{x_2}$, U**

$E(\mathbf{x_1}|\mathbf{x_3})$ = **expectation of $\mathbf{x_1}$ given $\mathbf{x_3}$, U**

$E(\mathbf{x_1}|\mathbf{x_2},\mathbf{x_3})$ = **expectation of $\mathbf{x_1}$ given $\mathbf{x_2}$ and $\mathbf{x_3}$, U**

$\mathbf{e}_n$ = m-**dimensional estimation error vector associated with the state vector $\mathbf{x}_n$ given the observations $\{\mathbf{z}_{n-1},\mathbf{z}_{n-2},\cdots,\mathbf{z}_1\}$, U**

e_{n+1} = m-**dimensional estimation error vector at state $n+1$, U**

$[F_n]$ = **known $m \times m$ gain matrix at discrete time index n, dimensionless**

$f(\mathbf{x})$ = **joint pdf of the random variable x, $\mathbf{U^{-n}}$**

$f_{12}(\mathbf{x_1},\mathbf{x_2})$ = **joint pdf for random variable vectors $\mathbf{x_1}$ and $\mathbf{x_2}$, $\mathbf{U^{-n}}$**

$f_1(\mathbf{x_1})$ = **pdf for the random variable vector $\mathbf{x_1}$, $\mathbf{U^{-k}}$**

$f_2(\mathbf{x_2})$ = **pdf for the random variable vector $\mathbf{x_2}$, $\mathbf{U^{-(n-k)}}$**

$F_{1|2}(\mathbf{x_1}|\mathbf{x_2})$ = **conditional pdf for the random variable $\mathbf{x_1}$ given the vector $\mathbf{x_2}$, $\mathbf{U^{-k}}$**

$[G_n]$ = **known gain $m \times r$ matrix at discrete time index n, dimensionless**

$g(\mathbf{y})$ = **pdf for the random variable vector y, $\mathbf{U^{-n}}$**

$g_{12}(\mathbf{y_1},\mathbf{y_2})$ = **joint pdf of $\mathbf{y_1}$ and $\mathbf{y_2}$, $\mathbf{U^{-n}}$**

$g_1(\bullet)$ = **abbreviation of $g_1(\mathbf{x}_1 - [\Lambda_{12}][\Lambda_{22}]^{-1}\mathbf{x_2})$, $\mathbf{U^{-k}}$**

$g_1(\mathbf{y_1})$ = **marginal (normal) pdf of $\mathbf{y_1}$, $\mathbf{U^{-k}}$**

$g_2(\mathbf{y_2})$ = **marginal (normal) pdf of $\mathbf{y_2}$, $\mathbf{U^{-(n-k)}}$**

$[H_n]$ = **finite sequence of known $s \times m$ matrices, $n \in \Gamma$, dimensionless**

$[I]$ = **identity matrix (main diagonal elements unity; all other elements zero), size determined by context, dimensionless**

i = **imaginary operator $\sqrt{-1}$, dimensionless**

i,j = $i,j = 1,2,\cdots,N\ (i,j \in \Gamma)$, **dimensionless**

$[K_n]$ = $m \times s$ **gain matrix, dimensionless**

$[\hat{K}_n]$ = $m \times s$ **estimated gain matrix, dimensionless**

$[\llcorner_1]$ = $k \times k$ **covariance matrix of y_1, $\mathbf{U^2}$**

$[\llcorner_2]$ = $(n-k) \times (n-k)$ **covariance matrix of y_2, $\mathbf{U^2}$**

$[M]$ = $m \times m$ covariance matrix associated with initial state of $\mathbf{x_1}$, $\mathbf{U}^2$

$\mathbf{m}$ = n-dimensional mean vector of pdf $f(\mathbf{x})$ with an MVND, $\mathbf{U}$

$\mathbf{m_1}$ = k-dimensional mean vector (of pdf $f_1(\mathbf{x_1})$), $\mathbf{U}$

$\mathbf{m_2}$ = $(n - k)$-dimensional mean vector (of pdf $f_2(\mathbf{x_2})$), $\mathbf{U}$

$\mathbf{m_3}$ = mean vector of pdf $f_3(\mathbf{x_3})$, dimension consistent with $\mathbf{x_3}$, $\mathbf{U}$

$\mathbf{m_4}$ = mean vector of pdf $f_4(\mathbf{x_4})$, dimension consistent with $\mathbf{x_4}$, $\mathbf{U}$

$\mathbf{m_{12}}$ = k-dimensional mean vector of pdf $f_{1|2}(\mathbf{x_1}|\mathbf{x_2})$, $\mathbf{U}$

N = uppermost value of the set of positive integers $\Gamma = 1,2,\cdots, N$, dimensionless

$N[\mu,[cm]]$ = MVND pdf of any mean vector μ and any covariance matrix $[cm]$, $\mathbf{U}^{-n}$

n = number of random variables in $\mathbf{x}$, dimensionless

n = state discrete time index, $n \in \Gamma$, dimensionless

$\mathbf{0}$ = zero vector (all elements are zero), size and unit depend on context

$[P_n]$ = $m \times m$ estimation error covariance matrix, $\mathbf{U}^2$

$[P_1]$ = initial estimate error covariance matrix, $\mathbf{U}^2$

Q_j = variance of ω, $\mathbf{U}^2$

$[Q_j]$ = $r \times r$ diagonal known covariance matrix, $\mathbf{U}^2$

$\mathbf{R}_j$ = variance of $\mathbf{v}_j$, $\mathbf{U}^2$

$[R_j]$ = $s \times s$ diagonal covariance matrix, $\mathbf{U}^2$

R^n = n-dimensional Euclidean space, $\mathbf{U}$

$\mathbf{t}$ = variable n-dimensional vector, an element of R^n, $\mathbf{U}^{-1}$

$\mathbf{u_1}$ = k-dimensional mean vector of $\mathbf{y_1}$, $\mathbf{U}$

$\mathbf{u_2}$ = $(n - k)$-dimensional mean vector of $\mathbf{y_2}$, $\mathbf{U}$

$\mathbf{u}_{n-1}$ = $(n - 1)s$-dimensional "giant" vector formed from the collection $\{\mathbf{z}_{n-1},\mathbf{z}_{n-2}, \cdots,\mathbf{z_1}\}$, $\mathbf{U}$

$\mathbf{v}_n$ = s-dimension finite sequence of zero mean independent Gaussian random variable vectors, $\mathbf{U}$

$\mathbf{x}$ = n-dimensional random variable column vector, $\mathbf{U}$

$x_1,x_2,\cdots,x_n$ = the n-scalar random variable components of $\mathbf{x}$, $\mathbf{U}$

$\mathbf{x_1}$ = k-dimensional random vector (upper partition of $\mathbf{x}$), $\mathbf{U}$

$\mathbf{x_2}$ = $(n - k)$-dimensional random vector (lower partition of $\mathbf{x}$), $\mathbf{U}$

$\mathbf{x_1},\mathbf{x_2},\mathbf{x_3}$ = jointly normal random variable vectors, $\mathbf{U}$

$\mathbf{x_4}$ = random variable vector comprising $\mathbf{x_2}$ and $\mathbf{x_3}$, $\mathbf{U}$

$\mathbf{x}_n$ = system state m-dimensional vector at discrete time index n, $\mathbf{U}$

$\mathbf{x}_{n+1}$ = system state m-dimensional vector at discrete time index $n + 1$, $\mathbf{U}$

$\hat{\mathbf{x}}_{n+1|n}$ = m-dimensional estimator vector of $\mathbf{x}_{n+1}$, $\mathbf{U}$

$\hat{\mathbf{x}}_{1|0}$ = m-dimensional initial system state estimate vector, $\mathbf{U}$

$\mathbf{y}$ = n-dimensional vector that satisfies $\forall\, \mathbf{y} \in R^n \ni \mathbf{y} \neq 0$, $\mathbf{U}$

$\mathbf{y_1}$ = k-dimensional random vector, $\mathbf{U}$

$\mathbf{y_2}$ = $(n - k)$-dimensional random vector, $\mathbf{U}$

$\mathbf{z}$ = convenient substitute for $\mathbf{x_1} - E(\mathbf{x_1}|\mathbf{x_2})$, $\mathbf{U}$

$\mathbf{z}_n$ = nth state observation of a system parameter random variable m-dimensional vector, $\mathbf{U}$

Γ = $\{1,2,\cdots,N\}$, dimensionless

δ_{ij} = Kronecker delta, = 0 for $i \neq j$, = 1 for $i = j$, dimensionless

$\delta(N)$ = m-dimensional vector function of the the set of observations $\{z_1,z_2,\cdots,z_N\}$, **U**

$[\Lambda]$ = $n \times n$ symmetric p.d. matrix, or covariance matrix of the MVND, $\mathbf{U}^2$

$[\Lambda_{11}]$ = $k \times k$ covariance matrix, $\mathbf{U}^2$

$[\Lambda_{12}]$ = $k \times (n-k)$ covariance matrix, $\mathbf{U}^2$

$[\Lambda_{21}]$ = $(n-k) \times k$ covariance matrix, $\mathbf{U}^2$

$[\Lambda_{22}]$ = $(n-k) \times (n-k)$ covariance matrix, $\mathbf{U}^2$

μ = a general vector of means, **U**

$\phi(\mathbf{t})$ = multivariate characteristic function of the MVND with parameters **m** and $[\Lambda]$, dimensionless

$\psi(\mathbf{x_1},\mathbf{x_2})$ = some function of $\mathbf{x_1}$ and $\mathbf{x_2}$, unit depends on function

ω_n = sequence of r-dimensional zero mean independent normal random variable vectors with known covariance matrix, $n \in \Gamma$, **U**

$\bigcirc$ = zero matrix (all elements are zero), size and unit determined by context

B-1 INTRODUCTION

This appendix develops the Kalman discrete-time filter in the following steps:

1. It considers the properties of the joint normal distribution, which is also referred to as the multivariate normal (or Gaussian) distribution (MVND).

2. It obtains the conditional density function.

3. It develops five lemmas to be used in the Kalman filter derivation.

4. It derives the Kalman discrete-time filter equations.

B-2 THE JOINT NORMAL DISTRIBUTION

B-2.1 DEFINITION

Let

$$\mathbf{x} \triangleq [x_1, x_2, \cdots, x_n]' = \begin{bmatrix} x_1 \\ x_2 \\ \vdots \\ x_n \end{bmatrix}, \quad \mathbf{U} \tag{B-1}$$

where

$\mathbf{x}$ = n-dimensional random variable column vector, **U**

$x_1, x_2, \cdots, x_n$ = the n-scalar random variable components of $\mathbf{x}$, **U**

n = number of random variables in $\mathbf{x}$, dimensionless.

The prime denotes the transpose of the column vector into the corresponding row vector and vice versa.

Let

$$f(\mathbf{x}) = f(x_1, x_2, \cdots, x_n), \quad \mathbf{U}^{-n} \tag{B-2}$$

where

$f(\mathbf{x})$ = joint probability density function (pdf) of the random variable $\mathbf{x}$, $\mathbf{U}^{-n}$.

The random variables in $\mathbf{x}$ have an MVND if $f(\mathbf{x})$ has the following form:

$$f(\mathbf{x}) = \frac{1}{\sqrt{(2\pi)^n \det[\Lambda]}} \exp\left[-\frac{1}{2}(\mathbf{x}-\mathbf{m})'[\Lambda]^{-1}(\mathbf{x}-\mathbf{m})\right], \quad \mathbf{U}^{-n} \tag{B-3}$$

where

$$
\begin{array}{rcl}
[\Lambda] & = & n \times n \text{ symmetric positive-definite (p.d.) matrix, } U^2 \\
\det[\Lambda] & = & \text{determinant of } [\Lambda],\ U^{2n} \\
[\Lambda]^{-1} & = & \text{inverse matrix of } [\Lambda],\ U^{-2} \\
\mathbf{m} & = & n\text{-dimensional vector of finite real elements, i.e., } \mathbf{m} \in R^n,\ U \\
R^n & = & n\text{-dimensional Euclidean space, } U.
\end{array}
$$

As discussed in Refs. 1 and 2, $[\Lambda]$ is symmetric if and only if (iff) $[\Lambda]' = [\Lambda]$. Also $[\Lambda]$ is positive-definite (p.d.) iff

$$ \mathbf{y}'\,[\Lambda]\,\mathbf{y} > \mathbf{0},\ \ U^4 \tag{B-4} $$

where

$$
\begin{array}{rl}
\mathbf{y} = & n\text{-dimensional vector that satisfies } \forall \mathbf{y} \in R^n \ni \mathbf{y} \neq \mathbf{0},\ U \\
\forall \mathbf{y} = & \text{for all vectors } \mathbf{y} \\
\in R^n = & \text{which belong to the space } R^n \\
\ni \mathbf{y} = & \text{such that the vector } \mathbf{y} \\
\mathbf{0} = & \text{zero vector (all elements are zero), size and unit depend on context.}
\end{array}
$$

It will be shown that $f(\mathbf{x})$ is a well-defined pdf and that

$$ E[\mathbf{x}] = \mathbf{m},\ \ U \tag{B-5} $$

where

$$
\begin{array}{rl}
E(\mathbf{x}) = & \text{mathematical expectation of } \mathbf{x},\ U \\
\mathbf{m} = & n\text{-dimensional mean vector of pdf } f(\mathbf{x}) \text{ with an MVND, } U
\end{array}
$$

and

$$ E\,[\,(\mathbf{x} - \mathbf{m})\,(\mathbf{x} - \mathbf{m})'\,]\ =\ [\Lambda],\ \ U^2 \tag{B-6} $$

where

$$
\begin{array}{rl}
E[(\mathbf{x} - \mathbf{m})(\mathbf{x} - \mathbf{m})'] = & \text{mathematical expectation of the vector product } (\mathbf{x} - \mathbf{m})(\mathbf{x} - \mathbf{m})',\ U^2 \\
[\Lambda] = & \text{covariance matrix of the MVND, } U^2.
\end{array}
$$

Strictly speaking, $[\Lambda]$ need not be p.d. in order to define the MVND. All that is really required is that $[\Lambda]$ be positive-semidefinite (p.s.d.), i.e.,

$$ \mathbf{y}'\,[\Lambda]\,\mathbf{y} \geq \mathbf{0},\ \forall \mathbf{y} \in R^n. \tag{B-7} $$

B-2.2 A MORE GENERAL DEFINITION

If $[\Lambda]$ is p.s.d. and not p.d., $[\Lambda]$ can be singular and therefore have no inverse, i.e., $[\Lambda]^{-1}$ does not exist. On the other hand, if $[\Lambda]$ is p.d., $[\Lambda]^{-1}$ must exist.

If $[\Lambda]$ is p.s.d. and not necessarily p.d., the MVND can be defined by its multivariate characteristic function:

$$
\begin{aligned}
\phi(\mathbf{t}) &\triangleq E[\exp(i\mathbf{t}'\mathbf{x})] \\
&= \exp\!\left(i\mathbf{t}'\mathbf{m} - \frac{1}{2}\mathbf{t}'\,[\Lambda]\,\mathbf{t} \right),\ \text{dimensionless}
\end{aligned}
\tag{B-8}
$$

where

$$
\begin{array}{rl}
\phi(\mathbf{t}) = & \text{multivariate characteristic function of the MVND with parameters } \mathbf{m} \text{ and } [\Lambda], \text{ dimensionless} \\
\mathbf{t} = & \text{variable } n\text{-dimensional vector, an element of } R^n,\ U^{-1} \\
i = & \text{imaginary operator } \sqrt{-1},\ \text{dimensionless.}
\end{array}
$$

$[\Lambda]^{-1}$ need not exist for $\phi(t)$ to be well-defined. In the remaining discussion it is assumed that $[\Lambda]^{-1}$ always exists, i.e., that $[\Lambda]$ is p.d. in all instances. This restriction will eliminate some nonessential complications from this introductory material.

B-2.3 THE PARTITIONING OF A NORMAL RANDOM VECTOR

In this subparagraph the decomposition or partitioning of a normal random vector is obtained. **x** is an *n*-dimensional random vector with MVND: $N[\mathbf{m},[\Lambda]]$ with the pdf of Eq. B-3. $N[\mathbf{m},[\Lambda]]$ is an abbreviation for an MVND with mean vector **m** and covariance matrix $[\Lambda]$.

The vector **x** is partitioned into two random vectors $\mathbf{x}_1$ and $\mathbf{x}_2$:

$$\mathbf{x} \triangleq \begin{bmatrix} \mathbf{x}_1 \\ --- \\ \mathbf{x}_2 \end{bmatrix}, \ \mathrm{U} \tag{B-9}$$

where

$\mathbf{x}_1$ = *k*-dimensional random vector, U
$\mathbf{x}_2$ = $(n-k)$-dimensional random vector, U.

The following quantities are defined:

$$\mathbf{m}_1 \triangleq E[\mathbf{x}_1], \ \mathrm{U} \tag{B-10}$$

where
$\mathbf{m}_1$ = *k*-dimensional mean vector, U;

$$\mathbf{m}_2 \triangleq E[\mathbf{x}_2], \ \mathrm{U} \tag{B-11}$$

where
$\mathbf{m}_2$ = $(n-k)$-dimensional mean vector (of pdf $f_2(\mathbf{x}_2)$), U;

$$[\Lambda_{11}] \triangleq E\left[(\mathbf{x}_1-\mathbf{m}_1)(\mathbf{x}_1-\mathbf{m}_1)'\right], \ \mathrm{U}^2 \tag{B-12}$$

where
$[\Lambda_{11}] = k \times k$ covariance matrix, U^2;

$$[\Lambda_{22}] \triangleq E\left[(\mathbf{x}_2-\mathbf{m}_2)(\mathbf{x}_2-\mathbf{m}_2)'\right], \ \mathrm{U}^2 \tag{B-13}$$

where
$[\Lambda_{22}] = (n-k) \times (n-k)$ covariance matrix, U^2;

$$[\Lambda_{12}] \triangleq E\left[(\mathbf{x}_1-\mathbf{m}_1)(\mathbf{x}_2-\mathbf{m}_2)'\right], \ \mathrm{U}^2 \tag{B-14}$$

where
$[\Lambda_{12}] = k \times (n-k)$ covariance matrix, U^2;
and

$$[\Lambda_{21}] \triangleq E\left[(\mathbf{x}_2-\mathbf{m}_2)(\mathbf{x}_1-\mathbf{m}_1)'\right]$$
$$= [\Lambda_{12}]', \ \mathrm{U}^2 \tag{B-15}$$

where
$[\Lambda_{21}] = (n-k) \times k$ covariance matrix, U^2.

Then

$$[\Lambda] = \left[\begin{array}{c|c} [\Lambda_{11}] & [\Lambda_{12}] \\ \hline [\Lambda_{21}] & [\Lambda_{22}] \end{array} \right], \ \mathbf{U}^2. \tag{B-16}$$

If $[\Lambda_{12}] = \bigcirc$, i.e., a matrix of all zeros, then $[\Lambda_{21}]$ is also $\bigcirc$. Also, as a consequence,

$$\det [\Lambda] = \det [\Lambda_{11}] \cdot \det [\Lambda_{22}], \ \mathbf{U}^{2n} \tag{B-17}$$

where

$\det[\Lambda_{11}]$ = determinant of $[\Lambda_{11}]$, $\mathbf{U}^{2k}$
$\det[\Lambda_{22}]$ = determinant of $[\Lambda_{22}]$, $\mathbf{U}^{2(n-k)}$

and

$$[\Lambda]^{-1} = \left[\begin{array}{c|c} [\Lambda_{11}]^{-1} & \bigcirc \\ \hline \bigcirc & [\Lambda_{22}]^{-1} \end{array} \right], \ \mathbf{U}^{-2} \tag{B-18}$$

where

$\bigcirc$ = zero matrix (all elements are zero), size and unit depend on context.

Further,

$$f(\mathbf{x}) = f_{12}(\mathbf{x}_1, \mathbf{x}_2) = f_1(\mathbf{x}_1) f_2(\mathbf{x}_2), \ \mathbf{U}^{-n} \tag{B-19}$$

where

$f_{12}(\mathbf{x}_1, \mathbf{x}_2)$ = joint pdf for random variable vectors $\mathbf{x}_1$ and $\mathbf{x}_2$, $\mathbf{U}^{-n}$
$f_1(\mathbf{x}_1)$ = pdf for random variable vector $\mathbf{x}_1$, $\mathbf{U}^{-k}$
$f_2(\mathbf{x}_2)$ = pdf for random variable vector $\mathbf{x}_2$, $\mathbf{U}^{-(n-k)}$.

$f_1(\mathbf{x}_1)$ and $f_2(\mathbf{x}_2)$ are

$$f_1(\mathbf{x}_1) = \frac{1}{\sqrt{(2\pi)^k |\Lambda_{11}|}} \exp\left[-\frac{1}{2}(\mathbf{x}_1 - \mathbf{m}_1)' [\Lambda_{11}]^{-1} (\mathbf{x}_1 - \mathbf{m}_1) \right], \ \mathbf{U}^{-k} \tag{B-20}$$

$$f_2(\mathbf{x}_2) = \frac{1}{\sqrt{(2\pi)^{n-k} |\Lambda_{22}|}} \exp\left[-\frac{1}{2}(\mathbf{x}_2 - \mathbf{m}_2)' [\Lambda_{22}]^{-1} (\mathbf{x}_2 - \mathbf{m}_2) \right], \ \mathbf{U}^{-(n-k)}. \tag{B-21}$$

Therefore, when $[\Lambda_{12}] = \bigcirc$, i.e., when $\mathbf{x}_1$ and $\mathbf{x}_2$ are uncorrelated, $\mathbf{x}_1$ and $\mathbf{x}_2$ are independent normal random vectors with distributions $N(\mathbf{m}_1, [\Lambda_{11}])$ and $N(\mathbf{m}_2, [\Lambda_{22}])$, respectively.

In general $[\Lambda_{12}] \neq \bigcirc$. To handle this more general case, two additional random vectors $\mathbf{y}_1$ and $\mathbf{y}_2$ are introduced and defined as follows:

$$\mathbf{y_1} \triangleq \mathbf{x_1} - [D]\,\mathbf{x_2}, \quad \mathbf{U} \tag{B-22}$$

where

$\quad\quad \mathbf{y_1}$ = k-dimensional random vector, U

$\quad\quad [D]$ = arbitrary $k \times (n-k)$ matrix (defined as $[\Lambda_{12}][\Lambda_{22}]^{-1}$), dimensionless

and

$$\mathbf{y_2} \triangleq \mathbf{x_2}, \quad \mathbf{U} \tag{B-23}$$

where

$\quad\quad \mathbf{y_2}$ = $(n-k)$-dimensional random vector, U.

By applying the previous definitions, Eqs. B-13 and B-14, it follows directly that

$$
\begin{aligned}
E&\left\{ \left[\mathbf{y_1} - E(\mathbf{y_1}) \right] \left[\mathbf{y_2} - E(\mathbf{y_2}) \right]' \right\} \\
&= E\left[(\mathbf{x_1} - [D]\,\mathbf{x_2} - \mathbf{m_1} + [D]\,\mathbf{m_2})\,(\mathbf{x_2} - \mathbf{m_2})' \right] \\
&= \left[\Lambda_{12} \right] - \left[D \right]\left[\Lambda_{22} \right], \quad \mathbf{U}^2.
\end{aligned}
\tag{B-24}
$$

$[D]$, which was an arbitrary matrix, is defined as follows:

$$[D] \triangleq \left[\Lambda_{12} \right]\left[\Lambda_{22} \right]^{-1}, \quad \text{dimensionless.} \tag{B-25}$$

Since $[\Lambda]$ was assumed to be p.d., $[\Lambda_{22}]^{-1}$ exists; therefore, $[D]$ is well-defined. Because of the definition of Eq. B-25, the random vectors $\mathbf{y_1}$ and $\mathbf{y_2}$ are uncorrelated since

$$
\begin{aligned}
E\left\{ \left[\mathbf{y_1} - E(\mathbf{y_1}) \right] \left[\mathbf{y_2} - E(\mathbf{y_2}) \right]' \right\} &= \left[\Lambda_{12} \right] - \left[D \right]\left[\Lambda_{22} \right] \\
&= \bigcirc, \quad \mathbf{U}^2
\end{aligned}
\tag{B-26}
$$

$\mathbf{y_1}$ and $\mathbf{y_2}$ are jointly normal random vectors and therefore form the results of Eqs. B-18 through B-21. The quantities $\mathbf{y_1}$ and $\mathbf{y_2}$ are independent normal random vectors and can be expressed in terms of $\mathbf{x_1}$ and $\mathbf{x_2}$ as follows:

$$
\begin{bmatrix} \mathbf{y_1} \\ \hline \mathbf{y_2} \end{bmatrix}
=
\left[
\begin{array}{c:c}
[I] & -\left[\Lambda_{12} \right]\left[\Lambda_{22} \right]^{-1} \\ \hline
\bigcirc & [I]
\end{array}
\right]
\begin{bmatrix} \mathbf{x_1} \\ \hline \mathbf{x_2} \end{bmatrix}, \quad \mathbf{U}
\tag{B-27}
$$

where

$\quad\quad [I]$ = identity matrix, dimensional obtained by context

$$
= \begin{bmatrix} 1 & 0 & 0 \\ 0 & 1 & 0 \\ 0 & 0 & 1 \end{bmatrix} \text{ (for example), dimensionless}
$$

and the matrix transformation is nonsingular. This particular transformation matrix is nonsingular because it is upper-block triangular and because the main diagonal blocks are both identity matrices.

Let $f(\mathbf{x})$ denote a general multivariate (say n-variate) density function (not necessarily normal). Let

$$\mathbf{y} = [A]\mathbf{x}, \quad \mathbf{U} \tag{B-28}$$

where

      $\mathbf{y}$ = n-dimensional random vector, U
      $\mathbf{x}$ = n-dimensional random vector of $f(\mathbf{x})$, U
    $[A]$ = $n \times n$ nonsingular transpose matrix, dimensionless.

The pdf $g(\mathbf{y})$ for the vector random variable $\mathbf{y}$ is found in the following three steps:

    1. Write

$$\mathbf{x} = [A]^{-1}\mathbf{y}, \quad \mathbf{U}. \tag{B-29}$$

    2. Then write

$$f(\mathbf{x})\, dx_1 \cdots dx_n = g(\mathbf{y})\, dy_1 \cdots dy_n, \quad \mathbf{U} \tag{B-30}$$

where

    $dy_1 \cdots dy_n = \big| \det[A] \big|\, dx_1 \cdots dx_n, \; \mathbf{U}^n$
    $\big| \det[A] \big|$ = absolute value of $\det[A]$, dimensionless
      $\det[A]$ = determinant of matrix $[A]$, dimensionless
        $g(\mathbf{y})$ = pdf for the random variable vector $\mathbf{y}$, $\mathbf{U}^{-n}$.

    3. Then

$$g(\mathbf{y}) = \frac{1}{|\det[A]|} f\left([A]^{-1}\mathbf{y}\right), \quad \mathbf{U}^{-n}. \tag{B-31}$$

If $f(\mathbf{x})$ is an MVND pdf, the pdf $g(\mathbf{y})$ can be shown to be an MVND pdf also. Let $f(\mathbf{x})$ be defined as in Eq. B-3. If Eq. B-29 exists,

$$g(\mathbf{y}) = \frac{\exp\left[-\frac{1}{2}\left([A]^{-1}\mathbf{y}-\mathbf{m}\right)'[\Lambda]^{-1}\left([A]^{-1}\mathbf{y}-\mathbf{m}\right)\right]}{|\det[A]|\sqrt{(2\pi)^n \det[\Lambda]}}, \quad \mathbf{U}^{-n}, \tag{B-32}$$

which can be rewritten as

$$g(\mathbf{y}) = \frac{\exp\left[-\frac{1}{2}(\mathbf{y}-[A]\mathbf{m})'\left([A]'\right)^{-1}[\Lambda]^{-1}[A]^{-1}(\mathbf{y}-[A]\mathbf{m})\right]}{\sqrt{(2\pi)^n}\,|\det[A]'|\cdot\det[\Lambda]\cdot|\det[A]|}, \quad \mathbf{U}^{-n} \tag{B-33}$$

where

    $\det[A]'$ = determinant of $[A]'$, dimensionless
    $|\det[A]'|$ = absolute value of $\det[A]'$, dimensionless.

In Eq. B-33, since $\det[A]' = \det[A]$, $|\det[A]|$ can be written as $\sqrt{|\det[A]'|\cdot|\det[A]|}$.

Eq. B-32 shows that $\mathbf{y}$ is a normal random vector with mean $[A]\mathbf{m}$ and covariance matrix $[A][\Lambda][A]'$. Therefore, $\mathbf{y} \in N[[A]\mathbf{m}, [A][\Lambda][A]']$. For this specific case

$$[A] = \left[\begin{array}{c|c} [I] & -\big[\Lambda_{12}\big]\big[\Lambda_{22}\big]^{-1} \\ \hline \bigcirc & [I] \end{array}\right], \quad \text{dimensionless,} \tag{B-34}$$

$$\mathbf{y} = [A]\mathbf{x}, \quad \mathbf{U}, \tag{B-35}$$

$$\det[A] = 1, \quad \text{dimensionless}, \tag{B-36}$$

and

$$\begin{bmatrix} \mathbf{y_1} \\ -- \\ \mathbf{y_2} \end{bmatrix} = \mathbf{y} \quad \text{and} \quad \begin{bmatrix} \mathbf{x_1} \\ -- \\ \mathbf{x_2} \end{bmatrix} = \mathbf{x}, \quad \mathbf{U}. \tag{B-37}$$

Since **y** has been shown to be a normal random vector and since $\mathbf{y} = [\mathbf{y_1}|\mathbf{y_2}]'$, $\mathbf{y_1}$ and $\mathbf{y_2}$ are jointly normal random vectors. Further, when Eq. B-25 applies, $\mathbf{y_1}$ and $\mathbf{y_2}$ are uncorrelated normal random vectors and are therefore statistically independent.

B-3 COMPUTATION OF CONDITIONAL DENSITY FUNCTION

This paragraph develops the density function and statistics for the conditional function $f_{1|2}(\mathbf{x_1}|\mathbf{x_2})$, $\mathbf{U}^{-n}$. The random variable vectors $\mathbf{x_1}$ and $\mathbf{x_2}$ are the result of partitioning the random variable vector **x** as described in subpar. B-2.3.

From Eqs. B-19 through B-21 the following equations can be written:

$$f_1(\mathbf{x_1}) = N\left(\mathbf{m_1}, [\Lambda_{11}]\right), \quad \mathbf{U}^{-k} \tag{B-38}$$

and

$$f_2(\mathbf{x_2}) = N\left(\mathbf{m_2}, [\Lambda_{22}]\right), \quad \mathbf{U}^{-(n-k)}. \tag{B-39}$$

From the definition of joint probability,

$$f_{12}(\mathbf{x_1},\mathbf{x_2}) = f_{1|2}(\mathbf{x_1}|\mathbf{x_2}) \, f_2(\mathbf{x_2}), \quad \mathbf{U}^{-l} \tag{B-40}$$

where

$f_{1|2}(\mathbf{x_1}|\mathbf{x_2})$ = conditional pdf for the random variable vector $\mathbf{x_1}$ given the vector $\mathbf{x_2}$, $\mathbf{U}^{-k}$.
Solving for the conditional pdf yields

$$f_{1|2}(\mathbf{x_1}|\mathbf{x_2}) = \frac{f_{12}(\mathbf{x_1},\mathbf{x_2})}{f_2(\mathbf{x_2})}, \quad \mathbf{U}^{-k} \tag{B-41}$$

where $f_2(\mathbf{x_2})$ does not vanish.

The conditional pdf $f_{1|2}(\mathbf{x_1}|\mathbf{x_2})$ is computed explicitly by applying this transformation:

$$\mathbf{y} \triangleq \begin{bmatrix} \mathbf{y_1} \\ -- \\ \mathbf{y_2} \end{bmatrix} = \begin{bmatrix} [I] & -[\Lambda_{12}][\Lambda_{22}]^{-1} \\ \bigcirc & [I] \end{bmatrix} \begin{bmatrix} \mathbf{x_1} \\ -- \\ \mathbf{x_2} \end{bmatrix}, \quad \mathbf{U}. \tag{B-42}$$

Since **y** is normal, $\mathbf{y_1}$ and $\mathbf{y_2}$ are marginally normal, i.e., each one is normal when considered alone. Therefore, $\mathbf{y_1}$ and $\mathbf{y_2}$ are completely specified by two mean vectors $\mathbf{u_1}$ and $\mathbf{u_2}$ and by two covariance matrices $[\llcorner_1]$ and $[\llcorner_2]$.

Define:

$$\mathbf{u_1} \triangleq E(\mathbf{y_1}) = \mathbf{m_1} - \left[\Lambda_{12}\right]\left[\Lambda_{22}\right]^{-1}\mathbf{m_2}, \text{ U} \qquad \text{(B-43)}$$

where

$\mathbf{u_1}$ = k-dimensional mean vector of $\mathbf{y_1}$, U;

$$\mathbf{u_2} \triangleq E(\mathbf{y_2}) = \mathbf{m_2}, \text{ U} \qquad \text{(B-44)}$$

where

$\mathbf{u_2}$ = $(n - k)$-dimensional mean vector of $\mathbf{y_2}$, U;

$$[\llcorner_1] = E\left[(\mathbf{y_1} - \mathbf{u_1})(\mathbf{y_1} - \mathbf{u_1})'\right]$$

$$= \left\{\left[(\mathbf{x_1} - \mathbf{m_1}) - \left[\Lambda_{12}\right]\left[\Lambda_{22}\right]^{-1}(\mathbf{x_2} - \mathbf{m_2})\right]\right.$$

$$\left.\times \left[(\mathbf{x_1} - \mathbf{m_1}) - \left[\Lambda_{12}\right]\left[\Lambda_{22}\right]^{-1}(\mathbf{x_2} - \mathbf{m_2})'\right]\right\} \qquad \text{(B-45)}$$

$$= \left[\Lambda_{11}\right] - \left[\Lambda_{12}\right]\left[\Lambda_{22}\right]^{-1}\left[\Lambda_{21}\right], \text{ U}^2$$

where

$[\llcorner_1]$ = $k \times k$ covariance matrix of $\mathbf{y_1}$, U^2;

and

$$\left[\llcorner_2\right] \triangleq \left[E(\mathbf{y_2} - \mathbf{u_2})(\mathbf{y_2} - \mathbf{u_2})'\right] = \left[\Lambda_{22}\right], \text{ U}^2 \qquad \text{(B-46)}$$

where

$[\llcorner_2]$ = $(n - k) \times (n - k)$ covariance matrix of $\mathbf{y_2}$, U^2.

The joint pdf $f_{12}(\mathbf{x_1},\mathbf{x_2})$ is now computed in terms of $\mathbf{y_1}$ and $\mathbf{y_2}$. It is already known in terms of $\mathbf{x_1}$ and $\mathbf{x_2}$. Using the reasoning of the steps associated with Eqs. B-29 through B-31, the following can be written:

$$f_{12}(\mathbf{x_1},\mathbf{x_2}) = g_{12}(\mathbf{y_1},\mathbf{y_2})\left|\det[A]\right|, \text{ U}^{-n} \qquad \text{(B-47)}$$

where

$g_{12}(\mathbf{y_1},\mathbf{y_2})$ = joint pdf of $\mathbf{y_1}$ and $\mathbf{y_2}$, U^{-n}

$[A]$ = $n \times n$ nonsingular transpose matrix of Eq. B-27, dimensionless.

Therefore,

$$\mathbf{y_1} = \mathbf{x_1} - \left[\Lambda_{12}\right]\left[\Lambda_{22}\right]^{-1}\mathbf{x_2}, \text{ U} \qquad \text{(B-48)}$$

and

$$\mathbf{y_2} = \mathbf{x_2}, \text{ U}. \qquad \text{(B-49)}$$

The transpose matrix $[A]$ is an upper-triangular matrix with all ones in the main diagonal; therefore, its determinant det$[A]$ is unity. Further, since $\mathbf{y_1}$ and $\mathbf{y_2}$ are independent random variable vectors by the choice of $[D] \triangleq [\Lambda_{12}][\Lambda_{22}]^{-1}$, as shown in Eq. B-25, $g_{12}(\mathbf{y_1},\mathbf{y_2})$ becomes

$$g_{12}(\mathbf{y_1},\mathbf{y_2}) = g_1(\mathbf{y_1})\, g_2(\mathbf{y_2}), \text{ U}^{-n} \qquad \text{(B-50)}$$

where

$g_1(\mathbf{y_1})$ = marginal (normal) pdf of $\mathbf{y_1}$, U^{-k}

$g_2(\mathbf{y_2})$ = marginal (normal) pdf of $\mathbf{y_2}$, $\text{U}^{-(n-k)}$.

Therefore,

$$f_{12}(\mathbf{x_1},\mathbf{x_2}) = g_1\left(\mathbf{x_1} - \left[\Lambda_{12}\right]\left[\Lambda_{22}\right]^{-1}\mathbf{x_2}\right) g_2(\mathbf{y_2}), \quad \mathbf{U}^{-n}. \tag{B-51}$$

Substituting Eq. B-49 into Eq. B-51 yields

$$f_{12}(\mathbf{x_1},\mathbf{x_2}) = g_1\left(\mathbf{x_1} - \left[\Lambda_{12}\right]\left[\Lambda_{22}\right]^{-1}\mathbf{x_2}\right) g_2(\mathbf{x_2}), \quad \mathbf{U}^{-n}. \tag{B-52}$$

Substituting Eq. (B-52) into Eq. (B-41) yields

$$f_{1|2}\left(\mathbf{x_1}\big|\mathbf{x_2}\right) = \frac{g_1\left(\mathbf{x_1} - \left[\Lambda_{12}\right]\left[\Lambda_{22}\right]^{-1}\mathbf{x_2}\right) g_2(\mathbf{x_2})}{g_2(\mathbf{x_2})}$$

$$= g_1\left(\mathbf{x_1} - \left[\Lambda_{12}\right]\left[\Lambda_{22}\right]^{-1}\mathbf{x_2}\right) \tag{B-53}$$

$$\triangle g_1\left(\bullet\right), \quad \mathbf{U}^{-k}$$

where

$g_1(\bullet)$ = abbreviation of $g_1(\mathbf{x} - [\Lambda_{12}][\Lambda_{22}]^{-1}\mathbf{x_2})$, $\mathbf{U}^{-k}$.

Because

$$g_1\left(\bullet\right) = N\left(u_1, \left[\mathsf{L}_1\right]\right), \quad \mathbf{U}^{-k} \tag{B-54}$$

and since

$$\mathbf{y_1} - \mathbf{u_1} = \left(\mathbf{x_1} - \left[\Lambda_{12}\right]\left[\Lambda_{22}\right]^{-1}\mathbf{x_2}\right) - \left(\mathbf{m_1} - \left[\Lambda_{12}\right]\left[\Lambda_{22}\right]^{-1}\mathbf{m_2}\right)$$

$$= \mathbf{x_1} - \left[\mathbf{m_1} + \left[\Lambda_{12}\right]\left[\Lambda_{22}\right]^{-1}\left(\mathbf{x_2} - \mathbf{m_2}\right)\right], \quad \mathbf{U}, \tag{B-55}$$

it follows by inspection that $f_{1|2}(\mathbf{x_1}|\mathbf{x_2})$ has the form

$$f_{1|2}\left(\mathbf{x_1}\big|\mathbf{x_2}\right) = N\left[\mathbf{m_{12}}, \left[\mathsf{L}_1\right]\right], \quad \mathbf{U}^{-k} \tag{B-56}$$

where $\mathbf{m_{12}}$ is defined as follows:

$$\mathbf{m_{12}} \triangleq \mathbf{m_1} + \left[\Lambda_{12}\right]\left[\Lambda_{22}\right]^{-1}\left(\mathbf{x_2} - \mathbf{m_2}\right), \quad \mathbf{U} \tag{B-57}$$

where

$\mathbf{m_{12}}$ = k-dimensional mean vector of pdf $f_{1|2}(\mathbf{x_1}|\mathbf{x_2})$, U.

Eq. B-56 can now be written as

$$f_{1|2}\left(\mathbf{x_1}\big|\ \mathbf{x_2}\right) = \frac{\exp\left[-\frac{1}{2}\left(\mathbf{x_1} - \mathbf{m_{12}}\right)'\left[\mathsf{L}_1\right]^{-1}\left(\mathbf{x_1} - \mathbf{m_{12}}\right)\right]}{\left(2\pi\right)^{k/2}\det\left[\mathsf{L}_1\right]^{1/2}}, \quad \mathbf{U}^{-k}. \tag{B-58}$$

$\mathbf{m_{12}}$, the conditional mean vector, depends on the "conditioning random variable vector" $\mathbf{x_2}$, but the conditional covariance matrix $[\mathsf{L}_1]$ does not depend upon the value of $\mathbf{x_2}$. These results are impor-

tant when the Kalman-Bucy filter is considered in the next paragraphs. See Ref. 3 for additional information on the Kalman-Bucy filter.

B-4 FIVE LEMMAS USED IN THE DERIVATION OF THE DISCRETE KALMAN FILTER

Several results can be derived directly from Eq. B-56 to obtain five lemmas that are used in the derivation of the discrete time Kalman filter.

B-4.1 LEMMA 1: THE CONDITIONAL MEAN

$$E\left(\mathbf{x}_1 \middle| \mathbf{x}_2\right) = \mathbf{m}_{12}$$

$$= \mathbf{m}_1 + \left[\Lambda_{12}\right]\left[\Lambda_{22}\right]^{-1}(\mathbf{x}_2 - \mathbf{m}_2), \quad \mathbf{U}$$

(B-59)

where

$E(\mathbf{x}_1 | \mathbf{x}_2)$ = mathematical expectation of $\mathbf{x}_1$ given $\mathbf{x}_2$, U.

B-4.2 LEMMA 2: THE CONDITIONAL COVARIANCE

$$E\left\{\left[\mathbf{x}_1 - E\left(\mathbf{x}_1 \middle| \mathbf{x}_2\right)\right]\left[\mathbf{x}_1 - E\left(\mathbf{x}_1 \middle| \mathbf{x}_2\right)\right]\mathbf{x}_2\right\} = \left[\llcorner_1\right]$$

$$= \left[\Lambda_{11}\right] - \left[\Lambda_{12}\right]\left[\Lambda_{22}\right]^{-1}\left[\Lambda_{21}\right], \quad \mathbf{U}^2$$

(B-60)

where the left side of Eq. B-60 is the conditional covariance of $\mathbf{x}_1 | \mathbf{x}_2$, U^2.

B-4.3 COMMENTS ON LEMMAS 1 AND 2

It is helpful to think of $f_{1|2}(\mathbf{x}_1 | \mathbf{x}_2)$ as a function of $\mathbf{x}_1$ parameterized by $\mathbf{x}_2$. Also

$$E\left[\psi\left(\mathbf{x}_1, \mathbf{x}_2\right) \middle| \mathbf{x}_2\right] \triangleq \int_{-\infty}^{\infty} \cdots \int_{-\infty}^{\infty} \psi\left(\mathbf{x}_1, \mathbf{x}_2\right) f_{1|2}\left(\mathbf{x}_1 \middle| \mathbf{x}_2\right) dx_1 dx_2 \cdots dx_k,$$

unit depends on $\psi(\mathbf{x}_1, \mathbf{x}_2)$

(B-61)

where

$\psi(\mathbf{x}_1, \mathbf{x}_2)$ = some function of $\mathbf{x}_1$ and $\mathbf{x}_2$, the unit depends upon function.

The proofs of Lemmas 1 and 2 follow by inspection of the form of $f_{1|2}(\mathbf{x}_1, \mathbf{x}_2)$.

B-4.4 LEMMA 3: INDEPENDENCE OF $\mathbf{x}_1 - E(\mathbf{x}_1 | \mathbf{x}_2)$ AND $\mathbf{x}_2$

The random variable $\mathbf{x}_1 - E[\mathbf{x}_1 | \mathbf{x}_2]$ is statistically independent of $\mathbf{x}_2$.

Proof: Recalling Lemma 1, let

$$\mathbf{z} \triangleq \mathbf{x}_1 - E\left(\mathbf{x}_1 \middle| \mathbf{x}_2\right)$$

$$= \mathbf{x}_1 - \mathbf{m}_1 - \left[\Lambda_{12}\right]\left[\Lambda_{22}\right]^{-1}(\mathbf{x}_2 - \mathbf{m}_2), \quad \mathbf{U}$$

(B-62)

where

$\mathbf{z}$ = convenient substitute for $\mathbf{x}_1 - E[\mathbf{x}_1 | \mathbf{x}_2]$, U.

Then

$$E(\mathbf{z}) = E\left(\mathbf{x}_1 - \mathbf{m}_1\right) - \left[\Lambda_{12}\right]\left[\Lambda_{22}\right]^{-1} E\left(\mathbf{x}_2 - \mathbf{m}_2\right)$$

$$= \mathbf{0}, \ \mathrm{U}$$

(B-63)

where

$E(\mathbf{x}_1 - \mathbf{m}_1) \triangleq \mathbf{0}, \ \mathrm{U}$

$E(\mathbf{x}_2 - \mathbf{m}_2) \triangleq \mathbf{0}, \ \mathrm{U}.$

Further, the random variable vectors **z** and $\mathbf{x}_2$ are jointly normal random variable vectors. This result follows from the observation that

$$\begin{bmatrix} \mathbf{z} \\ \hline \mathbf{x}_2 \end{bmatrix} = \begin{bmatrix} I & -\left[\Lambda_{12}\right]\left[\Lambda_{22}\right]^{-1} \\ \hline \bigcirc & I \end{bmatrix} \begin{bmatrix} \mathbf{x}_1 - \mathbf{m}_1 \\ \hline \mathbf{x}_2 - \mathbf{m}_2 \end{bmatrix} + \begin{bmatrix} \bigcirc \\ \hline \mathbf{m}_2 \end{bmatrix}, \ \mathrm{U}.$$

(B-64)

That is, $\begin{bmatrix} \mathbf{z} \\ \hline \mathbf{x}_2 \end{bmatrix}$ is an affine transformation of $\begin{bmatrix} \mathbf{x}_1 \\ \hline \mathbf{x}_2 \end{bmatrix}$.

Finally, the correlation matrix of **z** and $\mathbf{x}_2$ is evaluated as

$$\mathbf{cor}\left[\mathbf{z},\mathbf{x}_2\right] = E\left[\mathbf{z}\left(\mathbf{x}_2 - \mathbf{m}_2\right)'\right]$$

$$= E\left\{ \left[\mathbf{x}_1 - E\left(\mathbf{x}_1 \mid \mathbf{x}_2\right)\right]\left(\mathbf{x}_2 - \mathbf{m}_2\right)' \right\}$$

$$= E\left\{ \left[\mathbf{x}_1 - \mathbf{m}_1 - \left[\Lambda_{12}\right]\left[\Lambda_{22}\right]^{-1}\left(\mathbf{x}_2 - \mathbf{m}_2\right)\right]\left(\mathbf{x}_2 - \mathbf{m}_2\right)' \right\}$$

(B-65)

$$= E\left[\left(\mathbf{x}_1 - \mathbf{m}_1\right)\left(\mathbf{x}_2 - \mathbf{m}_2\right)'\right] - \left[\Lambda_{12}\right]\left[\Lambda_{22}\right]^{-1} E\left[\left(\mathbf{x}_2 - \mathbf{m}_2\right)\left(\mathbf{x}_2 - \mathbf{m}_2\right)'\right]$$

$$= \left[\Lambda_{12}\right] - \left[\Lambda_{12}\right]\left[\Lambda_{22}\right]^{-1}\left[\Lambda_{22}\right]$$

$$= \left[\Lambda_{12}\right] - \left[\Lambda_{12}\right] = \bigcirc, \ \mathrm{U}^2$$

where

$\mathbf{cor}[\mathbf{z},\mathbf{x}_2]$ = correlation matrix of **z** and $\mathbf{x}_2$, U^2.

The zero correlation result indicates that **z** and $\mathbf{x}_2$ are uncorrelated and, therefore, statistically independent.

B-4.5   LEMMA 4: COVARIANCE MATRIX OF $E(\mathbf{x}_1|\mathbf{x}_2)$

The covariance matrix of $E(\mathbf{x}_1|\mathbf{x}_2)$ is given by

$$\text{cov}\left[E\left(\mathbf{x}_1\middle|\ \mathbf{x}_2\right)\right] = \left[\Lambda_{12}\right]\left[\Lambda_{22}\right]^{-1}\left[\Lambda_{21}\right], \ \mathbf{U}^2 \tag{B-66}$$

where

$\text{cov}[E(\mathbf{x}_1|\mathbf{x}_2)]$ = covariance matrix of the expectation of $\mathbf{x}_1$ given $\mathbf{x}_2$, $\mathbf{U}^2$.

Proof: From Eqs. B-62 and B-63

$$E(\mathbf{z}) \ = \ E\left[\mathbf{x}_1 - E\left(\mathbf{x}_1\middle|\ \mathbf{x}_2\right)\right] = \ E(\mathbf{x}_1) - E\left[E\left(\mathbf{x}_1\middle|\ \mathbf{x}_2\right)\right] = \ \mathbf{0}, \ \mathbf{U}. \tag{B-67}$$

Therefore,

$$E\left[E\left(\mathbf{x}_1\middle|\ \mathbf{x}_2\right)\right] \ = \ E(\mathbf{x}_1) = \ \mathbf{m}_1, \ \mathbf{U}. \tag{B-68}$$

Then,

$$\begin{aligned}
\text{cov}\left[E\left(\mathbf{x}_1\middle|\ \mathbf{x}_2\right)\right] &= E\left\{\left[E\left(\mathbf{x}_1\middle|\ \mathbf{x}_2\right) - \mathbf{m}_1 E\left(\mathbf{x}_1\middle|\ \mathbf{x}_2\right) - \mathbf{m}_1\right]'\right\} \\[4pt]
&= E\left\{\left[\mathbf{m}_1 - \left[\Lambda_{12}\right]\left[\Lambda_{22}\right]^{-1}\left(\mathbf{x}_2 - \mathbf{m}_2\right) - \mathbf{m}_1\right]\right. \\[4pt]
&\quad \left.\times \left[\mathbf{m}_1 - \left[\Lambda_{12}\right]\left[\Lambda_{22}\right]^{-1}\left(\mathbf{x}_2 - \mathbf{m}_2\right) - \mathbf{m}_1\right]'\right\} \\[4pt]
&= E\left[\left[\Lambda_{12}\right]\left[\Lambda_{22}\right]^{-1}\left(\mathbf{x}_2 - \mathbf{m}_2\right)\left(\mathbf{x}_2 - \mathbf{m}_2\right)'\left(\left[\Lambda_{22}\right]^{-1}\right)'\left[\Lambda_{12}\right]'\right] \\[4pt]
&= \left[\Lambda_{12}\right]\left[\Lambda_{22}\right]^{-1}E\left[\left(\mathbf{x}_2 - \mathbf{m}_2\right)\left(\mathbf{x}_2 - \mathbf{m}_2\right)\right]\left(\left[\Lambda_{22}\right]^{-1}\right)'\left[\Lambda_{12}\right]' \\[4pt]
&= \left[\Lambda_{12}\right]\left[\Lambda_{22}\right]^{-1}\left[\Lambda_{22}\right]\left(\left[\Lambda_{22}\right]^{-1}\right)'\left[\Lambda_{12}\right]' \\[4pt]
&= \left[\Lambda_{12}\right]\left(\left[\Lambda_{22}\right]^{-1}\right)'\left[\Lambda_{12}\right]', \ \mathbf{U}^2.
\end{aligned} \tag{B-69}$$

From subpar. B-2.1 and Eq. B-16, $[\Lambda] = \begin{bmatrix} \left[\Lambda_{11}\right] & \vdots & \left[\Lambda_{12}\right] \\ ---- & + & ---- \\ \left[\Lambda_{21}\right] & \vdots & \left[\Lambda_{22}\right] \end{bmatrix}$ is a symmetric matrix. Therefore, $[\Lambda_{22}]$ is symmetric, and

$$\left(\left[\Lambda_{22}\right]^{-1}\right)' = \left(\left[\Lambda_{22}\right]'\right)^{-1} = \left[\Lambda_{22}\right]^{-1}, \ \mathbf{U}^{-2}. \tag{B-70}$$

Also

$$\left[\Lambda_{12}\right]' = \left[\Lambda_{21}\right], \ \mathbf{U}^2. \tag{B-71}$$

Substituting Eqs. B-70 and B-71 into Eq. B-69 yields

$$\text{cov}\left[E\left(x_1 \middle| x_2\right)\right] = \left[\Lambda_{12}\right]\left[\Lambda_{22}\right]^{-1}\left[\Lambda_{21}\right], \ U^2,$$

which proves Eq. B-66.

B-4.6   LEMMA 5: MULTIPLE CONDITIONAL

x_1, x_2, and x_3 **are jointly normal random variable vectors. In addition, it is assumed that** x_2 **and** x_3 **are statistically independent and that**

$$E\left(x_1\right) \ \underset{\triangle}{=} \ m_1 \ = \ 0, \ U. \tag{B-72}$$

Under these assumptions, it follows that

$$E\left(x_1 \middle| x_2, x_3\right) \ = \ E\left(x_1 \middle| x_2\right) + E\left(x_1 \middle| x_3\right), \ U \tag{B-73}$$

where

$E(x_1 | x_2, x_3)$ = **expectation of** x_1 **given** x_2 **and** x_3, U
$\quad E(x_1 | x_3)$ = **expectation of** x_1 **given** x_3, U
$\quad\quad x_1, x_2, x_3$ = **jointly normal random variable vectors, U.**

Proof: Let

$$x_4 \ = \ \begin{bmatrix} x_2 \\ \text{- -} \\ x_3 \end{bmatrix}, \ U \tag{B-74}$$

where

x_4 = **random variable vector comprising** x_2 **and** x_3, **U.**

$$E\left(x_1 \middle| x_4\right) \ = \ E\left(x_1 \middle| x_2, x_3\right)$$
$$= \ m_1 + \ \left[\Lambda_{14}\right]\left[\Lambda_{44}\right]^{-1}\left(x_4 - m_4\right), \ U \tag{B-75}$$

where

$$\left[\Lambda_{14}\right] \ = \ \left[\left[\Lambda_{12}\right] \ \vdots \ \left[\Lambda_{13}\right]\right], \ U^2 \tag{B-76}$$

and

$$\left[\Lambda_{44}\right] \ = \ \begin{bmatrix} \left[\Lambda_{22}\right] & \vdots & \bigcirc \\ \text{- - - -} & \text{+} & \text{- - - -} \\ \bigcirc & \vdots & \left[\Lambda_{33}\right] \end{bmatrix}, \ U^2 \tag{B-77}$$

where

$\quad[\Lambda_{22}]$, $[\Lambda_{33}]$, **and** $[\Lambda_{44}]$ = **square symmetric matrices whose dimensions depend on their selection,** U^2

$\quad[\Lambda_{12}]$, $[\Lambda_{13}]$, **and** $[\Lambda_{14}]$ = **rectangular matrices whose dimensions depend on their selection,** U^2.

Substituting Eqs. B-72, B-76, and B-77 into Eq. B-75 yields

$$E\left(\mathbf{x}_1 \middle| \mathbf{x}_4\right) = \left[\Lambda_{14}\right]\left[\Lambda_{44}\right]^{-1}\left(\mathbf{x}_4 - \mathbf{m}_4\right)$$

$$= \left[\left[\Lambda_{12}\right] \middle| \left[\Lambda_{13}\right]\right] \begin{bmatrix} \left[\Lambda_{22}\right]^{-1} & \bigcirc \\ \bigcirc & \left[\Lambda_{33}\right]^{-1} \end{bmatrix} \begin{bmatrix} \mathbf{x}_2 - \mathbf{m}_2 \\ \mathbf{x}_3 - \mathbf{m}_3 \end{bmatrix} \qquad \text{(B-75A)}$$

$$= \left[\Lambda_{12}\right]\left[\Lambda_{22}\right]^{-1}\left(\mathbf{x}_2 - \mathbf{m}_2\right) + \left[\Lambda_{13}\right]\left[\Lambda_{33}\right]^{-1}\left(\mathbf{x}_3 - \mathbf{m}_3\right)$$

$$= E\left(\mathbf{x}_1 \middle| \mathbf{x}_2\right) + E\left(\mathbf{x}_1 \middle| \mathbf{x}_3\right), \ \mathbf{U}$$

where

$\mathbf{m}_3$ = mean vector of pdf $f_3(\mathbf{x}_3)$, dimension consistent with $\mathbf{x}_3$, U

$\mathbf{m}_4$ = mean vector of pdf $f_4(\mathbf{x}_4)$, dimension consistent with $\mathbf{x}_4$, U,

which proves Eq. B-73.

B-5 THE DISCRETE TIME KALMAN FILTER

B-5.1 THE MODEL OF THE PLANT AND OBSERVATIONS

Let the state equation for a discrete linear time-varying system appear as

$$\mathbf{x}_{n+1} = \left[F_n\right]\mathbf{x}_n + \left[G_n\right]\boldsymbol{\omega}_n, \ \mathbf{U} \qquad \text{(B-78)}$$

where

$\mathbf{x}_{n+1}$ = system state m-dimensional vector at discrete time index $n+1$, U

$\mathbf{x}_n$ = system state m-dimensional vector at discrete time index n, U

$[F_n]$ = known $m \times m$ gain matrix at discrete time index n, dimensionless

$[G_n]$ = known $m \times r$ gain matrix at discrete time index n, dimensionless

$\boldsymbol{\omega}_n$ = part of $\{\boldsymbol{\omega}_n, n \in \Gamma\}$, which is assumed to be a sequence of zero mean, independent, Gaussian, r-dimensional random variable vectors with known covariance matrix, cov(ω), and constitutes a system stochastic disturbance, U

$\Gamma = \{1,2,\cdots,N\}$, dimensionless

n = state discrete time index, $n \in \Gamma$, dimensionless

and

$$\text{cov}\left(\omega\right) \triangleq E\left(\omega_i \omega_j{'}\right)$$
$$= Q_j \delta_{ij} = \left[Q_j\right], \ \mathbf{U}^2 \qquad \text{(B-79)}$$

where

cov(ω) = $m \times m$ diagonal covariance matrix of ω, $\mathbf{U}^2$

Q_j = variance of ω_j, $\mathbf{U}^2$

and

$$\delta_{ij} = \text{Kronecker delta} = 0 \ \text{ for } i \neq j, = 1 \ \text{ for } i = j, \ \text{dimensionless.} \qquad \text{(B-80)}$$

The initial state vector $\mathbf{x}_1$, i.e., the system initial condition, is assumed to be a zero mean Gaussian random variable vector with covariance matrix $[M]$, i.e.,

$$E\left(\mathbf{x}_1\right) = \mathbf{0}, \ \mathbf{U} \qquad \text{(B-81)}$$

where

$\mathbf{x}_1$ = assumed initial state random variable vector, U

$E(\mathbf{x}_1)$ = expectation or mean of $\mathbf{x}_1$, U

and

$$E\left(\mathbf{x}_1\mathbf{x}_1'\right) \triangleq [M], \ \mathbf{U}^2 \tag{B-82}$$

where

$[M]$ = $m \times m$ covariance matrix, $\mathbf{U}^2$.

In addition, it is assumed that the following system observations $\{\mathbf{z}_n, n \in \Gamma\}$ are made where

$$\mathbf{z}_n = [H_n]\mathbf{x}_n + \mathbf{v}_n, \ \mathbf{U} \tag{B-83}$$

where

$\mathbf{z}_n$ = nth state observation of a system parameter random variable m-dimensional vector, U

$[H_n]$ = finite sequence of known $s \times m$ matrices, i.e., the nth state member of $\{[H_n], n \in \Gamma\}$, dimensionless

$\mathbf{v}_n$ = s-dimension finite sequence of zero mean independent, Gaussian random variable vectors, U.

$\mathbf{v}_n$ is the nth state member of $\{\mathbf{v}_n, n \in \Gamma\}$ with

$$\mathbf{cov}\,(\mathbf{v}) = E\left(\mathbf{v}_i\mathbf{v}_j'\right) = [R_j] = \mathbf{R}_j\delta_{ij}, \ \mathbf{U}^2 \tag{B-84}$$

where

$\mathbf{cov(v)}$ = $s \times s$ covariance matrix of $\mathbf{v}$, $\mathbf{U}^2$

$[R_j]$ = $s \times s$ diagonal covariance matrix, $\mathbf{U}^2$

$\mathbf{R}_j$ = variance of $\mathbf{v}_j$, $\mathbf{U}^2$.

It is further assumed that $[R_j]^{-1}$ exists $\forall j \in \Gamma$ and that $\mathbf{v}_j$, ω_k, and $\mathbf{x}_1$ are statistically independent $\forall j, k \in \Gamma$.

B-5.2   ESTIMATION PROBLEM STATEMENT

Given the set of observations $\{\mathbf{z}_n, n \in \Gamma\}$, find the estimator:

$$\delta(N) \triangleq \delta(\mathbf{z}_1, \mathbf{z}_2, \cdots, \mathbf{z}_N), \ \mathbf{U} \tag{B-85}$$

where

$\delta(N)$ = m-dimensional vector function of the set of observations $\{\mathbf{z}_1, \mathbf{z}_2, \cdots, \mathbf{z}_N\}$, U

such that $\delta(N)$ minimizes $E\{[\mathbf{x}_{N+1} - \delta(N)]'[\mathbf{x}_{N+1} - \delta(N)]\}$. The estimator $\delta(N)$ can be written as

$$\delta(N) = E\left(\mathbf{x}_{N+1}\middle|\mathbf{z}_N, \mathbf{z}_{N-1}, \cdots, \mathbf{z}_1\right), \ \mathbf{U} \tag{B-86}$$

where

$E\left(\mathbf{x}_{N+1}\middle|\mathbf{z}_N, \mathbf{z}_{N-1}, \cdots, \mathbf{z}_1\right)$ = expectation of the system at state $N+1$ given the history of all observations through state N, U.

$E\left(\mathbf{x}_{N+1}\middle|\mathbf{z}_N, \mathbf{z}_{N-1}, \cdots, \mathbf{z}_1\right)$ will be computed recursively using an induction argument.

Let

$$\hat{\mathbf{x}}_{n+1|n} = \delta(n)$$
$$= E\left(\mathbf{x}_{n+1}\middle|\mathbf{z}_n, \mathbf{z}_{n-1}, \cdots, \mathbf{z}_1\right), \ \mathbf{U} \tag{B-87}$$

where

$\hat{\mathbf{x}}_{n+1|n}$ = m-dimensional estimator vector of $\mathbf{x}_{n+1}$ given $\{\mathbf{z}_n, \mathbf{z}_{n-1}, \cdots, \mathbf{z}_1\}$, U.

Assume $\hat{x}_{n/n-1}$ is known for $n > 1$, i.e., $x_{n/n-1}$ is assumed to be a known function of $\{z_{n-1}, z_{n-2}, \cdots, z_1\}$. Substituting Eq. B-78 into Eq. B-87 yields

$$
\begin{aligned}
\hat{x}_{n+1|n} &= E\left([F_n]\, x_n + [G_n]\, \omega_n \big| z_n, z_{n-1}, \cdots, z_1\right) \\
&= \Big[\, [F_n]\, E\left(x_n \big| z_n, z_{n-1}, \cdots, z_1\right) \\
&\quad + [G_n]\, E\left(\omega_n \big| z_n, z_{n-1}, \cdots, z_1\right)\Big], \ \ \mathbf{U}.
\end{aligned}
\tag{B-88}
$$

Since ω_n is statistically independent of $\{z_n, z_{n-1}, \cdots, z_1\}$ and since $E(\omega_n) = \mathbf{0}$,

$$
E\left(\omega_n \big| z_n, \cdots, z_1\right) = \mathbf{0}, \ \ \mathbf{U}.
\tag{B-89}
$$

ω_n is statistically independent of $\{z_n, z_{n-2}, \cdots, z_1\}$ because ω_n affects x_j only for $j \geq n+1$. Substituting Eq. B-89 into Eq. B-88 yields

$$
\hat{x}_{n+1|n} = [F_n]\, E\left(x_n \big| z_n, z_{n-1}, \cdots, z_1\right), \ \ \mathbf{U}.
\tag{B-90}
$$

Since it was assumed that $\hat{x}_{n/n-1}$ is a known function of $\{z_{n-1}, z_{n-2}, \cdots, z_1\}$, and that $[H_n]$ is a known matrix, it follows that

$$
E\left(x_n \big| z_n, z_{n-1}, \cdots, z_1\right) = E\left(x_n \big| z_n\right) - H_n\left(\hat{x}_{n|n-1}, z_{n-1}, z_{n-2}, \cdots, z_1\right), \ \ \mathbf{U}.
\tag{B-91}
$$

This equality holds because either side determines the other side of Eq. B-91. In other words,

$$
E(a|b,c) = E(a|b-d,c), \ \ \mathbf{U}
\tag{B-92}
$$

where
$\quad a,b,c = $ **random variables, U**
$\quad\quad d = $ **any known function of** c**, U.**

The vector $z_n - [H_n]\hat{x}_{n/n-1}$ can be shown to be statistically independent of the "giant" vector formed from the collection $\{z_{n-1}, z_{n-2}, \cdots, z_1\}$ and denoted by

$$
u_{n-1} \triangleq \left[z_{n-1} \,\big|\, z_{n-2} \,\big|\, \cdots \,\big|\, z_1\right]', \ \ \mathbf{U}.
\tag{B-93}
$$

The independence is shown as follows:

$$
\hat{x}_{n|n-1} = E\left(x_n \big| u_{n-1}\right), \ \ \mathbf{U}
\tag{B-94}
$$

and that

$$
z_n - [H_n]\,\hat{x}_{n|n-1} = v_n + [H_n]\left[x_n - E\left(x_n \big| u_{n-1}\right)\right], \ \ \mathbf{U}.
\tag{B-95}
$$

By Lemma 3 the vector $x_n - E(x_n|u_{n-1})$ is statistically independent of u_{n-1} since x_n and u_{n-1} are jointly normal random variable vectors. Therefore, $[H_n][x_n - E(x_n|u_{n-1})]$ is statistically independent of u_{n-1}. Since u_{n-1} does not include the measurement z_n, it follows that u_{n-1} is statistically independent of v_n. This last observation concludes the proof that $(z_n - [H_n]\hat{x}_{n/n-1})$ is statistically independent of u_{n-1}.

The last relationship is used to determine

$$\hat{\mathbf{x}}_{n+1|n} = [F_n]\, E\left(\mathbf{x}_n \big| \mathbf{z}_n - [H_n]\, \hat{\mathbf{x}}_{n|n-1}, \mathbf{u}_{n-1}\right),\ \mathbf{U}. \tag{B-96}$$

Since $\mathbf{x}_n$ is a linear combination of vectors, each of which has a zero mean, $\mathbf{x}_n$ has a zero mean. Since $\mathbf{x}_n$, $(\mathbf{z}_n - [H_n]\hat{\mathbf{x}}_{n/n-1})$ and $\mathbf{u}_{n-1}$ are jointly normal and $\mathbf{x}_n$ has a zero mean and $(\mathbf{z}_n - [H_n]\hat{\mathbf{x}}_{n/n-1})$ is statistically independent of $\mathbf{u}_n$, Lemma 5 can be applied to write

$$\hat{\mathbf{x}}_{n+1|n} = [F_n]\, E\left(\mathbf{x}_n \big| \mathbf{z}_n - [H_n]\, \hat{\mathbf{x}}_{n|n-1}\right)$$
$$+ [F_n]\, E\left(\mathbf{x}_n \big| \mathbf{u}_{n-1}\right),\ \mathbf{U}. \tag{B-97}$$

Substituting Eq. B-94 into Eq. B-97 yields

$$\hat{\mathbf{x}}_{n+1|n} = [F_n]\, \hat{\mathbf{x}}_{n|n-1} + [F_n]\, E\left(\mathbf{x}_n \big| \mathbf{z}_n - [H_n]\, \hat{\mathbf{x}}_{n|n-1}\right),\ \mathbf{U}. \tag{B-98}$$

Define

$$\mathbf{e}_n \triangleq \mathbf{x}_n - \hat{\mathbf{x}}_{n|n-1},\ \mathbf{U} \tag{B-99}$$

where

$\mathbf{e}_n = m$-dimensional estimation error associated with the state vector $\mathbf{x}_n$ given the observations $\{\mathbf{z}_{n-1}, \mathbf{z}_{n-2}, \cdots, \mathbf{z}_1\}$, U.

Eq. B-83 can be rewritten in terms of $\mathbf{e}_n$

$$\mathbf{z}_n - [H_n]\, \hat{\mathbf{x}}_{n|n-1} = [H_n]\left(\mathbf{x}_n - \hat{\mathbf{x}}_{n|n-1}\right) + \mathbf{v}_n$$
$$= [H_n]\, \mathbf{e}_n + \mathbf{v}_n,\ \mathbf{U}. \tag{B-100}$$

Define

$$[P_n] \triangleq E(\mathbf{e}_n \mathbf{e}_n'),\ \mathbf{U}^2 \tag{B-101}$$

where

$[P_n] = m \times m$ estimation error covariance matrix, $\mathbf{U}^2$.

$\mathbf{e}_n$ is statistically independent of $\mathbf{v}_n$ since $\mathbf{e}_n$ is only a function of the observations $\{\mathbf{z}_{n-1}, \mathbf{z}_{n-2}, \cdots, \mathbf{z}_1\}$; therefore,

$$E\left[\left([H_n]\mathbf{e}_n + \mathbf{v}_n\right)\left([H_n]\mathbf{e}_n + \mathbf{v}_n\right)'\right] = [H_n]\,[P_n]\,[H_n]' + [R_n],\ \mathbf{U}^2. \tag{B-102}$$

The $s \times s$ matrix $[H_n][P_n][H_n]' + [R_n]$ corresponds to the matrix $[\Lambda_{22}]$ in Lemma 1. Here, the mean vectors that correspond to $\mathbf{m}_1$ and $\mathbf{m}_2$ (of Lemma 1) are both zero, i.e.,

$$\mathbf{m}_1 \triangleq E(\mathbf{x}_n) = \mathbf{0},\ \mathbf{U} \tag{B-103}$$

and

$$\mathbf{m}_2 \triangleq E\left(\mathbf{z}_n - [H_n]\, \hat{\mathbf{x}}_{n|n-1}\right) = \mathbf{0},\ \mathbf{U}. \tag{B-104}$$

Since $E(\mathbf{z}_k) = \mathbf{0}$, $\forall k \in \Gamma$ and $\hat{\mathbf{x}}_{n/n-1}$ is a linear transformation on $\mathbf{u}_{n-1}$.

In Lemma 1 the matrix $[\Lambda_{12}]$ corresponds to $E[\mathbf{x}_n([H_n]\mathbf{e}_n + \mathbf{v}_n)']$. The procedure for evaluating this expectation follows. It can be observed that

$$E\left\{ \hat{\mathbf{x}}_{n\,|\,n\,-\,1}\left[\,[H_n]\,\left(\mathbf{x}_n - \hat{\mathbf{x}}_{n\,|\,n\,-\,1}\right) + \mathbf{v}_n\right]'\right\} = \mathbf{0},\ \mathbf{U}. \qquad \text{(B-105)}$$

Eq. B-105 follows by noting that

1. $\hat{\mathbf{x}}_{n/n-1}$ is functionally independent of $\mathbf{z}_n$ and therefore is statistically independent of the vector $\mathbf{v}_n$, by inspection.

2. $\hat{\mathbf{x}}_{n/n-1}$ is statistically independent of $(\mathbf{x}_n - \hat{\mathbf{x}}_{n/n-1})$. Since $\mathbf{x}_n - \hat{\mathbf{x}}_{n/n-1} = \mathbf{x}_n - E(\mathbf{x}_n\,|\,\mathbf{u}_{n-1})$ and $E(\mathbf{x}_n\,|\,\mathbf{u}_{n-1})$ is a linear transformation on $\mathbf{u}_{n-1}$, by Lemma 3, $\mathbf{x}_n - E(\mathbf{x}_n\,|\,\mathbf{u}_{n-1})$ is statistically independent of $\mathbf{u}_{n-1}$, and therefore, $\mathbf{x}_n - E(\mathbf{x}_n\,|\,\mathbf{u}_{n-1})$ is statistically independent of any linear transformation of $\mathbf{u}_{n-1}$. Thus by inspection and by using Points 1 and 2, it can be seen that Eq. B-105 is true.

Using Eq. B-105

$$[\Lambda_{12}]\ \triangleq\ E\left\{x_n\left[\,[H_n]\,\left(\mathbf{x}_n - \hat{\mathbf{x}}_{n\,|\,n\,-\,1}\right) + \mathbf{v}_n\right]'\right\},\ \mathbf{U}^2 \qquad \text{(B-106)}$$

can be written as

$$E\left\{\mathbf{x}_n - \hat{\mathbf{x}}_{n\,|\,n\,-\,1}\left[\,[H_n]\,\mathbf{x}_n - \hat{\mathbf{x}}_{n\,|\,n\,-\,1} + \mathbf{v}_n\right]'\right\} = [P_n]\,[H_n]',\ \mathbf{U}^2 \qquad \text{(B-107)}$$

since

$$E\,(\mathbf{e}_n\mathbf{e}_n')\ = \bigcirc,\ \mathbf{U}^2. \qquad \text{(B-108)}$$

Applying Lemma 1 yields

$$\begin{aligned} E\,(\mathbf{x}_n\,|\,\mathbf{z}_n - [H_n]\,\hat{\mathbf{x}}_{n\,|\,n\,-\,1}) &= [\Lambda_{12}]\,[\Lambda_{22}]^{-1}\,(\mathbf{z}_n - [H_n]\,\hat{\mathbf{x}}_{n\,|\,n\,-\,1}) \\ &= [P_n]\,[H_n]'\,(\,[H_n]\,[P_n]\,[H_n]' + [R_n]\,)' \\ &\quad \times (\mathbf{z}_n - [H_n]\,\hat{\mathbf{x}}_{n\,|\,n\,-\,1}),\ \mathbf{U}. \end{aligned} \qquad \text{(B-109)}$$

Define

$$[K_n]\ \triangleq\ [P_n]\,[H_n]'\,(\,[H_n]\,[P_n]\,[H_n]' + [R_n]\,)^{-1}, \qquad \text{(B-110)}^{*}$$

$$\textbf{dimensionless}$$

where

$\quad$ $[K_n] = m \times s$ **gain matrix, dimensionless.**

Substituting Eq. B-110 into Eq. B-98 yields

$$\hat{\mathbf{x}}_{n\,+\,1\,|\,n}\ =\ [F_n]\,\hat{\mathbf{x}}_{n\,|\,n\,-\,1} + [F_n]\,[K_n]\,(\mathbf{z}_n - [H_n]\,\hat{\mathbf{x}}_{n\,|\,n\,-\,1}),\ \mathbf{U}. \qquad \text{(B-111)}$$

---

[*] Since $[P_n] \triangleq E(\mathbf{e}_n\mathbf{e}_n')$, $[P_n]$ is nonnegative. Therefore, the matrix $[H_n][P_n][H_n]'$ is nonnegative. Hence, since $[R_n]$ was assumed to be p.d. $\forall\ n \in \Gamma$, it follows that $([H_n][P_n][H_n]' + [R_n])$ is p.d. and, therefore, not singular.

A recursive relation for $\mathbf{e}_n$ is obtained as follows. Let

$$[\hat{K}_n] \;=\; [F_n]\,[K_n]\,, \quad \textbf{dimensionless} \tag{B-112}$$

where

$[\hat{K}_n]$ = $m \times s$ **estimated gain matrix, dimensionless.**

Substituting Eq. B-112 into Eq. B-110 yields

$$
\begin{aligned}
\hat{\mathbf{x}}_{n+1|n} &= [F_n]\,\hat{\mathbf{x}}_{n|n-1} + [\hat{K}_n]\,\mathbf{z}_n - [\hat{K}_n]\,[H_n]\,\hat{\mathbf{x}}_{n|n-1} \\
&= ([F_n] - [\hat{K}_n]\,[H_n])\,\hat{\mathbf{x}}_{n|n-1} + [\hat{K}_n]\,\mathbf{z}_n, \quad \mathbf{U}.
\end{aligned}
\tag{B-113}
$$

Subtracting Eq. B-113 from Eq. B-78 and noting that $\mathbf{e}_n = \mathbf{x}_n - \hat{\mathbf{x}}_{n/n-1}$ and $\mathbf{z}_n = [H_n]\mathbf{x}_n + \mathbf{v}_n$ yield

$$
\begin{aligned}
\mathbf{x}_{n+1} - \hat{\mathbf{x}}_{n+1|n} &= [F_n]\,\mathbf{x}_n + [G_n]\,\boldsymbol{\omega}_n - ([F_n] - [\hat{K}_n]\,[H_n])\,\hat{\mathbf{x}}_{n|n-1} \\
&\quad - [\hat{K}_n]\,([H_n]\,\mathbf{x}_n + \mathbf{v}_n), \quad \mathbf{U}
\end{aligned}
\tag{B-114}
$$

or

$$
\begin{aligned}
\mathbf{e}_{n+1} &= ([F_n] - [\hat{K}_n]\,[H_n])\,(\mathbf{x}_n - \hat{\mathbf{x}}_{n|n-1}) + [G_n]\,\boldsymbol{\omega}_n - [\hat{K}_n]\,\mathbf{v}_n \\
&= ([F_n] - [\hat{K}_n]\,[H_n])\,\mathbf{e}_n + [G_n]\,\boldsymbol{\omega}_n - [\hat{K}_n]\,\mathbf{v}_n, \quad \mathbf{U}
\end{aligned}
\tag{B-115}
$$

where

$\mathbf{e}_{n+1}$ = m-**dimensional estimation error vector at state** $n+1$, U.

$\mathbf{e}_n$, $\boldsymbol{\omega}_n$, and $\mathbf{v}_n$ are pairwise independent random variable vectors. Specifically, $\mathbf{e}_n$ depends upon $\boldsymbol{\omega}_j$ and $\mathbf{v}_k$ only for $j,k \le n-1$. Also $\mathbf{e}_n$, $\boldsymbol{\omega}_n$, and $\mathbf{v}_n$ all have zero means.

Now by using Eq. B-115 and noting that

$$[P_{n+1}] \;\triangleq\; E(\mathbf{e}_{n+1}\mathbf{e}'_{n+1}), \quad \mathbf{U}^2 \tag{B-116}$$

where

$[P_{n+1}]$ = $m \times m$ **estimation error covariance matrix at state** $n+1$, $\mathbf{U}^2$,

$[P_{n+1}]$ **can be written as**

$$
\begin{aligned}
[P_{n+1}] &= ([F_n] - [\hat{K}_n]\,[H_n])\,[P_n]\,([F_n] - [\hat{K}_n]\,[H_n])' \\
&\quad + [G_n]\,[Q_n]\,[G_n]' + [\hat{K}_n]\,[R_n]\,[\hat{K}_n]', \quad \mathbf{U}^2.
\end{aligned}
\tag{B-117}
$$

Eq. B-117 is a nonlinear recursion relation for $[P_{n+1}]$ because $[\hat{K}_n] \triangleq [F_n][P_n][H_n]'([H_n][P_n][H_n]' + [R_n])^{-1}$.

B-5.3 SPECIFICATION OF INITIALIZING VARIABLES

The initializing variables are denoted by $\hat{\mathbf{x}}_{1|0}$ and $[P_1]$. The first is given by

$$
\begin{aligned}
\hat{\mathbf{x}}_{1|0} &= E(\mathbf{x}_1 | \text{no observations}) \\
&= E(\mathbf{x}_1) = \mathbf{0}, \quad \mathbf{U}
\end{aligned}
\tag{B-118}
$$

where

$$\hat{\mathbf{x}}_{1|0} = m\text{-dimensional initial system state estimate vector, U}$$

$$E(\mathbf{x}_1 | \text{no observations}) = \text{expected value of the first state vector given no observations, U}.$$

Since $\mathbf{x}_1$ is assumed to be a zero mean Gaussian vector with covariance matrix $[M]$, Eq. B-118 follows. The notation $\hat{\mathbf{x}}_{1|0}$ is, strictly speaking, not allowed in the notational setup because Γ does not include a zero element. However, it is easier to ignore this anomaly than to define two index sets.

The initial estimation error covariance matrix is given by

$$[P_1] = E\left[(\mathbf{x}_1 - \hat{\mathbf{x}}_{1|0}) (\mathbf{x}_1 - \hat{\mathbf{x}}_{1|0})' \right]$$

$$= E(\mathbf{x}_1 \mathbf{x}_1') = [M], \ \mathbf{U}^2$$

(B-119)

where

$[P_1]$ = initial estimate error covariance matrix, $\mathbf{U}^2$.

B-5.4 SUMMARY

The discrete Kalman filter relationships are summarized as follows:

1. The plant model, Eq. B-78:

$$\mathbf{x}_{n+1} = [F_n] \mathbf{x}_n + [G_n] \boldsymbol{\omega}_n, \ \mathbf{U}$$

2. The measurement model, Eq. B-83:

$$\mathbf{z}_n = [H_n] \mathbf{x}_n + \mathbf{v}_n, \ \mathbf{U}$$

3. The recursive state estimate, Eqs. B-113 and B-118:

$$\hat{\mathbf{x}}_{n+1|n} = ([F_n] - [\hat{K}_n][H_n]) \hat{\mathbf{x}}_{n|n-1} + [\hat{K}_n] \mathbf{z}_n, \ \mathbf{U}$$

where $\hat{\mathbf{x}}_{1|0} = \mathbf{0}$, U

4. The recursive estimate error covariance matrix, Eqs. B-117 and B-119:

$$[P_{n+1}] = ([F_n] - [\hat{K}_n][H_n])([F_n] - [\hat{K}_n][H_n])'$$

$$+ [G_n][Q_n][G_n]' + [\hat{K}_n][R_n][\hat{K}_n]', \ \mathbf{U}^2.$$

where $[P_1] = [M]$, $\mathbf{U}^2$.

These relationships are shown in Fig. B-1.
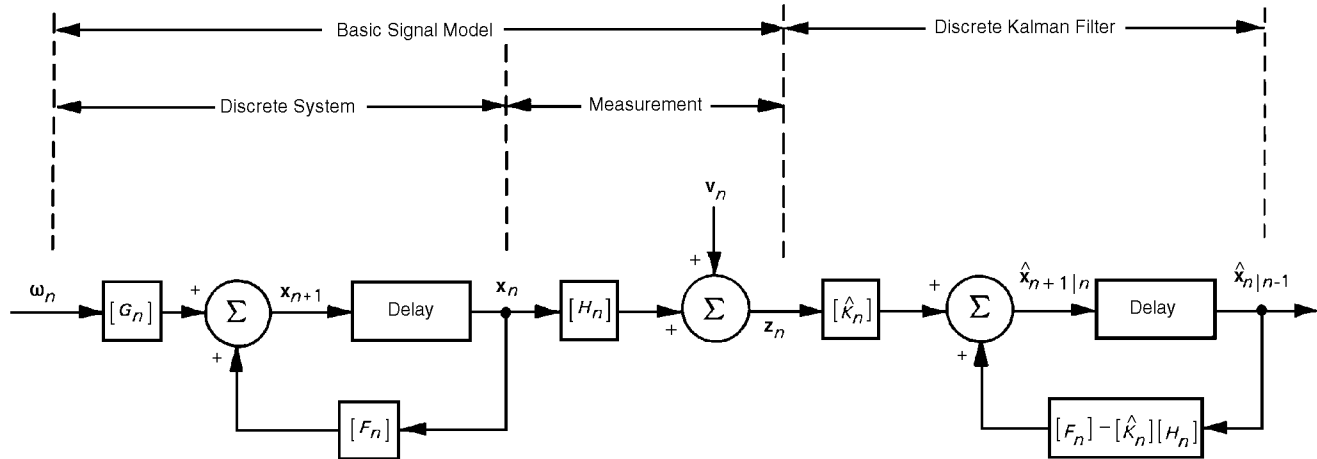
Figure B-1.   System Model and Discrete Kalman Filter

REFERENCES

1. The Analytic Sciences Corporation Technical Staff, Arthur Gelb, Ed., *Applied Optimal Estimation*, **The M.I.T. Press, Massachusetts Institute of Technology, Cambridge, MA, 1974.**

2. F. B. Hildebrand, *Methods of Applied Mathematics*, **Prentice-Hall, Inc., Englewood Cliffs, NJ, 1961.**

3. R. E. Kalman and R. S. Bucy, "New Results in Linear Filtering and Prediction Theory", Journal of Basic Engineering (ASME) **83D**, 95-108 (March 1961).

BIBLIOGRAPHY

B. D. O. Anderson and J. B. Moore, *Optimal Filtering*, **Prentice-Hall, Inc., Englewood Cliffs, NJ, 1979. (This is a graduate level text that develops Kalman filters, provides examples of their application, and discusses simplifying variations from optimality.)**

R. S. Bucy and P. D. Joseph, *Filtering for Stochastic Processes With Applications to Guidance*, **John Wiley & Sons, Inc., New York, NY, 1968.**

S. L. Fagin, "Recursive Linear Regression Theory, Optimal Filter Theory, and Error Analyses of Optimal Systems", Sperry Gyroscope Company (Now Unysis), Inertial Division, Great Neck, NY, *Proceedings of the IEEE International Convention*, **New York, NY, March 1964, The Institute of Electrical and Electronic Engineers, Inc., New York, NY.**

D. C. Fraser, *New Technique for Optimal Smoothing of Data*, **NASA Technical Brief 68-10060, National Aeronautics and Space Administration, Manned Spacecraft Center, Houston, TX, May 1968.**

K. Hoffman and R. Kunze, *Linear Algebra*, **Prentice-Hall, Inc., Englewood Cliffs, NJ, 1961.**

R. E. Kalman, "A New Approach to Linear Filtering and Prediction Problems", *Journal of Basic Engineering Transactions of the ASME*, **35-45 (March 1960).**

A. Papoulis, *Probability, Random Variables, and Stochastic Processes*, **McGraw-Hill Book Company, New York, NY, 1965.**

APPENDIX C
PROBABILITY THEORY

Detailed discussions of the following mathematical probability concepts are presented: random or chance events, definitions of probability, axiomatic probability, mutually exclusive events, independent events, joint probability, conditional probability, random variables (both discrete and continuous), probability cumulative distribution functions, probability density functions, stochastic processes, stationarity, ergodicity, time averages, ensemble averages (moments), the univariate and bivariate normal distributions, the central limit theorem, and the binomial distribution. Illustrative examples are provided for many of the concepts, and two combined statistics of sums of random variables are derived.

C-0   LIST OF SYMBOLS

In the general presentation of probability concepts, the units of the random variables, their statistics, and their probability density functions (if continuous) depend on the specific system to which they are applied. Until applied, "U" is used to stand in for the random variable units. Various powers of "U" are used for the various functions of the random variables.

The number of symbols used in this appendix is so large that a significant number have more than one definition. To avoid confusion, the appendix is divided into three distinct areas, and unique lists of symbols are used for each area.

C-0.1   SYMBOLS FOR PARAGRAPH C-2

A,B,C,D = general or specific events that may or may not occur, unit depends on event (**U**)

E = event of occurrence of (A and B) or (C and D), **U**

H = event of a hit in a round, dimensionless

H_k = event of a hit in the kth round, dimensionless

M = event of a miss in a round, dimensionless

M_1 = event of a miss in the first round, dimensionless

M_k = event of a miss in the kth round, dimensionless

n = number of trials, dimensionless

$n(A)$ = number of ways in which event A can occur, dimensionless

$n(\text{all})$ = total number of events that can occur, dimensionless

$P(A),P(B),P(C),P(D),P(E)$ = probability that the indicated event occurs at any trial, $\mathbf{U^{-1}}$

$P(AB)$ = joint probability that both events A and B will occur, $\mathbf{U^{-1}}$

$P(A+B)$ = probability that either event A or event B or, if not mutually exclusive, both occur, $\mathbf{U^{-1}}$

$P(AM_1)$ = joint probability that at least three rounds are required and that the first round is a miss, $\mathbf{U^{-1}}$

$P(A|M_1)$ = conditional probability that at least three rounds are required, given that the first round is a miss, $\mathbf{U^{-1}}$

$P(B|A)$ = conditional probability that event B occurs given that event A occurs, $\mathbf{U^{-1}}$

$P(CD)$ = joint probability that both events C and D occur, $\mathbf{U^{-1}}$

$P(H)$ = probability of a hit on any one round, $\mathbf{U^{-1}}$

$P(H_k)$ = probability of a hit on the kth round, $\mathbf{U^{-1}}$

$P(H+M)$ = probability of either a hit or a miss on any one round, $\mathbf{U^{-1}}$

$P(M)$ = probability of a miss on any one round, $\mathbf{U^{-1}}$

$P(M_k)$ = probability of a miss on the kth round, $\mathbf{U^{-1}}$

$P(\varepsilon_k)$ = probability that the first hit occurs on kth round, $\mathbf{U^{-1}}$

ε_k = event that first hit occurs on kth round, dimensionless

C-0.2 SYMBOLS FOR PARAGRAPHS C-3 THROUGH C-9

A = **event in Example C-4 that the potentiometer has lasted** $t = $ **30 days, dimensionless**

= **constant amplitude in Eq. C-65, U**

$\lceil a \rceil \triangleq$ **ceiling of** $a \triangleq$ **smallest integer** $\geq a$, **U**

B = **event that the potentiometer fails in the interval** $t < T \leq \Delta t$, **dimensionless**

$B(n,s)$ = **binomial cdf, U^{-1}**

$b(n,s)$ = **binomial pdf, U^{-1}**

C = **specified confidence probability, U^{-1}**

c = **constant of integration, day** $^{-1}$

$E(t)$ = **random variable instantaneous voltage across a resistance, V**

$\overline{E^2(t)}$ = **mean-square value of** $E(t)$, **V$^2/\Omega$**

$E^2(t)$ = **instantaneous power dissipated in resistor, W**

$E(X)$ = $\overline{X}$ = **expected value of random variable** X, **U**

$E(X^n) \triangleq$ **expected value of** X^n, **U^n**

$E[(X - \overline{X})^n]$ = **expected value of** $(X - \overline{X})^n$, **U^n**

e = **2.71828..., dimensionless**

$F_R(r)$ = **cdf of the Rayleigh random variable** R, **U^{-1}**

$F_R(\rho)$ = **continuous cdf of the normalized miss distance random variable** R/σ **(evaluated at** $R = \rho$**), U^{-1}**

$F_{R,\Theta}(\rho,\theta)$ = **continuous joint cdf of the random variables** R **and** Θ **(evaluated at** $R = \rho$ **and** $\Theta = \theta$**), U^{-1}**

$F_T(t)$ = **cdf of the time random variable** T **(evaluated at** $T = t$**), U^{-1}**

$F_X(x)$ = **continuous cdf of the random variable** X **as a function of** x, **U^{-1}**

$F_X(x;t)$ = **continuous cdf of the stochastic variable** $X(t)$ **(evaluated at** $X(t) = x$ **and at time** t**), U^{-1}**

$F_{X,Y}(u,v)$ = **continuous joint cdf of the random variables** X/σ_X **(evaluated at** u**) and** Y/σ_Y **(evaluated at** v**), U^{-1}**

$F_{X,Y}(x,y)$ = **continuous joint cdf of the random variables** X **and** Y **(evaluated at** $X = x$ **and** $Y = y$**), U^{-1}**

$F_{X|Y}(x|y)$ = **continuous conditional cdf of the random variable** X **given the random variable** Y **(evaluated at** $X = x$ **and** $Y = y$**), U^{-1}**

$F_Y(y)$ = **continuous cdf of the random variable** Y **(evaluated at** $Y = y$**), U^{-1}**

$F_Z(z)$ = **cdf of the random variable** Z **that can take on the values** $-\infty < z < \infty$, **U^{-1}**

$f_R(\rho)$ = **continuous pdf for the normalized miss distance, dimensionless**

$f_T(t)$ = **pdf of the random variable** T **(evaluated at** $T = t$**), U^{-1}**

$f_X(u)$ = **normal pdf for the random variable** X/σ, **dimensionless**

$f_X(x)$ = **continuous pdf of the random variable** X **as a function of** x, **U^{-1}**

$f_X(x;t)$ = **continuous pdf of the stochastic variable** $X(t)$ **(evaluated at** $X(t) = x$ **and at time** t**), U^{-1}**

$f_{X,Y}(u,v)$ = **continuous joint pdf of** X/σ_X **and** Y/σ_Y, **dimensionless**

$f_{X,Y}(x,y)$ = **continuous joint pdf of the random variables** X **(evaluated at** $X = x$**) and** Y **(evaluated at** $Y = y$**), U^{-2}**

$f_{X|Y}(\mathbf{x}|\mathbf{y})$ = **continuous conditional pdf of the random variable** X **given the random variable** Y, **U^{-1}**

$f_Y(v)$ = **normal pdf for the random variable** Y/σ_Y, **dimensionless**

$f_Y(y)$ = continuous pdf of the random variable Y (evaluated at $Y = y$), U^{-1}

$f_\Theta(\theta)$ = continuous pdf for the angular random variable Θ, rad^{-1}

K = normalizing factor, 1, m

$m^{(n)}$ = random variable moment of order n, U^n

n = number of trials (in a binomial distribution), dimensionless

= index integer, dimensionless

$P(X \leq x, Y \leq y)$ = joint probability that random variable $X \leq x$ and random variable $Y \leq y$, U^{-1}

$P(X \leq x \mid Y = y)$ = conditional probability that the random variable X is in $X_{min} \leq X \leq x \leq X_{max}$ given that the random variable $Y = y$, $Y_{min} \leq y \leq Y_{max}$, U^{-1}

$P(S = s)$ = probability that the random variable S will take on the value $s = 0, 1, 2, \cdots$, U^{-1}

P_{AV} = average power (equivalent dc) in a 1Ω resistance, W

p = probability of a success in any one trial, U^{-1}

$p_X(x)$ = discrete pdf of the Poisson random variable X, U^{-1}

q = probability of a failure in any one trial ($q = 1 - p$), U^{-1}

R = miss distance random variable that takes on the values of $0 \leq r < \infty$, m

r = values taken on by the random variable R, m

$\overline{S}_n$ = mean (or expected value) of the random variable S_n, U

S_n = sum of n random variables that can take on the values $S_{n_{min}} \leq s \leq S_{n_{max}}$, U

$S_{n_{max}}$ = maximum value the random variable S_n can take on, U

$S_{n_{min}}$ = minimum value the random variable S_n can take on, U

S_z = random variable that is the sum of the random variables X_1 and X_2, U

s = number of successes, dimensionless

s_n = value taken on by the random variable S_n, U

T = potentiometer life random variable that can take on the values $t \geq 0$, day

t = value taken on by the random variable T, day

= independent variable (usually time) in stochastic processes, s

t' = dummy variable of integration for t, day

u = value of normalized random variable x/σ, dimensionless

u' = dummy variable of integration for u, dimensionless

v = value of normalized random variable y/σ, dimensionless

v' = dummy variable of integration for v, dimensionless

X = random variable that takes on the values of x, U

X_i = ith random variable of the set $\{X_1, X_2, \cdots, X_n\}$, U

X_{max} = maximum value that the random variable X can take on, U

X_{min} = minimum value that the random variable X can take on, U

$\overline{X}$ = mean, or expected value, of the random variable X, U

$\overline{X}_n$ = mean, or expectation, of X_n, U

$X(t)$ = stochastic variable X as a function of the independent variable t, U

$\overline{X(t)}$ = time average of the stochastic variable $X(t)$, U

$\overline{X^2(t)}$ = mean-square time average for $X(t)$, U^2

x = values taken on by the random variable X, U

x_i = value taken on by the random variable X_i, U

x_t = value taken on by the stochastic variable $X(t)$, U

$x_{t+\tau}$ = value taken on by the stochastic variable $X(t + \tau)$, U

x' = dummy variable of integration for x, U

Y = random variable that can take on the values $Y_{min} \leq Y \leq y \leq Y_{max}$, U

Y_{max} = maximum value that the random variable Y can take on, U

Y_{min} = minimum value that the random variable Y can take on, U

$\bar{Y}$ = mean of the random variable Y, U

y = value taken on by the random variable Y, U

Z_i = ith normalized random variable, dimensionless

z' = dummy variable of integration for z, dimensionless

Δt = a time interval in Eq. C-66, s

= potentiometer operating interval, day

Θ = angle of line $\overline{TI}$ with respect to x-axis, rad

θ = values taken on by the random variable Θ, rad

θ' = dummy variable for θ, rad

μ = general symbol for the mean of a random variable, U

$\mu^{(n)}$ = central moment of order n, U^n ($\mu^{(1)}$ is usually written μ.)

μ_X = mean value of the random variable X, U

μ_Y = mean value of the random variable $Y = 0$, U

ρ = normalized range distance equivalent (R/σ or R/K_p), dimensionless

ρ_{pK} = value of the abscissa ρ at the peak of the Rayleigh pdf, dimensionless

ρ' = dummy variable for ρ, dimensionless

σ = standard deviation of a random variable, U

σ_{S_n} = standard deviation of the random variable S_n, U

σ_X = standard deviation of X, m

σ_{X_i} = variance of the random variable X_i, U^2

σ_Y = standard deviation of Y, m

$\sigma_{S_n}^2$ = variance of the random variable S_n, U^2

σ_X^2 = variance of the random variable X, U^2

τ = time offset or shift, s

Φ = random variable uniformly distributed over the interval $(0,2\pi)$, rad

ω = rotational frequency, $2\pi f$, rad/s

C-0.3   SYMBOLS FOR PARAGRAPHS C-10, C-11, AND C-12

c_1 = assumed constant factor, dimensionless

c_2 = assumed constant systematic error, V

c_3 = assumed constant factor, rad

$c_4 = -(c_1 + c_3)$, dimensionless (rad)

$c_5 = c_2 + d_2 + d_3$, V

d_1, d_2, d_3 = assumed constant systematic errors, V

e = error generated by the device or output error in the absence of input error, V

e_1 = Element 1 output error in the absence of input error, V

e_2 = Element 2 output error in the absence of input error, V

e_3 = Element 3 output error in the absence of input error, V

f_1 = performance function of Element 1, V

f_2 = performance function of Element 2, V

f_3 = performance function of Element 3, V

$f(x,y)$ = simple amplifier performance function, V

h_1 = nonideal performance function of Element 1, V

h_2 = nonideal performance function of Element 2, V

h_3 = nonideal performance function of Element 3, V

k = subscript index = 1,2,3, dimensionless

n = subscript index = 1,2,3, dimensionless

x = nominal input, V

x_1 = input to Element 1, V

x_2 = input to Element 2, V

x_3 = input to Element 3, rad

y = nominal input, V

y_1 = output of Element 1, V

y_2 = output of Element 2, V

y_3 = output of Element 3, V

z = normalized output variance $\sigma_{\varepsilon y1}^2 / \sigma_3^2$ of Element 1, dimensionless

z_{max} = maximum value of z

z_{min} = minimum value of z

α = nominal gain, dimensionless

Δ = fixed offset in amplifier output, V

δ = assumed value of ε_x, V

ε_x = input error, V

ε_{x_1} = error in input to Element 1, V

ε_{x_2} = error in input to Element 2, V

ε_{x_3} = error in input to Element 3, rad

ε_{x_n} = Element n input error, U

ε_y = output error, V

ε_{y_1} = error in output of Element 1, V

$\varepsilon_{y_{1S}}$ = systematic component of output error ε_{y_1}, V

ε_{y_2} = error in output of Element 2, V

ε_{y_3} = error in output of Element 3, V

ε_{y_k} = Element k total output error, V

ε_α = gain error, dimensionless

ρ_1 = σ_1/σ_3, dimensionless

ρ_2 = σ_2/σ_3, dimensionless

σ_1 = assumed random component factor of ε_{x_1}, V

σ_2 = assumed random component factor of e_1, V

σ_3 = assumed random component factor of e_2, V

$\sigma_{e_1}^2$ = variance of e_1, V^2

$\sigma_{e_2}^2$ = variance of $\dfrac{\sin x_3}{1 - \cos x_3} e_2$, V^2

$\sigma_{e_3}^2$ = variance of $\dfrac{\sin x_3}{1 - \cos x_3} e_3$, V^2

$\sigma_{\varepsilon x1}^2$ = variance of $-\varepsilon_{x_1}$, V^2

$$\sigma^2_{\varepsilon_{X2}} = \text{variance of } \frac{\sin x_3}{1 - \cos x_3}\varepsilon_{x_2}, \text{ V}^2$$

$$\sigma^2_{\varepsilon_{X3}} = \text{variance of } \frac{x_2}{1 - \cos x_3}\varepsilon_{x_3}, \text{ V}^2$$

$$\sigma^2_{\varepsilon_{y1}} = \text{variance of total output random error of Element 1, V}^2$$

$$\overline{\sigma^2_{\varepsilon_{y1}}} = \text{mean of } \sigma^2_{\varepsilon_{y1}} \text{ as a function of } x_3, \text{ V}^2$$

C-1 INTRODUCTION

Before proceeding to a detailed analysis of hit probability, it is important to introduce the basic mathematical concepts of probability theory as background information. These concepts are presented without any attempt at rigorous derivation because the necessary understanding of the fundamental concepts can be obtained from an intuitive approach, which avoids the introduction of additional mathematical theory. If rigorous derivation is desired, extensive discussions of probability theory are found in many excellent, books such as Refs. 1 through 6.

In par. C-2 the basic ideas of chance and probability are defined on an intuitive basis and then developed in connection with discrete events, i.e., events whose probabilities are limited to a finite or countably infinite number of values. Countably infinite means a one-to-one correspondence to the set of positive integers as described in Ref. 7. These basic ideas are more or less familiar to everyone from their application to games of chance. For convenience, the analogy of simple dice games is used to develop the definitions and axioms associated with the probability of discrete events.

The basic concepts of probability are then extended in par. C-3 to random variables with continuous probability functions and in par. C-4 to stochastic processes. The derivations become directly applicable to the fire control problem.

In par. C-5 a number of convenient statistics are defined. These statistics provide a numerical measure of the important statistical characteristics of a random event.

In the standard texts on probability theory, a large number of commonly encountered probability distributions are discussed in some detail. In fire control technology, the Gaussian, or normal, distribution and the bivariate normal distribution are the most commonly employed. These distributions are described in pars. C-6 and C-7, respectively.

C-2 PROBABILITY APPLIED TO DISCRETE EVENTS

C-2.1 PROBABILITY OF A SINGLE EVENT

A discrete event is an event whose probability of occurrence is limited to a finite or at most a countably infinite number of values. For now, a simple comparison can show the difference between discrete and continuous situations. The event that a weapon will miss its target with its nth round is represented by a discrete probability function, i.e., there are neither half rounds nor half hits. On the other hand, the event that the projectile-to-target miss distance is less than or equal to some value requires a continuous probability function in order to evaluate. Continuous probability functions are discussed in par. C-3.

The probability of occurrence of a specified discrete event can be defined in either of two ways. If it can be assumed that all events, i.e., all outcomes of a particular experiment, are equally likely, then the probability of a particular event—designated as A for this discussion—can be defined as the ratio of the number of ways in which A can occur to the total number of events that can occur. This definition is represented by

$$P(A) \;=\; \frac{n(A)}{n(\textbf{all})}, \;\; \textbf{per unit} \qquad\qquad \textbf{(C-1)}$$

where

A = an event that may or may not occur, no unit
$P(A)$ = probability that event A occurs at any trial, per unit
$n(A)$ = number of ways in which event A can occur, dimensionless
$n(\text{all})$ = total number of events that can occur, dimensionless.

For example, if a discrete event A is described as a four showing on the throw of a die,

$$P(A) = \frac{1}{6}, \text{ per unit}$$

$$= 16.666\ldots\%$$

where

A = event of throwing a four, no unit
$P(A)$ = probability of throwing a four, per unit
1 = number of ways event A can occur, dimensionless
6 = total events obtainable from one die, dimensionless.

The concept of probability defined in this way is sometimes called a priori probability.

A second way to define the concept of probability is as an "empirical" probability. If an experiment is performed a large number of times, the ratio between the number of occurrences and the number of trials is assumed to approach a limit defined as the probability of the occurrence. That is, based on what is known to have happened in the past, a prediction is made of what will happen in the future. The defining statement for an empirical probability is

$$\lim_{n \to \infty} \left[\frac{n(A)}{n(\text{all})} \right] = P(A), \text{ per unit} \tag{C-2}$$

where

n = number of trials, dimensionless.

If the die in the previous example is thrown a large number of times, experience has shown that the empirical probability approaches the a priori probability, or in this case, 1/6.

C-2.2 PROBABILITY OF MUTUALLY EXCLUSIVE EVENTS

Two or more events are said to be mutually exclusive if the occurrence of one precludes the occurrence of the other. For example, if a coin is tossed, heads and tails are mutually exclusive since it is possible to get one or the other but never both on a given toss.

If two events, A and B, are mutually exclusive, the probability that either A or B occurs is given by the following rule:

$$P(A + B) = P(A) + P(B), \text{ per unit} \tag{C-3}$$

where

$P(A+B) \triangleq P(A \text{ or } B)$ = probability that either event A or event B or, if not mutually exclusive, both will occur, dimensionless
$P(B)$ = probability that the event B will occur, dimensionless.

For example, if A is the event of tossing a four with a single die and B is the event of tossing a five, these events are mutually exclusive, and

$$P(A + B) = P(A) + P(B) = \frac{1}{6} + \frac{1}{6} = \frac{1}{3}, \text{ per unit.}$$

This expression states that on any single roll of the die, the probability that either a four or a five will show is 1/3 per unit, or 33.333...%.

C-2.3 PROBABILITY OF INDEPENDENT EVENTS

Two or more events are said to be independent if the occurrence or nonoccurrence of one in no way affects the occurrence of any of the others. For example, if A and B are the events of getting heads in two successive flips of a coin, then A and B are independent because the outcome of the second flip is in no way affected by what happened in the first flip and vice versa.

The probability that any two events, A and B, will both occur is called the joint probability of A and B and is given by the following rule.

If A and B are independent,

$$P(AB) = P(A) \, P(B), \text{ per unit} \tag{C-4}$$

where

$P(AB) \triangleq P(A \text{ and } B)$ = joint probability that both events A and B will occur, per unit.

For example, if A is the event of tossing a four on one die and B is the event of tossing a four on a second die and the dice are thrown simultaneously, these events are independent, and

$$P(AB) = P(A) \, P(B) = \frac{1}{6} \cdot \frac{1}{6} = \frac{1}{36}, \text{ per unit.}$$

This expression states that on any single roll of a pair of dice, the probability of two fours showing is 1/36 per unit. This can be intuitively understood since there are 36 possible permutations that could occur, but there is only one permutation that yields two fours.

C-2.4 PROBABILITY OF EVENTS THAT ARE NOT MUTUALLY EXCLUSIVE

Two or more events are said to be not mutually exclusive if the occurrence of one does not preclude the occurrence of the other and if the two events can occur jointly. If two events, A and B, are not mutually exclusive, the probability that A or B or both occur is given by the following rule:

$$P(A + B) = P(A) + P(B) - P(AB), \text{ per unit.} \tag{C-5}$$

For example, if A is the event of tossing four on one die and B is the event of tossing four on a second die and the dice are thrown simultaneously, the probability that either event A or event B occurs when the events are not mutually exclusive is

$$P(A + B) = P(A) + P(B) - P(AB)$$

$$= \frac{1}{6} + \frac{1}{6} - \frac{1}{36} = \frac{11}{36}, \text{ per unit.}$$

This expression states that on any single roll of a pair of dice, the probability of a four showing on one die or the other or both is 11/36 per unit. In this case of not mutually exclusive events, both $P(A)$ and $P(B)$ include $P(AB)$, which is not zero. Therefore, $P(A) + P(B)$ includes $2P(AB)$, so one $P(AB)$ must be subtracted from $P(A) + P(B)$ to eliminate this double inclusion. That is, the probability that A or B will occur includes the probability that A and B will occur but not twice the probability that A and B will occur.

C-2.5 CONDITIONAL PROBABILITY

For events that are to some extent interdependent, conditional probability is an important concept. The probability that event B will take place provided that event A has taken place (is taking place or will surely take place) is the conditional probability of B relative to A, and is shown symbolically as $P(B|A)$. Conditional probabilities make it possible to formulate a more general rule for the probability that two events, A and B, will both occur:

$$P(AB) = P(A) \, P(B|A), \text{ per unit} \tag{C-6}$$

or

$$P(B|A) = \frac{P(AB)}{P(A)} \text{ , per unit} \qquad (C\text{-}7)$$

where

$P(B|A)$ = conditional probability that event B occurs given that event A occurs, per unit.

For example, suppose that two cards are selected at random from a deck, and to know the probability of drawing two aces is desired. If the first card is replaced and the pack shuffled, the two events, i.e., of drawing an ace on the first or second draw, are independent. However, if A is the event of drawing an ace on the first draw and B is the event of drawing an ace on the second draw, the probability of drawing two aces is the joint probability, $P(AB)$. For replacement between draws

$$P(AB) = P(A)\ P(B), \text{ per unit}$$

but

$$P(A) = P(B) = \frac{4}{52}, \text{ per unit.}$$

Therefore,

$$P(AB) = \frac{4}{52} \cdot \frac{4}{52} = \frac{1}{169}, \text{ per unit.}$$

However, if the first card is not replaced, the two events are not independent. $P(A)$ remains $4/52$, but the conditional probability of B, given the prior occurrence of A, $P(B|A)$, is equal to $3/51$ because one card, an ace, is missing from the pack. Thus the joint probability is

$$P(AB) = P(A)\ P(B|A)$$
$$= \frac{4}{52} \cdot \frac{3}{51} = \frac{1}{221}, \text{ per unit.}$$

C-2.6   MULTIPLE PROBABILITY

The probability concepts that have been developed for two events can be extended to three or more events. Various combinations of the basic relationships are also possible. For example, a desired result might be obtained by different arrangements of two events. Thus, if desired event E can be obtained by the joint occurrence of A and B or by the joint occurrence of C and D, where events AB and CD are mutually exclusive, the following relationship applies:

$$P(E) = P(AB) + P(CD), \text{ per unit} \qquad (C\text{-}8)$$

where

C = an event which may or may not occur, no unit
D = an event which may or may not occur, no unit
$P(CD)$ = joint probability that both events C and D occur, per unit
E = event of occurrence of (A and B) or (C and D), no unit
$P(E)$ = probability of occurrence of event E, per unit.

If A, B, C, and D are independent,

$$P(AB) = P(A)\ P(B), \text{ per unit} \qquad (C\text{-}9)$$

and

$$P(CD) = P(C)\ P(D), \text{ per unit} \qquad (C\text{-}10)$$

where

$P(C)$ = probability of occurrence of event C, per unit

$P(D)$ = probability of occurrence of event D, per unit

then

$$P(E) = P(A)\ P(B) + P(C)\ P(D), \textbf{ per unit.} \tag{C-11}$$

For example, if the desired result is an 11 showing on a roll of a pair of dice, there are two possibilities: a six and a five or a five and a six. Use of Eq. C-11 shows that

$$P(E) = \left(\frac{1}{6} \cdot \frac{1}{6}\right) + \left(\frac{1}{6} \cdot \frac{1}{6}\right) = \frac{1}{18}, \textbf{ per unit}$$

where

E = event that 11 occurs on the roll on a pair of dice, no unit

$P(A)$ = probability of a six showing on the first die = 1/6, per unit

$P(B)$ = probability of a five showing on the second die = 1/6, per unit

$P(C)$ = probability of a five showing on the first die = 1/6, per unit

$P(D)$ = probability of a six showing on the second die = 1/6, per unit.

This example can also be solved intuitively since out of 36 possible permutations with the dice, there are two permutations that provide the desired result.

C-2.7   APPLICATION OF PROBABILITY TO FIRE CONTROL PROBLEMS

Following are two problems that illustrate application of the foregoing principles of probability for discrete events to simple fire control situations.

C-2.7.1   Illustrative Example C-1

A gun fires projectiles at a target until a first hit is scored. To determine the probability of the first hit occurring on any particular round is desired. This problem is from Ref. 8.
Solution:

It is assumed that the event of a hit or a miss on any one round is independent of the event of a hit or miss on any other round. The event of a hit on any one round is designated by the symbol H, and the event of a miss on any one round is designated by the symbol M. Since any one round must result either in a hit or a miss, the probability of either a hit or a miss is unity, i.e.,

$$P(H + M) = 1, \textbf{ per unit} \tag{C-12}$$

where

$P(H + M)$ = probability of either a hit or a miss on any one round, per unit

H = event of a hit in a round

M = event of a miss in a round.

Inasmuch as these two events are mutually exclusive, Eq. C-3 applies. From this equation it is apparent that

$$P(H + M) = P(H) + P(M), \textbf{ per unit} \tag{C-13}$$

where

$P(H)$ = probability of a hit on any one round (This probability is identical to the single-shot hit probability.), per unit

$P(M)$ = probability of a miss on any one round, per unit.

Therefore, from Eqs. C-12 and C-13 it is evident that

$$P(H) + P(M) = 1. \tag{C-14}$$

The event of a hit on any particular round k is denoted by H_k, and the event of a miss on that round is denoted by M_k. Because of the statistical independence of the hit or miss on any one round from the hit or miss on any other round, it is evident that

$$P(H_k) = P(H), \text{ per unit} \tag{C-15}$$

and

$$P(M_k) = P(M), \text{ per unit} \tag{C-16}$$

where
  $P(H_k)$ = probability of a hit on the kth round, per unit
  $P(M_k)$ = probability of a miss on the kth round, per unit.

Now, the event "the first hit occurs on the kth round", i.e., the first, second, ... and $(k-1)$st rounds all miss, and the kth round hits, is denoted by ε_k. The probability of the event ε_k is therefore identical with the multiple joint probability of the events contained between the dashes, i.e.,

$$P(\varepsilon_k) = P(M_1 \, M_2 \cdots M_{k-1} \, H_k), \text{ per unit} \tag{C-17}$$

where
  $P(\varepsilon_k)$ = probability that first hit occurs on kth round, per unit.

Since the events concerned are all statistically independent, the relationship for multiple joint probabilities that corresponds to Eq. C-4 applies and shows that

$$P(\varepsilon_k) = P(M_1) \cdot P(M_2) \cdots P(M_{k-1}) \cdot P(H_k), \text{ per unit.} \tag{C-18}$$

By virtue of Eqs. C-15 and C-16, Eq. C-18 can be rewritten as

$$P(\varepsilon_k) = [P(M)]^{k-1} \, P(H), \text{ per unit.} \tag{C-19}$$

Obviously, the probability that the first hit will occur on the kth round is less than the probability that the first hit will occur on the first round, which is $P(H)$. Eq. C-19 shows that the reduction factor is $[P(M)]^{k-1} = [1 - P(H)]^{k-1}$.

C-2.7.2 Illustrative Example C-2

Another problem of interest in connection with the fire control example in subpar. C-2.7.1 is determination of the probability that more than two rounds will be required to score a hit given the fact that the first round is a miss.
Solution:
First, the event that more than two rounds are required to score a hit is denoted by the symbol A. Then

$$P(A) = P(\varepsilon_3 + \varepsilon_4 + \cdots), \text{ per unit} \tag{C-20}$$

where
  $P(A)$ = probability that at least three rounds are required to score a hit, per unit
  ε_3 = event that the first hit occurs on the third round
  ε_4 = event that the first hit occurs on the fourth round.

This equation states that the probability that more than two rounds are required is the probability that

the first hit occurs either in round No. 3 or some succeeding round. Since events $\varepsilon_3, \varepsilon_4, \ldots$ are mutually exclusive, the relationship for multiple probabilities that corresponds to Eq. C-3 applies and shows that

$$P(A) \;=\; P(\varepsilon_3) \;+\; P(\varepsilon_4) \;+\; \cdots \;=\; \sum_{k=3}^{k=\infty} P(\varepsilon_k) \,, \;\; \textbf{per unit.} \tag{C-21}$$

Substitution of Eq. C-19 into Eq. C-21 shows that

$$
\begin{aligned}
P(A) \;&=\; \sum_{k=3}^{k=\infty} [\,P(M)\,]^{k-1} \; P(H) \\[4pt]
&=\; P(H)\,[P(M)]^{2} \;+\; P(H)\,[P(M)]^{3} \;+\; P(H)\,[P(M)]^{4} \;+\; \cdots \\[4pt]
&=\; P(H)\,[P(M)]^{2}\,\{\,1 + P(M) + [P(M)]^{2} + \cdots\,\}\,, \;\; \textbf{per unit.}
\end{aligned}
\tag{C-22}
$$

The series inside the braces can be recognized as a geometrical progression. The previous discussion shows that $P(M)$ must lie between 0 and 1, where 0 represents an improbable event and 1 represents a certain event, i.e., $0 < P(M) < 1$. Then $0 < [P(M)]^2 < 1$ also. In this case the limit of an infinite number of terms of the series is $1/[1 - P(M)]$, as described in Ref. 9. Substitution of $1/[1 - P(M)]$ for the geometrical progression inside the braces in Eq. C-22 yields

$$P(A) \;=\; \frac{P(H)\,[P(M)]^{2}}{1 - P(M)}\,, \;\; \textbf{per unit.} \tag{C-23}$$

After $1 - P(M)$ is substituted for $P(H)$ (See Eq. C-14.), Eq. C-23 becomes

$$P(A) = [P(M)]^2, \;\; \textbf{per unit.} \tag{C-24}$$

The result desired is the probability that more than two rounds are required, given the fact that the first round is a miss. This probability is a conditional probability that can be represented by the symbol $P(A|M_1)$. From Eq. C-7

$$P(A\,|\,M_1) \;=\; \frac{P(AM_1)}{P(M_1)}\,, \;\; \textbf{per unit} \tag{C-25}$$

where
    $P(A|M_1)$ = conditional probability that at least three rounds are required, given that the first round is a miss, per unit
    $P(AM_1)$ = joint probability that at least three rounds are required and that the first round is a miss, per unit.

The numerator of the right-hand side of Eq. C-25 is the joint probability of events A and M_1, i.e., the joint probability that (1) more than two rounds are required to score a hit and (2) the first round is a miss. It is obvious that the joint probability $P(AM_1)$ is the same as the probability $P(A)$ alone, i.e.,

$$P(A\,|\,M_1) = P(A), \;\; \textbf{per unit.} \tag{C-26}$$

Accordingly, substituting into Eq. C-25 from Eqs. C-16 and C-26 yields

$$P(A \mid M_1) = \frac{P(A)}{P(M)}, \text{ per unit.} \tag{C-27}$$

Substituting further from Eq. C-24 into Eq. C-27 shows that

$$P(A \mid M_1) = \frac{[P(M)]^2}{P(M)} = P(M), \text{ per unit.} \tag{C-28}$$

Of course, this result is exactly what is logically expected. That is, if it is known that the first round is a miss, more than two rounds will be required if, and only if, the second round is a miss also. The probability that the second round will be a miss is $P(M)$ by virtue of Eq. C-16.

So detailed a treatment of a simple problem would not be used in practice since the results are intuitively obvious. The intent of these examples is to demonstrate the application of the basic rules of probability in simple situations in which the solution is known in advance.

C-3 CONTINUOUS PROBABILITY FUNCTIONS

Par. C-2 presented probability concepts applied to the occurrence of a limited number of individual (or discrete) events. In general, these events (whether single, joint, or conditional) can be characterized by a variable that can take on a numerical value. For example, the event variable could be the number that comes up on a cast die. The event variable can have the value of the integers one through six, and there is a discrete probability associated with its taking on any one of the six values. In fact, could this event variable take on the values 4.5 or 7 or any number not in the set {1,2,3,4,5,6}? Clearly, the probability of such values is zero.

C-3.1 THE RANDOM VARIABLE

The event variable discussed in par. C-3 is called a random variable. It may also be called a stochastic variable when it occurs in stochastic processes, which are discussed in par. C-4.

A random variable is a real-valued variable whose values are the result of experimental chance. This chance is subject to a specific probability law (depending on the experiment), which may be discrete and/or continuous.

C-3.1.1 The Discrete Random Variable

When the random variable can take on only a specified, limited set of values, the random variable is discrete. The probabilities associated with the set of values must fall in the interval [0,1]. The number of values in the specified set must be finite or at most countably infinite. As mentioned in par. C-1, countably infinite (or countable) means a one-to-one correspondence with the set of positive integers, as described in Ref. 7.

The probability law associated with the discrete random variable may consist of a table of probabilities associated with each specified value of the random variable. The probability law may be a function that computes a probability for each specified value of the random variable. Such a function is called a discrete probability density function (pdf). An example of a discrete pdf that is important in queuing theory is the Poisson pdf:

$$p_X(x) = \frac{\mu^x e^{-\mu}}{x!}, \text{ per unit} \tag{C-29}$$

where

X = discrete random variable that takes on the values of x, U
x = 0, 1, 2, ... , U
e = 2.71828..., dimensionless
$p_X(x)$ = discrete pdf of the Poisson random variable X, $P(X = x)$, per unit
μ = mean value of the random variable X, U.

Because the factorial is defined only for positive integers, Eq. C-29 is a discrete pdf defined on the countable set of positive integers.

C-3.1.2 The Continuous Random Variable

When the random variable can take on any real value over some specified interval on a line segment, it is called a continuous random variable. Depending upon the experiment, the interval may include the entire real line $-\infty <$ random variable $< \infty$ or some part thereof. Further, the random variable may be composed of a mixture of continuous and discrete intervals. In this case, the random variable is considered to be continuous with at most a countable number of discontinuities. Such random variables may be manipulated by use of the Stieltjes integral, as explained in Ref. 2.

The probability law associated with a continuous random variable is a continuous function called the probability cumulative distribution function (cdf), or more familiarly, the probability distribution function. Again, this is a continuous function over the specified interval on a real line segment. An example of a continuous distribution function that is used to analyze the miss distance of a projectile is the Rayleigh distribution:

$$F_R(r) = 1 - e^{(r/K)^2} \qquad \text{(C-30)}$$

where

R = miss distance random variable that takes on the values of r $(0 \leq r \leq \infty)$, m
r = values taken on by the random variable R, m
K = normalizing factor 1, m
$F_R(r)$ = cdf of the Rayleigh random variable R, $P(0 \leq R \leq r)$, per unit.

This distribution is used in the illustrative example C-3 of subpar. C-3.4.2.

A random variable is designated continuous because its probability law, the cdf, is a continuous function of the values of the random variable. The continuous random variable may be a continuous function of some independent variable such as time or displacement. If so, the continuous random variable is involved in a stochastic process, which is discussed in par. C-4.

C-3.2 THE CONTINUOUS PROBABILITY DISTRIBUTION FUNCTION

In its most general form the probability cdf is defined as

$$F_X(x) \triangleq P(X \leq x) \text{ or } \triangleq P(X_{min} \leq X \leq x), \text{ per unit} \qquad \text{(C-31)}$$

where

X = continuous random variable that can take on the values of x, U
x = value taken on by the random variable X, U
$F_X(x)$ = continuous cdf of the random variable X as a function of x, per unit
$P(X_{min} \leq X \leq x)$ = probability that the random variable X falls in the interval $X_{min} \leq X \leq x$, per unit
X_{min} = minimum value that the random variable X can take on, U.

In Eq. C-31 the specified interval on the real line is $X_{min} \leq X \leq X_{max}$. The minimum value could be $-\infty$, and the maximum could be ∞ depending upon the experiment to which this random variable applies. Further, by definition

$$F_X(x \leq X_{min}) \triangleq 0, \text{ per unit}$$

and

$$F_X(x \geq X_{max}) \triangleq 1, \text{ per unit}$$

where

X_{max} = maximum value that the random variable X can take on, U.

The cdf $F_X(x)$ is continuous. However, it may have at most a countable number of instantaneous, i.e., abrupt, changes of slope.

C-3.3   THE CONTINUOUS PROBABILITY DENSITY FUNCTION

The continuous pdf in the interval $X_{min} \leq x \leq X_{max}$ is defined as follows:

$$f_X(x) = \frac{d}{dx}[F_X(x)], \quad U^{-1} \tag{C-32}$$

where

$f_X(x)$ = continuous pdf of random variable X as a function of x, U^{-1}
   $\triangleq$ instantaneous slope of the cdf as a function of x, U^{-1}.

There are several important characteristics of the continuous pdf:

1. Over the specified interval $X_{min} \leq x \leq X_{max}$ there may be at most a countable number of discontinuities corresponding to any abrupt changes in slope of the cdf.

2. Over the specified interval the area under the pdf is unity.

3. The continuous pdf is not a probability. In fact, it is the change in probability per unit change in the random variable X. The unit of the pdf is per unit/U. If the pdf were multiplied by 100, its unit would be %/U. For example, if the unit of the random variable were meters, the last unit would be %/m. However, since "per unit" is essentially dimensionless, the appropriate general unit for a univariate continuous pdf is simply U^{-1}.

Fig. C-1 provides an example of a continuous cdf and its corresponding pdf. The exponential distribution is used extensively in queuing analysis. Here, for example, the random variable X is the time between the arrivals of patrons into the queue.
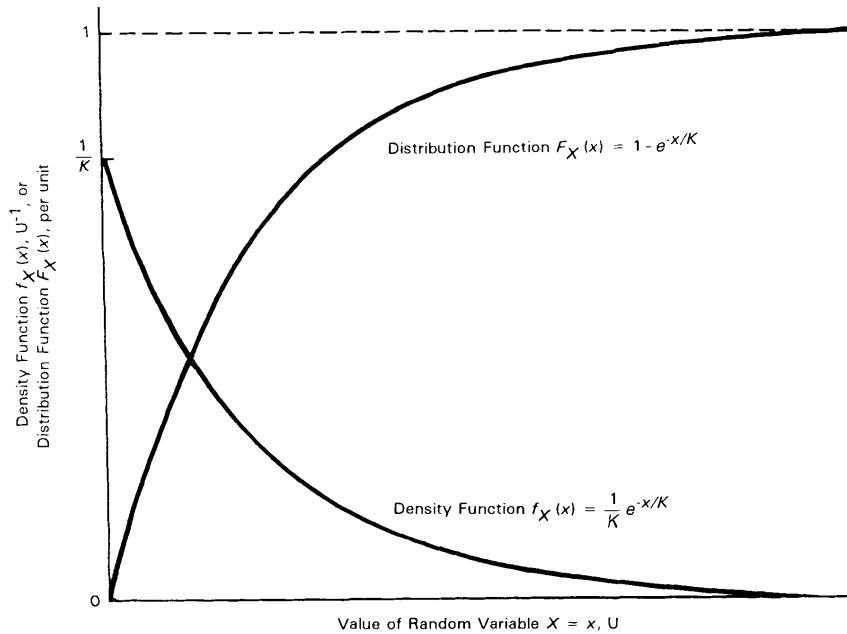
Figure C-1. Exponential Density and Distribution Functions

Eq. C-32 may be viewed as a differential equation. Solving for $F_X(x)$ yields

$$F_X(x) = \int_{X_{min}}^{x} f_X(x') \, dx', \quad \text{per unit} \tag{C-33}$$

where

x' = dummy variable of integration for x, U.

Then

$$F_X(x = X_{min}) = 0, \text{ per unit}$$

and

$$F_X(x = X_{max}) = 1, \text{ per unit.}$$

C-3.4 CONTINUOUS JOINT PROBABILITY DISTRIBUTION FUNCTIONS

C-3.4.1 Theory

Consider an experiment in which two continuous random variables X and Y are jointly distributed. The joint distribution function is given by (Ref. 10)

$$F_{X,Y}(x,y) = P(X \leq x, Y \leq y), \text{ per unit} \tag{C-34}$$

where

$F_{X,Y}(x,y)$ = **continuous joint cdf of the random variables X and Y evaluated at $X = x$ and $Y = y$, per unit**

$P(X \leq x, Y \leq y)$ = **joint probability that the random variables $X \leq x$ and $Y \leq y$, per unit**

Y = **random variable that can take on the values $Y_{min} \leq Y \leq y \leq Y_{max}$, U.**

The corresponding continuous pdf is given by

$$f_{X,Y}(x, y) \;=\; \frac{\partial^2}{\partial x\, \partial y}\, [F_{X,Y}(x, y)], \;\; \mathrm{U}^{-2}. \tag{C-35}$$

Conversely,

$$F_{X,Y}(x, y) \;=\; \int_{X_{min}}^{x} dx' \int_{Y_{min}}^{y} dy'\, f_{X,Y}(x', y'), \;\; \text{per unit.} \tag{C-36}$$

If the random variables X and Y are statistically independent, i.e., the value taken on by X has no effect on the value taken on by Y and vice versa, then

$$F_{X,Y}(x,y) = F_X(x) \cdot F_Y(y), \text{ per unit} \tag{C-37}$$

where

$F_Y(y)$ = **continuous cdf of the random variable Y evaluated at $Y = y$, per unit**

and

$$f_{X,Y}(x,y) = f_X(x) \cdot f_Y(y), \; \mathrm{U}^{-2} \tag{C-38}$$

where

$f_Y(y)$ = **continuous pdf of the random variable Y evaluated at $Y = y$, U^{-1}.**

So far, this subparagraph has considered bivariate continuous joint distribution functions. The extension to n-variate joint distribution functions from the bivariate case is clear. The unit for the continuous n-variate joint cdf is "per unit" since the cdf is always a probability. However, the unit of the continuous n-variate joint pdf is "U^{-n}", i.e., there is a U^{-1} for each of the n-variates. Thus the overall unit is $(\mathrm{U}^{-1})^n = \mathrm{U}^{-n}$.

C-3.4.2   Illustrative Example C-3

The following is an example of the application of continuous joint pdf's to a fire control problem.
Given: The errors in along-track range X and cross-track range Y are normally distributed.
Normal distributions are discussed in par. C-6. Further, these two random variables are independent and have the same statistics. That is, in the general normal pdf

$$f_X(x) \;=\; \frac{1}{\sigma_X\sqrt{2\pi}}\, e^{-\frac{1}{2}\left(\frac{x-\mu_X}{\sigma_X}\right)^2}, \;\; \text{m}^{-1} \tag{C-39}$$

where

$f_X(x)$ = normal pdf for the random variable X, m^{-1}

X = along-track error random variable that can take on the value of $-\infty < x < \infty$, m

σ_X = standard deviation of X, m

μ_X = mean (expected) value of X, m.

If $\mu_X = 0$ and $\sigma_X = 1/\sqrt{2}$, then Eq. C-39 for $u = x/\sigma_X$ reduces to

$$f_X(u) \;=\; \frac{1}{\sqrt{\pi}}\, e^{-u^2}, \;\; \text{dimensionless} \tag{C-40}$$

where

u = value of normalized x/σ_X, dimensionless

$f_X(u)$ = normal pdf for the random variable X/σ_X, dimensionless.

Similarly,

$$f_Y(v) \;=\; \frac{1}{\sqrt{\pi}}\, e^{-v^2}, \;\; \text{dimensionless} \tag{C-41}$$

where

$f_Y(v)$ = normal pdf for the random variable Y/σ_Y, dimensionless

Y = cross-track error random variable that can take on the value $-\infty < y < \infty$, m

μ_Y = mean (expected) value of $Y = 0$, m

v = value of normalized y/σ_Y, dimensionless.

Eqs. C-40 and C-41 are sketched in Fig. C-2.
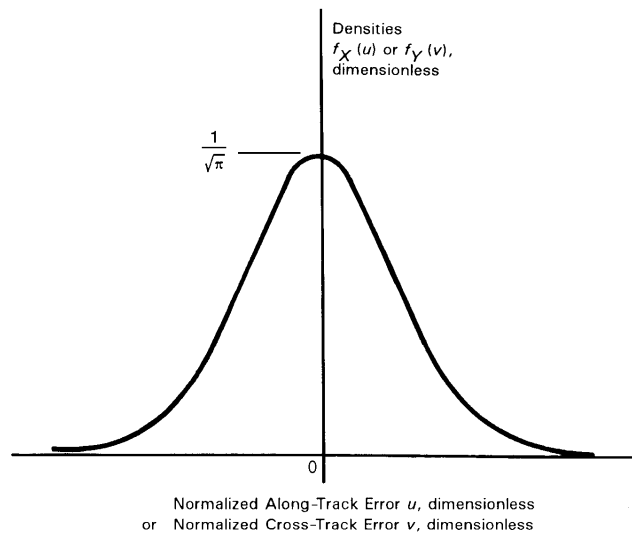
Figure C-2.   Probability Density Functions of Normalized Along-Track and Cross-Track Errors

To be found: **The probability distribution of the miss distance** R, **i.e., the distance from the target center to the point of impact of the projectile.**

Solution: **Because the random variables** X **and** Y **are statistically independent, Eqs. C-37 and C-38 apply. Therefore,**

$$f_{X,Y}(u, v) = f_X(u)\, f_Y(v)$$

$$= \frac{1}{\pi} e^{-(u^2 + v^2)}, \quad \textbf{dimensionless} \tag{C-42}$$

where

    $f_{X,Y}(u,v)$ = **continuous joint pdf of** X/σ_X **and** Y/σ_Y, **dimensionless.**

Further,

$$F_{X,Y}(u, v) = \int_{-\infty}^{u} f_X(u')\, du' \cdot \int_{-\infty}^{v} f_Y(v')\, dv'$$

$$= \int_{-\infty}^{u} \int_{-\infty}^{v} \frac{1}{\pi} e^{-(u'^2 + v'^2)}\, du'\, dv', \quad \textbf{per unit} \tag{C-43}$$

where

    $F_{X,Y}(u,v)$ = **continuous joint cdf of the random variables** X/σ_x **evaluated at** u **and** Y/σ_y **evaluated**
        at v, **per unit**
    u', v' = **dummy variables of integration for** u **and** v, **respectively, dimensionless.**

    The miss distance R **is obtained from transformation of the rectangular coordinates** X **and** Y **to the polar coordinate random variables** R **and** Θ. **Fig. C-3 depicts the coordinate relationships. The transformed**

R = miss distance random variable, m

Θ = angle of line $\overline{TI}$ with respect to X–axis, rad

X_I, Y_I = along-track and cross-track errors
    of the impact point with respect to
    the true target, m
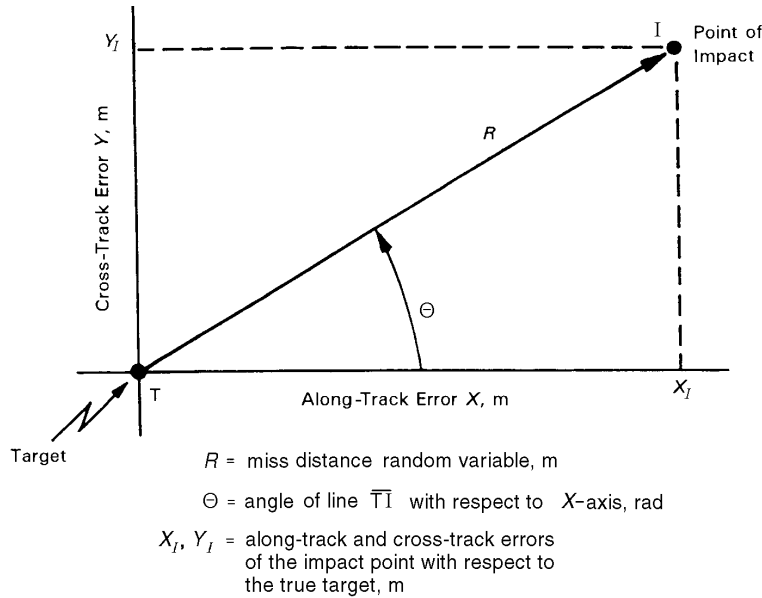
Figure C-3. Geometry of the Miss Distance

version of Eq. C-43 becomes

$$F_{R,\Theta}(\rho, \theta) = \int_0^\theta \int_0^\rho \frac{1}{\pi} e^{-\rho'^2} \rho' \, d\rho' \, d\theta'$$

$$= \int_0^\rho \rho' e^{-\rho'^2} d\rho' \cdot \int_0^\theta \frac{1}{\pi} d\theta' \qquad \text{(C-44)}$$

$$= \int_0^\rho f_R(\rho') \, d\rho' \cdot \int_0^\theta f_\Theta(\theta') \, d\theta', \quad \textbf{per unit}$$

where

$F_{R,\Theta}(\rho,\theta)$ = **continuous joint cdf of the random variables R and Θ evaluated at $R = \rho$ and $\Theta = \theta$**
   (which can take on values of $0 \le \rho \le \infty$ and $0 \le \theta \le 2\pi$, respectively), per unit

ρ = **normalized range distance equivalent, dimensionless**

ρ' = **dummy variable for ρ, dimensionless**

θ = **values taken on by the random variable Θ, rad**

θ' = **dummy variable for θ, rad**

du', dv = $\rho' d\rho' \, d\theta'$ **(This transformation is discussed in detail in Ref. 10, p. 421.)**

$f_R(\rho)$ = **continuous pdf for the normalized miss distance, dimensionless**

$f_\Theta(\theta)$ = **continuous pdf for the angular random variable Θ, dimensionless.**

   Since the problem is concerned only with the distribution of the miss distance (actually the normalized miss distance), it is necessary to obtain $F_{R,\Theta}(\rho,\theta)$ over the full range of Θ, $0 \le \theta \le 2\pi$. Therefore, in Eq. C-44

$$F_R(\rho) = F_{R,\Theta}(\rho, 2\pi)$$

$$= \int_0^\rho \rho' e^{-\rho'^2} d\rho' \int_0^{2\pi} \frac{1}{\pi} d\theta$$

$$= \frac{-e^{-\rho'^2}}{2} \bigg|_0^\rho \cdot \frac{\theta}{\pi} \bigg|_0^{2\pi} \qquad \text{(C-45)}$$

$$= \frac{1}{2} (1 - e^{-\rho^2}) \cdot \frac{2\pi}{\pi}$$

$$= 1 - e^{-\rho^2}, \quad \textbf{per unit}$$

where

$F_R(\rho)$ = **continuous cdf of the normalized miss distance random variable R/σ (which can take on the values $0 \le \rho \le \infty$), per unit.**

The related continuous pdf is found by differentiating Eq. C-45:

$$f_R(\rho) = \frac{d\left(1 - e^{-\rho^2}\right)}{d\rho} \qquad \text{(C-46)}$$

$$= 2\rho e^{-\rho^2}, \quad \textbf{dimensionless.}$$

   Eqs. C-45 and C-46 are plotted in Fig. C-4.
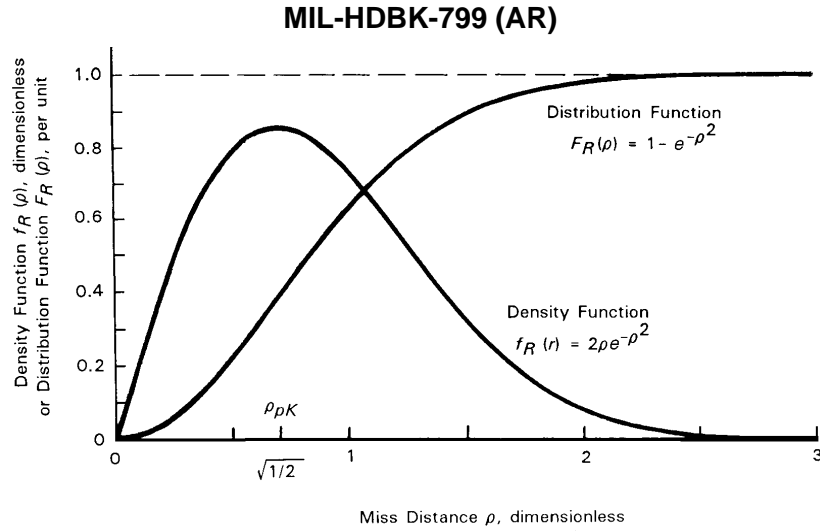
This is the Rayleigh distribution for peak location $\rho_{pK} = \sqrt{1/2}$.

Figure C-4. Probability Density and Distribution Functions of the Normalized Miss Distance

C-3.5 CONTINUOUS CONDITIONAL PROBABILITY DISTRIBUTION FUNCTIONS

C-3.5.1 Theory

The continuous conditional cdf is defined as

$$F_{X/Y}(x|y) \triangleq P(X \le x \,|\, Y = y), \text{ per unit} \tag{C-47}$$

where

$F_{X/Y}(x|y)$ = **continuous conditional cdf of random variable** X, **which can take on the values of** $X_{min} \le x \le X_{max})$ **given that the random variable** $Y = y$ **(where** $Y_{min} \le y \le Y_{max})$**, per unit**

$P(X \le x \,|\, Y = y)$ = **conditional probability that the random variable** X **is in** $X_{min} \le X \le x \le X_{max}$ **given that the random variable** $Y = y$, $Y_{min} \le y \le Y_{max}$, **per unit.**

Using the concept of Eq. C-32

$$f_{X|Y}(x|y) = \frac{\partial}{\partial x}[F_{X|Y}(x|y)], \; \mathbf{U}^{-1} \tag{C-48}$$

where

$f_{X/Y}(x|y)$ = **continuous conditional pdf of the random variable** X **given** Y, $\mathbf{U}^{-1}$.

Using the concept of Eq. C-7

$$f_{X|Y}(x|y) = \frac{f_{X,Y}(x,y)}{f_Y(y)}, \; \mathbf{U}^{-1}. \tag{C-49}$$

If X and Y are statistically independent random variables, then Eq. C-38 applies. Substituting Eq. C-38 into Eq. C-49 yields

$$f_{X|Y}(x|y) = \frac{f_X(x)\,f_Y(y)}{f_Y(y)}$$

$$= f_X(x), \; \mathbf{U}^{-1}$$

which shows that the pdf of X given Y is simply the pdf of X when X and Y are statistically independent.

C-3.5.2 Illustrative Example C-4

This illustrative example is of the use of continuous pdf's and cdf's in a conditional probability problem. This problem was obtained from Ref. 8, p. 39.

Given: A precision potentiometer used in a fire control computer has survived for t days. Its probability of failure within the next time period of operation Δt is $0.01\Delta t$, per unit and is independent of t.

Problem: If this potentiometer has lasted for 30 days, what is its probability of failure within the next 10 days?

Solution: The following can be written:

$$P(B|A) = P[\,(t < T \le t + \Delta t)\,|\,(T > t)\,]$$
$$= 0.01\ \Delta t,\ \text{per unit} \tag{C-50}$$

where

A = event, in Example C-4, that the potentiometer has lasted $t = 30$ days, dimensionless
B = event that the potentiometer fails in the interval $t < T \le \Delta t$, dimensionless
T = random variable representing the life of the potentiometer, day
t = value taken on by the random variable T, day
Δt = potentiometer operating interval (= 10), day
$P(B|A)$ = probability of event B given that event A has occurred, per unit.

If event B is to occur, then event A must occur so that

$$P(A|B) = 1,\ \text{per unit.}$$

Therefore,

$$P(AB) = P(A|B)\ P(B)$$
$$= P(B),\ \text{per unit} \tag{C-51}$$

where

$P(AB)$ = joint probability that both events A and B occur, per unit
$P(B)$ = probability that event B occurs, per unit.

Therefore,

$$P(B|A) = \frac{P(AB)}{P(A)} = \frac{P(B)}{P(A)},\ \text{per unit} \tag{C-52}$$

where

$P(A)$ = probability that event A occurs, per unit.

But

$$P(A) = P(T > t),\ \text{per unit.}$$

Therefore,

$$1 - P(A) = P(T \le t)$$
$$= F_T(t)\ \text{per unit} \tag{C-53}$$

where

$F_T(t)$ = cdf of the time random variable T evaluated at $T = t$, per unit.

Then $P(B)$ can be approximated by

$$P(B) \doteq \Delta t \cdot f_T(t), \text{ per unit} \tag{C-54}$$

where

$f_T(t)$ = **pdf of the random variable** T **evaluated at** $T = t$, **day**$^{-1}$.

This is a very good approximation since $f_T(t)$ changes gradually in the relatively small interval $t < T \le t + \Delta t$. Substituting Eqs. C-52, C-53, and C-54 into Eq. C-50 yields

$$P(B|A) = 0.01 \, \Delta t = \frac{\Delta t \, f_T(t)}{1 - F_T(t)}, \text{ per unit.} \tag{C-55}$$

From which

$$f_T(t) + 0.01 \, F_T(t) = 0.01, \text{ day}^{-1}. \tag{C-56}$$

Differentiating Eq. C-56 with respect to t yields

$$\frac{d}{dt} f_T(t) + 0.01 \frac{d}{dt} F_T(t) = 0$$

$$\text{or} \tag{C-57}$$

$$\frac{d}{dt} f_T(t) + 0.01 \, f_T(t) = 0, \text{ day}^{-2}.$$

Eq. C-57 is an ordinary first-degree linear differential equation with constant coefficients. Its solution (See Ref. 11 for discussion.) is

$$f_T(t) = c e^{-0.01t}, \text{ day}^{-1} \tag{C-58}$$

where

c = **constant of integration, day**$^{-1}$.

Since negative time is meaningless and the total area under $f_T(t)$ must be unity, the following must be true:

$$1 = \int_0^\infty f_T(t) \, dt = c \int_0^\infty e^{-0.01t} dt$$

$$= c \left[\frac{e^{-0.01t}}{-0.01} \right]_0^\infty = c \, \frac{1 - 0}{0.01}, \text{ dimensionless}$$

and

$$c = 0.01, \text{ day}^{-1}.$$

Therefore,

$$f_T(t) = 0.01 e^{-0.01t}, \text{ day}^{-1}$$

and

$$F_T(t) = \int_0^t f_T(t')\, dt' \tag{C-59}$$

$$= (1 - e^{-0.01\,t}), \quad \textbf{per unit}$$

where

t' = **dummy variable of integration for** t, **day.**

Then $P(B)$ **in this problem can be stated as the probability of failure between day 30 and day 40. This can be written as**

$$P(B) = F_T(40) - F_T(30), \textbf{ per unit.} \tag{C-60}$$

Also $P(A)$ **may be obtained from Eq. C-53:**

$$P(A) = 1 - F_T(30), \textbf{ per unit.} \tag{C-61}$$

Substituting Eqs. C-59, C-60, and C-61 into Eq. C-52 yields

$$P(B|A) = \frac{F_T(40) - F_T(30)}{1 - F_T(30)}$$

$$= \frac{(1 - e^{-0.4}) - (1 - e^{-0.3})}{1 - (1 - e^{-0.3})}$$

$$= \frac{e^{-0.3} - e^{-0.4}}{e^{-0.3}}$$

$$= 1 - e^{-0.1} = 0.0952, \textbf{ per unit.}$$

In summary: The probability that the potentiometer will fail within 40 days given that it lasted for 30 days is 0.0952 per unit, or 9.52%.

C-4   STOCHASTIC PROCESSES

The continuous random variable is so defined because its cdf is continuous over a specified region of the real line. This variable may be a function of some independent variable such as time or displacement, and in most realizable systems it is a continuous function of the independent variable. For convenience, in the following discussion it is assumed that the random variables are continuous functions of time.

C-4.1   ENSEMBLES

In general, the operation of the system that produces the random variable waveforms produces an ensemble or set of these waveforms. Fig. C-5 depicts an ensemble of continuous random variables. The process that produces the ensemble of random variables that are functions of time is called a stochastic process. The pdf's associated with these random variables are also functions of time. In fact, if the random variables are sampled at n times, the pdf's must be n-variate joint pdf's since each sample is a random variable.
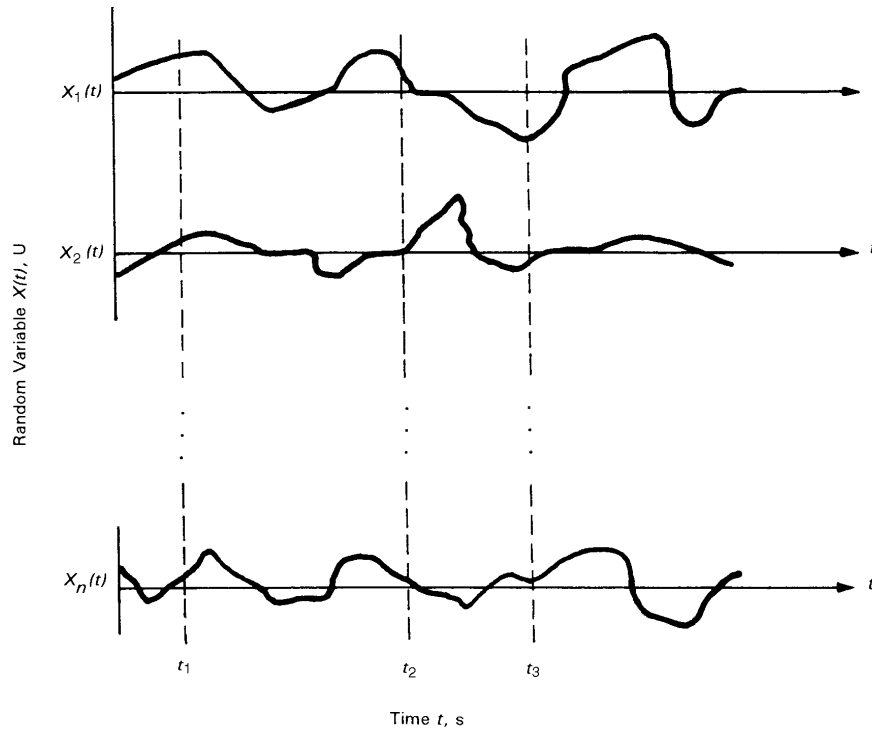
Any of the random variables X_1, X_2,···,X_n can be averaged with time, or the ensemble can be sampled at some particular time, such as t_1, t_2, or t_3, and the resulting time samples averaged.

Figure C-5. An Ensemble of Random Variable Functions of Time (Ref. 12)

A random variable function of time is generally designated $X(t)$. The corresponding continuous cdf is designated $F_X(x;t)$, and the corresponding pdf is obtained by

$$f_X(x;t) = \frac{\partial}{\partial x}[\,F_X(x;t)\,]\,, \ \mathbf{U}^{-1} \tag{C-62}$$

where

$f_X(x;t)$ = continuous pdf of the stochastic process $X(t)$, $\mathbf{U}^{-1}$
t = independent variable (usually time) in stochastic processes, s
$F_X(x;t)$ = continuous cdf of the stochastic process $X(t)$, per unit.

C-4.2 STATIONARY FUNCTIONS

The stationary random processes comprise an important class of stochastic processes. There are two major types of stationarity: strict sense (usually referred to as "stationary") and wide (or weak) sense.

C-4.2.1 Strict Sense Stationarity

Where strict sense stationarity occurs, $X(t)$ and $X(t+\tau)$ have the same statistics for any time shift τ, s. This implies that

$$f_X(x;t) = f_X(x;t+\tau) = f_X(x), \ \mathbf{U}^{-1} \tag{C-63}$$

where

τ = time offset or shift, s.

Eq. C-64 means that all statistics of $X(t)$ are entirely independent of where $X(t)$ is viewed (absolute time). Since the statistics are directly related to the moments of $X(t)$, the moments are independent of absolute time. The moments are defined in subpar. C-5.3.

C-4.2.2 Wide Sense or Weak Stationarity

Where wide sense stationarity occurs, $X(t)$ and $X(t+\tau)$ have the same first-order moment (mathematical mean), and the joint pdf's of these two samples can be written as

$$f_X(x_t,x_{t+\tau};t,t+\tau) = f_X(x_t,x_{t+\tau};t), \; \mathbf{U}^{-2} \tag{C-64}$$

where

$f_X(x_t,x_{t+\tau};t,t+\tau)$ = **joint pdf for** $X(t)$ **and** $X(t+\tau)$ **for any** t **and** τ, $\mathbf{U}^{-2}$

x_t = **value taken on by** $X(t)$

$x_{t+\tau}$ = **value taken on by** $X(t+\tau)$

$f_X(x,x_{t+\tau};\tau)$ = **joint pdf for** $X(t)$ **and** $X(t+\tau)$ **for any** τ, **i.e., independent of** t, $\mathbf{U}^{-2}$.

Eq. C-65 means that the joint pdf is independent of the absolute times of the samples but does depend only on their time difference .

C-4.2.3 Ergodicity

Another concept associated with stationary random processes is the ergodic hypothesis. This hypothesis claims that any statistic calculated by averaging all members of an ergodic ensemble at a fixed time can also be calculated by averaging over all time on a single, representative member of the ensemble. The key to this notion is the word "representative". If a particular member of the ensemble is to be statistically representative of all members, it must display at various points in time the full range of amplitude, rate of change in amplitude, etc., that are found among all the members of the ensemble. A classic example of a stationary ensemble that is not ergodic is the ensemble of functions that are constant in time. The failing in this case is that no member of the ensemble is representative of all members.

An example of a stationary ergodic random process is the ensemble of sinusoids of given amplitude and frequency with a uniform distribution of phase, i.e., all values of phase are equally probable. The member functions of this ensemble are all of the form

$$X(t) = A\,\mathbf{sin}(\omega t + \Phi) \tag{C-65}$$

where

A = **constant amplitude, U**

Φ = **a random variable uniformly distributed over the interval** $(0,2\pi)$, **rad**

ω = **rotational frequency,** $2\pi f$, **rad/s.**

Any average taken of the members of this ensemble at any fixed time would find all phase angles represented with equal probability density, but the same is true of an average over all time on any one member. For this process, then, all members of the ensemble qualify as "representative". Any distribution of the phase angle other than the uniform distribution over an integral number of cycles would define a nonergodic process.

There are three types of ergodicity: ergodicity of the mean, ergodicity of the autocorrelation, and ergodicity of the distribution function. The criteria used to determine ergodicity are beyond the scope of this handbook. A detailed discussion of the various types of ergodicity is included in Ref. 6.

As a general example of the ensemble method, consider a set (or ensemble) of simultaneously conducted experiments whose results $(X_1,X_2,\cdots,X_n)$ can be plotted as functions of time as shown in Fig. C-5. Each of these random time functions can be sampled at time intervals such as t_1, t_2, etc. Each sample at a specified time, e.g., t_1, can be averaged to obtain the ensemble average. Alternatively, any member of the set of random time functions can be averaged with time. If the random variable is ergodic, the ensemble average and the time average are the same. In general, whenever a random variable is ergodic, the statistical parameters of the ensemble or the corresponding statistical parameters of the time function are interchangeable.

Most statistical problems associated with fire control systems can be considered to be ergodic stationary because the parameters do not change rapidly with time. In contradistinction, problems associated with

ground-to-air guided missiles frequently result in nonstationary parameters because such rapidly chang-
ing factors as range and altitude cause continual change in the statistical parameters.

C-5   AVERAGES OR EXPECTATIONS OF RANDOM VARIABLES

Considerable insight into random variables is obtained from various statistics, or averages, that provide
a numerical measure of their important characteristics. The basic statistics are introduced here.

C-5.1   TIME AVERAGE

One of the most useful statistics parameters is the time average. The time average of a random variable
(or of any variable) function of time is defined by

$$\overline{X(t)} = \lim_{\Delta t \to \infty} \left[\frac{1}{\Delta t} \int_{t}^{t+\Delta t} X(t)\, dt \right], \ \mathbf{U} \qquad (C\text{-}66)$$

where
$\overline{X(t)}$ = time average of $X(t)$, **U**
Δt = a time interval, **s**.

In practical work, it is useful to take Δt of a duration for which the average does not change significantly
for a greater increase in Δt.

The symbol $\overline{X(t)}$ denotes the time average of the random time variable $X(t)$, this time average is a num-
ber anywhere on the real line, and the time average is not itself a function of time. The time average can
be computed analytically if an analytic expression for $X(t)$ is available. If a time record of $X(t)$ is available,
the time average can be computed either mechanically or numerically. Fig. C-6 is an example of the time
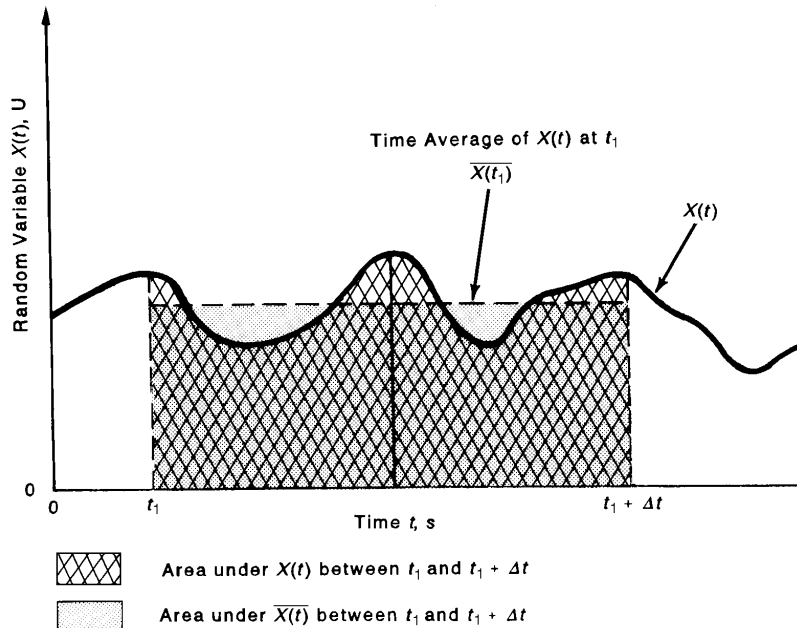
Figure C-6. Time Average of a Random Variable

average of a random variable and illustrates a graphical technique that may be used to compute the time
average. In Fig. C-6 the area under the curve over the interval $t_1 \le t \le t_1 + \Delta t$ is given by

$$\text{Area } \overline{X(t)} = \int_{t_1}^{t_1 + \Delta t} X(t)\, dt, \ \mathbf{U \cdot s}. \qquad (C\text{-}67)$$

If $\overline{X(t)}$ is the time average of $X(t)$ over this interval,

$$\text{Area } \overline{X(t)} = \overline{X(t)} \cdot \Delta t, \ \text{U} \cdot \text{s.} \tag{C-68}$$

Since Areas $X(t)$ and $\overline{X(t)}$ must be equal,

$$\overline{X(t)} = \frac{1}{\Delta t} \int_{t_1}^{t_1 + \Delta t} X(t) \, dt, \ \text{U.} \tag{C-69}$$

More generally,

$$\overline{X(t)} = \lim_{\Delta t \to \infty} \left[\frac{1}{\Delta t} \int_{t}^{t + \Delta t} X(t') \, dt' \right], \ \text{U} \tag{C-70}$$

where

t' = dummy variable of integration for t, s.

If the random variable should have negative values, the corresponding areas would be subtracted.

C-5.2 MEAN SQUARE

Another useful statistic is the mean-square time average. This quantity is used to express the average power of a random variable. Its usefulness is from the fact that when the random variable represents a voltage, displacement, or similar type of physical quantity—as is usually the case, the average power in the physical system is expressed by the mean-square time average. The mean-square time average is defined as the time average of the square of the random variable, i.e.,

$$\overline{X^2(t)} = \lim_{\Delta t \to \infty} \left(\frac{1}{\Delta t} \int_{t}^{t + \Delta t} X^2(t') \, dt' \right), \ \text{U}^2 \tag{C-71}$$

where

$\overline{X^2(t)}$ = mean-square time average of $X(t)$, U^2.

For example, assume a random instantaneous voltage $E(t)$ that is applied to a 1Ω resistor. The instantaneous power dissipated in the resistor is $E^2(t)$. A time average of the instantaneous power yields the average power and, as shown by Eq. C-71, turns out to be the mean-square time average of the voltage, i.e.,

$$P_{AV} = \lim_{\Delta t \to \infty} \left(\frac{1}{\Delta t} \int_{t}^{t + \Delta t} E^2(t') \, dt' \right) = \overline{E^2(t)}, \ \text{W} \tag{C-72}$$

where

P_{AV} = average power in a 1Ω resistance, W
$E(t)$ = random variable instantaneous voltage across a resistance, V
$\overline{E^2(t)}$ = mean-square value of $E(t)$, V^2/Ω
$E^2(t)$ = instantaneous power dissipated in resistor, W.

C-5.3 ROOT MEAN SQUARE

A final type of time average of importance is the root-mean-square (RMS) time average. This statistic is simply the square root of the mean-square time average. It is convenient because it is expressed in the same units as the random variable.

C-5.4 RANDOM VARIABLE ENSEMBLE MOMENTS

The moments or averages associated with an ensemble of random variables (as shown in Fig. C-5, for example) are important statistics. The main usefulness of these moments is their ability to specify completely any continuous pdf. The nth moment of a pdf $f_X(x)$ is defined by

$$m^{(n)} \triangleq E\left(X^n\right) \triangleq \int_{-\infty}^{\infty} x^n f_X(x) \ dx, \ \mathbf{U}^n \tag{C-73}$$

where

X = continuous random variable that can take on the values of x, U
$m^{(n)}$ = random variable moment of order n, $\mathbf{U}^n$
$E(X^n) \triangleq$ expected value of X^n (or nth moment of random variable X), $\mathbf{U}^n$.

The particular moments of significance to the fire control hit probability problem are discussed in the subparagraphs that follow.

The zero-order moment is the area under the entire probability density function and is therefore equal to unity, i.e.,

$$m^{(0)} = \int_{-\infty}^{\infty} x^0 f_X(x) \ dx = \int_{-\infty}^{\infty} f_X(x) \ dx \triangleq 1, \text{ per unit.} \tag{C-74}$$

C-5.4.1 First Moment or Mean

The first moment $m^{(1)}$, or simply m, is called the statistical mean, or expected value. It is also denoted by the symbol $\overline{X}$. Eq. C-73 shows that m is defined by

$$m = m^{(1)} = E(X) = \int_{-\infty}^{\infty} x f_X(x) \ dx, \ \mathbf{U} \tag{C-75}$$

where

$E(X) = \overline{X}$ = expected value of random variable X, U.

This moment is illustrated in Fig. C-7(A).

(A) Moments About the Zero Axis

(B) Second Moment About the Mean
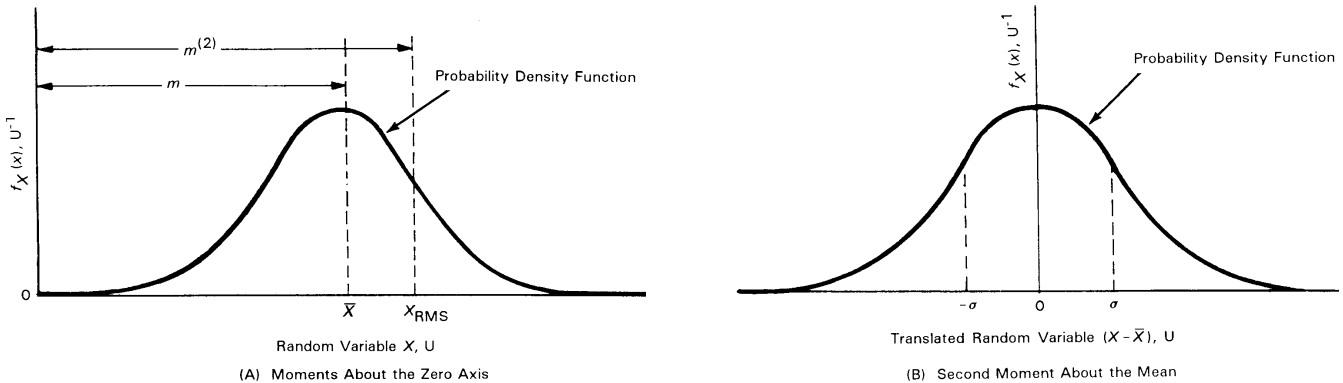
Figure C-7. Moments About the Zero Axis and the Mean

The time average given by Eq. C-66 and the ensemble average given by Eq. C-75 are identical when the random variable is an ergodic function of time.

C-5.4.2 Second Moment, or Mean Square

The second moment $m^{(2)}$ is called the mean-square value of X. In accordance with Eq. C-73, it is given by

$$m^{(2)} \triangleq \overline{X^2} = E(X^2) = \int_{-\infty}^{\infty} x^2 f_X(x) \ dx, \ \mathbf{U}^2 \tag{C-76}$$

where the symbol $\overline{X^2}$ is also used to represent the mean-square value, or second moment of X. The time average given by Eq. C-71 and the ensemble average given by Eq. C-76 are identical when the random variable is an ergodic function of time. This measurement is illustrated in Fig. C-7(A).

In the fire control hit probability analysis, the value of the mean of a set of firing errors is the bias error, i.e., the distance between the center of impact and the target (See Fig. 4-4.).

C-5.4.3 Second Central Moment, or Variance

The dispersion errors tend to scatter about the center of impact; therefore, a useful measure of dispersion is the second moment of a set of firing errors with respect to the mean value (the bias). Such moments about the mean (or center of impact), rather than about the zero axis (See Fig. C-7(B).), are called central moments and are defined by the general mathematical relationship

$$\mu^{(n)} \triangleq E[(X - \overline{X})]^n \triangleq \int_{-\infty}^{\infty} (x - \overline{X})^n f_X(x) \, dx, \; U^n \tag{C-77}$$

where

$E[(x - \overline{X})^n]$ = expected value of $(X - \overline{X})^n$ or nth central moment of the random variable X, U^n

$\mu^{(n)}$ = central moment of order n (nth central moment , i.e., the nth moment with respect to the mean value of the random variable), U^n.

The most significant central moment is the second $\mu^{(2)}$. This moment, which is called the variance, is the mean-square value of X about the mean. Since the units in which the variance is measured are the square of the units in which the random variable is measured (See Eq. C-76.), it is convenient to introduce a quantity that is the square root of the variance. This quantity is called the standard deviation and is denoted by σ_X. Accordingly, the variance is usually denoted by the symbol σ_X^2 and is given by

$$\sigma_X^2 = \mu^{(2)} = E[(X - \overline{X})^2] = \int_{-\infty}^{\infty} (x - \overline{X})^2 f_X(x) \, dx, \; U^2 \tag{C-78}$$

where

σ_X = standard deviation of the random variable X, U

σ_X^2 = variance of the random variable X, U^2

From this mathematical definition of the variance, it is possible to obtain the important relationship, i.e., the variance is the mean-square value of X minus the square of the mean.
By using Eqs. C-75, C-76, and C-78, the following equation is obtained:

$$\begin{aligned}
\sigma_X^2 &= E[(X - \overline{X})^2] \\
&= E(X^2 - 2\overline{X}X + \overline{X}^2) \\
&= E(X^2) - 2\overline{X}E(X) + \overline{X}^2 E(1) \\
&= E(X^2) - 2E(X)E(X) + E^2(X) \\
&= E(X^2) - E^2(X) \\
&= \overline{X^2} - (\overline{X})^2, \; U^2.
\end{aligned} \tag{C-79}$$

As stated previously, the primary value of the moment concept is that any continuous pdf function can be completely specified by its moments. Thus, in most cases, including fire control, the mean and the standard deviation are sufficient. For example, in fire control the mean is identical with the bias, and the standard deviation is a measure of the dispersion.

C-6 GAUSSIAN, OR NORMAL, DISTRIBUTION

C-6.1 USEFULNESS OF THE GAUSSIAN DISTRIBUTION

Although there are a number of common probability distributions, the one of greatest practical importance is the Gaussian, or normal, distribution. The Gaussian distribution is obtained in a large number of situations:

1. It has been empirically observed that most continuous random processes in nature can be described approximately by a Gaussian distribution.

2. Discrete random variables are often described by a binomial distribution, but for a large number of trials, the binomial distribution can be approximated by the Gaussian distribution.

3. If a random variable is derived from the sum of a large number of individual random variables, each of which may have any distribution, the resultant random variable approaches a Gaussian distribution as the number of random variables increases. This phenomenon is discussed in subpar. C-6.4.

C-6.2 DEFINITION OF THE GAUSSIAN DISTRIBUTION

The continuous pdf of a Gaussian distribution is defined by

$$f_X(x) \triangleq \frac{1}{\sigma_X\sqrt{2\pi}} \exp\left[-\frac{1}{2}\frac{(x-\bar{X})^2}{\sigma_X^2} \right], \; U^{-1} \qquad \text{(C-80)}$$

where
$\bar{X}$ = mean or expected value of the random variable X (See Eq. (C-75),) U.

From Eq. C-33 it is apparent that the associated Gaussian continuous cdf is given by

$$F_X(x) \triangleq \int_{-\infty}^{X} \frac{1}{\sigma_X\sqrt{2\pi}} \exp\left[-\frac{1}{2}\frac{(x-\bar{X})^2}{\sigma_X^2} \right] dx', \; \text{per unit.} \qquad \text{(C-81)}$$

The total area beneath a plot of $f_X(x)$ is unity. The Gaussian pdf and the associated Gaussian cdf are shown in Figs. C-8(A) and C-8(B), respectively. 68.3% of all values of the variable fall within $\pm 1\sigma$ of the mean, and practically all values (99.7%) fall within $\pm 3\sigma$ of the mean.

(A) Density Function

(B) Cumulative Distribution Function
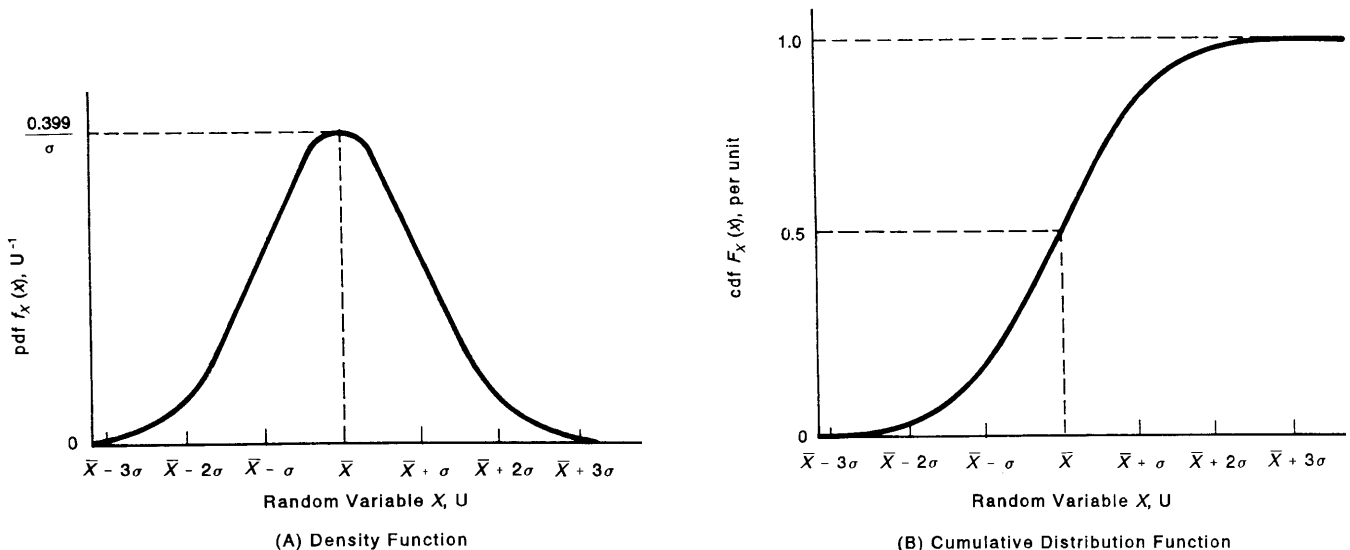
Figure C-8. The Gaussian, or Normal, Probability Function

C-6.3   THE CENTRAL LIMIT THEOREM

If the output of a system is affected by a number of random inputs and even though the input functions may individually depart greatly from normal distributions, the output is approximately a normal distribution. The mathematical justification for this observation is called the central limit theorem. Use of this theorem in connection with fire control systems enables the designer to combine errors as though all are Gaussian and without the necessity for detailed examination of the individual probability distributions.

The central limit theorem states that the sum of a set of random variables is a random variable whose pdf approaches the Gaussian form as the number of terms in the sum increases without limit. The theorem is valid with minor restrictions, e.g., the first and second moments of the individual probability density functions must exist, regardless of the form of the individual probability density functions. Additionally, it is assumed that no single error source, which might be nonnormal, dominates the system.

In symbolic form, assume a set of n random variables $\{X_1, X_2, \cdots, X_n\}$, each of which may have an arbitrary pdf. The sum of these is another random variable S_n defined by

$$S_n \triangleq \sum_{i=1}^{n} X_i, \ \mathbf{U} \qquad \text{(C-82)}$$

where

S_n = sum of n random variables that can take on the values $S_{n_{min}} \leq s \leq S_{n_{max}}$, **U**
$S_{n_{max}}$ = maximum value the random variable S_n can take on, **U**
$S_{n_{min}}$ = minimum value the random variable S_n can take on, **U**.

The random variable S_n will have a mean and variance $\overline{S}_n$ and $\sigma_{S_n}^2$, respectively. Define a new set of n normalized random variables $\{Z_1, Z_2, \cdots, Z_n\}$ as follows:

$$Z_i = \frac{X_i - \overline{S}_n}{\sigma_{S_n}}, \ \text{dimensionless} \qquad \text{(C-83)}$$

where

Z_i = ith normalized random variable, dimensionless
X_i = ith random variable of the set $\{X_1, X_2, \cdots, X_n\}$, **U**
$\overline{S}_n$ = mean (or expected value) of the random variable S_n, **U**
σ_{S_n} = standard deviation of the random variable S_n, **U**.

The central limit theorem states that

$$\lim_{n \to \infty} F_Z(z) = \int_{-\infty}^{z} \frac{1}{\sqrt{2\pi}} \exp\left(-\frac{1}{2} z'^2\right) dz', \ \text{per unit} \qquad \text{(C-84)}$$

where

$F_Z(z)$ = cdf of the random variable that can take on the values $-\infty < z < \infty$, per unit
z' = dummy variable of integration for z, dimensionless.

The right side of Eq. C-84 is the cdf of a Gaussian distribution with zero mean and unity variance. The proof of the central limit theorem is beyond the scope of this handbook, but it is included in Refs. 2 and 6.

C-7   THE BIVARIATE NORMAL DISTRIBUTION

If independent normal distributions exist along each of two orthogonal axes X and Y, the joint probability density function $f_{X,Y}(x,y)$ is found from Eqs. C-38 and C-80:

$$f_{X,Y}(x, y) = f_X(x) \ f_Y(y)$$

$$= \frac{1}{\sigma_X \sqrt{2\pi}} \ \exp\left[-\frac{1}{2} \left(\frac{x - \bar{X}}{\sigma_X} \right)^2 \right] \frac{1}{\sigma_Y \sqrt{2\pi}} \exp\left[-\frac{1}{2} \left(\frac{y - \bar{Y}}{\sigma_Y} \right)^2 \right] \qquad \text{(C-85)}$$

$$= \frac{1}{2\pi\sigma_X\sigma_Y} \ \exp\left\{ -\frac{1}{2} \left[\left(\frac{x - \bar{X}}{\sigma_X} \right)^2 + \left(\frac{y - \bar{Y}}{\sigma_Y} \right)^2 \right] \right\}, \ \mathbf{U}^{-2}$$

where

$\bar{X}, \bar{Y}$ = means of the random variables X and Y, respectively, **U**

σ_X, σ_Y = standard deviations of X and Y, respectively, **U**

$f_{X,Y}(x,y)$ = continuous joint pdf of the random variables X, which can take on values $-\infty < x < \infty$, and Y, which can take on values $-\infty < y < \infty$, $\mathbf{U}^{-1}$.

The joint pdf $f_{X,Y}(x,y)$ is termed the bivariate normal distribution because there are two variables involved. As shown by the representative plots in Fig. C-9, the bivariate normal distribution may be visualized in three dimensions as a "hill" that is based on the x,y-plane and has its center at $(\bar{X}, \bar{Y})$.
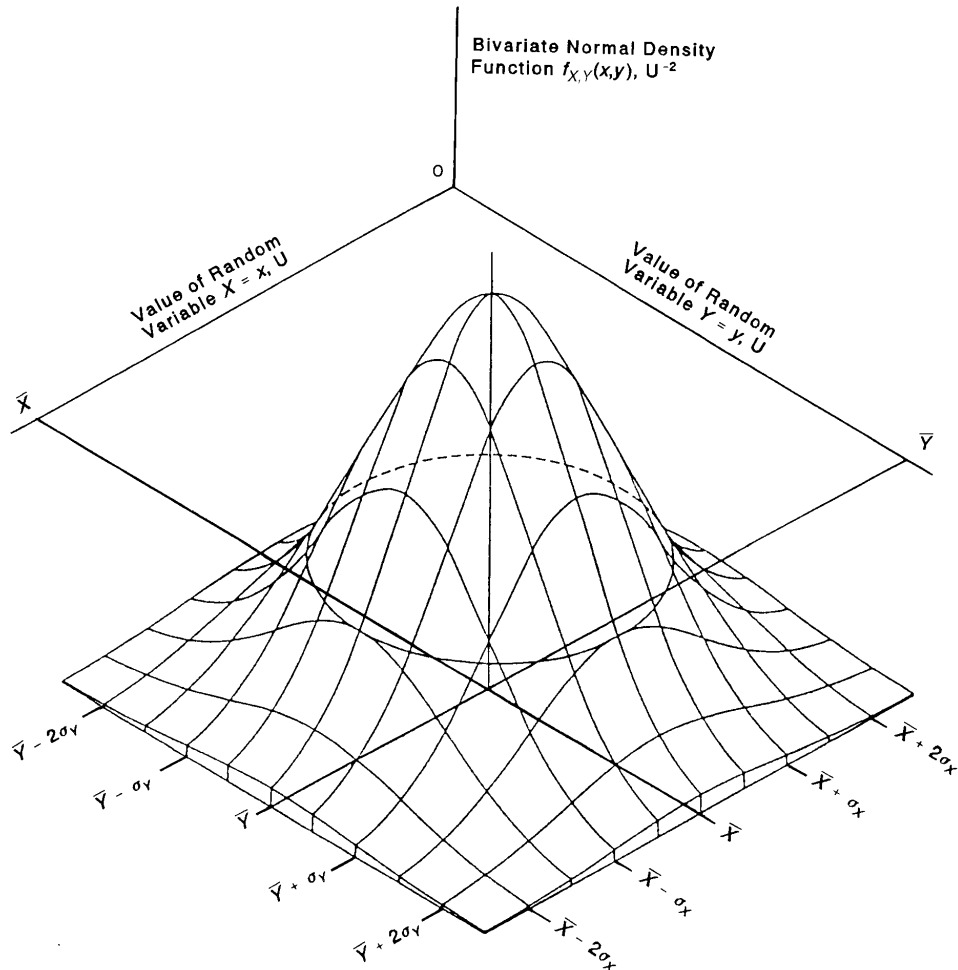
Figure C-9. Bivariate Normal Density Function

C-8 THE BINOMIAL DISTRIBUTION

C-8.1 DESCRIPTION

The binomial distribution is a useful discrete probability function. It deals with a sequence of n trials. The result of each trial is a success or a failure based upon some quality of the experiment result.

The binomial pdf is given by

$$
\begin{aligned}
b(n,s) &= P(S = s) \\
&= \binom{n}{s} p^s q^{n-s}, \quad \textbf{per unit}
\end{aligned}
\tag{C-86}
$$

where

$b(n,s)$ = **binomial pdf (of exactly s successes in n trials), per unit**
$P(S = s)$ = **probability that the random variable S will take on the value $s = 0,1,2, \cdots$, per unit**
n = **number of trials (in a binomial distribution), dimensionless**
s = **number of successes, dimensionless**
p = **probability of success in any one trial, per unit**
$q = 1 - p$ = **probability of failure in any one trial, per unit**

$\binom{n}{s}$ = **combination of n objects taken s at a time, $\dfrac{n!}{s!\,(n-s)!}$, dimensionless.**

The binomial cdf is given by

$$
\begin{aligned}
B(n, s) &\triangleq P(S \le s) \\
&= \sum_{i=0}^{s} \binom{n}{i} p^i q^{n-i}, \quad \textbf{per unit}
\end{aligned}
\tag{C-87}
$$

where

$B(n,s)$ = **binomial cdf (of $0,1,2,\cdots$, or s successes in n trials), per unit**
$P(S \le s)$ = **probability of $S = 0, S = 1, S = 2, \cdots$, or $S = s$, per unit.**

C-8.2 ILLUSTRATIVE EXAMPLE C-5

Problem: Find the number of trials required to achieve a specified probability of at least one success given the probability of success in any one trial p. The specified probability of at least one success is also called the confidence probability C.

Solution: From Eq. C-87

$$
\begin{aligned}
B(n, n) &= \sum_{i=0}^{n} \binom{n}{i} p^i q^{n-i} \\
&= (p + q)^n = 1^n = 1, \quad \textbf{per unit.}
\end{aligned}
\tag{C-88}
$$

Therefore,

$$
\begin{aligned}
C = P(S \ge 1) &= 1 - P(S = 0) \\
&= 1 - \binom{n}{0} p^0 q^{n-0} \\
&= 1 - q^n = 1 - (1 - p)^n, \quad \textbf{per unit}
\end{aligned}
\tag{C-89}
$$

where

C = **specified confidence probability, per unit**
$P(S \ge 1)$ = **probability of at least one success, per unit**
$P(S = 0)$ = **probability of no successes, per unit.**

Eq. C-89 may be written as

$$(1 - p)^n = 1 - C, \text{ per unit}$$

and

$$n = \frac{\log (1 - C)}{\log (1 - p)}, \quad \text{dimensionless.} \tag{C-90}$$

Since the number of trials n must be an integer, Eq. C-90 must be written as

$$n = \left\lceil \frac{\log (1 - C)}{\log (1 - p)} \right\rceil, \quad \text{dimensionless} \tag{C-91}$$

where
$\lceil a \rceil \triangleq$ **ceiling of $a \triangleq$ smallest integer $\geq a$, U.**

For example, specify that $C = 0.6$ for $p = 0.2$:

$$n = \left\lceil \frac{\log (1 - 0.6)}{\log (1 - 0.2)} \right\rceil = \lceil 4.106 \rceil = 5, \text{ trials.}$$

For example, specify that $C = 0.9$ for $p = 0.1$:

$$n = \left\lceil \frac{\log (1 - 0.9)}{\log (1 - 0.1)} \right\rceil = \lceil 21.854 \rceil = 22, \text{ trials.}$$

C-9 DERIVATION OF THE RANDOM ERROR THEOREM (Eq. 4-134)

Given: Two independent random variables X_1 and X_2 with known means $\overline{X_1}$ and $\overline{X_2}$, known variances $\sigma_{X_1}^2$ and $\sigma_{X_2}^2$, and known pdf's $f_{X_1}(x_1)$ and $f_{X_2}(x_2)$, respectively. Let

$$S_2 = X_1 + X_2, \text{ U} \tag{C-92}$$

where
$S_2 =$ **random variable that is the sum of the random variables X_1 and X_2, U.**

Because X_1 and X_2 are independent,

$$\begin{aligned} f_{S_2}(s_2) &= f_{X_1 X_2}(x_1, x_2) \\ &= f_{X_1}(x_1) \, f_{X_2}(x_2), \ \text{U}^{-2} \end{aligned} \tag{C-93}$$

where
$s_2, x_1, x_2 =$ **values that the random variables S, X_1, X_2 can take on, respectively, $-\infty < s_2, x_1, x_2 < \infty$, U.**

Applying the concept of Eq. C-75 yields

$$\begin{aligned} \overline{S_2} = E(S_2) &= E(X_1 + X_2) \\ &= E(X_1) + E(X_2) = \overline{X_1} + \overline{X_2}, \ \text{U} \end{aligned} \tag{C-94}$$

where

$\overline{S_2} = E(S_2) =$ **mean (or expectation) of random variable S_2, U**

$\overline{X_1} = E(X_1) =$ **mean (or expectation) of random variable X_1, U**

$\overline{X_2} = E(X_2) =$ **mean (or expectation) of random variable X_2, U.**

Applying the concept of Eq. C-78 yields

$$\sigma_{S_2}^2 = E\left[(S_2 - \bar{S}_2)^2\right]$$

$$= E\left\{\left[(X_1 - \bar{X}_1) + (X_2 - \bar{X}_2)\right]^2\right\} \tag{C-95}$$

$$= E\left[(X_1 - \bar{X}_1)^2\right] + E\left[(X_2 - \bar{X}_2)^2\right] + 2E\left[(X_1 - \bar{X}_1)(X_2 - \bar{X}_2)\right]$$

$$= \sigma_{X_1}^2 + \sigma_{X_2}^2 + 2E\left[(X_1 - \bar{X}_1)(X_2 - \bar{X}_2)\right]$$

where

$\sigma_{S_2}^2 = E[(S_2 - \bar{S}_2)]^2 = $ **variance of the random variable** S_2, U^2

$\sigma_{X_1}^2 = E[(X_1 - \bar{X}_1)]^2 = $ **variance of the random variable** X_1, U^2

$\sigma_{X_2}^2 = E[(X_2 - \bar{X}_2)]^2 = $ **variance of the random variable** X_2, U^2.

However, since X_1 and X_2 are independent (See Eq. C-93.),

$$E\left[(X_1 - \bar{X}_1)(X_2 - \bar{X}_2)\right] = \int_{-\infty}^{\infty}\int_{-\infty}^{\infty}(x_1 - \bar{X}_1)(x_2 - \bar{X}_2)\ f_{X_1}(x_1)\ f_{X_2}(x_2)\ dx_1 dx_2 \tag{C-96}$$

$$= \int_{-\infty}^{\infty}(x_1 - \bar{X}_1)\ f_{X_1}(x_1)\ dx_1 \int_{-\infty}^{\infty}(x_2 - \bar{X}_2)\ f_{X_2}(x_2)\ dx_2,\ U^2.$$

Consider the first integral in Eq. C-96:

$$\int_{-\infty}^{\infty}(x_1 - \bar{X}_1)\ f_{X_1}(x_1)\ dx_1 = \int_{-\infty}^{\infty}x_1\ f_{X_1}(x_1)\ dx_1 - \bar{X}_1 \int_{-\infty}^{\infty}f_{X_1}(x_1)\ dx_1,\ U \tag{C-97}$$

but

$$\int_{-\infty}^{\infty}x_1\ f_{X_1}(x_1)\ dx_1 \triangleq E(X_1) = \bar{X}_1,\ U. \tag{C-98}$$

Also

$$\int_{-\infty}^{\infty}f_{X_1}(x_1)\ dx_1 \triangleq 1,\ \text{per unit.} \tag{C-99}$$

Substituting Eqs. C-98 and C-99 into Eq. C-97 yields

$$\int_{-\infty}^{\infty}(x_1 - \bar{X}_1)\ f_{X_1}(x_1)\ dx_1 = \bar{X}_1 - \bar{X}_1 \times 1 = 0,\ U. \tag{C-100}$$

Similarly,

$$\int_{-\infty}^{\infty} \left(x_2 - \bar{X}_2\right) f_{X_2}(x_2)\, dx_2 = 0, \ \text{U.} \tag{C-101}$$

Substituting Eqs. C-100 and C-101 into Eq. C-96 and then into Eq. C-95 yields

$$\sigma_{S_2}^2 = \sigma_{X_1}^2 + \sigma_{X_2}^2 + 2 \times 0 = \sigma_{X_1}^2 + \sigma_{X_2}^2, \ \text{U}^2. \tag{C-102}$$

Expansion of S_2 to the sum of n independent variables $S_n = X_1, X_2, \cdots, X_n$ yields

$$S_n = \sum_{i=0}^{n} X_i, \ \text{U.} \tag{C-103}$$

Then Eqs. C-92 and C-102 expand to

$$\bar{S}_n = \sum_{i=1}^{n} X_i, \ \text{U} \tag{C-104}$$

and

$$\sigma_{S_n}^2 = \sum_{i=1}^{n} \sigma_{X_i}^2, \ \text{U}^2. \tag{C-105}$$

Q.E.D.

C-10 ILLUSTRATIVE EXAMPLE C-6

   This is an example of error analysis of a simple amplifier.
Given: A simple amplifier circuit as shown in Fig. C-10 where
   α = **nominal gain, dimensionless**
   ε_α = **gain error, dimensionless**
   x = **nominal input, V**
   ε_x = **input error, V**
   y = **nominal output, V**
   ε_y = **output error, V**
   Δ = **fixed offset in amplifier output, V.**
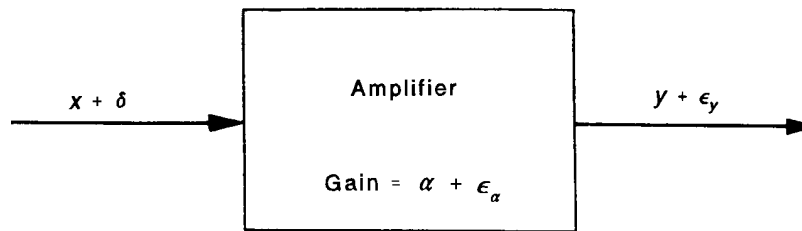
Figure C-10. Functional Diagram of a Simple Amplifier

Problem: Derive an expression for the total error ε_y in the output of the amplifier.
Solution A: The performance equation for the ideal (nominal) amplifier is

$$y = \alpha\, x, \ \text{V.} \tag{C-106}$$

The corresponding performance equation for the nonideal case is

$$y + \varepsilon_y = (\alpha + \varepsilon_\alpha)(x + \delta) + \Delta \tag{C-107}$$

where
        δ = **assumed value of ε_x, V.**

Since $\varepsilon_\alpha \delta$ is the product of two small quantities, it can be neglected. Therefore, the total output error is given by

$$\varepsilon_y = \varepsilon_\alpha\, x + \alpha\, \delta + \Delta, \textbf{ V.} \tag{C-108}$$

Solution B: Eq. C-106 in functional form converts to

$$f(x,y) = y - \alpha\, x = \textbf{0, V} \tag{C-109}$$

where

$f(x,y)$ = simple amplifier performance function, V.

This equation corresponds to Eq. 4-111. Taking partial derivatives of Eq. C-109 yields

$$\frac{\partial}{\partial x} f(x,\, y) \;=\; -\alpha, \textbf{ dimensionless} \tag{C-110}$$

and

$$\frac{\partial}{\partial y} f(x,\, y) \;=\; \textbf{1, dimensionless.} \tag{C-111}$$

The error due to the nonideal characteristic of the amplifier is

$$e = \varepsilon_\alpha\, x + \Delta, \textbf{ V} \tag{C-112}$$

where

e = error generated by the device.

When the errors are small, the performance equation for the nonideal amplifier with input errors is obtained by adding the error in Eq. C-112 to the output of the ideal amplifier:

$$y + \varepsilon_y = \alpha(x + \delta) + e, \textbf{ V.} \tag{C-113}$$

In functional form the performance equation for this nonideal case is

$$h(x,\delta,y,\varepsilon_y,e) = y + \varepsilon_y - \alpha(x + \delta) - e = \textbf{0, V.} \tag{C-114}$$

The complete set of error equations, Eq. 4-133, can now be applied to the simple amplifier. Since there is only one element involved, only one equation is required:

$$\frac{\partial}{\partial y} f(x,\, y)\, \varepsilon_y \;=\; -\frac{\partial}{\partial x} f(x,\, y)\varepsilon_x - e\, \frac{\partial}{\partial e} h(x,\, \delta,\, y,\, \varepsilon_y,\, e), \textbf{ V} \tag{C-115}$$

where

e = output error in the absence of an input error, V.

The partial derivative in the last term on the right-hand side of Eq. C-115 is obtained from Eq. C-114:

$$\frac{\partial}{\partial e} h(x,\, \delta,\, y,\, \varepsilon_y,\, e) \;=\; \textbf{-1.} \tag{C-116}$$

Substituting Eq. C-106 into Eq. C-113 yields

$$e = \varepsilon_\alpha\, x + \Delta, \textbf{ V.} \tag{C-117}$$

Substituting Eqs. C-110, C-111, C-112, and C-116 into Eq. C-115 and noting that $\varepsilon_X = \delta$ yield

$$\varepsilon_y = -(-\alpha)\,\delta - (\varepsilon_\alpha x + \Delta)\,(\textbf{-1})$$

$$= \varepsilon_\alpha x + \alpha\delta + \Delta, \textbf{ V}$$

which is identical to Eq. C-108 of Solution A.

C-11   ILLUSTRATIVE EXAMPLE C-7

This paragraph presents an example of error propagation through a simple computer circuit.
The computer circuit represented in Fig. C-11 has three inputs, one output, and three elements. (The
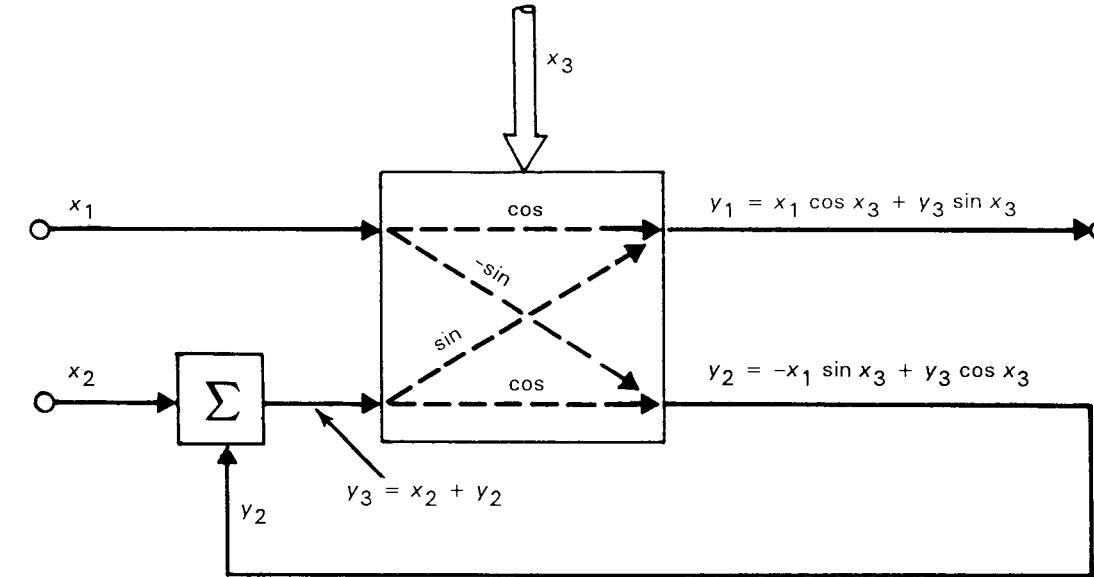
(A) Symbolic Representation
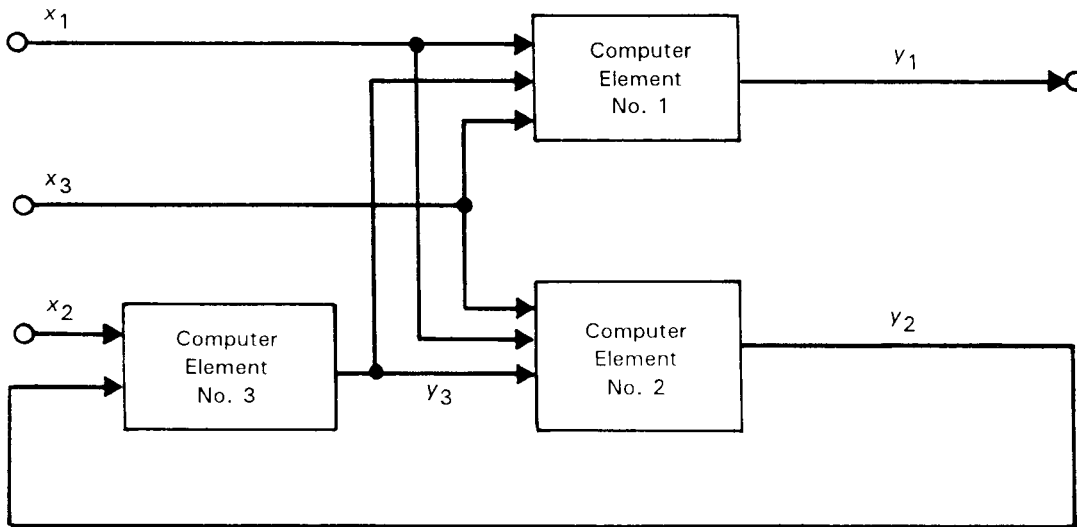
(B) Functional Representation

Figure C-11. Representations of a Simple Computer Circuit

resolver is considered to be made up of two elements since it has two outputs.) The circuit performance
equations are

$$f_1 = y_1 - x_1 \cos x_3 - y_3 \sin x_3 = 0, \text{ V} \tag{C-118}$$

$$f_2 = y_2 + x_1 \sin x_3 - y_3 \cos x_3 = 0, \text{ V} \tag{C-119}$$

$$f_3 = y_3 - x_2 - y_2 = 0, \text{ V} \tag{C-120}$$

where

x_1 = input to Element 1, V
x_2 = input to Element 2, V

x_3 = input to Element 3, rad
y_1 = output of Element 1, V
y_2 = output of Element 2, V
y_3 = output of Element 3, V
f_1 = performance function of Element 1, V
f_2 = performance function of Element 2, V
f_3 = performance function of Element 3, V.

The corresponding performance equations for the nonideal case are

$$h_1 = y_1 + \varepsilon_{y_1} - (x_1 + \varepsilon_{x_1})\ \cos(x_3 + \varepsilon_{x_3}) - (y_3 + \varepsilon_{y_3})\ \sin(x_3 + \varepsilon_{x_3}) - e_1 = 0,\ V \qquad \text{(C-121)}$$

$$h_2 = y_2 + \varepsilon_{y_2} + (x_1 + \varepsilon_{x_1})\ \sin(x_3 + \varepsilon_{x_3}) - (y_3 + \varepsilon_{y_3})\ \cos(x_3 + \varepsilon_{x_3}) - e_2 = 0,\ V \qquad \text{(C-122)}$$

$$h_3 = y_3 + \varepsilon_{y_3} - x_2 - \varepsilon_{x_2} - y_2 - \varepsilon_{y_2} - e_3 = 0,\ V \qquad \text{(C-123)}$$

where
h_1 = nonideal performance function of Element 1, V
h_2 = nonideal performance function of Element 2, V
h_3 = nonideal performance function of Element 3, V
ε_{x_1} = error in input to Element 1, V
ε_{x_2} = error in input to Element 2, V
ε_{x_3} = error in input to Element 3, rad
ε_{y_1} = error in output of Element 1, V
ε_{y_2} = error in output of Element 2, V
ε_{y_3} = error in output of Element 3, V
e_1 = Element 1 output error in the absence of input error, V
e_2 = Element 2 output error in the absence of input error, V
e_3 = Element 3 output error in the absence of input error, V.

Eqs. C-118, C-119, and C-120 can be solved in the following manner to give the output of the ideal computer circuit y_1 in terms of the three inputs x_1, x_2, and x_3. From Eq. C-120

$$y_3 = x_2 + y_2,\ V. \qquad \text{(C-124)}$$

From Eq. C-119

$$y_2 = y_3 \cos x_3 - x_1 \sin x_3,\ V. \qquad \text{(C-125)}$$

Substitution of Eq. C-125 into Eq. C-124 yields

$$y_3 = x_2 + y_3 \cos x_3 - x_1 \sin x_3,\ V. \qquad \text{(C-126)}$$

Rearrangement of terms gives

$$y_3(1 - \cos x_3) = x_2 - x_1 \sin x_3,\ V. \qquad \text{(C-127)}$$

Therefore,

$$y_3 = \frac{x_2 - x_1 \sin x_3}{1 - \cos x_3},\ V. \qquad \text{(C-128)}$$

From Eq. C-118

$$y_1 = x_1 \cos x_3 + y_3 \sin x_3,\ V. \qquad \text{(C-129)}$$

Substitution of Eq. C-128 into Eq. C-129 yields

$$y_1 = x_1 \cos x_3 + \frac{x_2 - x_1 \sin x_3}{1 - \cos x_3} \sin x_3$$

$$= \frac{x_1 \cos x_3 - x_1 \cos^2 x_3 + x_2 \sin x_3 - x_1 \sin^2 x_3}{1 - \cos x_3} \tag{C-130}$$

$$= -x_1 \frac{\sin^2 x_3 + \cos^2 x_3 - \cos x_3}{1 - \cos x_3} + \frac{x_2 \sin x_3}{1 - \cos x_3}, \quad \text{V.}$$

Therefore, since $\sin^2 x + \cos^2 x = 1$,

$$y_1 = -x_1 + \frac{x_2 \sin x_3}{1 - \cos x_3}, \quad \text{V.} \tag{C-131}$$

Eq. C-131 expresses the output of the computer circuit in terms of the three inputs.

 The required partial derivatives can be determined by successively differentiating Eq. C-118 with respect to y_1, y_2, y_3, x_1, x_2, and x_3 to obtain

$$\frac{\partial f_1}{\partial y_1}, \frac{\partial f_1}{\partial y_2}, \frac{\partial f_1}{\partial y_3}, \frac{\partial f_1}{\partial x_1}, \frac{\partial f_1}{\partial x_2}, \quad \text{and} \quad \frac{\partial f_1}{\partial x_3},$$

respectively, and then repeating the process with Eqs. C-119 and C-120 to yield the remaining partial derivatives. The results are tabulated

$$\frac{\partial f_1}{\partial y_1} = 1, \text{ dimless*} \qquad \frac{\partial f_2}{\partial y_1} = 0, \text{ dimless} \qquad \frac{\partial f_3}{\partial y_1} = 0, \text{ dimless}$$

$$\frac{\partial f_1}{\partial y_2} = 0, \text{ dimless} \qquad \frac{\partial f_2}{\partial y_2} = 1, \text{ dimless} \qquad \frac{\partial f_3}{\partial y_2} = -1, \text{ dimless}$$

$$\frac{\partial f_1}{\partial y_3} = -\sin x_3, \text{ dimless} \qquad \frac{\partial f_2}{\partial y_3} = -\cos x_3, \text{ dimless} \qquad \frac{\partial f_3}{\partial y_3} = 1, \text{ dimless}$$

$$\frac{\partial f_1}{\partial x_1} = -\cos x_3, \text{ dimless} \qquad \frac{\partial f_2}{\partial x_1} = \sin x_3, \text{ dimless} \qquad \frac{\partial f_3}{\partial x_1} = 0, \text{ dimless} \tag{C-132}$$

$$\frac{\partial f_1}{\partial x_2} = 0, \text{ dimless} \qquad \frac{\partial f_2}{\partial x_2} = 0, \text{ dimless} \qquad \frac{\partial f_3}{\partial x_2} = -1, \text{ dimless}$$

$$\begin{aligned}\frac{\partial f_1}{\partial x_3} &= x_1 \sin x_3 \\ &\quad -y_3 \cos x_3, \text{ V/rad}\end{aligned} \qquad \begin{aligned}\frac{\partial f_2}{\partial x_3} &= x_1 \cos x_3 \\ &\quad + y_3 \sin x_3, \text{ V/rad}\end{aligned} \qquad \frac{\partial f_3}{\partial x_3} = 0, \text{ V/rad}$$

———————

*dimless = dimensionless.

The partial derivatives needed from Eqs. C-121, C-122, and C-123 are

$$\frac{\partial h_1}{\partial e_1} = \frac{\partial h_2}{\partial e_2} = -\frac{\partial h_3}{\partial e_3} = -1, \text{ dimensionless.} \tag{C-133}$$

Eq. 4-133 shows that the error for computer Element No. 1 in Fig. C-11(B) can be expressed in the generalized form:

$$\sum_{k=1}^{3} \frac{\partial f_1}{\partial y_k} \varepsilon_{y_k} = -\sum_{n=1}^{3} \frac{\partial f_1}{\partial x_n} \varepsilon_{x_n} - e_1 \frac{\partial h_1}{\partial e_1}, \text{ V} \tag{C-134}$$

where

k = subscript index = 1,2,3, dimensionless
n = subscript index = 1,2,3, dimensionless
ε_{y_k} = Element k total output error, V
ε_{x_n} = Element n input error, unit depends on n.

Substitution of the values of the partial derivatives given by Eqs. C-132 and C-133 into Eq. C-134 yields the error equation

$$\varepsilon_{y_1} - (\sin x_3)\varepsilon_{y_3} = (\cos x_3)\varepsilon_{x_1} + (y_3 \cos x_3 - x_1 \sin x_3)\varepsilon_{x_3} + e_1, \text{ V.} \tag{C-135}$$

A similar procedure for computer Element Nos. 2 and 3 yields the respective error equations

$$\varepsilon_{y_2} - (\cos x_3)\varepsilon_{y_3} = -(\sin x_3)\varepsilon_{x_1} - (x_1 \cos x_3 + y_3 \sin x_3)\varepsilon_{x_3} + e_2, \text{ V} \tag{C-136}$$

and

$$-\varepsilon_{y_2} + \varepsilon_{y_3} = \varepsilon_{x_2} + e_3, \text{ V.} \tag{C-137}$$

Solving Eqs. C-135, C-136, and C-137 explicitly for ε_{y1}, ε_{y2}, and ε_{y3} yields

$$\varepsilon_{y_1} = (\sin x_3)\varepsilon_{y_3} + (\cos x_3)\varepsilon_{x_1} + (y_3 \cos x_3 - x_1 \sin x_3)\varepsilon_{x_3} + e_1, \text{ V} \tag{C-138}$$

$$\varepsilon_{y_2} = (\cos x_3)\varepsilon_{y_3} - (\sin x_3)\varepsilon_{x_1} - (x_1 \cos x_3 + y_3 \sin x_3)\varepsilon_{x_3} + e_2, \text{ V} \tag{C-139}$$

$$\varepsilon_{y_3} = \varepsilon_{y_2} + \varepsilon_{x_2} + e_3, \text{ V.} \tag{C-140}$$

The block diagram shown in Fig. C-12 can be readily formed from Eqs. C-138, C-139, and C-140. This diagram visualizes the effect of a given input error on the output error ε_{y_1}.

Eqs. C-138, C-139, and C-140 can also be solved to give the error in the output ε_{y_1} explicitly in terms of the input errors ε_{x_1}, ε_{x_2}, and ε_{x_3} and the element errors e_1, e_2, and e_3. Substitution of Eq. C-139 into Eq. C-140 yields

$$\varepsilon_{y_3} = (\cos x_3)\varepsilon_{y_3} - (\sin x_3)\varepsilon_{x_1} - (x_1 \cos x_3 + y_3 \sin x_3)\varepsilon_{x_3} + e_2 + \varepsilon_{x_2} + e_3, \text{ V.} \tag{C-141}$$

Solving for ε_{y_3} yields

$$\varepsilon_{y_3} = \frac{-(\sin x_3)\varepsilon_{x_1} - (x_1 \cos x_3 + y_3 \sin x_3)\varepsilon_{x_3} + e_2 + \varepsilon_{x_2} + e_3}{1 - \cos x_3}, \text{ V.} \tag{C-142}$$
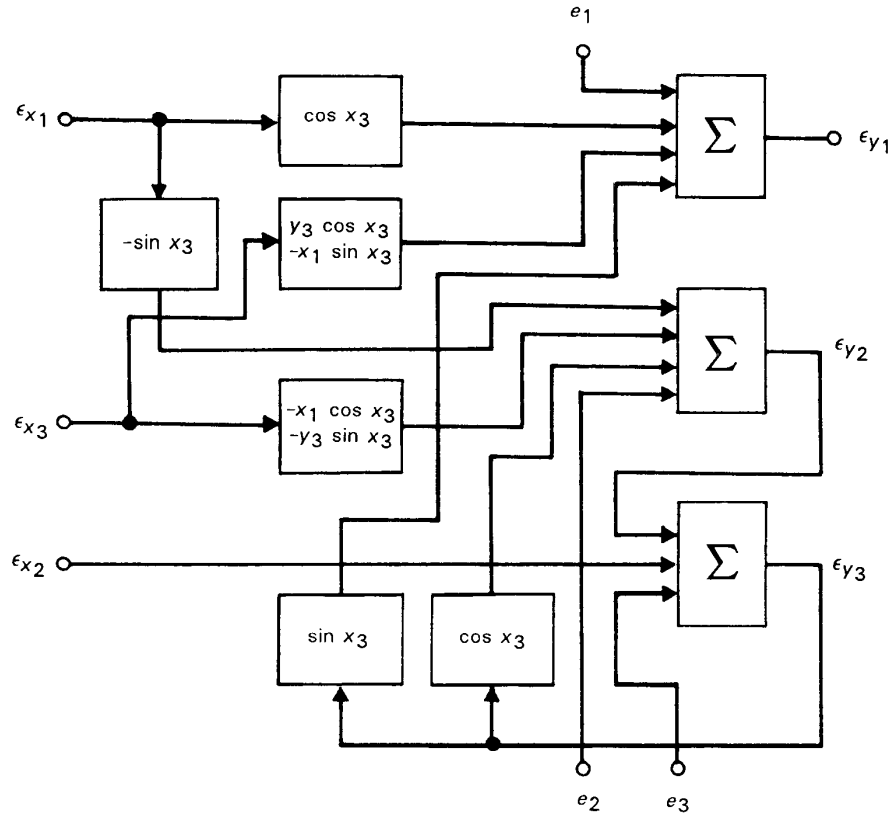
Figure C-12. Error Diagram for the Computer Circuit

Substitution of Eq. C-142 into Eq. C-138 shows that

$$\varepsilon_{y_1} = \frac{-(\sin^2 x_3)\,\varepsilon_{x_1} - (x_1 \sin x_3 \cos x_3)\,\varepsilon_{x_3} - (y_3 \sin^2 x_3)\,\varepsilon_{x_3} + (\sin x_3)\,e_2}{1 - \cos x_3}$$

$$+ \frac{(\sin x_3)\,\varepsilon_{x_2} + (\sin x_3)\,e_3}{1 - \cos x_3} + (\cos x_3)\,\varepsilon_{x_1} + (y_3 \cos x_3)\,\varepsilon_{x_3} - (x_1 \sin x_3)\,\varepsilon_{x_3} + e_1$$

$$= \frac{1}{1 - \cos x_3}\left[-(\sin^2 x_3)\,\varepsilon_{x_1} - (x_1 \sin x_3 \cos x_3)\,\varepsilon_{x_3} - (y_3 \sin^2 x_3)\,\varepsilon_{x_3} \right. \tag{C-143}$$

$$+ (\sin x_3)\,e_2 + (\sin x_3)\,\varepsilon_{x_2} + (\sin x_3)\,e_3 + (\cos x_3)\,\varepsilon_{x_1}$$

$$+ (y_3 \cos x_3)\,\varepsilon_{x_3} - (x_1 \sin x_3)\,\varepsilon_{x_3} + e_1 - (\cos^2 x_3)\,\varepsilon_{x_1}$$

$$\left. - (y_3 \cos^2 x_3)\,\varepsilon_{x_3} + (x_1 \sin x_3 \cos x_3)\,\varepsilon_{x_3} - (\cos x_3)\,e_1 \right], \text{ V.}$$

Removal of the terms of Eq. C-136 that cancel one another, simplification by use of the trigonometric identity $\sin^2 x + \cos^2 x = 1$, **and rearrangement of terms yield**

$$\varepsilon_{y_1} = \frac{1}{1 - \cos x_2}\left[-(1 - \cos x_3)\,\varepsilon_{x_1} + (\sin x_3)\,\varepsilon_{x_2} - y_3(1 - \cos x_3)\,\varepsilon_{x_3} \right.$$

$$\left. - (x_1 \sin x_3)\,\varepsilon_{x_3} + (1 - \cos x_3)\,e_1 + (\sin x_3)\,e_2 + (\sin x_3)\,e_3 \right], \text{ V.} \tag{C-144}$$

Substitution of Eq. C-128 into Eq. C-144 and simplification of terms yield

$$\varepsilon_{y_1} = -\varepsilon_{x_1} + \frac{\sin x_3}{1 - \cos x_3}\varepsilon_{x_2} - \frac{x_2}{1 - \cos x_3}\varepsilon_{x_3} + e_1 + \frac{\sin x_3}{1 - \cos x_3}e_2 + \frac{\sin x_3}{1 - \cos x_3}e_3, \text{ V.} \qquad \text{(C-145)}$$

Eq. C-145 expresses the error in the output of the computer circuit in terms of the errors in the elements and the errors in the inputs. The element error terms and the input error terms are all entirely separate, i.e., they are independent of one another.

C-12 ILLUSTRATIVE EXAMPLE C-8

This paragraph is an example of the error summation procedures described in subpar. 4-4.3.2.

Table C-1 gives assumed values of systematic and random component errors for the error equation derived in illustrative Example C-7 (See Eq. C-145.).

TABLE C-1. ASSUMED ERROR VALUES

ERROR	SYSTEMATIC COMPONENT (peak errors)	RANDOM COMPONENT (standard deviations)
ε_{x_1}, V	$c_1 x_2$, V	σ_1, V
ε_{x_2}, V	c_2, V	0, V
ε_{x_3}, rad	$c_3(1 - \cos x_3)$, rad	0, rad
e_1, V	d_1, V	$\sigma_2 \sin x_3$, V
e_2, V	d_2, V	$\sigma_3(1 - \cos x_3)$, V
e_3, V	d_3, V	0, V

c_1 = constant, dimensionless
c_3 = constant, rad
c_2, σ_1, σ_2, σ_3, d_1, d_2, and d_3 = constants, V

When the values of the systematic components given in Table C-1 are substituted into Eq. C-145 of Example C-7, the resulting relationship yields the systematic component of ε_{y_1}, which is designated as $\varepsilon_{y_{1S}}$, in the form

$$\varepsilon_{y_{1S}} = -c_1 x_2 + \frac{c_2 \sin x_3}{1 - \cos x_3} - c_3 x_2 + d_1 + \frac{d_2 \sin x_3}{1 - \cos x_3} + \frac{d_3 \sin x_3}{1 - \cos x_3}$$

$$= -(c_1 + c_3)\,x_2 + d_1\,(c_2 + d_2 + d_3)\,\frac{\sin x_3}{1 - \cos x_3}, \text{ V} \qquad \text{(C-146)}$$

where

$\varepsilon_{y_{1S}}$ = systematic component of output error ε_{y_1}, V
c_1 = assumed constant factor, dimensionless
c_2 = assumed constant systematic error, V
c_3 = assumed constant factor, rad
d_1, d_2, d_3 = assumed constant systematic errors, V.

This relationship can be rearranged and simplified to

$$\varepsilon_{y_{1S}} = c_4 x_2 + d_1 + c_5 \cot\frac{x_3}{2}, \text{ V}$$ (C-147)

where

$c_4 = -(c_1 + c_3)$, dimensionless (rad)
$c_5 = c_2 + d_2 + d_3$, V

and the trigonometric identity used is

$$\cot\frac{x_3}{2} = \frac{\sin x_3}{1 - \cos x_3}.$$

The dependent terms of Eq. C-147 are plotted in Fig. C-13. Obviously, the resolver computer circuit that is the subject of this example (See Figs. C-11 and C-12.) becomes useless for values of x_3 that approach

(A) Dependent Term $C_4 x_2$ versus x_2

(B) Dependent Term $C_5 \cot (x_3/2)$ versus x_3
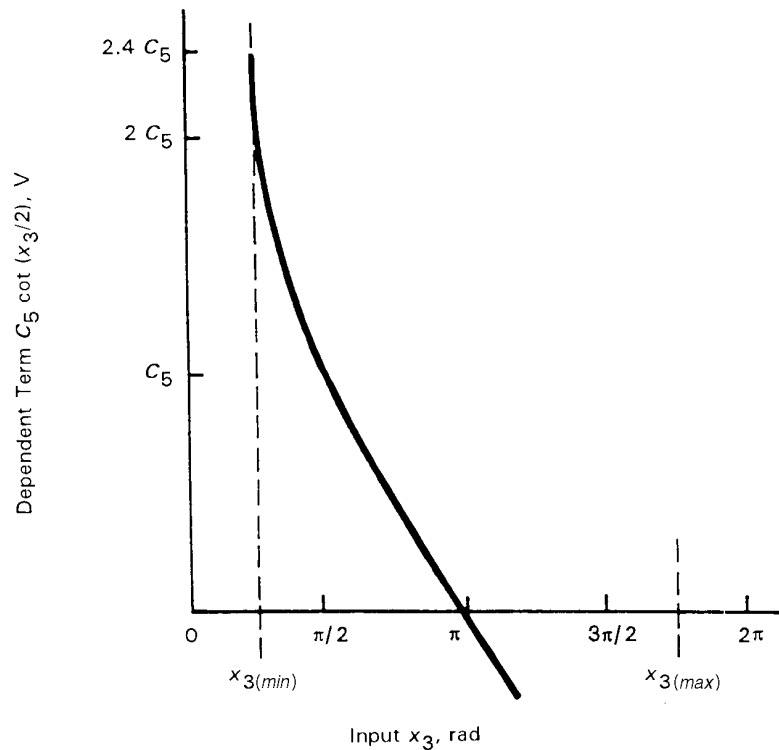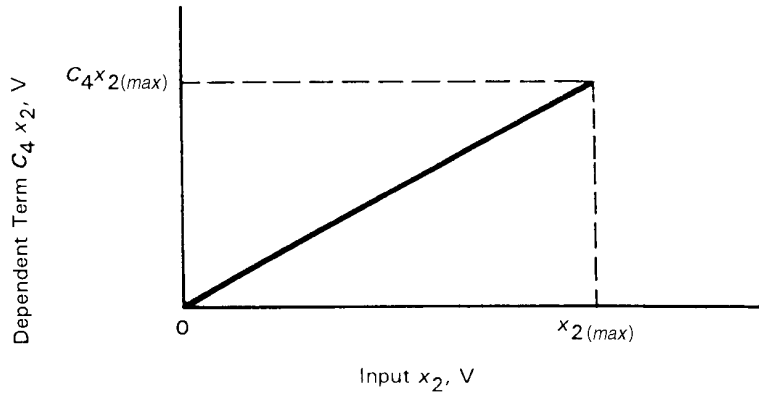
Figure C-13. Plots of Dependent Terms $C_4 x_2$ and $C_5 \cot (x_3/2)$

0 rad and 2π rad because the systematic component of ε_{y_1} then approaches an infinite magnitude. The variable x_3 must be limited to the minimum (min) and maximum (max) range $x_{3(min)} < x_3 < x_{3(max)}$, as shown in Fig. C-13(B). This range is determined explicitly by Eq. C-145 if the maximum value of ε_{y_1S} and the maximum value of x_2 (designated $x_{2(max)}$) are specified. On the other hand, if, for example, $x_{2(max)} = 1$, $x_{3(min)} = \pi/4$ rad, and $x_{3(max)} = 7\pi/4$ rad, the maximum value of ε_{y_1s} is either

$$\varepsilon_{y_{1S}} = c_4 + d_1 + 2.4\,c_5, \quad \mathbf{V}$$

for (C-148)

$$x_3 = x_{3\,(min)} = \frac{\pi}{4}, \quad \mathbf{rad}$$

or

$$\varepsilon_{y_{1S}} = c_4 + d_1 - 2.4\,c_5, \quad \mathbf{V}$$

for (C-149)

$$x_3 = x_{3\,(max)} = \frac{7\pi}{4}, \quad \mathbf{rad}.$$

Whether Eq. C-148 or Eq. C-149 yields the maximum systematic component of ε_{y_1} for a particular numerical example depends of course on the algebraic sign of $c_4 + d_1$.

The total random error is obtained from

$$\sigma_{\varepsilon y1}^2 = \sigma_{\varepsilon x1}^2 + \sigma_{\varepsilon x2}^2 + \sigma_{\varepsilon x3}^2 + \sigma_{e1}^2 + \sigma_{e2}^2 + \sigma_{e3}^2, \quad \mathbf{V} \tag{C-150}$$

where $\sigma_{\varepsilon y1}^2$ is the variance of the output error, $\sigma_{\varepsilon x1}^2$ is the variance of the first term of Eq. C-145 in Example C-7, and the remaining variances pertain to the remaining terms, respectively. $\sigma_{\varepsilon x3}^2$ is the variance of the entire $\dfrac{x_2}{1 - \cos x_3}\varepsilon_{x_3}$ term of Eq. C-145. As such, it has the unit volts, which is consistent with the other terms of Eq. C-150. Substitution of the values of the random component errors given in Table C-1 into Eq. C-150, which replaces Eq. C-145 of Example C-7 for random error summation, yields

$$\sigma_{\varepsilon y1}^2 = \sigma_1^2 + \sigma_2^2 \sin^2 x_3 + \sigma_3^2 (1 - \cos x_3)^2, \quad \mathbf{V}^2 \tag{C-151}$$

where

$\sigma_{\varepsilon y1}^2$ = variance of total output random error of Element 1, $\mathbf{V}^2$

σ_1 = assumed random component of ε_{x_1}, V

σ_2 = assumed random component factor of e_1, V

σ_3 = assumed random component factor of e_2, V.

For notational convenience, normalize Eq. C-151 with respect to σ_3^2 by dividing both sides by σ_3^2. Then

$$z = \rho_1^2 + \rho_2^2 \sin^2 x_3 + (1 - \cos x_3)^2, \quad \mathbf{dimensionless} \tag{C-152}$$

where

z = normalized output variance $\sigma_{\varepsilon y1}^2/\sigma_3^2$ of Element 1, dimensionless

$\rho_1^2 = \sigma_1^2/\sigma_3^2$, dimensionless

$\rho_2^2 = \sigma_2^2/\sigma_3^2$, dimensionless.

Fig. C-14 provides plots of the normalized output error variance z for four values of ρ_2. The minimum
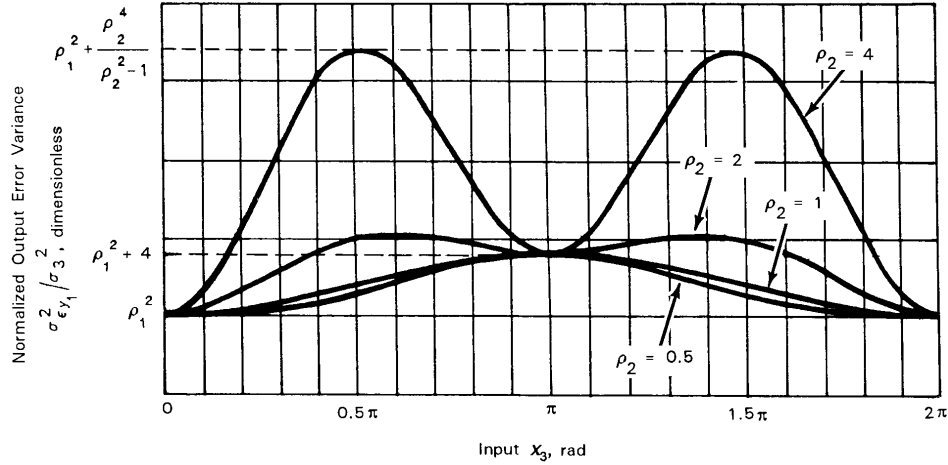
Figure C-14. Normalized Output Error Variance $\sigma^2_{\varepsilon_{y1}}/\sigma^2_3$ Versus Input x_3

and maximums of z were obtained as follows. Setting the slope of z with respect to x_3 equal to zero yields

$$\frac{dz}{dx_3} = 0 + 2\rho_2^2 \sin x_3 \cos x_3 + 2(1 - \cos x_3) \sin x_3 = 0, \text{ dimensionless} \qquad \text{(C-153)}$$

and

$$\sin x_3[1 + (\rho_2^2 - 1)\cos x_3] = 0, \text{ dimensionless.} \qquad \text{(C-154)}$$

Case 1: $\sin x_3 = 0$
Then

$$x_3 = \sin^{-1}(0) = \pm n\pi, \text{ rad} \qquad \text{(C-155)}$$

where
$n = 0,1,2,\cdots$, **dimensionless.**

Substituting the positive values of Eq. C-155 into Eq. C-152 yields

$$z\big|_{x_3 = n\pi} = \rho_1^2 + \rho_2^2 \cdot 0 + \Big[1 - \cos(n\pi)\Big]^2$$

$$= \begin{cases} \rho_1^2 & , n: \textbf{ even} \\ \rho_1^2 + 4 & , n: \textbf{ odd} \end{cases}, \text{ dimensionless.} \qquad \text{(C-156)}$$

The minimum value of z is ρ_1^2, and it occurs at $x_3 = 0, 2\pi, 4\pi, \cdots$. The maximum value of z is $\rho_1^2 + 4$, but this may change when Case 2 is analyzed.

Case 2: $\sin x_3 \neq 0$
  In this case the bracketed term of Eq. C-154 is set equal to zero and yields

$$\cos x_3 = \frac{-1}{\rho_2^2 - 1} = -(\rho_2^2 - 1)^{-1}, \text{ dimensionless.} \qquad \text{(C-157)}$$

However, $\cos x_3$ is defined only in the interval $-1 \leq \cos x_3 \leq 1$. Therefore, $\cos x_3$ is not defined for $0 \leq \rho_2^2 \leq 2$ and is defined for $\rho_2^2 > 2$. Further, in the region $\rho_2^2 > 2$

$$x_3 = \left\{ \begin{array}{l} \cos^{-1}[-(\rho_2 - 1)^{-1}] \\ \\ 2\pi - \cos^{-1}[-(\rho_2 - 1)^{-1}] \end{array} \right\}, \text{ rad.} \tag{C-158}$$

That is, in this region there are two values of x_3 that produce the peaks shown in Fig. C-14: $\pi/2 \le x^3 \le \pi$ and $3\pi/2 \le x_3 \le 2\pi$.

Thus for $\sin x_3 \ne 0$ and $\rho_2^2 \ge 2$, the maximum value of z is obtained by substituting Eq. C-157 into Eq. C-152:

$$z_{max} = \rho_1^2 + \rho_2^2 \left[1 - \left(\frac{-1}{\rho_2^2 - 1} \right)^2 \right] + \left(1 - \frac{-1}{\rho_2^2 - 1} \right)^2$$

$$= \rho_1^2 + \rho_2^2 \frac{\rho_2^4 - 2\rho_2^2}{(\rho_2^2 - 1)^2} + \left(\frac{\rho_2^2}{\rho_2^2 - 1} \right)^2$$

$$= \rho_1^2 + \frac{\rho_2^2}{(\rho_2^2 - 1)^2} (\rho_2^4 - 2\rho_2^2 + \rho_2^2) \tag{C-159}$$

$$= \rho_1^2 + \rho_2^4 \frac{(\rho_2^2 - 1)}{(\rho_2^2 - 1)^2}$$

$$= \rho_1^2 + \frac{\rho_2^4}{\rho_2^2 - 1}, \text{ dimensionless.}$$

In both cases

$$z_{min} = \rho_1^2 \tag{C-160}$$

and

$$z_{max} = \left\{ \begin{array}{ll} \rho_1^2 + 4 & , 0 \le \rho_2^2 < 2 \\ \\ \rho_1^2 + \dfrac{\rho_2^4}{\rho_2^2 - 1} & , \rho_2^2 \ge 2 \end{array} \right\}, \text{ dimensionless.} \tag{C-161}$$

If all values of x_3 are equally likely, the mean value of $\sigma^2_{\varepsilon_{y1}}$ is obtained as follows:

$$\overline{\sigma^2_{\varepsilon_{y1}}} = \frac{1}{\pi} \int_0^\pi \left[\sigma_1^2 + \sigma_2^2 \sin^2 x_3 + \sigma_3^2 (1 - \cos x_3)^2 \right] dx_3$$

$$= \frac{\sigma_1^2}{\pi} x_3 \Big|_0^\pi + \frac{\sigma_2^2}{\pi} \left[\frac{x_3}{2} - \frac{\sin(2x_3)}{4} \right]_0^\pi + \frac{\sigma_3^2}{\pi} x_3 \Big|_0^\pi$$

$$- \frac{2\sigma_3^2}{\pi} x_3 \Big|_0^\pi + \frac{\sigma_3^2}{\pi} \left[\frac{x_3}{2} + \frac{\sin 2x_3}{4} \right]_0^\pi$$ (C-162)

$$= \sigma_1^2 + \frac{\sigma_2^2}{2} + \sigma_3^2 - 0 + \frac{\sigma_3^2}{2}$$

$$= \sigma_1^2 + \frac{1}{2}\sigma_2^2 + \frac{3}{2}\sigma_3^2, \ V$$

where

$\overline{\sigma^2_{\varepsilon_{y1}}}$ = mean of $\sigma^2_{\varepsilon_{y1}}$ as a function of x_3, V^2.

REFERENCES

1. W. Feller, *An Introduction to Probability Theory and Its Applications*, Second Edition, John Wiley & Sons, Inc., New York, NY, 1957.

2. Emanuel Parzen, *Modern Probability Theory and Its Applications*, John Wiley & Sons, Inc., New York, NY, 1960.

3. John E. Freund, *Mathematical Statistics*, Prentice-Hall, Inc., Englewood Cliffs, NJ, 1962.

4. Daniel E. Bailey, *Probability and Statistics Models for Research*, John Wiley & Sons, Inc., New York, NY, 1971.

5. Kemeny, Snell, and Thompson, *Introduction to Finite Mathematics*, Prentice-Hall, Inc., Englewood Cliffs, NJ, 1957.

6. A. Papoulis, *Probability, Random Variables, and Stochastic Processes*, McGraw-Hill Book Company, New York, NY, 1965.

7. W. Rudin, *Principles of Mathematical Analysis*, Second Edition, McGraw-Hill Book Company, New York, NY, 1964, p. 22.

8. J. H. Laning and R. H. Battin, *Random Processes in Automatic Control*, McGraw-Hill Book Company, New York, NY, 1965, pp. 27, 28.

9. G. Korn and T. Korn, *Mathematical Handbook for Scientists and Engineers*, Second Edition, McGraw-Hill Book Company, New York, NY, 1968, p. 982.

10. Erwin Kreyszig, *Advanced Engineering Mathematics*, John Wiley & Sons, Inc., New York, NY, 1979.

11. Charles M. Close, *The Analysis of Linear Circuits*, Harcourt, Brace, and World, Inc., New York, NY, 1966, pp. 126, 127.

12. J. V. Beck and K. J. Arnold, *Parameter Estimation in Engineering and Science*, John Wiley & Sons, Inc., New York, NY, 1977.

BIBLIOGRAPHY

E. L. Crow, F. A. Davis, and M. W. Maxfield, *Statistics Manual With Examples Taken From Ordnance Development*, Dover Publications, Inc., New York, NY, 1960. (Reprint of NAVORD Report 3369-Nots 948).

DARCOM-P 706-103, Engineering Design Handbook, *Selected Topics in Experimental Statistics With Army Applications*, December 1983.

Technical Staff, The Analytic Sciences Corporation, Arthur Gelb, Ed., *Applied Optimal Estimation*, The M.I.T. Press, Massachusetts Institute of Technology, Cambridge, MA, 1974.

GLOSSARY

A

Aiming Post (Stake). **A 2.60-m pole with alternate 9.6-cm wide red and white stripes used to provide a suitable reference or zero point for indirect fire laying. Red and green lights are provided for night operation.**

Angle of Sight. **Angle of the weapon-target line with respect to horizontal; used in direct fire, in which the sights of a weapon are brought directly on the target.**

Angle of Site. **The vertical angle formed by the line of site and the base of the trajectory; used in indirect fire.**

Assembly Language. **An intermediate computer language that represents computer (machine) instructions by using mnemonic names and memory addresses by symbols rather than bit strings.**

Audition. **The ability to discriminate between different levels of pitch and loudness.**

B

Basic Reliability. **Refers to any failure that, should it occur, allows the system to continue to function, albeit with some degradation.**

Battle Range. **The range to a target within which an effective battle sight engagement can be conducted.**

Battle Sight. **A predetermined sight setting carried on a weapon for which a specific round type is preloaded into the gun and the target range is preindexed into the system and no aiming compensations are applied by the fire control computer. This is the most rapid method of engaging an enemy target and is the preferred method of engagement when quick reaction is required, the preloaded round is appropriate for the target being engaged, and the target is within the predetermined battle sight range.**

Beam Splitter. **An optical device used to divide a beam into two or more separate beams, e.g., a transparent plate coated with a very thin layer of aluminum that partially reflects the beam and partially transmits the beam.**

Binomial Distribution. **A discrete probability law stating the distribution of a binomial random variable with the chance of *s* successes in *n* trials of an experiment given the probability of success in one trial.**

Bivariate Normal Distribution. **The probability law stating the joint distribution of a pair of variates for continuous or discontinuous data; also referred to as the bell-shaped surface and the two-dimensional Gaussian distribution.**

Blasting Machine. **A manually operated item that generates an electrical impulse to initiate an explosive charge. The device allows tank main gun firing even with loss of vehicle electric power.**

Boresight. **A condition of alignment between a gun sight and the gun tube in which the optical axis of the sight (as defined by the sight reticle) intersects the axis of the gun tube (as defined by a chamber or muzzle scope) at some predefined distance from the weapon. A common boresight distance for tank gunnery is 1200 m.**

C

Caliber. **The diameter of a projectile or the diameter of the bore of a gun or launching tube. Also the length of the gun barrel measured in bore diameters (calibers), e.g., a naval 5-in./54 gun has a caliber (bore diameter) of 5 in. and a tube length of 54 calibers, or 22 ft.**

Cant. **The leaning or tilting to one side of a gun; equivalent to the roll of an airframe or missile.**

Cargo Projectile or Warhead. **A projectile that carries a cargo of submunitions that are expelled at some predetermined time of flight.**

Carriage. **A mobile or fixed support or mount for a cannon. It sometimes includes the elevating and tra-**

versing mechanisms.

Chamber Scope. An optical device that is inserted into the chamber of a gun tube and enables a test crew to determine the point of intersection of the axis of the gun tube with a distant target. The chamber scope is essentially an optical telescope whose optical axis is aligned with the axis of the bore of the gun tube at the breech end and allows a mechanic to view a distant target. The chamber scope is used when the alignments of the gun control system are being checked. The elevation control of the gun is based on sensors located at the gun trunnion, and the measurements obtained with a chamber scope accurately represent the angular position of the gun axis at the trunnion. *See also* **Muzzle Scope.**

Collimated Light or Radiation. Radiation in which every ray from any given object point is very nearly parallel to every other ray.

Conditional Probability. The probability that some event will occur given that some other specified events have occurred or will occur.

D

Dash Speed. Maximum burst speed of a vehicle for evasive maneuvering.

Dichroic Beam Splitter. An optical beam splitter that uses selective polarization to obtain two beams from a single beam.

Dimensional Analysis. Process of checking mathematical relationships for consistency of their unit dimensions.

Diopter. A measure of the refractive power of a lens system obtained by taking the reciprocal of the focal length measured in meters.

Direct Fire. Fire delivered on a target in which the sights of the weapon are brought directly on the target.

Direction Cosines. The cosines of the angles of a vector with respect to the coordinate axes. A vector may be specified by its length and its direction cosines.

Droop. The angular difference between the gun axis at the trunnion and at the muzzle.

Dynamics. Relates to the forces acting on a projectile.

E

Ergodicity. The property of stationary stochastic processes that results in the equivalence of time averages and their corresponding ensemble means.

Euler Angles. The angles of rotational transformation, e.g., the roll, pitch, and yaw angles used to transform an aircraft-referenced vector to an earth-referenced one.

Exit Pupil. The image of the objective formed by the eyepiece in a telescope or microscope.

Expected Values, Moments, Means. A subset of the statistics of a random variable that is analogous to the ensemble moments of mechanical systems; also the expected value or mean of the random variable or of functions of the random variable.

Exterior Ballistics. The study of projectile motion and orientation in flight after the projectile exits the gun muzzle and prior to target impact or fuze function.

F

Fire Control. Control over the direction, volume, and time of fire of guns or launchers by use of certain electrical, electronic, optical, thermal, or mechanical systems, devices, or aids.

Fire Control Aids. Simple mechanical devices used by the gunner to control the direction, volume, and time of fire of guns, e.g., rifle sights and tracer bullets.

Fire Control Equipment. Equipment required and used to aim guns directly at a particular target, e.g.,

radars, telescopes, laser range finders, directors, fire control computers, power plants, and the communication control systems connecting these elements.

Fire Control Instruments. Instruments that provide more exact fire control acquisition, processing, and application than aids, e.g., aiming circles, range finders, and telescopes.

Firing Tables. Tables containing the data needed to fire a gun accurately on a target under standard conditions and also the corrections that must be made for nonstandard conditions.

First-Return Logic. The logic used to select the closest target range when the laser range finder senses multiple returns.

Fly the Round Out. To obtain the complete trajectory solution.

Fragmentation Round. A projectile whose primary terminal ballistic effect is due to its breaking into fragments.

G

Gatling Gun. A machine gun with multiple barrels that fire in rotation and are mounted on a central cylinder.

Gauss-Markov Process. A continuous random process that has a normal or Gaussian probability distribution and is dependent only on the value that existed at one point in the immediate past.

Glint. Pulse-to-pulse variations in the relative phase of radar return signals from large targets and targets at close range due to the presence of multiple and physically separated radiation scattering centers on the target surface.

g-*Load.* The numerical ratio of centrifugal, acceleration, or deceleration forces to gravitational force on a maneuvering aircraft.

Grooves. The narrow channels in the bore of a rifled gun. (*Contrast with* **Lands.**) *See also* **Rifling.**

Gun Droop. See **Droop.**

H

High-Level Language. A computer language that allows common operations, such as expression evaluation, repetition, assignment, and condition at action, to be invoked in a single statement, e.g., BASIC, FORTRAN, C, JOVIAL, COBOL, and APL.

Horizontal Offset. The difference in angular orientation between the optical axis of an acquisition sight and the axis of the gun tube measured in a plane parallel to the plane of rotation of the gun turret.

Hunter-Killer Operation. A method of target engagement in which the tank commander searches for additional threat targets while the gunner fires on the current target until it is destroyed or disabled. (In classical methods of engagement the search for a new target is not started until the current engagement is completed.) Special fire control system configurations are required to perform hunter-killer operations because the commander must have a sighting system that is independent of the sight used by the gunner. In addition, the hunter sight must have the capability to direct the gunner's sight to a particular target.

I

Independent Random Variables. Discrete random variables for which the probability of one is completely unaffected by the probabilities of the others, i.e., $P(AB...Z) = P(A) \cdot P(B)...P(Z)$. Independent random variables are uncorrelated but not necessarily vice versa. However, normally distributed random variables are independent if they are uncorrelated and vice versa.

Indirect Fire. Gunfire delivered at a target that cannot be seen from the position of the gun; the procedure requires firing commands from a fire direction center.

Instantaneous Tangent to the Trajectory. The line of the slope of the trajectory at a specified point on the

trajectory.

Intervalometer. **An electrical device used to control rocket selection and rate of fire on a rocket launcher.**

J

Jerk. **The time rate of change of acceleration; it is the third time derivative of position.**

Joint Probability. **When an experiment involves more than one random variable, the joint probability density function provides the probability that each random variable takes on a value in some specified interval of the real line.**

K

Kalman Filter. **An optimal filtering technique used to estimate the state of a system in the presence of system noise and measurement errors. A member of a family of proficient, recursive, data-smoothing algorithms, which combine all the information up to and including the latest observation in an optimum fashion.**

Keepfull Anticavitators. **Hydraulic devices that prevent the pressure in the lines and chambers of a hydraulic system from falling below atmospheric pressure in order to prevent entrapped air in the hydraulic system from forming bubbles, which collapse when the pressure is suddenly raised and result in erosion and pitting of interior surfaces.**

Kinematics. **The study of the relative motion between points in space without reference to the forces that act on the system.**

L

Lands. **Raised ridges in the bore of a rifled gun. (***Contrast with*** Grooves.)** *See also* **Rifling.**

Last-Return Logic. **The logic used to select the farthest target range when the laser range finder senses multiple returns.**

Lay. **To direct the orientation of a weapon sighting system to position the sighting reticle onto the designated target.**

Least Squares. **One criterion for optimization: obtains estimates and statistics of parameters that minimize the sum of squared errors: (min $\sum_{i=1}^{n} \varepsilon_i^2$).**

Life Cycle Cost. **The total cost of acquisition and ownership to the Government over the life of the system; it includes the cost of development, acquisition, operation, support, and disposal.**

Line of Sight. **Straight line of vision from weapon station to target.**

Line of Site. **Straight line between the origin of the trajectory and the target.**

Logistics. **The branch of military science dealing with the procurement, maintenance, and movement of equipment, supplies, and personnel.**

M

Mach Number. **The ratio of the airspeed of a moving body to the speed of sound at the altitude of the body.**

Magnus Effect. *See* **Magnus Force** *or* **Magnus Moment.**

Magnus Force. **The component of the force of air resistance acting in a direction perpendicular to the plane of yaw. It is caused by the action between the boundary layer of air rotating with the projectile and the airstream.**

Magnus Moment. **The couple produced if the Magnus force line of action does not pass through the projectile centroid.**

Maintainability. A characteristic designed into the equipment; a measure of the ability of an item to be retained in or restored to a specified condition when maintenance is performed.

MANPRINT. A comprehensive management and technical program to improve total system (soldier and equipment) performance by focusing on soldier performance and reliability.

Markov Process. A stochastic process which assumes that in a series of random events the probability of an occurrence of each event depends only on the immediately preceding outcome.

Mirror Symmetry. Exact correspondence of form (configuration) with respect to a plane experienced as if the plane were a mirror.

Monte Carlo Technique. A method of simulation that uses appropriate random value generators to produce realistic random variable inputs and obtains statistics on the inputs and outputs.

Multiplexer. A device that divides a frequency or time interval into subintervals to provide many channels for the sampling or transmission of information.

Muzzle Scope. An optical device that is inserted into the muzzle end of a gun tube and enables a test crew to determine the point of intersection of the axis of the gun tube with a distant target. The muzzle scope is essentially an optical telescope whose optical axis is aligned with the axis of the bore of the gun tube at the muzzle end and allows a mechanic to view a distant target through an offset eyepiece. *See also* **Chamber Scope.**

Muzzle Reference Sensor (MRS). An optical or electro-optical device that is installed on a tank or howitzer to measure the droop of the gun tube.

N

Nap-of-the-Earth Flight. Flight at varying airspeeds as close to the surface of the earth as vegetation, obstacles, and vision devices will permit while generally following the contours of the earth.

Nutation. Oscillation of the yaw of a projectile. *See also* **Yaw Angle.**

O

Obturate. To seal the breech of a gun to prevent escape of propellent gases.

Off-Carriage Fire Control Equipment. Fire control items, e.g., range finders, radars, position locators, and computers, that are not carried on the weapon carriage.

On-Carriage Fire Control Equipment. Fire control items, e.g., sighting telescopes and range finders, that are carried on the weapon carriage.

P

Palm Switch. A safety device located on the gunner's hand controls. When the hand grips are squeezed, the palm switch is engaged and activates the gun control and firing circuitry.

Pendulous Cant Sensor. Gravity device that indicates deviation from the vertical.

Piecewise Linear Approximation. The process of dividing the domain of a nonlinear function into subdomains so that the function of each subdomain is approximately linear.

Pintle. Gun mounting pin.

Pitot Tube. A device used to measure local airspeed. It consists of a small tube which points in the upstream direction of an airflow. (Measuring the pressure inside the tube with respect to ambient pressure provides a means of measuring airspeed.)

Plane of Yaw. The plane that includes both the projectile velocity vector and the projectile longitudinal axis. (Yaw is caused by the action between the boundary layer of air rotating with the projectile and the airstream.)

Plant Equation. The set of differential equations which define the system that uses a Kalman filter.

Prediction Angle. Angle between line of sight and weapon line.

Probability. The real number assigned to a random event which indicates what chance that event has of occurring among all the possible events of the experiment. The probability ranges from zero (the impossible event) to unity (the certain event).

Probability Density Function (pdf). The continuous and/or discrete positive-valued function which describes the chance that a random variable will take on a particular value of its defined set of values. The pdf area must equal unity, and there must be no more than a countable number of discontinuities.

Projectile Jump. The offset between the center of impact and the aim point after corrections for the non-standard conditions and gravitational and drift effects have been applied. The magnitude of the jump for any weapon and projectile combination is determined from a mathematical representation of the center of impact of many rounds fired from a large number of vehicles under many different firing conditions.

Proprioception. The ability to sense through certain bodily receptors (muscles, tendons, etc.) the position of the body and its movements in space and time.

Pullover Gage. A gage that is pulled through the bore of a gun tube to measure tube wear. It is configured like a standard star gage but keeps the contact points of the gage on top of the lands of a rifled tube.

Pulse Doppler Radar. Pulse radar that uses the Doppler effect to obtain information about the velocity of a target.

Q

Quadrant Elevation. The vertical angle measured in mils between the gun axis at the trunnion and a plane that is normal to the local gravity vector. In indirect fire it is the elevation of the gun tube, which is required for the projectile to hit the aim point. This elevation accounts for nonstandard conditions, the propellant charge used, and the altitudes of the gun and target. *See also* **Superelevation.**

R

Random Variable (rv). A variable that may take on any value of a defined set or range of values. The chance that it takes on some particular value is described by its continuous and/or discrete, positive-valued probability density function (pdf). The area under the pdf must equal unity, and the pdf can have no more than a countable number of discontinuities. If the pdf has no continuous regions, it is discrete, and the random variable describes only discrete chance events.

Registration. That fire delivered to obtain corrections for nonstandard conditions in order to increase the accuracy of subsequent artillery fires.

Registration Point. The designated known spot for registration; it should be chosen so enemy target acquisition devices do not locate the registering unit.

Reliability. The probability that a device will function without failure over a specified time period or amount of usage.

Resolver. A device whose input is a vector quantity and whose outputs are components of the vector. Resolvers are generally bilateral, so inputs and outputs are interchangeable.

Reticle. An optical element located at an image plane; contains a pattern that assists in pointing an instrument or measuring target characteristics.

Retrograde Mission. An organized movement to the rear or away from the enemy. It may be forced by the enemy or may be made voluntarily. Such movements may be classified as withdrawal, retirement, or delaying operations. Retrograde missions, however, do not include the defensive operation of holding ground.

Rifling. The helical grooves cut in the bore of a rifled gun tube, beginning at the front face of the gun chamber and extending to the muzzle. The grooves produce a stabilizing spin on the projectile in flight.

Rotational Symmetry. Exact correspondence of form (configuration) with respect to an axis of rotation (spin).

S

Sabot. A lightweight carrier, whose diameter fills the bore of a weapon, in which a subcaliber projectile is centered to permit firing it in a larger caliber weapon. Discarding sabots are used in tank guns for hypervelocity armor-piercing depleted uranium or tungsten carbide projectiles.

Salvo Theory. The mathematical theory used to predict target hit probabilities for short bursts fired in rapid succession. Under these conditions all rounds in the burst share a common set of random error statistics. (*Contrast with* **Slow Rate of Fire Assumption.**)

Scratch Pad Memory. A special memory used for the temporary storage of manual control panel inputs.

Sight Synchronization. The process of measuring the loss in boresight between the gun sight and the axis of the gun tube as the sight elevation is increased or decreased from a zero reference position.

Six-Degree-of-Freedom Body. A body free to move in the three orthogonal translation directions (x, y, z) and in the three rotation orientations (roll, pitch, yaw).

Slow Rate of Fire Assumption. The mathematical theory used to predict target hit probability for the firing of single rounds. It is assumed that the gun is aimed before each round and that each round is considered to be statistically independent in terms of those random variables that vary from round to round. The rounds, however, may share a common set of statistics for those random variables that change slowly over time or from engagement to engagement. (*Contrast with* **Salvo Theory.**)

Snapshot Fire. A quick shot without using full fire control solution.

State Variable. One of the minimum set of numbers or variables that contains enough information about the history of a system to enable prediction of its future behavior.

Stationarity. The tendency in stochastic processes of the statistics of a stochastic variable to be independent of when the variable is observed; also referred to as strict stationarity.

Stationarity, Weak. The tendency in stochastic processes of the first two moments of a pair of stochastic variables to depend only upon their time difference and not on when they were observed; also referred to as wide-sense stationarity.

Stochastic Process. An ensemble of random variables or a process in which the random variables and their pdf's are functions of some independent variable, usually time. These random variables are called stochastic variables.

Subtenses. Regions subtended by the angular coverage of a sighting device, e.g., optical and thermal.

Superelevation. The angle between the line of sight to a target and the axis of the gun tube measured in a plane that is perpendicular to the gun trunnion axis. In direct fire it compensates for the fall of the projectile due to the pull of gravity. *See also* **Quadrant Elevation.**

Superposition, Principle of. A linear system characteristic which states that the output due to all inputs is the sum of all outputs obtained from each input taken one at a time.

T

Thermal Imaging Sight. An electro-optical sighting instrument that is sensitive to the thermal radiation generated by organic objects and reflected or radiated by inorganic objects. The device produces images that represent the thermal or temperature signature of a target.

Three-Degree-of-Freedom Body. A body (considered at a point) free to move in the three orthogonal translation directions (x, y, z).

Time of Flight. Elapsed time in seconds from the instant a projectile or other missile leaves a gun or launcher until the instant it strikes or bursts.

Time Averages. The mean or the mean-square value in stochastic processes obtained by integrating over the independent variable (usually time) of the stochastic variable; also referred to as time means.

Transpose. The matrix obtained from a given matrix by interchanging its rows and columns. The conversion of a column vector to a row vector and vice versa.

Trunnion. The bearing surfaces supporting a piece of artillery on its carriage and forming the horizontal axis about which the gun tube rotates when it is elevated.

Turret Bustle. An interior or exterior storage space at the rear of a turret.

U

Uniform Distribution. A continuous distribution in which all values of the random variable are equally probable over the specified interval on the real line.

V

Variance. The second central moment of a random variable; a measure of the square of the deviations of the values taken on by the random variable with respect to the mean of the random variable.

Vertical Zeroing Correction. The correction applied to the direction a gun points to compensate for the component of projectile jump in the vertical plane.

W

Weapon Fire Control or Weapon Control. *See* Fire Control.

Weapon Line. Extension of the weapon axis.

White Noise. A stochastic process whose power spectral density (psd) function is a constant, e.g., thermal noise.

White Noise, Band Limited. A stochastic process whose power spectral density (psd) function is a constant over a frequency range and essentially zero outside this range.

Y

Yaw Angle. In exterior ballistics, the angle between the rotational axis of symmetry of a projectile and the velocity vector of the projectile.

INDEX

A

D

E

V

W

Y

SUBJECT TERM (KEY WORD) LISTING

3- or 6-degree-of-freedom
Alpha-beta-gamma filtering
Ammunition
Ballistic reticle
Ballistics
Error budget
Filtering
Gun dynamics
Kalman filtering
Laser range finder
Miss distance
Modeling
Muzzle velocity
Optical sight
Prediction
Probability of hit
Probability of incapacitation
Reticle
Sensors
Simulation
Statistical analysis
Timeline
Tracking, autotracker
Weapon system analysis
Weapon system design

Custodian:
   Army—AR

Preparing activity:
   Army—AR
(Project 12GP-A004)

STANDARDIZATION DOCUMENT IMPROVEMENT PROPOSAL

INSTRUCTIONS

1. The preparing activity must complete blocks 1, 2, 3, and 8. In block 1, both the document number and revision letter should be given.

2. The submitter of this form must complete blocks 4, 5, 6, and 7.

3. The preparing activity must provide a reply within 30 days from receipt of the form.

NOTE: This form may not be used to request copies of documents, nor request waivers, or clarification of requirements on current contracts. Comments submitted on this form do not constitute or imply authorization to waive any portion of the referenced document(s) or to amend contractual requirements.

	1. DOCUMENT NUMBER	2. DOCUMENT DATE *(YYMMDD)*
	MIL-HDBK-799 (AR)	960405

3. DOCUMENT TITLE

FIRE CONTROL SYSTEMS—GENERAL

4. NATURE OF CHANGE *(Identify paragraph number and include proposed rewrite, if possible. Attach extra sheets as needed.)*

5. REASON FOR RECOMMENDATION

6. SUBMITTER

a. NAME *(Last, First, Middle Initial)*	b. ORGANIZATION	
c. ADDRESS *(Include Zip Code)*	d. TELEPHONE *(Include Area Code)*	7. DATE SUBMITTED *(YYMMDD)*

8. PREPARING ACTIVITY

a. NAME	b. TELEPHONE *(Include Area Code)*	
US Army Armament Research, Development, and Engineering Center	(1) Commercial 201-724-6671	(2) DSN 880-6671

c. ADDRESS *(Include Zip Code)*	IF YOU DO NOT RECEIVE A REPLY WITHIN 45 DAYS, CONTACT:
AMSTA-AR-EDE-S Picatinny Arsenal, NJ 07806-5000	Defense Quality and Standardization Office 5203 Leesburg Pike, Suite 1403, Falls Church, VA 22041-3466 Telephone (703) 756-2340 AUTOVON 289-2340